HARVARD UNIVERSITY

Library of the
Museum of
Comparative Zoology

VOL. 34, NO. 1–2 1992

MALACOLOGIA

nternational Journal of Malacology

Revista Internacional de Malacologia

Journal International de Malacologie

Международный Журнал Малакологии

Internationale Malakologische Zeitschrift

Publication dates

Vol. 28, No. 1–2	19 January 1988
Vol. 29, No. 1	28 June 1988
Vol. 29, No. 2	16 Dec. 1988
Vol. 30, No. 1–2	1 Aug. 1989
Vol. 31, No. 1	29 Dec. 1989
Vol. 31, No. 2	28 May 1990
Vol. 32, No. 2	7 June 1991
Vol. 33, No. 1–2	6 Sep. 1991

QL
417

VOL. 34, NO. 1–2 1992

MCZ
LIBRARY

SEP 1 5 1992

HARVARD
UNIVERSITY

MALACOLOGIA

International Journal of Malacology

Revista Internacional de Malacologia

Journal International de Malacologie

Международный Журнал Малакологии

Internationale Malakologische Zeitschrift

MALACOLOGIA

Editor-in-Chief:

GEORGE M. DAVIS

Editorial and Subscription Offices:

Department of Malacology
The Academy of Natural Sciences of Philadelphia
1900 Benjamin Franklin Parkway
Philadelphia, Pennsylvania 19103-1195, U.S.A.

Co-Editors:

EUGENE COAN
California Academy of Sciences
San Francisco, CA

CAROL JONES
Denver, CO

Assistant Managing Editor:

CARYL HESTERMAN

Associate Editors:

JOHN B. BURCH
University of Michigan
Ann Arbor

ANNE GISMANN
Maadi
Egypt

MALACOLOGIA is published by the INSTITUTE OF MALACOLOGY, the Sponsor Members of which (also serving as editors) are:

KENNETH J. BOSS
Museum of Comparative Zoology
Cambridge, Massachusetts

JOHN BURCH, *President-Elect*

MELBOURNE R. CARRIKER
University of Delaware, Lewes

GEORGE M. DAVIS
Secretary and Treasurer

CAROLE S. HICKMAN, *Vice-President*
University of California, Berkeley

JAMES NYBAKKEN, *President*
Moss Landing Marine Laboratory
California

CLYDE F. E. ROPER
Smithsonian Institution
Washington, D.C.

W. D. RUSSELL-HUNTER
Syracuse University, New York

SHI-KUEI WU
University of Colorado Museum, Boulder

Participating Members

EDMUND GITTENBERGER
Secretary, UNITAS MALACOLOGICA
Rijksmuseum van Natuurlijke
Historie
Leiden, Netherlands

JACKIE L. VAN GOETHEM
Treasurer, UNITAS MALACOLOGICA
Koninklijk Belgisch Instituut
voor Natuurwetenschappen
Brussel, Belgium

Emeritus Members

J. FRANCIS ALLEN, *Emerita*
Environmental Protection Agency
Washington, D.C.

ELMER G. BERRY,
Germantown, Maryland

ROBERT ROBERTSON
The Academy of Natural Sciences
Philadelphia, Pennsylvania

NORMAN F. SOHL
U.S. Geological Survey
Reston, Virginia

Copyright © 1992 by the Institute of Malacology

1992

EDITORIAL BOARD

J. A. ALLEN
Marine Biological Station
Millport, United Kingdom

R. BIELER
Field Museum
Chicago, U.S.A.

E. E. BINDER
Muséum d'Histoire Naturelle
Genève, Switzerland

A. J. CAIN
University of Liverpool
United Kingdom

P. CALOW
University of Sheffield
United Kingdom

J. G. CARTER
University of North Carolina
Chapel Hill, U.S.A.

R. COWIE
Bishop Museum
Honolulu, HI., U.S.A.

A. H. CLARKE, Jr.
Portland, Texas, U.S.A.

B. C. CLARKE
University of Nottingham
United Kingdom

R. DILLON
College of Charleston
SC, U.S.A.

C. J. DUNCAN
University of Liverpool
United Kingdom

D. J. EERNISSE
University of Michigan
Ann Arbor, U.S.A.

V. FRETTER
University of Reading
United Kingdom

E. GITTENBERGER
Rijksmuseum van Natuurlijke Historie
Leiden, Netherlands

F. GIUSTI
Università di Siena, Italy

A. N. GOLIKOV
Zoological Institute
Leningrad, U.S.S.R.

S. J. GOULD
Harvard University
Cambridge, Mass., U.S.A.

A. V. GROSSU
Universitatea Bucuresti
Romania

T. HABE
Tokai University
Shimizu, Japan

R. HANLON
Marine Biomedical Institute
Galveston, Texas, U.S.A.

J. A. HENDRICKSON, Jr.
Academy of Natural Sciences
Philadelphia, PA, U.S.A.

D. M. HILLIS
University of Texas
Austin, U.S.A.

K. E. HOAGLAND
Association of Systematics Collections
Washington, DC, U.S.A.

B. HUBENDICK
Naturhistoriska Museet
Göteborg, Sweden

S. HUNT
Lancashire
United Kingdom

R. JANSSEN
Forschungsinstitut Senckenberg,
Frankfurt am Main, Germany

R. N. KILBURN
Natal Museum
Pietermaritzburg, South Africa

M. A. KLAPPENBACH
Museo Nacional de Historia Natural
Montevideo, Uruguay

J. KNUDSEN
Zoologisk Institut & Museum
København, Denmark

A. J. KOHN
University of Washington
Seattle, U.S.A.

A. LUCAS
Faculté des Sciences
Brest, France

C. MEIER-BROOK
Tropenmedizinisches Institut
Tübingen, Germany

H. K. MIENIS
Hebrew University of Jerusalem
Israel

J. E. MORTON
The University
Auckland, New Zealand

J. J. MURRAY, Jr.
University of Virginia
Charlottesville, U.S.A.

R. NATARAJAN
Marine Biological Station
Porto Novo, India

J. ØKLAND
University of Oslo
Norway

T. OKUTANI
University of Fisheries
Tokyo, Japan

W. L. PARAENSE
Instituto Oswaldo Cruz, Rio de Janeiro
Brazil

J. J. PARODIZ
Carnegie Museum
Pittsburgh, U.S.A.

J. P. POINTER
Ecole Pratique des Hautes Etudes
Perpignan Cedex, France

W. F. PONDER
Australian Museum
Sydney

R. D. PURCHON
Chelsea College of Science & Technology
London, United Kingdom

QI Z. Y.
Academia Sinica
Qingdao, People's Republic of China

D. G. REID
The Natural History Museum
London, United Kingdom

N. W. RUNHAM
University College of North Wales
Bangor, United Kingdom

S. G. SEGERSTRÅLE
Institute of Marine Research
Helsinki, Finland

A. STAŃCZYKOWSKA
Siedlce, Poland

F. STARMÜHLNER
Zoologisches Institut der Universität
Wien, Austria

Y. I. STAROBOGATOV
Zoological Institute
Leningrad, U.S.S.R.

W. STREIFF
Université de Caen
France

J. STUARDO
Universidad de Chile
Valparaiso

S. TILLIER
Muséum National d'Histoire Naturelle
Paris, France

R. D. TURNER
Harvard University
Cambridge, Mass., U.S.A.

J.A.M. VAN DEN BIGGELAAR
University of Utrecht
The Netherlands

J. A. VAN EEDEN
Potchefstroom University
South Africa

N. H. VERDONK
Rijksuniversiteit
Utrecht, Netherlands

B. R. WILSON
Dept. Conservation and Land Management
Netherlands, Western Australia

H. ZEISSLER
Leipzig, Germany

A. ZILCH
Forschungsinstitut Senckenberg
Frankfurt am Main, Germany

MALACOLOGIA, 1992, 34(1–2): 1–24

BIOLOGY AND COMPARATIVE ANATOMY OF THREE NEW SPECIES OF COMMENSAL GALEOMMATIDAE, WITH A POSSIBLE CASE OF MATING BEHAVIOR IN BIVALVES

Paula M. Mikkelsen[1] & Rüdiger Bieler[2]

ABSTRACT

Three new galeommatid bivalves, *Divariscintilla octotentaculata*, *D. luteocrinita*, and *D. cordiformis*, are described as commensals occupying the burrows of the mantis shrimp *Lysiosquilla scabricauda* from central eastern Florida. Morphological comparisons are made with all other known members of the genus, comprising two previously described species from the same burrow system (*D. yoyo*, *D. troglodytes*) and the type species, *D. maoria*, from New Zealand. Key characters defining this genus (hinge morphology, flower-like organs, "hanging foot" structure) are discussed, especially with regard to their presence in other galeommatoidean genera. Intraspecific interaction resembling mating behavior is noted and discussed as one of the few possible examples in the Bivalvia.

Key words: *Divariscintilla*, Galeommatoidea, Bivalvia, systematics, anatomy, mating behavior, commensalism, Stomatopoda.

INTRODUCTION

Investigation of the organisms associated with the sand-burrowing mantis shrimp *Lysiosquilla scabricauda* (Lamarck, 1818) (Crustacea: Stomatopoda: Lysiosquillidae) in shallow waters of eastern Florida has revealed a community of seven molluscan species that appear highly dependent on this specialized habitat. Remarkably, all of these species were found to be either poorly known or undescribed. Accounts of the two species of vitrinellid gastropods—*Cyclostremiscus beauii* (Fischer, 1857) and *Circulus texanus* (Moore, 1965); Bieler & Mikkelsen, 1988—and two of the five species of bivalves—*Divariscintilla yoyo* Mikkelsen & Bieler, 1989, and *D. troglodytes* Mikkelsen & Bieler, 1989—have appeared elsewhere. This report deals with the remaining three species of galeommatoidean bivalves. Although superficially different from the two species previously described, and preliminarily treated as members of another genus (as *Scintilla* spp.; Mikkelsen & Bieler, 1989: 192; Eckelbarger et al., 1990), detailed study has revealed their proper placement in *Divariscintilla*, and has shown them to be in fact more similar to the New Zealand type species, *D. maoria* Powell, 1932, than were the two species previously described from Florida stomatopod burrows.

MATERIAL AND METHODS

Lysiosquilla burrows in shallow-water sand flats at several locations on the central eastern Florida coast were sampled using a stainless steel bait pump ("yabby pump") and sieves of 1-2 mm mesh. Sampling depths during extreme low water ranged from less than 0.5 m to supratidal, when the water level lay several centimeters below the level of the sand.

Living clams were maintained in finger bowls of seawater at ambient laboratory conditions (22-25°C), with variable lighting. Water was changed every 1-2 days, and an irregularly-supplied, unmeasured diet of mixed unicellular algae (e.g., *Isochrysis*, *Chlorella*, *Chaetoceras*) was provided. Behavioral studies were aided by video recordings taken of the living animals in aquaria using a standard commercial 1/2-inch-format video camera equipped with a macro lens.

Transfer of specimens between laboratory bowls was best accomplished using small spoons. The spoon could be applied against the glass from below the specimen to gently break the byssus threads while also cradling the clam. Handling these kinds of animals with forceps is awkward and frequently causes damage to fragile shells and tissue.

Relaxation prior to dissection or preservation was most effectively accomplished with

[1]Harbor Branch Oceanographic Museum, Harbor Branch Oceanographic Institution, 5600 Old Dixie Highway, Ft. Pierce, Florida 34946 U.S.A., and Department of Biological Sciences, Florida Institute of Technology, Melbourne, Florida 32901 U.S.A.
[2]Department of Zoology, Field Museum of Natural History, Roosevelt Road at Lake Shore Drive, Chicago, Illinois 60605 U.S.A.

crystalline magnesium sulfate, added directly to the finger-bowl water in unquantified small amounts. Methylene-blue/basic-fuchsin and neutral red were used to delineate tissues and organs in gross dissections.

For histological serial sections, animals were fixed in 5% buffered formalin (Humason, 1962: 14). Shells were decalcified using either dilute (approximately 0.5%) hydrochloric acid (complete decalcification within minutes) or a 1% solution of ethylenediamene tetraacetic acid (EDTA, adjusted to pH 7.2; decalcification complete in 5-6 days). Specimens were embedded in paraplast, sectioned at 8 μm and stained with Gomori's green trichrome (modified from Vacca, 1985). Staining reactions described in the text refer to this method. Colors referred to in the text are supplied for future use, that is, to infer homologies of the various glands. Photomicrographs of sections were taken with an Olympus BH-2 stereomicroscope fitted with an Olympus OM-2 camera with Kodak Panatomic-X (ASA 32) film.

For scanning electron microscopy (SEM), preserved specimens were passed through an ethanol-to-acetone series and critical-point dried. These and air-dried shells were coated with gold/palladium and examined using a Zeiss Novascan-30 scanning electron microscope.

All cited anatomical measurements were taken from specimens of average size (see under descriptions). Throughout the text, "relaxed" refers to the condition of an animal in normal crawling posture and does not refer to any chemical treatment.

Cited institutions are (* indicates location of type and other voucher material):

AMNH— American Museum of Natural History, New York, New York
DMNH— Delaware Museum of Natural History, Wilmington
*FMNH— Field Museum of Natural History, Chicago, Illinois
HBOI— Harbor Branch Oceanographic Institution, Ft. Pierce, Florida
*HBOM— Harbor Branch Oceanographic Museum [formerly Indian River Coastal Zone Museum], HBOI
*MCZ— Museum of Comparative Zoology, Harvard University, Cambridge, Massachusetts
*SBMNH—Santa Barbara Museum of Natural History, California
SMSLP— Smithsonian Marine Station at Link Port, Ft. Pierce, Florida
*USNM— National Museum of Natural History, Smithsonian Institution, Washington, D. C.

TAXONOMIC DESCRIPTIONS

Family GALEOMMATIDAE Gray, 1840

Genus *Divariscintilla* Powell, 1932

Type species: Divariscintilla maoria Powell, 1932: 66; by original designation. Recent, New Zealand.

Remarks: Redescribed by Mikkelsen & Bieler (1989: 193). See remarks concerning generic placement under Discussion.

Divariscintilla octotentaculata n. sp.
(Figs. 1, 4, 7-13, 23, 33)

Material examined

Holotype: 5.3 mm [shell length], FMNH 223401. Paratypes (31): 4.2, 4.2 mm, FMNH 223402; 3.2, 3.2, 3.2, 3.3, 3.3, 3.6, 3.8 mm, HBOM 064:01866; 4.2, 4.2, 3.6, 2.9 mm (preserved soft-bodies + shells coated for SEM), HBOM 064:01867; 3.9, 4.3, 4.3 mm, HBOM 064:01865; 3.0, 3.1, 3.2, 3.4, 3.6 mm, USNM 859443; 3.2, 3.2, 3.2, 3.4, 4.1 mm, MCZ 302510; 1.7, 3.4, 3.4, 3.8, 3.8 mm, SBMNH 35167. Total material: 262 specimens: FLORIDA: Ft. Pierce Inlet: 10 March 1987, 3; 2-3 May 1987, 73; 24 June 1987, 91; 03 August 1987, 2; 14 August 1987, 10; 31 August 1987, 1; 28 December 1987, 7; 11 March 1988, 7; 12 April 1988, 38; 16 October 1990, 2; 03 February 1991; 13. -Sebastian Inlet: 30 December 1987, 26. -St. Lucie Inlet: 18 February 1982, 2.

Type locality

Ft. Pierce Inlet, Indian River Lagoon, St. Lucie County, eastern Florida, 27°28.3'N, 80°17.9'W, occupying *Lysiosquilla scabricauda* burrows on intertidal sand flats with patches of the seagrass *Halodule wrightii* Ascherson. Paratypes all from type locality.

Diagnosis

Animal translucent white. Mantle thin, with retractable, papillose folds covering anterior and posterior thirds of shell. Tentacles originating at dorsal shell margin, two pairs anteriorly, two pairs posteriorly. Posterior foot-extension relatively short. Shell roundly

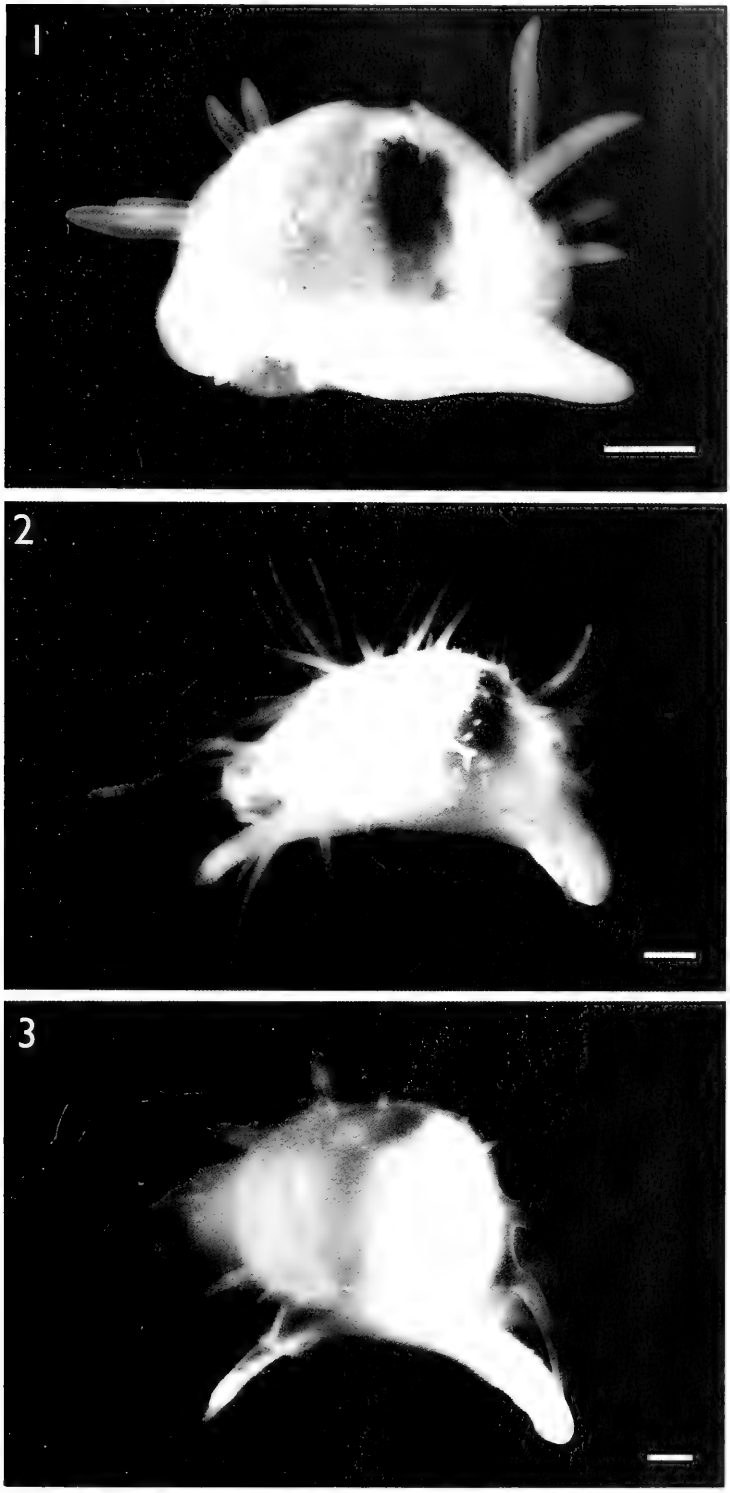

FIGS. 1-3. Photographs of living animals. 1. *Divariscintilla octotentaculata*. 2. *D. luteocrinita*. 3. *D. cordiformis*. Scale bars = 1.0 mm.

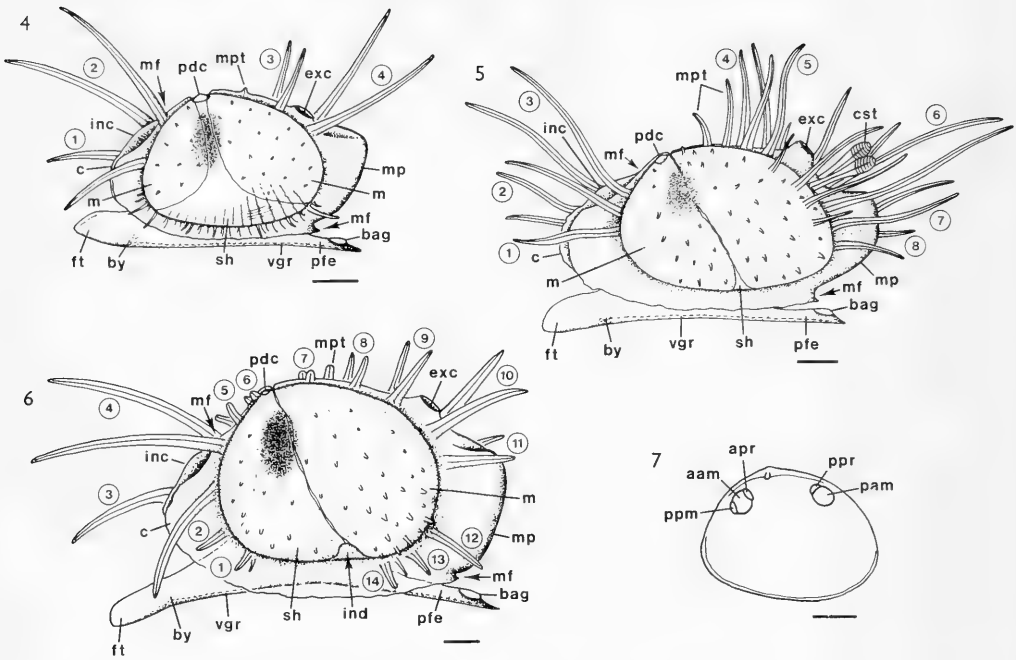

FIGS. 4-7. External appearance and internal shell morphology. Tentacle pairs numbered from anterior to posterior (for text reference only; identical numbers do not imply homology). 4. *Divariscintilla octotentaculata*, in crawling position, from left side. 5. *D. luteocrinita*, same as Fig 4. 6. *D. cordiformis*, same as Fig. 4. 7.*D. octotentaculata*, internal surface of right valve, showing approximate locations of muscle insertions. Scale bars = 1.0 mm. (aam, anterior adductor muscle scar; apr, anterior pedal retractor muscle scar; bag, byssus adhesive gland; by, location of byssus gland; c, cowl; cst, club-shaped tentacles; exc, excurrent "siphon"; ft, foot; inc, incurrent "siphon"; ind, shell indentation; m, mantle fold; mf, point of mantle fusion; mp, mantle pouch; mpt, median pallial tentacle; pam, posterior adductor muscle scar; pdc, prodissoconch; pfe, posterior foot-extension; ppm, pedal protractor muscle scar; ppr, posterior pedal retractor muscle scar; sh, shell; vgr, ventral pedal groove).

triangular, with umbo slightly anterior, smooth exteriorly, with weak radial ribs interiorly; length approximately 70% of extended mantle length. No "flower-like organ" on anterior surface of visceral mass.

Description

External Features and Mantle: Living extended animal (Figs. 1, 4) generally 5-7 mm in length, translucent white except for dark digestive gland within visceral mass. Shell largely external, with only anterior and posterior thirds of shell covered in life by mantle folds (Fig. 4, m), not meeting at lateral midline. Mantle folds fully retractable, finely papillose, with scattered larger papillae. Mantle thin, extending beyond shell edges; entire surface finely papillose, with fringe of longer papillae along ventral margin of shell. Two pallial openings: (1) anteropedal opening, from a point anterior to umbones to a point posterior to foot (Fig. 4, mf), forming extensive anterior cowl (Fig. 4, c), the edges of which are held together to form an effective incurrent "siphon" (Fig. 4, inc); and (2) posterodorsal excurrent opening (Fig. 4, exc) between posterior tentacle pairs, either as simple opening or on rounded protuberance forming distinct siphon; appearance dependent on degree of pallial expansion. Posterior mantle fusion forming a rounded, protruding pouch (Fig. 4, mp) containing the gills. Two pairs (one long, one short) retractable, anterior tentacles arising from near shell edge; dorsalmost pair longest. Two pairs (one long, one short) retractable tentacles in vicinity of excurrent siphon, also arising from near shell edge; posteriormost pair longest. A single,

short, mid-dorsal tentacle (Fig. 4, mpt), just posterior to umbo. An additional 1-2 pairs of short tentacles (=enlarged papillae?) in larger specimens (approximately 5 mm) at ventral shell edge at anterior and posterior ends of ventral papillose fringe. Each tentacle with papillose surface and central core of longitudinal muscle and nerve fibers, visible as an inner "thread" under low magnification. Inner pallial fold of non-shell areas (e.g., cowl, ventral mantle margin, posterior pouch) highly muscular.

Preserved specimens completely (or nearly so) retracted into shell, however, shell usually gaping, with tentacles (especially anterodorsal) slightly protruding beyond shell edges.

Shell (Figs. 7-11, 13): Shell generally 3-5 mm in length, roundly triangular, longer posteriorly, equivalve, rather compressed, glossy, iridescent, transparent, smooth except for fine concentric growth lines and weak radial ribs most evident interiorly at ventral margin (Fig. 9). Size large relative to mantle, comprising approximately 70% of extended mantle length. Valves held open at a 50-60x angle while crawling, capable of complete closure ventrally but gaping slightly anteriorly and posteriorly. Adductor muscle scars faint, subequal (Figs. 7, 9). Pallial line entire, indistinct. Periostracum colorless, most evident at ventral shell edge (Fig. 9, per).

Hinge line short (Fig. 10). One small, rounded cardinal tooth (Fig. 10, car) in each valve, that of left valve sometimes slightly bifid; lateral teeth absent. Cardinal teeth abutting, not interlocking. External ligament (Fig. 10, lig) weak, amphidetic, supported by nymph. Internal ligament (resilium; Fig. 10, res) stronger, opisthodetic.

Prodissoconch (Fig. 11) brownish-yellow, approximately 360 fm in length. Prodissoconch I corresponding in size to shell of newly released larva, approximately 32% of length of prodissoconch II; sculpture not discernible (surface abraded in adult shell). Prodissoconch II sculptured only with coarse and fine concentric growth lines. Prodissoconch I and II stages distinct, demarcated more by change in convexity than by sculpture or growth discontinuity (Fig. 11, single arrow). Demarcation between prodissoconch II and dissoconch abrupt (Figs. 8; 11, double arrow).

Shell microstructure (Fig. 13) cross-lamellar centrally, with thin prismatic layer covering each side, as in *Divariscintilla yoyo* (see Mikkelsen & Bieler, 1989).

Organs of the Pallial Cavity: Foot (Fig. 4, ft) as previously described for *Divariscintilla yoyo* (see Mikkelsen & Bieler, 1989), including hatchet-shaped anterior portion, narrowed posterior extension (Fig. 4, pfe), anterior byssus gland (Fig. 4, by), ciliated ventral groove (Fig. 4, vgr) supplied with numerous mucous glands, and terminal byssus adhesive gland (Fig. 4, bag). Byssus gland of undefined structure, staining turquoise in histological sections; byssus adhesive gland of branching lamellar folds, staining purplish-red. One to four byssus threads produced, emanating from extreme posterior tip of foot. Opaque white pigment band (of unknown function) along anterodorsal tip of foot, staining dark purplish-red in sections.

Anterior and posterior adductor muscles subequal, of moderate diameter. Anterior and posterior pedal retractor muscles smaller in diameter, inserting on shell just dorsal and medial to their respective adductor muscle scars. Very small pedal protractor muscle merging with anteroventral edge of anterior adductor muscle just before both attach to shell; inserting into anterior visceral mass just dorsal of labial palps. Muscles leaving very faint attachment scars on shell (Figs. 7, 9).

Overall morphologies of visceral mass, labial palps and ctenidia as in *Divariscintilla yoyo* (see Mikkelsen & Bieler, 1989). Palps with 6-8 lamellae each side. Ctenidia smooth, unpleated (appearing posteriorly loosely pleated in preserved specimens due to contraction). Outer demibranch approximately 50% smaller than inner; both demibranchs ventrally rounded and with both interfilamental and interlamellar connectives. Cilial currents on palps and ctenidia not verified.

Flower-like organ absent (see Discussion below).

Digestive System: Structure of digestive system (mouth, esophagus, stomach, midgut, hindgut, rectum) of same organization as that in *Divariscintilla yoyo* (see Mikkelsen & Bieler, 1989: fig. 28).

Suprabranchial Chamber: Arrangement of openings and presence of glandular patches (?hypobranchial glands; Fig. 23, hyp) adjacent to rectum as in *Divariscintilla yoyo* (see Mikkelsen & Bieler, 1989: fig. 29).

Nervous System: Arrangement of ganglia, statocysts, and major nerves as described for *Divariscintilla yoyo* (see Mikkelsen & Bieler, 1989: fig. 31). Left and right posterior tenta-

cles innervated by branches from the pallial nerve, adjacent to its junction with the visceral ganglion. Anterior tentacles similarly innervated but both from a common branch of the pallial nerve, adjacent to its junction with the cerebro-pleural ganglion.

Reproductive System: Simultaneous hermaphrodite. Ovotestis white, encompassing most of volume of visceral mass, as in *Divariscintilla yoyo* (see Mikkelsen & Bieler, 1989).

Mature spermatozoa morphologically indistinguishable from that of *D. yoyo* (see Eckelbarger et al., 1990: figs. 28-29, table 1; *D. octotentaculata* as *Scintilla* sp.), except smaller in relative size. Spermatogenesis fully described by Eckelbarger et al. (1990; as *Scintilla* sp.).

Brooding large number of small larvae for variable period; brooding time for individuals collected with larvae, 9-15 days (n = 4); total brooding time from set to release in laboratory, 9, 10, and 12 days (n = 3). Larvae held within both demibranchs and in suprabranchial chamber, where they are circulated via pallial expansions and contractions. During brooding, excurrent siphonal opening constricted by sphincter-like muscle, sometimes noted around free end of rectum, allowing digestive processes to continue. Larvae initially white, turning pink with shell development on day 5-7 (n = 2); released as straight-hinged "D" larvae with apical flagella, 115-123 μm in shell length ($\bar{x}$ = 119 μm, n = 40; Fig. 12). Larvae expelled through excurrent siphon via strong contractions of shell and pallial muscles. Adults brooding larvae collected in May, June, December 1987, and March, April 1988; additional adults setting larvae in laboratory in February, May, June 1982 and November 1990; one specimen setting two broods in laboratory, four months apart, with second brood approximately 20% quantity of first. No apparent seasonality.

Circulatory and Excretory Systems: As described for *Divariscintilla yoyo* (see Mikkelsen & Bieler, 1989).

Distribution and Abundance

Known from three locations, all on intertidal and shallow subtidal sand flats within the Indian River Lagoon, eastern Florida: the type locality, Ft. Pierce Inlet (St. Lucie County, 27°28.3'N, 80°17.9'W), just north of St. Lucie Inlet (Martin County, 27°11.4'N, 80°11.1'W), and Sebastian Inlet (Brevard County, 27°51.6'N, 80°27.0'W). May be quite numerous; largest number per burrow sample = 74.

Etymology

An adjective, *octotentaculatus, -a, -um*, from the Latin *octo* (eight) and the late Latin *tentaculum* (a "feeler"), referring to the eight long mantle tentacles, a diagnostic feature.

Remarks

This is the most common of the five *Divariscintilla* species in the *Lysiosquilla* burrows (see Ecology and Behavior).

Prior to the beginning of this study in March 1987, two individuals of this species were encountered, and are presently the only known specimens of any of the Floridian burrow galeommatoideans from previous collections. These were collected in a shovel-and-sieve sample from a sand bar in the Indian River Lagoon, north of St. Lucie Inlet, Martin County, Florida, 27°11.4'N, 80°11.1'W, on 18 February 1982. These individuals were maintained in the laboratory for approximately four months, providing material for notes and photographs on behavior, reproduction, and development.

Divariscintilla luteocrinita n. sp.
(Figs. 2, 5, 14-22, 24-25)

Material examined

Holotype: 5.0 mm (shell length), FMNH 223403. Paratypes (12): 4.6 mm, FMNH 223407; 4.4 mm (shell only), FMNH 223404; 3.2, 3.9 mm, HBOM 064:01863; 4.9, 4.5, 4.1, 2.9 mm (shells only, coated for SEM), HBOM 064:01864; 4.8 mm, USNM 860195; 5.5 mm (shell only), USNM 859444; 3.4 mm, MCZ 302517; 3.5 mm, SBMNH 35168. Total material: 16 specimens: FLORIDA: Ft. Pierce Inlet: 10 March 1987, 1; 2-3 May 1987, 5; 24 June 1987, 1; 03 August 1987, 1; 14 August 1987, 2; 31 August 1987, 1; 12 April 1988, 1; 03 February 1990; 4.

Type locality

Ft. Pierce Inlet, Indian River Lagoon, St. Lucie County, eastern Florida, 27°28.3'N, 80°17.9'W, occupying *Lysiosquilla scabricauda* burrows on intertidal sand flats with

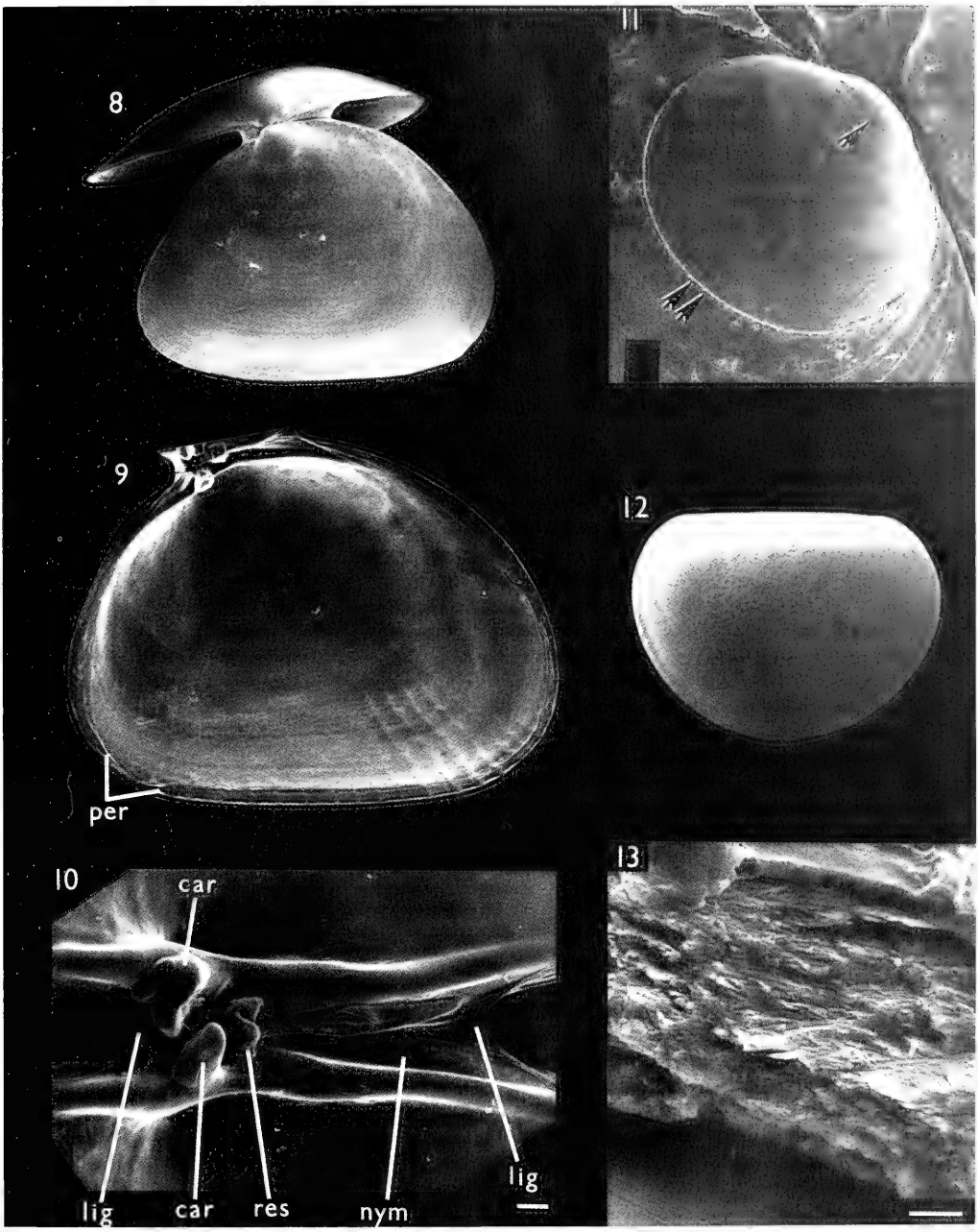

Figs. 8-13. Shell of *Divariscintilla octotentaculata* (SEM). 8. Left valve, external view, 2.9 mm length, paratype, HBOM 064:01867. 9. Right valve, internal view, 3.6 mm length, paratype, HBOM 064:01867. 10.Hinge, anterior to left, paratype, HBOM 064:01867. Scale bar = 100 μm. 11. Prodissoconch, 360 μm length. Single arrow = prodissoconch I-II boundary. Double arrow = prodissoconch II-dissoconch boundary. 12. Newly released larval shell, 119 μm length. 13. Microstructure, with internal surface at top. Scale bar = 5 μm. (car, cardinal tooth; lig, external ligament; nym, nymph; per, periostracum; res, resilium).

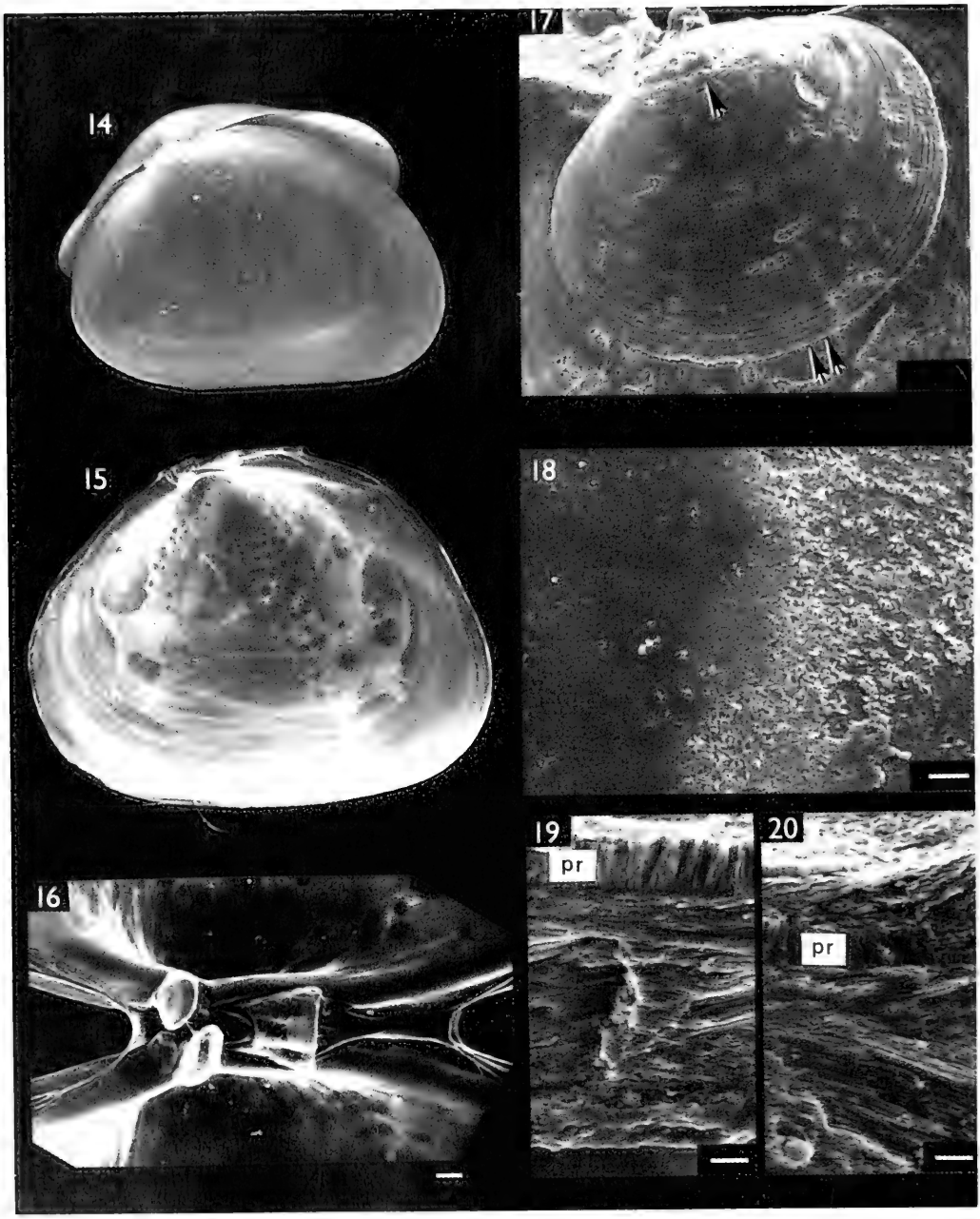

Figs. 14-20. Shell of *Divariscintilla luteocrinita* (SEM). 14. Left valve, external view, 2.9 mm length, paratype, HBOM 064:01864. 15. Right valve, internal view, 4.9 mm length, paratype, HBOM 064:01864. 16. Hinge, anterior to left, paratype, HBOM 064:01864. Scale bar = 100 μm. 17. Prodissoconch, 390 μm length. Single arrow = prodissoconch I-II boundary. Double arrow = prodissoconch II-dissoconch boundary. 18. Internal surface, showing smooth adductor muscle scar (left) and adjacent region of opaque thickening (right). Scale bar = 10 μm. 19. Microstructure in region of adductor muscle scar; internal surface at top. Scale bar = 5 μm. 20. Microstructure in region of opaque thickening, showing additional layer covering internal prismatic layer (pr); internal surface at top. Scale bar = 5 μm. (pr, internal prismatic layer).

patches of the seagrass *Halodule wrightii* Ascherson. Paratypes all from type locality.

Diagnosis

Animal translucent yellow. Mantle thin, with extensive, retractable, papillose folds completely covering shell, meeting at mid-line. Tentacles originating at shell edge, three pairs anteriorly, two singles and 9-11 pairs posteriorly, plus one pair club-shaped tentacles adjacent to excurrent opening. Posterior foot-extension relatively short. Shell roundly triangular, with umbo slightly anterior, smooth exteriorly, with opaque thickenings interiorly; length approximately 70% of extended mantle length. Single "flower-like organ" on anterior surface of visceral mass.

Description

External Features and Mantle: Living extended animal (Figs. 2, 5) generally 6-7 mm in length. Mantle and tentacles translucent pale yellow; foot white. Upper portion of digestive gland showing through mantle and shell as dark elongate-oval spot. Shell entirely covered in life by anterior and posterior mantle folds (Fig. 5, m), meeting at lateral dorso-ventral midline on each side. Mantle folds thin, incompletely retractable, entirely finely papillose, with scattered, elongated papillae especially posteroventrally. Mantle edge extending widely beyond shell edges; entire surface finely papillose. Pallial openings, musculature, and posterior pouch as in *Divariscintilla octotentaculata*. Numerous, long, retractile tentacles originating at shell edge: three pairs anterior to umbo; two singles plus five pairs posterior to umbo (= two singles on midline + two pairs + [excurrent siphon] + three pairs). Shorter accessory pairs posterior to umbo originating from mantle fold near, but ventrad of, shell edge: one to three pairs anterior, two to three pairs posterior to excurrent siphon. Structure of these tentacles as in *D. octotentaculata*; those on shell edge adjacent to cowl and posterior pouch (third and sixth, see numbers, Fig. 5) longest. One prominent pair of thicker, whitish, club-shaped tentacles (Fig. 5, cst) immediately posterior to excurrent siphon originating just inside shell edge; internal structure differing slightly from that of other tentacles (see Remarks).

Preserved specimens incompletely retracted into gaping shell; mantle folds contracted to narrow rim along shell edge, exposing most of shell surface; tentacles, cowl, posterior pouch, and foot contracted but still usually extending beyond shell edges.

Shell (Figs. 14-20): Shell generally 4-5 mm in length, roundly triangular to oval, longer posteriorly, equivalve, rather inflated, glossy, transparent to translucent white, smooth except for fine concentric growth lines and irregular opaque thickening interiorly, imparting a white-blotched pattern (Fig. 15). Size large relative to mantle, comprising approximately 70% of extended mantle length. Valves held open at approximately 40° angle while crawling, incapable of complete closure. Adductor muscle scars subequal, distinct due to presence of surrounding shell thickening (Fig. 15). Periostracum as in *Divariscintilla octotentaculata*.

Hinge line short (Fig. 16), similar to that of *Divariscintilla octotentaculata*. Both cardinal teeth rounded.

Prodissoconch (Fig. 17) brownish-yellow, approximately 390 μm in length. Prodissoconch I approximately 145 μm in length, approximately 37% of length of prodissoconch II; sculpture not discernible (surface abraded in adult shell). Prodissoconch II sculptured with coarse concentric growth lines. Demarcation between prodissoconch I and II stages (Fig. 17, single arrow), and between prodissoconch II and dissoconch (Figs. 14; 17, double arrow) as in *Divariscintilla octotentaculata*.

Shell microstructure as in *Divariscintilla octotentaculata*, except with additional layer of parallel crystals covering internal perpendicular prismatic layer, forming regions of opaque thickening (Figs. 18-20).

Organs of the Pallial Cavity: Foot (Fig. 5, ft) as in *Divariscintilla octotentaculata*. Adductor, pedal retractor, and pedal protractor muscles (including relative positions) as in *D. octotentaculata*. Muscles leaving distinct attachment scars on shell (Fig. 15).

Visceral mass, labial palps and ctenidia as in *Divariscintilla octotentaculata*. Palps with approximately 8 lamellae each side. Outer demibranch approximately 40% smaller than inner. Cilial currents on palps and ctenidia unknown.

A single "flower-like organ" (Figs. 21-22; see Mikkelsen & Bieler, 1989, for explanation of term) on anterior surface of visceral mass just ventral to labial palps. Size variable, not correlated with shell length.

Digestive System: As in *Divariscintilla octotentaculata*.

Suprabranchial Chamber: As in *Divariscintilla octotentaculata*, except that the whitish glandular patches (?hypobranchial glands) are much more extensive (Fig. 24).

Nervous System: Arrangement of ganglia, statocysts, and major nerves as described for *Divariscintilla yoyo* (see Mikkelsen & Bieler, 1989: fig. 31). Additional tentacular nerves arising (independently) from pallial nerve.

Reproductive System: Overall gross morphology as in *Divariscintilla octotentaculata*. Reproductive mode could not be determined from sectioned specimen, which showed no recognizable developed gametes. Adults brooding larvae have not been collected.

Circulatory and Excretory Systems: As in *Divariscintilla octotentaculata*.

Distribution and Abundance

Known only from the type locality, Ft. Pierce Inlet, St. Lucie County, Florida, 27°28.3'N, 80°17.9'W, on intertidal and shallow subtidal sand flats. Uncommon; only 16 specimens known.

Etymology

An adjective, *luteocrinitus*, *-a*, *-um*, from the Latin *luteus* (yellow) and the Latin *crinitus* (hairy), referring to the numerous, long, yellowish tentacles, imparting an overall "hairy" appearance.

Remarks

The single posterior pair of club-shaped tentacles is distinct and consistent in both living and preserved specimens. Normal tentacles (Fig. 25, nt; similar morphology in all five Floridian *Divariscintilla* spp.) show usually four haemocoelic compartments in cross section, each of these supplied with a longitudinal muscle bundle and nerve fiber, and separated by connective tissue septa. The muscle and nerve fibers form a more-or-less concentrated central core, appearing as a central thread under low magnification. Judd (1971: fig. 6) figured a similar internal morphology for tentacles of *Divariscintilla maoria*, but the individual compartmental muscle-plus-nerve bundles are not as concentrated at the core of the tentacle; this difference may not be real, but rather implied by Judd's interpretation of the histological sections. An additional difference is found in the outer surfaces of the tentacles of *D. luteocrinita*, which are highly papillose and convoluted rather than smooth as in *D. maoria* as shown by Judd (1971: fig. 6). Internally, the club-shaped tentacles of *D. luteocrinita* (Figs. 5, 25, cst) are identical in structure to normal tentacles except that the muscle fibers (Fig. 25, arrow) are dispersed over the surfaces of the septa instead of being concentrated at the core of the tentacle. This difference may allow this particular pair of tentacles to undergo stronger contraction, resulting in the club-like shape. Under full extension, the club shape and whitish coloration of these tentacles disappears, indicating that these features are products of the normally contracted state.

The function of the club-shaped tentacles is unknown. They are probably not homologous to the posterior "defensive appendages" of *D. maoria* (see Judd, 1971: fig. 7) or *Galeomma takii* (Kuroda, 1945) (see B. Morton, 1973a: fig. 5), which can be autotomized and possess only a single, central haemocoelic tube. No tentacles in *D. luteocrinita* have this morphology nor were they ever seen to autotomize. However, these tentacles were often observed to hyperelongate when the animals were disturbed, for example during specimen transfer between laboratory dishes. While most other tentacles contracted, the club-shaped tentacles elongated immediately to 2-3 times the shell length just as the transfer spoon made contact. This bears resemblance to the dymantic ("threatening") display of tentacles in *Galeomma polita* Deshayes, 1856 (see B. Morton, 1975), and *Ephippodonta oedipus* Morton, 1976 (see B. Morton, 1976), when disturbed, and suggests defensive function. Unlike the dymantic tentacles of the latter two species, however, the club-shaped tentacles of *D. luteocrinita* do not fully retract into the mantle at rest.

The large "?hypobranchial glands" of this species are located at sites similar to those of the smaller glands of other *Divariscintilla* species, i.e., adjacent to the rectum and the branchial nerves as they join the visceral ganglia. In histological sections, they bear striking resemblance to "seminal receptacles" described and figured for *Aligena elevata* (Stimpson, 1851) by Fox (1979: 101, 103, fig. 32), although in the single sectioned specimen of *D. luteocrinita*, they contained no sperm. The montacutid *Aligena elevata* is a protandrous hermaphrodite, and its seminal receptacles are present only during the fe-

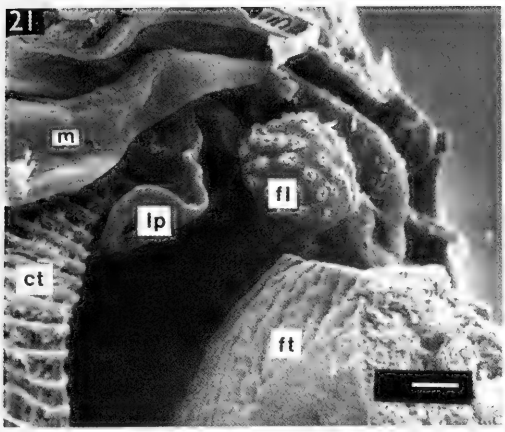

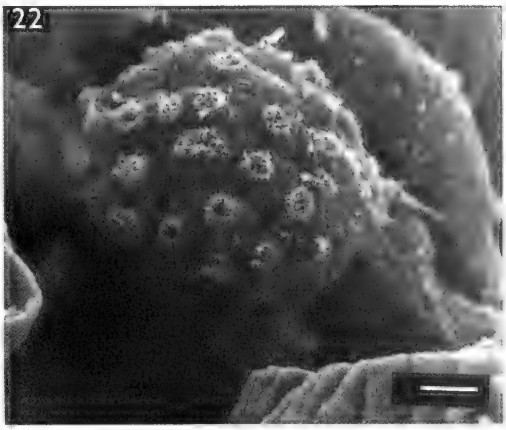

Figs. 21-22. Flower-like organ of *Divariscintilla luteocrinita* (SEM). Anterior tip of foot has been severed to enhance visibility. 21. Scale bar = 100 μm. 22. Scale bar = 50 μm. (ct, ctenidium; fl, flower-like organ; ft, foot; lp, labial palp; m, mantle).

male stage. The occurrence of such structures in Galeommatoidea was summarized by Fox (1979: table 8, as Leptonacea, 15 species), who noted that sperm storage organs were unknown outside of Montacutidae. However, protandry is known in members of other families (e.g. Lasaeidae: *Arthritica crassiformis* Powell, 1933 (see B. Morton, 1973b); see also Fox, 1979: table 11). The reproductive mode of *D. luteocrinita* is presently unknown, but seminal receptacles and/or protandry would be no surprise within the context of this reproductively complex superfamily.

Divariscintilla cordiformis n. sp.
(Figs. 3, 6, 26-32)

Material Examined

Holotype: 5.6 mm (shell length), FMNH 223405. Paratypes (4): 6.4 mm (sectioned on 29 microslides), FMNH 223406; 5.4 mm, HBOM 064:1861; 4.9 mm (partially dissected; prodissoconch coated for SEM), HBOM 064: 01862; 6.4 mm (shell only, coated for SEM), USNM 859445. Total material: 6 specimens: FLORIDA: Ft. Pierce Inlet: 24 June 1987, 2; -Peanut Island: 10 August 1987, 4.

Type locality

Peanut Island, near Lake Worth Inlet, Palm Beach County, eastern Florida, 26°46.6'N, 80°02.7'W, occupying *Lysiosquilla scabricauda* burrows on intertidal sand flats with patches of the seagrass *Halodule wrightii* Ascherson. Paratypes from type locality (FMNH, USNM, HBOM 064:01861) or Ft. Pierce Inlet (HBOM 064:01862).

Diagnosis

Animal translucent white. Mantle thin, with extensive, retractable papillose folds covering shell completely, meeting at midline. Tentacles originating at shell edge, six pairs anteriorly, eight pairs posteriorly. Posterior foot-extension relatively short. Shell oval, with umbo slightly anterior; length approximately 65% of extended mantle length. Small, ventral, anteriorly directed indentation in each valve. Coarse growth lines and slightly beaded radial ribs restricted to edges of otherwise-smooth shell. Single "flower-like organ" on anterior surface of visceral mass.

Description

External Features and Mantle: Living extended animal (Figs. 3, 6) generally 7-10 mm in length, translucent white except for dark digestive gland within visceral mass. Shell entirely covered in life by anterior and posterior mantle folds (Fig. 6, m) meeting at lateral dorso-ventral mid-line. Mantle folds thin, incompletely retractable, entirely finely papillose, with scattered larger papillae, which are longest at posteroventral section. Mantle edge extending widely beyond shell edges;

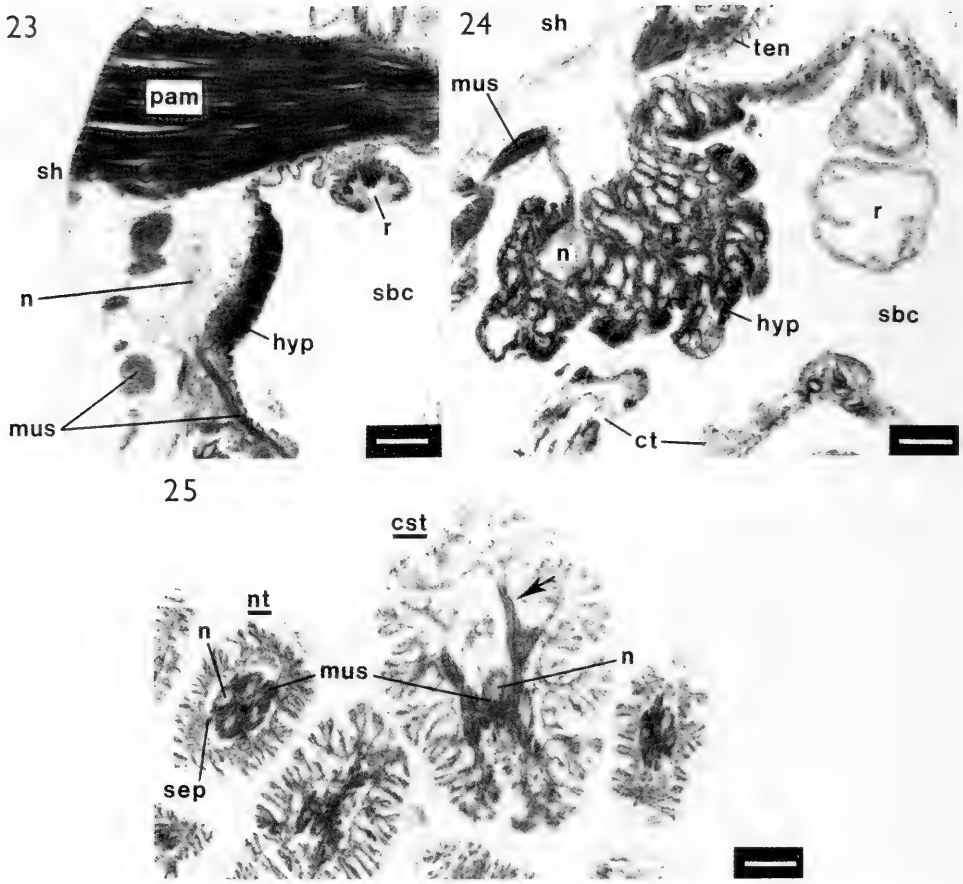

Figs. 23-25. Histological sections. 23. ?Hypobranchial gland adjacent to rectum in *D. octotentaculata*. 24. ?Hypobranchial gland adjacent to rectum in *D. luteocrinita*. 25. Cross-sections of normal and club-shaped tentacles in *D. luteocrinita*. Arrow = muscularized septum. Scale bars = 100 μm. (cst, club-shaped tentacle; ct, ctenidium; hyp, ?hypobranchial gland; mus, muscle fibers; n, nerve fiber; nt, normal tentacle; pam, posterior adductor muscle; r, rectum; sbc, suprabranchial chamber; sep, connective tissue septum; sh, shell; ten, tentacle).

entire surface finely papillose, with additional enlarged papillae near shell edge. Ventral mantle edge entire, not cleft in vicinity of ventral shell indentation. Pallial openings, musculature, and posterior pouch as in *Divariscintilla octotentaculata*. Paired, retractable, pallial tentacles numerous, originating near shell edge. Six anterior pairs, those adjacent to cowl area (third and fourth, see numbers, Fig. 6) longest. Eight posterior pairs, those adjacent to excurrent siphon (tenth) longest, but shorter than longest anterior tentacles. A single median tentacle (Fig. 6, mpt) between first and second posterior pairs (Fig. 6, nos. 7, 8). Structure of individual tentacles as in *D. octotentaculata*. Excurrent opening (Fig. 6, exc) between ninth and tenth tentacle pairs.

Preserved animals not fully retracted into gaping shell; mantle folds contracted to narrow rim along shell edge, exposing most of shell surface; tentacles, cowl, and posterior pouch contracted but still usually extending beyond shell edges; foot usually completely withdrawn into pallial cavity.

Shell (Figs. 26-30, 32): Shell generally 5-7 mm in length, nearly evenly oval, longer posteriorly, equivalve, compressed, glossy, transparent to translucent white. Small indentation (Figs. 6, ind; 27, arrow; 28) at mid-ventral

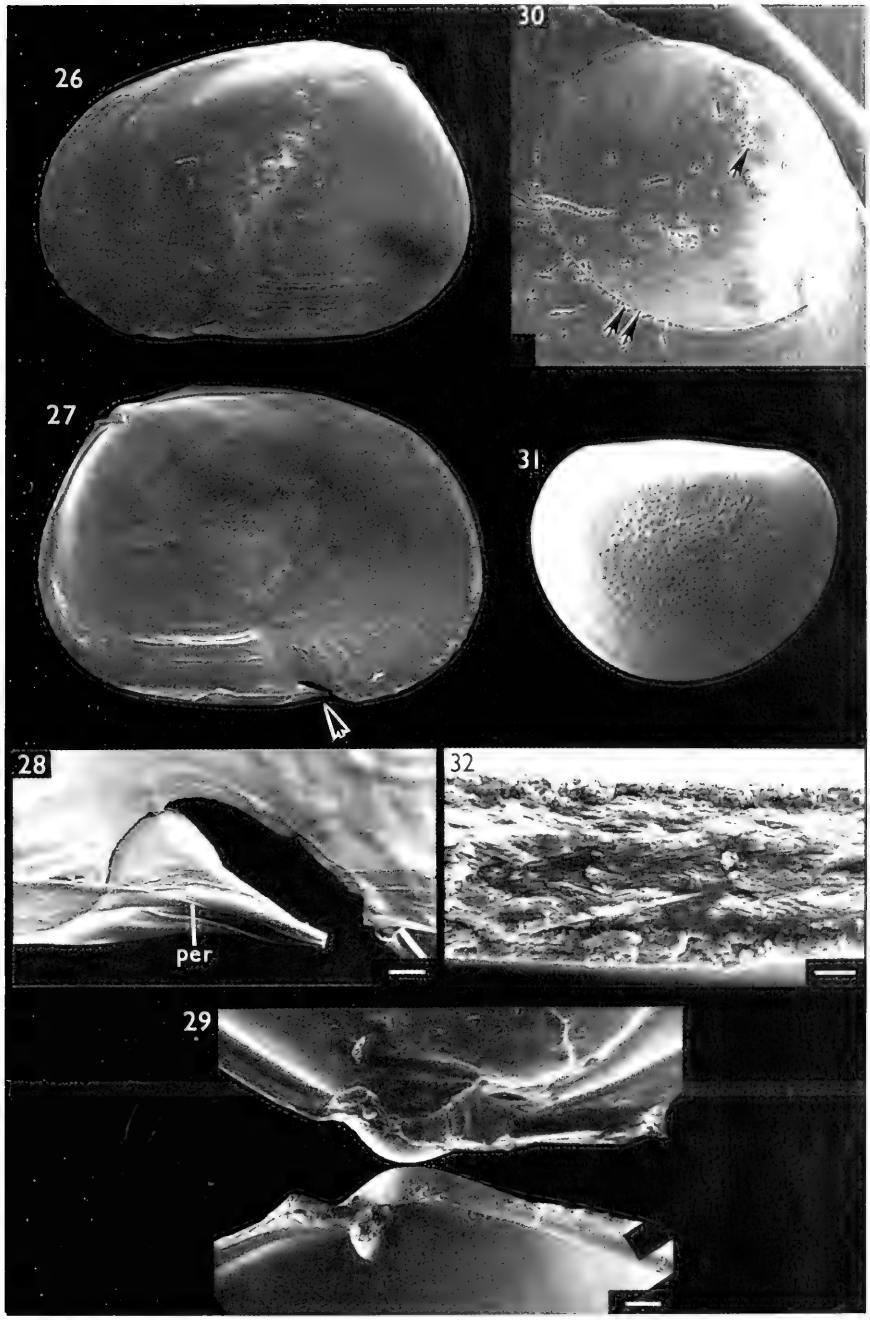

Figs. 26-32. Shell of *Divariscintilla cordiformis* (SEM). 26. Right valve, external view, 6.4 mm length, paratype, USNM 859445. 27. Right valve, internal view, 6.4 mm length, paratype, USNM 859445. Arrow = ventral indentation. 28. Close-up of ventral indentation, interior view. Scale bar = 100 μm. 29. Hinge, anterior to left. Scale bar = 200 μm. 30.Prodissoconch, 360 μm length, paratype, HBOM 064:01862. Single arrow = prodissoconch I-II boundary. Double arrow = prodissoconch II-dissoconch boundary. 31. Newly released larval shell, 146 μm length. 32.Microstructure, with internal surface at top. Scale bar = 5 μm. (per, periostracum).

margin, slanting anteriorly toward umbo, evident only on distal 1 mm or so of shell growth (as evidenced by growth lines). Exterior sculpture smooth except for fine concentric growth lines, heavier at anteroventral margin, anterior to indentation. Beaded radial ribs restricted to distal 1 mm or so of shell edge, most prevalent interiorly at posteroventral margin (Fig. 27) and exteriorly at antero- and posterodorsal margins (Fig. 26), forming distinct, fine crenulation at shell edge, absent only at ventral margin immediately anterior to indentation. Size large relative to mantle, comprising approximately 65% of extended mantle length. Valves held open at 20-30° angle while crawling, incapable of complete closure. Adductor muscle scars subequal, faint. Periostracum as in *Divariscintilla octotentaculata*; also evident covering ventral indentation (Fig. 28, per).

Hinge line (Fig. 29) short, as in *Divariscintilla octotentaculata*, with two small rounded cardinal teeth.

Prodissoconch (Fig. 30) brownish-yellow, approximately 360 μm in length. Prodissoconch I corresponding in size to shell of newly released larva, approximately 45% of length of prodissoconch II; sculpture not discernible (surface abraded in adult shell). Prodissoconch II sculptured with coarse concentric growth lines. Demarcation between prodissoconch I and II stages (Fig. 30, single arrow), and between prodissoconch II and dissoconch (Fig. 30, double arrow) as in *Divariscintilla octotentaculata*.

Organs of the Pallial Cavity: Foot and shell muscles (adductors, pedal retractors, pedal protractors, including relative positions) as in *Divariscintilla octotentaculata*. Muscles leaving very faint attachment scars on shell (Fig. 27).

Visceral mass, labial palps and ctenidia as in *Divariscintilla octotentaculata*. Palps with approximately seven lamellae each side. Outer demibranch approximately 35% smaller than inner. Cilial currents on palps and ctenidia unknown.

Single "flower-like organ" (see Mikkelsen & Bieler, 1989) on anterior surface of visceral mass just ventral to labial palps.

Digestive System: Similar to that of *Divariscintilla octotentaculata* (relative positions of gastric shield, style sac, digestive diverticula, midgut, etc.), based on histological sections. Limited number of specimens did not permit confirmation of structure through gross dissection.

Suprabranchial Chamber: As in *Divariscintilla octotentaculata*.

Nervous System: Arrangement of ganglia, statocysts, and major nerves as described for *Divariscintilla yoyo* (see Mikkelsen & Bieler, 1989: fig. 31). Additional tentacular nerves arising (independently) from pallial nerve.

Reproductive System: Simultaneous hermaphrodite. Overall gross morphology as in *Divariscintilla octotentaculata*.

One specimen brooding larvae collected in August 1987. Larvae released one day after collection. Newly-released larval shells 136-148 μm in length ($\bar{x}$ = 143 μm, n = 40; Fig. 31). Adult preserved and subsequently sectioned; apparently intact larvae found in suprabranchial chamber and throughout digestive system, including intestine and rectum (therefore not being digested).

Circulatory and Excretory Systems: As in *Divariscintilla octotentaculata*.

Distribution and Abundance

Known from the type locality at Peanut Island, Palm Beach County, and from sand flats at Ft. Pierce Inlet, St. Lucie County, Florida, 27°28.3'N, 80°17.9'W. Rare; only 6 specimens known.

Etymology

An adjective, *cordiformis*, *-e*, from the Latin *cordis* (heart) and the Latin *forma* (shape), referring to the ventrally indented shell outline.

Remarks

As in *Divariscintilla maoria* (see Judd, 1971), the ventral indentation in the shell of this species does not seem to be functionally important. In both species, it is present in both valves, anteriorly inclined, not developed in juveniles, and not reflected by soft anatomy.

ECOLOGY AND BEHAVIOR

As in the two previously described commensal galeommatids (Mikkelsen & Bieler, 1989), no specimens of the newly described species were ever found physically attached

to a mantis shrimp, either in the field or in museum specimens (HBOM). They are assumed to be free-living within the vertical portions of the U-shaped burrow, although specimens were never visible at the opening prior to pumping. Again as with the previous species (Mikkelsen & Bieler, 1989), these clams were never found free-living outside of the burrows or associated with any other burrowing invertebrate in the area (e.g. other mantis shrimps, callianassid shrimps, polychaetes, sipunculans), nor were any empty shells located in dry collections (AMNH, DMNH, FMNH, HBOM, USNM), probably because of their fragile nature.

Divariscintilla octotentaculata was the most frequently encountered commensal mollusk in the *Lysiosquilla* burrows; of the 35 burrows containing mollusks, 31 contained *D. octotentaculata*, 20 *D. yoyo*, 19 *D. troglodytes*, 8 *D. luteocrinita*, 6 *Cyclostremiscus beauii*, 7 *Circulus texanus*, and only 2 *D. cordiformis*. *Divariscintilla octotentaculata* was usually collected with other commensals, occurring alone in only 6 of the 31 samples. *Divariscintilla luteocrinita* was always collected with other commensals. *Divariscintilla cordiformis* was collected once with *D. octotentaculata*, and once alone. Densities of *D. octotentaculata* varied greatly, ranging from 1-74 per sample ($x = 8.3$, $n = 31$). *Divariscintilla luteocrinita* was usually present in numbers of only one or two specimens per burrow; one sample contained four specimens. *Divariscintilla cordiformis* was encountered only twice, once as two specimens, once as four. Only a small number of burrows sampled contained commensals. And, as previously reported (Mikkelsen & Bieler, 1989), it must be emphasized that in no case could an entire burrow be sampled using the yabby pump, which only effectively samples its own length (0.5-1.0 m) of the vertical parts of the U-shaped burrow. Estimates of occurrence and/or density of any clams living in the deeper horizontal section of the burrow was thus not possible.

Animals of all three species spent most of their time in the laboratory attached to the glass surface of laboratory bowls by up to four byssus threads, and it is assumed that this is also their habit on the smooth walls of the *Lysiosquilla* burrow. When dislodged, they actively crawl about using an even, gliding motion produced by ciliary action on the central surface of the foot. This was equally effective on the underside of the water surface as on glass. They made no attempts to burrow when offered a substrate of loose sand in the laboratory.

All three *Divariscintilla* species previously described (*D. maoria*, Judd, 1971: fig. 4; *D. yoyo* and *D. troglodytes*, Mikkelsen & Bieler, 1989: fig. 32) are known to "hang" from a vertical substrate by the posterior foot-extension, which in these species is extremely long and elastic; byssus threads secreted by the anteriorly located byssus gland are laid down within the ventral groove of the foot and emerge from the terminus to attach to the substrate. The threads are secured within the groove by secretions of the posteriorly located byssus adhesive gland. Byssus and byssus adhesive glands of similar morphologies are present in each of the three new species described here and are assumed to function in the same way. This has been confirmed for *D. octotentaculata* and *D. luteocrinita*, in which secretion of byssus threads, accompanied by distinct pulsing of the byssus gland area, was observed as described for *D. yoyo* and *D. troglodytes* (Mikkelsen & Bieler, 1989). Following this activity, the clam hangs from the posterior foot-extension, with the byssus threads emerging from the posterior terminus of the foot in the vicinity of the byssus adhesive gland. The posterior foot-extension of these species, as well as of *D. cordiformis*, is not as elongated and extensible as in those previously described, therefore the distinctive "hanging" posture, wherein the clam "dangles" from an elongated foot, is not as pronounced.[3]

A peculiar interaction between pairs of *Divariscintilla* species was observed in the laboratory on three occasions. In two instances involving *D. octotentaculata*, one animal of a pair was noted reaching its foot into the mantle cavity of the second specimen, either from in front of or behind its partner. On one of these occasions, the two individuals performed this activity simultaneously, "facing" one another, with each one reaching around the visceral mass of the other to contact the posterior surface with the tip of its foot (Fig. 33). Two specimens of *D. yoyo* have been

[3]Careful notes were not recorded on the behavior of *D. cordiformis* in the early phase of the study, and the inavailability of additional living specimens prevented confirmation of the presence or absence of "hanging" behavior. Morphology suggests that this behavior does occur, however, the shorter posterior extension and the absence of any mention in our preliminary written observations indicates that the "hanging" posture was inconspicuous, as in *D. octotentaculata* and *D. luteocrinita*.

Fig. 33. Mating (?) behavior between two specimens of *Divariscintilla octotentaculata*, as observed in laboratory.

noted performing this same type of activity. In all three instances, the interaction was initiated by the smaller of the two specimens of the pair, and the activity was sustained for 3-7 minutes. Although there is no direct evidence, it seems likely that this observed interaction is part of some sort of reproductive activity, perhaps stimulation of sperm transfer (external gonadal openings are located on the posterodorsal surface of the visceral mass). Each of the two specimens involved in the simultaneous behavior described above had larvae in their suprabranchial chambers within three weeks of the noted activity. (If this behavior is in fact copulatory in function, then this confirms simultaneous hermaphroditism in these species.)

Observed animals of these *Divariscintilla* species do not respond to changes in light intensity (e.g. photographic strobes) and did not seek darkness when offered "artificial burrows" (in the form of black plastic tubes) in the laboratory.

DISCUSSION

Generic Placement

The genus *Divariscintilla* was redescribed in a previous part of this study on *Lysiosquilla*-associated mollusks (Mikkelsen & Bieler, 1989). Major emphasis was placed on two features, the presence of flower-like organs and a bipartite foot with both byssus and byssus-adhesive glands, shared between these species and the type species, *D. maoria* Powell, 1932 (the latter described by Judd, 1971). We regarded the presence of an apparently functionless (Judd, 1971) shell notch in *D. maoria*, as well as the difference in degree of shell coverage by the mantle, as species-level rather than generic characters. At the time, we also considered placement of *D. yoyo* and *D. troglodytes* in the monotypic genus *Phlyctaenachlamys* Popham, 1939, based on *P. lysiosquillina* Popham, 1939. However, there are a number of anatomical characters that distinguish the *Divariscintilla* species (flower organs, hindgut typhlosole, interlamellar ctenidial junctions, relative size of adductor muscles, hinge teeth; compare data of Popham, 1939, and Mikkelsen & Bieler, 1989).

Divariscintilla luteocrinita and *D. cordiformis* fit well within *Divariscintilla*, as redescribed. In fact, these new species actually bridge several morphological gaps between *D. maoria* and *D. yoyo*/*D. troglodytes*, that is shell notch, posterior shell prolongation, less shell internalization, and more numerous posterior tentacles. *Divariscintilla octotentaculata* does not possess the flower-like organs; however, in all other taxonomic characters (hinge, mantle, ctenidia, etc.), it does conform to the redefined genus. The hinge teeth of this species, comprised (as in other *Divariscintilla* species) of only one small cardinal tooth in each valve, was an important element in deciding generic placement. Hinge structure is presently considered taxonomically important at the generic level in Galeommatoidea (P. H. Scott, in litt., October 1990). Most members of the superfamily possess more than one cardinal tooth in at least one valve; some show distinct lateral teeth as well. The genus *Scin-*

TABLE 1. Distinguishing characteristics of all described species of *Divariscintilla*: an expansion of table 1 from Mikkelsen & Bieler (1989).

	D. maoria (from Judd, 1971)	*D. yoyo*	*D. troglodytes*	*D. octotentaculata*	*D. luteocrinita*	*D. cordiformis*
Shell:						
General shape	oval	elongate-pointed	oval	roundly triangular	roundly triangular	oval
Ventral indentation	present	absent	absent	absent	absent	present
Prolongation	posterior	anterior	anterior	posterior	posterior	posterior
Internal sculpture	unribbed	unribbed	radially ribbed (marginally)	radially ribbed (marginally)	unribbed, with internal thickening	radially ribbed (marginally)
Length relative to extended mantle length	68%	40%	50%	70%	70%	65%
Prodissoconch length (μm)	"small"	360	380	360	390	360
Mean newly-released larval shell length (μm)	unknown	132	126	119	unknown	143
Mantle:						
Color, thickness	(not given)	whitish, thick	yellowish, thin	whitish, thin	yellowish, thin	whitish, thin
Extent covering shell	margins only	entire, umbonal foramen	entire, anterior slit	anterior and posterior thirds	entire, midline overlap	entire, midline overlap
Papillae	very small	sparse, very small	numerous, small, evenly-distributed	numerous, small, longer at ventral edge	numerous, small, evenly-distributed	numerous, small, evenly-distributed
Anterior tentacles	2 pairs	1 pair	2 pairs	2 pairs	3 pairs	6 pairs
Posterior tentacles	1 single	1 single	1 single, 1 pair	1 single, 2–3 pairs	2 singles, 5 pairs, + 3–6 pairs accessory, + 1 pair club-shaped	1 single, 8 pairs
Defensive appendages	6–8 present	absent	absent	absent	absent	absent
Pedal protractor muscle insertion relative to anterior adductor muscle	(not given)	dorsal	dorsal	ventral	ventral	ventral
Flower-like organs: number	1	3–7 (usually 5)	1	0	1	1
Labial palps: Lamellae per palp	approx. 9	10–14	14–20	6–8	approx. 8	approx. 7
Ctenidia:	smooth	pleated	pleated	smooth	smooth	smooth?
Geographical range:	New Zealand	eastern Florida	eastern Florida	eastern Florida	eastern Florida	eastern Florida

tillona Finlay, 1927, is the only other genus known to us in which members have a single cardinal tooth in each valve. However, members of the latter genus are all attached ectocommensals on echinoderms, and in addition, are distinguished by a highly specialized,

laterally compressed and furrowed foot. Both of these considerations exclude the new species described here. In view of the taxonomic confusion present in this group, we prefer to use an existing genus until a generic revision of this superfamily based on both shell and anatomical characters can be accomplished.

Coney (1990), in a review of "ventrally notched galeommatid genera," assigned *Divariscintilla yoyo* and *D. troglodytes* to the genus *Phlyctaenachlamys*, and reinstated *Divariscintilla* as a monotypic genus. His reasoning revolved around (1) the shell notch, (2) hinge teeth and ligament morphology, (3) shell ultrastructure, (4) mantle tentacles, (5) degree of shell coverage by the mantle, and (6) ctenidial morphology. We disagree with his taxonomic decisions and address these points as follows:

(1) Shell notch: The newly described species *Divariscintilla cordiformis* has an apparently functionless ventral shell notch very similar to that of the type species *D. maoria*, and agrees well anatomically with the "unnotched" species assigned to *Divariscintilla*. Importantly, the notch does not influence mantle or other soft-part morphology.

(2) Hinge and ligament: Coney (1990: 131, 135) offered conflicting statements regarding hinge teeth. His table of generic characters and description of *Divariscintilla maoria* stated that there was one cardinal tooth in the right valve, whereas his generic description indicated two. Although his scanning photomicrograph of the right hinge (Coney, 1990: fig. 11) seemed on first examination to reveal two cardinal teeth, comparison with our photomicrographs as well as Coney's subsequent text indicated that the posteriormost "knob" was actually the resilium, not a second cardinal tooth. Coney (1990) upheld the original interpretation by Powell (1932) that the left valve was edentulous, although his scanning photomicrograph (Coney, 1990: fig. 12) featured a small structure that may correspond to Powell's (1932: 67) "minute and shapeless vestige" of a left cardinal. Additionally, Coney (1990) noted a ridge in the left valve that he called a posterior lateral tooth. All *Divariscintilla* species (by our definition) possess strengthened or thickened hinge lines to varying degrees, but without development into distinct and/or interlocking lateral teeth/lamellae. As we lack relevant ontogenetic data on shell development, we do not wish to infer homology in this instance and prefer not to call these structures "lateral teeth."

According to Popham (1939: 66, text-fig. 6), the hinge of *Phlyctaenachlamys lysiosquillina* has two discrete cardinal teeth in the right valve, one cardinal in the left, and an interlocking set of posterior laterals. This is distinctly different from the situation in *Divariscintilla yoyo*, *D. troglodytes*, and *D. maoria*.

Ligament morphology in all *Divariscintilla* species (by our definition) consists of an external amphidetic ligament (inappropriately called "periostracal webbing" at one point in our earlier paper; Mikkelsen & Bieler, 1989: 178) supported by a nymph, and an internal opisthodetic resilium. The resilium is also apparently present in *Phlyctaenachlamys lysiosquillina*, but the external ligament was not mentioned by Popham (1939).

In total, these findings do not agree with Coney's (1990: 142) statement that "the hinge teeth and ligament are remarkably similar between the three species [*lysiosquillina*, *yoyo*, *troglodytes*], but are quite different than those of *Divariscintilla maoria*. . . ."

(3) Shell ultrastructure: This feature was also utilized by Coney (1990) in his discussion of distinguishing characteristics of *Divariscintilla* and *Phlyctaenachlamys* species, although he also (1990: 142) admitted that the "shell ultrastructure of *Phlyctaenachlamys lysiosquillina* is unknown". Studies of the three new species described here (Figs. 13, 19-20, 32), as well as a reevaluation of this character in *D. yoyo* and *D. troglodytes* (see Mikkelsen & Bieler, 1989: figs. 11, 15), indicate that both the inner and outer noncross-lamellar layers may be prismatic rather than "homogenous" as previously labelled by us. Variability in thickness and/or presence of the various layers among individuals and among different locations on a single valve (e.g. extra internal layer in *D. luteocrinita*, see above) has also been noted. A more exacting study using more appropriate methodology (e.g. sections rather than fractions, see Taylor et al., 1973) is necessary before differences at this level should be employed in taxonomic decisions.

(4) Mantle tentacles: Coney (1990: 142) maintained that "number and placement of mantle tentacles and defensive appendages is strongly similar between *P[hlyctaenachlamys] lysiosquillina* and those of *P. yoyo* and *P. troglodytes*," noting that none of these species possess the numerous posterior defensive tentacles seen in *Divariscintilla maoria*.

The three new species described here in *Divariscintilla* all possess a number of posterior tentacles, albeit none "defensive." The two primary anterior tentacles, also mentioned specifically by Coney (1990: 142) to combine *P. lysiosquillina*, *D. yoyo*, and *D. troglodytes*, are in fact also present in *Divariscintilla maoria*.

(5) Shell coverage: Although there is a distinct difference in the degree of shell coverage by the mantle between the type species and *Divariscintilla yoyo* and *D. troglodytes*, the three newly described species show intermediate conditions. All *Divariscintilla* species (by our definition) show at least some degree of shell exposure, thus differing from the condition in *Phlyctaenachlamys lysiosquillina* ("the shell is completely embedded"; Popham, 1939: 65). A similar range of variability was described for the genus *Ephippodonta* Tate, 1889, by Arakawa (1960: 57), and can also be found in *Entovalva* Völtzkow, 1890, *sensu lato*, wherein the genus *Devonia* was distinguished by Winckworth (1930: 14) for a species with incomplete shell coverage.

(6) Ctenidial morphology: Coney (1990: 142) noted that the ctenidia in *Divariscintilla maoria* are smooth, whereas those of *Phlyctaenachlamys lysiosquillina*, *D. yoyo* and *D. troglodytes* have been described as pleated. However, unlike pleated (= plicate) gills in other bivalve groups (e.g. *Pecten*; see Rice, 1897), pleating in these species is not based on structural differences in the filaments (pers. obs.; Popham, 1939: 71). Some degree of "pleating" caused by contraction in preserved specimens has been noted during the present study. An additional ctenidial character separates *P. lysiosquillina* and the five Floridian species of *Divariscintilla*, in that the latter have interlamellar junctions (unknown for New Zealand *D. maoria*).

Comparative characteristics for all six known species of *Divariscintilla* are presented in Table 1. The three new species described here more closely resemble the type species, *D. maoria* (see Judd, 1971: fig. 1), in general morphology than do the other species previously described during this study (*D. yoyo* and *D. troglodytes*, see Mikkelsen & Bieler, 1989: figs. 1, 2). Like *D. maoria*, the three new species have posteriorly prolonged, relatively large shells and smooth ctenidia (differences in percent reduction of the outer demibranch as cited in the text may not be reliable, as they were taken from preserved specimens and were affected by contraction). One species, *D. octotentaculata*, has a shell that is similarly incompletely covered by the mantle. Another species, *D. cordiformis*, shows a similar ventral indentation that is likewise apparently functionless. These similarities effectively remove most of the dissimilarity between the New Zealand type species and the included eastern Florida species that existed at the completion of the previous paper (Mikkelsen & Bieler, 1989). *Divariscintilla maoria* is the only species in the genus for which detachable defensive papillae have been described.

Distribution

The peculiar pattern of geographic distribution of *Divariscintilla* species, with now five members in the western Atlantic and one in New Zealand, is most likely a result of insufficient sampling of burrow fauna. No ecological niche separation between the five sympatric species was recognized, leaving interesting questions for future research.

Comparison with Other Genera

Divariscintilla was formerly treated as a subgenus of *Vasconiella* Dall, 1899, by Chavan (1969), apparently on the basis of notched shells. However, members of *V. jeffreysiana* (P. Fischer, 1873), type and sole species of the genus, possess a deep indentation only in the comparatively smaller right valve, and importantly, there are modifications in the right mantle and ctenidial tissues corresponding to the notch (Cornet, 1982). This species is also the only other galeommatoidean with a published account of a "flower-like organ" (Table 2). Unfortunately, although recognizably illustrated by Cornet (1982: fig. 5), no details on structure or possible function were provided for the briefly mentioned "rounded tubercle just under the labial palps" (Cornet, 1982: 39). *Vasconiella jeffreysiana* is probably also commensally associated with a mantis shrimp, *Lysiosquilla eusebia* (Risso, 1816) (Table 2; Cornet, 1982). Differences of *Vasconiella* from *Divariscintilla* (i.e. two cardinal teeth in the left valve, lack of a posterior foot-extension, ?lack of ctenidial interlamellar junctions) prevent synonymy of the two genera as currently defined, but clearly, their relationship should be investigated further.

Mention has been made several times above to the relationships of galeommatoideans with certain phyla of host invertebrates (e.g. echinoderms versus stomatopods). Evi-

TABLE 2. Galeommatoidean species, hosts, and occurrences of flower-like organs and hanging foot structure (x = presence; – = absence).

	Host	Flower-like organs	Hanging foot structure	References(s)
Divariscintilla maoria Powell, 1932	*Heterosquilla tricarinata* (Claus)	x	x	Judd, 1971
D. yoyo Mikkelsen & Bieler, 1989	*Lysiosquilla scabricauda* (Lamarck)	x	x	Mikkelsen & Bieler, 1989
D. troglodytes Mikkelsen & Bieler, 1989	*Lysiosquilla scabricauda* (Lamarck)	x	x	Mikkelsen & Bieler, 1989
D. octotentaculata n. sp.	*Lysiosquilla scabricauda* (Lamarck)	–	x	This study
D. luteocrinita n. sp.	*Lysiosquilla scabricauda* (Lamarck)	x	x	This study
D. cordiformis n. sp.	*Lysiosquilla scabricauda* (Lamarck)	x	x	This study
Parabornia squillina Boss, 1965	*Lysiosquilla scabricauda* (Lamarck)	x	x	Boss, 1965a; this study
Vasconiella jeffreysiana (P. Fischer, 1873)	?*L. eusebia* (Risso)	x	–	Cornet, 1982
Phlyctaenachlamys lysiosquillina Popham, 1939	*L. maculata* (Fabricius)	–	x	Popham, 1939
Ceratobornia longipes (Stimpson, 1855)	*Callianassa major* Say or *Upogebia affinis* (Say)	–	x	Jeffreys, 1863; Dall, 1899; Norman, 1891; Jenner & McCrary, 1968
C. cema Narchi, 1966	*Callianassa major* Say	–	x	Narchi, 1966

dence suggests that host specificity applies mainly to those cases where modifications for locomotion and attachment have occurred. Most "generalist" species (*sensu* B. Morton & Scott, 1989; e.g. *Mysella bidentata* (Montagu, 1803), associated with a wide variety of invertebrates [Boss, 1965b]) possess a simple foot structure consisting of a strong crawling portion (similar to the anterior foot of *Divariscintilla* spp.) ending in a bluntly rounded "heel" from which byssus threads emanate (B. Morton & Scott, 1989: fig. 1 [*Lasaea*], figs. 9-10 [*Pseudopythina*]). This is probably the plesiomorphic condition in the superfamily, compared to the more derived states seen in some of the host specialists. For example, the flattened foot of *Scintillona* spp. (J. E. Morton, 1957) may be a modification for laterally applied locomotion among the vertical spines and papillae of echinoderms to which they attach (Dall et al., 1938: 145; Yamamoto & Habe, 1974; Ó Foighil & Gibson, 1984: 75). Also, the sucker-like anterior foot of *Entovalva* (= *Devonia*) *perrieri* (Malard, 1903) (see Anthony, 1916) allows attachment to the smooth, outer body walls and/or inner cloacal walls (Bruun, 1938) of burrowing holothurians.

An elongate posterior foot-extension for attachment to a smooth vertical substrate is found in three specialist genera: *Divariscintilla*, *Phlyctaenachlamys* Popham, 1939, and *Ceratobornia* Dall, 1899 (Table 2). All species involved are associated with crustaceans that produce smooth-walled burrows in sand (Table 2). Most are believed to live attached to the crustacean burrow walls (*Ceratobornia. cema* may also "temporarily" attach to its host (Narchi, 1966); the biology of *C. longipes* is unknown). Although insufficiently studied in *Phlyctaenachlamys* and *Ceratobornia*, all species apparently possess the same "hanging apparatus" comprised of an anterior byssus gland, ventral groove, and posterior byssus adhesive gland (see Popham, 1939: fig. 2, *P. lysiosquillina*, hanging behavior not specifically described; Narchi, 1966: figs. 1, 5, *C. cema*; Dall, 1899: pl. 88, figs. 10-11, 13, *C. longipes*). They also all possess similar general morphologies of the pallial, ctenidial, digestive, circulatory, excretory, and nervous systems (*C. longipes* incompletely known).

TABLE 3. Distinguishing characteristics for the three galeommatoidean genera possessing the "hanging foot." See text for included species and sources of data. [L, left; R, right]

	Divariscintilla	*Phlyctaenachlamys*	*Ceratobornia*
Shell internalization	incomplete	complete	incomplete
Hinge:			
Cardinal teeth	1 R, 1 L	2 R, 1 L	2 R, 2 L
Lateral teeth	absent	1 posterior, reduced	1 posterior, reduced
Retraction into shell	yes (1 sp.) no (5 spp.)	no	yes
Adductor muscles	subequal	posterior reduced	subequal
Flower-like organs	present (5 spp.) absent (1 sp.)	absent	absent
Interlamellar ctenidial junctions:	present	absent	absent
Hindgut typhlosole	present	absent	absent
Hypobranchial gland	present?	absent	absent
Supportive chondroid edge in foot	absent	absent	present

The anatomical differences among the three genera that presently prevent their synonymy are listed in Table 3. Until the importance of each of these characters can be reassessed, it is uncertain whether possession of a "hanging foot" reflects convergence or phylogenetic relationship, and the three genera are best treated separately.

Another possible difference between *Divariscintilla* on one hand and *Phlyctaenachlamys* and *Ceratobornia* on the other lies in the mode of reproduction. Members of *Divariscintilla* for which such data are available (*D. yoyo*, *D. troglodytes*, *D. octotentaculata*, *D. cordiformis*) are known to be simultaneous hermophrodites. From literature data, it seems that *Phlyctaenachlamys lysiosquillina* and *Ceratobornia cema* are forms with separate sexes (Popham, 1939, p. 80: "specimen sectioned was a male"; and Narchi, 1966, p. 521: "sectioned specimen was a female"). However, while simultaneous hermaphroditism can be documented from individuals without observations over extended periods of time, "males" or "females" could belong to forms with consecutive hermaphroditism. Protandrous and protogynous hermaphroditism have both been reported for the superfamily (summarized by Fox, 1979: tab. 11, as Leptonacea).

Rhamphidonta Bernard, 1975, represented by the single species *R. retifera* (Dall, 1899), also possesses a bipartite foot but one which is different from that discussed above, both morphologically and functionally. According to Bernard (1975), the foot of *R. retifera* is anteriorly elongated, with the main enlarged crawling portion located posteriorly. Members of this species are not known to hang; they burrow into sand to avoid illumination, and are apparently free-living. The hinge of *R. retifera* (see Bernard, 1975: fig. 1) is distinctly "montacutid." Close relationship with the three genera discussed above is unlikely.

The mantis shrimp *Lysiosquilla scabricauda* also serves as host to *Parabornia squillina* Boss, 1965, a galeommatoidean that attaches to the inner surface of the abdominal sclera of the shrimp (Table 2). *Parabornia squillina* has been collected in the region of this study (Sebastian Inlet, Peanut Island), but has not been collected in burrows containing *Divariscintilla* species. Interestingly, the animal of *P. squillina* also possesses a single "flower-like organ" (pers. obs.), although this was not mentioned in the original species description based on preserved material. (Boss, 1965a: fig. 3 shows an unexplained five-part zig-zag outline for the visceral mass below the gills and labial palps.) Its foot (Boss, 1965a: fig. 3) appears morphologically similar to the "hanging type" described above; a deep ventral groove ends with an opaque white area at the end of a very short posterior extension (pers. obs.). Boss (1965a: 4) interpreted the white area at the end of the foot as the byssus gland (as did Judd [1971] for *D. maoria*, and Narchi [1966] for *Ceratobornia cema*). In view of the byssus adhesive gland described here and previously (Mikkelsen & Bieler, 1989), this organ (which was depicted with internal lamellae by Boss, 1965a: fig. 3)

warrants reinvestigation. If this structure is the primary byssus gland, what is the function of the ventral groove? (Histological study of the structure of the entire foot, and observations of living animals producing byssus threads would resolve this question.) Boss (1965a) placed *Parabornia* in the Erycinidae (Erycininae), in part, because its hinge has two cardinal teeth in each valve and a central resilium. If hinge structure is eventually confirmed as a reliable taxonomic character based on phylogeny of the group, the "hanging foot" and "flower-like organs" would need to be explained as results of evolutionary convergence and/or symplesiomorphies.

Mating Behavior in Bivalves

The observed "mating" behavior (Fig. 33) between individuals of *Divariscintilla octotentaculata* as well as of *D. yoyo* is of special interest. Mating behavior has not been confirmed for bivalves (Mackie, 1984: 362). Mackie (1984: 363) summarized the reported cases of associations between females and dwarf males in bivalves and concluded that those interactions would qualify as mating behavior if it can be shown that the associations are confined to a breeding period.

True copulatory behavior is absent in bivalves because they lack copulatory organs. However, several authors (Clapp, 1951: 7; Townsley et al., 1966: 49) have observed male teredinids (*Bankia* spp.) inserting their exhalent siphons into the inhalent siphons of females during sperm release. Purchon (1977: 295), and subsequently Mackie (1984: 362), interpreted this as the use of an intromittant organ, the development of which would be of "great survival value to species ... living in isolated pieces of drift wood (Purchon, 1977: 295). Similarly, quasi-copulatory behavior in *Divariscintilla* would be advantageous for these small bivalves with limited gamete production, living in restricted, relatively isolated populations within the burrows of their hosts. Selective mating in burrows that contain several other congeneric species would guarantee successful fertilization and make conservative use of male gametes. In our previous discussion of flower-like organs, now known from five species of *Divariscintilla*, we (Mikkelsen & Bieler, 1989: 191) speculated that these organs might emit a pheromone for attracting reproductive partners (another possibility, if they are indeed pheromone-emitting organs, would be the attraction of larvae to settlement sites).

ACKNOWLEDGMENTS

The following are gratefully acknowledged: Dr. Raymond B. Manning (USNM), for bringing this interesting fauna to our attention; William D. ("Woody") Lee (SMSLP), for invaluable field help; Paul H. Scott (SBMNH), for comments on generic placement; Patricia A. Linley and Pamela Blades-Eckelbarger (both HBOI) for SEM assistance; Tom Smoyer (HBOI) for photographic work; Dr. Kerry B. Clark (Florida Institute of Technology, Melbourne) and John E. Miller (formerly HBOI) for the use of and help with video recording equipment; Paul S. Mikkelsen (formerly HBOI), for behavioral and developmental notes and the photograph in Fig. 1; Chris Bauman (Vero Beach, Florida) for the illustration in Fig. 33; Paul H. Scott (SBMNH), Dr. Kenneth J. Boss (MCZ), and two anonymous reviewers for valuable comments on the manuscript.

This research was supported in part by the Smithsonian Marine Station at Link Port; the cooperation of Dr. Mary E. Rice and her staff is gratefully acknowledged. Funding for this project was derived in part from a National Capital Shell Club scholarship to P. M., and a NATO Postdoctoral Research Fellowship at SMSLP to R. B. This is Harbor Branch Oceanographic Institution Contribution no. 862 and Smithsonian Marine Station Contribution no. 273.

LITERATURE CITED

ANTHONY, R., 1916, Contribution a l'étude de l'*Entovalva* (*Synapticola*) *perrieri* Malard, mollusque acéphale commensal des synaptes. *Archives de Zoologie Expérimentale et Générale*, 55: 375-391, pls. 6-7.

ARAKAWA, K. Y., 1960, Ecological observations on an aberrant lamellibranch, *Ephippodonta murakamii* Kuroda. *Venus, Japanese Journal of Malacology*, 21(1): 50-60, pls. 7-8.

BERNARD, F. R., 1975, *Rhamphidonta* gen. n. from the northeastern Pacific (Bivalvia, Leptonacea). *Journal de Conchyliologie*, 112(3-4): 105-115.

BIELER, R. & P. M. MIKKELSEN, 1988, Anatomy and reproductive biology of two western Atlantic species of Vitrinellidae, with a case of protan-

drous hermaphroditism in the Rissoacea. *The Nautilus*, 102(1): 1-29.

BOSS, K. J., 1965a, A new mollusk (Bivalvia, Erycinidae) commensal on the stomatopod crustacean *Lysiosquilla*. *American Museum Novitates*, no. 2215: 11 pp.

BOSS, K.J., 1965b, Symbiotic erycinacean bivalves. *Malacologia*, 3(2): 183-195.

BRUUN, A. F., 1938, A new entocommensalistic bivalve, *Entovalva major* n.sp., from the Red Sea. *Videnskabelige Meddelelser fra Dansk naturhistorisk Forening i København*, 102: 163-167.

CHAVAN, A., 1969, Superfamily Leptonacea Gray, 1847. Pp 518-537, in: R. C. MOORE, ed., *Treatise on Invertebrate Paleontology, Part N. Mollusca 6. Bivalvia 2.* Geological Society of America (Boulder, Colorado) & University of Kansas (Lawrence), ii + N491-N952 pp.

CLAPP, W. F., 1951, Observations on living Teredinidae. *Fourth Progress Report on Marine Borer Activity in Test Boards Operated during 1950.* Report no. 7550, W. F. Clapp Laboratories, Inc., Duxbury, Massachusetts, 9 pp.

CONEY, C. C., 1990, *Bellascintilla parmaleeana* new genus and species from the tropical eastern Pacific, with a review of the other, ventrally notched galeommatid genera (Bivalvia: Galeommatacea). *The Nautilus*, 104(4): 130-144.

CORNET, M., 1982, Anatomical description of *Vasconiella jeffreysiana* (P. Fischer, 1873) (Mollusca, Bivalvia, Leptonacea). *Journal of Molluscan Studies*, 48(1): 36-43.

DALL, W. H., 1899, Synopsis of the Recent and Tertiary Leptonacea of North America and the West Indies. *Proceedings of the United States National Museum*, 21(1177): 873-897, pls. 87-88.

DALL, W. H., P. BARTSCH & H. A. REHDER, 1938, A manual of the Recent and fossil marine pelecypod mollusks of the Hawaiian Islands. *Bernice P. Bishop Museum Bulletin*, 153: iv + 233 pp., 58 pls.

ECKELBARGER, K. J., R. BIELER & P. M. MIKKELSEN, 1990, Ultrastructure of sperm development and mature sperm morphology in three species of commensal bivalves (Mollusca: Galeommatoidea). *Journal of Morphology*, 205: 63-75.

FOX, T. H., 1979, *Reproductive adaptations and life histories of the commensal leptonacean bivalves.* Ph.D. dissertation, University of North Carolina, Chapel Hill, ix + 207 pp.

HUMASON, G. L., 1962, *Animal Tissue Techniques.* W. H. Freeman & Co., San Francisco & London, xv + 468 pp.

JEFFREYS, J. G., 1863, *British Conchology, or an account of the Mollusca which now inhabit the British Isles and the surrounding seas. Vol. II. Marine Shells, comprising the Brachiopoda, and Conchifera from the family of Anomiidae to that of Mactridae.* London, John Van Voorst, xiv + 465 pp., 8 pls.

JENNER, C. E. & A. B. McCRARY, 1968, A "gastropod" bivalve, commensal on *Squilla empusa* (Abstract). *Annual Report for 1968, American Malacological Union:* pp. 20-21.

JUDD, W., 1971, The structure and habits of *Divariscintilla maoria* Powell (Bivalvia: Galeommatidae). *Proceedings of the Malacological Society of London*, 39: 343-354.

MACKIE, G. L., 1984, Bivalves. Pp. 351-418, in: A. S. TOMPA, et al., *The Mollusca, Vol. 7, Reproduction.* Academic Press, Orlando, xix + 486 pp.

MIKKELSEN, P. M. & R. BIELER, 1989, Biology and comparative anatomy of *Divariscintilla yoyo* and *D. troglodytes*, two new species of Galeommatidae (Bivalvia) from stomatopod burrows in eastern Florida. *Malacologia*, 31(1): 1-21.

MORTON, B., 1973a, The biology and functional morphology of *Galeomma* (*Paralepida*) *takii* (Bivalvia: Leptonacea). *Journal of Zoology*, 169(2): 133-150.

MORTON, B., 1973b, Some factors affecting the location of *Arthritica crassiformis* (Bivalvia: Leptonacea) commensal upon *Anchomasa similis* (Bivalvia: Pholadidae). *Journal of Zoology*, 170: 463-473.

MORTON, B., 1975, Dymantic display in *Galeomma polita* Deshayes (Bivalvia: Leptonacea). *Journal of Conchology*, 28: 365-369.

MORTON, B., 1976, Secondary brooding of temporary dwarf males in *Ephippodonta* (*Ephippodontina*) *oedipus* sp. nov. (Bivalvia: Leptonacea). *Journal of Conchology*, 29: 31-39.

MORTON, B. & P. H. SCOTT, 1989, The Hong Kong Galeommatacea (Mollusca: Bivalvia) and their hosts, with descriptions of new species. *Asian Marine Biology*, 6: 129-160.

MORTON, J. E., 1957, The habits of *Scintillona zelandica* (Odhner) 1924 (Lamellibranchia: Galeommatidae). *Proceedings of the Malacological Society of London*, 32(5): 185-188.

NARCHI, W., 1966, The functional morphology of *Ceratobornia cema*, new species of the Erycinacea (Mollusca, Eulamellibranchiata). *Anais da Academia Brasileira de Ciências*, 38(3-4): 513-524.

NORMAN, A. M., 1891, *Lepton squamosum* (Montagu), a commensal. *Annals and Magazine of Natural History*, (6) 7(39): 276-278.

Ó FOIGHIL, D. & A. GIBSON, 1984, The morphology, reproduction and ecology of the commensal bivalve *Scintillona bellerophon* spec. nov. (Galeommatacea). *The Veliger*, 27(1): 72-80.

POPHAM, M. L., 1939, On *Phlyctaenachlamys lysiosquillina* gen. and sp. nov., a lamellibranch commensal in the burrows of *Lysiosquilla maculata. British Museum (Natural History), Great Barrier Reef Expedition 1928-29, Scientific Reports,* 6(2): 549-587.

PURCHON, R. D., 1977, *The Biology of the Mollusca, 2nd ed.* Pergamon Press, Oxford, xxv + 560 pp.

RICE, E. L., 1897, Die systematische Verwertbarkeit der Kiemen bei den Lamellibranchiaten.

Jenaische Zeitschrift für Naturwissenschaft, 31 (N.F. 24): 29-89, pls. 3-4.

TAYLOR, J. D., W. J. KENNEDY & A. HALL, 1973, The shell structure and mineralogy of the Bivalvia. II. Lucinacea—Clavagellacea, conclusions. *Bulletin of the British Museum (Natural History)*, 22(9): 253-294, pls. 1-15.

TOWNSLEY, P. M., R. A. RICHY & P. C. TRUSSELL, 1966, The laboratory rearing of the shipworm, *Bankia setacea* (Tryon). *Proceedings of the National Shellfisheries Association*, 56: 49-52.

VACCA, L. L., 1985, *Laboratory manual of histochemistry*. Raven Press, New York, xvii + 578 pp.

WINCKWORTH, R., 1930, Notes on nomenclature. *Proceedings of the Malacological Society of London*, 19(1): 14-16.

YAMAMOTO, T. & T. HABE, 1974, *Scintillona stigmatica* (Pilsbry) new to Japan. *Venus, Japanese Journal of Malacology*, 33(3): 116.

Revised Ms accepted 1 August 1991

MALACOLOGIA, 1992, 34(1–2): 25–32

EMBRYONIC DEVELOPMENT OF *BIOMPHALARIA GLABRATA* (SAY, 1818) (MOLLUSCA, GASTROPODA, PLANORBIDAE): A PRACTICAL GUIDE TO THE MAIN STAGES

Toshie Kawano (Camey),[1] Kayo Okazaki[2] & Lillane Ré[1]

ABSTRACT

The morphology of the gastropod mollusk *Biomphalaria glabrata* (Say, 1818) from the stage proceeding the first egg cleavage to the hippo stage is presented. The morphogenetic changes along its development were followed by *in vivo* observation and by cell lineage studies, with description of the origin and function of the main structures that characterize the embryonic and larval phases.

Key Words: *Biomphalaria glabrata,* Planorbidae, cleavage, embryonic, development.

INTRODUCTION

The studies of cell lineages in mollusks are of great interest for research in experimental embryology. The first ones date back to the end of the last century, when different species were investigated by many authors, such as *Neritina fluviatilis* by Blochmann (1882), *Umbrella mediterranea* by Heymons (1893), *Ischnochiton* sp. by Heath (1899), *Planorbis trivolvis* by Holmes (1900), *Physa fontinalis* by Wierzejski (1905), *Littorina obtusata* by Delsman (1912, 1914), *Limnaea stagnalis* by Raven (1946, 1958) and Verdonk (1965) and *Dentalium* sp. by Dongen (1976). Camey & Verdonk (1970) carried out studies on cell lineage of the gastropod *Biomphalaria glabrata* (Say, 1818); they analyzed its embryonic stages, with emphasis on the cephalic region, from the first egg cleavages to the veliger stage.

This guide was prepared in order to describe the various stages of the embryonic and larval development of *B. glabrata* and was also especially planned for those initiating research activities or attending or giving lectures on embryology. It covers the stages between the first egg cleavages, which are characterized by the spiral (helicoidal) type, and the trochophore and veliger stages, all of them occurring within the egg capsule.

MATERIAL AND METHODS

Egg masses of *Biomphalaria glabrata* (Say, 1818) were picked up in Belo Horizonte, State of Minas Gerais, Brazil, and maintained for several years in the laboratory, at 25°C, in a climatic chamber.

The developmental stages were followed and photographed *in vivo* by using a Zeiss photomicroscope. From the first to the fourth cleavages, the stages were photographed at intervals of 1 to 30 minutes. From the fourth cleavage on, the time intervals were of 5 hours. From the early trochophore stage on, the larvae were immobilized with ethyl ether for photography. These time intervals were decided upon based on data obtained in previous observations of the embryonic development of this species.

Stage 1 (Fig. 1B) was considered as the starting point for the determination of the embryo age due to the variation of the time intervals elapsing between egg laying and first egg cleavage, as pointed out by Raven (1946). Due to the asynchrony of egg division in the same egg-mass, zero time was considered to be the time when 50% of the eggs were in stage 1.

For the cell lineage study, the embryos were prepared according to the technique described by Verdonk (1965), which basically consists of the following steps: the embryos were decapsulated, fixed with 0.75% $AgNO_3$ for a few seconds until the cell contours became sharp, dehydrated in an alcohol series, cleared with xylene, and mounted with Permount between a slide and a coverslip. Embryos and larvae were drawn using a Zeiss camera lucida, and the nomenclature adopted was that of Conklin (1897).

[1]Serviço de Zoonoses Parasitárias e Parasitologia, Instituto Butantan Cx.Postal 065, CEP 01000, São Paulo, SP, BRAZIL.
[2]Divisão de Radiobiologia, Departamento de Aplicações em Ciências Biológicas, Instituto de Pesquisas Energéticas e Nucleares, Comissão Nacional de Energia Nuclear/SP, São Paulo, SP, BRAZIL

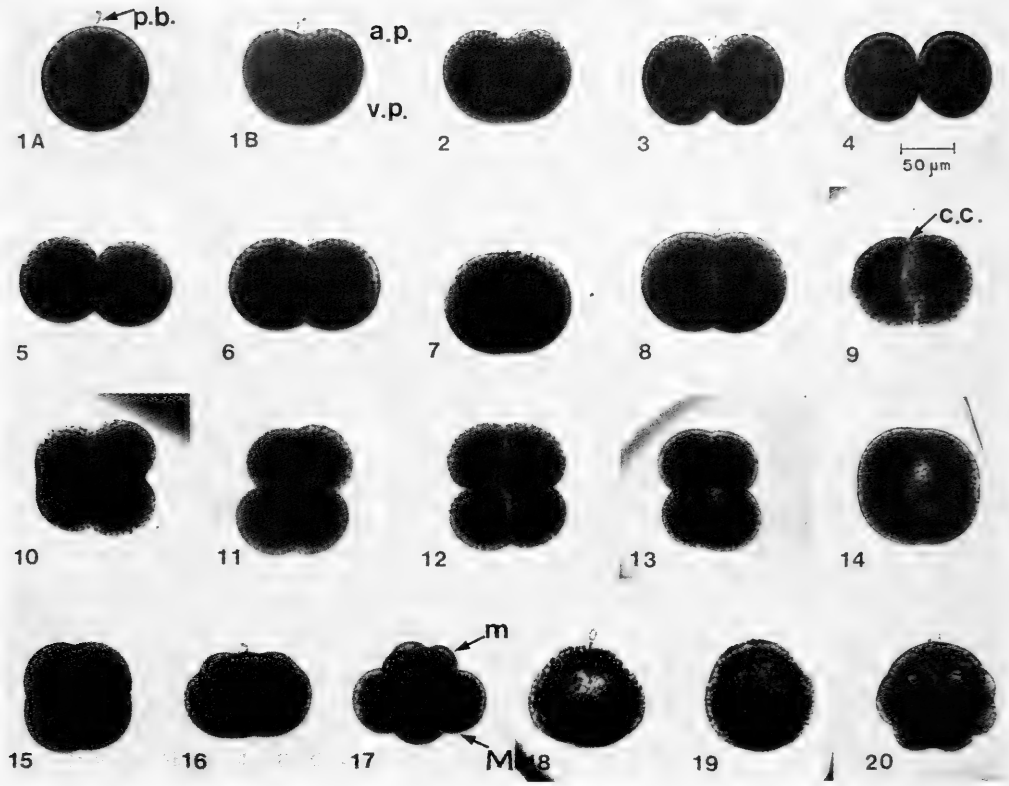

FIG. 1. Early development of *Biomphalaria glabrata.* (1A) Undivided egg with two polar bodies. (1B) Beginning of first cleavage, with appearance of the cleavage furrow in the animal pole (0 hr). (2) Appearance of the cleavage furrow, after 3 min. (3) After 4 min. (4) Two blastomeres attached to each other by a small cytoplasmic area, after 10 min. (5), (6) and (7) the blastomeres present a gradually larger contact surface: after 21, 26 and 38 min., respectively, (8) Emergence of the cleavage cavity after 45 min. (9) Cleavage cavity appearing more clearly, after 75 min. (10) Second cleavage, after 80 min. (11) Four blastomere stage, after 91 min. (12) Beginning of the appearence of the cleavage cavity, at 98 min. (13) After 103 min. (14) After 123 min. (15) Almost rounded surface of the blastomeres, at 134 min. (16) Third cleavage with formation of the first quartette of micromeres, at 160 min. (17) At 165 min. (18) At 173 min. (19) At 181 min. (20) Fourth cleavage, at 230 min. p.b. = polar body, a.p. = animal pole, v.p. = vegetative pole, c.c. = cleavage cavity, m = micromere, M = macromere.

RESULTS

Table 1 shows the main stages of the embryonic development of *B. glabrata,* from the beginning of the first cleavage to the hippo stage.

The morphological features of *B. glabrata* during the main stages of its embryonic and larval development are illustrated in Figures 1-3. The embryonic and larval cells are schematically presented in Figure 4.

Figure 1 presents a sequence of morphogenetic alterations covering the period of time between the zygote (or fertilized egg) and the fourth cleavage stage. Stage 1A shows the zygote before the first cleavage; two polar bodies (p.b.) can be seen at the upper apical region, exactly in the animal pole. The diameter of a viable egg is approximately 100 µm long. Stages from 1 to 19 are equivalent to those described for *Limnaea stagnalis* by Raven (1946). The first cleavage furrow appears during stage 1B in the animal pole. This phase corresponds to the beginning of the first cleavage, which is total and passes through the animal and vegetative poles. Stages 2 and 3 occur approximately 3 or 4 minutes after stage 1B, respectively, with

TABLE 1. Main stages of the embryonic development of *B. glabrata* at 25°C.

Embryonic stage	Time interval between observations	Number of stage in figures
Beginning of the 1st cleavage	0	1B
2nd cleavage	80 min.	10
3rd cleavage	160 min.	16
4th cleavage	230 min.	20
blastula	15 hrs.	21
gastrula	26 hrs.	23
early trochophore	43 hrs.	25
late trochophore	66 hrs.	27
early veliger	96 hrs.	28
late veliger	120 hrs.	29
hippo stage	144 hrs.	30

cleavage furrow becoming gradually more predominant; the cleavage of the animal pole region is more rapid than that of the vegetative one. At stage 4 the cleavage furrow almost completely divides the zygote into two blastomeres, both of them presenting a well-rounded surface and linked to each other by only a small cytoplasmic bridge. This phase occurs approximately 10 minutes after stage 1B (Fig. 1, stage 4; Fig. 4, stage 31). After stage 5, at approximately 21 minutes from the beginning of zero time, the two blastomeres approach each other, increasing their contact surface, that is, they flatten against each other, with the formation of a separating blastomeric membrane (Fig. 1, stage 5). During stages 6 and 7 (Fig. 1), the boundaries of the blastomeres can hardly be defined; these stages occur approximately 26 and 38 minutes after stage 1B, respectively.

The cleavage cavity, the function of which is osmotic regulation, can be seen between the two blastomeres at stage 8, approximately 45 minutes after stage 1B (Fig. 1). This cavity increases in size, and both blastomeres have an egg shape (Fig. 1, stages 8 and 9).

The beginning of the second cleavage (Fig. 1, stage 10) occurs 80 minutes after the first cleavage. Because the blastomeres do not divide synchronously, the cleavage furrow of one of the blastomeres appears before the other, so that this stage presents an asymmetrical shape (Fig. 1, stage 10). This cleavage is meridional and total.

During stage 11 (Fig. 1), after approximately 91 minutes, the blastomeres show a rounded shape but are not on the same plane when observed obliquely; that is, blastomeres A and C (Fig. 4, stage 32) are linked to each other by the furrow in the animal pole, and blastomeres B and D by the furrow in the vegetative pole.

At stage 12 (Fig. 1), after approximately 98 minutes, the cleavage furrow linking the alternate blastomeres in the animal and vegetative poles of the egg can be seen more clearly (Fig. 1, stage 12; Fig. 4, stage 32). At stages 13 (after 103 min) and 14 (after 123 min) (Fig. 1), the blastomeres are already more closely joined, and the cleavage cavity between them begins to appear. Material from the cleavage cavity then starts coming out, with contraction of the whole egg causing a visible reduction in diameter (Fig. 1, stage 15).

The third cleavage is laeotropic and occurs in the subequatorial plane of the egg, with the formation of the first micromere quartette (1a to 1d), approximately 160 minutes after the beginning of the first cleavage (Fig. 1, stage 16; Fig. 4, stage 33). A gradual increase of the cleavage cavity is observed during stages 17 (after 165 min), 18 (after 173 min) and 19 (Fig. 1).

Stage 20 (Fig. 1) illustrates the egg at the fourth cleavage stage, which is dexiotropic. The fourth cleavage is subequatorial and occurs approximately 230 minutes after stage 1B (Fig. 4, stage 34), originating the second micromere quartette (2a to 2d).

The embryo reaches the blastula stage approximately 10 to 23 hours after the 1st cleavage (Figs. 21, 22).

Stages 35 and 36 (Fig. 4) show the embryo with about 64 and 130 cells, respectively, and presenting a set of cells forming a cross-like figure ($1a^{11}$ to $1d^{11}$, $1a^{12}$ to $1d^{12}$ and $2a^{11}$ to $2d^{11}$ cell lineages) in the animal pole, which gives origin to almost the whole head region.

Gastrulation occurs about 24 to 39 hours after the first cleavage (Fig. 2, stages 23, 24A,

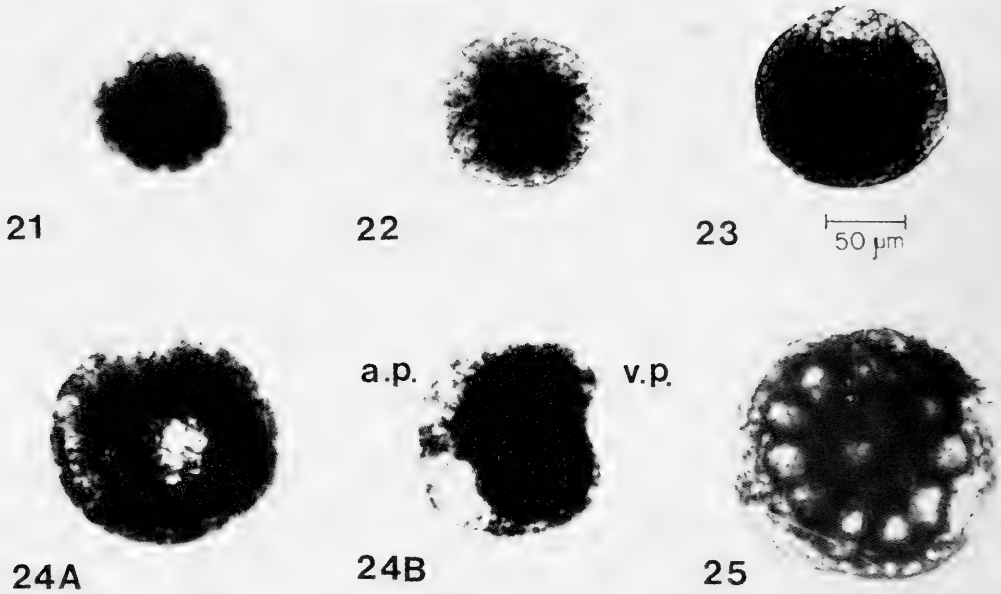

FIG. 2. Different stages of development of *Biomphalaria glabrata.* (21) Blastula, 15 hrs. after 1st cleavage. (22) Blastula, 21 hrs. and 30 min. after 1st cleavage (23) Gastrula, 26 hrs. after 1st cleavage. (24A) Late gastrula as seen from the vegetative pole after 34 hrs. (24B) Lateral view of the 34 hrs. gastrula stage. (25) Early trochophore, after 43 hrs. a.p. = animal pole, v.p. = vegetative pole.

24B; Fig. 4, stages 37 and 38). Flattening of the vegetative pole region towards the animal pole then occurs, followed by the invagination of this region, with the formation of a spherical opening, the blastopore, which then becomes gradually smaller.

The early trochophore stage appears approximately 40 to 65 hours after the first cleavage, and is characterized by the first larval movements (Fig. 2, stage 25; Fig. 3, stage 26) by means of the ciliated cells of the prototroch, which divides the larva in the pretrochal region, characterized by the presence of an apical plate, head vesicle and cephalic plates, and the posttrochal region, characterized by the presence of a shell gland, stomodeum and foot (Fig. 4, stage 39). The prototroch shows a double row of cells, an upper one formed by $2d^{111}$, $2b^{112}$, $1a^{21}$, $1a^{22}$, $1b^{21}$ and $1b^{22}$ cells, and a lower ciliated one consisting of $2b^{211}$ and $2b^{121}$ cells and of cells descending from $2b^{122}$ and $2b^{212}$ cells (Fig. 4, stage 39).

The late trochophore stage occurs approximately 65 to 80 hours after the first cleavage, with the larva having a slightly elongated, kidney-like shape. In this phase, cells responsible for the formation of the head and foot can be seen in its anterior region, and in the dorsal region one can see the shell gland (Fig. 3, stage 27). Stage 40 (Fig. 4) shows a greater development of the prototroch, leading to more active larval movements. The pretrochal region, located above the prototroch, is formed by a set of cells that gives rise to such larval structures as the apical plate ($1a^{111}$ to $1d^{111}$, $1a^{1121}$, $1b^{1121}$ and $1b^{1211}$), cephalic plates (cells located laterally to the apical plate), and the head vesicle ($1c^{21}$, $1d^{21}$, $1c^{22}$, $1d^{22}$, $1a^{122}$, $1c^{122}$, $1d^{122}$, $1d^{1211}$, $1d^{1212}$, $2a^{11}$, $2c^{11}$, $2d^{11}$), which in turn will form the head. In the posttrochal region, below the prototroch, are the stomodeum (M), which will give origin to the mouth, and cells that will form the foot and the shell gland.

The time interval between 80 and 100 hours after the first cleavage corresponds to the early veliger stage. The shell and foot are then more developed (Fig. 3, stage 28). The prototroch has evolved into the velum (Fig. 4, stage 41). In this stage, the shell gland shifts towards the right side.

The veliger stage occurs about 120 hours after the first egg cleavage. The eyes become more visible, and the elevation of the tentacle regions can be observed, as well as the mouth, foot and shell (Fig. 3, stage 29). Stage

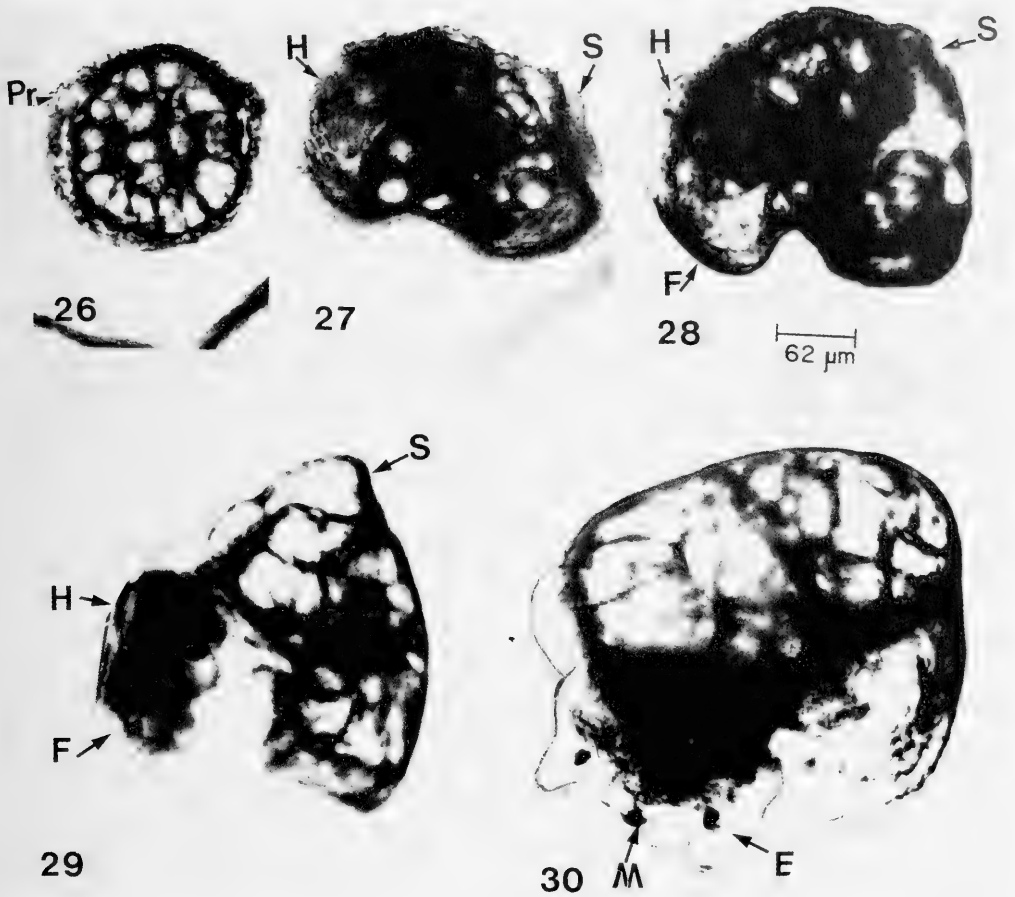

FIG. 3. Different stages of development of *Biomphalaria glabrata*. (26) Early trochophore, 55 hrs. after 1st cleavage. (27) Trochophore, after 66 hrs. (28) Early veliger, after 96 hrs. (29) Veliger, after 120 hrs. (30) Hippo stage, 144 hrs. after first cleavage. E = eyes, F = foot, H = head, M = mouth, S = shell, Pr = prototroch.

42 (Fig. 4) shows that the apical plates and head do not undergo any changes, while the cephalic plates go on dividing to form the tentacles and eyes.

The hippo stage is a phase of larval development that occurs within the egg capsule approximately 144 hours after the first cleavage. At this stage, the eyes and tentacles in the pretrochal region are already well developed, and in the posttrochal region the foot has grown in size and is much more differentiated. The shell starts coiling and covers almost the whole body (Fig. 3, stage 30). At 25°C, the young snail hatches from the egg capsule between the sixth and ninth day after the first cleavage.

DISCUSSION

Due to their semi-transparence and easy maintenance in the laboratory, the eggs of *B. glabrata* represent a suitable material for studies on embryology, allowing a good *in vivo* observation. At egg-laying, its egg-masses already contain fertilized eggs and, after approximately 30 minutes (at 25°C), the emission of the first polar body occurs, as a result of the first meiotic division. Approximately 60 minutes later, the second polar body emerges. Both polar bodies remain in the animal pole during the first cleavages. Within 60 minutes after the emission of the second polar body, the fusion of the male and

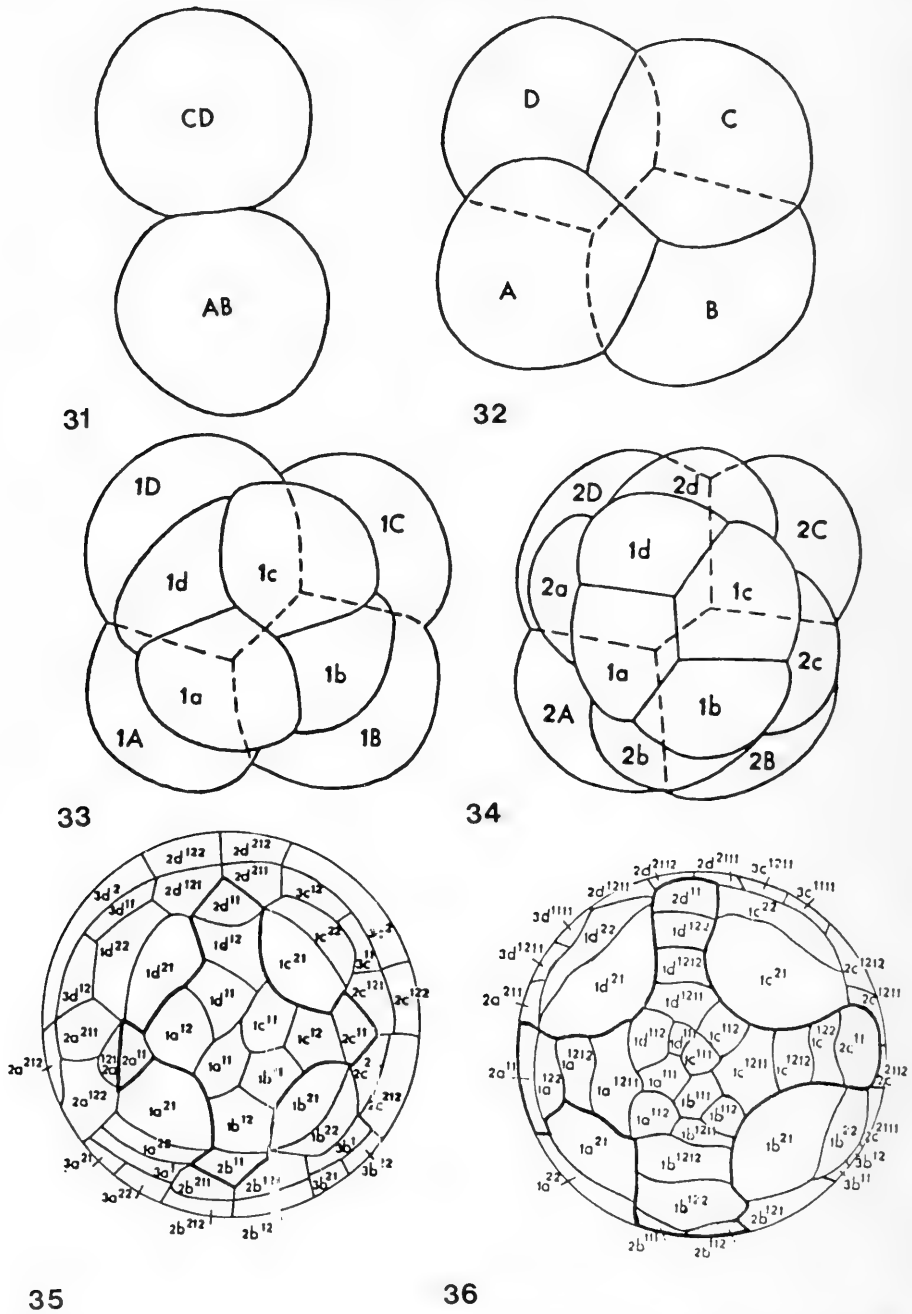

FIG. 4. Outline of cell boundaries on developing eggs of *Biomphalaria glabrata*. (31) 1st cleavage with 2 blastomeres. (32) 2nd cleavage with 4 blastomeres, 80 min. after 1st cleavage. (33) 3rd cleavage with 1st quartette of micromeres (1a to 1d) and with 8 blastomeres, after 160 min. (34) 4th cleavage with 2nd quartette of micromeres (2a to 2d) and 12 blastomeres, after 230 min. (35) Blastula stage with 64 blastomeres, showing the cross figure at the animal pole after 15 hrs. (36). Blastula with 130 cells (animal pole) after 21 hrs. and 30 min. (37). Gastrula, after 26 hrs. (38) Gastrula after 34 hrs. (39) Early trochophore after 34 hrs. (40) Trochophora after 66 hrs. (41) Early veliger after 96 hrs. (42) Veliger stage after 120 hrs. M = mouth, A.P. = apical plate, H.V. = head vesicle, C.P. = cephalic plate, V = velum, T = Tentacle, E = eyes, F = foot, Pr. = prototroch.

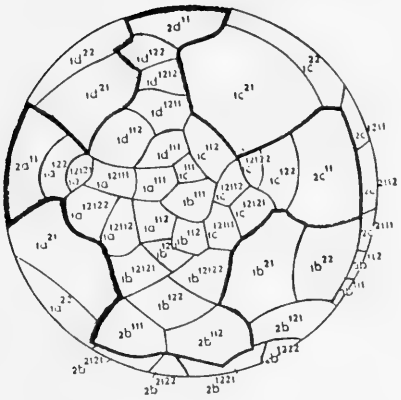

37

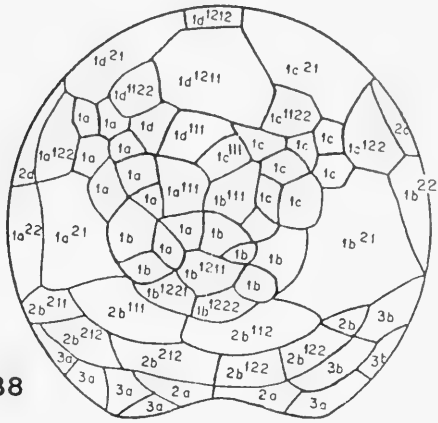

38

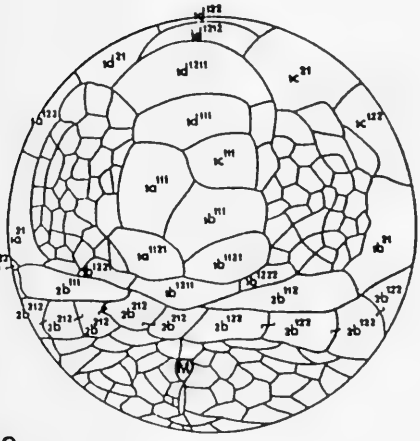

39

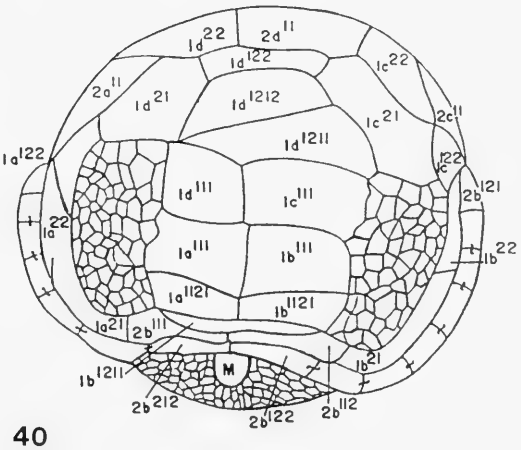

40

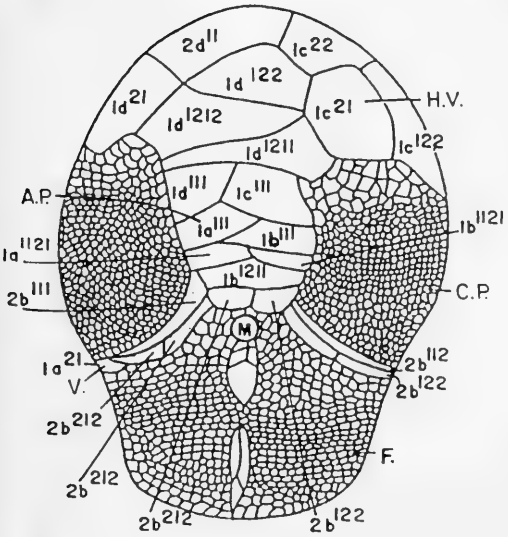

41

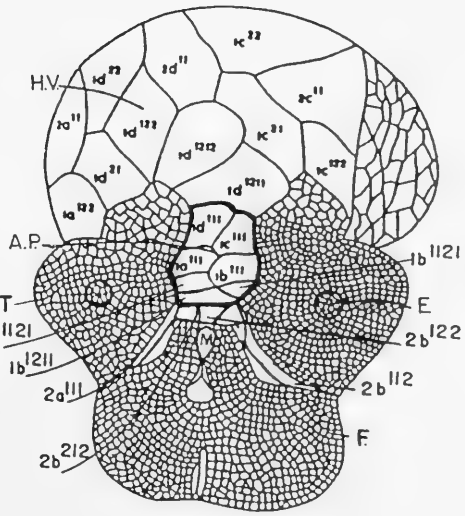

42

female pronuclei occurs, the egg now being ready for the first cleavage (Camey, 1968).

Except for cephalopods, the cleavage pattern of mollusks is of the spiral type; that is, blastomere cleavage is oblique in relation to its axis and is of the determinative type, because the different egg regions are going to form the future organs (Raven, 1958).

The developmental stages described here are similar to those of *Limnaea stagnalis,* with some differences. Cleavage is laeotropic or reverse in *B. glabrata* (Camey & Verdonk, 1970) and dexiotropic in *L. stagnalis* (Verdonk, 1965). The differentiation of the type of cleavage occurs according to the orientation of the division spindle. When this is oblique in relation to the axis of the egg in clockwise direction, cleavage is dexiotropic, and when the spindle is oblique but in a counterclockwise direction, cleavage is laeotropic. The first indication of the orientation of the cleavage spindle in *B. glabrata* occurs during the third cleavage (Camey & Verdonk, 1970).

In the trochophore stage, the shell gland is shifted to the right side in *B. glabrata* (Camey, 1968) and to the left side in *L. stagnalis* (Verdonk, 1965).

When the helicoidal shell of an adult of *L. stagnalis* is placed with the apex turned up, it can be seen that the opening is towards the right side. In *B. glabrata,* with a planispiral shell, it is difficult to determine the direction of the shell opening, except for its shift in a direction opposite to that of *L. stagnalis* during larval development. It may be concluded, therefore, that the cleavage pattern and shell opening of *B. glabrata* are laeotropic.

ACKNOWLEDGEMENTS

Thanks are due to Dr. Kaoru Hiroki for the critical reading of this paper and to Miss. Vera Helena Monezi for typing this manuscript.

LITERATURE CITED

BLOCHMANN, F., 1882, Ueber die Entwicklung der *Neritina fluviatilis.* Mull. *Zeitschrift für Wissenshaftliche Zoologie.* Leipzig. 36: 125–174.

CAMEY, T., 1968, Estágios iniciais do desenvolvimento embrionario da *Biomphalaria glabrata* (Say, 1818). Tese de Doutoramento. Belo Horizonte, MG, Brasil.

CAMEY, T. & N. H. VERDONK, 1970, The early development of the snail *Biomphalaria glabrata* (Say) and the origin of the head organs. *Netherlands Journal of Zoology,* Leiden, 20(1): 93–121.

CONKLIN, E. G., 1897, The embryology of *Crepidula. Journal of Morphology,* 13: 1–226.

DELSMAN, H. C., 1912, Ontwikkelingsgeschiedenis van *Littorina obtusata.* Thesis, Univ. of Amsterdam, Amsterdam, The Netherlands.

DELSMAN, H. C., 1914, Cf. Entwicklungsgeschichte von *Littorina obtusata. Tijdschrift Netherlandsche Dierkundige Vereeniging.* Leiden, 13(2): 170–340.

DONGEN, C. A. M. VAN, 1976, The development of *Dentalium* with special reference to the significance of the polar lobe. Utrecht, Rijksuniversiteit, 92 pp. PhD. Thesis.

HEATH, H., 1899, The development of *Ischnochiton. Zoologische Jahrbucher, Anatomie,* 12: 567–656.

HEYMONS, R., 1893, Zur Entwicklungsgeschichte von *Umbrella mediterranea* Lam. *Zeitschrift für Wissenschaftliche Zoologie,* 36: 245–298.

HOLMES, S. J., 1900, The early development of *Planorbis. Journal of Morphology.* 16: 369–458.

RAVEN, C. P., 1946, The development of the egg of *Lymnaea stagnalis* L. from the first cleavage till the trochophore stage, with special reference to its "chemical embriology". *Archives Neerlandaises de Zoologie,* Leiden, 7(3–4): 353–434.

RAVEN, C. P., 1958, *Morphogenesis: the analysis of molluscan development.* London, Pergamon Press. 311 pp. (International series of monographs on pure and applied biology. Division Zoology, v. 2)

VERDONK, N. H., 1965, Morphogenesis of the head region in *Lymnaea stagnalis* L. Utrecht, 133 pp. PhD. Thesis.

WIERZEJSKI, A., 1905, Embryologie von *Physa fontinalis* L. *Zeitschrift für Wissenchaftliche Zoologie,* 83: 502–706.

Revised Ms. accepted 31 August 1991

MALACOLOGIA, 1992, 34(1–2): 33–61

ALLOZYME FREQUENCIES IN *ALBINARIA* (GASTROPODA: PULMONATA: CLAUSILIIDAE) FROM THE IONIAN ISLANDS OF KEPHALLINIA AND ITHAKA

Th. C. M. Kemperman & G. H. Degenaars[1]

Systematic Zoology Section, Population Biology Department, Rijksuniversiteit Leiden, c/o National Museum of Natural History, P.O. Box 9517, 2300 RA Leiden, The Netherlands

ABSTRACT

In 42 samples comprising 11 of the 12 subspecies of the four species of *Albinaria* occurring on the islands of Kephallinia and adjoining Ithaka, Greece, allozyme variation was studied at 28 gene loci by starch gel electrophoresis. To serve as outgroups, single samples of two Cretan *Albinaria* species and both an *Albinaria* and an *Isabellaria* species from the Peloponnese were included. The various taxa varied at 0.0% to 35.7% of the loci, with an average of 12.2%. In 71% of the populations, a deficiency of heterozygosity was found. Taxa differ in the number of populations that must be analysed to reach a point where further addition of populations does not increase the genetic variation. The results show relatively low genetic distances between the taxa from Kephallinia; between the subspecies of the two non-endemic species hardly any allozyme differentiation is found. In the two endemic species, however, the subspecies are less similar to each other and show conspicuous genetic resemblances with different non-endemic species. The taxon from Ithaka differs markedly from all Kephallinian taxa and thus geographical isolation seems to be an important factor with respect to genetic differentiation. There is evidence for introgressive hybridization. In at least one case, we found indications for hybrizymes. A Hennigian analysis did not result in a resolved phylogeny. The present classification of species and subspecies, based on morphological and biogeographical data, is maintained only with some doubt.

Key words: systematics, allozymes, genetic variation, hybridization, electrophoresis, *Albinaria,* Pulmonata.

INTRODUCTION

General Notes

Within the context of a study on the systematics and evolutionary history of the pulmonate genus *Albinaria* Vest, 1867 (Gittenberger, in press), special attention has been given to the *Albinaria* species of the neighboring Ionian islands Kephallinia and Ithaka. The aims of this subproject are (1) to unravel the pattern of taxonomic relationships among the various taxa and (2) to get some insight into the population genetics and the evolutionary history of these pulmonates. This goal is approached by using shell morphology (Kemperman & Gittenberger, 1988), radula morphology (Kemperman et al., in prep.), genital morphology, distributional patterns, and allozyme variation (Degenaars, in press). In addition to the latter preliminary report, the present paper deals with the biochemical data in more detail.

The value of electrophoretic techniques for systematic study is widely recognized (Avise, 1974; Buth, 1984; Richardson et al., 1986; Ferguson, 1988; Nevo, 1988; Murphy et al., 1990). Allozyme variation among samples of different populations provides a data-set that may be considered virtually independent of the morphological data (Avise, 1974; Emberton, 1988). *Albinaria* has been the subject of electrophoretic studies before. Ayoutanti et al. (1988) reported on an allozyme analysis of 23 *Albinaria* populations from 12 Aegean islands, including Crete. Using 27 loci, these authors tried to unravel the genetic affinities among a group of *Albinaria* species from many islands with generally only one or two *Albinaria* taxa each. We limited our study to the rich *Albinaria* fauna of only two, neighboring islands. The studies show some overlap in

[1]Present address: Hugo de Vries Lab., University of Amsterdam, Kruislaan 318, 1098 SM Amsterdam, The Netherlands.

that we used, for example, Cretan material as outgroup and partly analyzed the same enzyme systems.

Geography of Kephallinia and Ithaka

The largest island, Kephallinia (Fig. 1), measures about 50 km from north to south and somewhat more than 20 km across the middle of the main part of the island (that is, without the Paliki Peninsula), which is dominated by a mountain ridge, reaching 1,628 m altitude. All over the island are areas with limestone rocks and/or rock faces inhabited by *Albinaria*. Ithaka is only 23 km long and up to 6 km wide. It consists of two large peninsulas joined by a narrow, high isthmus.

The present 130 m isobath can probably be looked upon as the Pleistocene shore line of approximately 18,000 B.P., when sea level reached its lowest point (Andel & Shackleton, 1982: 447–448) during the Würm. Judging from the isobaths on Admiralty Chart no. 203 (1988) and data given by Bird (1984: 81, fig. 41), we may assume that between approximately 29,000 and 12,000 years ago there was a minimally 1 km-broad land connection between Kephallinia and Ithaka, running from Cape Dichalia, northeast of Sami on Kephallinia, and the south-southwest coast of Ithaka. At present, this is a stretch of approximately 4 km sea water. North of this area, there have not been relatively recent land bridges, because there the sea between Kephallinia and Ithaka is over 145 m deep, with a depth of 182 m near Fiskardo, northeastern Kephallinia. Thus, Ithaka and Kephallinia have been separate islands for at least 12,000 years.

Because the sea between Lixouri and Argostoli is at present only 25 m deep, we have to accept that during glacial sea-level lowerings the entire Gulf of Argostoli between the Paliki Peninsula and the main island was land.

Distribution of *Albinaria* on Kephallinia and Ithaka

In Figure 1, the ranges of the *Albinaria* taxa from Kephallinia and Ithaka are indicated, based on our data from approximately 800 localities (Kemperman, in prep. A). Different shadings indicate different species, whereas broken thick lines separate the ranges of subspecies. Based on classical conchological characters, four species are distinguished, each with at least two subspecies.

On Kephallinia, two species are endemic, both with limited ranges, namely *A. jonica* and *A. adrianae*. On Ithaka no endemic *Albinaria* species have been found.

Albinaria contaminata ranges on the Ionian islands from Lefkas to Zakynthos and on the mainland from the southern Epirus to the province of Phocis. It is the only *Albinaria* known from Ithaka. On Kephallinia it is the most widely distributed species, occurring almost everywhere, except for places along the west coast and the Paliki Peninsula. The second widespread species is *A. senilis,* occurring on all the Ionic islands, except for Zakynthos, and from the Epirus southward to the mainland opposite Lefkas.

MATERIALS AND METHODS

Species Sampled

In total, 46 populations are examined electrophoretically, 42 of which were from Kephallinia and Ithaka, representing the following taxa (between square brackets, the number of investigated populations: individuals is given): *Albinaria contaminata contaminata* (Rossmässler, 1835) [7: 128], *A. c. incommoda* (Boettger, 1878) [4: 36], *A. c. odysseus* (Boettger, 1878) [4: 53], *A. c. liebetruti* (Charpentier, 1852) [1: 18], *A. senilis senilis* (Rossmässler, 1836) [12: 140], *A. s. flavescens* (Boettger, 1878) [2: 27], *A. s. kolpomyrtensis* Kemperman & Gittenberger, 1990 [1: 15], *A. adrianae adrianae* Gittenberger, 1979 [4: 52], *A. a. dubia* Gittenberger, 1979 [1: 19], *A. jonica assicola* Kemperman & Gittenberger, 1990 [2: 36], and *A. j. jonica* (Pfeiffer, 1866) [2: 16].

All specimens from Kephallinia and Ithaka were collected by the first author in March 1988. See Appendix for detailed information on the localities indicated in Figure 2.

As outgroups we used populations of *A. teres nordsiecki* Zilch, 1977 [1: 8] and *A. rebeli* Wagner, 1924 [1: 13] from Crete, and *Albinaria* spec. [1: 20] and *Isabellaria edmundi* Gittenberger, 1987 [1: 20] from the Peloponnese (Parnon) (see Appendix). The outgroup material was collected by E. Gittenberger in April and June 1988.

In total 613 individuals are examined, an average of 13 specimens per population.

Collecting and Transport

Populations were sampled at a location limited to 1 to 20 m^2. The snails could be col-

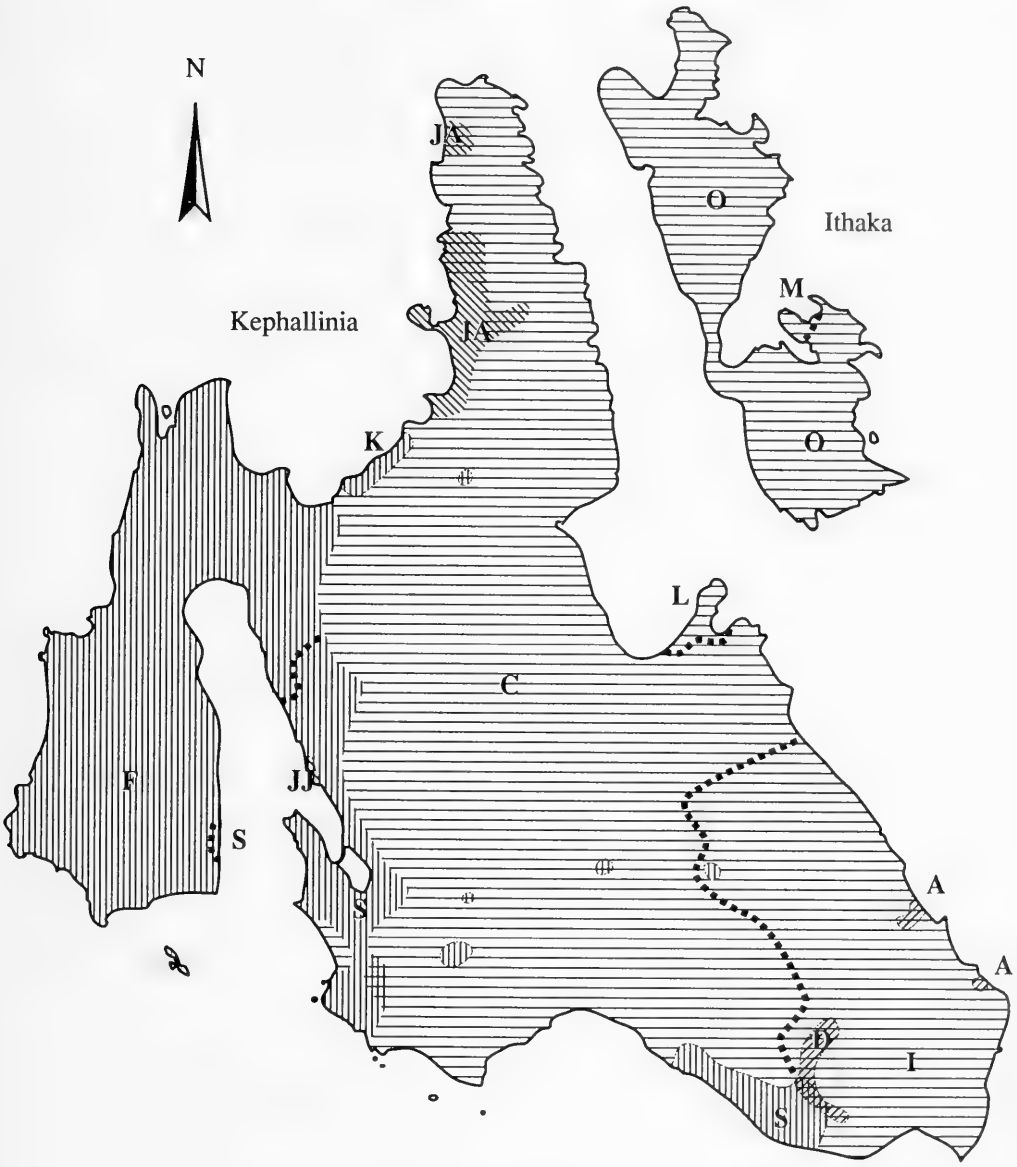

FIG. 1. Map of Kephallinia and Ithaka, with distributions of *Albinaria* taxa.

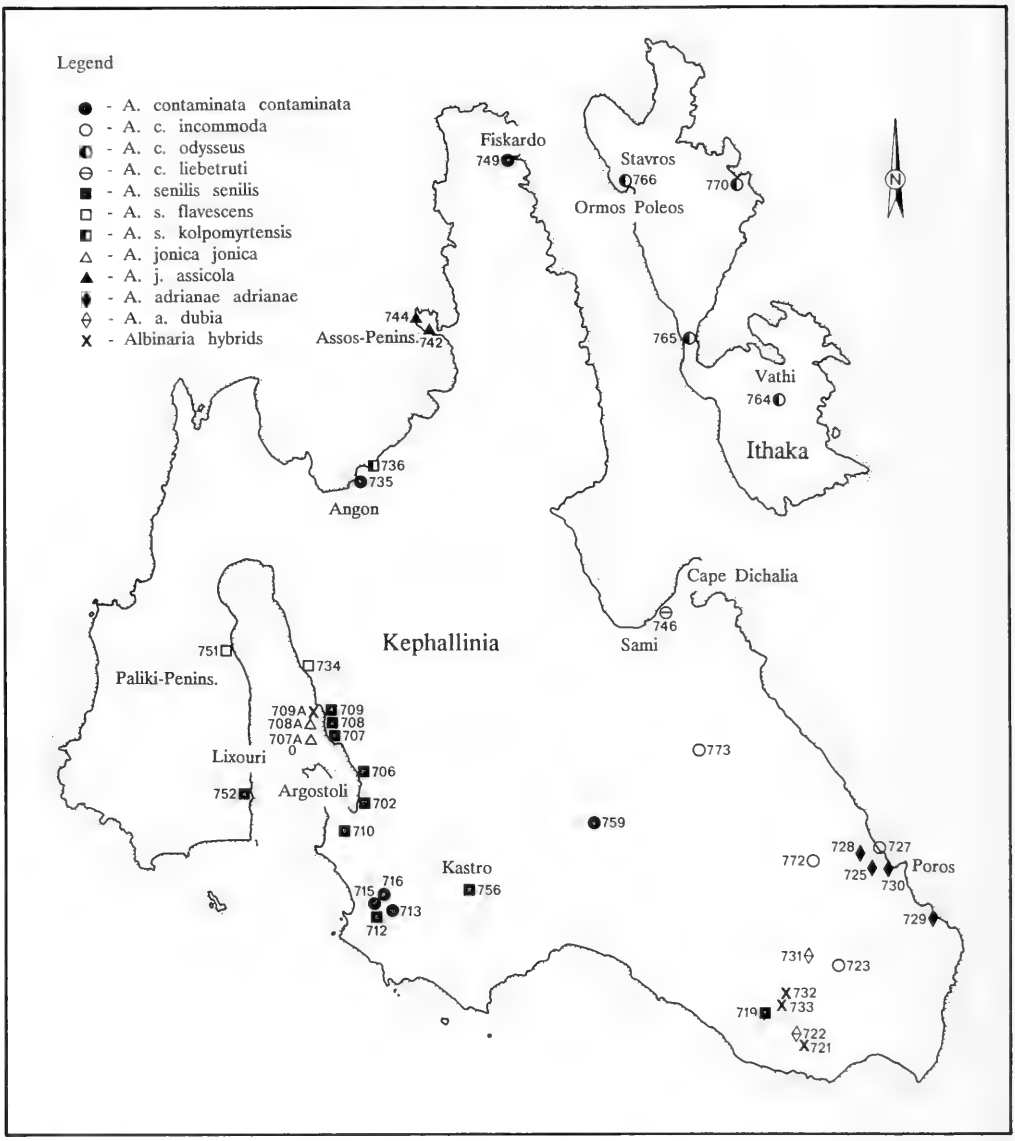

FIG. 2. Map of Kephallinia and Ithaka, with collection sites of material used in allozyme studies.

lected easily, without any special device. Forced into aestivation, they are not very demanding during transport. Plastic sandwich-bags with some dry paper wipes proved to be adequate for storage of several weeks.

Electrophoresis

Complete animals, including shells, were ground in two drops of distilled water in ice-cooled porcelain cups. Wicks (Whatman no. 3 filter paper; 2 × 5 mm) were used to apply the homogenate on the gels. After 15 initial running minutes at approximately 16 V/cm, the wicks were removed and the electric field was raised to approximately 19 V/cm. Running times depended on the buffer system that was used (Table 1). The gel/buffer system was ice-cooled. The complete set of enzyme systems of a specimen was tested, usually in

TABLE 1. Enzymatic systems and loci scored for electrophoretic analysis, with buffer systems employed and stain references.

Enzymatic system (E.C.)	Loci	Migration	Buffer*	Stain reference
Adenylate kinase (2.7.4.3)	*Ak*	anodic	TC 7	Shaw & Prasad (1970)
Aldehyde oxidase (1.2.3.1)	*Ao*	anodic	Poulik	Ayala et al. (1972)
Alkaline phosphatase (3.1.3.1.)	*Aph*	anodic	TC 7	Shaw & Prasad (1970)
Aspartate aminotransferase (2.6.1.1)	*Aat-1,2*	cathodic/anodic	TEB 9	Selander et al. (1971)
α-Esterase (3.1.1.1)	*Est-1,2,3*	cathodic/anodic	TC 7	Shaw & Prasad (1970)
Glucose-6-phosphate dehydr. (1.1.1.49)	*G6pd*	anodic	TEB 9	Shaw & Prasad, mod. Brewer (1970)
Glucophosphate isomerase (5.3.1.9)	*Gpi*	anodic	Poulik	Shaw & Prasad (1970)
α-Glycerophosphate dehydrog. (1.1.1.8)	*α-Gpdh-1,2*	anodic	TEB 8	Shaw & Prasad (1970)
Hexokinase (2.7.1.1)	*Hk*	anodic	TEB 8	Shaw & Prasad (1970)
L-Iditol dehydrogenase (1.1.1.14)	*Idh*	anodic	TEB 9	Shaw & Prasad (1970)
Isocitrate dehydrogenase (1.1.1.42)	*Isdh-1,2*	anodic	TC 7	Shaw & Prasad (1970)
Lactate dehydrogenase (1.1.1.27)	*Ldh*	anodic	TEB 8	Shaw & Prasad (1970)
Leucine aminopeptidase (3.4.11.1)	*Lap*	anodic	TEB 8	Shaw & Prasad (1970)
Malate dehydrogenase (1.1.1.37)	*Mdh-1,2*	cathodic/anodic	TC 7	Shaw & Prasad (1970)
Mannose phosphate isomerase (5.3.1.8)	*Mpi*	anodic	TEB 9	Nichols et al. (1973)
NADH dehydrogenase (1.6.99.3)	*Nadd-1,2*	anodic	Poulik	Menken (1980)
Phosphoglucomutase (5.4.2.2)	*Pgm*	anodic	Poulik	Shaw & Prasad (1970)
Phosphogluconate dehydrog. (1.1.1.43)	*Pgd*	anodic	TEB 9	Shaw & Prasad (1970)
Superoxide dismutase (1.15.1.1)	*Sod-1,2*	anodic	TEB 8	Shaw & Prasad (1970)
Xanthine dehydrogenase (1.2.1.37)	*Xdh*	anodic	TEB 8	Shaw & Prasad (1970)

*) TC 7 = Tris—Citrate, pH 7, running time (rt) 2 h (Shaw & Prasad, 1970); Poulik = Poulik, gel pH 8.75–8.9 & electrode pH 7.6–8.0, rt 3 h (Poulik, 1957); TEB 8 = Tris—EDTA—borate, pH 8, rt 3.5 h (Shaw & Prasad, 1970); TEB 9 = Tris—EDTA—borate, pH 9, rt 4.5 h (Ayala et al., 1973). All at 350 V or 35 mA.

two days, for which the homogenate had to be stored overnight at −80°C. For references concerning the histochemical staining procedures, see Table 1. All samples were scanned for 28 loci from 20 enzyme systems. In Table 1 a list of the enzyme systems is given, with the abbreviations used in the present article. Because of the risk of a substantial decline in detectability of the weaker enzyme systems, we analyzed freshly prepared homogenates only.

Data Analyses

Scoring of the loci resulted in a "single-individual" genotype dataset. Doubtful pairs of bands were by convention scored as single bands, and in case of a doubtful position of a single band the alternative with the highest frequency was accepted. Data analyses were performed with the BIOSYS-1 computer program, release 1.7 (Swofford & Selander, 1989). To assess the degree of genetic variability, we calculated per population and per subspecies the mean observed heterozygosity per locus (Ho), the mean heterozygosity per locus based on Hardy-Weinberg expectations (He), the accompanying standard deviations, as well as the percentage of polymorphic loci (Pp and Pt). Also allelic frequencies were estimated per population and per subspecies. In the latter case, populations with morphologically determined hybrids have not been taken into account. On the basis of the allele frequencies, the genetic similarity coefficients were computed for each pair of populations or taxa, according to Nei's (1972) genetic distance (D) and Rogers' (1972) genetic distance (R). On the resulting genetic distance coefficient matrices, a UPGMA cluster analyses (Sneath & Sokal, 1973) was performed.

To achieve a phylogeny, we also carried out a Hennigian analysis following Richardson et al. (1986: 337), Mooi (1989) and Emberton (1990). We used the computerprogram HENNIG86 (Farris, 1988).

The ingroup is not polyphyletic, but consists of a representative sample of subspecies of the wide-spread species *A. contaminata* and *A. senilis* and all the known subspecies of the endemic species *A. jonica* and *A. adrianae*. It is hypothesized that these species form a monophyletic group and that both *A. adrianae* and *A. jonica* have evolved on Kephallinia, sharing a common ancestor with one of the other species. Although our ingroup—all the *Albinaria* species and subspecies from

Kephallinia and Ithaka, except for *A. contaminata muraria*—does not consist of all the known members of the clade, this does not invalidate its use as a monophyletic group. In principle one can never be sure whether all its extinct and extant members are known. Many valuable phylogenetic revisions have been published in monographs dealing with incomplete ingroups due to geographical or practical restrictions. Our outgroup is composed of not too closely related congeneric species from relatively distant localities (Peloponnese and Crete) and, in the case of *Isabellaria edmundi,* a species of a genus of doubtful status that is at least very closely related to *Albinaria* (Gittenberger, 1987).

Classification on Shell Morphology and Distribution

It should be emphasized that we primarily classified the various taxa according to shell morphology and distribution, following Nordsieck (1977) and Kemperman & Gittenberger (1990). From the shell characters we mention (1) the sculpture of the protoconch, (2) the sculpture of the teleoconch (without cervix), (3) the cervical sculpture, (4) the cervical structures, (5) the microsculpture, (6) the general shell shape, (7) the shell size, (8) the apertural shape, (9) the shape of the apertural lip, (10) the apertural attachment to the teleoconch, (11) the shape of the columellaris, (12) the length of the parietalis, (13) the length of the spiralis, (14) the presence of a paralellis, (15) the shape of the palatalis, (16) the shape of the lunella, and (17) the shape of the clausilium. These characters, which proved to vary independently among the species and subspecies, will be discussed in detail in Kemperman (in prep. A). It turned out that *A. contaminata* differs in eight independent characters from *A. senilis,* in ten from *A. jonica* and in eleven from *A. adrianae*. *A. senilis* differs in nine characters from *A. jonica* and in four from *A. adrianae,* whereas *A. jonica* differs in seven characters from *A. adrianae*. These morphological data, in combination with the distributional patterns and the fact that intermediate forms are an extreme minority found only in a few contact zones lead us to consider these forms separate species.

RESULTS

Among all taxa, including the outgroups, variation was found at 16 of the 28 loci (57%), namely, *Aat-1, Ak, Aph, Est-3, Gpi, Hk, Idh, Lap, Ldh, Mdh-1, Mdh-2, Mpi, Nadd-1, Nadd-2, Pgd,* and *Pgm*. All the taxa, except for *A. a. dubia,* of which only a single population could be analysed, are polymorphic to some extent. At up to 35.7% of the loci, with an average of 12.2% (± 10.4%), variation has been demonstrated (Table 2). The observed percentage polymorphic loci per taxon (Pt) depends to some extent on the number of scanned populations. In a single population, only a part of the specific allozyme variation is found. Therefore, to estimate the amount of polymorphic loci in a certain taxon, a minimum number of populations must be studied. For *A. c. contaminata* and *A. s. senilis,* we computed the percentage polymorphic loci for one population, for two combined populations, and so on, each time adding randomly specimens of one more population. This procedure was repeated three times, starting and continuing with different populations. The averaged values for the different numbers of populations are indicated in Figure 3. From this figure it becomes obvious that in *A. s. senilis* from four populations on, the growth in variation is very low. In *A. c. contaminata,* however, there is still no important reduction in increase of variation after the addition of six populations.

The polymorphic loci per population (Pp) varies between 0.0% and 17.9%, with an average of 7.5% (± 4.9%). Two of sixteen populations of *A. contaminata* and four of five populations of *A. adrianae* proved to be invariable. The averaged values of Pp per taxon vary between 0.0% for *A. a. dubia* and 10.7% for *A. j. jonica*.

In Figure 4, we plotted the Pp of the analysed populations of the various species against the number of analysed individuals. It turned out that there is only a limited relation between the number of analysed individuals and the Pp of that population (Table 2).

In all taxa that could be investigated, the level of heterozygosity was low (Table 2). With Ho = 0.030, *A. s. senilis* was the most variable subspecies. No genetic variation was found in the population of *A. a. dubia,* and only very little was found in *A. c. liebetruti* (Ho = 0.003), *A. c. odysseus* (Ho = 0.005) and *A. a. adrianae* (Ho = 0.001). In all subspecies, except for *A. s. kolpomyrtensis,* the mean observed heterozygosity was below the mean expected heterozygosity. The differences were often considerable, as in *A. c. liebetruti* (Ho = 0.003 versus He = 0.017) and *A. c. odysseus* (Ho = 0.005 versus He =

TABLE 2. Percentages polymorphic loci per taxon and per population and the mean heterozygosity. For abbreviations, see Results; "s" in an abbreviation means standard deviation. *: based on 702, 706–708, 710 and 712 only.

Taxon/loc. nr.	P_t	P_p	$\overline{P_p}$	sP_p	$\overline{H_o}$	sH_o	$\overline{H_e}$	sH_e
contaminata	32.1		9.2	5.8	0.013	0.006	0.026	0.013
713		14.3			0.020	0.012	0.032	0.020
715		17.9			0.024	0.013	0.039	0.021
716		7.1			0.005	0.004	0.018	0.015
721		10.7			0.037	0.024	0.031	0.019
735		7.1			0.000	0.000	0.019	0.013
749		0.0			0.000	0.000	0.000	0.000
759		7.1			0.012	0.008	0.012	0.008
incommoda	14.3		4.4	3.4	0.009	0.006	0.014	0.009
723		7.1			0.022	0.018	0.019	0.015
727		7.1			0.008	0.006	0.015	0.012
772		0.0			0.000	0.000	0.000	0.000
773		3.6			0.009	0.009	0.019	0.019
liebetruti	3.6	3.6			0.003	0.003	0.017	0.017
odysseus	17.9		8.0	3.4	0.005	0.003	0.044	0.021
764		3.6			0.000	0.000	0.013	0.013
765		7.1			0.003	0.003	0.012	0.010
766		10.7			0.015	0.009	0.023	0.014
770		10.7			0.000	0.000	0.029	0.019
senilis	32.1*		9.9	4.9	0.030	0.010	0.050	0.016
702		7.1			0.020	0.018	0.020	0.015
706		14.3			0.036	0.023	0.045	0.025
707		14.3			0.018	0.011	0.030	0.017
708		7.1			0.023	0.018	0.033	0.024
709		3.6			0.018	0.018	0.018	0.018
710		3.6			0.000	0.000	0.019	0.019
712		3.6			0.030	0.030	0.023	0.023
719		14.3			0.022	0.011	0.031	0.018
732		14.3			0.042	0.022	0.044	0.023
733		10.7			0.009	0.007	0.034	0.021
752		10.7			0.029	0.018	0.037	0.021
756		17.9			0.065	0.030	0.061	0.028
flavescens	14.3		7.2	5.0	0.010	0.005	0.028	0.016
734		3.6			0.004	0.004	0.004	0.004
751		10.7			0.016	0.011	0.039	0.026
kolpomyrtensis	10.7		10.7		0.022	0.013	0.020	0.012
jonica	17.9		10.7	0.0	0.028	0.015	0.035	0.016
707		10.7			0.021	0.013	0.027	0.016
708		10.7			0.048	0.027	0.057	0.032
assicola	10.7		8.9	2.6	0.011	0.009	0.018	0.014
742		10.7			0.010	0.008	0.019	0.014
744		7.1			0.013	0.010	0.018	0.015
adrianae	3.6		0.9	1.8	0.001	0.001	0.001	0.001
725		0.0			0.000	0.000	0.000	0.000
728		0.0			0.000	0.000	0.000	0.000
729		0.0			0.000	0.000	0.000	0.000
730		3.6			0.002	0.002	0.002	0.002
dubia	0.0				0.000	0.000	0.000	0.000
teres	3.6				0.000	0.000	0.015	0.015
rebeli	7.1				0.005	0.005	0.024	0.017
Albinaria sp.	7.1				0.002	0.002	0.016	0.014
Isabellaria	3.6				0.000	0.000	0.018	0.018

0.044). From the individual population samples in which Ho and He are not equal to zero (Table 2), 13% have Ho > He, whereas 16% have Ho = He. So, in 71% of the populations there is a deficiency of heterozygosity.

Among the various taxa there is only little allozymic differentiation (Table 3). All taxa show the same allele at highest frequency for all but nine loci, namely, *Aat-1, Hk, Idh, Lap, Ldh, Mdh-1, Mdh-2, Mpi* and *Pgm*. Of these loci, only *Aat-1, Mdh-1* and *Mdh-2* concern *Albinaria*s from Kephallinia or Ithaka. Although *Aat-1, Mdh-2* and *Lap* are highly polymorphic, there is always a most common allele.

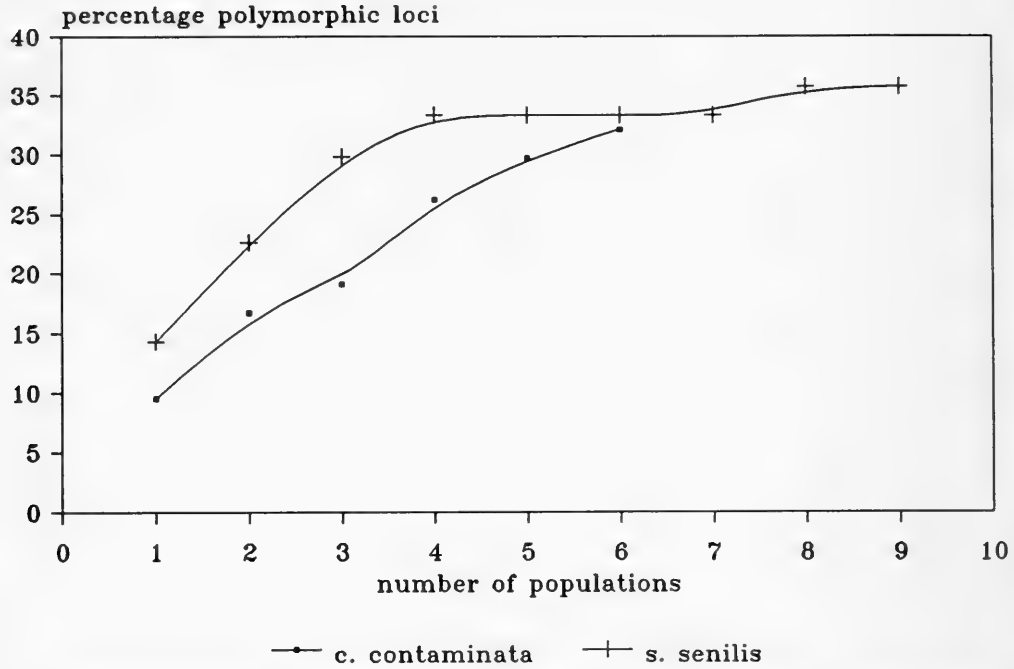

FIG. 3. Allozyme variation in *Albinaria* subspecies at increasing number of populations. For explanation, see Discussion.

Albinaria a. adrianae is monomorphic at the *Mdh-1* locus for an allele that is rare or absent in the other taxa. *Albinaria a. dubia* is monomorphic at the *Mdh-2* locus for an allele that is not found in any other Kephallinian taxon, but occurs in the Ithakian *A. c. odysseus* and in the outgroup species, namely, *Albinaria* sp. and *Isabellaria edmundi* from the Peloponnese and *A. teres nordsiecki* and *A. rebeli* from Crete. No other Kephallinian or Ithakian taxa are monomorphic for rare alleles. The outgroup species, however, have at the loci *Aat-1, Lap, Ldh, Mdh-1, Mdh-2, Mpi, Nadd-1, Idh* either unique alleles or alleles that they share with other outgroup species.

Based on the estimated allelic frequencies, coefficients of genetic distances (D & R) were calculated for all pair-wise combinations of populations as well as taxa (Table 4). The results of the UPGMA cluster analyses, which are based on the various matrices are given in Figures 5 and 6, the population dendrograms, and Figures 7 and 8, the taxon dendrograms. Intraspecific genetic distances in the non-endemic species *A. contaminata* and *A. senilis* on Kephallinia are very low, whereas the differentiation among both the subspecies of the endemic *A. adrianae* and *A. jonica* is large enough to cluster them separately with different groups of the non-endemic species. The interspecific variation of the non-endemic species is limited, but large enough to enable a complete partition. The genetic distance between the endemic species is larger than that between the endemic and the non-endemic species.

There may be a correlation between genetic distance and geographical isolation, which is demonstrated by the genetic distance between the fully isolated subspecies of both *A. adrianae* and *A. jonica,* as well as by the allelic composition of the Ithakian *A. c. odysseus*. The latter is genetically more differentiated from the combined other Kephallinian taxa than these are from each other. The distance between the Kephallinian-Ithakian taxa and the Cretan-Peloponnesian outgroup species also reflects the geographical isolation. However, among the outgroup species, the differentiation between taxa from Crete on the one hand and the Peloponnese on the other hand does not strictly conform to the geographical distances.

To test the goodness of fit of the trees we

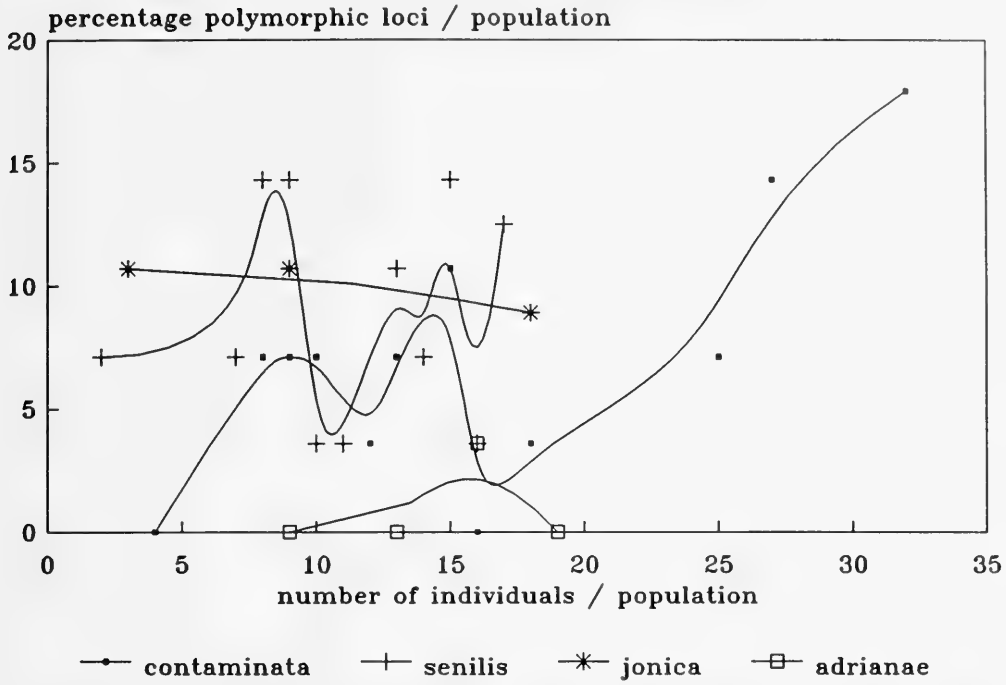

FIG. 4. Allozyme variation in *Albinaria* species within samples of different size. For explanation, see Discussion.

repeatedly calculated Nei's D and ran a UPGMA cluster analysis while each time a different subspecies was removed from the data set. This procedure resulted in two types of trees that differ only in the position of *A. c. odysseus* and *A. a. adrianae*. When either *A. c. contaminata, A. c. incommoda* or *A. a. dubia* was removed, a tree was obtained with *A. c. odysseus* as the sister group of the combined *A. contaminata* subspecies and *A. j. jonica*. In case of the removal of *A. c. contaminata* and *A. c. incommoda, A. a. adrianae* switched from the *A. contaminata* cluster to the *A. senilis* cluster. However, when either *A. c. liebetruti, A. s. senilis, A. s. flavescens, A. s. kolpomyrtensis, A. j. jonica, A. j. assicola* or *A. a. dubia* were removed the dendrogram was identical to the one obtained when all subspecies are included (Fig. 7). It can be concluded from this "jackknife" procedure that the complete dendrogram is very stable except for the position of *A. c. odysseus* and *A. a. adrianae*.

To be used in a Hennigian analysis, Table 5 gives the characters of the various taxa, as they are derived from the allele frequencies (Table 3). There are 17 informative alleles. The apomorphic character states are determined by outgroup comparison. Table 5 shows that a plesiomorphic state or states have been proposed for 15 of the 16 polymorphic loci. *Mdh-2* defines a large group to which only *A. a. dubia* is not linked. *Albinaria a. dubia* has no synapomorphies with any of the other taxa. The goal of separating the taxa into groups that are characterized by derived character states turned out to be impracticable. This means that a Hennigian analysis of the entire group does not produce a resolved phylogeny. The low number of synapomorphies distributed among the loci even troubles partial analyses.

Some alleles are very locally distributed in a certain species, sometimes exclusively where its range comes close to that of another species. This shared presence of alleles may be considered then the result of introgression. This applies to (1) the *Nadd-1* c- and d-allele in *A. j. jonica* at loc. 708, and in the adjoining populations of *A. s. senilis* at locs. 702 and 706; (2) *Gpi* alleles in *A. s. senilis* at locs. 756 and 706, and *A. c. contam-*

TABLE 3. Allele frequencies in populations for 16 polymorphic loci. N = number of individuals sampled at the locus. For taxon abbreviations, see Figure 5.

	Population														
Locus	sen 702	sen 706	sen 707	jon 707	jon 708	sen 708	sxj 709	sen 709	sen 710	sen 712	con 713	con 715	con 716	sen 719	cxs 721
Aat-1															
(N)	6	9	12	5	3	4	3	2	10	16	20	24	17	12	5
a	1.000	1.000	0.917	1.000	1.000	1.000	1.000	1.000	1.000	1.000	0.975	1.000	1.000	1.000	1.000
b	0.000	0.000	0.000	0.000	0.000	0.000	0.000	0.000	0.000	0.000	0.000	0.000	0.000	0.000	0.000
c	0.000	0.000	0.083	0.000	0.000	0.000	0.000	0.000	0.000	0.000	0.000	0.000	0.000	0.000	0.000
d	0.000	0.000	0.000	0.000	0.000	0.000	0.000	0.000	0.000	0.000	0.025	0.000	0.000	0.000	0.000
e	0.000	0.000	0.000	0.000	0.000	0.000	0.000	0.000	0.000	0.000	0.000	0.000	0.000	0.000	0.000
Ak															
(N)	6	9	12	5	2	5	3	1	1	6	9	24	5	11	5
a	1.000	1.000	0.708	1.000	0.750	1.000	1.000	1.000	1.000	1.000	1.000	1.000	1.000	0.909	1.000
b	0.000	0.000	0.000	0.000	0.000	0.000	0.000	0.000	0.000	0.000	0.000	0.000	0.000	0.000	0.000
c	0.000	0.000	0.292	0.000	0.250	0.000	0.000	0.000	0.000	0.000	0.000	0.000	0.000	0.000	0.000
d	0.000	0.000	0.000	0.000	0.000	0.000	0.000	0.000	0.000	0.000	0.000	0.000	0.000	0.091	0.000
Aph															
(N)	8	6	12	5	2	5	3	1	8	10	21	21	22	12	5
a	1.000	1.000	1.000	1.000	1.000	1.000	1.000	1.000	1.000	1.000	1.000	1.000	1.000	1.000	1.000
b	0.000	0.000	0.000	0.000	0.000	0.000	0.000	0.000	0.000	0.000	0.000	0.000	0.000	0.000	0.000
Est-3															
(N)	8	6	12	8	3	5	3	1	8	10	17	21	22	12	5
a	1.000	1.000	1.000	1.000	1.000	1.000	1.000	1.000	1.000	1.000	1.000	1.000	1.000	1.000	1.000
b	0.000	0.000	0.000	0.000	0.000	0.000	0.000	0.000	0.000	0.000	0.000	0.000	0.000	0.000	0.000
Gpi															
(N)	1	6	12	5	2	5	3	1	8	10	17	18	14	12	5
a	1.000	0.833	1.000	1.000	1.000	1.000	1.000	1.000	1.000	1.000	0.676	0.667	0.750	0.917	1.000
b	0.000	0.000	0.000	0.000	0.000	0.000	0.000	0.000	0.000	0.000	0.029	0.028	0.179	0.000	0.000
c	0.000	0.083	0.000	0.000	0.000	0.000	0.000	0.000	0.000	0.000	0.059	0.056	0.000	0.000	0.000
d	0.000	0.000	0.000	0.000	0.000	0.000	0.000	0.000	0.000	0.000	0.000	0.056	0.000	0.000	0.000
e	0.000	0.083	0.000	0.000	0.000	0.000	0.000	0.000	0.000	0.000	0.000	0.000	0.000	0.083	0.000
f	0.000	0.000	0.000	0.000	0.000	0.000	0.000	0.000	0.000	0.000	0.059	0.056	0.000	0.000	0.000
g	0.000	0.000	0.000	0.000	0.000	0.000	0.000	0.000	0.000	0.000	0.176	0.139	0.071	0.000	0.000
Hk															
(N)	6	3	1	3	1	1	1	1	10	16	9	7	13	1	1
a	1.000	1.000	1.000	1.000	1.000	1.000	1.000	1.000	1.000	1.000	1.000	1.000	1.000	1.000	1.000
b	0.000	0.000	0.000	0.000	0.000	0.000	0.000	0.000	0.000	0.000	0.000	0.000	0.000	0.000	0.000
c	0.000	0.000	0.000	0.000	0.000	0.000	0.000	0.000	0.000	0.000	0.000	0.000	0.000	0.000	0.000
Idh															
(N)	5	9	14	6	2	6	4	2	11	15	23	23	17	17	7
a	1.000	1.000	1.000	1.000	1.000	1.000	1.000	1.000	1.000	1.000	0.913	1.000	1.000	1.000	1.000
b	0.000	0.000	0.000	0.000	0.000	0.000	0.000	0.000	0.000	0.000	0.087	0.000	0.000	0.000	0.000
c	0.000	0.000	0.000	0.000	0.000	0.000	0.000	0.000	0.000	0.000	0.000	0.000	0.000	0.000	0.000
Lap															
(N)	1	1	12	6	2	4	3	1	10	10	21	16	13	12	5
a	1.000	1.000	0.917	0.833	0.750	0.500	0.500	0.000	0.500	1.000	1.000	0.906	0.962	0.958	1.000
b	0.000	0.000	0.000	0.167	0.250	0.000	0.500	1.000	0.500	0.000	0.000	0.000	0.038	0.042	0.000
c	0.000	0.000	0.083	0.000	0.000	0.000	0.000	0.000	0.000	0.000	0.000	0.000	0.000	0.000	0.000
d	0.000	0.000	0.000	0.000	0.000	0.500	0.000	0.000	0.000	0.000	0.000	0.000	0.000	0.000	0.000
e	0.000	0.000	0.000	0.000	0.000	0.000	0.000	0.000	0.000	0.000	0.000	0.094	0.000	0.000	0.000
f	0.000	0.000	0.000	0.000	0.000	0.000	0.000	0.000	0.000	0.000	0.000	0.000	0.000	0.000	0.000
g	0.000	0.000	0.000	0.000	0.000	0.000	0.000	0.000	0.000	0.000	0.000	0.000	0.000	0.000	0.000
Ldh															
(N)	6	9	12	9	3	4	3	2	10	6	24	25	10	12	5
a	1.000	1.000	1.000	1.000	1.000	1.000	1.000	1.000	1.000	1.000	1.000	1.000	1.000	1.000	1.000
b	0.000	0.000	0.000	0.000	0.000	0.000	0.000	0.000	0.000	0.000	0.000	0.000	0.000	0.000	0.000
c	0.000	0.000	0.000	0.000	0.000	0.000	0.000	0.000	0.000	0.000	0.000	0.000	0.000	0.000	0.000
d	0.000	0.000	0.000	0.000	0.000	0.000	0.000	0.000	0.000	0.000	0.000	0.000	0.000	0.000	0.000

(*continued*)

inata at locs. 713, 715 and 716; (3) the c-allele of the *Ak* locus in *A. s. senilis* at locs. 756 and 707 and in *A. j. jonica* at loc. 708; (4) the b-allele of *Aat-1* in *A. c. liebetruti* at loc. 746, in *A. c. incommoda* at loc. 773 and in all Ithakian populations (Table 5). Therefore, a Hennigian phylogenetic analysis has also been performed on data in which the alleles probably acquired by introgression were removed. This, however, did not result in an obvious improvement of the analyses.

DISCUSSION

General

There is still much debate on the relevance of various algorithms determining genetic distance coefficients and the combination of these coefficients with clustering methods (Nei et al., 1983; Buth, 1984; Richardson et al., 1986; Emberton, 1988; Ferguson, 1988). For a phenetic comparison of the allozyme

TABLE 3. (Continued)

Locus	inc 723	adr 725	inc 727	adr 728	adr 729	adr 730	dub 731	sxd 732	sxd 733	fla 734	con 735	kol 736	ass 742	ass 744	lie 746
							Population								
Mdh-1															
(N)	6	9	14	8	3	7	4	1	9	6	19	29	1	17	7
a	0.000	0.000	0.000	1.000	1.000	0.000	1.000	0.000	0.000	0.167	1.000	0.931	1.000	0.000	0.857
b	0.750	1.000	1.000	0.000	0.000	1.000	0.000	1.000	1.000	0.583	0.000	0.017	0.000	1.000	0.143
c	0.000	0.000	0.000	0.000	0.000	0.000	0.000	0.000	0.000	0.000	0.000	0.000	0.000	0.000	0.000
d	0.000	0.000	0.000	0.000	0.000	0.000	0.000	0.000	0.000	0.000	0.000	0.017	0.000	0.000	0.000
e	0.250	0.000	0.000	0.000	0.000	0.000	0.000	0.000	0.000	0.083	0.000	0.000	0.000	0.000	0.000
f	0.000	0.000	0.000	0.000	0.000	0.000	0.000	0.000	0.000	0.167	0.000	0.034	0.000	0.000	0.000
Mdh-2															
(N)	6	9	14	8	3	7	4	1	9	6	20	29	2	17	7
a	1.000	0.889	1.000	0.063	0.000	0.786	0.250	1.000	1.000	1.000	1.000	0.897	1.000	0.676	1.000
b	0.000	0.111	0.000	0.000	0.000	0.214	0.000	0.000	0.000	0.000	0.000	0.103	0.000	0.324	0.000
c	0.000	0.000	0.000	0.000	0.000	0.000	0.000	0.000	0.000	0.000	0.000	0.000	0.000	0.000	0.000
d	0.000	0.000	0.000	0.938	1.000	0.000	0.750	0.000	0.000	0.000	0.000	0.000	0.000	0.000	0.000
Mpi															
(N)	1	6	12	6	2	4	3	2	10	1	23	15	14	12	5
a	1.000	1.000	0.958	1.000	1.000	1.000	1.000	0.750	1.000	1.000	1.000	1.000	1.000	1.000	0.700
b	0.000	0.000	0.042	0.000	0.000	0.000	0.000	0.250	0.000	0.000	0.000	0.000	0.000	0.000	0.000
c	0.000	0.000	0.000	0.000	0.000	0.000	0.000	0.000	0.000	0.000	0.000	0.000	0.000	0.000	0.300
d	0.000	0.000	0.000	0.000	0.000	0.000	0.000	0.000	0.000	0.000	0.000	0.000	0.000	0.000	0.000
Nadd-1															
(N)	14	9	14	8	3	7	4	1	9	16	18	26	22	17	7
a	0.929	0.611	1.000	1.000	0.667	1.000	1.000	1.000	1.000	1.000	0.917	1.000	1.000	1.000	0.929
b	0.000	0.000	0.000	0.000	0.000	0.000	0.000	0.000	0.000	0.000	0.000	0.000	0.000	0.000	0.000
c	0.036	0.167	0.000	0.000	0.167	0.000	0.000	0.000	0.000	0.000	0.000	0.000	0.000	0.000	0.000
d	0.036	0.111	0.000	0.000	0.167	0.000	0.000	0.000	0.000	0.000	0.000	0.000	0.000	0.000	0.000
e	0.000	0.000	0.000	0.000	0.000	0.000	0.000	0.000	0.000	0.000	0.083	0.000	0.000	0.000	0.000
f	0.000	0.111	0.000	0.000	0.000	0.000	0.000	0.000	0.000	0.000	0.000	0.000	0.000	0.000	0.000
g	0.000	0.000	0.000	0.000	0.000	0.000	0.000	0.000	0.000	0.000	0.000	0.000	0.000	0.000	0.071
Nadd-2															
(N)	14	9	14	8	3	7	4	1	9	15	15	23	22	17	7
a	1.000	1.000	1.000	0.813	1.000	1.000	1.000	1.000	1.000	1.000	1.000	1.000	1.000	1.000	1.000
b	0.000	0.000	0.000	0.188	0.000	0.000	0.000	0.000	0.000	0.000	0.000	0.000	0.000	0.000	0.000
Pgd															
(N)	6	9	14	9	3	6	4	2	11	16	24	23	17	4	2
a	1.000	0.944	1.000	1.000	1.000	1.000	1.000	1.000	1.000	1.000	1.000	1.000	1.000	1.000	1.000
b	0.000	0.056	0.000	0.000	0.000	0.000	0.000	0.000	0.000	0.000	0.000	0.000	0.000	0.000	0.000
c	0.000	0.000	0.000	0.000	0.000	0.000	0.000	0.000	0.000	0.000	0.000	0.000	0.000	0.000	0.000
Pgm															
(N)	6	9	14	3	3	2	4	1	9	16	20	17	14	5	2
a	1.000	1.000	1.000	1.000	1.000	1.000	1.000	1.000	1.000	1.000	1.000	0.971	1.000	1.000	1.000
b	0.000	0.000	0.000	0.000	0.000	0.000	0.000	0.000	0.000	0.000	0.000	0.029	0.000	0.000	0.000
c	0.000	0.000	0.000	0.000	0.000	0.000	0.000	0.000	0.000	0.000	0.000	0.000	0.000	0.000	0.000
Aat-1															
(N)	9	6	9	9	12	16	19	6	12	8	13	15	18	17	13
a	1.000	1.000	1.000	1.000	1.000	1.000	1.000	1.000	1.000	1.000	0.846	1.000	0.944	1.000	0.692
b	0.000	0.000	0.000	0.000	0.000	0.000	0.000	0.000	0.000	0.000	0.000	0.000	0.000	0.000	0.269
c	0.000	0.000	0.000	0.000	0.000	0.000	0.000	0.000	0.000	0.000	0.000	0.000	0.056	0.000	0.000
d	0.000	0.000	0.000	0.000	0.000	0.000	0.000	0.000	0.000	0.000	0.000	0.000	0.000	0.000	0.000
e	0.000	0.000	0.000	0.000	0.000	0.000	0.000	0.000	0.000	0.000	0.154	0.000	0.000	0.000	0.038
Ak															
(N)	9	6	9	3	3	6	8	4	11	8	8	6	1	1	16
a	1.000	1.000	1.000	1.000	1.000	1.000	1.000	1.000	1.000	1.000	1.000	1.000	1.000	1.000	1.000
b	0.000	0.000	0.000	0.000	0.000	0.000	0.000	0.000	0.000	0.000	0.000	0.000	0.000	0.000	0.000
c	0.000	0.000	0.000	0.000	0.000	0.000	0.000	0.000	0.000	0.000	0.000	0.000	0.000	0.000	0.000
d	0.000	0.000	0.000	0.000	0.000	0.000	0.000	0.000	0.000	0.000	0.000	0.000	0.000	0.000	0.000
Aph															
(N)	6	8	9	5	10	10	14	4	11	1	10	8	9	10	10
a	1.000	1.000	1.000	1.000	1.000	1.000	1.000	1.000	1.000	1.000	1.000	1.000	1.000	1.000	1.000
b	0.000	0.000	0.000	0.000	0.000	0.000	0.000	0.000	0.000	0.000	0.000	0.000	0.000	0.000	0.000

(*continued*)

data, we have chosen the well known Nei's Genetic Distance (D). This index measures the mean number of electrophoretically detectable substitutions per locus, which accumulated because the two populations diverged from a common ancestor (Buth, 1984). Nei's D might also enable assumptions concerning the period of time after the taxa evolved from their most recent common ancestor, presuming that constant rates of evolution occur within the lineages. No agreement exists, however, on the translation of genetic distances into time-spans (Richardson et al., 1986). After a comparison of

TABLE 3. (Continued)

Est-3															
(N)	9	8	9	1	10	10	6	4	11	1	10	8	16	18	18
a	1.000	1.000	1.000	1.000	1.000	1.000	1.000	1.000	1.000	1.000	1.000	1.000	1.000	1.000	1.000
b	0.000	0.000	0.000	0.000	0.000	0.000	0.000	0.000	0.000	0.000	0.000	0.000	0.000	0.000	0.000
Gpi															
(N)	6	6	9	3	13	16	8	4	11	1	10	8	10	10	10
a	1.000	1.000	1.000	1.000	1.000	0.969	1.000	1.000	0.909	1.000	1.000	0.938	1.000	1.000	1.000
b	0.000	0.000	0.000	0.000	0.000	0.031	0.000	0.000	0.000	0.000	0.000	0.000	0.000	0.000	0.000
c	0.000	0.000	0.000	0.000	0.000	0.000	0.000	0.000	0.000	0.000	0.000	0.000	0.000	0.000	0.000
d	0.000	0.000	0.000	0.000	0.000	0.000	0.000	0.000	0.000	0.000	0.000	0.000	0.000	0.000	0.000
e	0.000	0.000	0.000	0.000	0.000	0.000	0.000	0.000	0.091	0.000	0.000	0.063	0.000	0.000	0.000
f	0.000	0.000	0.000	0.000	0.000	0.000	0.000	0.000	0.000	0.000	0.000	0.000	0.000	0.000	0.000
g	0.000	0.000	0.000	0.000	0.000	0.000	0.000	0.000	0.000	0.000	0.000	0.000	0.000	0.000	0.000
Hk															
(N)	6	6	9	3	12	16	2	1	1	8	13	15	18	8	12
a	1.000	1.000	1.000	1.000	1.000	1.000	1.000	1.000	1.000	1.000	1.000	1.000	1.000	1.000	1.000
b	0.000	0.000	0.000	0.000	0.000	0.000	0.000	0.000	0.000	0.000	0.000	0.000	0.000	0.000	0.000
c	0.000	0.000	0.000	0.000	0.000	0.000	0.000	0.000	0.000	0.000	0.000	0.000	0.000	0.000	0.000
Idh															
(N)	9	1	10	6	9	10	17	8	14	10	13	15	9	10	16
a	1.000	1.000	1.000	1.000	1.000	1.000	1.000	1.000	1.000	0.950	1.000	0.867	1.000	1.000	1.000
b	0.000	0.000	0.000	0.000	0.000	0.000	0.000	0.000	0.000	0.050	0.000	0.133	0.000	0.000	0.000
c	0.000	0.000	0.000	0.000	0.000	0.000	0.000	0.000	0.000	0.000	0.000	0.000	0.000	0.000	0.000
Lap															
(N)	6	1	8	1	9	10	2	6	1	1	10	9	10	10	10
a	0.750	1.000	0.813	1.000	1.000	1.000	1.000	0.917	1.000	1.000	1.000	0.889	1.000	1.000	1.000
b	0.250	0.000	0.000	0.000	0.000	0.000	0.000	0.083	0.000	0.000	0.000	0.111	0.000	0.000	0.000
c	0.000	0.000	0.000	0.000	0.000	0.000	0.000	0.000	0.000	0.000	0.000	0.000	0.000	0.000	0.000
d	0.000	0.000	0.000	0.000	0.000	0.000	0.000	0.000	0.000	0.000	0.000	0.000	0.000	0.000	0.000
e	0.000	0.000	0.000	0.000	0.000	0.000	0.000	0.000	0.000	0.000	0.000	0.000	0.000	0.000	0.000
f	0.000	0.000	0.000	0.000	0.000	0.000	0.000	0.000	0.000	0.000	0.000	0.000	0.000	0.000	0.000
g	0.000	0.000	0.188	0.000	0.000	0.000	0.000	0.000	0.000	0.000	0.000	0.000	0.000	0.000	0.000
Ldh															
(N)	9	6	9	9	12	6	19	6	12	1	13	9	17	8	18
a	1.000	1.000	1.000	1.000	1.000	1.000	1.000	1.000	1.000	1.000	1.000	1.000	1.000	1.000	1.000
b	0.000	0.000	0.000	0.000	0.000	0.000	0.000	0.000	0.000	0.000	0.000	0.000	0.000	0.000	0.000
c	0.000	0.000	0.000	0.000	0.000	0.000	0.000	0.000	0.000	0.000	0.000	0.000	0.000	0.000	0.000
d	0.000	0.000	0.000	0.000	0.000	0.000	0.000	0.000	0.000	0.000	0.000	0.000	0.000	0.000	0.000
Mdh-1															
(N)	9	6	10	8	13	6	16	6	13	10	13	14	9	8	8
a	0.944	0.000	1.000	0.000	0.000	0.000	0.000	0.000	0.000	0.000	1.000	0.000	0.000	0.000	1.000
b	0.056	0.000	0.000	0.000	0.000	0.000	1.000	0.917	1.000	1.000	0.000	1.000	1.000	1.000	0.000
c	0.000	0.000	0.000	0.000	0.000	0.000	0.000	0.000	0.000	0.000	0.000	0.000	0.000	0.000	0.000
d	0.000	1.000	0.000	1.000	1.000	1.000	0.000	0.000	0.000	0.000	0.000	0.000	0.000	0.000	0.000
e	0.000	0.000	0.000	0.000	0.000	0.000	0.000	0.000	0.000	0.000	0.000	0.000	0.000	0.000	0.000
f	0.000	0.000	0.000	0.000	0.000	0.000	0.000	0.083	0.000	0.000	0.000	0.000	0.000	0.000	0.000
Mdh-2															
(N)	9	6	10	8	13	6	16	6	13	10	13	14	9	8	8
a	1.000	1.000	1.000	1.000	1.000	1.000	0.000	0.750	0.846	1.000	0.846	1.000	0.222	0.250	1.000
b	0.000	0.000	0.000	0.000	0.000	0.000	0.000	0.250	0.154	0.000	0.154	0.000	0.000	0.000	0.000
c	0.000	0.000	0.000	0.000	0.000	0.000	1.000	0.000	0.000	0.000	0.000	0.000	0.000	0.000	0.000
d	0.000	0.000	0.000	0.000	0.000	0.000	0.000	0.000	0.000	0.000	0.000	0.000	0.778	0.750	0.000
Mpi															
(N)	3	6	9	9	12	6	19	6	12	1	10	9	9	10	10
a	1.000	1.000	1.000	1.000	1.000	1.000	1.000	0.333	1.000	1.000	1.000	1.000	1.000	1.000	1.000
b	0.000	0.000	0.000	0.000	0.000	0.000	0.000	0.000	0.000	0.000	0.000	0.000	0.000	0.000	0.000
c	0.000	0.000	0.000	0.000	0.000	0.000	0.000	0.667	0.000	0.000	0.000	0.000	0.000	0.000	0.000
d	0.000	0.000	0.000	0.000	0.000	0.000	0.000	0.000	0.000	0.000	0.000	0.000	0.000	0.000	0.000
Nadd-1															
(N)	9	14	10	8	13	16	16	6	13	10	13	6	18	18	18
a	1.000	1.000	0.950	1.000	1.000	1.000	1.000	1.000	0.500	1.000	1.000	1.000	0.972	0.944	1.000
b	0.000	0.000	0.000	0.000	0.000	0.000	0.000	0.000	0.000	0.000	0.000	0.000	0.000	0.000	0.000
c	0.000	0.000	0.000	0.000	0.000	0.000	0.000	0.000	0.000	0.000	0.000	0.000	0.028	0.000	0.000
d	0.000	0.000	0.000	0.000	0.000	0.000	0.000	0.000	0.500	0.000	0.000	0.000	0.000	0.056	0.000
e	0.000	0.000	0.000	0.000	0.000	0.000	0.000	0.000	0.000	0.000	0.000	0.000	0.000	0.000	0.000
f	0.000	0.000	0.000	0.000	0.000	0.000	0.000	0.000	0.000	0.000	0.000	0.000	0.000	0.000	0.000
g	0.000	0.000	0.050	0.000	0.000	0.000	0.000	0.000	0.000	0.000	0.000	0.000	0.000	0.000	0.000

(*continued*)

various combinations of genetic coefficients and clustering methods, Nei et al. (1983) concluded that Nei's D in combination with an UPGMA is the best choice for phylogenetic analysis. However, a phylogenetic interpretation of the Nei's D dendrograms is seriously affected by (a) the failure of Nei's D to satisfy the triangle of equality, which may result in biologically impossible negative branch-lengths, and (b) the fact that the dendrograms only show phenetic similarity or dissimilarity. Rogers' R (1972) meets the metrical requirements, which is therefore also applied in combination with UPGMA cluster analyses.

TABLE 3. (Continued)

Locus	Population														
	con 749	fla 751	sen 752	sen 756	con 759	ody 764	ody 765	ody 766	ody 770	inc 772	inc 773	ter	reb	Isa	par
Nadd-2															
(N)	3	14	10	8	13	16	16	6	13	10	13	14	18	18	6
a	1.000	1.000	1.000	1.000	1.000	1.000	1.000	1.000	1.000	1.000	1.000	1.000	1.000	1.000	1.000
b	0.000	0.000	0.000	0.000	0.000	0.000	0.000	0.000	0.000	0.000	0.000	0.000	0.000	0.000	0.000
Pgd															
(N)	9	1	10	6	7	10	17	2	14	2	13	9	17	18	18
a	1.000	1.000	1.000	1.000	1.000	1.000	1.000	1.000	1.000	1.000	1.000	1.000	1.000	1.000	1.000
b	0.000	0.000	0.000	0.000	0.000	0.000	0.000	0.000	0.000	0.000	0.000	0.000	0.000	0.000	0.000
c	0.000	0.000	0.000	0.000	0.000	0.000	0.000	0.000	0.000	0.000	0.000	0.000	0.000	0.000	0.000
Pgm															
(N)	6	1	10	5	10	10	14	2	13	2	13	8	18	18	12
a	1.000	1.000	1.000	1.000	1.000	1.000	1.000	1.000	1.000	1.000	1.000	1.000	1.000	1.000	1.000
b	0.000	0.000	0.000	0.000	0.000	0.000	0.000	0.000	0.000	0.000	0.000	0.000	0.000	0.000	0.000
c	0.000	0.000	0.000	0.000	0.000	0.000	0.000	0.000	0.000	0.000	0.000	0.000	0.000	0.000	0.000
Aat-1															
(N)	8	17	11	15	8	12	13	13	12	1	4	8	12	20	20
a	1.000	0.735	0.227	1.000	0.938	0.000	0.000	0.000	0.583	1.000	0.625	0.000	0.750	0.000	1.000
b	0.000	0.000	0.773	0.000	0.000	1.000	0.962	1.000	0.417	0.000	0.375	1.000	0.250	1.000	0.000
c	0.000	0.265	0.000	0.000	0.000	0.000	0.000	0.000	0.000	0.000	0.000	0.000	0.000	0.000	0.000
d	0.000	0.000	0.000	0.000	0.000	0.000	0.038	0.000	0.000	0.000	0.000	0.000	0.000	0.000	0.000
e	0.000	0.000	0.000	0.000	0.063	0.000	0.000	0.000	0.000	0.000	0.000	0.000	0.000	0.000	0.000
Ak															
(N)	12	7	3	15	3	11	13	13	11	1	11	4	5	12	12
a	1.000	1.000	1.000	0.767	1.000	1.000	1.000	1.000	1.000	1.000	1.000	1.000	1.000	1.000	1.000
b	0.000	0.000	0.000	0.000	0.000	0.000	0.000	0.000	0.000	0.000	0.000	0.000	0.000	0.000	0.000
c	0.000	0.000	0.000	0.033	0.000	0.000	0.000	0.000	0.000	0.000	0.000	0.000	0.000	0.000	0.000
d	0.000	0.000	0.000	0.200	0.000	0.000	0.000	0.000	0.000	0.000	0.000	0.000	0.000	0.000	0.000
Aph															
(N)	12	10	10	12	4	6	10	10	10	1	13	8	13	8	8
a	1.000	1.000	1.000	1.000	1.000	1.000	1.000	0.000	1.000	1.000	1.000	1.000	1.000	1.000	1.000
b	0.000	0.000	0.000	0.000	0.000	0.000	0.000	1.000	0.000	0.000	0.000	0.000	0.000	0.000	0.000
Est-3															
(N)	16	10	10	12	3	12	13	13	15	1	13	8	13	20	20
a	1.000	1.000	1.000	1.000	1.000	1.000	1.000	1.000	1.000	1.000	1.000	1.000	0.154	0.400	0.750
b	0.000	0.000	0.000	0.000	0.000	0.000	0.000	0.000	0.000	0.000	0.000	0.000	0.846	0.600	0.250
Gpi															
(N)	12	10	10	12	4	6	10	10	10	1	10	4	10	13	12
a	1.000	1.000	1.000	0.833	1.000	1.000	1.000	1.000	1.000	1.000	1.000	1.000	1.000	1.000	1.000
b	0.000	0.000	0.000	0.083	0.000	0.000	0.000	0.000	0.000	0.000	0.000	0.000	0.000	0.000	0.000
c	0.000	0.000	0.000	0.042	0.000	0.000	0.000	0.000	0.000	0.000	0.000	0.000	0.000	0.000	0.000
d	0.000	0.000	0.000	0.042	0.000	0.000	0.000	0.000	0.000	0.000	0.000	0.000	0.000	0.000	0.000
e	0.000	0.000	0.000	0.000	0.000	0.000	0.000	0.000	0.000	0.000	0.000	0.000	0.000	0.000	0.000
f	0.000	0.000	0.000	0.000	0.000	0.000	0.000	0.000	0.000	0.000	0.000	0.000	0.000	0.000	0.000
g	0.000	0.000	0.000	0.000	0.000	0.000	0.000	0.000	0.000	0.000	0.000	0.000	0.000	0.000	0.000
Hk															
(N)	4	17	12	3	8	7	10	10	10	1	1	4	10	1	1
a	1.000	1.000	1.000	1.000	1.000	1.000	1.000	1.000	1.000	1.000	1.000	0.000	1.000	1.000	1.000
b	0.000	0.000	0.000	0.000	0.000	0.000	0.000	0.000	0.000	0.000	0.000	0.750	0.000	0.000	0.000
c	0.000	0.000	0.000	0.000	0.000	0.000	0.000	0.000	0.000	0.000	0.000	0.250	0.000	0.000	0.000
Idh															
(N)	11	17	12	15	8	11	13	13	15	4	11	4	10	12	12
a	1.000	1.000	1.000	1.000	1.000	1.000	1.000	1.000	1.000	1.000	1.000	1.000	0.000	1.000	0.000
b	0.000	0.000	0.000	0.000	0.000	0.000	0.000	0.000	0.000	0.000	0.000	0.000	1.000	0.000	0.000
c	0.000	0.000	0.000	0.000	0.000	0.000	0.000	0.000	0.000	0.000	0.000	0.000	0.000	0.000	1.000
Lap															
(N)	11	10	9	12	5	1	10	10	10	1	10	4	10	12	12
a	1.000	0.950	0.833	0.750	1.000	1.000	1.000	0.950	0.900	1.000	1.000	1.000	0.000	0.000	1.000
b	0.000	0.000	0.167	0.167	0.000	0.000	0.000	0.050	0.100	0.000	0.000	0.000	0.000	1.000	0.000
c	0.000	0.000	0.000	0.000	0.000	0.000	0.000	0.000	0.000	0.000	0.000	0.000	0.000	0.000	0.000
d	0.000	0.000	0.000	0.083	0.000	0.000	0.000	0.000	0.000	0.000	0.000	0.000	1.000	0.000	0.000
e	0.000	0.000	0.000	0.000	0.000	0.000	0.000	0.000	0.000	0.000	0.000	0.000	0.000	0.000	0.000
f	0.000	0.050	0.000	0.000	0.000	0.000	0.000	0.000	0.000	0.000	0.000	0.000	0.000	0.000	0.000
g	0.000	0.000	0.000	0.000	0.000	0.000	0.000	0.000	0.000	0.000	0.000	0.000	0.000	0.000	0.000

(*continued*)

The percentages of polymorphic loci per population (Pp) (Table 2) are generally below the values given by Nevo (1978: 126) for other stylommatophoran gastropods. The average Pp of Kephallinian and Ithakian *Albinaria* taxa is 7.5% (± 4.9%). Nevo listed mean estimates of polymorphism which range from 6% to 100% with an average of 31.5% (± 26.6%) (excluding *Rumina decollata*). However, it is not clear from his data what is

TABLE 3. (Continued)

Ldh															
(N)	15	10	12	15	5	11	13	13	15	1	13	8	13	20	20
a	1.000	1.000	1.000	1.000	1.000	1.000	1.000	0.885	0.933	1.000	1.000	0.000	0.000	1.000	1.000
b	0.000	0.000	0.000	0.000	0.000	0.000	0.000	0.000	0.000	0.000	0.000	1.000	1.000	0.000	0.000
c	0.000	0.000	0.000	0.000	0.000	0.000	0.000	0.115	0.000	0.000	0.000	0.000	0.000	0.000	0.000
d	0.000	0.000	0.000	0.000	0.000	0.000	0.000	0.000	0.067	0.000	0.000	0.000	0.000	0.000	0.000
Mdh-1															
(N)	16	7	13	15	6	5	13	13	5	4	13	8	3	20	18
a	1.000	0.000	0.000	0.000	1.000	1.000	1.000	1.000	1.000	1.000	1.000	0.000	0.000	0.000	0.000
b	0.000	1.000	1.000	1.000	0.000	0.000	0.000	0.000	0.000	0.000	0.000	0.000	0.000	0.000	0.000
c	0.000	0.000	0.000	0.000	0.000	0.000	0.000	0.000	0.000	0.000	0.000	1.000	1.000	1.000	1.000
d	0.000	0.000	0.000	0.000	0.000	0.000	0.000	0.000	0.000	0.000	0.000	0.000	0.000	0.000	0.000
e	0.000	0.000	0.000	0.000	0.000	0.000	0.000	0.000	0.000	0.000	0.000	0.000	0.000	0.000	0.000
f	0.000	0.000	0.000	0.000	0.000	0.000	0.000	0.000	0.000	0.000	0.000	0.000	0.000	0.000	0.000
Mdh-2															
(N)	16	7	13	15	6	5	13	13	5	4	13	8	3	20	20
a	1.000	0.500	1.000	1.000	1.000	0.800	0.154	0.192	0.000	1.000	1.000	0.000	0.000	0.000	0.000
b	0.000	0.429	0.000	0.000	0.000	0.000	0.000	0.000	0.000	0.000	0.000	0.000	0.000	0.000	0.000
c	0.000	0.000	0.000	0.000	0.000	0.200	0.846	0.808	1.000	0.000	0.000	1.000	1.000	1.000	1.000
d	0.000	0.071	0.000	0.000	0.000	0.000	0.000	0.000	0.000	0.000	0.000	0.000	0.000	0.000	0.000
Mpi															
(N)	11	10	9	12	5	6	10	10	10	1	11	4	10	12	12
a	1.000	1.000	1.000	0.958	1.000	1.000	1.000	1.000	1.000	1.000	1.000	1.000	1.000	1.000	0.000
b	0.000	0.000	0.000	0.000	0.000	0.000	0.000	0.000	0.000	0.000	0.000	0.000	0.000	0.000	1.000
c	0.000	0.000	0.000	0.000	0.000	0.000	0.000	0.000	0.000	0.000	0.000	0.000	0.000	0.000	0.000
d	0.000	0.000	0.000	0.042	0.000	0.000	0.000	0.000	0.000	0.000	0.000	0.000	0.000	0.000	0.000
Nadd-1															
(N)	16	17	3	15	7	11	13	13	15	4	13	4	13	20	20
a	1.000	1.000	1.000	1.000	1.000	1.000	1.000	1.000	1.000	1.000	1.000	1.000	1.000	1.000	0.000
b	0.000	0.000	0.000	0.000	0.000	0.000	0.000	0.000	0.000	0.000	0.000	0.000	0.000	0.000	1.000
c	0.000	0.000	0.000	0.000	0.000	0.000	0.000	0.000	0.000	0.000	0.000	0.000	0.000	0.000	0.000
d	0.000	0.000	0.000	0.000	0.000	0.000	0.000	0.000	0.000	0.000	0.000	0.000	0.000	0.000	0.000
e	0.000	0.000	0.000	0.000	0.000	0.000	0.000	0.000	0.000	0.000	0.000	0.000	0.000	0.000	0.000
f	0.000	0.000	0.000	0.000	0.000	0.000	0.000	0.000	0.000	0.000	0.000	0.000	0.000	0.000	0.000
g	0.000	0.000	0.000	0.000	0.000	0.000	0.000	0.000	0.000	0.000	0.000	0.000	0.000	0.000	0.000
Nadd-2															
(N)	16	17	13	15	7	11	13	13	5	4	13	4	13	20	20
a	1.000	1.000	1.000	1.000	1.000	1.000	1.000	1.000	1.000	1.000	1.000	1.000	1.000	1.000	1.000
b	0.000	0.000	0.000	0.000	0.000	0.000	0.000	0.000	0.000	0.000	0.000	0.000	0.000	0.000	0.000
Pgd															
(N)	15	10	12	15	5	11	13	13	15	4	13	8	13	20	20
a	1.000	1.000	1.000	0.500	0.900	1.000	1.000	1.000	1.000	1.000	1.000	1.000	1.000	1.000	1.000
b	0.000	0.000	0.000	0.500	0.000	0.000	0.000	0.000	0.000	0.000	0.000	0.000	0.000	0.000	0.000
c	0.000	0.000	0.000	0.000	0.100	0.000	0.000	0.000	0.000	0.000	0.000	0.000	0.000	0.000	0.000
Pgm															
(N)	16	10	13	3	4	6	10	10	10	4	13	8	13	20	20
a	1.000	1.000	0.769	1.000	1.000	1.000	1.000	1.000	1.000	1.000	1.000	1.000	1.000	1.000	0.025
b	0.000	0.000	0.192	0.000	0.000	0.000	0.000	0.000	0.000	0.000	0.000	0.000	0.000	0.000	0.975
c	0.000	0.000	0.038	0.000	0.000	0.000	0.000	0.000	0.000	0.000	0.000	0.000	0.000	0.000	0.000

meant by a population. According to our findings, the genetic variability depends on the extent of the area which is considered to be inhabited by a single population (Fig. 3). It is uncertain, therefore, whether Nevo's P values are comparable with our averaged Pp values for each taxon.

Detailed results on mobility, dispersion and homing in *Albinaria* are not yet available. However, we have observed individuals moving on rockfaces for at least one meter during a single rainy night. Baur (1988) found in bedrock-inhabiting *Chondrina clienta* (Westerlund), on the island of Öland, Sweden, an average distance of 291 cm was bridged during six months, with a maximum of 814 cm. Except for the more temporate climate to which *Chondrina clienta* is confined, this species is very well comparable with *Albinaria* species in habitat preferences (Gittenberger, pers. com.). In view of these data, and because our samples are collected from an area limited to 1 to 20 m^2 of substratum, each sample is considered to belong to a panmictic population.

Genetic differences within a subspecies proved to be present within distances less than 200 m, for example in *A. j. assicola* at locs. 744 and 742, in *A. s. senilis* and in *A. j. jonica* at locs. 707 and 708, as well as in *A. c. contaminata* at locs. 713, 715 and 716. Nevo's (1978: 126) values for populations are approximately of the same magnitude as what we find within some whole subspecies (Pt = of all populations together), namely, 32.1% for *A. c. contaminata,* 17.9% for *A. c. odysseus,* but only 3.6% for *A. c. liebetruti* and *A. a. adrianae.* In *A. s. senilis,* we looked separately at the central west coast range

TABLE 4. Matrix of genetic distance coefficients: above diagonal Roger's R, below diagonal Nei's D.

Subspecies	1	2	3	4	5	6	7	8	9	10	11	12	13	14	15
1 senilis	*****	0.028	0.026	0.058	0.053	0.062	0.115	0.087	0.046	0.058	0.056	0.187	0.220	0.165	0.235
2 flavescens	0.003	*****	0.023	0.054	0.052	0.054	0.102	0.089	0.033	0.052	0.041	0.171	0.212	0.158	0.227
3 kolpomyrtensis	0.002	0.004	*****	0.051	0.047	0.057	0.114	0.090	0.041	0.046	0.047	0.186	0.213	0.167	0.226
4 contaminata	0.037	0.039	0.038	*****	0.015	0.021	0.077	0.058	0.071	0.046	0.079	0.181	0.221	0.169	0.228
5 incommoda	0.036	0.039	0.037	0.001	*****	0.013	0.070	0.051	0.069	0.042	0.077	0.177	0.214	0.159	0.228
6 liebetruti	0.039	0.041	0.042	0.004	0.002	*****	0.061	0.061	0.074	0.047	0.082	0.165	0.211	0.154	0.233
7 odysseus	0.085	0.083	0.093	0.051	0.049	0.037	*****	0.088	0.108	0.107	0.088	0.128	0.211	0.116	0.239
8 jonica	0.071	0.069	0.075	0.035	0.036	0.040	0.062	*****	0.059	0.087	0.088	0.191	0.224	0.167	0.234
9 assicola	0.022	0.017	0.023	0.058	0.059	0.062	0.091	0.041	*****	0.066	0.035	0.172	0.215	0.162	0.219
10 adrianae	0.038	0.040	0.038	0.037	0.037	0.040	0.091	0.074	0.059	*****	0.072	0.176	0.218	0.165	0.223
11 dubia	0.036	0.032	0.038	0.073	0.074	0.078	0.070	0.076	0.030	0.074	*****	0.139	0.182	0.129	0.187
12 teres	0.184	0.179	0.194	0.189	0.186	0.170	0.114	0.194	0.183	0.190	0.147	*****	0.161	0.125	0.255
13 rebeli	0.225	0.226	0.221	0.232	0.229	0.234	0.210	0.231	0.228	0.234	0.189	0.161	*****	0.143	0.244
14 Isabellaria sp.	0.151	0.158	0.165	0.168	0.159	0.151	0.093	0.159	0.164	0.171	0.129	0.122	0.142	*****	0.226
15 Albinaria sp.	0.242	0.241	0.242	0.243	0.245	0.250	0.244	0.245	0.236	0.244	0.199	0.284	0.264	0.249	*****

populations (locs. 702, 706–708, 710 and 712), which resulted in a Pt of 32.1%. Taking all *A. s. senilis* material into account (thus including 719, 752 and 756) leads to only a very slight increase of Pt to 35%. The wide range of the Pt values for the various taxa is to a certain extent due to differences in the number of populations that could be investigated (Table 2). A percentage of 3.6 in *A. c. liebetruti* is based on a single population. In fact, this value cannot be compared with, for example, 32.1% in *A. s. senilis,* because the latter number is based on six populations. As is obvious from Table 2, the range of variation of species and subspecies is not reached in a single population. This cannot be a consequence of simply a larger number of specimens that is studied when more populations are investigated. Figure 4 shows that there is, except for *A. contaminata,* only a small trend towards an increasing P at populations with higher numbers of analysed individuals. According to the results presented in Figure 3, a minimal number of populations is needed to reach a point where the addition of more populations contributes relatively little to the genetic variability. In case of *A. s. senilis,* this number is five populations, whereas in case of *A. c. contaminata* it is at least more than six populations. This indicates that for *A. c. contaminata* the total variation has not yet been established. It is concluded that there can be important differences in genetic variability throughout the range of *Albinaria* subspecies, which recommends, at least in the case of subspecies with large ranges, the use of minimally six populations. Because of the lack of a sufficient amount of living material, we were not able to investigate equal numbers of individuals per population and six or more populations for all taxa.

Nevo (1978) investigated the correlation between several biological parameters and the genetic variability observed in over 200 species of plants and animals. Some of his parameters are briefly discussed here.

One might expect that the genetic variability depends on the mode of reproduction. In our material, there is a considerable deficiency of heterozygosity in most populations (Table 2). This pattern has also been found in other hermaphroditic Mollusca (Selander & Kaufman, 1973; Nevo, 1978; Hillis et al., 1987; Boato, 1988). A deficiency of heterozygosity and a low proportion of polymorphic loci are considered indicative of a breeding system with incomplete panmixia. It has been reported that a complete or near absence of genetic variability within populations may occur in facultative self-fertilizing breeding systems, as is known, for example, for *Rumina decollata* (see Selander & Kaufman, 1973), *Partula gibba* (see Johnson et al., 1977) and some *Arion* species (see McCracken & Selander, 1980). The fact that most populations of *A. adrianae* proved to be invariable (Table

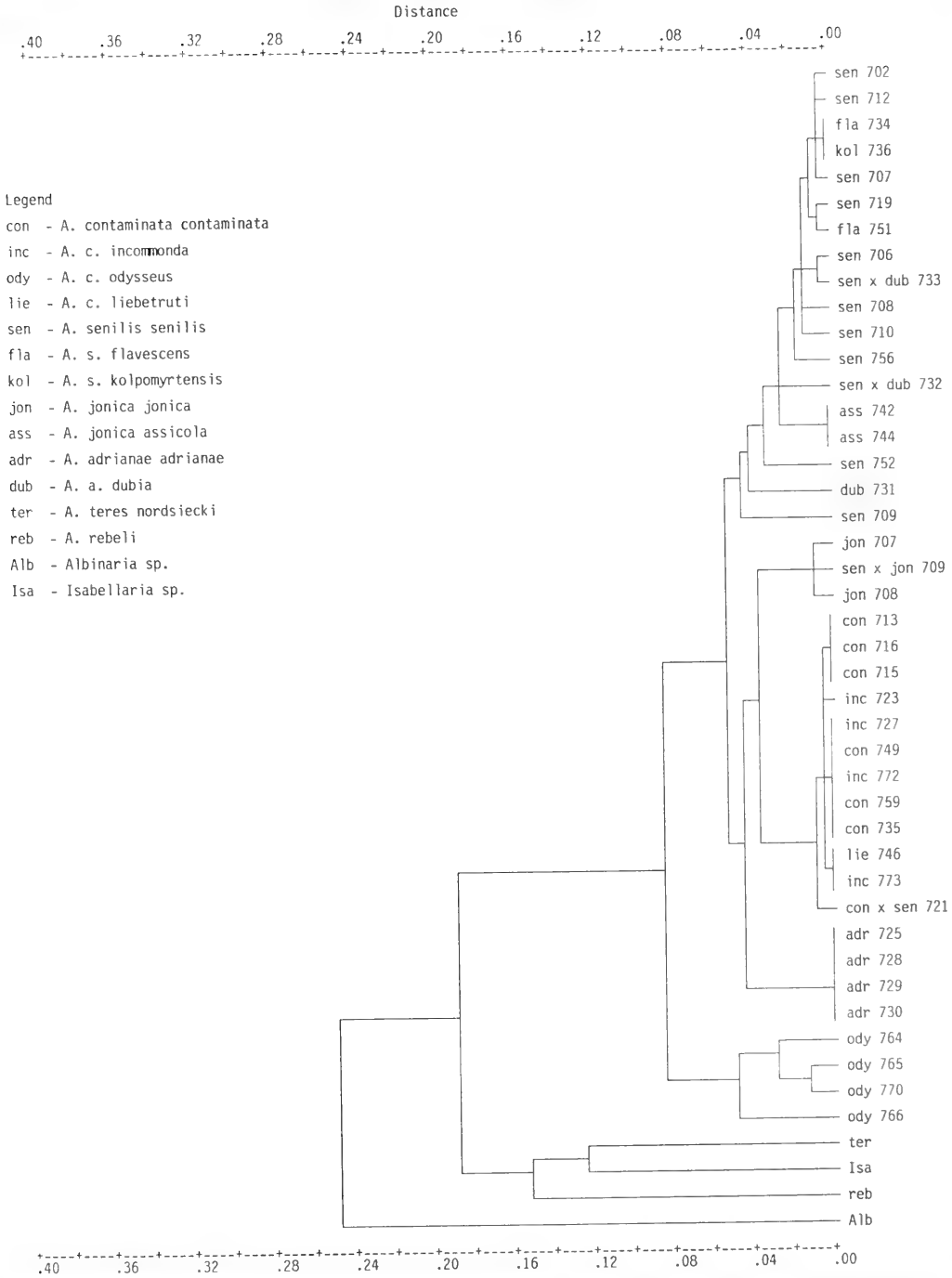

FIG. 5. Dendrogram of UPGMA cluster analysis on Nei's (1972) genetic distance coefficients. Cophenetic correlation = 0.947.

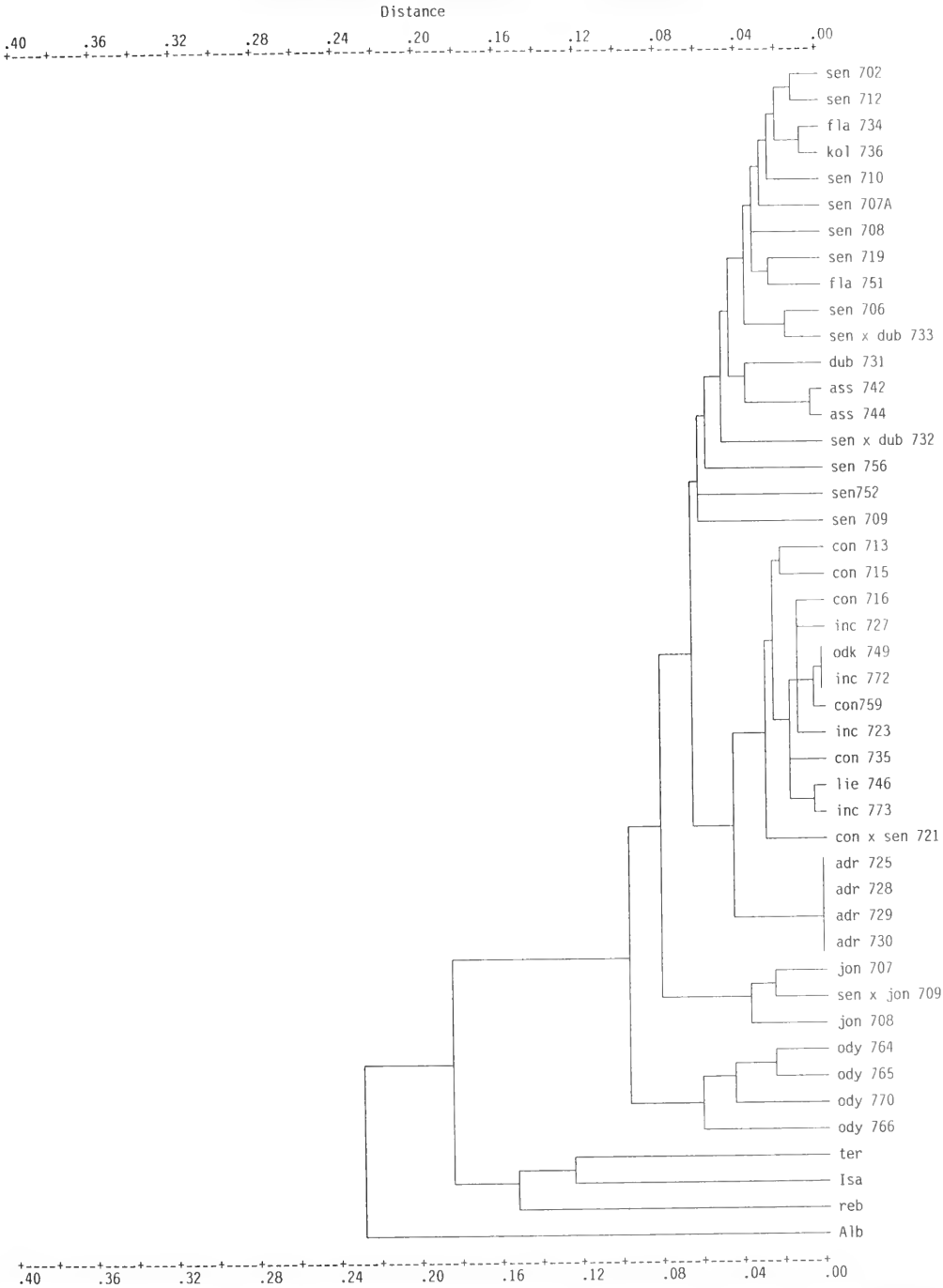

FIG. 6. Dendrogram of UPGMA cluster analysis on Rogers' (1972) genetic distance coefficients. Cophenetic correlation = 0.941. For legend, see Figure 5.

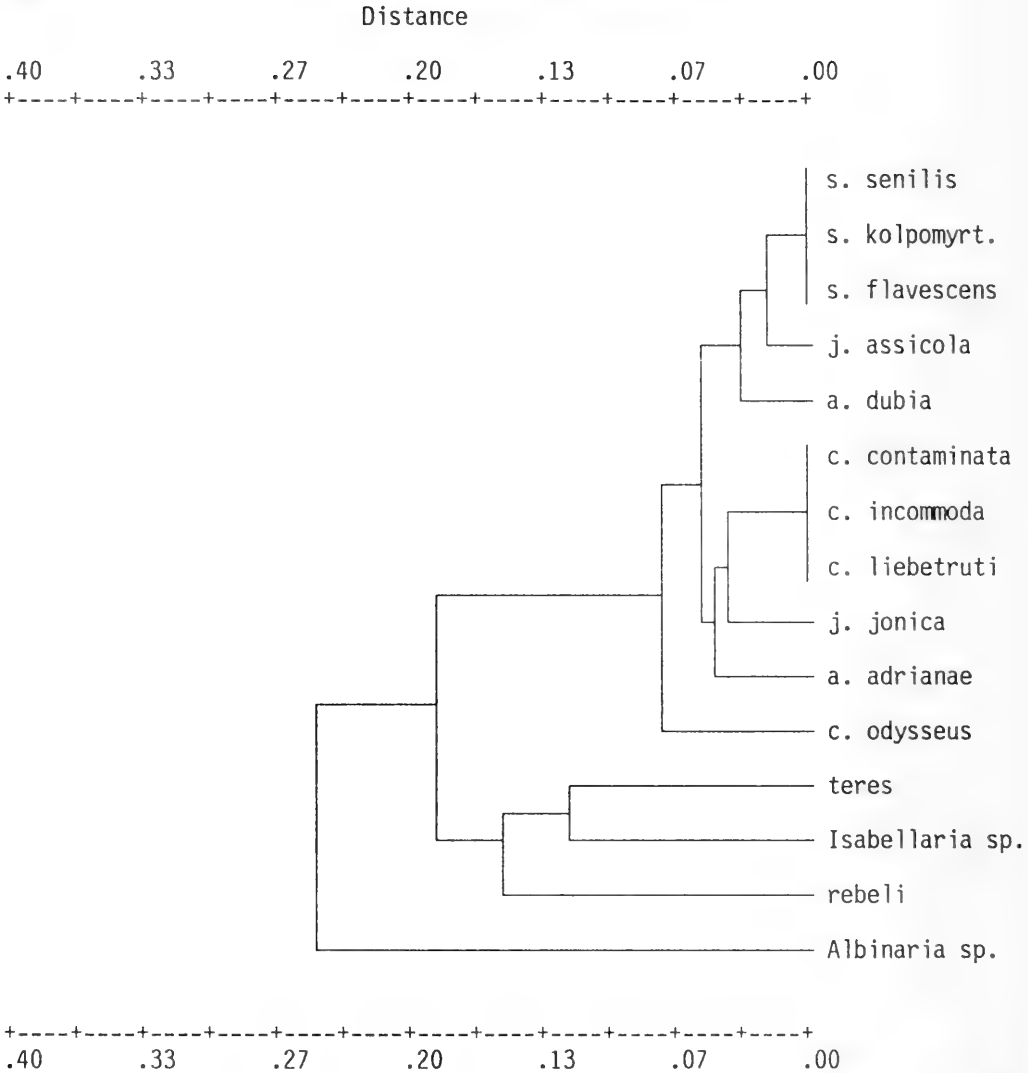

FIG. 7. Dendrogram of UPGMA cluster analysis on Nei's (1972) genetic distance coefficients. Cophenetic correlation = 0.960.

2) might be an indication for apomixis. However, there is no additional information that could support this. The observations within, for example, *A. c. contaminata* (namely, P = 17.9 in loc. 715 and P = 0.0 in loc. 749) show that populations of a single *Albinaria* subspecies may be strikingly different in genetic variability. Whether this is caused by multiple reproductive systems or by one or more other reasons, remains unknown. Because no information on the breeding system of Kephallinian and Ithakian *Albinaria* is present, it also remains unclear whether the observed deficiency of heterozygosity in the majority of the sampled populations is caused by facultative apomixis or by inbreeding. As has been stated before, a sample is considered to belong to a panmictic population. Hence, it is concluded that the Wahlund effect (Richardson et al., 1986) is probably not partly responsible for the paucity of the mean heterozygosity. It can also be suggested that the convention of scoring doubtful pairs of bands as single bands might have contributed to the

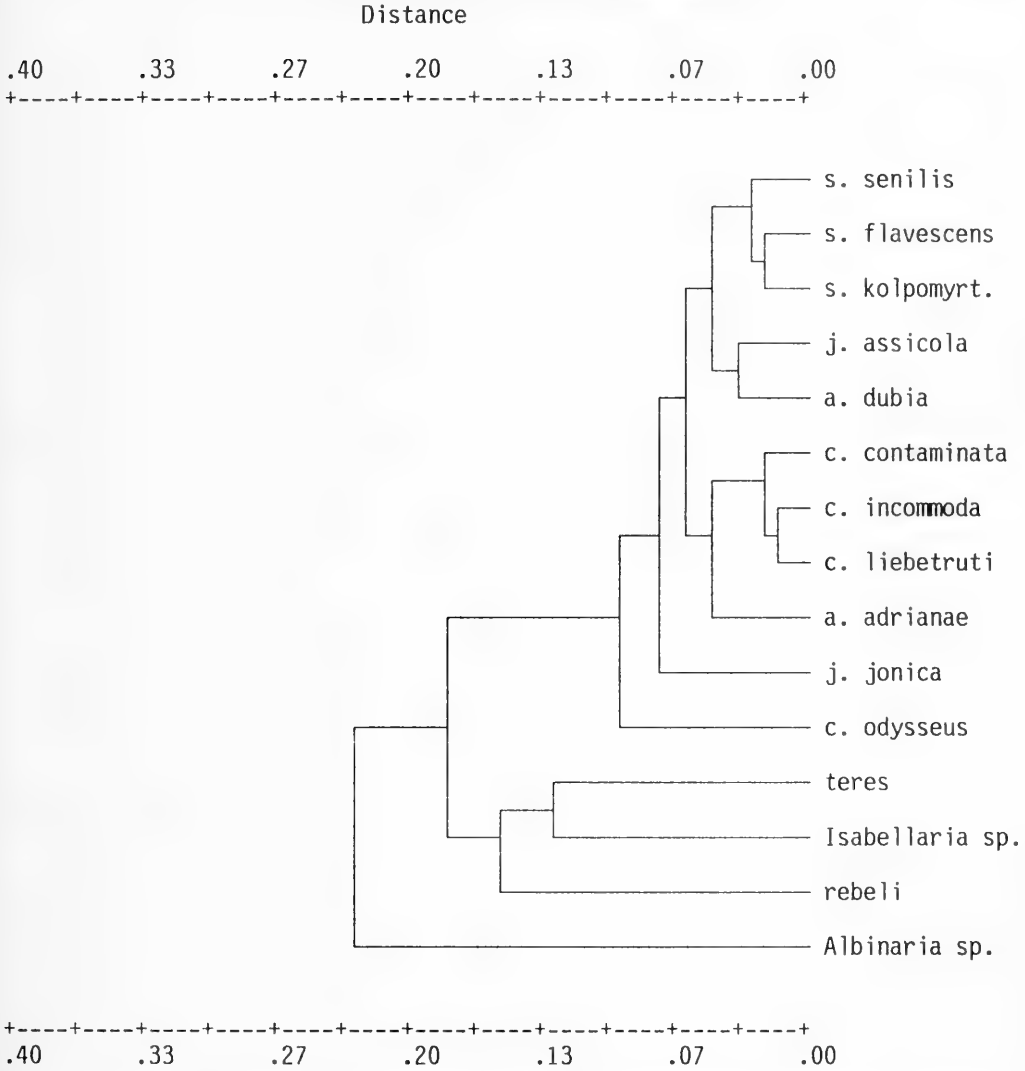

FIG. 8. Dendrogram of UPGMA cluster analysis on Rogers' (1972) genetic distance coefficients. Cophenetic correlation = 0.963.

observed deficiency of heterozygotes. However, this cannot have influenced our values substantially. Moreover, the effect is also reduced by the acceptance of the most frequent alternative in case of a doubtful position of a single homozygous band.

Most *Albinaria* habitats on Kephallinia and Ithaka are seasonally subject to heat and drought. Therefore, in summer at least, most snails are in aestivation. Relatively long periods of severe drought and/or very high temperatures might cause a high mortality, its extent depending on the local microclimate. Especially in small populations, a high mortality could result then in a bottleneck effect and, therefore, a low genetic variability. Because we could not make reliable estimations of population size, correlations between this factor and allozyme variation cannot be investigated.

It is suggested (Nevo, 1978: 162) that a relatively low genetic variability (low P value) is characteristic for geographically restricted habitat specialists, whereas a high variability

TABLE 5. Character states for 16 polymorphic loci, showing the plesiomorphic states for the ingroup taxa. Synapomorphies are underlined, autapomorphies are in italics. For taxon abbreviations, see Figure 5.

Taxon	Locus as taxonomic character															
	Aat-1	Ak	Aph	Est-3	Gp1	Hk	Idh	Lap	Ldh	Mdh-1	Mdh-2	Mp1	Nadd-1	Nadd-2	Pgd	Pgm
Ingroup:																
sen	abc	a*bc*d	a	a	abcde	a	a	abcd	a	abef	ab	abe	acd*f*	a	ab	abc
fla	ac	a	a	a	a	a	ab	a*f*	a	b	abd	a	a	a	a	a
kol	a	a	a	a	ae	a	ab	ab	a	b	a	a	a	a	a	a
con	ade	a	a	a	abcd*fh*	a	ab	abe	a	abdf	ab	a	ae	a	ac	ab
inc	ab	a	a	a	a	a	a	a	a	a	a	a	a*g*	a	a	a
lie	abe	a	a	a	a	a	a	a	a	a	a	a	a	a	a	a
ody	abd	a	a*b*	a	a	a	a	ab	a*cd*	a	ac	a	a	a	a	a
jon	a	ac	a	a	a	a	a	ab	a	a	ad	a	acd	a*b*	a	a
ass	ac	a	a	a	a	a	a	a	a	b	ad	a	acd	a	a	a
adr	a	a	a	a	ab	a	a	a	a	d	a	a	a	a	a	a
dub	a	a	a	a	a	a	a	a	a	b	c	a	a	a	a	a
Outgroup:																
ter	b	a	a	a	a	*bc*	a	a	*b*	c	c	a	a	a	a	a
reb	ab	a	a	ab	a	■	b	d	*b*	c	c	a	a	a	a	a
Isa	b	a	a	ab	a	a	a	b	a	c	c	a	a	a	a	■
Alb	a	a	a	ab	a	a	*c*	a	a	c	c	b	b	a	a	ab
Plesiomorphic state:																
	ab	a	a	a	a	a	ab	abd	a		c	ab	a	a	a	ab

is associated with more wide-spread habitat generalists. This rule can be checked in our material, consisting of two endemic habitat specialists and two non-endemic, much more wide-spread, less stenoecious species. In populations of *A. contaminata* and *A. senilis,* the mean P values vary between 3.6% and 10.7%, with an average of 8.0% for *A. contaminata* and 9.6% For *A. senilis* (Table 2). In the endemic habitat specialist *A. adrianae,* we found no polymorphic loci in one population of *A. a. dubia* and three populations of *A. a. adrianae*; in a fourth population of the latter subspecies, a P of 3.6% was found. Although these differences are small, the data support Nevo's rule. However, P values in the second endemic species *A. jonica* contradict it. The habitat specialist *A. j. jonica,* known only from barren rock faces, has a mean P of 8.9%, and the more catholic *A. j. assicola* has a mean P of 10.7%, both moderately high values. Also, the low P value of 3.6% for *A. c. liebetruti,* which is considered a habitat generalist, does not support Nevo's suggestion. We do not consider Nevo's rule falsified by our results, however. It could equally well be argued that there are only minor ecological differences in the habitats of the various subspecies; they are all represented in relatively warm, dry limestone areas.

Apparently a certain genetic distance does not reflect a divergence on either population, subspecies, species or genus level. Generally, electrophoretic data alone are not sufficient for final decisions on this matter (Gould & Woodruff, 1978: 407; Gould & Woodruff, 1986: 464; Richardson et al., 1986: 308; Menken & Ulenberg, 1987: 318). It may be impossible to distinguish subspecies or even reproductively isolated species on the basis of biochemical characters (Avise, 1975; Johnson et al., 1977). Several authors list ranges of Nei's D corresponding with various taxonomic ranks (e.g., Davis et al., 1981; Menken & Ulenberg, 1987; Thorpe, 1982). It becomes obvious from these publications that the rank indications for a certain group of taxa do not necessarily hold for another group (Davis, 1984). The genetic distances found in *Albinaria* are very low, but, on the whole, the grouping of populations by UPGMA cluster analyses of Nei's D and Rogers' R is in congruence with the results of the classical, morphological approach.

The amount of genetic divergence among the Kephallinian and Ithakian *Albinaria* taxa can be considered indicative of a recent radiation of the group, assuming that a clear genetic differentiation is secondary to the speciation process. The occurrence of different fixed alleles in several species, which are defined on conchological and biogeographical data, demonstrates that these taxa also have individuality with regard to allozyme composition.

A Hennigian analysis of the allozyme data did not result in a resolved phylogeny. The results are contradictory and often inconsistent with the conchological data (Kemperman, in prep. A) and biogeographical patterns. It is considered premature to discuss these differences in detail here.

There are several possible reasons for the poor outcome of the Hennigian analyses. Generally, the number of apomorphic characters states is too low to validate dichotomies (Table 5). This number is even lowered when alleles are removed from which the shared presence is suspected to result from introgression, rather than being based on apomorphy. Although, the resulting phylogeny should become more realistic when the "pseudo"-apomorphic characters based on introgression are removed, the results did not improve. Another source of discrepancies might be the use of characters based on very low allele frequencies that are given the same weight as characters based on high frequencies. Characters based on low allele frequencies are considered the least supportive, mostly because they are more error prone.

Albinaria spp. on Kephallinia and Ithaka

Albinaria contaminata: The subspecies *A. c. contaminata, A. c. incommoda,* and *A. c. liebetruti,* cannot be recognized as separate entities in the UPGMA cluster dendrograms of Nei's D and Rogers' R (Figs. 5, 6). Material from locs. 727 (*A. c. incommoda*), 735, 749 and 759 (*A. c. contaminata*) and 772 (*A. c. incommoda*), situated in various quarters of the species range, is even identical according to Nei's D dendrogram.

All phenetic analyses illustrate the relatively high genetic distance between populations from Ithaka on the one hand and those from Kephallinia on the other hand. The cause of this divergence is difficult to find out. Ithaka is geologically older than Kephallinia (Hagn et al., 1962: 185), but it has been unified with Kephallinia several times in the past due to sea-level oscillations. Nothing is known yet about the early history of *Albinaria* in this region. The present situation on Kephallinia and Ithaka is certainly affected by a series of separations and secondary contacts. It may be questioned whether each geographical separation resulted in genetic divergence and to what extent the secondary contacts reestablished a fully mixed gene-pool. The present genetic divergence is at least the result of the postglacial separation of minimally 12,000 years. It cannot be excluded that it is the effect of an accumulation of smaller divergences caused by the repetitive splitting and fusion of ranges.

It remains a puzzling fact that, according to both Nei's and Rogers' genetic distance coefficients, *A. c. odysseus,* from Ithaka, gets a position in the UPGMA dendrograms (Figs. 5–8) opposite all Kephallinian *Albinaria* taxa, thus including the not conspecific ones. This implies that the amount of allozyme divergence cannot be correlated with taxonomic status, that is, with species boundaries. It must be stressed here, however, that the position of *A. c. odysseus* is relatively unstable. This is demonstrated by the jackknife procedure, resulting in dendrograms in which *A. c. odysseus* is grouped either among the other *A. contaminata* subspecies or opposite the combined Kephallinian taxa. Except for *A. a. adrianae* in two cases, the subspecies remain always in the same position.

An explanation for the large genetic distance between Ithakian and Kephallinian taxa might be that, due to, for example, extensive introgressive hybridization, a certain amount of gene flow continues between all Kephallinian taxa, opposing the genetic differentiation among them. Although introgression among Kephallinian taxa occurs, our biochemical data are insufficient to demonstrate the level of gene flow.

A population of *A. contaminata* sampled near Fiskardo, northern Kephallinia (loc. 749), was identified as *A. c. odysseus* by Rähle (1979: 215). Although the shells show some resemblance to Ithakian *A. c. odysseus,* the allozyme data indicate no genetic difference with other Kephallinian *A. contaminata* populations. The conchological similarity might result from convergent evolution only. However, because of the location of loc. 749, it can also be hypothesized that ancient shipments between the harbour of Fiskardo

and the opposite Mycenean harbour in the Ormos Poleos on Ithaka caused human transport of *A. c. odysseus* from Ithaka to Kephallinia, followed by hybridization with the local *A. c. contaminata*. If that is the case, only some shell characters still witness the introgression.

The range of *A. c. liebetruti* on Kephallinia is very small, comprising probably less than one km^2 along the coast east of Sami. This area is situated close to the former land bridge to Ithaka. Nevertheless, *A. c. liebetruti* is not found on Ithaka. Maybe this is because it could not penetrate an area occupied by another conspecific taxon. It is also possible that this subspecies is only a relatively recent human introduction on Kephallinia. If so, *A. c. liebetruti* did not occur close to the Pleistocene land bridge until recently. Most conchological characters of *A. c. liebetruti* from Kephallinia are very similar to those of this subspecies from Zakynthos, where it is widely distributed (Rähle, 1979; Kemperman, in prep. A). This supports the second view. Meanwhile, the results of the allozyme analyses, especially with regard to the populations of locs. 746 and 773, and conchological data suggest that there is introgressive hybridization between *A. c. liebetruti* and *A. c. incommoda*. Unfortunately, there are no allozyme data for populations of the former subspecies from Zakynthos.

There are no synapomorphies defining *A. contaminata* as a monophyletic group (Table 5). Within *A. contaminata, A. c. contaminata* shares a synapomorphic allele (d) of the *Aat-1* locus with *A. c. odysseus* and a synapomorphic allele (e) of the same locus with *A. c. liebetruti*; the shared presence of the b-allele of the *Aat-1* locus in *A. c. incommoda, A. c. liebetruti* and *A. c. odysseus* is considered to be based on introgression, as discussed below. No other synapomorphies were found within *A. contaminata*. With other species, however, *A. contaminata* has several apomorphies in common. The apomorphic b-allele of the *Gpi* locus is shared with *A. s. senilis* and *A. a. adrianae,* whereas the apomorphic alleles c and d of *Gpi* are exclusively found in *A. c. contaminata* and *A. s. senilis*. The presence of the *Gpi* alleles b, c and d in *A. c. contaminata* and *A. s. senilis* is further discussed below. The b-allele at *Mdh-2* is the synapomorphic character state for *A. c. contaminata, A. s. senilis* and *A. s. flavescens*. Because these synapomorphies result in conflicting conclusions, they do not allow decisions on phylogenetic relations with respect to *A. contaminata*.

Albinaria senilis: According to all distance coefficients, only minor genetic variation occurs among the various populations of *A. senilis*. There is no differentiation between the subspecies. In both population dendrograms (Figs. 5, 6), *A. s. senilis* from loc. 709 is the sister group of the combined other *A. senilis* samples. At locs. 708 and 709, *A. s. senilis* lives truly sympatrically with *A. j. jonica* (locs. 707, 708). At those sites, some specimens have been found that are morphologically intermediate between *A. s. senilis* and *A. j. jonica*; allozyme analyses, however, group these intermediate specimens with *A. j. jonica* (Fig. 5). The position in the UPGMA-dendrograms of *A. s. senilis* of loc. 709, of which only two specimens could be analysed, results from the fixation of both the *Mdh-1* b-allele and the *Lap* b-allele. For *Mdh-1* b, most other *A. s. senilis* populations are also fixed; this allele is absent in *A. j. jonica*. The *Lap* b-allele occurs in some other populations of *A. s. senilis, A. c. contaminata* and *A. j. jonica*. Although according to the shell morphology this material was convincingly identified as *A. s. senilis,* the analysed enzyme systems indicate that the specimens were hybrids between *A. s. senilis* and *A. j. jonica*.

Within *A. s. senilis* two geographically isolated populations, namely, loc. 752 on the Paliki-Peninsula and loc. 756 from Kastro, southeast of Argostoli, exhibit relatively high genetic distances from the other *A. senilis* populations. Both populations are not clearly differentiated morphologically.

The results of the allozyme frequency analyses did not support the taxonomic distinction of *A. s. kolpomyrtensis* Kemperman & Gittenberger, 1990, which was based on conchological and distributional data. In the dendrograms, this subspecies is closely linked to *A. s. flavescens* (Figs. 5–8), which is the geographically adjoining subspecies.

There are no apomorphic character states that point to *A. senilis, s.l.,* as a monophyletic group. This is not affected by limiting the analyses to a subset of the outgroup species. The apomorphic allele e of the *Gpi* locus is the only derived character state defining a subgroup within *A. senilis,* namely, the combined *A. s. senilis* and *A. s. kolpomyrtensis*. All other apomorphies are shared with one or more other species, which results in conflicting phylogenetic trees. The apomorphic c-allele of

Aat-1 defines *A. s. senilis, A. s. flavescens* and *A. j. assicola* as a monophyletic group. The c-allele of *Ak* groups *A. s. senilis* and *A. j. jonica* together; however, the presence of this allele in both taxa is considered to be the result from introgression, as discussed below. Both apomorphic alleles c and d of *Nadd-1* would point to the combined *A. s. senilis, A. j. jonica* and *A. j. assicola* as a monophyletic group, but the presence of these alleles in *A. s. senilis* is regarded too as being due to introgression. The cause of the distribution of the "synapomorphic" alleles b, c and d of *Gpi* in both *A. s. senilis* and *A. c. contaminata* is further discussed below. The status of the b-allele of *Gpi* with respect to *A. a. adrianae* and *A. s. senilis* is unclear. The d-allele of *Mdh-2* is shared by *A. s. flavescens, A. j. jonica* and *A. j. assicola,* whereas the b-allele of *Mdh-2* could be a synapomorphy for *A. s. senilis, A. s. flavescens* and *A. c. contaminata.*

Albinaria jonica: The endemic *A. jonica* is divided into two widely disjunct subspecies. *Albinaria j. assicola* occurs along the Kephallinian northwest coast, including the Assos Peninsula. Its range overlaps partly with that of *A. c. contaminata* (Fig. 1), but the two species remain separate in habitat. *Albinaria j. jonica* is known from 3 to 4 km north of Argostoli, along the west coast of the main island. It is found on the rocks along about 500 m of the coastal road, where it occurs in a mixed population with *A. s. senilis.* Morphologically intermediate specimens have occasionally been found between *A. j. assicola* and *A. c. contaminata,* as well as between *A. j. jonica* and *A. s. senilis.*

With respect to both subspecies of *A. jonica,* there is a striking contrast between the results of morphological studies and those of allozyme analyses. The taxa have been recognized as conspecific on the basis of conchological features (Kemperman & Gittenberger, 1990). Quite different from what is found among subspecies of *A. senilis* and *A. contaminata,* all UPGMA analyses demonstrate a relatively large genetic distance between *A. j. assicola* (locs. 742 and 744) and *A. j. jonica* (locs. 707 and 708). Moreover, the affinities between these and other taxa, as indicated by the results of the UPGMA cluster analyses, suggest that *A. jonica* is not a monophyletic entity. *Albinaria j. assicola* is grouped among *A. senilis* subgroups, although it is partly sympatric not with this species, but with *A. contaminata.* The position of *A. j. jonica* is less constant. Nei's D (Figs. 5, 7) suggests that *A. j. jonica* and *A. c. contaminata* are sister groups; combined they are the sister group of *A. a. adrianae.* After Rogers' R (Figs. 6, 8), *A. j. jonica* is the sister group of the combined Kephallinian taxa.

Contrary to the results of the UPGMA analyses is the outcome of a Hennigian analysis defining *A. jonica, s.l.,* as a monophyletic group. At the *Nadd-1* locus, c (present in locs. 708 and 742) and d (present in locs. 708 and 744) are synapomorphic alleles (Table 5); it is assumed that the occurrence of both alleles in *A. s. senilis* is the result of introgressive hybridization. Another synapomorphy for *A. jonica* would be the d-allele of *Mdh-2,* if one considers its occurrence in *A. s. flavescens* (loc. 751 only) due to introgression. This could then date back to times when the present floor of the Gulf of Argostoli was dry land. The c-allele of *Ak* in *A. j. jonica,* shared with *A. s. senilis* (Table 5), will be discussed below. The presence of the apomorphic c-allele of *Aat-1* in *A. j. assicola* as well as in *A. s. senilis* and *A. s. flavescens,* might result from convergent evolution.

Albinaria adrianae: The endemic *A. adrianae* is subdivided into two subspecies. This subdivision, primarily based on shell characters, is also strongly supported by the allozyme data. The four analyzed samples of *A. a. adrianae* (locs. 725, 728, 729 and 730), proved to be genetically very similar. According to UPGMA population dendrograms based on Nei's D and Rogers' R (Figs. 5, 6), these populations are even identical. Material from loc. 730, with a P value of 3.6%, differs only slightly from the other three localities, which were found to be monomorphic. *Albinaria a. adrianae* has not a stable position within the various dendrograms. According to Rogers' R, *A. a. adrianae* and *A. contaminata* are sister groups. Corresponding to Nei's D, *A. a. adrianae* is the sister group of the combined *A. contaminata* and *A. j. jonica.* When Nei's D is calculated while either *A. c. contaminata* or *A. c. incommoda* are removed from the dataset in a jackknife procedure, *A. a. adrianae* switches from this position and becomes the sister group of the combined *A. senilis, A. j. jonica* and *A. a. dubia.* The second subspecies, *A. a. dubia,* is clustered either as the sister group of the combined *A. senilis* subspecies and *A. j. assicola* (Nei's D) or as the sister group of *A. j. assicola* alone (Rogers' R). This results from the fixation of the *Mdh-1*

allele b in *A. a. dubia,* as well as in *A. j. assicola, A. s. flavescens* and *A. s. kolpomyrtensis*. However, no phylogenetic conclusions can be drawn on this allele distribution as no plesiomorphic character state can be determined for this locus (Table 5).

The allozyme analyses did not reveal one or more synapomorphic character states characterizing *A. adrianae* as a monophyletic group (Table 5). Moreover, the absence of the a-allele of MDH-2, which is a synapomorphy for all subspecies but *A. a. dubia,* points to the paraphyletic origin of *A. a. adrianae* and *A. a. dubia*. With the b-allele of the *Gpi* locus, *A. a. adrianae* has an apomorphic character state in common with both *A. s. senilis* and *A. c. contaminata*. Because the presence of this allele in both *A. s. senilis* and *A. c. contaminata* is considered to be the result of introgression from *A. c. contaminata* to *A. s. senilis,* it is a synapomorphic character state for *A. c. contaminata* and *A. a. adrianae*. Because in our analyses *A. a. dubia* has no apomorphic character states at all, its phylogenetic position remains puzzling.

Hybridization and Introgression: Among *Albinaria* species both hybridization and introgression are known to occur (e.g. Fuchs & Käufel, 1936; Nordsieck, 1983; Gittenberger, 1991). For Kephallinian taxa, these phenomena are reported by Rähle (1979), Gittenberger (1979) and Nordsieck (1979), who based their conclusions on morphological characters. We found some biochemical data pointing to introgression (Table 3).

(1) As mentioned above, the c- and d-alleles of the *Nadd-1* locus are characteristic for *A. jonica, s.l.*; in *A. j. jonica* they are present in loc. 708. These alleles occur also in the adjoining *A. s. senilis* populations 702 and 706. It is assumed, therefore, that their very local presence in *A. s. senilis* results from introgression.

(2) The c-allele of the *Ak* locus is only known from *A. s. senilis* at locs. 756 and 707, as well as from *A. j. jonica* at loc. 708. As localities 707 and 708 are adjoining, introgression of the *Ak* c-allele is hypothesized between *A. s. senilis* and *A. j. jonica*. Although the distribution of this allele in *A. s. senilis* is less local than it is in *A. j. jonica,* the direction of the introgression is unclear.

(3) The b-allele of *Aat-1* occurs in all Ithakian populations as well in *A. c. liebetruti* of loc. 746 and *A. c. incommoda* of population 773. This is in roughly an area constituting Ithaka and the central eastern part of Kephallinia. During the late Würm sea-level lowering, Kephallinia and Ithaka were connected by a land bridge located close to this area. Therefore, introgression is a possible explanation. *Albinaria c. liebetruti* might have received the allele either during the late Würm period directly from the same Ithakian source, or secondarily from local Kephallinian *A. c. incommoda*. Thus, whether or not *A. c. liebetruti* is a recent invader in Kephallinia cannot be decided on the basis of these data. For the presence of the *Aat-1* b-allele in *A. s. senilis* of loc. 752, introgression cannot be hypothesized. We have to accept either convergent evolution or indistinguishable, yet different electromorphs.

(4) The b-, c- and d-alleles of the *Gpi* locus are found in the adjoining *A. c. contaminata* populations at locs. 713 (alleles b and c), 715 (alleles b, c and d) and 716 (allele b). These alleles are also found in the nearby *A. s. senilis* populations at locs. 756 (alleles b, c, and d) and 706 (allele b). Their local presence in both species can be seen as the result of introgression, but it can also be hypothesized that the b-, c- and d-alleles of *Gpi* are examples of what Woodruff (1989: 282) called hybrizymes, "unexpected allelic electromorphs associated with hybrid zones." We found morphologically intermediate specimens, indicative of hybridization, in this area. Only the presence of the *Gpi*-b allele in *A. a. adrianae* of loc. 730 is not in agreement with the hypothesis that hybrizymes are involved.

(5) Locally, both in *A. c. contaminata* population 715 and in *A. s. senilis* population 752, the b-allele of the *Pgm* locus occurs. This can hardly be the result of introgression, unless ancestral populations once met during a glacial sea-level lowering.

(6) At loc. 732, specimens morphologically intermediate between *A. s. senilis* and *A. a. dubia* are found, whereas at the nearby loc. 721, we collected specimens intermediate between *A. s. senilis* and *A. c. contaminata*. Only at these two localities we found the c-allele of the *Mpi* locus. Because loc. 732 is situated in a hybrid zone, the *Mpi* c-allele might be a hybrizyme (Woodruff, 1989). With respect to the material of loc. 721, one might postulate introgression between loc. 732 and loc. 721.

(7) Some specimens of loc. 709 are conchologically intermediate between *A. s. senilis* and *A. j. jonica*; the shells have the slen-

derness of *A. j. jonica,* the apertural shape of *A. s. senilis,* and an intermediate sculpture. In contrast, the allozyme analyses point to a genetic similarity with *A. j. jonica* (Figs. 5, 6). This is, for example, indicated by the presence of the *Mdh-2* d-allele, which might be considered typical for *A. j. jonica.*

Apparently there are several localities on Kephallinia and Ithaka where introgression might explain the distribution of rare alleles (1–4). As an alternative for introgression, the presence of hybrizymes is suggested (4, 6). Again, in all cases, one must remember the possibility of convergent or parallel evolution or the presence of electromorphs that are indistinguishable by our methods.

The Outgroup Species

All dendrograms (Figs. 5–8) show the same topology for the species serving as outgroups, namely, *Albinaria* sp. and *Isabellaria edmundi* from the Peloponnesos, and *A. teres nordsiecki* and *A. rebeli* from Crete. They are linked outside the cluster formed by the species from Kephallinia and Ithaka, with a genetic distance varying between 0.18 and 0.41. *Albinaria t. nordsiecki* is the sister group of *Isabellaria edmundi*; the combination of *A. t. nordsiecki* and *I. edmundi* is the sister group of *A. rebeli.* This cluster is the sister group of the combined Kephallinian and Ithakian *Albinaria* taxa. The *Albinaria* sp. is grouped as the sister group of all other taxa.

The grouping of *Isabellaria edmundi* within a cluster of *Albinaria* species, with a genetic distance far below the distance between a Cretan and a Peloponnesian *Albinaria* species, supports the view that *Isabellaria sensu auctt.* might be of polyphyletic origin and partly synonymous with *Albinaria* (Gittenberger, 1987: 79).

Electrophoretic Data, Morphology and Classification

In this paper, we do not discuss in detail the results of morphological and morphometrical analyses; these will be presented in a forthcoming article. Nevertheless, some remarks concerning electrophoretic data in relation to morphology can be made already.

The genetic distance ($\bar{D} = 0.05$ for Kephallinian and Ithakian taxa, and $D \leq 0.284$ when including the outgroup-species) are very low with regard to their status as separate species (Menken & Ulenberg, 1987; Thorpe, 1982). Apparently we are dealing with most closely related "young" species, clearly characterized by their distribution and a series of independent conchological characters, among which some localized introgression still occurs. This reminds one of what is described for five *Partula* species by Johnson et al. (1977: 122, 125), who found an $\bar{D}$ of 0.09. Davis et al. (1981) mentioned $0.01 < D < 0.1$ for the *Elliptio complanata* species group (Bivalvia: Unionidae). For *Cerion* species, the following values are reported in the literature: $\bar{D} = 0.015$ ($D < 0.056$) (Gould & Woodruff, 1978: 407); $\bar{D} < 0.06$ (Woodruff & Gould, 1980: 397); $\bar{D} \pm 0.05$ (Gould & Woodruff, 1986: 464); and $D < 0.01$ (Gould & Woodruff, 1987: 343). Evidently, "taxonomic decisions do not follow directly from the estimation of D" (Gould & Woodruff, 1986: 466).

Preliminary results of allozyme analyses of several *Albinaria* taxa from Crete are in line with this statement. Although both the distributional patterns and the conchological diversification strongly remind one of what is reported for the Kephallinian and Ithakian taxa here, genetic distances between the Cretan taxa were seven times larger ($\bar{D} = 0.35$). This is considered indicative of speciation events that occurred further back in geological time (Schilthuizen, pers. com., 1991).

For the *Albinaria* under study, the taxonomic relationships, derived from morphological and biogeographical data, are not in close congruence with the patterns found in allozyme variation. This becomes obvious several times independently. Illustrative are the widely separate positions of the subspecies of both *A. jonica* and *A. adrianae* among different clusters of *A. contaminata* and *A. senilis,* according to the allozyme data. Despite the fact that *A. c. odysseus* from Ithaka is only slightly different morphologically from the Kephallinian *A. c. contaminata,* the Ithakian subspecies has to be placed opposite the total group of four polytypic *Albinaria* species represented in Kephallinia according to its allozymes. In some cases, forms that are considered hybrid origin by morphological and distributional data, cannot be recognized as such electrophoretically.

Despite the puzzling facts that remain, the electrophoretic analyses were an important tool in the multidisciplinary approach towards an understanding of the differentiation of Kephallinian and Ithakian *Albinaria.*

ACKNOWLEDGMENTS

We are indebted to Prof. Dr. E. Gittenberger, who initiated and supervised this project and gave critical comments on the various versions of this text. The second author wishes to express her gratitude to Dr. G. M. Davis for teaching her the ins and outs of allozyme analyses on molluscs at his laboratory at the Academy of Natural Sciences of Philadelphia, USA; many thanks are due also to C. Hesterman, who gave the daily technical support there. At Amsterdam, we were guests of Prof. Dr. S. B. J. Menken, who helped us adapting and continuing our runs and also commented on this paper. At Amsterdam, daily technical support was given by W. van Ginkel, Dr. J. W. Arntzen and Dr. W. M. Scheepmaker, for which we are very grateful. Dr. J. W. Arntzen also helped us with debugging the data-set and introduced us to BIOSYS. Dr. T. Backeljau of Brussels, Belgium, is kindly acknowledged for his introduction to biochemical molluscan systematics.

LITERATURE CITED

ANDEL, T. H. VAN & J. C. SHACKLETON, 1982. Late Paleolithic and Mesolithic coastlines of Greece and the Aegean. *Journal of Field Archaeology,* 9: 445–454.

AVISE, J. C., 1974. Systematic value of electrophoretic data. *Systematic Zoology,* 23: 465–481.

AYALA, F. J., J. R. POWELL, M. L. TRACY, C. A. MOURÃO & S. PÉREZ-SALAS, 1972. Enzyme variability in the *Drosophila willistoni* group. IV. Genic variation in natural populations of *Drosophila willistoni*. *Genetics,* 70: 113–139.

AYALA, F. J., D. HEDGECOCK, G. S. ZUMWAULT & J. W. VALENTINE, 1973. Genetic variation of *Tridacna maxima,* an ecological analog of some unsuccessful evolutionary lineages. *Evolution,* 27: 117–191.

AYOUTANTI, A., C. KRIMBAS, S. TSAKAS & M. MYLONAS, 1988. Genetic differentiation and speciation in the Greek Archipelago: the genus *Albinaria*. *Biologia Gallo-Hellenica,* 13: 155–160.

BAUR, B., 1988. Microgeographical variation in shell size of the land snail *Chondrina clienta*. *Biological Journal of the Linnean Society,* 35: 247–259.

BIRD, E. C. F., 1984. *Coasts. An introduction to coastal geomorphology*. 3rd ed., Basil Blackwell, New York, xv + 320 pp.

BOATO, A., 1988. Microevolution in *Solatopupa* landsnails (Pulmonata: Chondrinidae): genetic diversity and founder effects. *Biological Journal of the Linnean Society,* 34: 327–348.

BREWER G. J., 1970. *An introduction to isozyme techniques*. Academic Press, New York, xii + 186 pp.

BUTH, D. G., 1984. The application of electrophoretic data in systematic studies. *Annual Review of Ecology and Systematics,* 15: 501–522.

DAVIS, G. M., 1984. Introduction to the second international symposion on molluscan genetics.— *Malacologia,* 25(2): 265–269.

DAVIS, G. M., W. H. HEARD, D. L. H. FULLER & C. HESTERMAN, 1981. Molecular genetics and speciation in *Elliptio* and its relationships to the taxa of North American Unionidae (Bivalvia). *Biological Journal of the Linnean Society,* 15: 131–150.

DEGENAARS, G. H. Allozyme variation analysis in *Albinaria* (Gastropoda Pulmonata: Clausiliidae). In: C. MEIER-BROOK, ed., *Proceedings of the Tenth International Malacological Congress,* Tübingen, 1989. In press.

EMBERTON, K. C., 1988. The genitalic, allozymic, and conchological evolution of the eastern north american Triodopsinae (Gastropoda: Pulmonata: Polygyridae). *Malacologia,* 21(1–2): 159–273.

EMBERTON, K. C., 1990. Acavid land snails of Madagascar: subgeneric revision based on published data (Gastropoda: Pulmonata: Stylommatophora). *Proceedings of the Academy of Natural Sciences at Philadelphia,* 142: 101–117.

FARRIS, J. S., 1988. *Hennig86 reference, version 1.5*. James S. Farris, Port Jefferson Station, New York, 18 pp.

FERGUSON, A., 1988. Isozyme studies and their interpretation. In: D. L. HAWKSWORTH, ed., *Prospects in systematics*. Systematics Association, Spec. Vol. 36: 185–201.

FUCHS, A. & F. KÄUFEL, 1936. Anatomische und systematische Untersuchungen an Land- und Süßwasserschnecken aus Griechenland und von den Insel des Ägäischen Meeres. *Archiv für Naturgeschichte* (n.f.) 5(4): 541–662.

GITTENBERGER, E., 1979. Eine neue *Albinaria* Art (Gastropoda, Clausiliidae) der Insel Kephallinia. *Zoologische Mededelingen Leiden,* 54(2): 83–85.

GITTENBERGER, E., 1987. Neue Taxa der sogenannten Gattung *Isabellaria* (Gastropoda Pulmonata: Clausiliidae) vom Peloponnes. *Basteria,* 51: 79–84.

GITTENBERGER, E.. Diversification in *Albinaria* (Gastropoda, Clausiliidae). In: C. MEIER-BROOK, ed., *Proceedings of the Tenth International Malacological Congress,* Tübingen, 1989. In press.

GITTENBERGER, E., 1991. What about non-adaptive radiation? *Biological Journal of the Linnean Society,* 43: 263–272.

GOULD, S. J. & D. S. WOODRUFF, 1978. Natural history of *Cerion* VIII: Little Bahama Bank—a revision based on genetics, morphometrics and geographic distribution. *Bulletin of the Museum of Comparative Zoology,* 148(8): 371–415.

GOULD, S. J. & D. S. WOODRUFF, 1986. Systematics of *Cerion* on New Providence Island: A rad-

ical revision. *Bulletin of the American Museum of Natural History,* 182: 389–490.

GOULD, S. J. & D. S. WOODRUFF, 1987. Systematics and levels of covariation in *Cerion* from the Turks and Caicos Islands. *Bulletin of the Museum of Comparative Zoology,* 151(6): 321–363.

HAGN, H., H. BERGMANN, B. BISCHOFF, K. BRAUNE, G. DREMEL, G. HUG & W. OTT, 1968. Zur Neogen-Stratigraphie von Kephallinia und Ithaka. *Giornale di Geologia,* 2a, 35(2): 179–188.

HILLIS, D. M., D. S. ROSENFELD & M. SANCHEZ, 1987. Allozymic variability and heterozygote deficiency within and among morphologically polymorphic populations of *Liguus fasciatus* (Mollusca: Pulmonata: Bulimulidae). *American Malacological Bulletin,* 5(2): 153–157.

JOHNSON, M. S., B. CLARKE & J. J. MURRAY, 1977. Genetic variation and reproductive isolation in *Partula*. *Evolution,* 31: 116–126.

KEMPERMAN, TH. C. M.. *Systematics and evolutionary history of the genus Albinaria (Gastropoda: Pulmonata: Clausiliidae) on the Ionian islands of Kephallinia and Ithaka.* Thesis, in preparation A.

KEMPERMAN, TH. C. M.. Genitalia of *Albinaria* of the Ionian Islands Kephallinia and Ithaka. In preparation B.

KEMPERMAN, TH. C. M. & E. GITTENBERGER, 1988. On morphology, function and taxonomic importance of the shell ribs in Clausiliidae (Mollusca: Gastropoda Pulmonata), with special reference to those in *Albinaria*. *Basteria,* 52: 77–100.

KEMPERMAN, TH. C. M. & E. GITTENBERGER, 1990. Two new *Albinaria* subspecies (Gastropoda: Pulmonata: Clausiliidae) from Kephallinia and Ithaka. *Basteria,* 54: 143–150.

KEMPERMAN, TH. C. M. & G. D. E. POVEL & P. H. F. BOR. Differentiation in radulae of closely related pulmonates: a pilot study in *Albinaria* (Gastropoda: Clausiliidae). In preparation.

MCCRACKEN, G. F. & R. K. SELANDER, 1980. Self-fertilization and monogenic strains in natural populations of terrestrial slugs. *Proceedings of the National Academy of Sciences of the USA,* 77(1): 684–688.

MENKEN, S. B. J., 1980. *Allozyme polymorphism and the speciation process in small ermine moths (Lepidoptera, Yponomeutidae).* Thesis, University of Leiden.

MENKEN, S. B. J. & S. A. ULENBERG, 1987. Biochemical characters in agricultural entomology. *Agricultural Zoology Reviews,* 2: 305–360.

MOOI, R., 1989. The outgroup criterion revisited via naked zones and alleles. *Systematic Zoology,* 38(3): 283–290.

MURPHY, R. W., J. W. SITES, Jr., D. G. BUTH & C. H. HAUFLER, 1990. Proteins I: Isozyme electrophoresis. In: D. M. Hillis & C. Moritz, eds., *Molecular systematics.* Sinauers Associates, Inc., Sunderland, Massachusetts, pp. 45–126.

NEI, M., 1972. Genetic distance between populations. *American Naturalist,* 106: 283–292.

NEI, M., F. TAJIMA & Y. TATENO, 1983. Accuracy of estimated phylogenetic trees from molecular data. II. Gene frequency data. *Journal of Molecular Evolution,* 19: 153–170.

NEVO, E., 1978. Genetic variation in natural populations: patterns and theory. *Theoretical Population Biology,* 13: 121–177.

NEVO, E., 1988. Genetic diversity in nature, patterns and theory. In: M. K. Hecht, B. Wallace & G. T. Prance, eds., *Evolutionary biology,* vol. 18: 217–246. Plenum Press, New York.

NICHOLS, E. A., V. M. CHAPMAN & F. H. RUDDLE, 1973. Polymorphism and linkage for mannosephosphate isomerase in *Mus musculus*. *Biochemical Genetics,* 8(1): 47–53.

NORDSIECK, H., 1977. Zur Anatomie und Systematik der Clausilien, XVII. Taxonomische Revision des Genus *Albinaria* Vest. *Archiv für Molluskenkunde,* 107(4/6): 285–307.

NORDSIECK, H., 1979. Eine neue *Albinaria*-art von Kefallinia (Gastropoda: Clausiliidae). *Archiv für Molluskenkunde,* 110(1/3): 63–66.

NORDSIECK, H., 1983. Neue Taxa rezenter europäischer Clausilien, mit bemerkungen zur Bastardierung bei Clausilien (Gastropoda: Clausiliidae). *Archiv für Molluskenkunde,* 114(4/6): 189–211.

POULIK, M. D., 1957. Starch gel electrophoresis in a discontinuous system of buffers. *Nature,* 180: 1477–1479.

RÄHLE, W., 1979. Land- und Süßwassermollusken von Kephallinia und Zakynthos (Ionische Inseln). *Archiv für Molluskenkunde,* 110(4/6): 199–224.

RICHARDSON, B. J., P. R. BAVERSTOCK & M. ADAMS, 1986. *Allozyme electrophoresis. A handbook for animal systematics and population studies.* Academic Press, Sydney, xii + 410 pp.

ROGERS, J. S., 1972. Measures of genetic similarity and genetic distance. *Studies in Genetics,* 7: 145–153.

SELANDER, R. K., M. H. SMITH, S. Y. YONG, W. E. JOHNSON & F. B. GENTRY, 1971. Biochemical polymorphism and systematics in the genus *Peromyscus*. I. Variation in the old-field mouse (*Peromyscus polinotus*). *Studies in Genetics,* 4: 49–90.

SELANDER, R. K. & D. W. KAUFMAN, 1973. Self-fertilization and genetic population structure in a colonizing land snail. *Proceedings of the National Academy of Sciences of the USA,* 70(4): 1186–1190.

SHAW, C. R. & R. PRASAD, 1970. Starch gel electrophoresis, a compilation of recipes. *Biochemical Genetics,* 4: 297–320.

SNEATH, P. H. A. & R. R. SOKAL, 1973. *Numerical taxonomy.* San Francisco, Freeman. xv + 573 pp.

SWOFFORD, D. L. & R. B. SELANDER, 1989. *BIOSYS-1. A computer program for the analyses of allelic variation in population genetics and bio-*

chemical systematics, release 1.7. Illinois Natural History Survey, Champaign. v + 43 pp.

THORPE, J. P., 1982. The biological clock hypothesis: Biochemical evolution, genetic differentiation and systematics. *Annual Reviews of Ecology and Systematics,* 13: 139–168.

WOODRUFF, D. S., 1989. Genetic anomalies associated with *Cerion* hybrid zones: the origin and maintenance of new electromorphic variants called hybrizymes. *Biological Journal of the Linnean Society,* 36: 281–294.

WOODRUFF, D. S. & S. J. GOULD, 1980. Geographic differentiation and speciation in *Cerion*—a preliminary discussion of patterns and processes. *Biological Journal of the Linnean Society,* 14: 389–416.

Revised Ms. received 18 September 1991

APPENDIX: LIST OF COLLECTION LOCALITIES

Unless otherwise stated, the locality is on Kephallinia island. Locality numbers correspond with those on the map of Figure 2.

319 *A. senilis senilis* (Rossmässler)—Near junction to Moni Theotokou Sision (= 17.4 km SE of Argostoli), on rock, 210 m alt., DH7017; 24-04-1987

702 *A. senilis senilis* (Rossmässler)—1 km E of Argostoli, W of junction Angon—Sami/Poros, on walls along road, 10 m alt., DH5626; 16-03-1988

706 *A. senilis senilis* (Rossmässler)—400 m N of Ag. Konstantinos (= 1.5 km NE of Argostoli) on rocks along road, 10 m alt., DH5627; 17-03-1988

707 *A. jonica jonica* (L. Pfeiffer)—Akros Kokkinos Vrachos, most western rocks along road, (= 3.5 km N of Argostoli), 50 m alt., DH5429; 17-03-1988

707 *A. senilis senilis* (Rossmässler)—Akros Kokkinos Vrachos (= 3.5 km N of Argostoli), most western rocks along road, 50 m alt., DH5429; 17-03-1988

708 *A. senilis senilis* (Rossmässler)—200 m N of Akros Kokkinos Vrachos (= 3.7 km N of Argostoli); on rocks along road, 50 m alt., DH 5429; 17-03-1988

708 *A. jonica jonica* (L. Pfeiffer)—200 m N of Akros Kokkinos Vrachos (= 3.7 km N of Argostoli), on rocks along road, 50 m alt., DH5429; 17-03-1988

709 *A. senilis senilis* (Rossmässler)—500 m N of Akrcs Kokkinos Vrachos (= 4 km N of Argostoli), along road on rocks, 55 m alt., DH5429; 17-03-1988

710 *A. senilis senilis* (Rossmässler)—Spilia, S exit village (= 1.7 km S of Argostoli), along road on rocks covered with vegetation, 120 m alt., DH5524; 18-03-1988

712 *A. senilis senilis* (Rossmässler)—Lakythra, 50 m N of northern entrance (= 6.2 km SSE of Argostoli), on rocks in field and on low rock-face, W side of road, 230 m alt., DH5720; 18-03-1988

713 *A. contaminata contaminata* (Rossmässler)—Lakythra, 50 m N of northern entrance (= 6.2 km SSE of Argostoli), on rocks in field and on low rock-face, E side of road, 230 m alt., DH5720; 18-03-1988

715 *A. contaminata contaminata* (Rossmässler)—0.5 km NW of Lakythra, in road-cleft on hill-top (= 5.3 km SSE of Argostoli), W side of road on rock-face, 240 m alt., DH5721; 18-03-1988

716 *A. contaminata contaminata* (Rossmässler)—0.5 km NW of Lakythra, in road-cleft on hill-top (= 5.3 km SSE of Argostoli), E side of road on rock-face, 240 m alt., DH5721; 18-03-1988

719 *A. senilis senilis* (Rossmässler)—Atsoupades, 200 m NW of junction for Arginia (= 22.1 km ESE of Argostoli), on rocks along road, 290 m alt., DH7416; 21-03-1988

722 *A. adrianae dubia* Gittenberger—W exit of Markopoulon (= 24.1 km ESE of Argostoli), on rocks along road, 285 m alt., DH7615; 21-03-1988

723 *A. contaminata incommoda* (Boettger)—300 m N of Ag. Georgios (= 24.3 km ESE of Argostoli), on wet soft sand-'stone', 220 m alt., DH7818; 21-03-1988

725 *A. adrianae adrianae* Gittenberger—Poros, rock-faces N side of bridge in cleft (25.1 km E of Argostoli), type loc., 10 m alt., DH8023; 21-03-1988

727 *A. contaminata incommoda* (Boettger)—180 m N of Poros-town bridge (= 25 km E of Argostoli), on isolated rocks between houses along coastal road, 1 m alt., DH8023; 21-03-1988

728 *A. adrianae adrianae* Gittenberger—200 m N of Poros-town bridge (= 25 km E of Argostoli), on isolated rocks between houses along coastal road, 1 m alt., DH8023; 21-03-1988

729 *A. adrianae adrianae* Gittenberger—Gorge 3.8 km SE of Poros (= 28.3 km ESE of Argostoli) on lower and higher rocks of gorge, 2–10 m alt., DH8220; 21-03-1988

730 *A. adrianae adrianae* Gittenberger—Poros, N rocks along river E from bridge in cleft (= 25.1 km E of Argostoli), 5–15 m alt., DH8023; 21-03-1988

731 *A. adrianae dubia* Gittenberger—2.5 km NW of Ag.Georgios, type loc. (= 22.8 km ESE of Argostoli) on high rock faces, 400 m alt., DH7618; 21-03-1988

734 *A. senilis flavescens* (Boettger)—1 km W of Kourouklata (= 6.4 km N of Argostoli), on

rocks along road, 140 m alt., DH5432; 22-03-1988

735 *A. contaminata contaminata* (Rossmässler)—1 km NE of N exit of Angon (= 14 km NNE of Argostoli); on rocks along road, 250 m alt., DH5641; 22-03-1988

736 *A. s. kolpomyrtensis* Kemperman & Gittenberger—2 km NE of N exit of Angon (= 15.3 km N of Argostoli), on rocks along road, 260 m alt., DH5641; 22-03-1988

742 *A. j. assicola* Kemperman & Gittenberger—Assos Peninsula, rocks along lower part of road to main entrance fortress (= 22.5 km NNE of Argostoli), 2–5 m alt., DH5948; 22-03-1988

744 *A. j. assicola* Kemperman & Gittenberger—Assos Peninsula (= 22.5 km NNE of Argostoli), fortress and southern rocks, 100 m alt., DH5948; 22-03-1988

746 *A. contaminata liebetruti* (Boettger)—1 km NE of Sami (= 17.2 km ENE of Argostoli), on rocks W of Tomb-cave, 35 m alt., DH7035; 22-03-1988

749 *A. contaminata* (Rossmässler)—1 km S of Fiskardo (= 30.8 km NNE of Argostoli), on rocks along bay, 10 m alt., DH6356; 24-03-1988

751 *A. senilis flavescens* (Boettger)—1.5 km S of Livadi, = 1 km N of Ag. Dimitrios (= 8.5 km NW of Argostoli), on sand-stone wall along road, 5 m alt., DH5033; 23-03-1988

752 *A. senilis senilis* (Rossmässler)—Lepada, 2.5 km S of Lixouri (= 4.5 km W of Argostoli), 100 m N of beach entrance on low rocks along coast, 2 m alt., DH5125; 23-03-1988

756 *A. senilis senilis* (Rossmässler)—Kastro Ag. Georgios, inside fortress on stone walls (= 7.0 km SE of Argostoli), 290 m alt., DH6021; 24-03-1988

759 *A. contaminata contaminata* (Rossmässler)—4 km NW of broadcasting plant on Megas Oros (= Oros Aenos)(= 14.3 km E of Argostoli), on rocks along road, 1260 m alt., DH6723; 25-03-1988

764 *A. contaminata odysseus* (Boettger)—Ithaka Isl., Perachori, in/on ruin Venetian Church in lower part village (= 1.7 km S of Vathi), 170 m alt., DH7545; 26-03-1988

765 *A. contaminata odysseus* (Boettger)—Ithaka Isl., 600 m S of Agros, on rock face along road-curve (= 4.5 km W of Vathi), 160 m alt., DH7147; 26-03-1988

766 *A. contaminata odysseus* (Boettger)—Ithaka Isl., W side of Poly-bay (= 11.2 km NW of Vathi), on rocks and walls, 1–5 m alt., DH6855; 26-03-1988

770 *A. contaminata odysseus* (Boettger)—Ithaka Isl., Kioni, most eastern port of town (= 9 km N of Vathi), along coastal road on wall, 5 m alt., DH7355; 26-03-1988

772 *A. contaminata incommoda* (Boettger)—2 km NW of Tzanata (= 21.8 km E of Argostoli), near bridge on sediment wall along old road to Mon. Atrou, 130 m alt., DH7623; 27-03-1988

773 *A. contaminata incommoda* (Boettger)—1.1 km E of Koulourata (= 16.9 km E of Argostoli), on high rock-faces along road, 420 m alt., DH7128; 27-03-1988

Outgroup species, locality-numbers are not on Figure 2.

1 *A. teres nordsiecki* Zilch—Greece, Crete, Province of Lasithi, Kavousi ravine, 50 m alt; 28-04-1988

2 *A. rebeli* Wagner—Greece, Crete, Province of Lasithi, NW of Orino, 620 m alt.; 6-04-1988

3 *A.* nov. spec.—Greece, Peloponnesos, Province of Arkadhia, E slope Parnon Mountain at 8.5 km SW of Astros, shadowed rocks in coniferious forest, 400 m alt., UTM FG43; 27-07-1988

4 *Isabellaria edmundi* Gittenberger—Greece, Peloponnesos, Province of Arkadhia, high rock-face along the forest road, 5 km (6 km along the road) N of Kosmas, 975 m alt., UTM FG51; 27-07-1988

MALACOLOGIA, 1992, 34(1–2): 63–73

EFFECT OF STARVATION AND HIBERNATION ON THE FINE STRUCTURAL MORPHOLOGY OF DIGESTIVE GLAND CELLS OF THE SNAIL *HELIX LUCORUM*

Vasilis K. Dimitriadis & Dimitris Hondros

School of Biology, Faculty of Sciences, Aristotle University of Thessaloniki, Thessaloniki 540 06, Greece

ABSTRACT

Thirty seven days hibernation resulted in significant changes in the morphology of the digestive gland epithelium of *Helix lucorum* compared to control animals: the number of the digestive cells significantly decreased, but the number of the other cell types of digestive gland, calcium and excretory cells significantly increased. The apical granules and the cisternae with dense cores of the digestive cells significantly increased in number and size, while the calcium granules of the calcium cells increased in number and showed more intense concentric rings compared to those of the control animals. In the excretory cells, the large vacuoles significantly increased in size, while in all the digestive gland cells the lipid inclusions decreased in number as hibernation proceeded. In some cases, cytoplasmic material was extruded into the lumen, and intercellular spaces appeared to be very dilated.

Forty days of starvation induced similar but less intense phenomena in the digestive gland of *Helix lucorum.* The possible physiological function of the crop epithelial cells and the digestive gland cells of *Helix lucorum* is discussed.

Key words: *Helix lucorum,* snail, digestive gland, fine structure, starvation, hibernation.

INTRODUCTION

Snails exposed to starvation or hibernation respond by minimizing their energy requirements (Prosser, 1973). Carbohydrate metabolism is the principal energy source during hibernation, whereas during starvation oxygen uptake decreases sharply during the first day and more slowly later (von Brand, 1931; von Brand et al., 1948). However, little is known about the biochemistry and the physiology, as well as the fine structural morphology of snails exposed to such conditions as hibernation and starvation. There is little information about the fine structure of the gut and digestive gland epithelium and other visceral tissues of snails exposed to starvation and hibernation (Sumner, 1965; Oxford & Fish, 1979; Janssen, 1985; Roldan, 1987). The majority of the data available deals with the fine structure and the physiology of the digestive gland mainly under normal conditions (see, for example, Sumner, 1965, 1966; Owen, 1966; Walker, 1970; Bowen & Davies, 1971; Oxford & Fish, 1979; Pipe, 1986; Roldan, 1987).

In the present study, the cells of the digestive gland of *Helix lucorum* were studied with the light and electron microscope under normal conditions. In addition, the morphology of the digestive gland was studied in starving and hibernating animals and was compared with the morphology existing under normal conditions.

MATERIALS AND METHODS

Adult snails of *Helix lucorum* (Gastropoda, Pulmonata, Helicidae) were collected from Edessa, northern Greece. The shell diameter of the snails used in the present study varied from 41 to 43 mm and the body weight from about 19 to 21.5 g.

Snails, deprived of food, were kept in a cold room at 4±1°C under a 9 h light (L): 15 h dark (D) photoperiod for 8, 12, 22 and 37 days, in order to be exposed to hibernating conditions (Lazaridou-Dimitriadou & Saunders, 1986). Control feeding snails were kept at 19±1°C and 13L:11D photoperiod. Starved snails were kept at 19±1°C and 13L:11D photoperiod for 15, 25 and 40 days. Four animals from each experimental group were dissected late morning, and the digestive gland was fixed in Karnovsky's fixative (Karnovsky, 1965), postfixed in 2% osmium tetroxide, dehydrated and embedded in Spurr's resin. Sections were cut

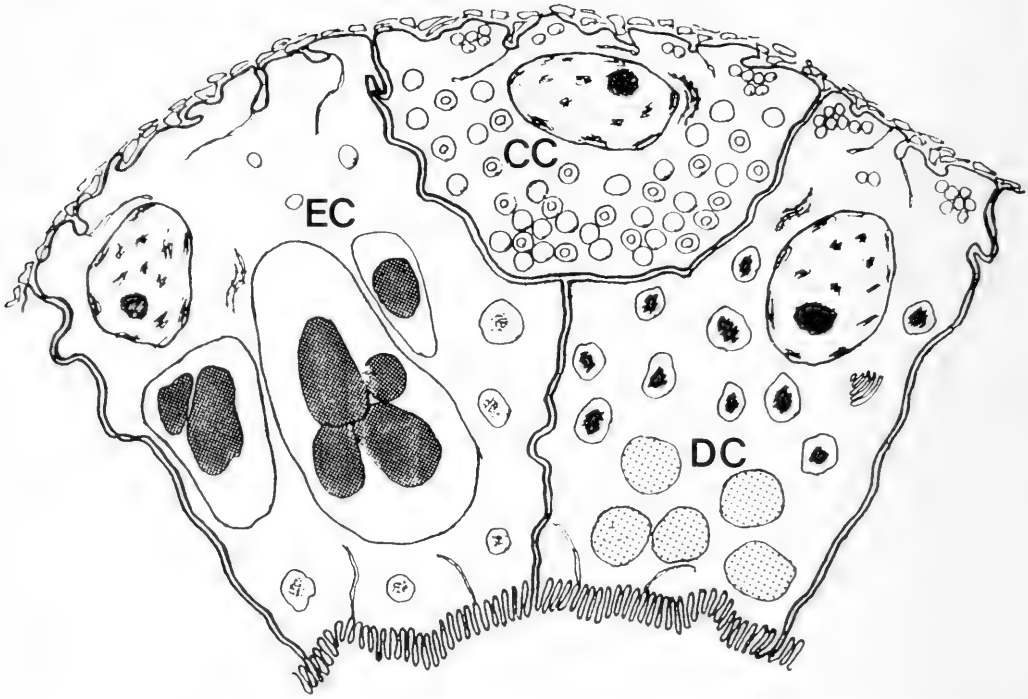

FIG. 1. Drawing of the various cell types observed in the digestive gland epithelium of *H. lucorum*. CC, calcium cell; DC, digestive cell; EC, excretory cell.

using a Reichert Om U3 ultramicrotome. The sections were poststained with lead citrate and uranyl acetate and examined under a Japan Electron Optics Laboratory Co. 100B electron microscope operating at 80 KV. For light microscopic observations, thick sections were stained with 1% toluidine blue.

Morphometric evaluation was performed according to Weibel (1979) and Steer (1981). Samples of five cells were counted from every digestive gland section of four different snails. The volume densities of certain morphometric parameters of crop and digestive gland organelles were determined from point counting stereology, using a test square lattice with a period d = 10 mm, equivalent to 1 μm on the specimen. A minimum of 480 points were counted per cell. The mean absolute volume of the various cells were estimated using the mean absolute volumes of the nuclei (using, depending of the cell type, the formula for a spheroid of prolate spheroid) and the ratio of nuclear/cytoplasmic volume. The mean total volume per cell of the various cell components were determined by their volume densities and the absolute volumes of the corresponding cells. The percentages of the various epithelial cell types within the digestive gland epithelium were determined from measurements on light microscopic micrographs at a final magnification of ×500. Cells were identified on the basis of morphologic criteria given in the Results section. Mean values and standard deviations of the morphometric parameters were calculated and statistically compared using Student's t-test, significant level $P < 0.05$.

RESULTS

Morphology of the Digestive Gland Epithelium

The digestive gland epithelium of *Helix lucorum* consisted of three cell types: digestive cells, calcium and excretory cells (Fig. 1). In cross sections of the gland tubules, the cells were located around a central lumen, and the whole structure was surrounded by connective tissue, muscular layers and a sys-

tem of haemocoelic spaces surrounded by amoebocytes.

Digestive cells were the most frequent cell type found in the digestive gland (Fig. 6). They usually appeared in a columnar shape, varied in size, and usually prossessed microvilli (Fig. 2). Digestive cells were characterized by numerous granules and cisternae of varying size and electron density. In the apical portion of these cells, there was usually a number of granules filled with a homogeneous material of a low electron density (Figs. 2, 3). In the middle region of the cells, smaller cisternae were also observed containing two or more intracisternal cores (Figs. 2, 3). At the base of the digestive cells, a few lipid inclusions were concentrated in clusters (Fig. 4). The nuclei of the digestive cells were usually located in the basal or in the middle regions of the cell and were usually well defined.

Calcium cells were the second cell type found in the digestive gland epithelium of *H. lucorum*. Their number was smaller than that of the digestive cells (Fig. 6). They were usually pyramidal in shape and did not usually protrude into the lumen, but they were located at the base of the epithelium. Their height was less than that of the digestive cells (Fig. 6). Calcium cells were usually filled with calcium granules which were located mainly in the basal region of the cells. Calcium granules were spherical in shape (Fig. 5) and were of a similar size throughout each cell. In high magnification, the calcium granules showed inner concentric rings. The nuclei of the calcium cells were usually located in their basal region, where lipid inclusions were often observed.

Excretory cells were the third cell type found in the digestive gland epithelium of *H. lucorum* (Figs. 12, 14). Their size was larger than that of digestive cells, their shape varied between ovoid and columnar, and their cytoplasm was characterized by one or more large cisternae containing cores or amorphous mass of high electron density. These cisternae occupied a large portion of the cell volume (Fig. 12). The nucleus was usually positioned at the basal region of the excretory cells and in their apical portion small vacuoles of low electron density were observed.

Morphology of the Digestive Gland Epithelium under Starving Conditions

Snails exposed to starving conditions showed modified morphology of the digestive cells compared to the control animals. After 40 days of starvation, a significant decrease in the number of these cells were noticed (Fig. 6). A significant increase in the total volume per cell of the apical granules located in the digestive cells compared to the control animals was also noticed in the same period (Figs. 7, 8). In contrast, the cisternae with the electron dense cores did not change significantly their total volume per cell after 40 days of starvation compared to the control animals (Fig. 7). Lipid inclusions decreased in number and almost disappeared after 40 days of starvation compared to control animals, while calcium granules increased their number and consequently their total volume per cell (Figs. 6, 7). In high magnification, the calcium granules also showed more concentric rings in starved snails (Fig. 11). However, the diameter of the calcium granules was similar in both starved and control animals.

Excretory cells significantly increased in number and volume after 40 days of starvation compared to the control animals (Figs. 6, 9). Moreover, the large cisternae of these cells significantly increased in size (Figs. 7, 9) so that they occupied over than half of the cell volume. Generally, the Golgi complexes and the rough endoplasmic reticulum of these cells were quite distinguishable and well organised in this stage.

After 25 and 40 days of starvation, extrusions of cytoplasm of whole cells into the gland lumen were apparent. Degeneration phenomena were rarely observed, while no of autophagic vacuoles were visible. The membrane infoldings appeared more intense, mainly in the basal region, and the intercellular spaces were more dilated than that of the control animals.

Morphology of the Digestive Gland Epithelium under Hibernating Conditions

After eight days of dormancy, the digestive gland cells did not show significant morphological changes. The only change noticed concerned the calcium cells, which showed more electron-dense concentric rings compared to those in control animals.

Thirty seven days exposure of *H. lucorum* in hibernating conditions induced fine structural modification of digestive gland cells. The digestive cells significantly increased in size, while their number decreased by about 25% (Fig. 6) compared to the control animals. The total volume per digestive cell of the apical

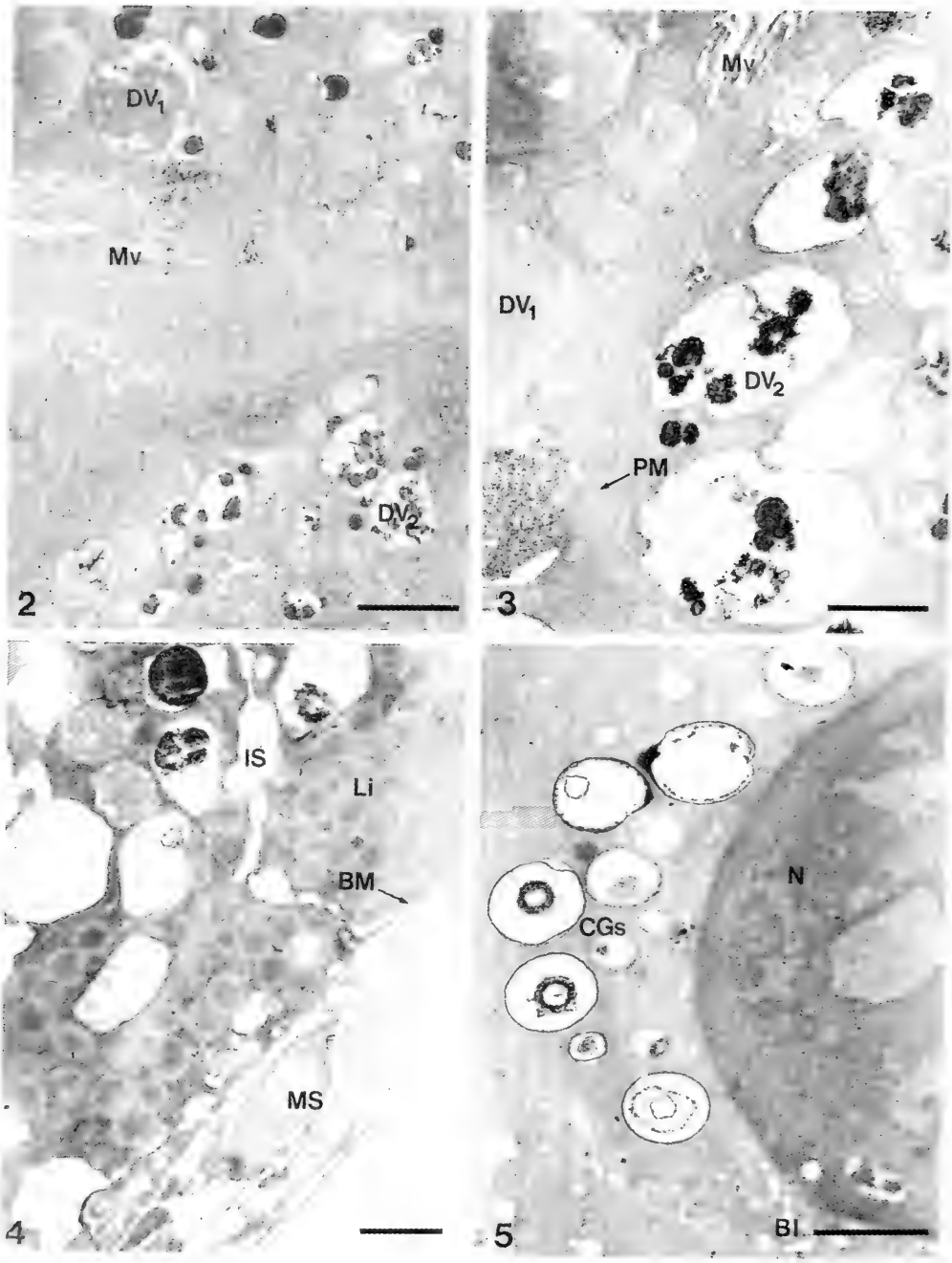

FIG. 2. Digestive cells contain apical granules with homogenous material (DV_1) and smaller cisternae with electron dense cores (DV_2). Mv, microvilli. Bar = 4 μm.
FIG. 3. Higher magnification view of the apical granules (DV_1) and of the cisternae with dense cores (DV_2) located in the apical portion of digestive cells. Mv, microvilli; Pm, plasma membranes. Bar = 6 μm.
FIG. 4. Numerous lipid inclusions (Li) appear in clusters at the base of digestive cells. BM, basement membrane, IS, intercellular space; MS, muscles. Bar = 3 μm.
FIG. 5. Calcium cells contain numerous calcium granules (CGs) with inner concentric rings. BI, basal infoldings; N, nucleus. Bar = 3 μm.

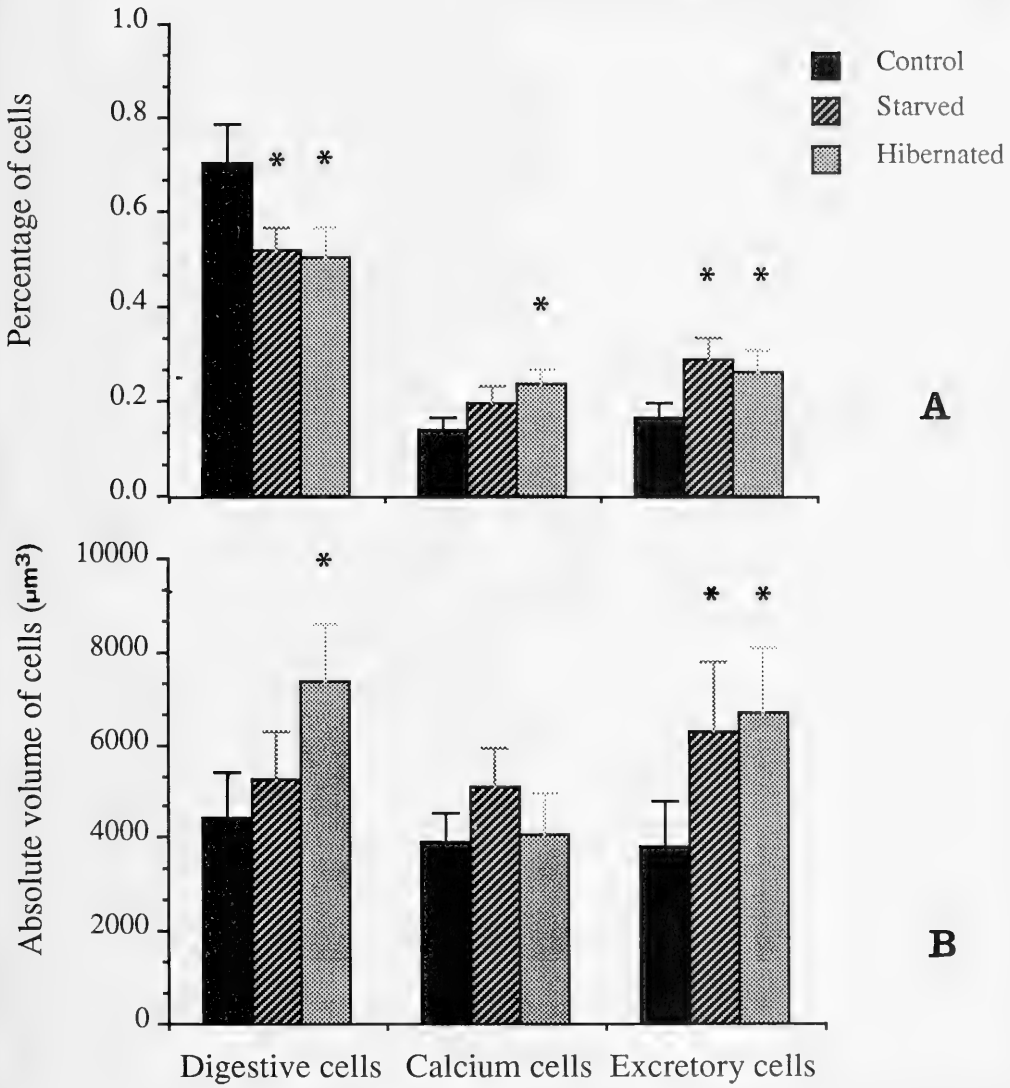

FIG. 6. Distribution (%) (A) and absolute volumes (B) of the various cell of control, starved (40 days) or hibernated animals (37 days) observed in the digestive gland of *H. lucorum*. Significantly different values ($P < 0.05$) among control and starved or control and hibernated animals are indicated by asterisks.

granules, as well as of the cisternae with the electron dense cores, significantly increased compared to the control animals (Fig. 7). Calcium cells significantly increased in number and slightly in size at that period (Fig. 6). As hibernation proceeded, calcium granules increased in number (Fig. 7) and appeared in clusters. The concentric rings in the calcium granules also had a higher electron density and increased in number in relation to the control animals (Fig. 11).

Another morphological effect of hibernation was a significant increase in the absolute volumes of the excretory cells compared to the control animals (Fig. 6). After 37 days of hibernation, the large cisternae of the latter cells also greatly increased in size and often occupied more than half of their cell volume

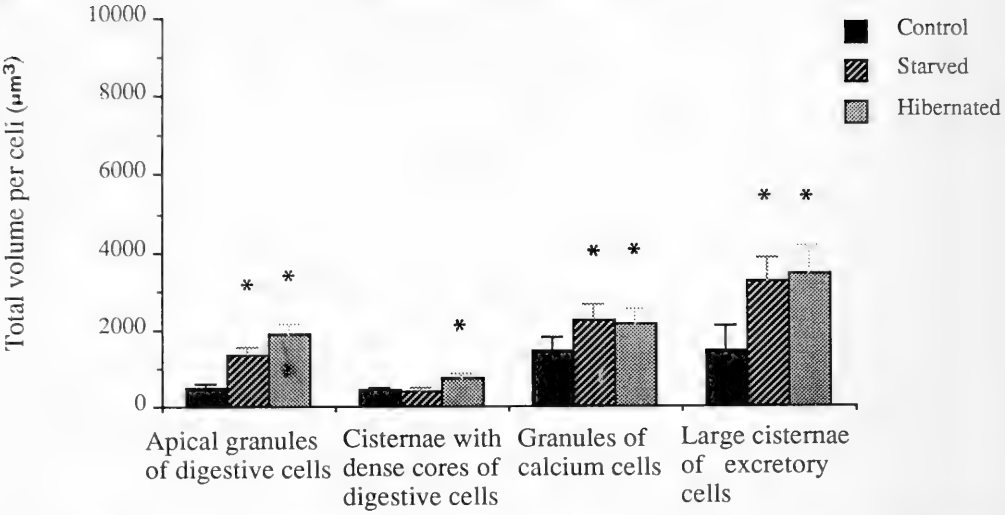

FIG. 7. Total volume per cell of cell components of digestive, calcium and excretory cells of control, starved (40 days) or hibernated cells (37 days) of digestive gland of *H. lucorum*. Significantly different values ($P < 0.05$) among control and starved or control and hibernated animals are indicated by asterisks.

(Figs. 7, 12, 13, 15). In all the cells studied, the number of lipid inclusions observed at the basal region greatly decreased 37 days after the exposure of the animals to hibernation, while the extracellular spaces formed by the infoldings of the basal plasma membrane and the intercellular spaces appeared very dilated in relation to the control animals. Cytoplasmic regions often extruded into the lumen. In addition, whole cells appeared to have degenerated and been released into the lumen (Fig. 10).

DISCUSSION

There are numerous studies on the morphology and physiology of epithelial cells in the digestive gland of the Pulmonata (Sumner, 1965, 1966; Walker, 1970; Bowen & Davies, 1971; Oxford & Fish, 1979) that are consistent with the fact that this, the largest organ, participates in digestion, absorption and storage of food material previously digested in the crop and stomach lumen. However, there are conflicting reports about the cell types that constitute the digestive gland epithelium of Pulmonata. Thus, Krijgsman (1925, 1928) considered digestive and excretory cells as different cell types. David & Götze (1963) distinguished one category of digestive calcium cells, whereas Billett & McGee-Russell (1955) considered calcium and excretory cells as distinct forms of digestive cells. Other studies supported the existence of three types of digestive gland cells in slugs: digestive, calcium and thin cells (Abolins-Krogis, 1961; Morton, 1979), considering excretory cells as digestive cells.

After 40 days of starvation or 37 days of hibernation, there was an increase in the volume of the digestive cells, as well as an increase in the total volume per cell of the apical granules in the digestive cells. This fact is consistent with the results of Sumner (1965), who reported that starvation resulted in vacuolisation of the digestive cells of *Helix aspersa,* as well as in an increase in size of the green granules compared to the control animals. Similar granules to the apical granules of digestive cells of *H. lucorum* were reported in the digestive glands of *Arion hortensis, Littorina littorea* and *Cepaea nemoralis* (Bowen & Davies, 1971; Oxford & Fish, 1979; Pipe, 1986) and were characterized as heterophagic, phagolysosomal or heterolysosomal cisternae. On the contrary, Krijgsman (1925, 1928), Walker (1970) and Sumner (1965), in *Helix pomatia* and *Agriolimax reticulatus,* referred to similar granules as green vacuoles due to their staining with light green. There are also histochemical results in other snails indicating that these cisternae display a positive PAS (Walker, 1969), acid phosphatase,

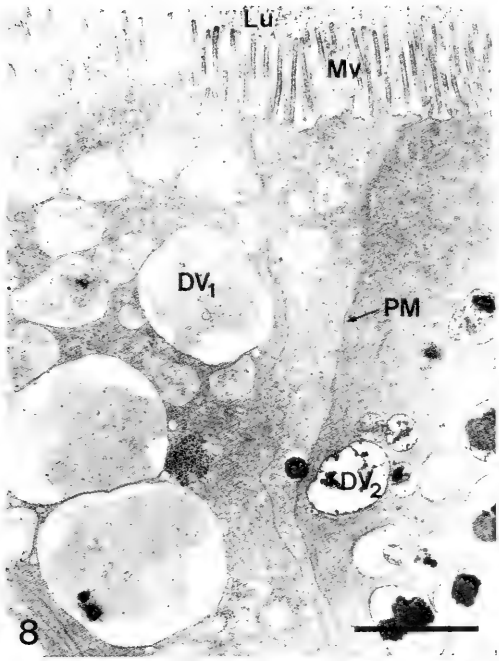

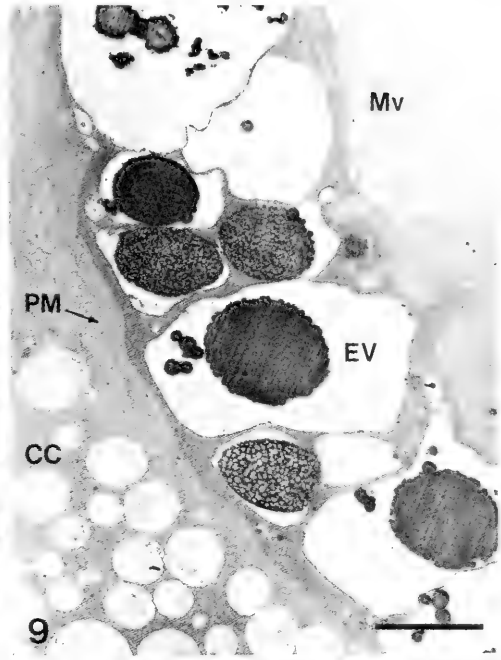

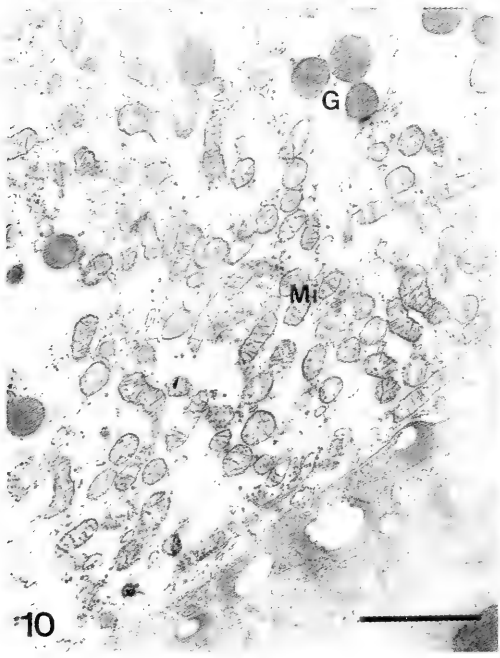

FIG. 8. 40 days' starvation. Apical portion of digestive cells possessing large number of apical granules (DV_1). DV_2, cisternae with dense cores; Lu, lumen; Mv, microvilli; PM, plasma membrane. Bar = 3 μm.
FIG. 9. 40 days' starvation. Excretory cells display many large cisternae (EV) with large electron dense cores. Mv, microvilli; PM, plasma membrane; CC, calcium cell. Bar = 5 μm.
FIG. 10. 22 days' hibernation. Part of the cytoplasm of a digestive gland cell shows degenerating phenomena. Mi, mitochondria; G, granules. Bar = 3 μm.
FIG. 11. 37 days' hibernation. Calcium granules containing two or more inner concentric rings (CRs). Bar = 1 μm.

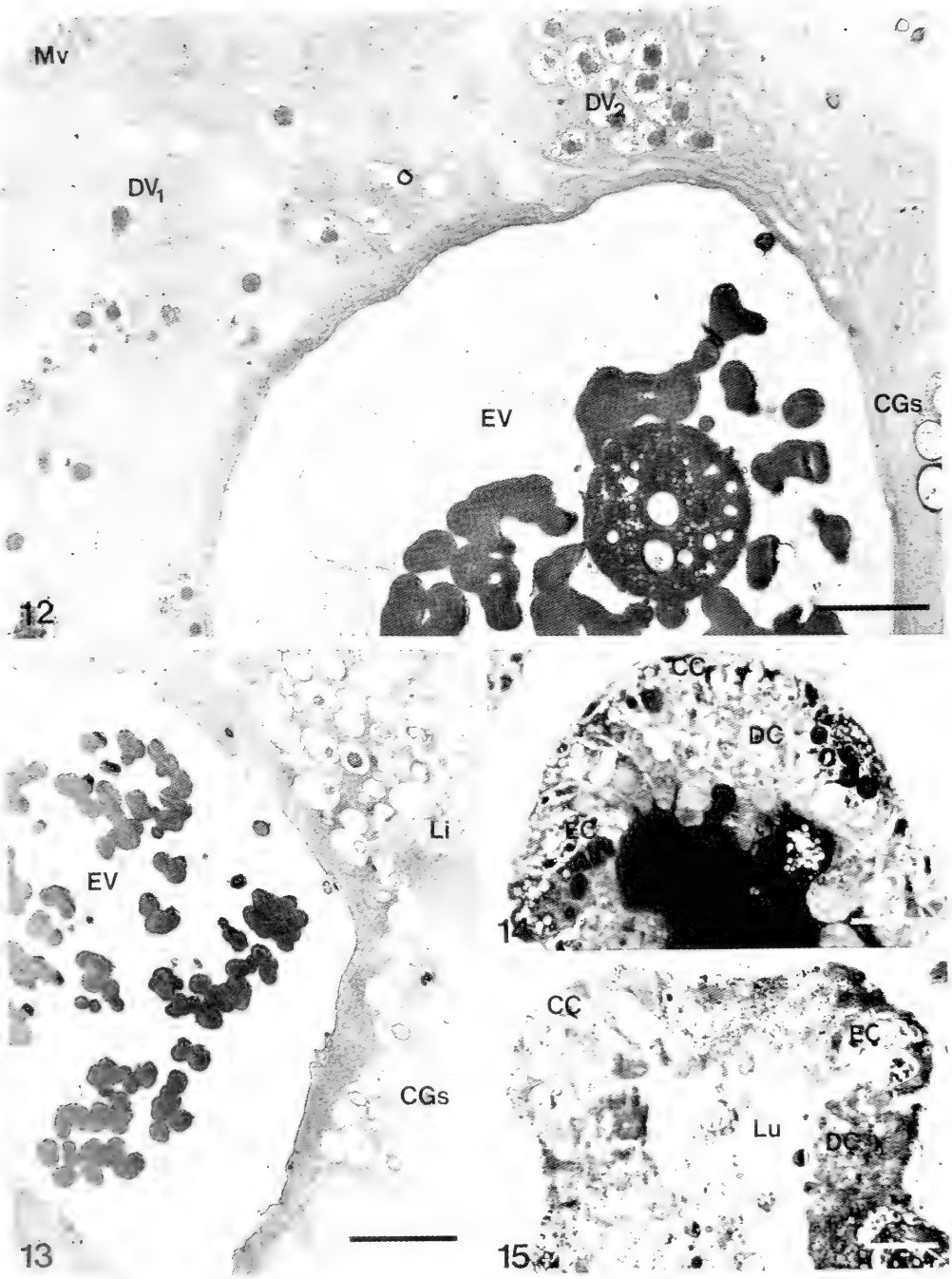

FIGS. 12. 13. 37 days' hibernation. Part of large cisternae (EV) with large electron-dense cores occupying great cytoplasmic areas of excretory cells. CGs, calcium granules; DV_1, apical granules; DV_2, cisternae with dense cores; Li, lipid inclusions; Mv, microvilli. Fig. 12 Bar = 5 μm. Fig. 13 Bar = 6 μm.
FIGS. 14, 15. Light microscopic view of digestive gland epithelium of control (Fig. 14) and hibernating animals (Fig. 15). Many excretory cells (EC) and calcium cells (CC) are observed in the epithelium of the hibernating snails, compared to the control ones. DC, digestive cells; Lu, lumen. Fig. 14 Bar = 20 μm. Fig. 15 Bar = 20 μm.

esterase (Bowen, 1970; Bowen & Davies, 1971) and B-glucuronidase reactions (Billett & McGee-Russell, 1955). This fact probably indicates that elaboration of material with certain enzymes inside these cisternae occurs.

After 37 days of hibernation, the total volume per digestive cell of the cisternae with dense cores, which probably correspond to the green granules of *Helix aspersa,* was found to have increased. Similar cisternae have been reported in the equivalent cells of *H. aspersa,* where they were characterized as yellow granules and exhibited positive reactions for calcium and lipofuscin, as well as positive PAS activity (Sumner, 1965). Also, Pipe (1986) observed similar cisternae in the digestive cells of *Littorina littorea* and suggested that they probably were cut off from heterolysosomal vesicles and filled with waste material. Sumner (1965) also supported the view that similar cisternae could contain remnants of intracellular digestion that must be extruded to the central lumen.

From the above-mentioned reports it could be concluded that the apical granules and cisternae with dense cores in digestive gland cells are structures involved in endocytotic processes. There are reports supporting the existence of phagocytosis in the digestive glands of most Gastropoda (Owen, 1966; Oxford & Fish, 1979). Owen (1966) claimed that the existence of phagocytosis in certain species of Mollusca may be an adaptation to functional needs. In the present study, the fine structural characteristics of digestive cells of *H. lucorum* support the view that these cells are responsible for absorption and digestion of food material, as well as production and secretion of digestive enzymes. However, phagocytosis of solid food material by the cells examined was not observed. It is possible that nutrients are absorbed by small pinocytotic vesicles forming the apical granules and consequently are degraded by lysosomal action, producing the cisternae with dense cores. Thus, the increase of the total volume per cell of the apical granules and of the cisternae with dense cores could probably be attributed to the accumulation of residual indigestible material inside the digestive cell, reflecting decreased digestive and excretory functions of these cells due to hibernation.

The absolute volume of the excretory cells, and the volume of their large cisternae, increased during hibernation. There is a controversy about the origin and the function of excretory cells. Thiele (1953) and Sumner (1965) suggested that they are degenerating calcium cells, as they contained only a small quantity of DNA in their nuclei, little cytoplasm and a small number of mitochondria. Fretter (1952), Billett & McGee-Russell (1955) and Walker (1970) proposed that they are differentiated forms of digestive cells. Abolins-Krogis (1961) found mucopolysaccharides, proteins, lipids and small quantities of RNA in similar vacuoles of *Helix aspersa* and suggested that this material is used for shell repair. In *H. lucorum,* the increase in size of the large cisternae, is probably a result of accumulation of excretory material inside the excretory cells, which probably reflects the minimizing of their excretory processes during hibernation.

In the present study, the electron microscopic examination of *H. lucorum* digestive glands revealed the presence of three cell types: digestive cells, calcium cells and excretory cells. The morphological features suggest that excretory cells constitute a distinct cell type. Morton (1975, 1979) supported the view that excretory cells of Pulmonata are digestive cells in different stages of a sequence of cytological changes over the course of 24 hours. Also Walker (1970) supported the view that excretory cells of *Agriolimax reticulatus* digestive glands are degenerating cells full of lipofuscin, which are formed from digestive cells. If this hypothesis can be supported, the excretory cells should be the final step in the development of the digestive cells. In that case, the excretory cells contain the digestive remnants of ingested material, which are degraded by lysosomal action and are finally discharged into the gland lumen. Arising from this hypothesis are the following questions: (1) Why is the population density of the excretory cells in *H. lucorum* digestive glands apparently smaller than that of the digestive cell? (2) Why are there no cell types intermediate between digestive and excretory cells in the examined digestive glands?

Another characteristic feature that 37 days hibernation induced was an increase in the number of calcium cells. This is evidently due to the participation of these cells in the formation of the calcareous epiphragm that covers the peristome of the snail during hibernation. The role of calcium in gastropods and other molluscs is multiple: it is regarded as a component being implicated in pH homeostasis (Sminia et al., 1977; Akberalli et al., 1977; Jokumsen & Fyhn, 1982), in reproduction (Tompa & Wilbur, 1977; Fournié & Chetail,

1982), in regulation of freezing tolerance (Murphy, 1977), as a component of mucus (Barr, 1928), in metabolic waste production (Kniprath, 1975), and in shell regeneration and formation of the epiphragm during hibernation (Abolins-Krogis, 1961, 1965; Wagge, 1951). In pulmonates, calcium appears as carbonate (Wagge, 1951) or phosphate (Krijgsman, 1928; Oxford & Fish, 1979), in a crystalline form or as an amorphous mass (Wagge, 1951). In the hepatopancreas of *Helix aspersa* (Howard et al., 1981), calcium granules contain $CaMgP_2O_7$. These granules are sites for accumulation of a wide variety of cations, acting as a detoxification mechanism that traps a number of dietary metals. However, the wide functions of these granules are largely unknown (Taylor et al., 1988).

Autolysis and extrusions of cytoplasmic material into the digestive gland lumen of *H. lucorum* were increased significantly as starvation and hibernation proceeded. A similar cell response is also referred to by Bowen & Davies (1971) and Oxford & Fish (1979) in *Arion hortensis* and *Cepaea nemoralis,* where release of hydrolytic enzymes from the cytoplasm of digestive cells was related to an increase in the rate of cell autolysis. In *H. lucorum,* the extrusion of cytoplasmic pieces into the lumen was possibly related to the reduction of energy requirements of the epithelium and the maintenance of low function activity of the digestive gland cells.

By using light and electron microscopic observations and stereological evaluation, the present study provides fine structural information about how hibernation and starvation affects the cells of the digestive gland of *H. lucorum.* However, more information, especially from the use of cytochemical methods, is needed for a better understanding of the physiology of the phenomenon of hibernation in snails.

ACKNOWLEDGEMENTS

This work was supported financially by the Greek Ministry of Agriculture. We are grateful to Dr. M. Lazaridou-Dimitriadou, who provided the snails and kept them under normal, starvation and hibernation conditions.

LITERATURE CITED

ABOLINS-KROGIS, A., 1961, The histochemistry of the hepatopancreas of *Helix pomatia* (L.) in relation to the regeneration of the shell. *Arkiv für Zoologie,* 13:159–201.

ABOLINS-KROGIS, A., 1965, Electron microscope observations on calcium cells in the hepatopancreas of the snail *Helix pomatia* (L.). *Arkiv für Zoologie,* 18:85–92.

AKBERALLI, H. B., K. R. M. MARRIOTT & E. R. TRUEMAN, 1977, Calcium utilization during anaerobiosis induced by osmotic shock in a bivalve mollusc. *Nature,* 266:852–853.

BARR, R. A., 1928, Some notes on the mucus and skin glands of *Arion ater. Quarterly Journal of Microscopical Science,* 71:503–526.

BILLETT, F. & S. M. McGEE-RUSSELL, 1955, The histochemical localization of β-glucuronidase in the digestive gland of the Roman snail (*Helix pomatia*). *Quarterly Journal of Microscopical Science,* 96:35–48.

BOWEN, I. D., 1970, The fine structure localization of acid phosphatase in the gut epithelium cells of the slug *Arion ater* (L.). *Protoplasma,* 70:247–270.

BOWEN, I. D. & P. DAVIES, 1971, The fine structure distribution of acid phosphatase in the digestive gland of *Arion hortensis* (F.). *Protoplasma,* 73:78–81.

DAVID, H. & J. GÖTZE, 1963, Electronenmikroskopische befunde an der Mitterdarmdruse von Schmenken. *Zeitschrift für Microscopisch-anatomische Forschung,* 70:252–272.

FOURNIÉ, G. & M. CHETAIL, 1982, Evidence for a mobilization of calcium reserves for reproduction requirement in *Deroceras reticulatum. Malacologia,* 22:285–291.

FRETTER, V., 1952, Experiments with ^{32}P and ^{131}I on species of *Arion* and *Agriolimax. Quarterly Journal of Microscopical Science,* 93:133–146.

HOWARD, B., P. C. M. MITCHELL, A. RITCHIE, K. SIMKISS & M. G. TAYLOR, 1981, The composition of intracellular granules from the metal-accumulating cells of the common garden snail (*Helix aspersa*). *Biochemical Journal,* 194:307–311.

JANSSEN, H. H., 1985, Some histophysiological findings on the midgut gland of the common garden snail, *Arion rufus* (L.). *Zoologischer Anzeiger,* (Jena) 215:33–51.

JOKUMSEN, A. & H. J. FYHN, 1982, The influence of aerial exposure upon respiratory and osmotic properties of hemolymph from two intertidal mussels, *Mytilus edulis* and *Modiolus modiolus. Journal of Experimental Marine, Biology and Ecology,* (B)61:189–203.

KARNOVSKY, M. J., 1965, A formaldehyde-glutaraldehyde fixative of high osmolarity for use in electron microscopy. *Journal of Cell Biology,* 27: 137A–138A.

KNIPRATH, E., 1975, Das Wachstum des Mantels von *Lymnaea stagnalis* (Gastropoda). *Cytobiologie,* 10:260–267.

KRIJGSMAN, B. J., 1925, Arbeitsrhythmus der Verdauungsdrüsen bei *Helix pomatia.* 1. Die naturlichen bedingungen. *Zeitschrift für Vergleichende Physiologie,* 2:264–296.

KRIJGSMAN, B. J., 1928, Arbeitsrhythmus der Verdauungsdrusen bei *Helix pomatia.* 2. Sekretion, Resorption und Phagocytose. *Zeitschrift für Vergleichende Physiologie,* 8:187–280.

LAZARIDOU-DIMITRIADOU, M. & D. S. SAUNDERS, 1986, The influence of humidity, photoperiod, and temperature on the dormancy and activity of *Helix lucorum* L. (Gastropoda, Pulmonata). *Journal of Molluscan Studies,* 52: 180–189.

MORTON, B., 1975, The seasonal variation in the feeding and digestive cycle of *Amphibola crenata* (Martin 1784) (Gastropoda: Pulmonata). *Forma et Functio,* 8:175–190.

MORTON, B., 1979, The diurnal rhythm and the cycle of feeding and digestion in the slug *Deroceras carnuanae. Journal of Zoology,* 187:135–152.

MURPHY, D. J., 1977, A calcium dependent mechanism responsible for increasing freezing tolerance of the bivalve mollusc *Modiolus demissus. Journal of Experimental Biology,* 69:13–21.

OWEN, G., 1966, Digestion. In: *Physiology of Mollusca,* Vol. 2, K. M. WILBUR & C. M. YONGE, eds. Academic Press, New York, San Francisco.

OXFORD, G. S. & L. J. FISH, 1979, Ultrastructural localization of esterase and acid phosphatase in digestive gland cells of fed and starved *Cepaea nemoralis* (L.). *Protoplasma,* 101:186–196.

PIPE, R. K., 1986, Light and electron microscopic localization of β-glucuronidase activity in the stomach and digestive gland of the marine gastropod *Littorina littorea. Histochemical Journal,* 18:175–186.

PROSSER, C. L., 1973, *Comparative animal physiology.* W. B. Saunders Company, London.

ROLDAN, C., 1987, Ultrastructural modifications of the epithelium in the anterior digestive tract in starved specimens of *Theba pisana. Iberus,* 7: 153–164.

SMINIA, T., N. D. de WITH, J. L. BOS, M. E. Van NIEUMEGEN, M. P. WITTER & J. WONDERGEM, 1977, Structure and function of the calcium cells of the fresh water pulmonate snail *Lymnaea stagnalis. Netherland Journal of Zoology,* 27: 195–208.

STEER, M. W., 1981, *Understanding cell structure.* Cambridge University Press, Cambridge.

SUMNER, A. T., 1965, The cytology and cytochemistry of the digestive gland cells of *Helix. Quarterly Journal of Microscopical Science,* 106:173–192.

SUMNER, A. T., 1966, The fine structure of the digestive gland cells of *Helix, Succinea* and *Testacella. Journal of the Royal Microscopical Society,* 85:185–192.

TAYLOR, M. G., K. SIMKISS, G. N. GREAVES & J. HARRIES, 1988, Corrosion of intracellular granules and cell death. *Proceedings of the Royal Society of London,* B234:463–476.

THIELE, G., 1953, Vergleichende unterschuchungen uber den Feinbau und die Funktion der mitterdarmdrüse einheimischer Gastropoden. *Zeitschrift für Zellforschung und Microscopische Anatomie,* 38:87.

TOMPA, A. S. & K. M. WILBUR, 1977, Calcium mobilization during reproduction in snail *Helix pomatia* (L.). *Nature,* 270:53–54.

VON BRAND, T., 1931, Der Jahreszyklus im Stoffbestand der Weinbergschnecke (*Helix pomatia*). *Zeitschrift für Vergleichende Physiologie,* 14: 200–264.

VON BRAND, T., M. O. NOLAN & E. R. MANN, 1948, Observations of the respiration of *Australorbis glabratus* and some other aquatic snails. *Biological Bulletin,* 95:199–213.

WAGGE, L. E., 1951, The activity of amoebocytes and of alkaline phosphatases during the regeneration of the shell of the snail *Helix aspersa. Quarterly Journal of Microscopical Science,* 92: 307–321.

WALKER, G., 1969, *Studies on digestion of the slug Agriolimax reticulatus* (*M.*). Ph. D. Thesis, University of Wales.

WALKER, G., 1970, The cytology, cytochemistry and ultrastructure of the cell types found in the digestive gland of the slug *Agriolimax reticulatus* (M.). *Protoplasma,* 71:91–109.

WEIBEL, E. R., 1979, *Stereological methods.* Vol 1: Practical methods for biological morphometry. Academic Press, New York and London

Revised Ms. accepted 19 September 1991

MALACOLOGIA, 1992, 34(1–2): 75–86

SUPRASPECIFIC NAMES OF MOLLUSCS: A QUANTITATIVE REVIEW

Philippe Bouchet & Jean-Pierre Rocroi

Muséum National d'Histoire Naturelle, 55 Rue de Buffon, Paris 75005, France

ABSTRACT

The number of nomenclaturally available genus-group taxa described since 1758 for Recent and fossil molluscs has been estimated by two methods. One result stands at 28,400 names; another at 24,900 names, of which 12,700 are gastropods, 6,000 are cephalopods, 5,100 are bivalves and 1,100 are in the smaller classes. The yearly increment appears to have remained relatively stable since the late 19th century. It is presently at an average of 224 new genus-group names per year, with Cephalopoda representing precisely one-third of the names. At least 20% of the recently introduced taxa escape the *Zoological Record,* with the Soviet and paleontological literatures especially underrepresented. In the last 30 years, journals and books published in USSR, USA, and China contain altogether 50% of the new names. The total number of nomenclaturally available genus-group names of Recent molluscs is on the order of 12,000. It is estimated that the number of family-group names for molluscs is over 5,000.

Key words: genus-group names, family-group names, numbers, nomenclature, nomenclators, trends, literature coverage.

INTRODUCTION

Although estimates of molluscan species diversity (Nicol, 1969; Boss, 1971; for a criticism, see Solem, 1978) exist, genus-group names, as defined by Article 42 of the *International Code of Zoological Nomenclature,* have not received similar attention for many years. In molluscs, as in other large groups of Recent and fossil animals, taxonomic work is hampered by the lack of adequate, up-to-date, comprehensive manuals, and by the vast number of journals and books containing descriptions of new taxa. The fate of every family- or genus-level taxonomic treatise is to be incomplete or outdated the very year it is published. In malacology, the currently available taxonomic academic treatises are 20–50 years old (Wenz, 1938–1944; Zilch, 1959–1960; Moore, 1960–1971). In 1987, as a result of this frustration, we started to compile a loose-leaf index to the new supraspecific names proposed since 1960 for Recent and fossil molluscs, exclusive of cephalopods. As this work is now being extended to encompass the older literature, we have found it interesting to quantify the abundance of names involved, to identify trends in current taxonomic literature, and to evaluate the efficiency of the supposedly most complete indexing system, the *Zoological Record.* The present paper documents these findings and discusses their implications.

Taxonomic research in malacology demonstrates a strong division between cephalopod and non-cephalopod literature. In particular, ammonoid research is almost totally separated from other fields of molluscan research: malacological journals only exceptionally contain papers on ammonites; ammonite and other cephalopod specialists rarely interact with other malacologists in national and international congresses. Our index, which reflects our own research interests, excludes cephalopods and is itself an illustration of this dichotomy. As a consequence, while some of our results are concerned with Mollusca in general, others deal only with Mollusca exclusive of cephalopods.

METHODS

The number of genus-group taxa in Mollusca is based on an evaluation of the number of names contained in various catalogues, nomenclators and checklists. Names enumerated in the sources listed in Table 1 were counted. For the *Nomenclator Zoologicus,* we counted the molluscan names in 50 pages (chosen from five consecutive pages in ten random samples) per volume. The total of 250 pages sampled represents about 5% of 4,816 pages included in the *Nomenclator.* Only original spellings were considered.

To index the supraspecific names proposed after 1960, we first scanned the Mollusca volumes of the *Zoological Record* for the relevant years. For Cephalopoda, only genus-group names were considered: we simply counted them without further checking. For classes other than cephalopods, genus-group and family-group names were considered separately. The original publications were consulted, and all newly introduced names were checked and recorded.

In a second phase, we used a combination of approaches to find names (of non-Cephalopods) omitted in the *Zoological Record:* (a) We scanned biographical compilations of malacologists containing their lists of papers and taxa (e.g. Powell by Cernohorsky, 1988; Habe by Inaba & Oyama, 1977), and yearly or cumulative indices for malacological journals (e.g. Anonymous, 1979); (b) We searched malacological and regional journals not covered by the *Zoological Record* that we knew contained new malacological taxa (e.g. *Notiziario del CISMA,* Roma; *Schriften zur Malakozoologie,* Cismar); (c) We used library facilities in Paris (Muséum National d'Histoire Naturelle, Société Géologique de France, Centre National de la Recherche Scientifique, Université Pierre et Marie Curie and several personal libraries), Leningrad (Zoological Institute of the Academy of Sciences and All-Union Geological Institute of the Ministry of Geology), London (The Natural History Museum), Stockholm (Naturhistoriska Riksmuseet and University Library) and Frankfurt (Senckenberg Library), including browsing through collections of reprints in departmental libraries; (d) We reviewed available papers for secondary uses of supraspecific names published elsewhere in unrecorded places; this method proved particularly useful with the Soviet literature; (e) The recent (since 1985) Chinese paleontological literature is covered by the quarterly *Gushengwuxue Wenzhai* (English subtitle: Paleontological Abstracts), and we discovered many names in this abstracting journal; (f) Recently published catalogues of names (such as Vokes, 1980, 1990; Vaught, 1989) were also scanned for omissions, and several colleagues provided references to obscure names.

Our data base is therefore far more complete for non-cephalopods than for cephalopods. Even for non-cephalopods, it is admittedly still a little incomplete but provides the best available source of supraspecific names for the years 1960–1989.

RESULTS

Number of Genus-Group Taxa in Mollusca

We estimated the total number of genus-group names by two independant methods. One method relies primarily on a statistical analysis of the names listed in *Nomenclator Zoologicus.* The other is based on the various catalogues and checklists available for selected classes of the phylum.

Evaluation Based on *Nomenclator Zoologicus*

(a) 1758–1965: We counted molluscan genus-group names in a set of 250 pages of the *Nomenclator Zoologicus,* selected as described under "Methods." Excluding incorrect subsequent spellings, there is an average 4.77 molluscan names per page, and the total number of nomenclaturally available genus-group names can be estimated at 23,000 for the period 1758–1965. This number is a minimum because some names certainly have escaped the *Nomenclator Zoologicus.* It is our experience, however, that while omissions appear to become more numerous with recent volumes, as we document below, the coverage of the *Nomenclator Zoologicus* is fairly good for the years 1758–1935. We therefore believe 23,000 names to be a reliable estimate.

(b) 1966–1989: Using the combination of methods outlined above, our index of non-cephalopod names for the period 1966–1989 contains 3,644 genus-group taxa. For the same period, the *Zoological Record* lists 1,448 genus-group names of Cephalopoda. If it is conservatively assumed that 20% of the cephalopod names have escaped the *Zoological Record* (see below), then the total number of cephalopod names introduced during that period would be 1,810. The total number of molluscan genus-group names introduced in the years 1966–1989 is therefore approximately 5,400.

The total number of genus-group names in Mollusca therefore amounts to circa *28,400 names.*

Evaluation Based on Catalogues

A number of catalogues or counts are available for selected classes or subclasses of Mollusca. We have counted the number of genus-group names in comprehensive works,

TABLE 1. Number of genus-group names of molluscs, partitioned by class

	Total	Recent
Aplacophora	80 (a)	80 (a)
Monoplacophora	267 (b)	9
Polyplacophora	282 (c)	205 (a,c)
Bivalvia	5090 (d)	2043 (d)
Scaphopoda	63 (e)	57 (a)
Gastropoda	12721	9004 (a,g), 10451 (a)
Prosobranchia	7149 (f)	4112 (g), 5559 (a)
Opisthobranchia	982 (h)	817 (a)
Pulmonata	4590 (i)	4075 (a)
Hyolitha, Rostroconchia, etc..	362 (j)	0
Cephalopoda	6000 (k)	305 (l)
Total	24865	11703–13150

Sources:
(a) after Vaught (1989); (b) after Knight & Yochelson, and Knight, Batten & Yochelson, in Moore (1960), plus increment; (c) after van Belle (1975–78), plus increment; (d) after Vokes (1980), plus increment; (e) after Ludbrook, in Moore (1960), plus increment; (f) after Schilder (1947) for the period 1758–1932, an estimated increment of 45.5 names/yr. for the period 1933–1959 (see Table 4), and our own counts for 1960–1989; (g) same as (f), but estimated increment 24.3 names/yr; (h) after Zilch (1959–60), Russell (1971, 1986), and increment; (i) after Zilch (1959–60), plus increment; (j) Hyolitha and Tentaculitida after Fisher, in Moore (1962), plus increment; Rostroconchia after Vokes (1980), plus increment; (k) Ammonoida and Nautilida after Hewitt (1989), modified; (l) after Nesis (1987).

handbooks and catalogues, as listed in Table 1. Because none of these sources is complete to 1989, we have added an increment, based on our own index for the more recent years. When these independent subcounts are added, the result is *24,900* names (Figs. 1, 3).

Number of Genus-Group Names of Recent Mollusca

In this analysis, a name is classified as Recent if it is based on a Recent type species. Therefore, Recent and fossil constitute two mutually exclusive categories: we are fully aware that this is only an approximation of the actual situation.

From the sources listed in Table 1, we conclude the number of genus-group names of Recent Mollusca (Fig. 2; see also Fig. 4) to be approximately 12,000, or 42% of all molluscan genus-group names. As a comparison, Vaught (1989), who also listed incorrect subsequent spellings, chresonyms (one name may be tabulated several times), and some genus-group names with fossil type species, ennumerated approximately 15,000 names.

Discussion

The two estimates, 28,400 and 24,900, are consistent with each other and differ only by 12%. We believe that the discrepancy between the two figures arises mainly from our use of Schilder (1947) for an evaluation of the number of names in the Prosobranchia. Schilder's data were based on Wenz (1938–44), which is fairly complete only for names published before 1933. We do not know to what extent Schilder corrected his counts with the literature published in 1933–1947, and this fact alone could explain a "loss" of several hundred names.

Our results are intermediate between two previously published estimates: (1) Schilder (1949) estimated that there were 11,260 genera established for "living and fossil shells." Because he did not explain how he obtained his results, or what he meant with "shells," it is difficult to comment. We consider that this very low figure is a gross underestimation of the actual number of names involved, even when one appreciates that Schilder made his statement more than 40 years ago.

(2) Vokes (1967) stated he had a card file containing 40,000 names of Mollusca extracted from volumes 1–5 of *Nomenclator Zoologicus,* a much higher figure than our own results indicates. We corresponded with Dr. Vokes to discuss this difference, and we have had access to the card-index that was the basis for his 1967 and 1980 catalogues, which he generously donated in 1991.

It appears that Vokes listed incorrect subsequent spellings as well as original spellings: on average, 22.5% of the names enumerated in Vokes (1980) are incorrect subsequent spellings, and as many as 37.9% of the 8,200 cards in his bivalve card-index are for nomenclaturally unavailable names (incorrect subsequent spellings, chresonyms, etc.). From this evidence, we conclude that 40,000 was a gross overestimate, and that it should not be regarded as an accurate number of molluscan genus-group names.

Naming Activity in the Last 30 Years

In the period 1960–1989, 6,720 new molluscan genus-group names have been introduced. Numbers for classes other than ceph-

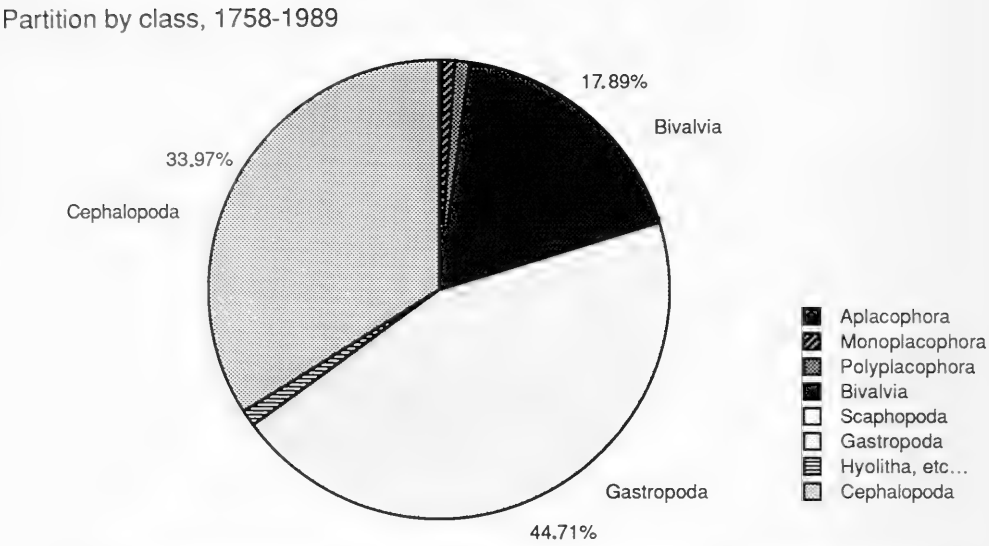

FIG. 1. Number of genus-group names of Mollusca introduced since 1758, partitioned by class.

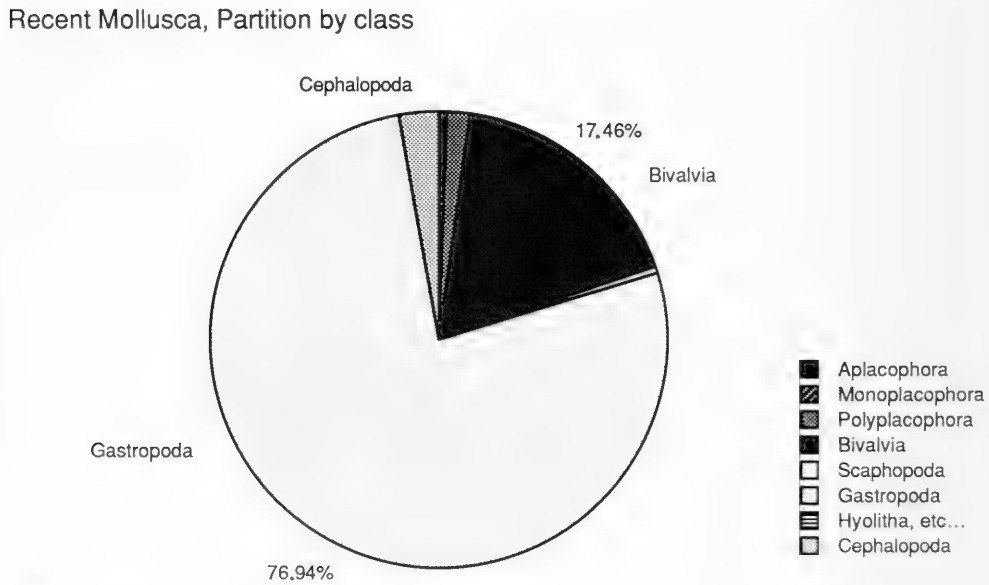

FIG. 2. Number of genus-group names of Recent Mollusca introduced since 1758, partitioned by class.

alopods represent genus-group names actually found by us. For the Cephalopoda, we use the count of names recorded by the *Zoological Record,* corrected on the basis of an estimated 20% omission rate by the *Zoological Record.*

The breakdown by class, and Recent vs. fossil, is presented in Table 2 and Figure 5. For simplicity, Caudofoveata and Solenogastra have been grouped under "Aplacophora," and the minor fossil classes are grouped under a single entry. For the controversial contents of the Monoplacophora, we have followed Runnegar & Pojeta (1985).

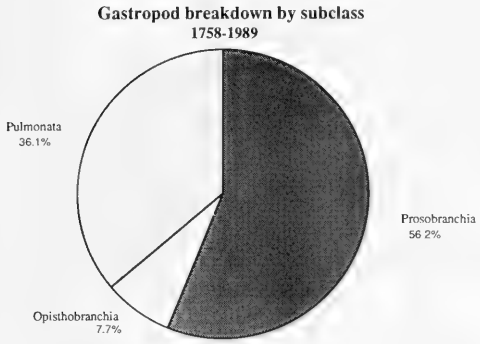

FIG. 3. Number of genus-group names of Gastropoda introduced since 1758, partitioned by subclass.

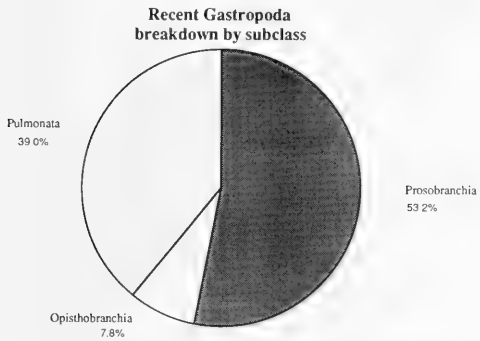

FIG. 4. Number of genus-group names of Recent Gastropoda introduced since 1758, partitioned by subclass.

These results lead to several observations:

1. Cephalopod names can be estimated at 33% of the total on the basis of volume 7 of *Nomenclator Zoologicus,* the only one that indicates class level. Counts for the entire period 1960–1989 give 33.3%. It is remarkable that 98.2% of all cephalopod genus-group names are based on fossils.
2. Within the Gastropoda, which comprises 37.5% of the total, the number of taxa can be further subdivided by subclass as presented in Table 3 and Figure 6.

   Of all gastropod names, 62.6% are based on Recent species, 37.4% on fossil species. It is interesting to note that 61.7% of Archaeogastropoda names, which date back to the early Paleozoic, are based on fossils, whereas only 40.9% of Neogastropoda, which date back to the Cretaceous, are based on fossils. Considering that there are many more taxonomists working on Recent gastropods than on Paleozoic ones, this would tend to indicate that name counts do reflect some pattern of overall diversity, rather than the activity of taxonomists.
3. Bivalves are, to a considerable extent, dominated by paleontological research: 79.6% of all bivalve genus-group names are based on fossil species.

Zoological Record Coverage

We have estimated the *Zoological Record* coverage by two alternative methods.

1. Volume 7 (1956–1965) of the *Nomenclator Zoologicus* is largely based on the *Zoological Record* (the same typographical errors that crept in the *Zoological Record* also appear in the *Nomenclator,* e.g. *Apollonia* misspelled *Appollonia*). We searched for 311 names (all the names beginning with A, B or C) known to us, published during this span of years—56 names (18.0%) were found missing in that volume.
2. For the period 1966–1989, the *Zoological Record* listed some 2,848 genus-group names of Mollusca exclusive of Cephalopoda. (Names published in the 1950s but recorded by the *ZR* in the 1960s were not counted by us in this total. Names published in 1989 and recorded by the *ZR* in the 1989–90 volume were counted.) Our own index contains 3,644 names for the same period. This indicates a coverage by the *Zoological Record* of 78.2%, or an omission rate of 21.8%.

   This is admittedly an optimistic estimate, because our own index has also certainly missed a number of names. For instance, we know of another 85 names with incomplete references or no references at all, which we have not yet been able to trace to their primary source. If these 85 names are considered when calculating the omission rate, it then jumps to 23.7%.

Therefore, it seems fair to conclude that at least 20% of new genus-group names have been omitted in the last 35 years by a nomen-

TABLE 2. Breakdown, by class, of new genus-group names introduced in 1960–1989

	Paleozoic	Mesozoic	Cenozoic	Total Fossil	Recent	Total	Increment (names/yr.)
Aplacophora	—	—	—	—	32	32	1.1
Monoplacophora	173	1	—	174	7	181	6.0
Polyplacophora	30	2	1	33	15	48	1.6
Bivalvia	301	525	275	1101	282	1383	46.1
Scaphopoda	7	1	1	9	24	33	1.1
Gastropoda	164	293	477	934	1566	2500	83.3
Hyolitha, Rostroconchia, etc.	305	2	1	308	—	308	10.3
Cephalopoda				2197	38	2235	74.5
Grand Total				4756	1964	6720	224

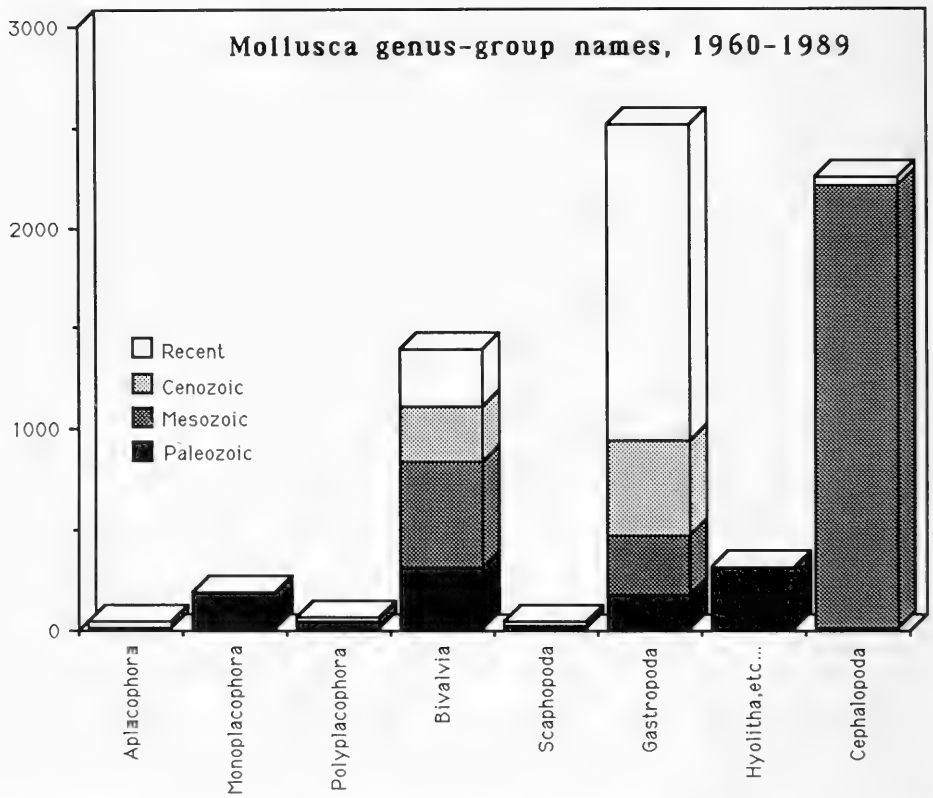

FIG. 5. Number of genus-group names of Mollusca introduced in the period 1960–1989, partitioned by class. All fossil Cephalopoda have been plotted under Mesozoic, which is admittedly an oversimplification.

clator considered to be the most complete in terms of coverage of the taxonomic literature.

It is important to emphasize that omission by the *Zoological Record* is not random. The most imperfect coverage is of the Soviet literature, in particular the coverage of paleontological monographs. Altogether, probably as much as one-third of names proposed in the Soviet literature escapes the *Zoological Record*. Other imperfectly covered literatures are those from China, Japan, South America and southern Europe. We confirm the generally accepted belief that books are much more poorly recorded than journals.

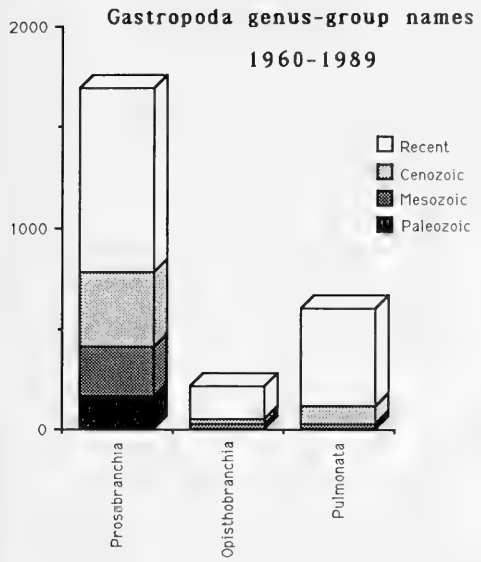

FIG. 6. Number of genus-group names of Gastropoda introduced in the period 1960–1989, partitioned by subclass.

Temporal Variation in Names Output

The year of publication of genus-group names has been extracted from the samples of the *Nomenclator Zoologicus* described above, and grouped by periods of 30 years. Table 4 shows the total number of genus-group names proposed for each period of 30 years, and the yearly rate within each of these eight periods.

An examination of the number of supraspecific names contained per volume of *Zoological Record* for the period 1960–1989 reveals considerable variability in the yearly output and indicates that no single randomly selected year can be considered representative for the period.

Table 4 and Figure 7 show a regular growth of the yearly increment during the first 100 years, with a faster growth in the latter part of the 19th century. The yearly output has subsequently remained remarkably stable at 170–200 genus-group names per year since 1880, with a slight minimum in the period 1936–1965 (also noted by Solem, 1978).

Hewitt (1989) stated that the recent decades are characterized by important "monographic bursts" in nautiloid and ammonoid taxonomy. Such bursts have certainly occurred elsewhere in selected groups and faunas, such as the Aplacophora, for which 40% of the names have been introduced in the last 30 years. However, contrary to a rather general belief among many molluscan taxonomists, Table 4 and the graph suggest only a moderate increase, not an overall explosion, in the output of names over this 30-year period.

Which Country Produces the Most Molluscan Taxa?

To answer this question we have plotted for 1960–1989 the number of new genus-group names (non Cephalopods only) by country of origin of the author (Fig. 8), and separately by country of publication. When multiple authorship is involved, each author is counted for 0.5 (two authors), 0.33 (three authors), etc.

In the period 1960–1989, authors from 53 countries are involved, with those from USSR, USA and China accounting for a little over half (50.3%) of the names. Below the 6th rank (New Zealand, 4.1%), the percentage is already below 5%, and the 1% mark is reached at the 17th rank (Cuba).

National output should **not** be used as a key to overall molluscan biological diversity of the different parts of the world. While it is true that, to some extent, the vast majority of the Japanese naming activity focuses on the Japanese (paelo)fauna, the naming activity of many countries involves faunas from several oceans or continents: a marine snail from the Caribbean is just as likely to be named by an American or a European author. In other words, there is no immediate biological explanation for the differences in numbers of mollusc genus-group names described in each country.

It is remarkable that New Zealand, Australia and Czechoslovakia, with national populations of respectively 3.4, 16.8 and 15.6 million, rank among the 10 countries with the highest output. New Zealand is then not only the country with the highest number of sheep per capita, but also the country with by far the highest output of mollusc genus-group names per capita!

Ranking by country of publication (Table 6) is not significantly different from the ranking by country of origin of authors. This means that authors do not, as a rule, "expatriate" their papers in journals of other countries. However, Germany and, to a lesser extent, Great Britain rank higher as publishers than

TABLE 3. Breakdown, by subclass, of new gastropod genus-group names introduced in 1960–1989

	Paleozoic	Mesozoic	Cenozoic	Total Fossil	Recent	Total
Prosobranchia	163	245	364	772	916	1688
Archaeogastropoda	148	61	26	235	146	381
Mesogastropoda	15	167	156	338	482	820
Neogastropoda	—	17	182	199	288	487
Opisthobranchia	—	24	21	45	168	213
Pulmonata	1	24	92	117	482	599
Total	164	293	477	934	1566	2500

TABLE 4. Estimates of number of genus-group names introduced during 30-year periods

period	1758–1787	1788–1817	1818–1847	1848–1877	1878–1907	1908–1935	1936–1965	1966–1989 (1)	1966–1989 (2)
time (yr)	30	30	30	30	30	28	30	24	
names	171	874	2755	3002	5643	5947	5115	4333	5454
increment	5.7	29.1	91.8	100.1	188.1	212.4	170.5	180.5	227.3

(1) Names actually recorded by the *Zoological Record* (2) Names found by us (non-cephalopods) + cephalopod names estimated on the basis of a 20% omission rate.

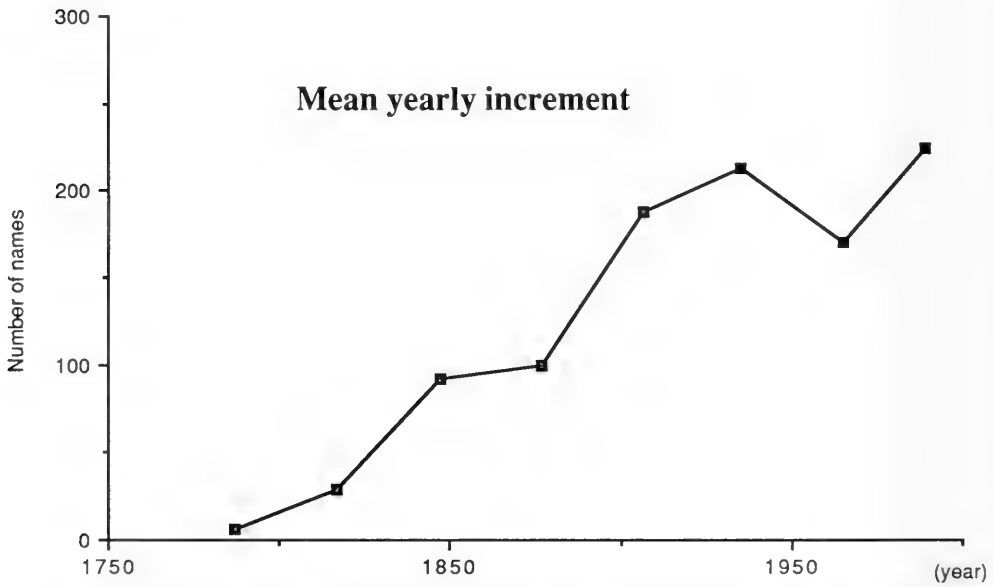

FIG. 7. Mean yearly increment of new genus-group names of Mollusca, calculated over 30-year periods.

as authors, whereas the opposite is true for New Zealand.

Family-Group Names

No estimate of the number of family-group names, as defined by Article 35 of the *Code*, available for molluscs has ever been published. A fact well known to taxonomists is that a new family may be erected without even mentioning that a new name is being introduced. For that reason, we believe that our data base is slightly less complete for family-group names than for genus-group names.

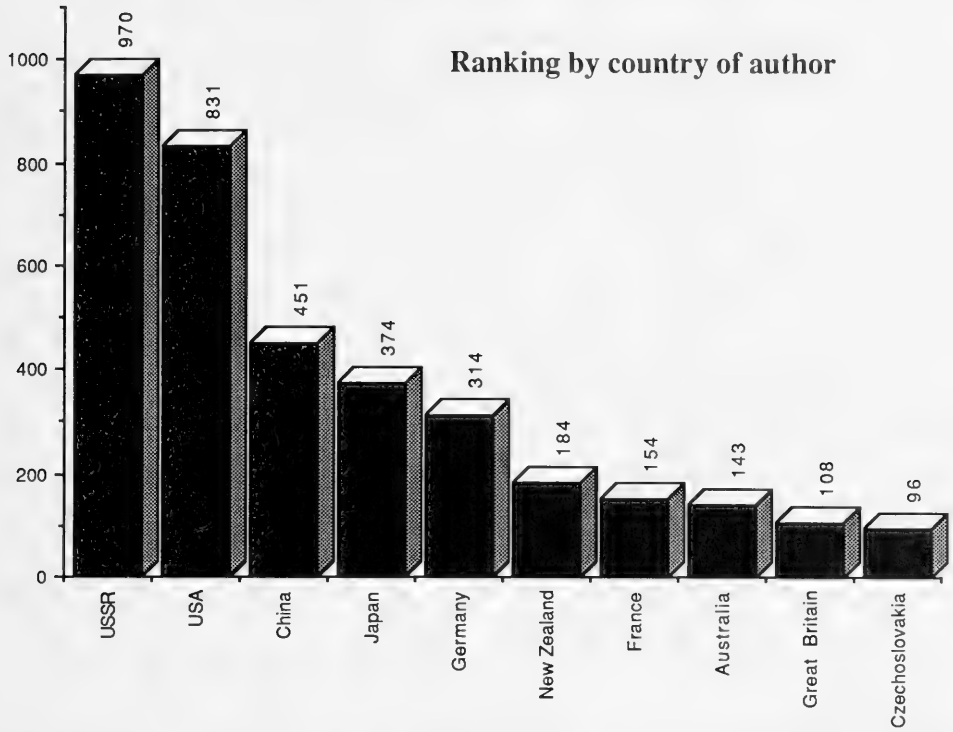

FIG. 8. Ranking of number of genus-group names of Mollusca (exclusive of Cephalopoda) introduced in 1960–1989, partitioned by country of origin of author.

TABLE 5. Ranking of country of origin of author as a function of total number of genus-group names.

1 Country	2 no. of names	3 %	4 Rank
USSR	970	21.6	1
USA	831	18.5	2
China	451	10.1	3
Japan	374	8.3	4
Germany	314	7.0	5
New Zealand	184	4.1	6
France	154	3.4	7
Australia	143	3.2	8
Great Britain	108	2.4	9
Czechoslovakia	96	2.1	10
Total	3625	80.7	

TABLE 6. Ranking of number of genus-group names arranged by place of publication (1960–1989)

Rank	Country	no. of names	%
1	USSR	955	21.3
2	USA	901	20.1
3	China	446	9.9
4	Germany	415	9.3
5	Japan	390	8.7
6	Australia	154	3.4
7	France	146	3.3
8	Great Britain	143	3.2
9	New Zealand	133	3.0
10	Italy	99	2.2
1–10		3782	84.4

The only partial checklist of family-group names is that by Ponder & Warén (1988) for the Caenogastropoda and Heterostropha. It lists 833 names, of which 187 were introduced in the period 1960–1987.

Our own index lists 1,102 new family-group names proposed for molluscs exclusive of cephalopods in the period 1960–1989. If we assume that the ratio of names published before and after 1960 is the same for Caeno-

gastropoda + Heterostropha as for the rest of the molluscs, then **the total number of family-group names available for molluscs exclusive of cephalopods can be estimated at 4,900.** No similar figure is available for Cephalopoda, but Hewitt (1989) counted 409 nautiloid and ammonoid families.

In our view, this demonstrates the need for a new nomenclatural tool that would be to family-group names what the *Index Animalium* (Sherborn, 1902; 1922–1932) and the *Nomenclator Zoologicus* are to species-group and genus-group names respectively.

Epilogue

The sheer magnitude of the numbers discussed in this paper will certainly draw contrasting opinions among malacologists. Two extreme views can be expected. In one view, the newly named taxa are deemed to represent taxonomically valid units, and the current naming activity simply demonstrates the gross incompleteness of the knowledge on the diversity of this phylum. In the opposite view, most of the newly created names are synonyms and the current naming activity is the symptom of a system gone crazy.

Superfluity in molluscan nomenclature appears to be a recurrent concern among professional taxonomists (e.g. Schilder, 1949; Nicol, 1958; Boss, 1971, 1978). Schilder (1949) estimated that 34% of the names available to classify prosobranchs were synonyms. However, whereas 49% of the names established in 1808–1857 were synonyms, the synonymy ratio decreased to 37%, 34% and 21% respectively for the next consecutive 25-year periods (Schilder, 1949). This can be interpreted in two ways: either taxonomists have been doing better work since the early 19th century, or it takes a long period of time (in excess of 75 years) before the value of a genus-group name can be properly assessed. It is likely that both elements reflect the actual situation, an opinion already expressed by Schilder & Schilder (1947). Schilder (1947) had also suggested that genus-group names of Recent and fossil prosobranchs, described and undescribed, would amount to about approximately 20,000, of which 5,000 would still be extant. This prediction may not be as unrealistic as it may first seem: in bivalves, fossils outnumber Recent genus-group names in the proportion of 2–3 to 1; and there are already in the order of 5,000 Recent prosobranch genus-group names. If Schilder was correct, this would mean that more than 10,000 fossil prosobranch genera still await naming, a daunting perspective!

Naming activity strongly reflects national traditions. There used to be a time when malacologists from Australia and New Zealand did not expect that their fauna might already have been described by workers in other parts of the world, and consequently engaged in overnaming what they considered to be entirely endemic faunas. The expression "another creation" was even used for the Australian biota. It is clear that this scientific isolation has now ended, and that the high level of molluscan naming activity in New Zealand and Australia is the result of a healthy descriptive malacology there in a worldwide context.

Notwithstanding our unfamiliarity with Paleozoic and Mesozoic faunas, we remain greatly concerned by the introduction of new taxa at the genus and family levels based on poorly preserved fossils or molds. Certain branches of malacology are also undoubtedly suffering from "inbreeding," a case in point being the immense literature on the Neogene Ponto-Caspian basins.

Despite these reservations, we do not share the view that overnaming is the single most important factor explaining yearly increments of 224 molluscan genus-group names, and 40+ family-group names. In the last 30 years, whole new faunas have been discovered, either Recent (e.g. oceanic hydrothermal vents) or fossil (e.g. lower Cambrian of China); old faunas have been readressed using new techniques (e.g. scanning electron microscopy, SCUBA diving) and new characters (e.g. anatomy of minute species). And, perhaps most importantly, the phase of intellectual stagnation that followed Thiele's epoch-making *Handbuch* is giving way to stimulating and provocative ideas. In this process, superfluous names undoubtedly become introduced, but we are convinced that these do not minimize the considerable amount of genuine discoveries being made every year.

The unexpectedly high omission rate of *Zoological Record* should cause concern to all taxonomists. Because this nomenclator is the main bibliographical source of many (paleo)zoologists, this factor alone poses an important threat to nomenclatural stability. We believe that this justifies the establishment of new criteria of availability of zoological names, whereby a published name would have to be registered by the International Commission of Zoological Nomenclature be-

fore it is declared nomenclaturally available (Bouchet, in press).

ACKNOWLEDGMENTS

For assistance with literature and/or calling our attention to names not listed in the *Zoological Record,* we thank A. Bogan (Academy of Natural Sciences, Philadelphia), S. Freneix (Institut de Paléontologie, Paris), R. Janssen (Senckenberg Museum, Frankfurt), A. Kabat (National Museum of Natural History, Washington, D.C.), T. Kase (National Science Museum, Tokyo), I. Loch (Australian Museum, Sydney), A. Lum (Natural History Museum, London), Z.-G. Ma (Institute of Geology and Paleontology, Academia Sinica, Nanjing), A. Matsukuma (National Science Museum, Tokyo), R. Petit (North Myrtle Beach, South Carolina), Yu. Starobogatov and M. Dolgolenko (Zoological Institute, Leningrad), H. Vokes (Tulane University, New Orleans) and A. Warén (Naturhistoriska Riksmuseet, Stockholm). For assistance in English, we thank A. Kabat. A. Foubert helped generating computer-produced figures.

LITERATURE CITED

ANONYMOUS, 1979, *Venus: Japanese Journal of Malacology. Volumes 1–36 (1928–1977).* The Malacological Society of Japan, Tokyo.

BOSS, K. J., 1971, Critical estimate of the number of Recent Mollusca. *Occasional Papers on Mollusks,* 3(40):81–135.

BOSS, K. J., 1978, Taxonomic concepts and superfluity in bivalve nomenclature. *Philosophical Transactions of the Royal Society of London,* (B)284:417–424.

BOUCHET, P. (in press), Proposal that a zoological name becomes nomenclaturally available from the date when the work containing its introduction is received by the Secretariat of ICZN. *Bulletin of Zoological Nomenclature*

CERNOHORSKY, W. O., 1988, Arthur William Baden Powell (1901–1987). A brief biography and bibliography with a list of molluscan taxa. *Records of the Auckland Institute and Museum,* 25:1–38.

EDWARDS, M. A. & A. T. HOPWOOD, 1966, *Nomenclator Zoologicus,* vol. 6. The Zoological Society of London, London.

EDWARDS, M. A. & H. G. VEVERS, 1975, *Nomenclator Zoologicus,* vol. 7. The Zoological Society of London, London.

GUSHENGWUXUE WENZHAI [= Paleontological Abstracts], 1986–1991. Quarterly. Institute of Geology and Paleontology, Nanjing.

HEWITT, R. A., 1989, Recent growth of nautiloid and ammonite taxonomy. *Paläontologische Zeitschrift,* 63:281–296.

INABA, T. & K. OYAMA, 1977, *Catalogue of molluscan taxa described by Tadashige Habe during 1939–1975, with illustrations of hitherto unfigured species.* Tokyo.

MOORE, R. C. (ed). *Treatise on invertebrate paleontology.* Part I, *Mollusca 1* (1960); Part N, *Mollusca 6* (vol. 1, 1969; vol. 2, 1969; vol. 3, 1971); Part W, *Miscellanea* (1962). The Geological Society of America & The University of Kansas.

NEAVE, S. A., 1939–1940, *Nomenclator Zoologicus,* vols 1–2 (1939), vols 3–4 (1940), vol. 5 (1950). The Zoological Society of London, London.

NESIS, K. N., 1987, *Cephalopods of the world.* TFH Publications, Neptune City.

NICOL, D., 1958, Trends and problems in pelecypod classification (the genus and subgenus). *Journal of the Washington Academy of Sciences,* 48(9):285–293.

NICOL, D., 1969, The number of living species of molluscs. *Systematic Zoology,* 18:251–254.

NOMENCLATOR ZOOLOGICUS. See Neave; Edwards & Hopwood; Edwards & Vevers.

PONDER, W. & A. WARÉN, 1988, Classification of the Caenogastropoda and Heterostropha. A list of the family-group names and higher taxa. *Malacological Review,* Supplement 4:288–326.

RUNNEGAR, B. & J. POJETA, 1985, Origin and diversification of the Mollusca. In: E. R. TRUEMAN & M. R. CLARKE, eds; *The Mollusca,* vol. 10, *Evolution,* 1–58. Academic Press, Orlando.

RUSSELL, H. D., 1971, *Index Nudibranchia (1554–1965).* Delaware Museum of Natural History, Greenville.

RUSSELL, H. D., 1986, *Index Nudibranchia. Supplement I, 1966–1975.* Department of Mollusks, Harvard University. Special Occasional Publication 7.

SCHILDER, F. A., 1947, Die Zahl der Prosobranchier in Vergangenheit und Gegenwart. *Archiv für Molluskenkunde,* 76:37–44.

SCHILDER, F. A., 1949, Statistical notes on malacology. *Proceedings of the Malacological Society of London,* 27(6):259–261.

SCHILDER, M. & F. A. SCHILDER, 1947, Zur Entwicklung der Molluskenkunde. *Archiv für Molluskenkunde,* 76:163–166.

SHERBORN, C. D., 1902, 1922–1932, *Index Animalium. Sectio I (1758–1800),* 1902, Cambridge; *Sectio II (1801–1850),* 1922–1932 (29 parts). British Museum, London.

SOLEM, A., 1978, Classification of the land mollusca. In: V. FRETTER & J. PEAKE, eds, *Pulmonates,* vol. 2A. *Systematics, evolution and ecology,* 49–97. Academic Press, London.

VAN BELLE, R. A., 1975–78, Sur la classification des Polyplacophora. *Informations de la Société Belge de Malacologie,* (4)5:121–134 (1975);

(4)6:135–152 (1975); 5(2):15–42 (1977); 6(1): 3–28 (1978); 6(2):35–44 (1978).

VAUGHT, K. C., 1989, *A classification of the living Mollusca.* American Malacologists, Melbourne, Florida.

VOKES, H. E., 1967, Genera of the Bivalvia: a systematic and bibliographic catalogue. *Bulletin of American Paleontology,* 51(232):1–394.

VOKES, H. E., 1980, *Genera of the Bivalvia: a systematic and bibliographic catalogue (Revised and updated).* Paleontological Research Institution, Ithaca.

VOKES, H. E., 1990, Genera of the Bivalvia: a systematic and bibliographic catalogue—Addenda and errata. *Tulane Studies in Geology and Paleontology,* 23(4):97–120.

WENZ, W., 1938–1944, *Handbuch der Paläozoologie.* Band 6, *Gastropoda.* Teil 1, *Allgemeiner Teil und Prosobranchia.* Borntraeger, Berlin.

ZILCH, A., 1959–1960, *Handbuch der Paläozoologie.* Band 6, *Gastropoda* Teil 2, *Euthyneura.* Borntraeger, Berlin.

ZOOLOGICAL RECORD for the years 1960–1989, 1963–1990, Part 9, Mollusca. The Zoological Society of London (1963–1980); BioSciences Information Service and the Zoological Society of London (1981–1990).

Revised Ms. accepted 2 January 1992

MALACOLOGIA, 1992, 34(1–2): 87–97

SHELL PATTERN POLYMORPHISM IN A 13-YEAR STUDY OF THE LAND SNAIL *THEBA PISANA* (MÜLLER) (PULMONATA: HELICIDAE)

Robert H. Cowie

Bishop Museum, P.O. Box 19000A, Honolulu, Hawaii 96817-0916, U.S.A.

ABSTRACT

Shell pattern gene frequencies in the helicid *Theba pisana* at Tenby, South Wales, did not change over a 13-year period at a range of sites differing in frequency. This apparent stability and the differences among sites may be maintained by selection, although the selective agent(s) is(are) unknown. Alternatively, selection may be absent (or too weak to be detected), and the differences among sites may be random due to the founder effect; in this case, stochastic fluctuations in gene frequency would be small in these large populations and directional changes would not be expected. The need for long-term ecological studies in order to address such questions is emphasized.

Key words: Pulmonata, *Theba pisana,* genetics, polymorphism, selection, founder effect.

INTRODUCTION

Long-term field studies are essential in evolutionary biology yet are rarely possible (Cain, 1983; Cowie, 1989). Subtle but important changes in the composition of communities, the relative distributions of species or the morph frequencies in polymorphic populations, or indeed the absence of such changes, can only be demonstrated by studies pursued over many years.

In the extensively studied European land snails *Cepaea nemoralis* (L.) and *C. hortensis* (Müller), stability in morph frequencies over periods of 5–50 years, as well as significant changes over such periods, have been found and attributed to natural selection (Cain, 1983; Murray & Clarke, 1978; Wall et al., 1980). Other studies have failed to detect selection (Cain & Cook, 1989; Cain et al., 1990). Striking changes in the relative distributions of the two species have also been reported (Cowie & Jones, 1987). Longer-term studies also have demonstrated significant changes in morph frequencies, attributable to both natural selection and historical factors (Cain, 1983; Cameron & Dillon, 1984).

The rather strict criteria for the successful study of gene frequencies over time (Murray & Clarke, 1978; and see also Endler, 1986, pp. 73–75) are that (i) accurately dated and localised data be available; (ii) the genetic control of the polymorphism be understood sufficiently to allow accurate scoring of genotypes; (iii) there be genetic continuity over the period of the study; and (iv) the selective significance of the characters be understood. The present study of morph frequencies in the land snail *Theba pisana* (Müller) fulfills all these criteria: the samples were all taken by the author from the same group of sites on specific dates and using the same collecting techniques (Cowie, 1984a, b); the genetics of the polymorphism have been elucidated by breeding experiments (Cowie, 1984a); samples were taken from continuously extant populations with overlapping generations every year from 1977 to 1989 (except 1982); and both visual selection by predators and climatic selection appear to influence both this polymorphism (Hazel & Johnson, 1990; Heller, 1981; Heller & Gadot, 1984; Johnson, 1980, 1981) and other aspects of visually detectable variation in *T. pisana* (Cowie, 1990).

Theba pisana is a coastal Mediterranean land snail, the distribution of which extends along the Atlantic coasts of north Africa and western Europe as far north as the southwestern parts of England and Wales and the east coast of Ireland. It has been introduced to Australia, South Africa and California. A five-year study of morph frequencies at six sites at Tenby, South Wales (Cowie, 1984a), failed to demonstrate any changes in morph frequencies over this period despite a hint that selection was acting against the unbanded (i.e. pale) morphs. The aims of the present study were to confirm or discount the possible selection and to assess the stability or otherwise of the morph frequencies over a longer period. All shells are deposited in the Mollusca Section of The Natural History Mu-

seum (London) (Mollusca Section accession number: 2355).

METHODS

Samples were collected from up to six sites between 24 May and 31 August of each year from 1977 to 1989 (except 1982) following the precise protocols of Cowie (1984a, b). All snails in a sample area were collected, so no bias in morph frequency, due to differential collection of certain morphs, was introduced. A map of the site locations is given by Cowie (1984a). *Theba pisana* is biennial at Tenby, breeding only once at the end of its second year and then dying. Summer samples taken prior to the start of the late summer/early autumn breeding season therefore have distinctly bimodal size frequency distributions, allowing easy separation of two-year-old adults from one-year-old juveniles by simple graphical analysis (Cowie, 1984b). Morph scores of the two age classes could, therefore, be analysed separately.

The data of Cowie (1984a) have been incorporated in the present analysis. The regular taking of more than one sample from some of the six sites, sometimes on more than one occasion during the 24 May–31 August period, was discontinued from 1983 onwards as being redundant: one sample only was taken from each site, and on only one occasion (between 24 May and 31 August) in each year. From 1986 onwards, a single sample only was taken from each of three sites, representing the three broad sampling areas at Tenby (see Cowie, 1984a).

Morphs were scored according to Cowie (1984a). The discussion over whether *T. pisana* is pentataeniate or tetrataeniate (Cowie, 1984a; Gittenberger & Ripken, 1987; Heller, 1981) does not affect the scoring of the polymorphism. The polymorphism in the Tenby populations is controlled by three loci with two alleles showing dominance at each. Epistasy allows only four main phenotypes to appear: plain unbanded, dotty unbanded (with a row of dots along the mid-line of the shell), dark five-banded and yellow five-banded; these are illustrated by Cowie (1984a). There is some blurring of the boundaries between the dark and yellow five-banded morphs such that it has been necessary to include an "intermediate" five-banded category (Cowie, 1984a). The blurred distinctions between the five-banded categories, combined with the variable shell size at which the dark banding lineolations appear, allow only limited conclusions to be drawn regarding this aspect of the variation, and indeed juveniles were scored simply as banded without distinction into dark, intermediate and yellow. However, the distinction between banded and unbanded shells, in both adults and juveniles, is clear since, in these populations, the apex (in fact the protoconch) of banded shells is always darker than that of unbanded shells. This association of banding pattern and apex colour is due to the very close linkage of the banded/unbanded and apex colour loci, combined with strong linkage disequilibrium, due presumably to selection (Cain, 1984; Cowie, 1984a). Mistakes in scoring are considered, then, to be insignificant.

RESULTS

Morph scores for all samples are given in Table 1. The differences between sites in the proportion of unbandeds, indicated by Cowie (1984a), have been maintained. Sites 2, 3 and 4, which are less than 100 m apart and more or less connected by suitable habitat with *T. pisana* present, show similar frequencies, most samples having 25–45% unbandeds (average about 34%). Sites 1, 5 and 6, the last two of which are close together but separated from site 1 by about 0.5 km of cliffs with no *T. pisana,* also have similar frequencies, most samples having 10–25% unbandeds (average about 17%).

Percentages of unbandeds through the course of the study at each site, for adults and juveniles separately, are shown in Figures 1–6. Regression analyses (Feldman et al., 1987) of these percentage data (arcsinh square root transformed) on year reveal no significant change ($p>0.05$ in all cases) in frequencies of unbandeds in either adults or juveniles at any site throughout the course of the study, either when all samples or only those of 30 or more individuals are included (Table 2). Morph frequencies have not changed significantly for 13 years. Two-way log-likelihood G-statistic analyses (Sokal & Rohlf, 1969) of the actual frequencies of unbandeds by year for each site separately (Table 3) indicate some heterogeneity among years (as detected by Cowie (1984a)) but no obvious trend, and do not contradict the overall absence of change. (Because of the lack of

TABLE 1. Morph scores for all samples.

Site	Year	Adults						Juveniles				
		unbanded		banded			Total adults	unbanded		banded	Total juveniles	Total
		plain	dotty	dark	intermed	yellow		plain	dotty			
1	1977	48	26	258	81	20	433	45	16	360	421	854
	1978	27	9	150	36	4	226	42	22	294	358	584
	1979	5	2	37	7	2	53	4	4	65	73	126
	1980	7	4	43	8	5	67	6	6	66	78	145
	1981	3	3	31	10	3	50	17	4	72	93	143
	1983	8	2	29	1	2	42	5	0	37	42	84
	1984	5	3	24	1	1	34	7	2	55	64	98
	1985	4	1	22	4	3	34	2	1	24	27	61
	1986	3	1	22	1	2	29	8	4	91	103	132
	1988	0	0	9	1	0	10	2	0	23	25	35
	1989	3	1	12	3	4	23	2	0	13	15	38
2	1977	203	42	269	63	18	609*	245	43	372	660	1269
	1978	133	51	204	67	21	476	90	22	164	276	752
	1979	21	12	52	9	4	98	32	11	89	132	230
	1981	81	39	159	59	20	358	47	16	88	151	509
	1983	24	8	36	3	11	82	32	11	57	100	182
	1984	14	7	35	4	4	64	36	20	129	185	249
	1985	77	28	115	10	13	243	17	3	51	71	314
	1986	18	5	35	5	4	67	43	6	91	140	207
	1987	43	11	60	9	17	140	22	0	63	85	225
	1988	39	15	57	12	12	135	25	11	50	86	221
	1989	28	10	54	9	6	107	18	7	38	63	170
3	1977	24	12	62	20	4	122	33	12	79	124	246
	1978	38	6	70	16	6	136	37	18	113	168	304
	1979	1	0	1	1	0	3	23	15	88	126	129
	1980	9	5	23	7	2	46	20	10	65	95	141
	1981	5	2	14	4	1	26	1	0	5	6	32
	1983	19	5	26	8	10	68	5	5	35	45	113
	1984	18	6	50	8	13	95	30	17	90	137	232
	1985	32	14	81	14	10	151	14	0	30	44	195
4	1977	51	23	104	29	8	215	66	6	106	178	393
	1978	55	35	143	33	7	273	106	65	297	468	741
	1979	12	5	30	5	3	55	52	15	132	199	254
	1980	34	17	44	13	2	110	42	15	110	167	277
	1981	26	21	83	21	11	162	16	10	43	69	231
	1983	17	4	39	8	10	78	17	12	77	106	184
	1984	59	9	146	9	9	232	23	15	59	97	329
	1985	65	15	115	9	10	214	8	0	32	40	254
5	1977	24	7	119	38	15	203	13	2	53	68	271
	1978	14	5	78	17	9	123	20	14	157	191	314
	1979	1	0	10	2	2	15	3	2	6	11	26
	1980	4	3	35	8	3	53	1	2	11	14	67
	1981	4	1	16	1	3	25	1	1	2	4	29
	1983	4	1	11	2	2	20	1	0	11	12	32
6	1977	23	10	139	39	10	221	16	4	104	124	345
	1978	19	2	87	18	7	133	20	7	219	246	379
	1979	0	0	16	12	1	29	3	2	29	34	63
	1981	10	2	57	21	7	97	21	5	94	120	217
	1983	11	1	103	14	13	142	7	1	57	65	207
	1984	13	8	86	15	17	139	7	1	88	96	235
	1985	22	5	82	5	9	123	10	3	130	143	266
	1986	11	3	61	7	4	86	12	2	89	103	189
	1987	9	4	49	7	12	81	28	2	111	141	222
	1988	5	1	57	15	8	86	29	12	165	206	292
	1989	10	5	57	18	11	101	33	10	253	296	397
	Total	1443	517	3807	847	415	7043	1465	494	5232	7191	14234

In certain years, samples were not collected as follows: 1980—sites 2, 6; 1982—all sites; 1984–1989—site 5; 1986–1989—sites 3, 4; 1987—sites 1, 3, 4, 5.

*There were 14 banded adults that were not scored as dark, intermediate or yellow. These have been included in analyses of banded/unbanded but excluded from analyses within the banded class.

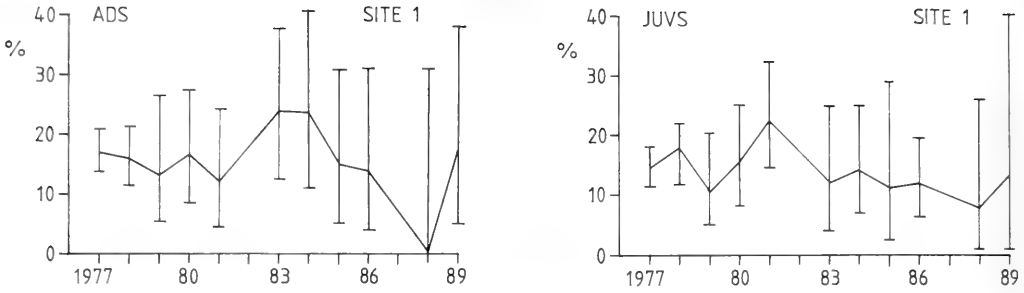

FIG. 1. Percent unbandeds in adults (ADS) and juveniles (JUVS) at site 1 for 1977–1989, with 95% confidence limits derived using the tables of Sokal & Rohlf (1973) supplemented by Goldstein (1964).

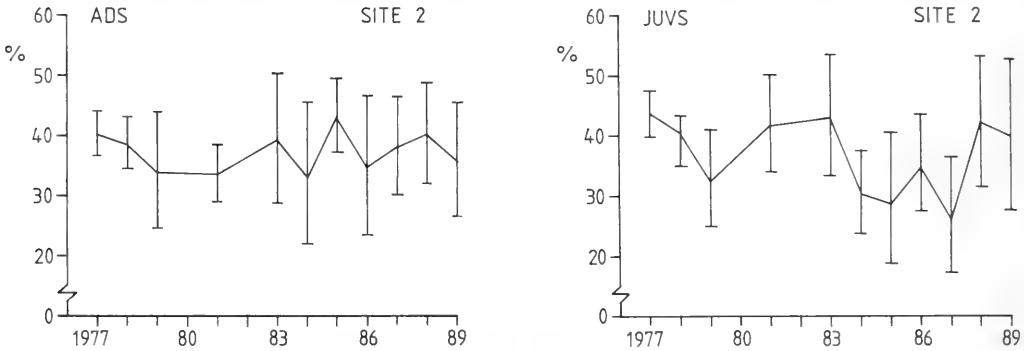

FIG. 2. Percent unbandeds at site 2; details as in Fig. 1.

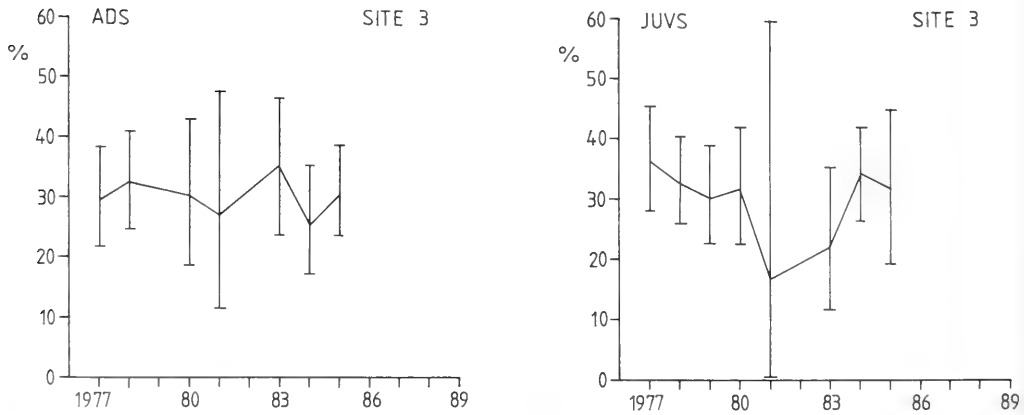

FIG. 3. Percent unbandeds at site 3; details as in Fig. 1. (The 1979 adult value is omitted as the sample was too small to allow calculation of confidence limits.)

samples from some sites in some years, an overall three-way G-statistic analysis of frequency by year by site was not performed).

The suggestion that selection was operating against unbandeds, at least during the second year of life (Cowie, 1984a), is rejected. Comparisons of unbanded frequencies in adults with those in juveniles of the

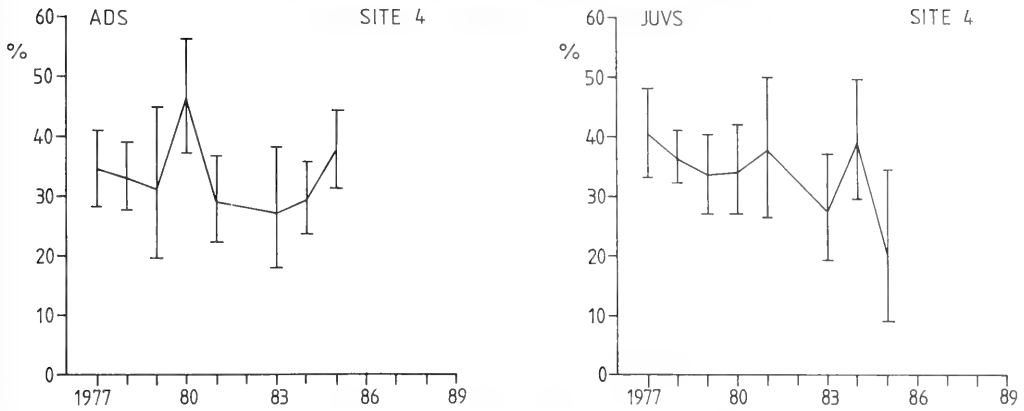

FIG. 4. Percent unbandeds at site 4; details as in Fig. 1.

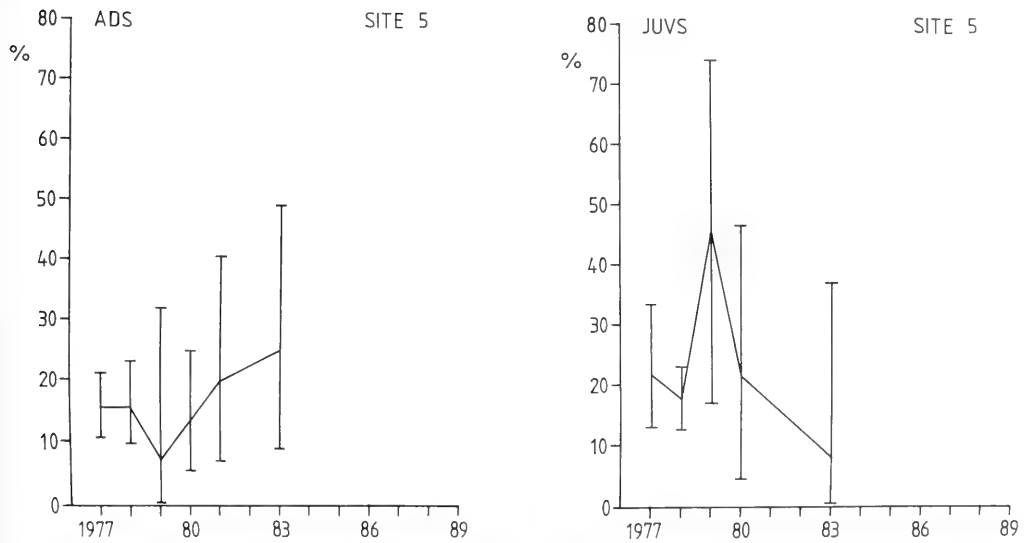

FIG. 5. Percent unbandeds at site 5; details as in Fig. 1. (The 1981 juvenile value is omitted as the sample was too small to allow calculation of confidence limits.)

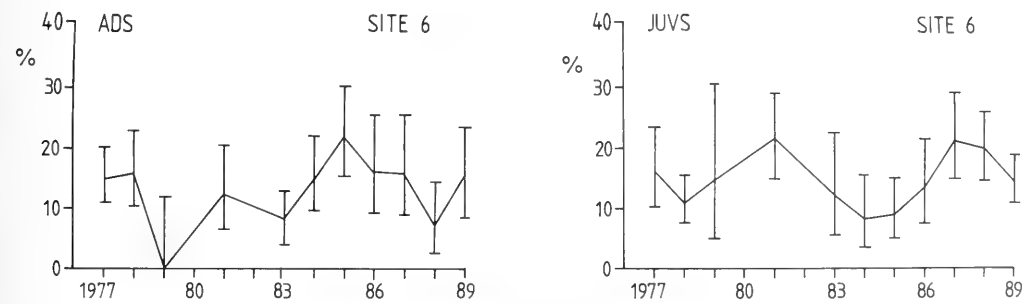

FIG. 6. Percent unbandeds at site 6; details as in Fig. 1.

TABLE 2. Values of r^2 and p from the regression analyses of morph frequency (transformed) on year. If any sample(s) or sub-sample(s) (e.g. unbanded adults when considering percent plain among adults) contained fewer than 30 individuals, the regression was also computed omitting these samples and the results are given in parentheses.

Site	Adults								Juveniles			
	% unbanded		% plain		% dark		% yellow		% unbanded		% plain	
	r^2	p	r^2	p	r^2	p	r^2	p	r^2	p	r^2	p
1	0.160	0.222	0.109	0.351	0.012	0.747	0.006	0.828	0.286	0.090	0.351	0.055
	(0.124)	(0.392)			(0.305)	(0.256)	(0.234)	(0.332)	(0.103)	(0.439)		
2	0.001	0.930	0.021	0.674	0.009	0.785	0.356	0.053	0.095	0.356	0.001	0.934
			(0.015)	(0.753)							(0.133)	(0.375)
3	0.086	0.481	0.035	0.657	0.011	0.807	0.264	0.193	0.044	0.620	0.025	0.711
	(0.029)	(0.749)	(0.064)	(0.838)	(0.047)	(0.680)	(0.588)	(0.075)	(0.117)	(0.453)	(0.267)	(0.373)
4	0.033	0.667	0.430	0.077	0.174	0.304	0.175	0.303	0.411	0.087	0.006	0.859
			(0.418)	(0.165)							(0.414)	(0.241)
5	0.281	0.279	0.000	0.972	0.228	0.338	0.219	0.349	0.101	0.540	0.006	0.888
	(0.961)	(0.127)			(0.708)	(0.364)	(0.893)	(0.212)	(-)	(-)*		
6	0.096	0.354	0.071	0.458	0.033	0.593	0.469	0.020	0.012	0.750	0.092	0.364
	(0.017)	(0.716)			(0.015)	(0.732)	(0.403)	(0.049)			(0.472)	(0.518)

*There were only two samples with 30 or more juveniles at site 5, so a regression based on just these two points has not been calculated.

previous year (i.e. the population from which those adults were derived) at each site (40 possible comparisons) do not show a significant trend; the points in Figure 7 fall more or less evently on either side of the line of equal percent unbanded, and a Wilcoxon's signed ranks test detected no significant difference ($p>0.1$) in the frequencies of unbandeds between these adult and juvenile samples. (On checking the data on which Table 3 of Cowie (1984a) is based, the percent unbanded in that table for juveniles in 1979 at site 1 was found to be incorrect; the correct value is 11.0, not 32.6. Recalculation of the Wilcoxon's tests of Cowie (1984a) but incorporating this correction, in fact, indicates no significant difference for the comparison of adults with juveniles of the previous year—$p>0.05$; although the less biologically meaningful comparison of adults and juveniles of the same year remains significant, but less strongly so—$p<0.05$.)

Within the unbandeds, there are no apparent differences among sites in the proportion of plain as opposed to dotty shells, most samples having 60–85% plain (average about 74%). As above, regression analysis (Table 2) detected no significant trends, while G-statistic analysis (Table 3) indicated some heterogeneity among years but without suggesting any trends. Again, morph frequencies show no consistent change.

Within the bandeds, there are no apparent differences among sites in the proportions of dark, intermediate and yellow shells. Most samples had 65–85% dark and 0–20% yellow (average about 75% and 9%, respectively), with the remainder made up of intermediates. Regression analysis revealed a single significant change in morph frequen-

TABLE 3. G-statistic analysis of morph frequencies by year.

Site	G		d.f.		p	
	adults	juveniles	adults	juveniles	adults	juveniles
			unbanded vs. banded			
1	4.714	9.800	9*	10	n.s.	n.s.
2	9.694	27.172	10	10	n.s.	<0.01
3	1.215	4.426	7	7	n.s.	n.s.
4	14.446	11.010	7	7	<0.05	n.s.
5	2.890	7.430	5	5	n.s.	n.s.
6	17.646	23.762	9*	10	<0.05	<0.01
			plain vs. dotty			
1	3.502	7.340	9	6*	n.s.	n.s.
2	16.858	18.416	10	9*	n.s.	<0.05
3	6.164	2.942	6*	5*	n.s.	n.s.
4	24.900	30.184	7	6*	<0.001	<0.001
5	0.866	4.794	4*	3*	n.s.	n.s.
6	9.730	9.030	9	10	n.s.	n.s.
			dark vs. intermediate/yellow			
1	17.248	-	9*	-	<0.05	-
2	22.400	-	10	-	<0.05	-
3	5.690	-	6*	-	n.s.	-
4	25.072	-	7	-	<0.001	-
5	2.180	-	5	-	n.s.	-
6	24.520	-	10	-	<0.01	-

*Some years pooled to give adequate cell values.

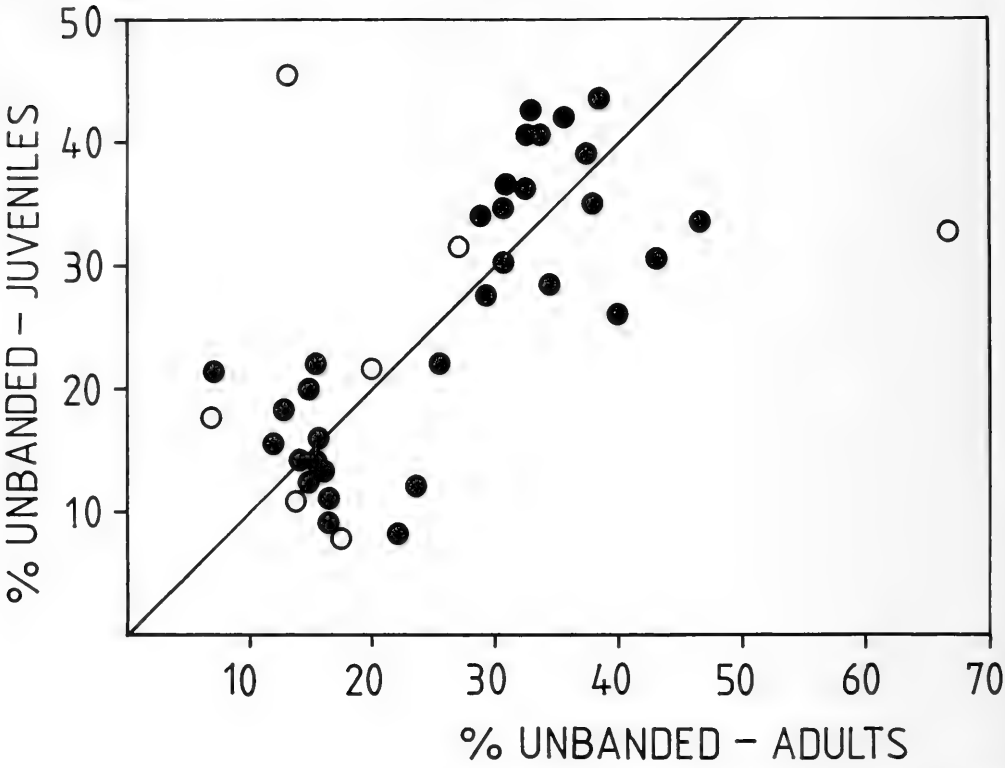

FIG. 7. Scatter diagram of percent unbanded in adult samples against juvenile samples of the previous year (see text for explanation). The diagonal indicates equal percentages. Open circles represent cases in which the adult or juvenile sample, or both, contained fewer than 30 individuals.

cies—an increase in percent yellow at site 6—which is only just significant ($p = 0.049$) when those samples of fewer than 30 individuals are omitted from the analysis (Table 2). This one significant result can be attributed to chance, given the large number of regression analyses performed, and does not indicate a real change. G-statistic analysis (Table 3, with frequencies of yellow and intermediate shells combined) again indicates heterogeneity among years (including at site 6, where the regression analysis indicated a significant trend) but this probably also reflects stochastic effects associated with multiple testing, combined with the difficulty, and consequent inconsistency, of scoring morphs within the banded class (see above). It is reasonable to conclude, once again, that there has been no consistent change in morph frequency over the course of the study.

In the absence of any trends, selection coefficients have not been calculated (cf. Murray & Clarke, 1978; Wall et al., 1980).

DISCUSSION

Theba pisana was probably introduced artifically to the U.K. during the eighteenth century (Cowie, 1984a; Turk, 1966, 1972). Cowie (1984a) suggested that selection acting since that time (over about 100 generations) may have given rise to the characteristic appearance of the morphs at Tenby and nearby localities in South Wales. While this may or may not be true, the current differences among sites in morph frequency, yet the lack of detectable morph frequency change over the 13 years of the study, can be explained in a number of ways (cf. Endler, 1986: 73–75), involving both selection and stochastic processes:

(1) Directional selection, following the initial introduction, produced the differences among sites; these differences are now being maintained by stabilising selection. While visual selection by predators and climatic selection are known to influence variation in shell pat-

tern and colour of soft parts in *T. pisana* (Cowie, 1990; Hazel & Johnson, 1990; Heller, 1981; Heller & Gadot, 1984; Johnson, 1980, 1981), as in the better known helicids *Cepaea nemoralis* and *C. hortensis* (Cain, 1983; Cowie & Jones, 1985; Jones et al., 1977), it is difficult to see what selective differences exist among the three sampling areas (site 1, sites 2, 3 and 4, sites 5 and 6) because all occur along a short length (about 0.75 km) of cliff face in apparently fairly similar habitat; any putative selective agent(s) is(are) unknown. Nevertheless, subtle and arcane habitat differences may be important, as has been suggested as one of a number of explanations of "area effects" in *Cepaea* (Cain & Currey, 1963a, b), and an influence of selection on morph frequencies in *T. pisana* at Tenby cannot be ruled out.

(2) The differences among sites arose from founder effects; frequent extinction of local populations, followed by recolonisation, at this, the climatic edge of the species' range (Cowie, 1987), leads to morph frequencies being the results of a succession of founding events; directional selection operating similarly at all sites has never been able to bring the populations to equilibrium. None of the present populations became extinct during the course of the study, although numbers were low at sites 1 and 5; selection may not be sufficiently strong to have been detected during the 13 years of the study. The suggestion that apparently strong directional selection was operating over all sites against unbandeds, and perhaps against plain morphs within the unbanded class (Cowie 1984a), is rejected, with the explanation that the initial five-year study was not long enough and the apparent selection was a statistical artefact, exagerated by a computational error (see above). At this cold extreme of the range of *T. pisana,* selection for darker colour (i.e. increased banding) might be expected, and indeed, at all other localities in this part of South Wales (Cowie, 1986), only five-banded (no unbanded) snails are found (Cowie, 1984a, 1987; Fowles & Cowie, 1989). (The absence of unbandeds at these other localities may also be due to the founder effect if these smaller populations are all derived ultimately from the much larger and well-established Tenby populations via small propagules consisting only of banded snails—Cowie, 1984a; Fowles & Cowie, 1989.)

(3) The differences among sites are due to founder effects; selection is not operating; and the differences are being maintained, or at least changing only slowly, because large population sizes prevent significant genetic drift. Cowie (1984c) estimated effective neighbourhood numbers as ranging up to 4130 individuals, large enough for drift to be insignificant.

It is not possible to distinguish between these various scenarios. Even though at least some aspects of the biology of *T. pisana,* especially at Tenby, are fairly well understood, there remain major gaps in our knowledge of the selective pressures to which the snails are subject, pressures that will differ from locality to locality, so that studies of *T. pisana* in Israel (Heller, 1981; Heller & Gadot, 1984), South Africa (Hickson, 1972) and Australia (Baker & Vogelzang, 1988; Hazel & Johnson, 1990; Johnson, 1980, 1981) can only be of broad, and not specific, relevance to our understanding of factors controlling the polymorphism in South Wales. Furthermore, Cain & Cook (1989) and Cain et al. (1990), studying *Cepaea nemoralis* over periods of 18 years and 23 years, respectively, have indicated the considerable difficulties involved in distinguishing among systematic changes in gene frequencies due to selection, maintenance of unchanging frequencies by selection, and stochastic fluctuations (see also Endler, 1986, ch. 4); Cain & Cook (1989) suggest that studies of 250 years or more may be necessary. The unanswered questions posed by the present study, reinforce the view (Endler, 1986; Wade & Kalisz, 1990) that only with detailed ecological knowledge, necessarily involving long-term studies, combined with experimentation, can the factors influencing polymorphisms in natural populations be thoroughly understood.

ACKNOWLEDGEMENTS

This work was begun at Liverpool University and continued, in part, at University College London. Scoring of post-1982 samples, new analyses presented here and writing up were done at the Bishop Museum. I thank these institutions for the opportunities and facilities provided. I also thank Professor A. J. Cain and Dr. M. S. Johnson for comments on the manuscript, Dr. L. A. Mehrhoff for computational and statistical assistance and the various friends and colleagues, especially C. T. French and A. M. Cassin, who assisted with field work.

LITERATURE CITED

BAKER, G. H. & B. K. VOGELZANG, 1988, Life history, population dynamics and polymorphism of *Theba pisana* (Mollusca: Helicidae) in Australia. *Journal of Applied Ecology,* 25: 867–887.

CAIN, A. J., 1983, Ecology and ecogenetics of terrestrial molluscan populations. In: W. D. RUSSELL-HUNTER, ed., *The Mollusca.* Volume 6. *Ecology.* Academic Press, London. pp. 597–647.

CAIN, A. J., 1984, Genetics of some morphs in the land snail *Theba pisana. Malacologia,* 25: 381–411.

CAIN, A. J., & L. M. COOK, 1989, Persistence and extinction in some *Cepaea* populations. *Biological Journal of the Linnean Society,* 38: 183–190.

CAIN, A. J., L. M. COOK & J. D. CURREY, 1990, Population size and morph frequency in a long-term study of *Cepaea nemoralis. Proceedings of the Royal Society of London, Series B, Biological Sciences,* 240: 231–250.

CAIN, A. J., & J. D. CURREY, 1963a, Area effects in *Cepaea. Philosophical Transactions of the Royal Society of London, Series B, Biological Sciences,* 246: 1–81.

CAIN, A. J., & J. D. CURREY, 1963b, The causes of area effects. *Heredity,* 18: 467–471.

CAMERON, R. A. D. & P. J. DILLON, 1984, Habitat stability, population histories and patterns of variation in *Cepaea. Malacologia,* 25: 271–290.

COWIE, R. H., 1984a, Ecogenetics of *Theba pisana* (Pulmonata: Helicidae) at the northern edge of its range. *Malacologia,* 25: 361–380.

COWIE, R. H., 1984b, The life-cycle and productivity of the land snail *Theba pisana. Journal of Animal Ecology,* 53: 311–325.

COWIE, R. H., 1984c, Density, dispersal and neighbourhood size in the land snail *Theba pisana. Heredity,* 52: 391–401.

COWIE, R. H., 1986, Reduction in the distribution of the land snail *Theba pisana* in the Tenby area, Dyfed. *Nature in Wales,* New Series, 4: 66–70.

COWIE, R. H., 1987, Rediscovery of *Theba pisana* at Manorbier, South Wales. *Journal of Conchology,* 32: 384–385.

COWIE, R. H., 1989, Of moths, snails and population genetics. *Bulletin of the British Ecological Society,* 20: 266–269.

COWIE, R. H., 1990, Climatic selection on body colour in the land snail *Theba pisana* (Pulmonata: Helicidae). *Heredity,* 65:123–126.

COWIE, R. H. & J. S. JONES, 1985, Climatic selection on body colour in *Cepaea. Heredity,* 55: 261–267.

COWIE, R. H. & J. S. JONES, 1987, Ecological interactions between *Cepaea nemoralis* and *Cepaea hortensis:* competition, invasion but no niche displacement. *Functional Ecology,* 1: 91–97.

ENDLER, J. A., 1986, *Natural selection in the wild.* Princeton University Press, Princeton. xiii + 336 pp.

FELDMAN, D. S., R. HOFFMANN, J. GAGNON & J. SIMPSON, 1987, *Statview II.* Abacus Concepts, Inc., Berkeley.

FOWLES, A. P. & R. H. COWIE, 1989, Westward extension of the distribution of *Theba pisana* in South Wales. *Journal of Conchology,* 33: 186–187.

GITTENBERGER, E. & T. E. J. RIPKEN, 1987, The genus *Theba* (Mollusca: Gastropoda: Helicidae), systematics and distribution. *Zoologische Verhandelingen,* 241: 1–59.

GOLDSTEIN, A., 1964, *Biostatistics: an introductory text.* Macmillan, New York, ix + 272 pp.

HAZEL, W. N. & M. S. JOHNSON, 1990, Microhabitat choice and polymorphism in the land snail *Theba pisana* (Müller). *Heredity,* 65: 449–454.

HELLER, J., 1981, Visual versus climatic selection of shell banding in the landsnail *Theba pisana* in Israel. *Journal of Zoology,* 194: 85–101.

HELLER, J. & M. GADOT, 1984, Shell polymorphism of *Theba pisana*—the effects of rodent distribution. *Malacologia,* 25: 349–354.

HICKSON, T., 1972, A possible case of genetic drift in colonies of the land snail *Theba pisana. Heredity* 45: 7–14.

JOHNSON, M. S., 1980, Association of shell banding and habitat in a colony of the land snail *Theba pisana. Heredity,* 45: 7–14.

JOHNSON, M. S., 1981, Effects of migration and habitat choice on shell banding frequencies in *Theba pisana* at a habitat boundary. *Heredity,* 47: 121–133.

JONES, J. S., B. H. LEITH & P. RAWLINGS, 1977, Polymorphism in *Cepaea:* a problem with too many solutions? *Annual Review of Ecology and Systematics,* 8: 109–143.

MURRAY, J. J. & B. C. CLARKE, 1978, Changes of gene frequency in *Cepaea nemoralis* over fifty years. *Malacologia,* 17: 317–330.

SOKAL, R. R. & F. J. ROHLF, 1969, *Biometry.* Freeman, San Francisco, xxi + 776 pp.

SOKAL, R. R. & F. J. ROHLF, 1973, *Introduction to biostatistics.* Freeman, San Francisco, xiii + 368 pp.

TURK, S. M., 1966, The rediscovery of *Theba pisana* (Müller) in Cornwall. *Journal of Conchology,* 26: 19–25.

TURK, S. M., 1972, A study of the white sand-hill snail, *Theba pisana. Devon Trust for Nature Conservation Journal,* 4: 138–142.

WADE, M. J. & S. KALISZ, 1990, The causes of natural selection. *Evolution,* 44: 1947–1955.

WALL, S., M. A. CARTER & B. C. CLARKE, 1980, Temporal changes of gene frequencies in *Cepaea hortensis. Biological Journal of the Linnean Society,* 14: 303–317.

Revised Ms. accepted 16 December 1991

MALACOLOGIA, 1992, 34(1–2): 99–106

NULL ALLELES AND HETEROZYGOTE DEFICIENCIES AMONG MUSSELS (*MYTILUS EDULIS* AND *M. GALLOPROVINCIALIS*) OF TWO SYMPATRIC POPULATIONS

J. P. A. Gardner[1]

School of Biological Sciences, University College of Swansea, Swansea, SA2 8PP, United Kingdom

ABSTRACT

The frequencies of null (enzymatically inactive) alleles estimated from two-banded phenotypes at an esterase-D (dimeric enzyme) locus among two sympatric *Mytilus edulis/Mytilus galloprovincialis* populations (Croyde and Whitsand) in southwestern England are 0.00823 and 0.00751 respectively. These values fall in the range of null allele frequencies predicted for British mussel populations. At Croyde, there were significantly more *M. galloprovincialis* than *M. edulis* null heterozygotes. This is thought to result from linkage of *M. edulis* null alleles to genes at a selective disadvantage compared with *M. galloprovincialis*, which indirectly reduces null allele frequency. Observed and predicted frequencies of null alleles are used to test the hypothesis that heterozygote deficiencies (compared to Hardy-Weinberg expectations), which are often observed among marine molluscan populations, might be caused by null alleles.

Key words: null alleles, heterozygote deficiency, *Mytilus edulis, Mytilus galloprovincialis.*

INTRODUCTION

Null (enzymatically inactive) alleles at loci encoding enzymes have been reported in populations of plants (Allendorf et al., 1982; Lafiandra et al., 1987) and animals (Voelker et al., 1980a, b; Langley et al., 1981; Skibinski et al., 1983; Foltz, 1986; Katoh & Foltz, 1989). Null alleles usually occur only rarely, often <0.005 (Ayala et al., 1972; Voelker et al., 1980a; Langley et al., 1981; Allendorf et al., 1982), although higher frequencies have been reported (Selander & Yang, 1969; Coyne & Felton, 1977; Freeth & Gibson, 1985).

In southwestern England, the marine mussels *Mytilus edulis* and *M. galloprovincialis* occur sympatrically and hybridize (Skibinski, 1983; Gardner & Skibinski, 1988). The systematic status of *M. galloprovincialis* has been reviewed by Seed (1978), Gosling (1984) and Koehn (1991). One of the best methods for distinguishing between the two mussel types is electrophoresis of an esterase-D (*Est-D*) locus, which has a genetic identity (*I* value; Nei, 1972) of 0.039 in comparisons between *M. edulis* from south Wales and *M. galloprovincialis* from Italy (Skibinski et al., 1980). *Est-D* is a dimeric enzyme (Harris & Hopkinson, 1976) that produces a three-banded heterozygote phenotype. It is a particularly good locus for observing null alleles not only because it is the most effective locus for detecting differences between the two mussel types, but also because two-banded null allele phenotypes are easily scored. However, estimates of this sort will tend to underestimate overall null allele frequency if the null allele produces a protein that fails to dimerize with the normal protein, that is, no heterodimer is produced, or if the heterodimer is formed but is not enzymatically expressed, that is, it is not visible on the gel. Although the frequency of such events can be determined by pedigree analysis and biochemical methods, these techniques generally preclude investigations of the large numbers (several thousands) of individuals necessary for population studies.

A phenomenon often observed among marine molluscan populations is a significant deficit of heterozygotes compared to Hardy-Weinberg expectations (Milkman & Beaty, 1970; Berger, 1983; Skibinski et al., 1983; Singh & Green, 1984; Zouros & Foltz, 1984; Gaffney et al., 1990). It has been suggested that null heterozygotes are one of the possible explanations for this deficit (Skibinski et

[1]Present address: Marine Sciences Research Laboratory, Memorial University of Newfoundland, St. John's, Newfoundland, A1C 5S7, Canada

TABLE 1. Allele distributions in pure *M. edulis* and *M. galloprovincialis* populations, after Skibinski et al. (1980) and Sanjuan et al. (1990).

Allele	*M edulis*[1]	*M. edulis*[2]	*M. galloprovincialis*[3]	*M. galloprovincialis*[4]
Est-D				
76	0	0	0.019	0
82	0	0.005	0.048	0.038
90	0.036	0.024	0.905	0.950
93	0	0.001	0	0
100	0.946	0.941	0.016	0.013
103	0	0	0.013	0
107	0.004	0.004	0	0
110	0.015	0.020	0	0
118	0	0.003	0	0
Odh				
80	0		0.012	
100	0.020		0.396	
115	0.930		0.131	
129	0.050		0.459	
140	0		0.004	

[1]Mean allele frequency of *M. edulis* from Holland and Denmark (Sanjuan et al., 1990).
[2]Allele frequencies of *M. edulis* from Swansea, South Wales (Skibinski et al., 1980).
[3]Mean allele frequency of *M. galloprovincialis* from Spanish Mediterranean (Sanjuan et al., 1990).
[4]Allele frequencies of *M. galloprovincialis* from Venice, Italy (Skibinski et al., 1980).

al., 1983; Beaumont et al., 1985; Mallet et al., 1985; Gaffney et al., 1990). Despite the fact that few data exist concerning null allele frequencies, it is usually assumed that null alleles do not occur at sufficiently high frequencies to explain the observed heterozygote deficits.

In this paper, genotype-dependent differences in the frequencies of two-banded null heterozygotes are reported. Observed and predicted frequencies of null alleles are applied to data from mussel populations to test if null alleles can explain heterozygote deficiencies.

MATERIALS AND METHODS

During the period from October 1986 to June 1989, 3,159 mussels from Croyde Bay, north Devon, and 2,929 mussels from Whitsand Bay, south Cornwall, southwestern England, were collected from locations as previously reported (Skibinski, 1983; Gardner & Skibinski, 1988). Mussels were electrophoresed, and stained for the esterase-D (EST-D; EC 3.1.1.1) and octopine dehydrogenase loci (ODH; EC 1.5.1.11). Some mussels were also stained for the mannose phosphate isomerase locus (MPI; EC 5.3.1.8). Tissue samples were prepared from hepatopancreas (liver) homogenized in an equal volume of distilled water. Following centrifugation at 0°C and 3000 rpm for 15 min, the supernatant was used as the enzyme source. EST-D, ODH and MPI were run on a Tris-citric acid (pH 6.9) buffered gel (Grant & Cherry, 1985). The following staining methods were employed; that of Ahmad et al. (1977) for EST-D, Beaumont et al. (1980) for ODH, and Grant & Cherry (1985) for MPI.

The migratory position (identity) of a null allele cannot be determined because it can be anodal or cathodal to the two-banded null phenotype. Similarly, the identity of the expressed allele in the heterozygous state with the null allele cannot be determined because it is unknown which band of the phenotype is the allele and which the heterodimer. It is therefore not possible to determine individual null allele frequencies, nor to determine the frequencies of *Est-D* alleles in the heterozygous state with the null alleles. For this reason, the synthetic compound allele system described by Skibinski (1983) was used to classify null genotypes. At a given locus, the compound *E* allele is obtained by pooling those alleles at highest frequency in *M. edulis,* and the compound *G* allele by pooling those alleles at highest frequency in *M. galloprovincialis.* For example, the *Est-D*^{E} allele occurs at frequencies of 0.01 and 0.96 at Bude and Swansea, "pure" *M. galloprovincialis* and *M. edulis* populations, respectively

(Edwards & Skibinski, 1987). The allele distributions among the two mussel types (Table 1) have been established by Skibinski et al. (1980) and Sanjuan et al. (1990). Although most alleles at a locus occur in both mussel types, the frequency differences are quite pronounced for the most common alleles. Frequency differences of rare alleles are less pronounced, but rare alleles contribute less often to compound alleles. The compound genotype of *Est-D* null heterozygotes was estimated by reference to the genotype at the *Odh* locus, which is in tight linkage disequilibrium with the *Est-D* locus. There are significant excesses of the *E/E E/E* (*M. edulis*-like) and *G/G G/G* (*M. galloprovincialis*-like) dilocus compound genotypes (Skibinski, 1983; Gardner & Skibinski, 1988). Mussels with *Est-D* null alleles were classified as *M. edulis*-like if they possessed the *Odh E/E* compound genotype, as intermediate or putative F1 hybrid if they exhibited the *Odh E/G* compound genotype, and as *M. galloprovincialis*-like if they possessed the *Odh G/G* compound genotype. For one null heterozygote, genotype was assigned on the basis of the compound genotype at the *Mpi* locus (which is also in tight linkage disequilibrium with the *Est-D* locus; Gardner & Skibinski, 1988) because the *Odh* genotype was not easily scored. Analysis was carried out to determine if null alleles occur at significantly greater frequency among *M. edulis, M. galloprovincialis,* or hybrid mussels.

Finally, null allele frequencies for three loci were predicted for the Croyde and Whitsand populations from the equation $F_{IT} = 2x/(1+x)$ (where x is null allele frequency and F_{IT} is a measure of deviation from Hardy-Weinberg expectations in the compound population obtained by pooling all subdivisions) if Hardy-Weinberg equilibrium (HWE) is assumed and if null heterozygotes are scored as homozygotes and null homozygotes are inviable. F_{IT} estimates have been obtained for British *M. edulis* and *M. galloprovincialis* populations, and for "pure" *M. edulis* populations by Skibinski et al. (1983). The observed *Est-D* two banded null phenotype frequencies and the predicted null allele frequencies were both applied to estimates of the *D* statistic ($D = (H_o/H_e)-1$, where H_o is the observed, and H_e the expected heterozygote frequencies), which is commonly used to estimate deviations from Hardy-Weinberg expectations (a negative *D* value indicates a deficiency of heterozygotes compared with expectations). *D* statistics for the Croyde and Whitsand populations are given by Gardner & Skibinski (1988), and have been recalculated to determine if heterozygote deficiencies are attributable to observed and predicted null allele frequencies. New estimates of H_o have been calculated by multiplying the original H_o values of Gardner & Skibinski (1988) by $1+x$, where x is null allele frequency. Null allele frequencies (x values) give a direct estimate of the underestimation of observed heterozygote frequency and the overestimation of observed homozygote frequency. New H_e estimates should be greater than the original H_e estimates because with the inclusion of null heterozygotes, heterozygosity will increase when mussels incorrectly scored as homozygotes are now correctly scored as heterozygotes. However, the original estimates of H_e have been used because the identities of the null alleles remain unknown, so new estimates of H_e have not been calculated. This then gives a conservative test, in the sense that (1) the calculated *D* values are slightly greater than they should be, that is, the heterozygote deficiency at each locus is estimated to be slightly smaller than it really is, and (2) the corresponding X^2 and P (significance) values are slightly less significant than they should be. Because the method of estimating null allele frequency assumes HWE, the F_{IT} values of Skibinski et al. (1983) for "pure" *M. edulis* populations (which, on the whole, are in HWE), and F_{IT} values for *M. edulis* and *M. galloprovincialis* populations (which are in HWE less often) have both been employed (Table 3).

RESULTS

At Croyde, two-banded null allele phenotypes occurred at an average frequency of 0.00823. There were 1.93 times as many *M. galloprovincialis* null heterozygotes as expected, based upon an hypothesis of equal null allele frequency for all genotypes ($G = 10.508$, $df = 2$, $P = 0.003$). The *E/E* and *E/G* compound genotypes showed null heterozygote frequencies that were 55.1% and 53.8% of their expected frequencies (Table 2). At Whitsand, null alleles were observed at a mean frequency of 0.00751. There was no significant association between null heterozygote frequency and compound genotype ($G = 0.816$, $df = 2$, $P = 0.672$). There were non-significant excesses of *E/G* and *G/G,* and

TABLE 2. Frequencies of compound genotypes and null heterozygotes at an esterase-D locus for mussels from Croyde and Whitsand.

Site	Croyde			Whitsand		
Compound genotype	*E/E*	*E/G*	*G/G*	*E/E*	*E/G*	*G/G*
No. of null heterozygotes	6	3	17	7	7	8
No. of mussels without null alleles	1473	647	1013	1194	831	822
Observed % frequency of null heterozygotes	0.473	0.462	1.650	0.583	0.835	0.899
Expected number of null heterozygotes*	12.104	5.317	8.324	8.968	6.242	6.625

*assuming equal frequencies of null heterozygotes for all compound genotypes

a non-significant deficit of *E/E* null heterozygotes compared with expectations (Table 2). Inter-population comparisons reveal that there were no significant differences between the two populations in the total number of null heterozygotes, or in the frequencies of *M. edulis* null heterozygotes, hybrid (*E/G*) null heterozygotes, and *M. galloprovincialis* null heterozygotes.

D values calculated by Gardner & Skibinski (1988) for the *Ap, Est-D* and *Pgi* loci at Croyde and Whitsand are shown in Table 3. In all cases, there were significant deficiencies of heterozygotes compared with expectations. Recalculation of *D* for the *Est-D* locus based upon the observed two-banded null heterozygote frequencies does not reduce the significance of the deficiencies at either site. Changes in the associated X^2 values are very small and do not have a significant effect upon probability levels (Table 3). With the exception of the *Ap* locus at Whitsand, the same is true when predicted null allele frequencies (firstly for "pure" *M. edulis* populations, and secondly for *M. edulis* and *M. galloprovincialis* populations) estimated from the equation $F_{IT} = 2x/(1+x)$ are used to re-calculate *D* values of the *Ap, Est-D* and *Pgi* loci.

DISCUSSION

Est-D null heterozygotes occur significantly more often among *M. galloprovincialis* than among *M. edulis* at Croyde. This is in line with the findings of Skibinski et al. (1983), who predicted an *Est-D* null allele mean frequency of 0.018 in *M. edulis* populations and a mean frequency of 0.071 in *M. edulis* and *M. galloprovincialis* populations. Null alleles most frequently result from single point mutations (Schwartz & Sofer, 1975; Voelker et al., 1980b; Scallon et al., 1987), but can also be due to small insertions that diminish transcription (Burkhart et al., 1984; Gibson & Wilks, 1989; but see Jiang et al., 1988). Two separate explanations can account for the lower frequency of nulls in *M. edulis* than in *M. galloprovincialis*. First, the *M. edulis* genome might be less susceptible to the mutational events that give rise to null alleles. Second, tight linkage of *M. edulis* nulls to other loci in the *M. edulis* genome, which experiences a significantly higher age-dependent mortality rate than *M. galloprovincialis* (Gardner & Skibinski, submitted), might indirectly reduce the frequency of nulls in *M. edulis*. At Croyde, comparison of the mean shell length of *M. edulis* versus *M. galloprovincialis* with null alleles (mean ± SD of 21.2 mm ± 6.20, n = 6, versus 39.7 mm ± 4.02, n = 17) indicates that *M. edulis* null alleles occur among smaller, younger mussels. No *M. edulis* larger than 30 mm length were found with null alleles, supporting the suggestion that increased mortality experienced by *M. edulis* compared to *M. galloprovincialis* acts indirectly to reduce null allele frequency among *M. edulis*. This second explanation is preferred because of supporting data, whereas the first explanation requires the invoking of differential mutation rates, for which there is no direct evidence. Evidence of length-dependent change in genotype frequencies (Gardner & Skibinski, 1988) indicates that *M. edulis* viability with regard to *M. galloprovincialis* is greater at Whitsand than at Croyde, providing an explanation for the non-significant differences in genotype-dependent null allele frequencies at Whitsand.

Few estimates of null allele frequencies exist for marine molluscan populations. Gaffney et al. (1990) estimated mean null allele frequencies in the coot clam, *Mulinia lateralis*, to

TABLE 3. Recalculation of *D* values to take into consideration (a) the observed two banded null heterozygote frequencies at the esterase-D locus, and the predicted frequencies of null heterozygotes at three loci for (b) "pure" *M. edulis* populations, and (c) for *M. edulis* and *M. galloprovincialis* populations.

	CROYDE			WHITSAND		
	Ap	*Est-D*	*Pgi*	*Ap*	*Est-D*	*Pgi*
[1]Ho	0.379	0.196	0.457	0.417	0.277	0.516
[1]He	0.462	0.505	0.651	0.493	0.485	0.687
[1]*D*	−0.179*	−0.611***	−0.298***	−0.153*	−0.430***	−0.250***
[1]n	422	474	501	381	376	411
[2]x	—	0.00823	—	—	0.00751	—
[2]Ho	—	0.198	—	—	0.284	—
[2]He	—	0.505	—	—	0.485	—
[2]*D*	—	−0.608***	—	—	−0.425***	—
[2]n	—	474	—	—	376	—
[3]x	0.0101	0.0304	0.0163	0.0101	0.0304	0.0163
[3]Ho	0.383	0.202	0.465	0.422	0.285	0.524
[3]He	0.462	0.505	0.651	0.493	0.485	0.687
[3]*D*	−0.171*	−0.600***	−0.287***	−0.145*	−0.413***	−0.237***
[3]n	422	474	501	381	376	411
[4]x	0.0225	0.2903	0.0482	0.0225	0.2903	0.0482
[4]Ho	0.388	0.253	0.479	0.427	0.357	0.541
[4]He	0.462	0.505	0.651	0.493	0.485	0.687
[4]*D*	−0.161*	−0.499***	−0.264***	−0.134[NS]	−0.264***	−0.213***
[4]n	422	474	501	381	376	411

x null allele frequency
Ho observed number of heterozygotes
He expected number of heterozygotes
D heterozygote deviation compared with Hardy-Weinberg expectations, calculated as $D = (Ho/He)-1$
NS not significant
*$P<0.05$
***$P<0.001$
n number of mussels
[1]Data from Gardner & Skibinski (1988).
[2]Data from Gardner & Skibinski (1988) recalculated incorporating the observed frequencies of two banded null heterozygote phenotypes.
[3]Data from Gardner and Skibinski (1988) recalculated incorporating frequencies of predicted null alleles for "pure" *M. edulis* populations (Skibinski et al., 1983).
[4]Data from Gardner & Skibinski (1988) recalculated incorporating frequencies of predicted null alleles for *M. edulis* and *M. galloprovincialis* populations (Skibinski et al., 1983).

be 0.001 at the GPI locus and 0.0003 at the AP2 locus. In common with other large studies, the null allele frequencies reported by Gaffney et al. (1990) are for two-banded phenotypes of dimeric enzymes, and as in the present study, must therefore be viewed as minimum estimates. Because of the difficulty of distinguishing one-banded null heterozygotes from homozygotes, no null allele frequency data are given for monomeric enzymes for the coot clam. No null heterozygotes were observed at the other dimeric loci. Skibinski et al. (1983) predicted that null allele frequency in British populations of *M. edulis* and *M. galloprovincialis* should be in the range 0.003 to 0.102 for 11 allozyme loci. The observed null allele frequencies reported here (0.00823 at Croyde and 0.00751 at Whitsand) are therefore consistent with predicted values over several loci (Skibinski et al., 1983).

Mean null allele frequency estimated from the equation $F_{IT} = 2x/(1+x)$ for seven *Est-D* alleles is 0.102 for *M. edulis* and *M. galloprovincialis,* and for the pure *M. edulis* is 0.019 (Skibinski et al., 1983); that is, both values are substantially greater than the observed frequencies of two-banded null heterozygotes. This might be accounted for by the undetectable presence of null alleles that do not produce a heterodimer, such individuals being scored as homozygotes. This is particularly important because it is often suggested that

null alleles might be responsible for observed heterozygote deficiencies (Boyer, 1974; Skibinski et al., 1983; Beaumont et al., 1985; Mallet et al., 1985; Foltz, 1986; Gaffney et al., 1990). However, estimates from natural populations suggest that null alleles are not common enough, often by orders of magnitude, to account for homozygote excesses, and recalculation of *D* statistics (Table 3) seems to confirm this. *D* values increase (heterozygote deficiencies decrease) in all cases as expected when observed or predicted null allele frequencies are used to re-estimate observed and expected heterozygote frequencies. However, changes in significance levels are generally small and only effect probability values in one case. This indicates that null alleles generally do not occur at sufficient frequency to significantly effect heterozygote deficiencies. At Whitsand, the heterozygote deficiency at the *Ap* locus reported by Gardner & Skibinski (1988) is small but significant ($X^2 = 4.389$, df = 1, P = 0.0362). Recalculation of *D,* adjusting for predicted null allele frequency among "pure" *M. edulis* populations, reduces the X^2 value to 3.909 (df = 1, P = 0.048), that is, to borderline significance. Further recalculation adjusting for null allele frequency among *M. edulis* and *M. galloprovincialis* populations reduces the X^2 value to 3.361 (df = 1, P = 0.0668), that is, a non-significant deficiency of heterozygotes. It seems likely that only in such cases as this, where heterozygote deficiencies are small but (borderline) significant, can observed or predicted null allele frequencies contribute significantly to heterozygote deficiencies.

In the single case among marine bivalves where very high frequencies of null alleles have been observed (Foltz, 1986), it was suggested (Gaffney et al., 1990) that the producton of aneuploid gametes (i.e., gametes with one or more chromosomes, or chromosome segments, absent) might better explain the high frequency of apparent null alleles. There is thus still no evidence from natural populations to indicate that heterozygote deficiencies result solely from high frequencies of null alleles. Although null alleles appear likely to contribute to heterozygote deficiencies, more significant causes include selection, the Wahlund effect, aneuploidy or imprinting, that is, the differential expression of genetic material, at the chromosomal or allelic level, depending on whether the genetic material was derived from the male or female parent (Gaffney et al., 1990). In the case of the sympatric *Mytilus* populations of southwestern England, selection and the Wahlund effect are the most likely explanations for significant heterozygote deficiencies (Skibinski, 1983; Gardner & Skibinski, 1988).

ACKNOWLEDGEMENTS

Thanks to Eric Roderick for help in the field; to Donna Gardner for data collation; to Andy Beaumont, David Skibinski and three anonymous reviewers for helpful comments. The research was supported in part by a NERC Studentship to the author.

LITERATURE CITED

AHMAD, M., D. O. F. SKIBINSKI & J. A. BEARDMORE, 1977, An estimate of the genetic variation in the common mussel *Mytilus edulis. Biochemical Genetics,* 15: 833–846.

ALLENDORF, F. W., K. L. KNUDSEN & G. M. BLAKE, 1982, Frequencies of null alleles at enzyme loci in natural populations of ponderosa and red pine. *Genetics* 100: 497–504.

AYALA, F. J., J. R. POWELL, M. L. TRACEY, C. MOURAO & S. PEREZ-SALAS, 1972, Enzyme variability in the *Drosophila willistoni* group. IV. Genic variation in natural populations of *Drosophila willistoni. Genetics,* 70: 113–139.

BEAUMONT, A. R., T. R. DAY & G. GADE, 1980, Genetic variation at the octopine dehydrogenase locus in *Cerastoderma edule* (L.) and six other bivalve species. *Marine Biology Letters,* 1: 137–148.

BEAUMONT, A. R., E. M. GOSLING, C. M. BEVERIDGE, M. D. BUDD & G. M. BURNELL, 1985, Studies on heterozygosity and size in the scallop, *Pecten maximus.* Pp. 443–454, in: P. E. GIBBS, ed., *Proceedings of the 19th European Marine Biology Symposium,* Cambridge University Press.

BERGER, E. M., 1983, Population genetics of marine gastropods and bivalves. Pp. 563–596, in: W. D. RUSSELL-HUNTER, ed., *The Mollusca,* Volume 6, *Ecology,* Academic Press, New York.

BOYER, J. F., 1974, Clinal and size-dependent variation at the *Lap* locus in *Mytilus, edulis. Biological Bulletin of the Woods Hole Oceanographic Institute, Woods Hole, Mass.,* 147: 535–549.

BURKHART, B. D., E. MONTGOMERY, C. H. LANGLEY & R. A. VOELKER, 1984, Characterization of allozyme null and low activity alleles from two natural populations of *Drosophila melanogaster. Genetics,* 107:295–306.

COYNE, J. A. & A. A. FELTON, 1977, Genic heterogeneity at two alcohol dehydrogenase loci in

Drosophila pseudoobscura and *Drosophila persimilis*. *Genetics,* 87:285–304.

EDWARDS, C. A. & D. O. F. SKIBINSKI, 1987, Genetic variation of mitochondrial DNA in mussel (*Mytilus edulis* and *M. galloprovincialis*) populations from South West England and South Wales. *Marine Biology,* 94: 547–556.

FOLTZ, D. W., 1986, Null alleles as a possible cause of heterozygote deficiencies in the oyster *Crassostrea virginica* and other bivalves. *Evolution,* 40: 869–870.

FREETH, A. L. & J. B. GIBSON, 1985, Alcohol dehydrogrenase and sn-glycerol-3-phosphate dehydrogenase null activity alleles in natural populations of *Drosophila melanogaster. Heredity,* 55: 369–374.

GAFFNEY, P. M., T. M. SCOTT, R. K. KOEHN & W. J. DIEHL, 1990, Interrelationships of heterozygosity, growth rate and heterozygote deficiencies in the coot clam, *Mulinia lateralis. Genetics,* 124: 687–699.

GARDNER, J. P. A. & D. O. F. SKIBINSKI, 1988, Historical and size-dependent genetic variation in hybrid mussel populations. *Heredity,* 61: 93–105.

GARDNER, J. P. A. & D. O. F. SKIBINSKI, submitted, Growth and mortality differences between the mussels *Mytilus edulis* (L.), *Mytilus galloprovincialis* (Lmk.) and their hybrids from two sympatric populations in S.W. England. *Biological Bulletin of the Woods Hole Oceanographic Institute, Woods Hole, Mass.*

GIBSON, J. B. & A. V. WILKS, 1989, Molecular structure of a naturally occurring alcohol dehydrogenase null activity allele in *Drosophila melanogaster. Biochemical Genetics,* 27: 679–688.

GOSLING, E. M., 1984, The systematic status of *Mytilus galloprovincialis* in western Europe: a review. *Malacologia,* 25: 551–568.

GRANT, W. S. & M. I. CHERRY, 1985, *Mytilus galloprovincialis* Lmk. in southern Africa. *Journal of Experimental Marine Biology and Ecology,* 90: 179–191.

HARRIS, H. & D. A. HOPKINSON, 1976, Handbook of enzyme electrophoresis in human genetics. North Holland Publishing Company, Amsterdam.

JIANG, C., J. B. GIBSON, A. V. WILKS & A. L. FREETH, 1988, Restriction endonuclease variation in the region of the alcohol dehydrogenase gene: a comparison of null and normal alleles from natural populations of *Drosophila melanogaster. Heredity,* 60: 101–108.

KATOH, M. & D. W. FOLTZ, 1989, Biochemical evidence for the existence of a null allele at the leucine aminopeptidase-2 (*Lap-2*) locus in the oyster *Crassostrea virginica* (Gmelin). *Genome,* 32: 687–690.

KOEHN, R. K., 1991, The genetics and taxonomy of the species in the genus *Mytilus. Aquaculture,* 94: 125–145.

LAFIANDRA, D., G. COLAPRICO, D. D. KASARDA & E. PORCEDDU, 1987, Null alleles for gliadin blocks in bread and durum wheat cultivars. *Theoretical and Applied Genetics,* 74: 610–616.

LANGLEY, C. H., R. A. VOELKER, A. J. LEIGH BROWN, S. OHNISHI, B. DICKSON & E. MONTGOMERY, 1981, Null allele frequencies at allozyme loci in natural populations of *Drosophila melanogaster. Genetics,* 99: 151–156.

MALLET, A. L., E. ZOUROS, K. E. GARTNER-KEPKAY, K. R. FREEMAN & L. M. DICKIE, 1985, Larval viability and heterozygote deficiency in populations of marine bivalves: evidence from pairs of matings of mussels. *Marine Biology,* 87: 165–172.

MILKMAN, R. & L. D. BEATY, 1970, Large-scale electrophoretic studies of allelic variation in *Mytilus edulis. Biological Bulletin of the Woods Hole Oceanographic Institute, Woods Hole, Mass.,* 139: 430.

NEI, M., 1972, Genetic distance between populations. *American Naturalist,* 106: 283–292.

SANJUAN, A., H. QUESADA, C. ZAPATA & G. ALVAREZ, 1990. On the occurrence of *Mytilus galloprovincialis* Lmk. on the N.W. coast of the Iberian Peninsula. *Journal of Experimental Marine Biology and Ecology,* 143: 1–14.

SCALLON, B. J., C. D. DICKINSON & N. C. NIELSEN, 1987, Characterization of a null-allele for the Gy_4 glycinin gene from soybean. *Molecular and General Genetics,* 208: 107–113.

SCHWARTZ, M. & W. SOFER, 1976, Alcohol dehydrogenase-negative mutants in *Drosophila:* defects at the structural locus? *Genetics,* 83: 125–136.

SEED, R., 1978, The systematics and evolution of *Mytilus galloprovincialis* (Lmk.). Pp. 447–468, in: B. Battaglia & J. A. Beardmore, eds., *Marine organisms: genetics, ecology and evolution.* Plenum Press, New York.

SELANDER, R. K. & S. Y. YANG, 1969, Protein polymorphism and genic heterozygosity in a wild population of the house mouse (*Mus musculus*). *Genetics,* 63: 653–667.

SINGH, S. M. & R. H. GREEN, 1984, Excess of allozyme heterozygosity in marine molluscs and its possible biological significance. *Malacologia,* 25: 569–581.

SKIBINSKI, D. O. F., 1983, Natural selection in hybrid mussel populations. Pp. 283–298, in: G.S. Oxford & D. Rollinson eds., *Protein polymorphism: adaptive and taxonomic significance.* Systematics Association Special Volume No. 24, Academic Press, London & New York.

SKIBINSKI, D. O. F., J. A. BEARDMORE & T. F. CROSS, 1983, Aspects of the population genetics of *Mytilus* (Mytilidae; Mollusca) in the British Isles. *Biological Journal of the Linnean Society,* 19: 137–183.

SKIBINSKI, D. O. F., T. F. CROSS & M. AHMAD, 1980, Electrophoretic investigation of systematic relationships in the marine mussels *Modiolus modiolus* L., *Mytilus edulis* L., and *Mytilus galloprovincialis* Lmk. (Mytilidae; Mollusca). *Biological Journal of the Linnean Society,* 13: 65–73.

VOELKER, R. A., C. H. LANGLEY, A. J. LEIGH BROWN, S. OHNISHI, B. DICKSON, E. MONTGOMERY & S. C. SMITH, 1980a, Enzyme null alleles in natural populations of *Drosophila melanogaster:* frequencies in a North Carolina population. *Proceedings of the National Academy of Sciences, U.S.A.,* 77: 1091–1095.

VOELKER, R. A., H. E. SCHAFFER & T. MUKAI, 1980b, Spontaneous allozyme mutations in *Drosophila melanogaster:* rate of occurrence and nature of the mutants. *Genetics,* 94: 961–968.

ZOUROS, E. & D. W. FOLTZ, 1984, Possible explanations of heterozgote deficiencies in bivalve molluscs. *Malocologia,* 25: 583–591.

Revised Ms. accepted 29 August 1991

MALACOLOGIA, 1992, 34(1–2): 107–128

A NEW PROBLEMATICAL HYGROMIIDAE FROM THE AEOLIAN ISLANDS (ITALY) (PULMONATA: HELICOIDEA)[1]

Folco Giusti[2], Giuseppe Manganelli[2] & Jorge V. Crisci[3]

ABSTRACT

Helicotricha n. gen. is proposed for a very small hygromiid from the Aeolian Islands, Italy: *H. carusoi* n. sp. The new species has a shell with persistent postembrional hairs and is characterized anatomically by: a right ommatophore retractor independent of the genitalia; a penial nerve originating from the right cerebral ganglion; a vaginal complex with digitiform glands and dart-sac complex consisting of two couples of stylophores disposed on opposite sides of the vagina (each couple is formed by a larger dart-bearing outer stylophore and a smaller dartless inner stylophore); and a penial complex with a very peculiar penial papilla. Direct anatomical comparison of the new genus with other genera of the Hygromiidae suggested that it may be very closely related to *Microxeromagna.* This hypothesis was subsequently found to be supported by the results of cladistic analysis. New evidence is thus provided to confirm that the distinction between the Hygromiinae and the Trichiinae is artificial. A neotype is designated for *Helix aetnea* Benoit, 1857, a junior synonym of *Xerotricha conspurcata* (Draparnaud, 1801), and the presence of *Helicopsis* (s. str.) in western North Africa is confirmed.

Key words: Hygromiidae, Aeolian Islands, Italy, western Mediterranean, *Helicella, Xerotricha, Helicopsis,* systematics.

INTRODUCTION

Recent insular equilibrium theory studies based on analytical comparison of the malacofaunas of the Tuscan and Aeolian archipelagos, Italy (Piantelli et al., 1990), have motivated new field research and study of the material collected from the various islands. As happened for the islands of the Tuscan Archipelago (Giusti & Manganelli, 1989, 1990), new data emerged for the Aeolians. A new species of the Hygromiidae was identified amongst material of *Xerotricha conspurcata* (Draparnaud, 1801) collected in all the Aeolian Islands. The Hygromiidae are a group of helicoids of western Palaearctic distribution recently separated from the Helicidae as a distinct family and characterized by a bursa copulatrix duct free from the diaphragm wall and a variable number of stylophores.

The peculiar structure of the genitalia made it difficult to establish relationships and generic status of the new species. Although the 2 + 2 structure of the dart-sac complex associated with the vagina, and the right ommatophore retractor free of penis and vagina, at first glance suggested a relationship with the genus *Helicopsis,* details of the penial complex suggested other possibilities. In particular, as in the case of *Helicella* (one large, evident and one vestigial, externally invisible, stylophore on opposite sides of the vagina) and *Xerolenta* (one normal and one modified stylophore on opposite sides of the vagina) which appear to form monophyletic groups respectively with *Candidula* (one large, evident and one vestigial, externally invisible, stylophore on one side of the vagina) and *Xeromunda* (one normal and one modified stylophore on one side of the vagina) respectively (Hausdorf, 1988, 1990a; Giusti & Manganelli, 1989; Manganelli & Giusti, 1989), it seems highly probable that the new genus (one larger outer stylophore and one smaller dartless inner stylophore on opposite sides of the vagina) is a member of the monophyletic group to which also *Microxeromagna* (one larger outer stylophore and one smaller dartless inner stylophore on one side of the vagina) belongs. Accordingly, in view of the fact that *Helicella, Xerolenta, Candidula, Xeromunda* are unanimously regarded as distinct generic taxa and in view also of our considerations on character weighting in establish-

[1]Notulae Malacologicae, LI.

[2]Dipartimento di Biologica Evolutiva, Università degli Studi di Siena, Via Mattioli 4, I-53100 Siena, Italy
[3]Laboratorio de Sistematica y Biologia Evolutiva, Museo de La Plata, Paseo del Bosque 1900, La Plata, Argentina

ing systematic rank in the Hygromiidae (Manganelli & Giusti, 1988), a new genus is introduced for the new species.

MATERIALS AND METHODS

Empty shells and whole specimens were collected in the litter or under stones and wood on rocky slopes of the islands (locality data follows species description). Living specimens were left in water to drown for 24 h then preserved in ethanol 75%. Relaxed material was studied by optical microscopy (Wild M5A). Bodies were isolated then dissected using thin, pointed watchmaker's forceps. Images of isolated portions of body and genitalia were drawn using a Wild camera lucida. Radulae were manually extracted from buccal bulbs, then washed in pure 75% ethanol, mounted on copper blocks with electron-conductive glue, sputter-coated with gold and photographed using a Philips 505 SEM.

All shell parameters—shell maximum diameter, shell height, aperture maximum diameter, aperture height—were measured in variable numbers of shells from the different islands using a Wild M5A microscope and a millimetric lens. Whole shells were photographed under optical microscope. Whole shells and shell surface details were photographed under optical and scanning electron microscopes using the procedure described for the radulae.

Detailed study of the genitalia followed, particularly the distal portion (penis and vagina), the external and internal details of which proved to be diagnostic characters in similar previous studies (see literature cited in the Discussion) (Table 2).

The entire set of character states was used for classical evolutionary and cladistic analysis to define the new genus.

Cladistic analysis was performed using the method of phylogenetic systematics as originally developed by Hennig (1966), who maintained that only strictly monophyletic taxa may be regarded as historical entities and demonstrated that the only logical basis for inferring monophyly is by showing synapomorphies. The distribution of the synapomorphies is determined by the parsimony criterion (minimizing homoplasy). On the basis of these synapomorphies, the taxa are ordered into a specific pattern represented by a hierarchical branching diagram.

The new genus *Helicotricha* belongs to the family Hygromiidae, which is delimited by the following unique combination of features: bursa copulatrix free from diaphragm; variable number of stylophores (2 + 2; 0 + 2; 1 + 1; 0 + 1; 0 + 0); stylophores, when present and not extremely regressed or modified, forming dart-sac complex consisting of one or two double units with a common base and distinct distal sacs lying side by side in the same plane; diverticulum of bursa copulatrix absent; digitiform gland tufts variable in number inserted on proximal vagina not close to where dart sacs, when present, open into vagina. Helicidae are characterized by: bursa copulatrix inserted into diaphragm; dart-sac complex consisting of a single stylophore; diverticulum of bursa copulatrix duct present. Helicidae and Hygromiidae share the following characters: dart-sac complex, vaginal digitiform glands.

Twenty (Table 1) genera are considered to be the terminal taxa. The minute details of the distal genitalia of some have recently been reviewed (Schileyko, 1978a, 1978b; Giusti & Manganelli, 1987, 1989; Hausdorf, 1988, 1990a, 1990b; Manganelli & Giusti, 1988, 1989).

In the case of the two sets of genera reviewed by Schileyko and Hausdorf, some characters were uncertain or not discussed. A question mark sometimes follows or substitutes the character states in Table 3. A question mark also substitutes the character states when one character is known to be present with more than two states in the same taxa (character 5 in *Xeromunda* and *Cernuella* (s. str.); character 16 in *Xerotricha*). Character polarity was determined by outgroup comparison methods (Watrous & Wheeler, 1981; Maddison et al., 1984) using the family collectively Helicidae as outgroup, because there is no single genus that is a clear sister group. Three out fifteen characters (5, 10, 15) had more than two character states. These characters were treated as nonadditive. Two characters (11, 14) were autoapomorphies, with an additional autoapomorphy in a multistate nonadditive character (10).

The data was analyzed using a Wagner parsimony algorithm from Farris's phylogenetic program HENNIG86, applying the implicit enumeration option for calculating trees (version 1.5; Farris, 1989; see also Platnick, 1989) run on a IBM AT computer. When cladistic analysis yielded more than one tree, the Nelsen consensus method was applied (Nelsen, 1979). We also used the successive weighting procedure (Farris, 1989), which calculates weights from the best fits to the most parsimonious trees, and applied them in the

TABLE 1. Acronyms, genus-group taxa, type species and bibliographical sources of anatomical data. Some of the genera listed have a subgeneric division. For cladistic analysis, only species of nominotypical subgenera have been considered.

Acronyms	Genus-group taxa	Type-species	Sources
CAND	*Candidula* Kobelt, 1871	*Glischrus (Helix) candidula,* Studer, 1820, = *Helix unifasciata* Poiret, 1801	Hausdorf, 1988: (*C. unifasciata, C. gigaxii);* personal unpublished data on *C. spadae, C. intersecta, C. unifasciata*
CAUC	*Caucasigena* Lindholm, 1927	*Helix eichwaldi* Pfeiffer, 1846	Schileyko, 1978a, 1978b
CERN	*Cernuella* Schluter, 1838	*Helix variabilis* Draparnaud, 1801, = *Cochlea virgata* Da Costa, 1778	Hausdorf, 1988; Manganelli & Giusti, 1988
EDEN	*Edentiella* Polinski, 1929	*Helix edentula* Draparnaud, 1805	Schileyko, 1978a, 1978b
HELL	*Helicella* Férussac, 1821	*Helix itala* Linnaeus, 1758; cf. Opinion 431	Hausdorf, 1988; Giusti & Manganelli, 1989
HELP	*Helicopsis* Fitzinger, 1833	*Helix striata* Müller, 1774	Giusti & Manganelli, 1989; Schileyko, 1978b; Hausdorf, 1990b
HELT	*Helicotricha* Giusti & Manganelli, 1992	*Helicotricha carusoi* Giusti, Manganelli & Crista, 1992	this paper
HYGR	*Hygromia* Risso, 1826	*Helix cinctella* Draparnaud, 1801	Giusti & Manganelli, 1987
HYGH	*Hygrohelicopsis* Schileyko, 1978a	*Hygrohelicopsis darevskii* Schileyko, 1978a	Schileyko, 1978a, 1978b
KOKO	*Kokotschashvilia* Hudec & Lezhawa, 1969	*Helix holotricha* O. Boettger, 1884	Schileyko, 1978a, 1978b
LEUC	*Leucozonella* Lindholm, 1927	*Helix rubens* von Martens, 1874	Schileyko, 1978a, 1978b
MICR	*Microxeromagna* Ortiz de Zarate Lopez, 1950	*Helix stolismena* Bourguignat, in Servain, 1880, = *Helix armillata* Lowe, 1852	Hausdorf, 1988, 1990c; Manganelli & Giusti, 1988
NANA	*Nanaja* Schileyko, 1978b	*Nanaja cumulata* Schileyko, 1978b	Schileyko, 1978b
PLIC	*Plicuteria* Schileyko, 1978a	*Helix lubomirskii* Slosarski, 1881	Schileyko, 1978a, 1978b
PXER	*Pseudoxerophila* Westerlund, in Westerlund & Blanc, 1879	*Helix (Pseudoxerophila) bathytera* Westerlund, in Westerlund & Blanc, 1879	Hausdorf, 1988
TRIC	*Trichia,* Hartmann, 1840	*Helix hispida* Linnaeus, 1758	Schileyko, 1978a, 1978b
XERL	*Xerolenta* Monterosato, 1892	*Helix obvia* Menke, 1828	Hausdorf, 1988
XERM	*Xeromunda* Monterosato, 1892	*Helix turbinata,* sensu Monterosato, 1892, *non* De Cristofori & Jan, 1832) (cf. Hausdorf, 1988; Manganelli & Giusti, 1988; 1989; an application to the I.C.Z.N. is in progress by Giusti & Manganelli	Hausdorf, 1988, 1990a; Manganelli & Giusti, 1989
XERS	*Xerosecta* Monterosato, 1892	*Helix explanata* Müller, 1774	Manganelli & Giusti, 1988
XERT	*Xerotricha* Monterosato, 1892	*Helix conspurcata* Draparnaud, 1801	Hausdorf, 1988; Giusti & Manganelli, 1989

weighting procedure until there were no changes in successively produced trees.

SYSTEMATIC DESCRIPTION

Helicotricha n. gen

Diagnosis

Very small hygromiid with shell having persistent postembronial hairs; anatomically characterized by right ommatophore retractor independent of genitalia; penial nerve from right cerebral ganglion; vaginal complex with digitiform glands and dart-sac complex consisting of two pairs of stylophores, each couple comprising a larger dart-bearing outer stylophore and a smaller dartless inner stylophore; penial complex having a very peculiar penial papilla.

Description

Shell: Small, hairy, opaque-brown in colour, with white flecks. Spire consisting of approx-

TABLE 2. List of characters

1—Penial nerve.
—From right cerebral ganglion = 0
—From right pedal ganglion = 1
Remarks: no data for *Caucasigena, Edentiella, Hygrohelicopsis, Kokotschashvilia, Leucozonella, Nanaja, Plicuteria.* In Manganelli & Giusti (1989: 4) was wrongly reported for *Xeromunda* "from right pedal ganglion." Revision of original data indicates that penial nerve comes out of right cerebral ganglion.

2—Right ommatophore retractor.
—Between penis and vagina = 0
—Independent of penis and vagina = 1
Remarks: No data for *Psudoxerophila.*

3—Number of stylophores and/or their derivates forming the dart-sac complex.
—2 + 2 = 0
—0 + 2 = 1

4—Shape and position of stylophore groups in relation to vagina.
—Stylophores *Trichia* type: each stylophore group (each composed of an outer and an inner stylophore) slender and entering vagina through a slender neck (Manganelli & Giusti, 1988: fig. 14 E) = 0
—Stylophores not *Trichia* type: each stylophore group (each composed of an outer and an inner stylophore) wide and fused to inner walls of vagina for a long tract (Manganelli & Giusti, 1988: fig. 14 A) = 1
Remarks: *Helicopsis:* based on the type species only (Giusti & Manganelli, 1989). Schileyko (1978b) and Hausdorf (1990b) show drawings of the genitalia of *H. striata* and of some other species (*H. likharevi, H. retowskii*) in which the situation is slightly different. A slightly different situation also occurs in the species studied in the present paper and referred to as *Helicopsis* sp.

5—Shape and dimensions of stylophore groups.
—Each group formed by an inner and an outer stylophore of similar dimensions (Manganelli & Giusti, 1988: fig. 14 A) = 0
—Each group consisting of large outer stylophore and small externally visible inner stylophore (Giusti & Manganelli, 1989: fig. 9 A) = 1
—Each group consisting of large outer stylophore and externally visible residues of the inner stylophore (Manganelli & Giusti, 1989: fig. 1 E) = 2
—Each group consisting of larger outer stylophore and very small, not externally visible, inner stylophore (Schileyko, 1987a: fig. 43) = 3
—Each group consisting of large outer stylophore and extremely reduced not externally visible inner stylophore (Giusti & Manganelli, 1989: fig. 9 C) = 4
Remarks: the scheme of the dart-sac complex in *Helicella* reproduced by Hausdorf (1988: fig. 8) is incorrect: the inner stylophore, referred to as "Nebensack," appears too large and externally visible.

6—Digitiform glands.
—All around vagina = 0
—On one side of vagina = 1
Remarks: situation not clear enough in drawings by Schileyko (1978a, 1978b) of the genitalia of *Edentiella, Nanaja* and *Plicuteria.* The situation in *Hygrohelicopsis* and *Leucozonella* showed by the same author (Schileyko, 1978a, 1978b) seems to indicate digitiform glands all around vagina. Species of *Cernuella* (s. str.) show digitiform glands all around vagina (*C. caruanae*) or on one side of the vagina (*C. virgata*).

7—Basal portion
—Stylophore groups opening directly into vagina without a wide basal dilated portion (Manganelli & Giusti, 1988: fig. 14 E) = 0
—Stylophore groups opening in a wide dilated basal portion (Manganelli & Giusti, 1989: fig. 1 E) = 1

8—Inner stylophores.
—With thin muscular walls and large internal cavity (Manganelli & Giusti, 1988: fig. 14 E) = 0
—With thick muscular walls and small internal cavity (Manganelli & Giusti, 1988: fig. 14 A) = 1
Remarks: transverse and longitudinal sections of dart-sac complex in *Edentiella, Kokotschashvilia, Leucozonella, Nanaja, Plicuteria* unknown. Situation as reported by Schileyko (1978a, 1978b) for *Caucasigena* and *Hygrohelicopsis* not clear enough.

9—Opening of stylophores.
—Openings of inner and outer stylophore cavities into vagina close to each other (Manganelli & Giusti, 1988: fig. 14 E) = 0
—Openings of inner and outer stylophore cavities into vagina very far apart (Manganelli & Giusti, 1988: fig. 14 A) = 1

10—Inner vaginal accessory structures.
—Opening of stylophores in a groove bordered by folds (Manganelli & Giusti, 1988: fig. 8 A) = 0
—Opening of stylophores bordered by rows of papillae (Schileyko, 1987b: fig. 215) = 1
—Vagina with one tongue-like structure for each stylophore group (two tongue-like structures when 2 stylophore groups present) (Giusti & Manganelli, 1989: figs. 3, 9A) = 2
—Vagina with a groove-like structure for each stylophore group (unique tube-like structure when 2 stylophore groups present) (Giusti & Manganelli, 1989: figs. 7, 9 C) = 3
—Vagina with dart-gun through which dart is shoot (Manganelli & Giusti, 1989: figs. 4 E, 14 A) = 4

11—Joint of penis and vagina
—Penis joins vagina distally with respect to stylophores (Manganelli & Giusti, 1989: Fig. 5 F) = 0
—Penis joins distal vagina level with stylophores (Manganelli & Giusti, 1989: fig. 8 B) = 1

12—Proximal penis.
—Proximal penis *Helicopsis* type: transverse sections reveal a duct in the lumen; this duct joins the epiphallus lumen directly with the ejaculatory canal of the penial papilla (Giusti & Manganelli, 1989: fig. 8 F, H) = 0.
—Proximal penis simple: transverse sections only show the penial walls (Manganelli & Giusti, 1988: fig. 11 F) = 1.
Remarks: A structure, only apparently similar to those in *Helicopsis,* seems present in drawings by Manganelli & Giusti (1990: figs. 2C, 3A, 4E for *Xeromunda*), Schileyko (1978b: Fig. 253 for "*Helicella candicans*)", Schileyko, in Damjanov & Likharev (1975: fig. 274, for "*Helicella candicans*" and fig. 278 for "*Helicella spiruloides*"). This is due to the fact that the thin external layer of the penis has been detached during dissection.

13—Glandular area on one side of terminal penis walls.
—absent = 0
—present (this paper: Fig. 3) = 1
Remarks: no data for *Caucasigena, Edentiella, Hygrohelicopsis, Kokotschashvilia, Leucozonella, Nanaja, Plicuteria, Pseudoxerophila;* for *Microxeromagna* unpublished personal data.

14—Frenula.
—Penial papilla with no frenula joining it to the distal penis walls (Manganelli & Giusti, 1988: fig. 7 F–H) = 0
—Penial papilla joined by frenula to the distal penis walls (Manganelli & Giusti, 1988: fig. 6 C–D) = 1

15—Sections of penial papilla.
—*Trichia* type (Schileyko, 1978b: fig. 221) = 0
—*Caucasigena* type (Schileyko, 1978b: fig. 199) = 1
—*Xerosecta* type (Manganelli & Giusti, 1988: fig. 8 C) = 2
—*Helicotricha* type (this paper: Fig. 3C) = 3
—*Microxeromagna* type (Manganelli & Giusti, 1988: fig. 11 E) = 4
—*Leucozonella* type (Schileyko, 1978b: fig. 146) = 5
—*Cernuella* type (Manganelli & Giusti, 1988: fig. 7 G) = 6
Remarks: Species of *Xerotricha* have sections of penial papilla of *Trichia* type (*X. apicina*) and of *Cernuella* type (*X. conspurcata*). Due to variability, *Leucozonella* is based only on the type-species.

---

imately 4 whorls separated by deep sutures, last whorl angled at periphery. Umbilicus open, wide approximately 1/5 of maximum shell diameter. Aperture oblique, oval, lacking internal rib. Peristome not thickened or reflexed. External surface of protoconch with few faint growth lines and microsculpture consisting of fine close longitudinal grooves. External surface of teleoconch with superficially reticulated periostracal layer and transverse rows of very short hairs.

Genitalia: Vaginal complex with relatively long distal vagina; dart-sac complex consisting of

TABLE 3. Original data matrix used for cladistic analysis. All characters with more than two states are treated as not additive.

	Character														
Taxa	1	2	3	4	5	6	7	8	9	10	11	12	13	14	15
Outgroup	0	0	?	?	?	0	0	?	?	0	0	?	0	0	?
Candidula	1	1	1	1	4	1	0	1	0	3	0	1	0	0	6
Caucasigena	?	0	0	0	0	1	0	0	0	0	0	1	?	0	1
Cernuella	1	1	1	1	0	?	0	0	1	4	1	1	0	1	6
Edentiella	?	0	0	0	0	?	0	?	0	0	0	1	?	0	1
Helicella	1	1	0	1	4	1	0	1	0	3	0	1	0	0	6
Helicopsis	0	1	0	0	0	1	0	0	0	0	0	0	0	0	0
Helicotricha	0	1	0	0	0	1	0	1	0	0	0	1	1	0	3
Hygrohelicopsis	?	1	0	1	3	1	0	0	0	0	0	?	?	0	0
Hygromia	0	0	1	1	0	1	0	0	1	4	0	1	0	0	6
Kokotschashvilia	?	0	0	0	0	1	0	?	0	0	0	?	?	0	0
Leucozonella	?	0	0	1	0	1	0	?	0	0	0	?	?	0	5
Microxeromagna	0	1	1	0	0	0	0	1	0	0	0	1	1	0	4
Nanaja	?	0	0	1	1	?	0	?	0	2	0	1	?	0	6
Plicuteria	?	0	0	0	0	?	0	?	0	1	0	?	?	0	0
Pseudoxerophila	0	1	0	1	0	1	1	1	0	0	0	?	?	0	?
Trichia	0	0	0	0	0	1	0	1	0	0	0	0	0	0	0
Xerolenta	0	1	0	1	2	1	1	1	0	0	0	1	0	0	6
Xeromunda	0	1	1	1	2	?	1	1	0	0	0	1	0	0	6
Xerosecta	0	1	1	0	0	1	0	1	0	0	0	1	0	0	2
Xerotricha	0	1	0	1	1	1	0	1	0	2	0	1	1	0	?

two pairs of stylophores disposed on opposite sides of vagina, each pair consisting of a smaller inner and a larger outer stylophore; outer stylophore containing slightly curved darts of circular section near base and oval or rhombic section thereafter; each inner stylophore (called "accessory sacs" by Nordsieck, 1987, and Hausdorf, 1988; see Giusti & Manganelli, 1989: 51, for a discussion of homology and terminology of this structure) showing wide, totally dartless internal cavity; cavities of outer and inner stylophore of each couple in communication and opening into vagina in a single opening bordered by two large anteriorly fused pleats. Digitiform glands forming two groups, each of two glands, sometimes apically branched, arising from opposite sides of distal vagina close to point where bursa copulatrix duct arises. Bursa copulatrix duct of medium length, with initial portion slightly flared. Penial complex with flagellum almost as long as epiphallus plus penis. Epiphallus (from end of vas deferens to point of attachment of penial retractor) long, almost twice penis length. Penis (from point of attachment of penial retractor to genital atrium) lacking distinct penial sheath and distally enlarged. Wide area yellow in colour and covered with glandular tissue, on external side of terminal portion of penis walls. Penial papilla cylindrical, formed by a wide tube with thin walls. Penial papilla lumen continuous with that of proximal penis and epiphallus. T-shaped (in transverse section) pilaster running entire length of penial papilla and joined to it by a peduncle, so that cross section of papilla plus pilaster resembles card figure spades.

Right ommatophore retractor free of penis and vagina.

Penial nerve apparently arising in the right cerebral ganglion (according to Franc, 1968: 473, even if it comes from cerebral ganglion the penial nerve originates in the pedal ganglion).

Origin of the Name

Helicotricha, gender feminine.

The small helicoid shell with hairy periostracum suggested the name of the new genus.

Type species

Helicotricha carusoi n. sp.

Helicotricha carusoi n. sp.
[Figs. 1A–C, 2A–D, 3A–D, 4A–D, 5A–D, G, 6A–C]

Helicella (Xerotricha) conspurcata,—Giusti, 1973: 259–260 [partim, *non* Draparnaud, 1801].

FIG. 1. Shells of *Helicotricha carusoi* n. gen. n. sp. Holotype (A) and one paratype (B) from Alicudi Island: Perciato, F. G. leg. 24.10.69. A shell from Salina Island: Pollara, R. Arcidiacono leg. 21.9.66 (C).

Helicopsis sp.,—Piantelli et al., 1990: Table 5 et passim.

Diagnosis

At present the only species of the genus *Helicotricha* known. Specific coincides with generic diagnosis.

Description

Shell (Figs. 1A–C, 2A–D): Shell small (Figs. 1A–C), hairy, low conical above, convex below, opaque brown in colour, with white flecks. White flecks widely distributed over shell surface, concentrated above (near sutures and near periphery of last whorl) to form irregularly spaced spots of variable shape, below (from periphery of last whorl to umbilicus) to form white spiral bands of variable width and number (2–6). Spire depressed-conical, consisting of 4–4½ convex, regularly increasing whorls separated by deep sutures; last whorl angled at periphery, dilated, sometimes descending slightly near aperture. Umbilicus open and wide, approximately 1/5 of maximum shell diameter. Aperture markedly oblique, oval, lack-

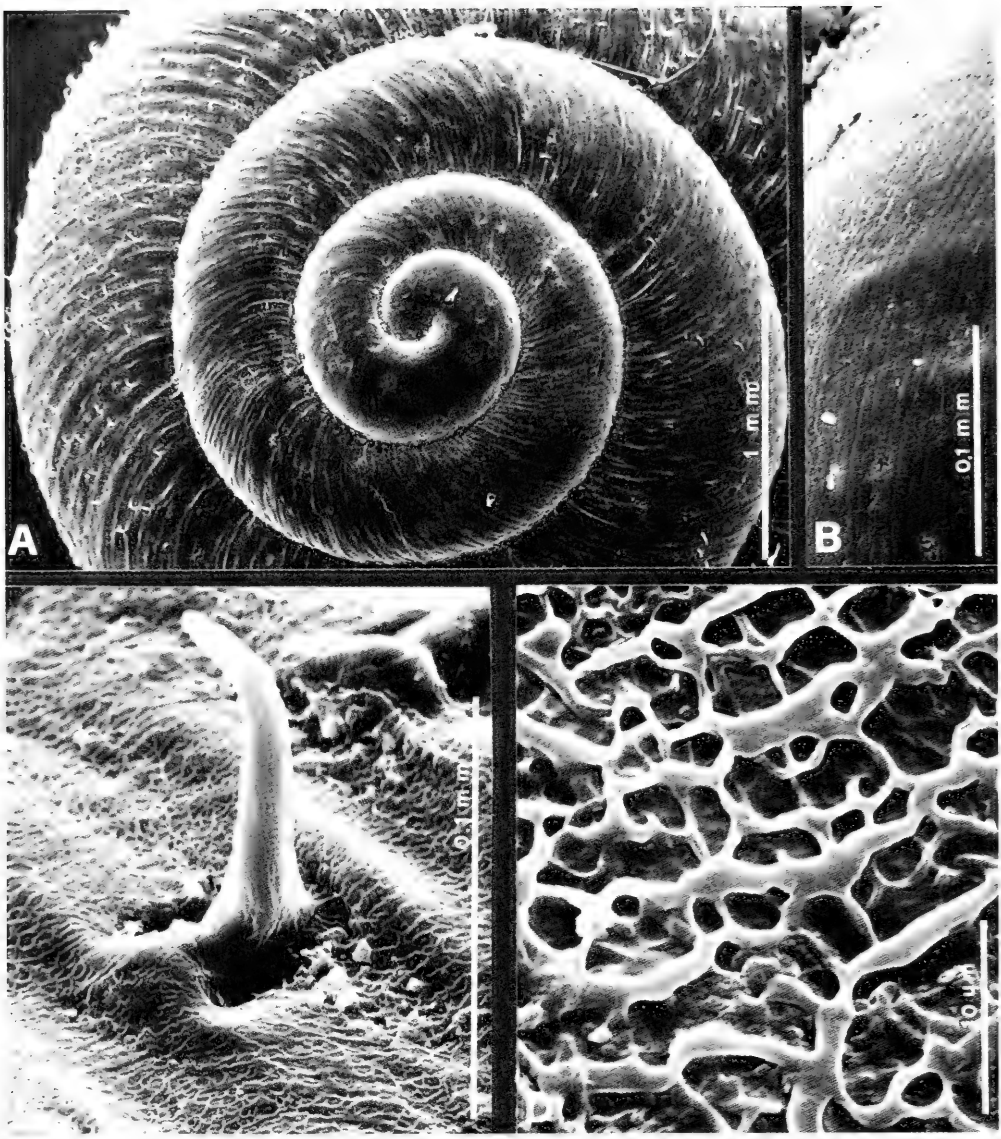

FIG. 2. External shell surface of specimens of *Helicotricha carusoi* n. gen. n. sp. collected on Panarea Island, D. Caruso & I. Marcellino leg. 27.5.67 (A–B) and Lipari Island: Monte Sant'Angelo, F.G. leg. 23.10.69 (C–D). A: A view of first whorls. B: Detail of protoconch showing longitudinal grooves. C: Detail of last whorl with one hair and reticular microsculpture of teleoconch. D: Detail of reticular microsculpture of teleoconch.

ing internal rib; peristome not thickened, slightly reflexed at its columellar margin.

External surface of protoconch with few faint growth lines near its end (Fig. 2A) and microsculpture consisting of fine close spiral grooves (Fig. 2B). External surface of teleoconch (Fig. 2A) with many growth lines, more marked near sutures. Periostracal layer (Fig. 2C–D), superficially reticulated (Fig. 2D) to form transverse rows of very short, often hook-shaped hairs 0.1 mm in length (Fig. 2C). Reticulation and hairs of caducous appearance, absent in large portions of surface. Surface of mineralized portion of shell (in areas devoid of periostracal layer) seems to be crossed by fine close spiral grooves.

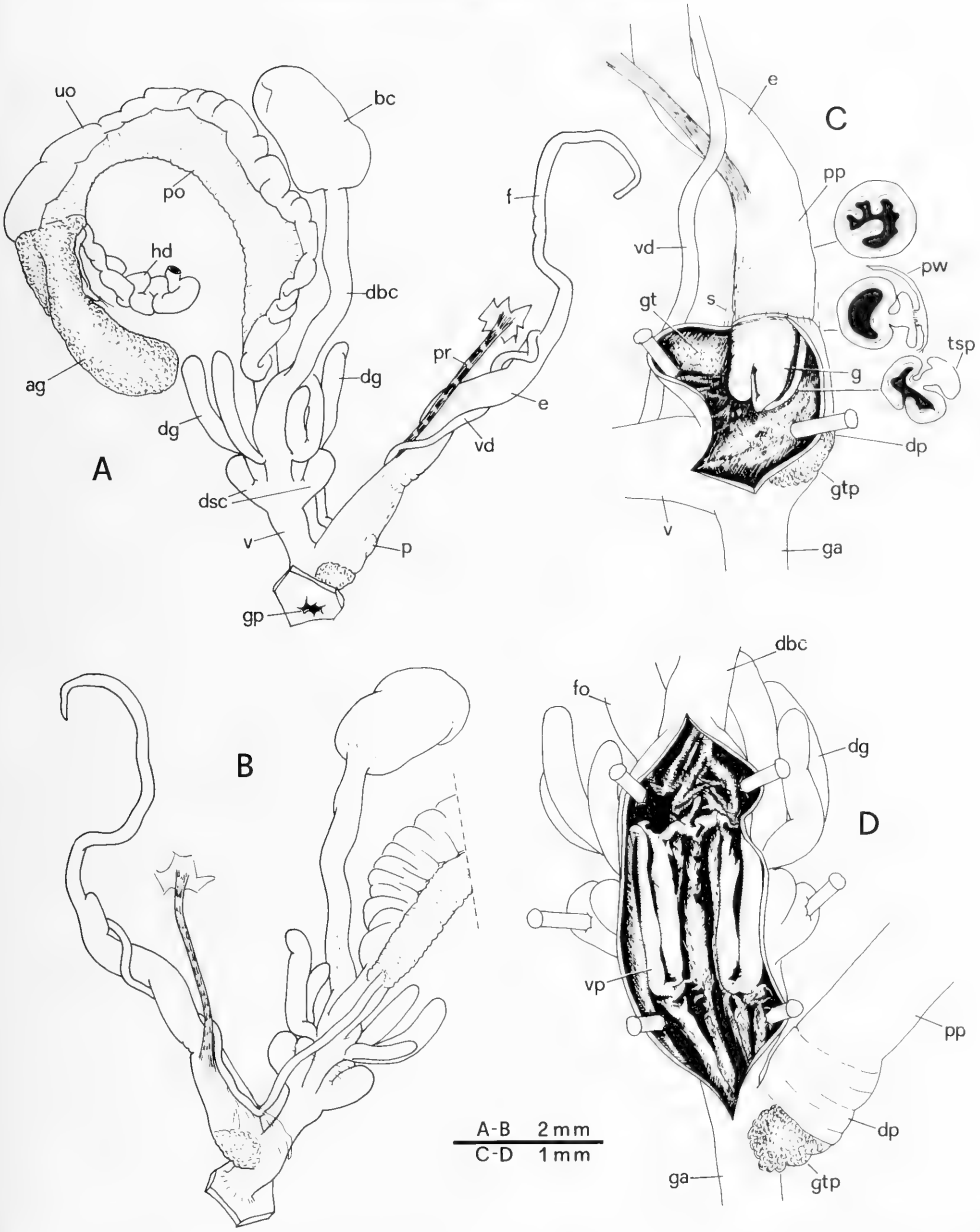

FIG. 3. Genitalia of *Helicotricha carusoi* n. gen. n. sp. in specimens collected on Basiluzzo Islet, F. G. leg. 5.11.69. A–B: Two opposite views of the same genital apparatus (gonad excluded in A; gonad and part of ovispermiduct excluded in B). C: Part of penial complex with distal penis opened to show penial papilla, a section of proximal penis and two sections of penial papilla. D: Vagina opened to show its inner structure. Explanations of the symbols used in Figures 3–5, 8: ag, albumen gland; bc, bursa copulatrix (gametolytic gland); dbc, duct of bursa copulatrix; dg, digitiform glands; dsc, dart-sac complex; dp, distal penis; e, epiphallus; f, flagellum; fc, fertilization chamber; fn, fenestration; fo, free oviduct; fr, frenula; g, penial papilla (glans); ga, genital atrium; gp, genital pore; gt, glandular tissue; gtp, gland of the terminal penis; hd, hermaphrodite duct; p, penis; po, prostatic portion of ovispermiduct; pp, proximal penis; pr, penial retractor muscle; pv, proximal vagina; pw, penial wall; s, stripes; sr, seminal receptacle; t, talon; tsp, t-shaped pilaster of the penial papilla; uo, uterine portion of ovispermiduct; v, vagina; vd, vas deferens.

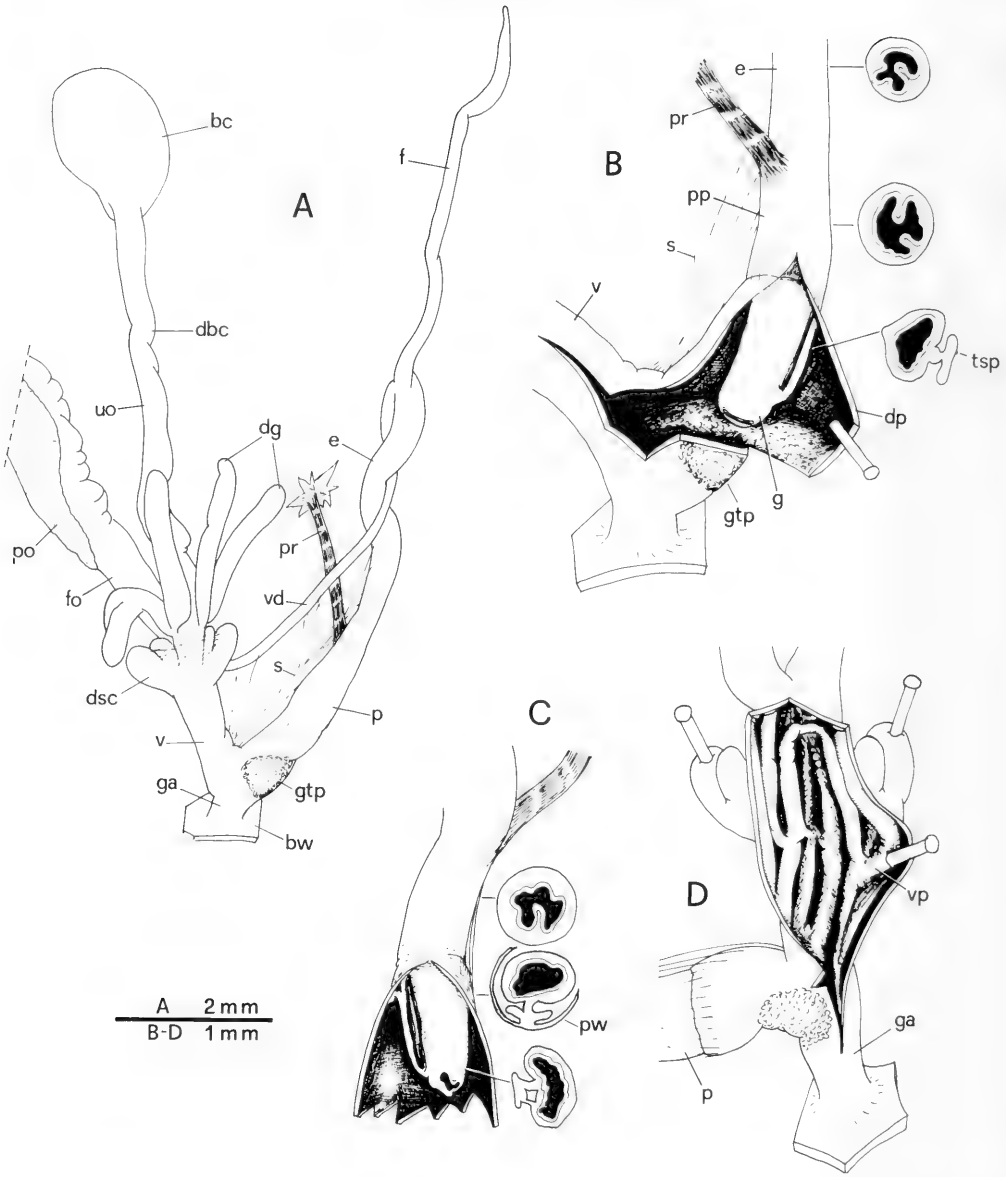

FIG. 4. Genitalia of *Helicotricha carusoi* n. gen. n. sp. in specimens collected on Filicudi Island: Stimpagnato, F. G. leg. 28.10.69. A: Genital apparatus (gonad and part of ovispermiduct excluded). B–C: Part of two penial complexes with distal penis opened to show penial papilla, section of epiphallus, proximal penis and penial papilla (B), Section of proximal penis and two sections of penial papilla (C). D: Vagina opened to show its inner structure.

Dimensions (N = 10): shell max. diam.: 4.5–5.4 mm; shell height: 2.5–3.4; aperture max. diam.: 2.0–2.5 mm; aperture height: 1.7–2.1.

Dimensions of the holotype: shell max. diam.: 5.3 mm; shell height: 2.8; aperture max.: diam. 2.1 mm; aperture height: 2.1

Genitalia (Figs. 3A–D, 4A–D, 5A–D, G): Convoluted first hermaphrodite duct arising from

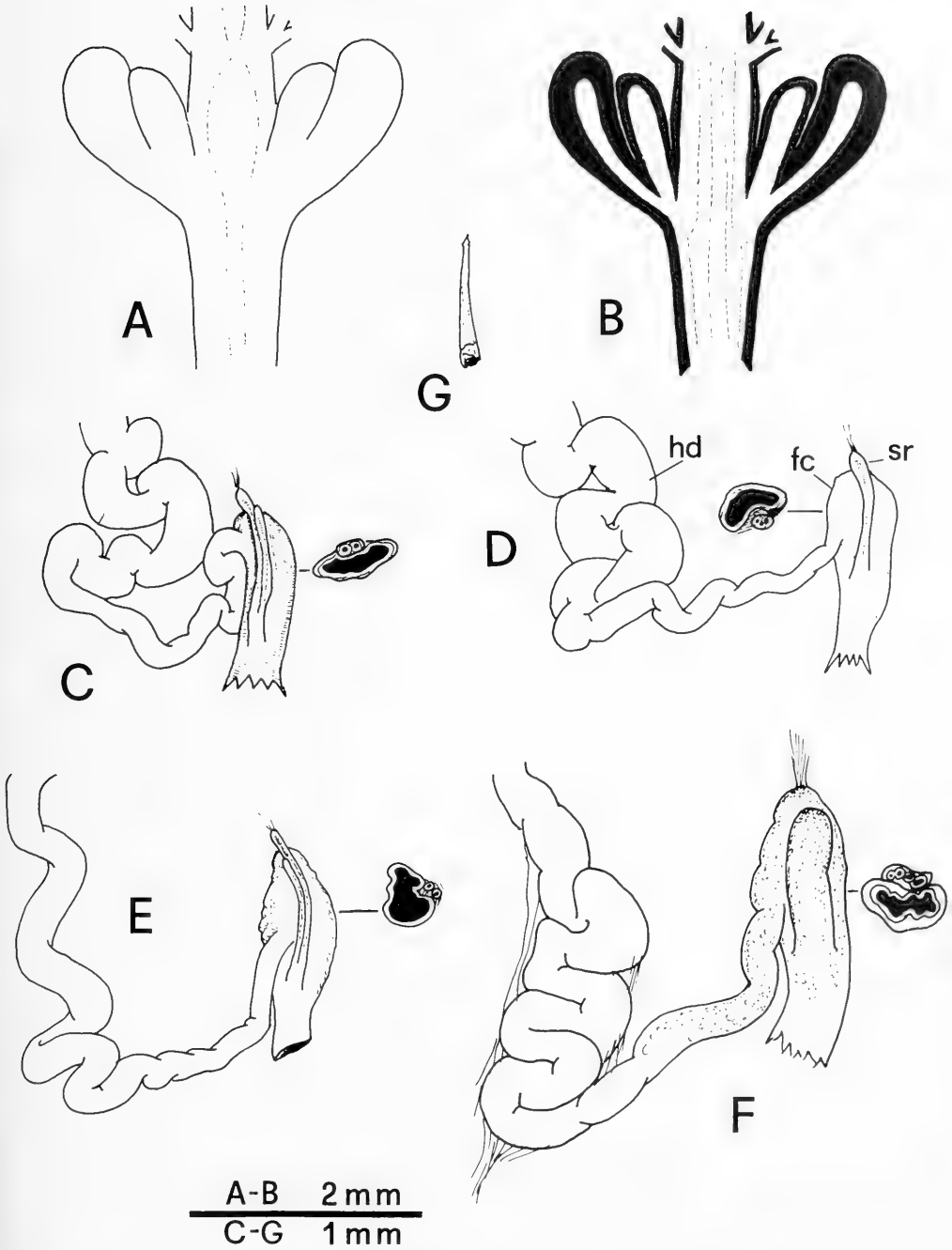

FIG. 5. Outline and scheme of dart-sac complex (darts omitted) (A–B), talon (C–D) and dart (G) of *Helicotricha carusoi* n. gen. n. sp. in specimens collected on Filicudi Island: Stimpagnato, F. G. leg. 28.10.69, talon (E) of *Microxeromagna armillata* from Corsica: Olmeto, F.G. & G.M. leg. 1.12.83 and talon (F) of *Helicopsis striata* from Öland, parish Persnäsa (Jordhamn, Sweden).

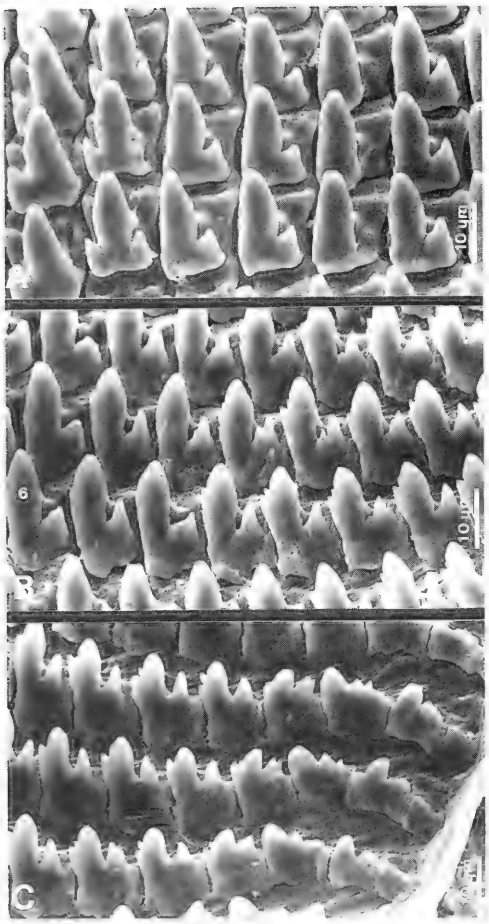

FIG. 6. Radula of *Helicotricha carusoi* n. gen. n. sp. in a specimen collected on Basiluzzo Islet, F. G. leg. 5.11.69. A: Central tooth and first lateral teeth. B: 6th–12th lateral teeth. C: Extreme marginal teeth.

multilobate gonad (not illustrated) and ending in talon (i.e. fertilization chamber plus seminal receptacle complex); talon lying on surface of inner side of large albumen gland. Talon (Fig. 5C–D) with wide lateral fertilization chamber embracing basal portion of seminal receptacle complex. Receptacle complex very slender, only slightly enlarged apically and containing 2–3 very small distinct sperm tubes. Ovispermiduct wide, plurilobate, consisting of prostatic and uterine portions. Prostatic portion continuing anteriorly into vas deferens and proximal portion of penis complex. Penis complex (Figs. 3A–B, 4A) consisting of penial flagellum, epiphallus (i.e. from end of vas deferens to point of attachment of penial retractor muscle) and penis (i.e. from point of attachment of penial retractor muscle to genital atrium). Penial flagellum long (4.9–5.5 mm; N = 3) and slender along entire length. Epiphallus longer (3.0–4.0 mm; N = 3) than penis (2.0–2.3 mm; N = 3) and narrower. Penis lacking distinct penial sheath but with thin bands of tissue arising where penial retractor muscle ends and terminating near penis end. Penis distally enlarged where it contains penial papilla (= glans). Wide area yellow in colour and covered with glandular tissue (also evident internally) on external side of terminal portion of penis walls. Penis walls level with base of penial papilla sometimes appear to contain glandular tissue. Penial papilla (Figs. 3C, 4B–C) cylindrical, consisting of a wide tube. Penial papilla lumen continuous with proximal penis and epiphallus. T-shaped (in transverse section) pilaster running alongside penial papilla for entire length, joined to it by a peduncle. Ejaculatory pore at apex of penial papilla, slit-like, variable in width. T-shaped pilaster basally connected to penis wall for short distance at penial papilla base (Figs. 3C, 4C). Penial retractor muscle usually short. Uterine portion of ovispermiduct continuing anteriorly into short (approximately 1 mm; N = 3), wide uterine canal (i.e. free oviduct) ending in vagina level with point of entry of duct (4–6 mm in length; N = 3) of bursa copulatrix. Bursa copulatrix (i.e. gametolytic gland) (Figs. 3A–B, 4A) sac-like and variable in shape. Duct of bursa copulatrix 4–6 mm long (N = 3), its initial portion slightly flared, internally figured with series of fine pleats. Dart-sac complex consisting of two pairs of stylophores, each pair consisting of a smaller inner dartless stylophore and a larger outer dart-bearing stylophore. Opening of each pair of stylophores clearly visible half way along vagina on opposite sides (Figs. 3A–B, 4A, 5A–B). Two pairs of digitiform glands also opening on opposite sides of proximal vagina close to dart-sac complex. Digitiform glands irregular in shape and sometimes apically bifurcated. Each digitiform gland and dart-sac pair opens into the vagina within a furrow laterally bordered by two large, distally fused folds (Figs. 3D, 4D). Other smaller folds run longitudinally on the internal vagina walls between two systems of larger folds. All folds taper distally to end on internal genital atrium walls. Dart of each outer stylophore very small (1 mm in length; N = 2), basally circular

in transverse section, apically flattened-oval or rhombic, tip arrowhead-shaped (Fig. 5G).

Other Anatomical Characters: Penial nerve apparently originating in right cerebral ganglion (according to Franc, 1968: 473, even if it comes from cerebral ganglion the penial nerve originates in the pedal ganglion).

Right ommatophore retractor independent of penis and vagina (i.e. not passing between the penis and vagina).

Radula (Fig. 6A–C): Radula consisting of many rows of teeth each according to formula 20–22 + C + 20–22. Central tooth with wide basal plate and raised pointed upper vertices. Body of tooth with very large mesocone and two small ectocones, 1/3 of mesocone length. First lateral teeth having wide basal plate but with inner vertex missing; body with large pointed mesocone and small pointed ectone 1/4 of mesocone length. At about 6th or 7th lateral tooth, inner side of mesocone showing slight protuberance developing into pointed cusp in following lateral and marginal teeth. Moving laterally, teeth maintaining same shape but progressively smaller, with more pointed cusps and reduced basal plates. Last marginal teeth having mesocone apex with 2–3 cusps and ectotone split into 2–4 smaller points.

Jaw: Jaw odontognathous, strongly ribbed and devoid of central denticle.

Type Locality

Aeolian Islands, Alicudi Island: Perciato [UTM references: 33SVC4465].

Typical Series

Holotype (shell) (Fig. 1A) and 7 paratypes (2 shells + 3 dissected specimens + 2 spirit specimens) from the type locality, F. G. leg. 24.10.69. Holotype and all the paratypes in Giusti Collection, Dipartimento di Biologia Evolutiva, Università degli Studi di Siena, Via Mattioli 4; I-53100 Siena, Italy. Other material examined (all from Aeolian Islands [UTM ref.: 33SVC, WC])

Alicudi Island [33SVC46]: Spano [[4467], F. G. leg. 26.10.69 (2 spirit specimens + 2 dissected specimens).

Basiluzzo Islet [33SWC07]: S. Bruno leg. 25.2.67 (7 spirit specimens), F. G. leg. 5.11.69 (1 spirit specimen + 1 dissected specimen); F. G. leg. 31.3.71 (3 spirit specimens).

Filicudi Island [33SVC66, 67]: Siccagni [6070], F. G. leg. 29.10.69 (1 spirit specimen); Stimpagnato [6168], F. G. leg. 28.10.69 (4 spirit specimens + 2 dissected specimens); Between Canale and Monte Guardia [6268, 6368], F. G. leg. 28.10.69 (3 spirit specimens); Zucco Grande [6270, 6370], F. G. leg. 30.10.69 (2 spirit specimens + 1 shell), F. G. leg. 23.3.72 (2 shells).

Lipari Island [33SVC95, 96]: G. Marcuzzi leg. 13.4.68 (1 shell + 1 spirit specimen); Capistello [9556, 9656], F. G. leg. 27.4.70 (1 shell); Monte Sant'Angelo [9360, 9460], F. G. leg. 23.10.69 (5 shells).

Lisca Bianca Islet [33SWC07]: F. G. leg. 5.10.69 (7 spirit specimens)

Panarea Island [33SWC07]: D. Caruso & I. Marcellino leg. 27.5.67 (5 shells), Punta del Corvo [0576], F. G. leg. 30.3.71 (1 shell + 1 spirit specimen); Punta Milazzese [0575], F. G. leg. 5.11.69 (1 spirit specimen + 1 dissected specimen).

Salina Island [33SVC86, 87]: Capo Faro [8870], F. G. leg. 25.4.70 (2 spirit specimens); Lingua [8865], F. G. leg. 25.4.70 (2 spirit specimens + 1 dissected specimen); Malfa [8570], R. Arcidiacono leg. 17.9.66 (1 spirit specimen); Monte dei Porri [8368, 8468], F. G. leg. 26.4.70 (3 spirit specimens); Pollara [8369], R. Arcidiacono leg. 21.9.66 (1 shell), F. G. leg. 25.4.70 (1 spirit specimen); Rinella [8566], F. G. leg. 26.4.70 (1 shell); Valle del Santuario [8568], F. G. leg. 25.4.70 (1 spirit specimen).

Stromboli Island [33SWC19, 20]: G. Marcuzzi leg. 16.4.68 (28 spirit specimens).

Vulcano Island [33SVC95]: G. Marcuzzi leg. 12.4.68 (2 shells); Porto [9652], F. G. leg. 27.4.70 (2 spirit specimens + 1 shell).

All the material in Giusti Collection, Dipartimento di Biologia Evolutiva, Università degli Studi di Siena, Via Mattioli 4; I-53100 Siena, Italy.

Locality names and UTM references based on the Official Map of Italy 1:25.000 Series M 891.

Origin of the Name

The new species is dedicated to Prof. Domenico Caruso, Director of the Department of Animal Biology, University of Catania, Italy, in token of highest esteem and companionship.

DISCUSSION

Generic Status

As outlined in the introduction, the supraspecific status of the new species was difficult to establish. Some anatomical features (2 + 2 stylophores and right ommatophore retractor independent of penis and vagina) suggested relationships with more than one genera of Hygromiidae found in the western Mediterranean and Europe: *Xerotricha* Monterosato, 1892 (type species: *Helix conspurcata* Draparnaud, 1801), *Helicella* Fèrussac, 1821 (type species: *Helix itala* Linnaeus, 1758) and *Helicopsis* Fitzinger, 1833 (type species: *Helix striata* Müller, 1774) (see Gittenberger, 1969; Gittenberger & Manga, 1977; Schileyko, 1978a; Gittenberger & Raven, 1982; Giusti & Manganelli, 1989; Gittenberger et al., 1989; Hausdorf, 1988).

Following the scheme of classical evolutionary systematics a first comparison was made with *Xerotricha,* the type species of which, *X. conspurcata* (Draparnaud, 1801), has a small hairy shell that differs from *Helicotricha carusoi* n. sp. only by virtue of its longer periostracal hairs and its narrower umbilicus.

Xerotricha conspurcata, like both its congeneric species, *X. apicina* (Lamarck, 1822) and *X. nubivaga* (Mabille, 1882) (Hausdorf, 1988; Gittenberger et al., 1989, Giusti & Manganelli, 1989), shows a differently structured vaginal complex characterized by a large dart-sac complex consisting of two pairs of stylophores, each constituted by a larger outer dart-bearing stylophore and a very small inner dartless stylophore (i.e. 2 + 2) (see Giusti & Manganelli, 1989: 51, for a discussion of homology and terminology of these structures). The latter open into the vagina inside the slit delimited by two large tongue-like structures that are apically independent of each other (Hausdorf, 1988: fig. 9; Giusti & Manganelli, 1989: figs. 3, 5, 9A–B). The penial papilla in *Xerotricha* is also different, being simple and without lateral pilaster (Giusti & Manganelli, 1989: figs. 2D, 4E).

Anatomically the new species is also similar to some small *Helicella* with shells that have persistent postembryonic hairs (e.g. *H. corderoi* Gittenberger & Manga, 1977—see Gittenberger & Manga, 1977; Manga Gonzales, 1983; *H. mangae* Gittenberger & Raven, 1982—see Gittenberger & Raven, 1982; according to Prieto, 1986, this nominal species is a junior synonym of *H. gonzalei* Azpeitia, 1924). Nevertheless, *Helicella* has a dart-sac complex which, although similar (consisting of two opposite pairs of stylophores, each formed by a very large apically pointed outer stylophore and a very reduced, almost vestigial, inner dartless stylophore, i.e. 2 + 2), opens internally into a continuous pleated tube-like structure contained in the vagina (Hausdorf, 1988: fig. 8; Giusti & Manganelli, 1989: figs. 6A,E, 7, 9C). In *Helicella,* the penial papilla is also different, being simple and without lateral pilaster (Hausdorf, 1988: fig. 8; Giusti & Manganelli, 1989: fig. 6F).

Detailed comparison was then made with *Helicopsis*[4], the species of which have a very similar genital scheme (Hesse, 1934; Gittenberger, 1969; Damjanov & Likharev, 1975; Schileyko, 1978a; Grossu, 1983; Giusti & Manganelli, 1989; present paper: Figs. 5F, 8A–C). *Helicopsis* (s. str.) has so far been identified with certainty only in central and oriental Europe, and subgenus *Xeroleuca* Kobelt, 1877 (type species: *Helix turcica* Holten, 1802) has been reported in northwestern Africa (Hesse, 1934; Zilch, 1960). There are two records of *Helicopsis* (s. str.), one in Tunisia (Ktari & Rezig, 1976) and one at Huelva, Spain, (Gasull, 1972, 1985) that must be checked. The species briefly studied by Ktari & Rezig (1976) may correspond to a species found by one of us in Morocco (Figs. 7A, 8A–C). *Helicopsis* (s. str.) has a small, thick, robust, ribbed and hairless shell and a vagina with a dart-sac complex constituted by two opposite pairs of stylophores, each formed by an outer and an inner stylophore (i.e. 2 + 2). The outer stylophores are smaller and more slender than those in *Xerotricha* and *Helicella* and are more clearly distinguished from the inner dartless stylophores which, in their turn, are larger than those in *Xerotricha* and *Helicella.* Moreover, the vagina in *Helicopsis* is clearly different from that in *Xerotricha* and *Helicella,* being internally devoid of tongue-like or tube-like structures into which the stylophores open (Giusti & Manganelli, 1989: figs. 8C, 9D). In view of the above and because the new species and those of *Helicop-*

[4]While the paper was in press, Hausdorf (1990b) described the genitalia of three species-group taxa supposed to belong to genus *Helicopsis: H. gittenbergeri* n. sp., *H. s. subcalcarata* (Naegele, 1903) and *H. subcalcarata neuberti* n. subsp. Comparison with the latter taxa has been omitted because no information about the penial papilla structure, the only sure diagnostic character for *Helicopsis,* was furnished.

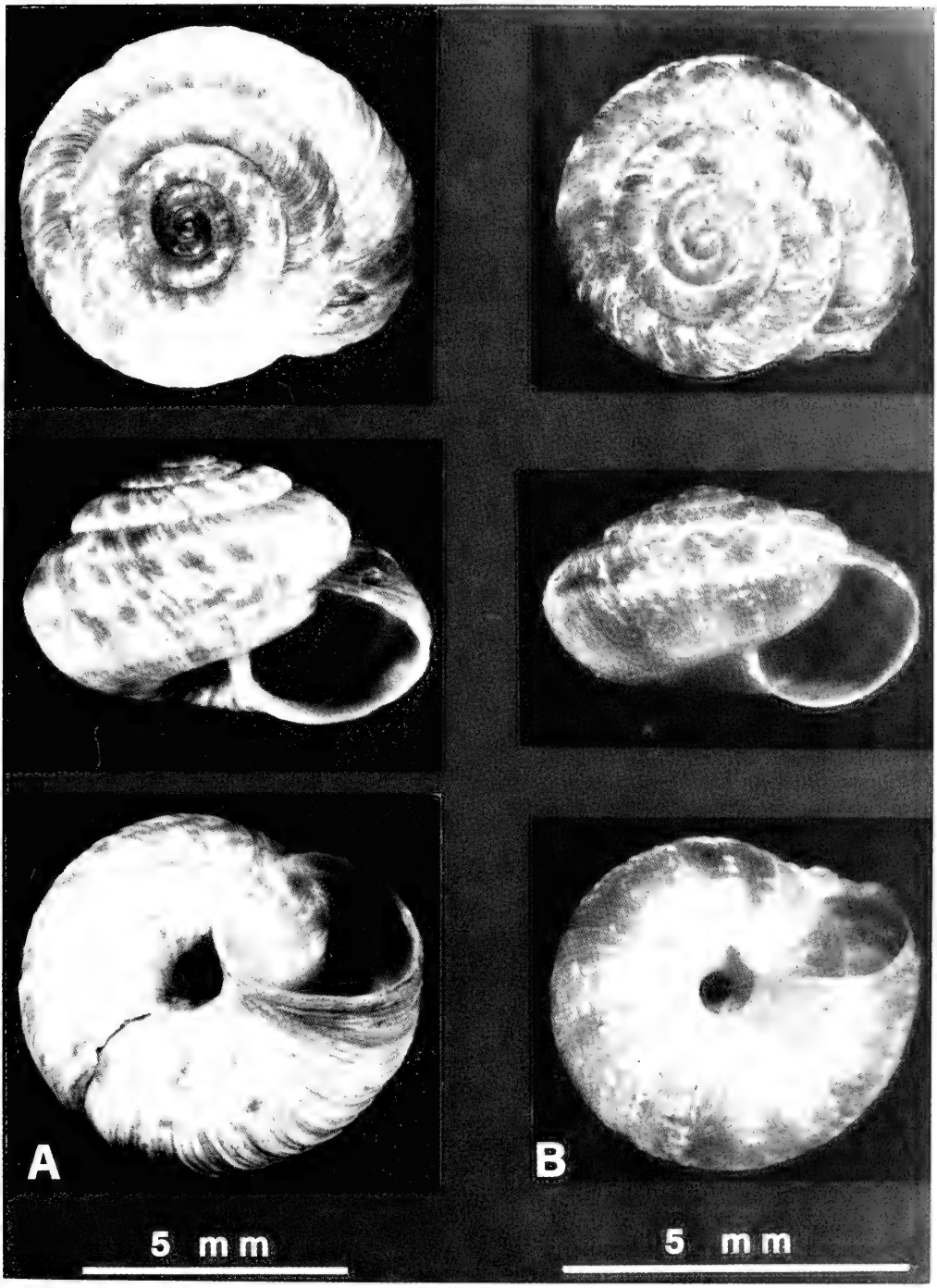

FIG. 7. A: Shell of *Helicopsis* sp. collected at the foot of Mount Zerboum, Moulay Idris (Morocco). B: Neotype of *Helix aetnea* Benoit, 1857, Nicolosi sull'Etna, C. Caroti leg. 1877 (Museum of Zoology, University of Florence, Italy, MZUF no. 5049/1).

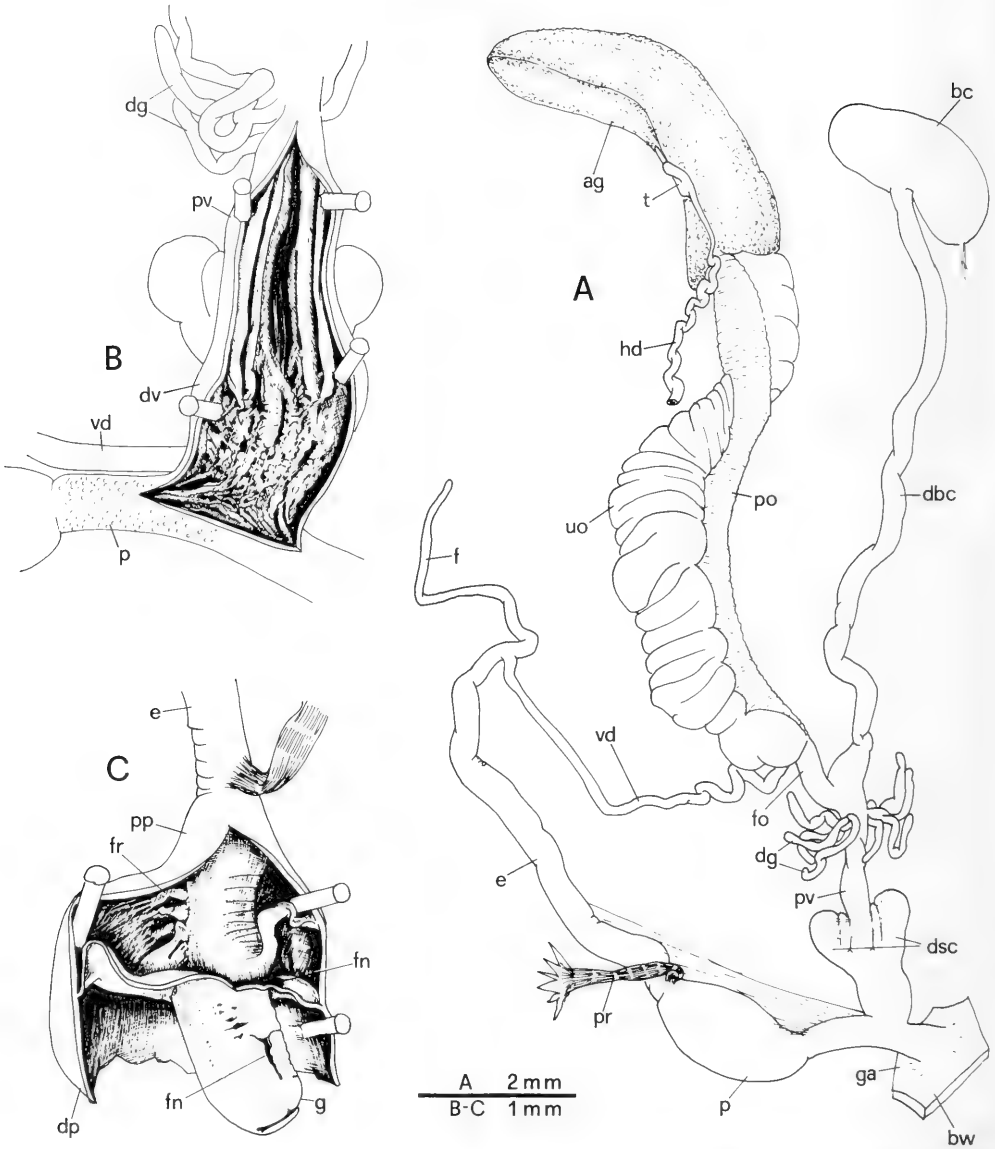

FIG. 8. Genitalia of *Helicopsis* sp. in specimens collected at the foot of Mount Zerboum, Moulay Idris (Morocco). A: Genital apparatus (gonad excluded). B: Vagina opened to show its inner structure. C: Part of the penial complex with the penis opened to show the penial papilla.

sis (Schileyko, 1978a: fig. 237; Giusti & Manganelli, 1989: fig. 8C) have stylophores opening in a slit bordered by two large but simple pleats running along the vagina walls, it seems plausible to include the new species in the genus *Helicopsis*. Nevertheless, the structure of the penial complex in the new species differs from that in *Helicopsis*. The species of the latter genus, about which there is detailed knowledge of genital structure, have a penial papilla consisting of a central tube wrapped in an external sheath that is more or less laterally and basally fenestrated and which basally expands to reach and to fuse with the penial walls (Schileyko, 1978a: figs. 235, 238–242, 244; Giusti & Manganelli,

1989: figs. 8D, F–H; present paper: Fig. 8C). In so doing, the sheath distinguishes the cavity of the distal penis (containing the penial papilla) from that of the proximal penis, although it does not impede communication through its fenestrations. The cavity of the proximal penis is traversed by a tube that has sometimes a lateral pilaster connected by frenula to the penis walls and which is basally continuous with the epiphallus and apically with the central tube of the penial papilla. This peculiar penis structure, present not only in the European species but also in the Maghrebian species studied herein, can be considered diagnostic for *Helicopsis.* Consequently, the present new species cannot be included in the genus *Helicopsis.*

One can argue that the penis structure in the present new species may be derived from that in *Helicopsis* through the reduction of the penial papilla sheath (the lateral T-section pilaster may be a residue of the sheath) and the loss the peculiar inner structure of the proximal penis. However this hypothesis seems less probable than the following one.

Helicotricha carusoi n. sp. has a shell clearly resembling in overall structure, microsculpture and colour that of a well-known Mediterranean species: *Microxeromagna armillata* (Lowe, 1852) (Giusti & Manganelli, 1989: pl. 7, figs. A–E). The latter species, moreover, has a genital structure corresponding to that of *H. carusoi* n. sp. (similar talon, similar length and proportions of the parts of the penial complex, a yellow glandular area on distal penis walls; see Ortiz de Zarate Y Lopez, 1950: fig. 22; Forcart, 1976: fig. 3; Clerx & Gittenberger, 1977: figs. 102–103; Falkner, 1981: fig. 2; Aparicio, 1982: fig. 3; Manga Gonzales, 1983: fig. 12; Hausdorf, 1988: fig. 13; Manganelli & Giusti, 1988: figs. 11A–F, 14H; present paper: Fig. 5E). It only differs in the dart-sac complex, which has 0 + 2 stylophores (instead of 2 + 2), and in some details of the penial papilla. Other monophyletic groups have been hypothesized to be formed by genera with 2 + 2 and 0 + 2 stylophores (i.e. *Helicella-Candidula* and *Xerolenta-Xeromunda;* Hausdorf, 1988, 1990a, Giusti & Manganelli, 1989; Manganelli & Giusti, 1989). Similarly, we hypothesize that *Helicotricha* n. gen. forms a monophyletic group with *Microxeromagna.* The former genus can have originated the latter by reduction of the dart-sac complex; the origin of *Helicotricha* from *Microxeromagna* by duplication of the dart-sac complex seems less probable according to Schileyko's (1978a, 1984) reconstruction of the phylogenetic relationships in the Hygromiidae.

Many other genera of the European and Russian Hygromiidae resemble *Helicotricha* n. gen. in having the vaginal complex with digitiform glands and dart-sac complex constituted by two opposite pairs of stylophores, each formed by a large, dart-bearing outer stylophore and a smaller dartless inner stylophore (i.e. 2 + 2): *Hygrohelicopsis* Schileyko, 1977 (type species: *H. darevskii* Schileyko, 1977), *Leucozonella* Lindholm, 1927 (type species: *Helix rubens* von Martens, 1874), *Kokotschashvilia* Hudec & Lezhawa, 1969 (type species: *Helix holotricha* Boettger, 1874), *Caucasigena* Lindholm, 1927 (type species: *Helix eichwaldi* Pfeiffer, 1846), *Plicuteria* Schileyko, 1977 (type species: *Helix lubomirskii* Slosarski, 1881), *Trichia* Hartmann, 1840 (type species: *Helix hispida* Linnaeus, 1758), and *Edentiella,* Polinski, 1929 (type species: *Helix edentula* Draparnaud, 1801) (see Schileyko, 1978a, 1978b). Of these, the genus closest to *Helicotricha* n. gen. is *Hygrohelicopsis* because it shows the right ommatophore retractor independent of penis and vagina. Nevertheless, *Hygrohelicopsis* can be easily distinguished by the structure of distal genitalia showing inner stylophores extremely reduced, not visible from outside, distal vagina absent, and penial papilla bulbous but simple without external sheath or lateral pilaster. All the other genera are more distinguished from *Helicotricha* n. gen. because they have the right ommatophore retractor passing between penis and vagina, different and larger shells, different penial papillae and many other minor differences in the structure of the genitalia (Schileyko, 1978a, 1978b).

Cladistic Analysis

The entire set of character states (Table 2) utilized in the traditional approach was used for cladistic analysis. The latter was attempted even if the characters were few and limited to genitalia structure. To avoid complicating the analysis, only a limited number of eastern European genera was considered: those for which better description exist and which are at least apparently more closely related to the new genus.

A total of 105 most parsimonious hypotheses were generated by our data matrix. All have 37 steps with a consistency index of 0.67 and rescaled retention index of 0.72 after non-informative characters were excluded.

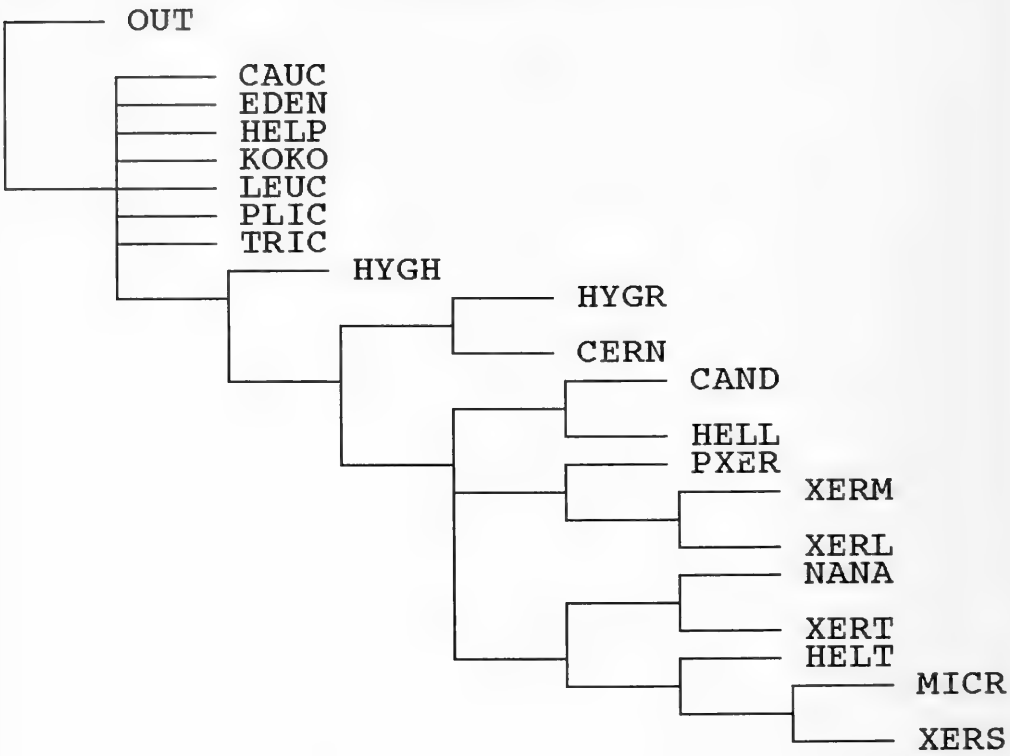

FIG. 9. The Nelsen consensus tree of 105 cladograms.

The successive weighting procedure did not discriminate among them, the main difference being the position of the set of taxa HELP-LEUC. The Nelsen consensus tree of 105 cladograms (Fig. 9) showed that 11 monophyletic groups appear in all of them, listed with their synapomorphies as follows:

(1) All the taxa, except HELP, TRIC, KOKO, PLIC, CAUC, EDEN, LEUC: 2 (1) (parallel with HELP and a reversion in HYGM).
(2) All the taxa, except HELP, TRIC, KOKO, PLIC, CAUC, EDEN, LEUC, HYGH: 15 (6).
(3) HYGM, CERN: 3 (1), 9 (1), 10 (4) (the first parallel with CAND, XERM, MICR, XERS).
(4) CAND, HELL, PXER, XERL, XERM, XERT, NANA, HELT, MICR, XERS: 8 (1) (parallel with HELP, TRIC).
(5) CAND, HELL: 1 (1), 5 (4), 10 (3) (the first parallel with CERN).
(6) PXER, XERL, XERM: 7 (1).
(7) XERL, XERM: 5 (2).
(8) XERT, NANA, HELT, MICR, XERS: 13 (1) (with a reversion in XERS).
(9) XERT, NANA: 5 (1), 10 (2).
(10) HELT, MICR, XERS: 4 (0), 15 (2) (the former is a reversion).
(11) MICR, XERS: 3 (1) (parallel with HYGM, CERN, CAND, XERM).

Character 6 represented a synapomorphy for the entire set of terminal taxa with a reversion in MICR. Figure 10 is one of the 105 minimum-length trees. It is not a preferred tree and is simply given to illustrate the evolution of the characters.

As is evident, the main result of cladistic study has been that of apparently supporting the conclusion reached in the preceeding paragraph, i.e. that *Helicotricha* is a sister group of *Microxeromagna-Xerosecta*. It also appeared to confirm that *Helicotricha* is not closely related to *Helicopsis* as hypothesized in the same paragraph.

Relationships with *Xerosecta* suggested by cladogram seem logical: *Xerosecta* is very

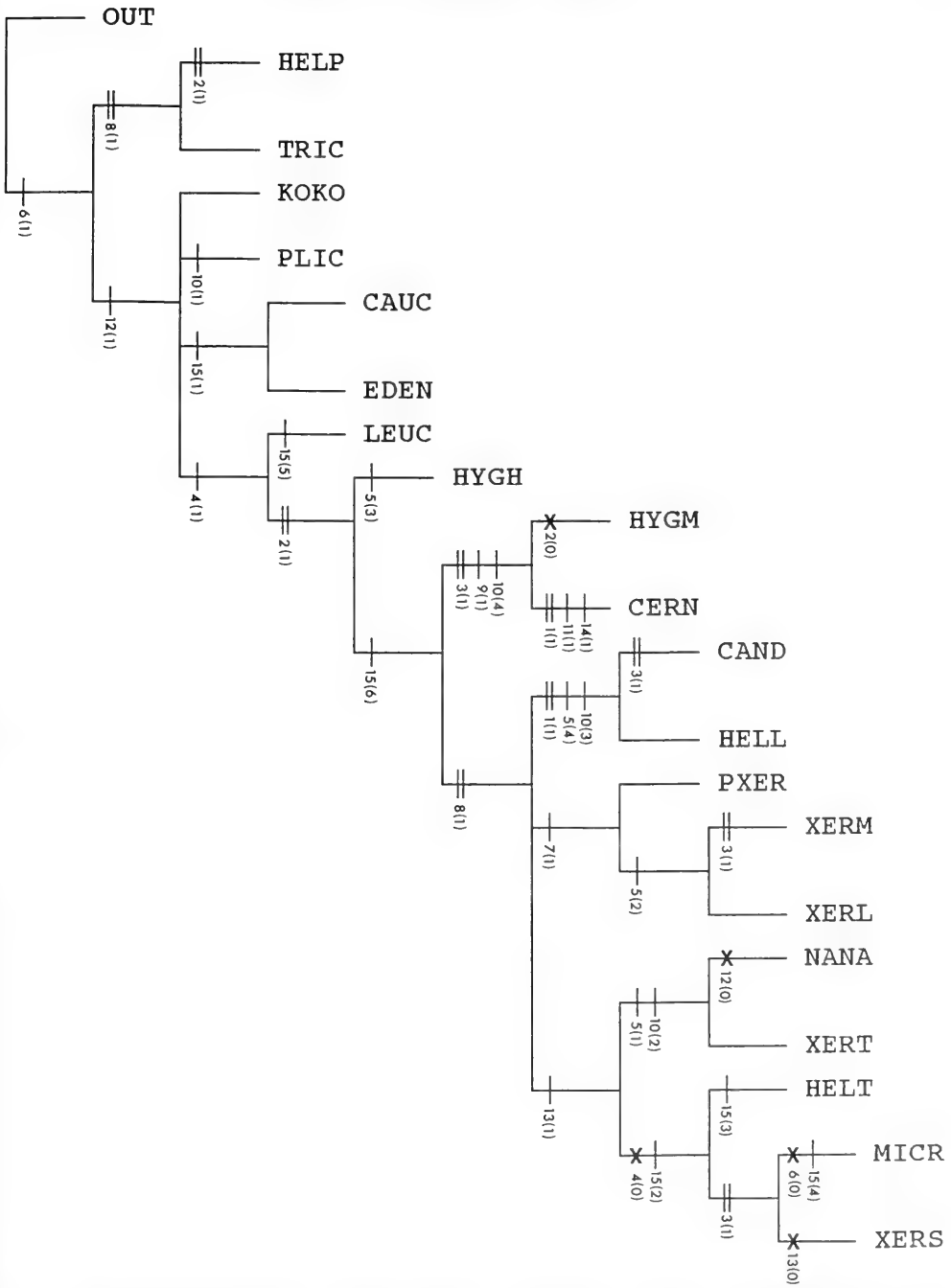

FIG. 10. One of the most parsimonious trees generated by the data matrix given by way of illustration of the evolution of the characters (lines: synapomorphies; double lines: homoplasies; X reversions).

close to *Microxeromagna* (Hausdorf, 1988, 1990c; Manganelli & Giusti, 1988).

The Suprageneric Systematics of the Hygromiidae

The phylogenetic hypothesis concerning *Helicotricha* n. gen. formulated above, in addition to those concerning *Xerolenta-Xeromunda* and *Helicella-Candidula,* disagrees with Schileyko's proposal to distinguish the Trichiinae (hygromiids with 2 + 2 stylophores) from the Hygromiinae (hygromiids with 0 + 2 stylophores).

The present data supports the idea that the supposed members of one of these "subfamilies" independently evolved from supposed members of the other so that their derived status is due to parallelism (Giusti & Manganelli, 1987).

The consideration of a larger number of characters, when eventually available (genetic, cytological, etc.) could promote better understanding of the phylogeny of Hygromidae (and Helicoidea in general) and verify the contention of Giusti et al. (1991) who, on the basis of spermatozoa fine morphology, suggested there are too many family group categories in the Helicoidea and that it is inopportune to produce new schemes and create new taxa on the basis of old and insufficient anatomical (or even shell!) characters.

Comparison with Old and Uncertain Taxa of the Species Group

A search of the taxa described for Sicilian fauna did not produce positive results. Apart from *Xerotricha conspurcata, X. apicina* and the two species recently revised by us and recognized to belong to a distinct genus—*Schileykiella: S. reinae* Pfeiffer, 1856, and *S. parlatoris,* Bivona, 1839 (Manganelli et al., 1989)—only one small hygromiid with a hairy shell, *Helix aetnea* Benoit, 1857, is known in Sicily.

Some shells were found in the Paulucci Collection which, according to the label, were collected in the type locality of *H. aetnea,* studied by Benoit himself, and confirmed by him to fully correspond to his *H. aetnea* (Museum of Zoology, University of Florence, Italy, MZUF no. 5049). Our study of the minute shell characters confirms Paulucci's (1878: 6, 32) and Westerlund's (1889: 302) identification of *H. aetnea* as a juvenile of *X. conspurcata.* Because Benoit's typical series is untraceable and there is no other possible typical material in the principal malacological collections, and because Benoit clearly confirmed that Paulucci's material totally corresponded to his species, we have selected a neotype for this species (MZUF no. 5049/1) illustrated in Figure 7B. *Helix aetnea* Benoit, 1857, consequently becomes a junior synonym of *X. conspurcata.*

Geographic Distribution

All the Aeolian Islands. A few shells from the island of Ustica (NW of Sicily) [UTM ref.: 33SUC38, 48] may belong to the new species, but since they are sexually immature and anatomical study is impossible, no conclusions can be drawn. Although its presence in Sicily is highly probable, a search of the literature and of our materials from Sicily, and some Sicilian and Maltese Islands did not bring to light any useful information.

Ecology

Helicotricha carusoi n. sp. has been found to live under stones, dry leaves and pieces of wood in many different places on single islands, frequently together with *Xerotricha conspurcata.* Like the latter species, the present species is thus a xeroresistant element, well adapted to Mediterranean habitats.

ACKNOWLEDGMENTS

We thank Mr. L. Gamberucci and Mrs. A. Daviddi for technical assistance and Mrs. H. Ampt for linguistic revision. This research was supported by CNR, MPI 40% and MPI 60% grants, and was carried out as part of a project of the Escuela de Specialization en Ambiente y Patologia Ambientale of the Universidad Nacional de La Plata, Argentina, and Università di Siena, Italy.

Thanks also to two anonymous revisers for the detailed analysis of manuscript which improved the quality of the paper.

LITERATURE CITED

APARICIO, M. T., 1982, Observations on the anatomy of some Helicidae from central Spain. *Malacologia,* 22 (1–2): 621–626.

BENOIT, L., 1857, *Illustrazione sistematica critica iconografica de' testacei estramarini della Sicilia*

Ulteriore e delle isole circostanti. i–xvi + 1–52 (+ 1–9 pls. ?), Napoli.

CLERX, J. P. M. & E. GITTENBERGER, 1977, Eniger über *Cernuella* (Pulmonata, Helicidae). *Zoologische Mededelingen (Leiden),* 52: 27–56, pls. 1–2.

DAMJANOV, S. G. & I. LIKHAREV, 1975, Gastropoda terrestria. *Fauna Bulgarica,* 4: 425 pp.

FALKNER, G., 1981, *Lehmannia valentiana* und *Microxeromagna vestita* bei Grimaldi—neu für die italienische Fauna. *Mitteilungen der Zoologischen Gesellschaft Braunau,* 3: 388–391.

FARRIS, J. S., 1989, The retention index and the rescaled consistency index. *Cladistics,* 5: 417–419.

FORCART, L., 1976, Die Cochlicellinae und Helicellinae von Palästina und Sinai. *Archiv für Molluskenkunde,* 106 (4/6): 123–189.

FRANC, A., 1968, Sous-classe des pulmonés.—In P. P. GRASSE, *Traité de zoologie. Anatomie, systématiques, biologiques,* 5 *mollusques gastéropodes et scaphopodes* (3): 325–607.

GASULL, L., 1972, Descripcion de una nueva especie de *Helicella* de la provincia de Huelva, *Helicopsis (Helicopsis) altenai* n. sp. (Gastrop. Pulmon.). *Boletin de la Sociedad de Historia Natural de Baleares,* 17: 73–75.

GASULL, L., 1985, Fauna malacologica continental de la provincia de Huelva. *Miscellania Zoologica,* 9: 127–143.

GITTENBERGER, E., 1969, Eine neue Art der Gattung *Helicopsis* (Gastropoda, Helicidae, Helicellinae) aus Niederösterreich. *Basteria,* 33 (1–4): 63–68.

GITTENBERGER, E., M. R. ALONSO & M. IBANEZ, 1989, *Helix pavida* Mousson, 1872, and *H. nubivaga* Mabille, 1882 (Gastropoda, Helicidae, Helicellinae) poorly known Helicellinae from the Canary Islands. *Basteria,* 53 (4–6): 117–125.

GITTENBERGER, E. & M. Y. MANGA, 1977, Some new species of the genus *Helicella* (Pulmonata: Helicidae) from the province Leon. *Zoologische Mededelingen (Leiden),* 51 (11): 177–189, pls. 1–2.

GITTENBERGER, E. & J. G. M. RAVEN, 1982, A new *Helicella* (Helicidae, Helicellinae) from the Cantabrian Mountains, Spain. *Basteria,* 46 (1–4): 79–83.

GIUSTI, F., 1973, Notulae malacologicae, XVIII. I molluschi terrestri e salmastri delle Isole Eolie. *Lavori della Società Italiana di Biogeografia,* (n.s.), 3: 113–306, pls. 1–16.

GIUSTI, F. & G. MANGANELLI, 1987, Notulae malacologicae XXXVI. On some Hygromiidae (Gastropoda: Helicoidea) living in Sardinia and in Corsica. (Studies on the Sardinian and Corsican malacofauna VI). *Bollettino Malacologico,* 23: 123–206.

GIUSTI, F. & G. MANGANELLI, 1989, Notulae malacologicae, XLV. A new Hygromiidae from the Tyrrhenian islands of Capraia and Sardinia with notes on the genera *Xeromicra* and *Xerotricha* (Pulmonata: Helicoidea). *Bollettino Malacologico,* 25 (1/4): 23–62.

GIUSTI, F. & G. MANGANELLI, 1990, *Ciliellopsis oglasae* a new Hygromiidae from Montecristo Island (Pulmonata: Hygromiidae). *Journal of Conchology,* 33: 269–277, pls. 27–29.

GROSSU, A. V., 1983, *Gastropoda Romaniae 4. Ordo Stylommatophora Suprafam.: Arionacea, Zonitacea, Ariophantacea si Helicacea.* Bucuresti, Editura Litera, 564 pp.

HAUSDORF, B., 1988, Zur Kenntnis der systematischen Beziehungen einiger Taxa der Helicellinae Ihering 1909 (Gastropoda: Hygromiidae). *Archiv für Molluskenkunde,* 119 (1/3): 9–37.

HAUSDORF, B., 1990a, Die *Xeromunda*-Arten des griechischen Festlandes (Gastropoda: Hygromiidae). *Archiv für Molluskenkunde,* 119 (4/6): 407–432.

HAUSDORF, B., 1990b, Zur Kenntnis einiger Arten der Gattung *Helicopsis* Fitzinger aus Griechenland und der Türkei (Gastropoda: Hygromiidae). *Archiv für Molluskenkunde,* 120 (1/3): 57–71.

HAUSDORF, B., 1990c, Über die Verbreitung von *Microxeromagna armillata* (Lowe, 1852) und *Xerotricha conspurcata* (Draparnaud, 1801) in Griechenland und der Türkei (Gastropoda, Pulmonata: Hygromiidae). *Malakologische Abhandlungen,* 15: 55–62.

HENNIG, W., 1966, *Phylogenetic systematics.* University of Illinois Press, Urbana, 263 pp.

HESSE, P., 1934, Zur Anatomie und Systematik palaearktischer Stylommatophoren. *Zoologica (Stuttgart),* 33 (1), Heft 85: 1–59, pls. 1–9.

KTARI, M. H. & M. REZIG, 1976, La faune malacologique de la Tunisie septentrionale. *Bulletin de la Societè des Sciences Naturales de la Tunisie,* 11: 31–74.

MADDISON, W. P., M. J. DONOGHUE & R. MADDISON, 1984, Outgroup analysis and parsimony. *Systematic Zoology,* 33: 83–103.

MANGA GONZALES, M. Y., 1983. *Los Helicidae (Gastropoda: Pulmonata) de la provincia de Leon.* Leon, 394 pp.

MANGANELLI, G. & F. GIUSTI, 1988, Notulae malacologicae, XXXVIII. A new Hygromiidae from Italian Apennines and notes on the genus *Cernuella* and related taxa (Pulmonata: Helicoidea). *Bollettino Malacologico,* 23: 327–379.

MANGANELLI, G. & F. GIUSTI, 1989, Notulae malacologicae, XLIII. *Xeromunda* Di Maria Di Monterosato in Italy (Pulmonata: Hygromiidae). *Bollettino Malacologico,* 25 (1–4): 1–22.

MANGANELLI, G., I. SPARACIO & F. GIUSTI, 1989, New data on the systematics of two Sicilian land snails, *Helix parlatoris* Bivona, 1839 and *Helix reinae* L. Pfeiffer, 1856 and description of *Schileykiella* n.gen. (Pulmonata: Hygromiidae). *Journal of Conchology,* 33: 141–156, pls. 10–16.

NELSEN, G. I., 1979, Cladistic analysis and synthesis: principles and definitions, with a historical note on Adanson's "Familles des plantes" (1763–1764). *Systematic Zoology,* 28: 1–21.

NORDSIECK, H., 1987, Revision des System der

Helicoidea (Gastropoda: Stylommatophora). *Archiv für Molluskenkunde,* 118: 9–50.

ORTIZ DE ZARATE Y LOPEZ, A., 1950, Observaciones anatomicas y position sistematica de varios helicidos espanoles. *Boletin de la Real Sociedad Española de Historia Natural,* 43: 21–85, pls. 1–2.

PAULUCCI, M., 1878, *Matériaux pour servir a l'étude de la faune malacologique terrestre et fluviatile de l'Italie et des ses îsles.* iv + 54 pp. Paris.

PIANTELLI, F., F. GIUSTI, F. BERNINI & G. MANGANELLI, 1990, The mollusc and oribatid fauna of the Aeolian and Tuscan Archipelagos and the island equilibrium theory. In: Proceeding of the international symposium "Biogeografical aspects of insularity" (Roma 18–22 May 1987). *Accademia Nazionale dei Lincei, Atti dei Convegni Lincei,* 85: 117–154.

PLATNICK, N. I., 1989, An empirical comparison of microcomputer parsimony programs. II. *Cladistics,* 5: 145–161.

PRIETO, C. P., 1986, *Estudio sistematico y biogeografico de los Helicidae (sensu Zilch, 1959–60) (Gastropoda: Pulmonata: Stylommatophora) del Pais Vasco y regiones adyacentes.* Universidad del Pais Vasco, Facultad de Ciencias, doctoral thesis, 393 pp., 10 pls.

SCHILEYKO, A. A., 1978a, Molluscs. Land molluscs of the superfamily Helicoidea. *Fauna SSSR,* (n.s.) 17: 1–348 [in Russian].

SCHILEYKO, A. A., 1978b, On the systematics of *Trichia* s. lat. (Pulmonata: Helicoidea: Hygromiidae). *Malacologia,* 17: 1–56.

SCHILEYKO, A. A., 1984, Molluscs. Terrestrial molluscs of the suborder Pupillina of the fauna of the USSR (Gastropoda, Pulmonata, Geophila). *Fauna SSSR,* (n.s.) 130: 1–399. [in Russian].

WATROUS, L. & Q. WHEELER, 1981, The outgroup comparison method of character analysis. *Systematic Zoology,* 30: 1–11.

WESTERLUND, C. A., 1889, *Fauna der in der palaarktischen Region lebenden Binnenconchylien. II. Genus Helix,* 2, 473 + 30 pp. R. Friedländer & Sohn., Berlin.

ZILCH, A., 1960, Euthyneura. In W. WENZ: Gastropoda. Handbuch der Paläozoologie, 6 (2, 4th part): 601–835 + i–xii.

Revised Ms. accepted 2 December 1991

MALACOLOGIA, 1992, 34(1–2): 129–141

STRUCTURE AND COMPOSITION OF THE SHELL OF THE ARCHAEOGASTROPOD LIMPET *LEPETODRILUS ELEVATUS ELEVATUS* (MCLEAN, 1988)

Stephen Hunt

Department of Biological Sciences, University of Lancaster, Bailrigg, Lancaster, LA1 4YQ England

ABSTRACT

Shells from the hydrothermal vent-dwelling archaeogastropod limpet *Lepetodrilus elevatus elevatus* are described in terms of their mineralogy, fine structure and composition. The shell is mainly crossed-lamellar aragonite, with narrow inner and outer prismatic layers and no nacre. The thick proteinaceous periostracum has an unusually high glycine content. Sulphur, detected in the periostracum by X-ray microprobe analysis, cannot be attributed to either sulphur-containing amino acids or free elemental sulphur. Periostracum and shell both contain phosphorus, but metals other than calcium are present in traces only. Most shells examined show erosion in the form of pits rich in sulphur and phosphorus. The significance of the unusual periostracal composition in relation to the shell mineralogy, the propensity for shell erosion, and the chemistry of the vent water environment, is discussed.

Key words: archaeogastropod, *Lepetodrilus,* shell, calcification, aragonite, cross-lamellar, periostracum, polyglycine.

INTRODUCTION

Exploration of deep ocean hydrothermal sites discovered in the 1980s revealed an unexpected rich fauna with molluscs well represented. While large bivalves attracted much attention, gastropods are most numerous, mainly as small limpet forms, new and unique to this special environment. Hickman (1983) noted the presence in the Galapagos Rift and East Pacific Rise (13°N and 21°N) sites of three new archaeogastropod groups that could not be assigned to then-recognised superfamilies. These have been described by McLean (1985, 1988) and by Fretter (1988). Here I describe the architecture and composition of the shell of *Lepetodrilus elevatus elevatus,* a member of the archaeogastropod superfamily Lepetodrilacea (McLean, 1988).

MATERIALS AND METHODS

Specimens of *L. elevatus elevatus* (see McLean, 1988, for the systematic description and list of the principal repositories of the type material) were collected by Dr. F. Gaill of the Centre du Biologie Cellulaire, CNRS, Ivry sur Seine, France, at 2600 m depth during the 1984 Biocyarise cruise using the submersible Cyana at 12°48′N, 103°56′W.

Scanning electron microscopy was carried out on shells that had been rinsed with distilled water, air dried, mounted with graphite paste cement onto aluminium support stubs, and sputter coated with gold. Microscopy was performed with a Jeol JSM50A scanning electron microscope at 15kv. For microprobe analysis, specimens were mounted on graphite support stubs and were rotary coated with carbon. Analyses were carried out at 15kv excitation voltage by a Kevex energy dispersive analysis system at 20ev per channel gain with a preset live time of 100 sec.

For thin sectioning, periostracum was obtained by shell dissolution with 0.1M hydrochloric acid, washed in distilled water, fixed overnight in pH 7.0, 0.1M cacodylate buffer containing 5% glutaraldehyde, and post-fixed in cacodylate-2% osmium tetroxide for 30 min. Following dehydration through alcohols, fixed material was embedded in Spurr's resin and sectioned at 50 nm or less using a diamond knife. Sections were stained with uranyl acetate and Reynold's lead citrate for 30–60 min each. Sections were examined at 100kv in a Jeol 100CX STEM microscope.

X-ray diffraction patterns were determined using finely ground specimens of whole shell held in glass capillaries mounted in a helium-filled flat camera of working distance 3.5 cm with Ni-filtered Cu/Kα radiation and pinhole

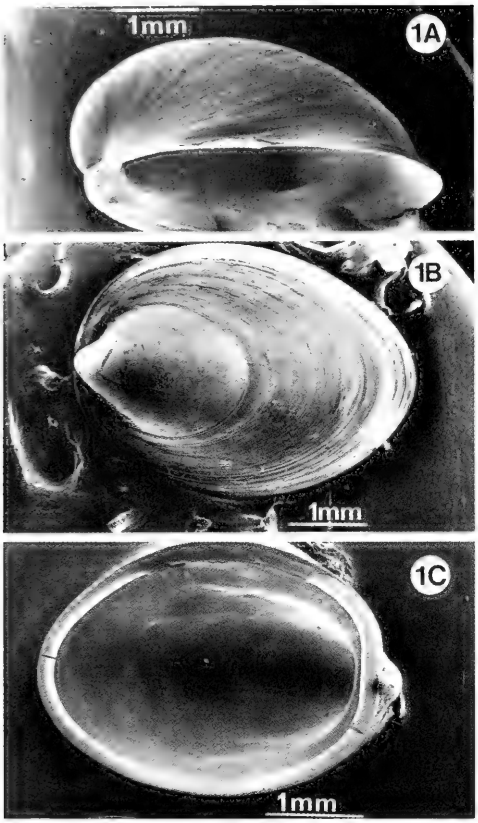

FIG. 1. *Lepetodrilus elevatus elevatus*. A. Lateral view. B. Dorsal view. C. Ventral view.

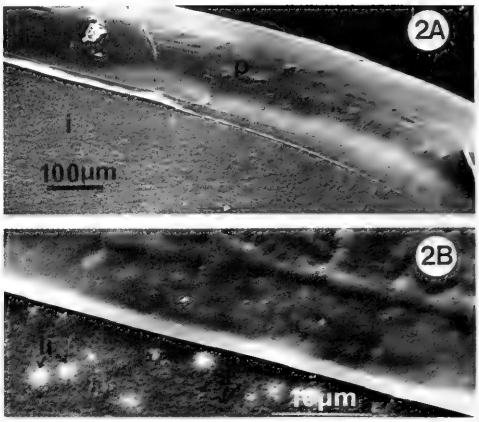

FIG 2. Inner surface of the shell (i) showing the folding over of the periostracum (p) at the shell edge and the granular structure of the shell with large and small scale irregularities (li and si) arrowed. A. Low magnification. B. Same region at a higher power.

collimation. Fibre diffraction patterns were made using small strips of wet material clamped in holders and slightly tensioned before drying. Standard patterns were made with powdered calcite (Iceland spar) and aragonite (scleractinian exoskeleton).

Amino acid analyses were carried out on specimens hydrolysed in evacuated tubes with 3M methane sulphonic acid containing 0.2% w/v tryptamine at 100°C for 48 hours. Neutralized aliquots were analysed using an LKB model 4101 amino acid analyser.

RESULTS

General Description of the Shells

Shells of *L. elevatus elevatus* are typically about 2.25 mm high, with an oval aperture about 4 mm by 3 mm (Fig. 1A–C). The external surface has low concentric, closely spaced growth ridges and a smoother apex. An olive-brown periostracum folds over the lip of the shell with a 0.2–0.3 mm inner overlap (Figs. 1C, 2A). The inner surface of the shell is smooth though higher magnifications reveal regularly distributed granules and shallow pitted irregularities (Fig. 2A, B).

Shell Mineralogy

Figure 3 shows the diffraction pattern of powdered shell. The principal reflections are aragonitic, with little or no calcitic contribution.

Ultrastructure of the Mineral Phase

Fractured edges of the shell show three major shell layers—outer, middle and inner, of which the middle is the major and composed quite uniformly of the crossed-lamellar structure type (Figs. 4–6). Between this layer and the periostracum is a columnar layer of irregular fibrous prismatic organization (Fig. 7). The innermost shell layer is columnar in irregular simple prismatic form (Fig. 8). Here a thin zone, no more than 2 µm deep and formed of either short prisms or granules, demarcates this layer from the crossed lamellar.

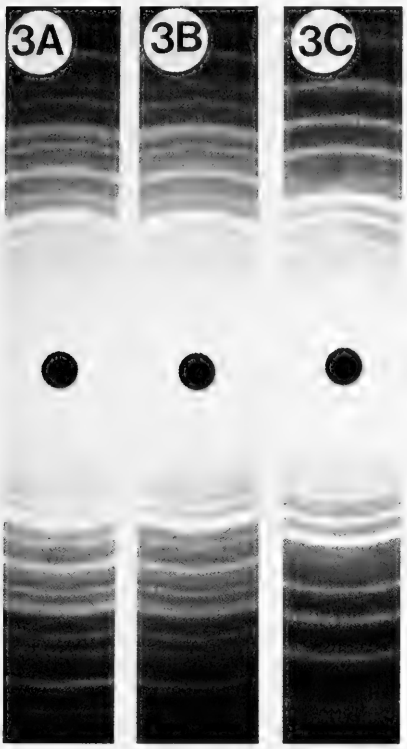

FIG 3. Powder diffraction patterns of A. Aragonite. B, *Lepetodrilus* shell. C. Calcite.

There is no evidence of an innermost nacreous layer being present.

Elemental Analysis

X-ray microprobe analyses of the main mineralized layers show calcium to be the only detectable element present in significant amounts (Fig. 9, Table 1), presumably as the carbonate. The traces of sulphur and phosphorous would be unlikely to make an important contribution to shell mineralogy even if they were present as calcium phosphate and sulphate. Although vent waters are transition and heavy metal rich, none are detectable in the shell mineral. Traces of magnesium, silicon and aluminium could indicate chance incorporation clay-forming suspensates. Roux et al. (1985) have noted that concentrations of trace elements in the aragonitic shell of the hydrothermal vent bivalve *Calyptogena* did not reflect vent-water trace element concentrations but were similar to those found in aragonitic shell of other marine bivalves.

Periostracum

Figure 10 is a low-power transmission electron micrograph of sectioned periostracum. No laminated, orthogonal or helicoidal fibrous architecture of the type found in some marine and terrestrial prosobranch gastropod periostraca (Bevelander & Nakahara, 1970; Hunt & Oates, 1970, 1978, 1985) was found. The faint bands in the plane of the periostracum are probably depositional irregularities without compositional or orientational significance. The darker and more homogeneous zone adjacent to the shell may represent a phase of rapid deposition and tanning. The inner surface has an irregular profile and forms a thin, more electron-luscent layer than the main body of periostracal protein into which it merges via a narrow, more densely staining zone. The outer surface is also irregular. What may be knobs or ridges adhere to a thick layer of vacuolated granular material that may be a deposit of microorganisms and detritus. The remnants of bacteria are present in the vacuoles.

Table 2 gives the amino acid analysis of the periostracum, and Table 3 lists values for key features of the composition enabling comparisons with other structural proteins. The periostracum has a high glycine content, over 70 residue percent. Glycine-rich proteins are common among structural proteins, and whereas many periostracal proteins are of this type, it is unusual for those of marine gastropods to be glycine-rich. Figures 11 and 12 show the composition of this periostracum placed in relation to other gastropod periostraca. Its glycine content is higher than in any other gastropod (62 species) recorded by us. This, coupled with its hydrophobic index (+47), ranks it with those of terrestrial prosobranchs. The only periostraca with higher glycine levels (over 80 residue percent) are from bivalve molluscs at hydrothermal vent sites. But, unlike the latter, the sulphur-containing amino acid levels here are low or absent (Hunt, 1987). The high beta turn potential value, coupled with low values for helix and beta sheet potential, point to a protein secondary structure high in random folding.

Figure 13A shows the typical X-ray emission profile of the periostracum probed to avoid surface deposits. Noteworthy is the large sulphur peak. There are traces of iron and copper and a little phosphorus (Table 4). In the absence of calcium, the latter cannot be accounted for as hydroxyapatite, though this

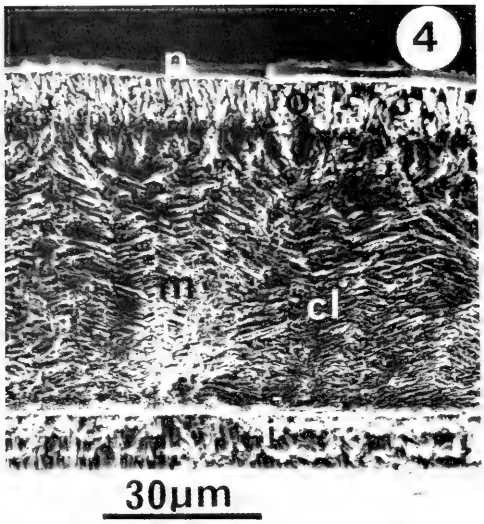

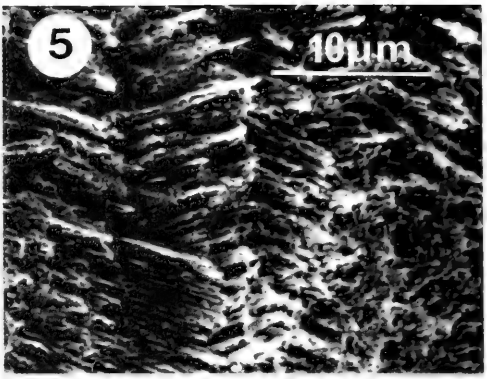

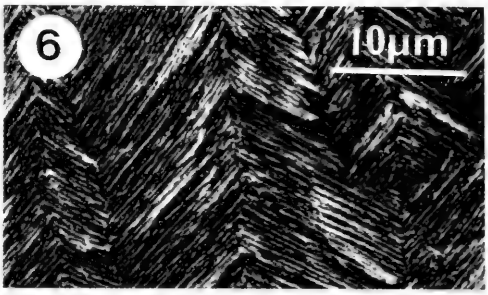

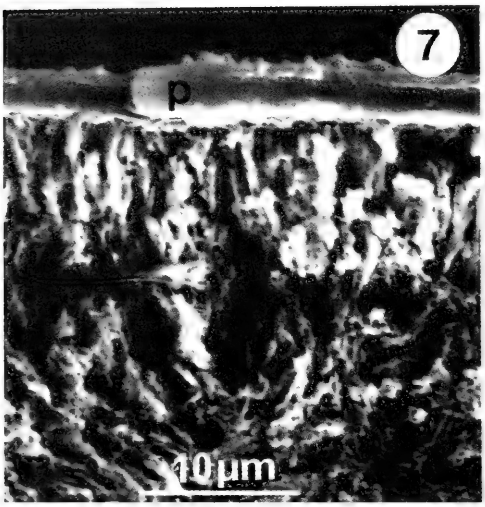

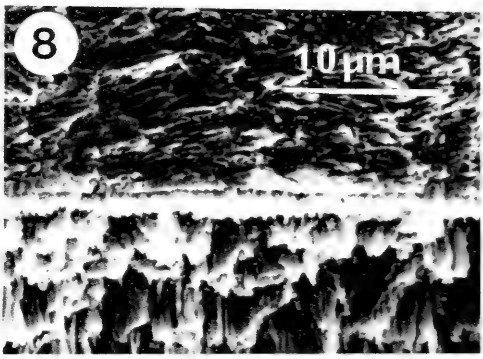

FIG. 4. Fractured edge of shell with the dorsal surface at the top and showing the periostracum (p) and the three main calcified layers, outer (o), middle (m) and inner (i). Cross-lamellation (cl) is evident in the deeper middle layer.
FIGS. 5, 6. Two views of the crossed-lamellar organization of the middle layer of the shell.
FIG. 7. The outer layer of the shell with the periostracum (p) overlying an irregular layer of aragonite columns.
FIG. 8. The innermost layer of the shell composed of irregular columns sharply separated from the overlying cross-lamellar material by a narrow zone of short prisms or granules.

is present in some bivalve periostraca (Waller, 1983). The absence of sulphur-containing amino acids demands another explanation of the high sulphur content. Many microorganisms present at the hydrothermal vents have an energy metabolism based on oxidation of sulphur compounds. Deposition of elemental sulphur as part of this process is common and occurs in the gills of *Calyptogena* as part of a symbiotic relationship (Felbeck et al., 1985). Extraction, however, of the periostracum with carbon disulphide only removes traces of elemental sulphur (Fig. 13B,C, Table 4).

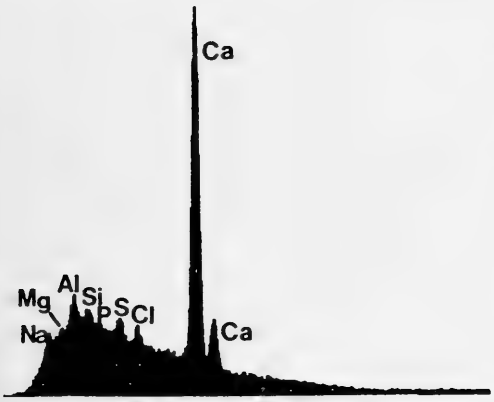

FIG. 9. Analysis of the shell by X-ray microprobe. For this analysis, the beam was centred in the crossed-lamellar layer, but closely similar patterns were obtained for the outer and inner calcified layers. The analysis is energy dispersive, and the abscissal axis is in terms of X-ray energy and is a measure of increasing atomic number, whereas the ordinate axis is a measure of received X-ray photon counts at the detector.

X-ray diffraction patterns prepared from flattened strips of periostracum show no oriented fibre reflections. There is considerable diffuse scatter and a weak ring corresponding to a 0.387 nm spacing, which tends to confirm the secondary structure as being a compact and highly folded random coil. The helical coiled polyglycines I and II are absent.

Shell Erosion

All specimens examined had erosion pits, most commonly near the shell apex. Many of these pits penetrate the shell and are usually partially filled or closed by brown or black material. Figure 14 shows several such pits with characteristic rounded profiles around single or multiple coalescing sites of penetration. The pitting is often associated with areas of periostracal cracking that follow the pit profile (Fig. 15).

Pits penetrate the shell in a series of terraced steps. In several, the first layer revealed beneath the periostracum is more finely granular than the deeper terraces or the coarser pit-bottom material (Figs. 16, 17).

Figure 18 and Table 5 show X-ray microprobe analyses of eroded and pitted areas. A characteristic feature are the high levels of sulphur and phosphorus in the pits and, as might be expected, increasingly high calcium counts from lower within them.

DISCUSSION

Leptodrilus elevatus elevatus is found in huge numbers in close association with the giant vestimentiferan tube worm *Riftia* at depths of around 2600 m, close to the hydrothermal vents, where the sea water has high concentrations of such reduced gases as hydrogen sulphide, together with dissolved sulphides of iron, manganese, zinc and copper and low oxygen tension. Many of the animals living there take advantage of chemolithotrophic bacteria that base their metabolism on oxidation of hydrogen sulphide and other reduced forms of sulphur. Endosymbiotic relationships exist between vent bacteria and bivalve molluscs (Felbeck et al., 1985), in which hydrogen sulphide, concentrated from the sea water by the mollusc, is transferred to bacteria in the gills and used as the energy source for synthesis of organic compounds used by the animal. De Burgh & Singla (1984) describe how a vent archaeogastropod limpet also obtains nutrients by endocytosis of bacteria growing upon its gills.

The need to absorb oxygen at low concentrations from waters containing high metal concentrations, as well as nutritional strategies involving consumption of bacteria, which may have absorbed metallic elements in their cell coats (Juniper et al., 1986), might lead to expectation that mineralization would yield shells reflecting the sea water chemistry, but this seems not to be so. Although traces of magnesium, aluminium and silicon are nearly always present in the shells, none of the

TABLE 1. Elemental composition of the main mineralized layer of the *Lepetodrilus* shell determined by X-ray microprobe analysis. Values are as emitted X-ray counts for each integrated elemental peak as a percentage of total counts integrated across the whole energy spectrum. For conditions, see text. These values relate to Figure 9, on which the traces of magnesium and phosphorus barely show.

Element	Na	Mg	Al	Si	P	S	Cl	Ca
counts %total	1.11	0.54	3.67	1.19	0.48	4.75	1.28	86.99

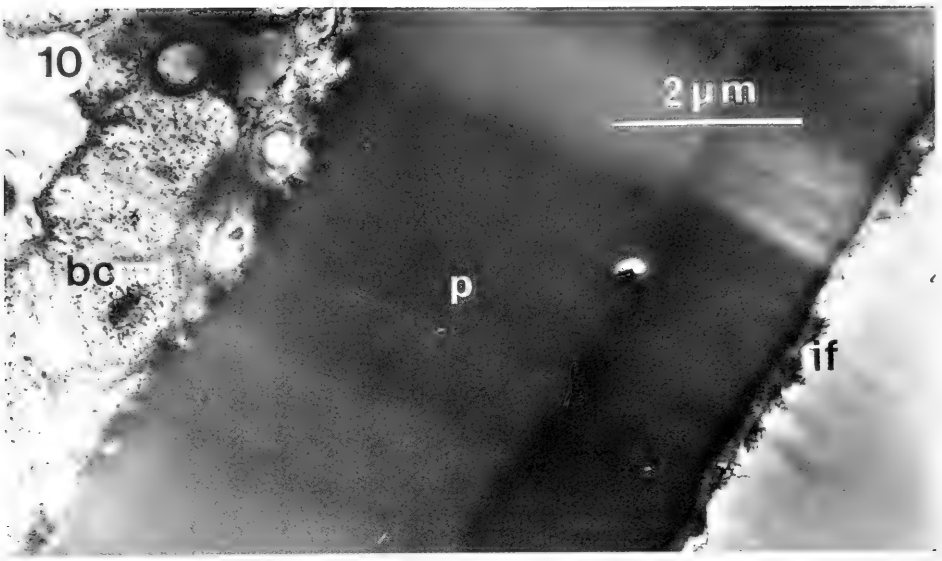

FIG. 10. Transmission electron micrograph of a transverse section through the periostracum (p). The outer surface with bacterial debris contamination (bc) is at the left and the inner shell contact surface (if) at the right. The specimen has been decalcified.

TABLE 2. Amino acid composition of the periostracum of *L. elevatus elevatus* reported as residues of each amino acid per thousand total amino acid residues.

Aspartic acid	17	Alanine	10	Tyrosine	30
Threonine	6	Cysteine	0	Phenylalanine	12
Serine	8	Valine	34	Histidine	14
Glutamic acid	11	Methionine	2	Lysine	41
Proline	8	Isoleucine	23	Arginine	22
Glycine	713	Leucine	49	Tryptophan—Not determined	

heavier metallic elements appear to be included during calcification. The only elements achieving any prominence against the dominant calcium component are phosphorus and sulphur.

Traces of phosphorous in the shells might be accounted for by phosphoprotein in the matrix. Petit et al. (1980) have found calcium "spherites" containing phosphorus in the vascular channels and connective tissue immediately adjacent to mantle edge cells of the freshwater bivalve *Amblema,* implicating these in shell formation. Marsh & Sass (1983) have demonstrated calcium-binding phosphoprotein particles in the extrapalial fluid and innermost shell lamella of estuarine and marine bivalves.

Shell sulphur could be due either to traces of calcium sulphate or perhaps sulphated polysaccharides. *Nautilus* shell, for example, contains polysaccharide sulphates in the membrane overlying the nacreous crystals (Crenshaw & Ristedt, 1976). *Crassostrea* has sulphated proteins in the matrix (Wilbur & Salleuddin, 1983). Organic ester sulphate could also account for the high sulphur content of the periostracum.

Aragonite appears to be the predominant form of crystaline calcium carbonate in the shell. There are no precedents that would indicate if very high hydrostatic pressures can affect shell mineralization in molluscs, though in vitro work shows that calcium carbonate crystalization equilibria are pressure sensitive—aragonite becomes the most stable form at higher pressure and temperature (Mellor,

TABLE 3. Side-chain characteristics and conformational predisposing properties of the amino acid composition of the *Lepetodrilus* and other molluscan periostracal proteins calculated from the data of Table 2.

Side Chain	*Lepetodrilus*	Av. other marine gastropods[9]	Av. marine bivalves[10]
Acidic[1]	28	237	60
Basic[2]	77	103	71
Polar[3]	149	501	264
Apolar[4]	136	300	189
Polar/Apolar	1.1	1.6	1.4
Hydrophobic index[5]	+47	−226	+235
Helix potential[6]	215	513	270
Sheet potential[7]	229	428	352
Turn potential[8]	746	420	620

[a]Asp + Glu. [2]His + Lys + Arg. [3]Acidic + Basic + Thr + Ser + Tyr. [4]Pro + Ala + Val + Ile + Leu + Phe. [5]Calculated according to the method of Andersen (1979) by ranking each residue according to the characteristic energy change involved in transfer of it between water and ethanol. Hydrophilic residues have negative values and hydrophobic positive. Summation of the product of the i_{th} amino acid content and ΔG for the i_{th} transfer, for all amino acids, gives the hydrophobic index. [6]Calculated from data in Chou & Fasman (1977) using the conformational frequency parameters *P* as weighting factors to load the overall numbers of helix-promoting amino acids in the periostracal proteins. Thus, "helix potential" is given by the number of residues (per 1000 total) of an amino acid multiplied by its $P\alpha$ value and summed for the residues Glu, Met, Ala, Leu, Lys, Phe, Ile and Val (in decreasing order of helix-promoting ability). Typical values for a "random coil" protein (resilin), a nearly 100% α-helical protein (tropomyosin), and a globular protein with low helix (2%) and high beta sheet (57%) content (concanavalin A) are 350, 956 and 561, respectively (calculated from amino acid compositions in residues per 1000 total residues) (Andersen & Weis-Fogh, 1964; Huddart & Hunt, 1975; Wang et al., 1971; Reeke et al., 1975). [7]As for [6], but using the beta sheet-promoting conformational parameters P_β to weight and sum the contents of Val, Ile, Tyr, Phe, Leu, Cys, Thr and Met (Chou & Fasman, 1977). Values for resilin, tropomyosin and concanavalin A are 226, 344, and 532, respectively. [8]Asp + Ser + Pro + Gly. These residues show high frequency in the four amino acids at a beta turn (Chou & Fasman, 1977). Values for resilin, tropomyosin and concanavalin A are 636, 174 and 388, respectively. [9]38 non-hydrothermal species (Hunt, 1987). [10]29 non-hydrothermal species (Hunt, 1987).

1960). Probably the chemistry of the organic matrix is more important. Commenting upon the entirely aragonitic form of the shell in the hydrothermal vesicomyid *C. magnifica* and the mixed aragonitic and calcitic form of a hydrothermal mytilid, Lutz (1982) observes that in the eastern Pacific regions, the depths of 2000–3000 m, where sampling has taken place, are well above reported calcite compensation depths but substantially below those for aragonite compensation.

Because the limpet is in a chemically hostile niche, the aragonitic mineralogy might seem to be a disadvantage being less stable and slightly more soluble than the calcitic. The unreliability of aragonite is seen where the periostracum has been damaged and rapid dissolution begins to penetrate the shell.

Clearly the periostracum offers much protection for the shell and probably because its composition is atypical of marine gastropods. Hunt & Oates (1985) note that there are probably two main families of periostracal proteins in gastropods—those with a low glycine content and negative hydrophobic index, and those with a medium to high glycine content and positive hydrophobic index. The latter is typical also of most marine and freshwater lamellibranchs. The former have easily wetted periostraca with high permeabilities to water and ions; the latter have the opposite characteristics. I have commented elsewhere (Hunt, 1987) on the resistance of shells of the latter type to attack by 2M hydrochloric acid through an intact periostracum; *Lepetodrillus* behaves in this way, showing only periostracal blistering, carbon dioxide evolution, and shell erosion where the periostracum is already damaged.

Marine prosobranch periostraca, for which we have analyses available, do fall into both groups, but the hydrophilic class are more common. Assuming that the primary role of periostraca is in shell deposition, then given the type of massive calcitic shell formed by many marine gastropods, an ion-impermeable barrier would not normally be an essential protective feature where acid pH is a less frequently encountered environmental pressure. But here the environment is more

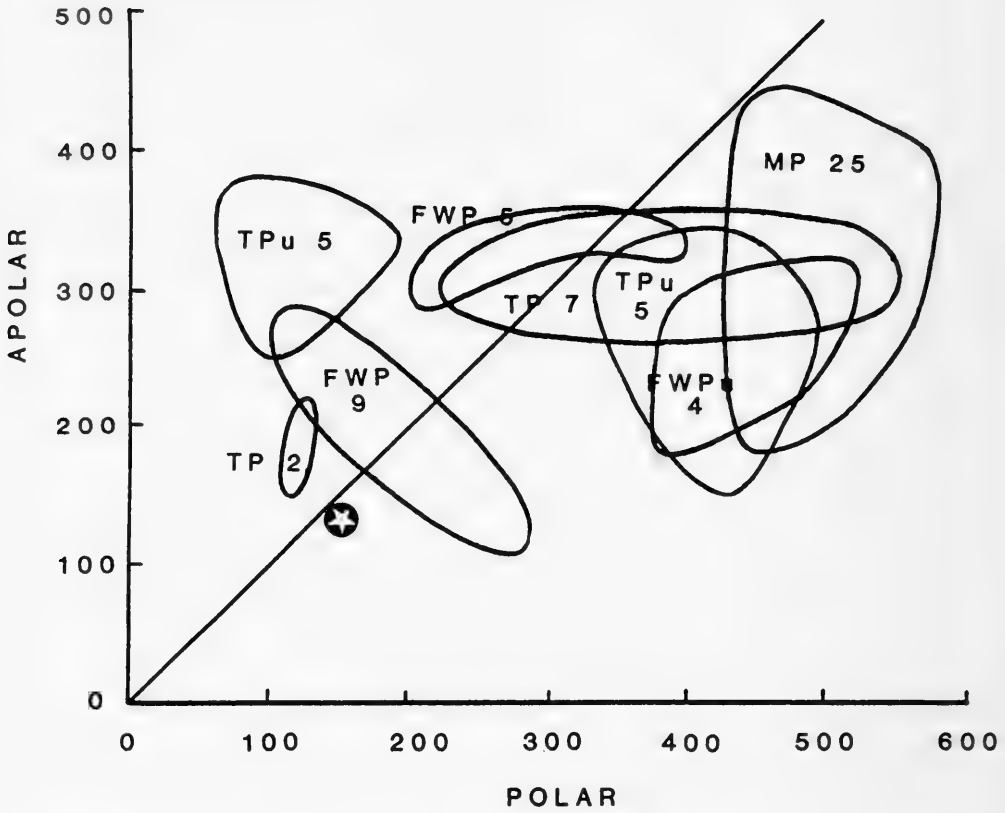

FIG. 11. The relationship between apolar and polar amino acids, as defined in Table 3, for gastropod periostraca. The different groups of gastropod are designated as follows:- TP, terrestrial prosobranchs; TPu, terrestrial pulmonates; FWP, freshwater prosobranchs; FWPu, freshwater pulmonates; MP, marine prosobranchs. Amino acid analyses are drawn partly from Meenakshi et al. (1969) and Degens et al. (1967) and from analyses performed in this laboratory but not yet published. Numerals after the designations represent numbers of species sampled, and the enclosed areas are the limits of apolar/polar value clusters—some gastropod groups have periostraca of more than one type. The graphical line demarcates apolar periostraca on the left from polar on the right. The star represents the position of the *Lepetodrilus* analysis.

extreme and shell mineralology unstable, demanding an impermeable and strong periostracum.

Account may also have to be taken of the lower oxygen tension at which the limpets function. Operating metabolism partly anaerobically may mean that consistently elevated levels of succinic acid could form in the extrapallial fluid within the shell (Crenshaw & Neff, 1969; Lutz & Rhoads, 1980), demanding a constant internal regeneration of the shell to compensate for acid dissolution. Better exterior protection would then be advantageous.

Although the composition of the periostracum is unusual, its hydrophobicity is still inside the range for marine gastropods (Fig. 12). It is the glycine content that pulls it away from the major groupings, and this factor too contributes to the anomalous position on the polarity distribution diagram. The almost equal balance of polar and apolar character is shared with some terrestrial and freshwater prosobranchs, though not with most marine species (Fig. 11). A high glycine content may promote a densely packed, highly folded random structure that density of which could be as helpful in reducing ion-permeability as hydrophobicity. Lamellibranch periostraca from hydrothermal species also have unusual amino acid compositions with high glycine

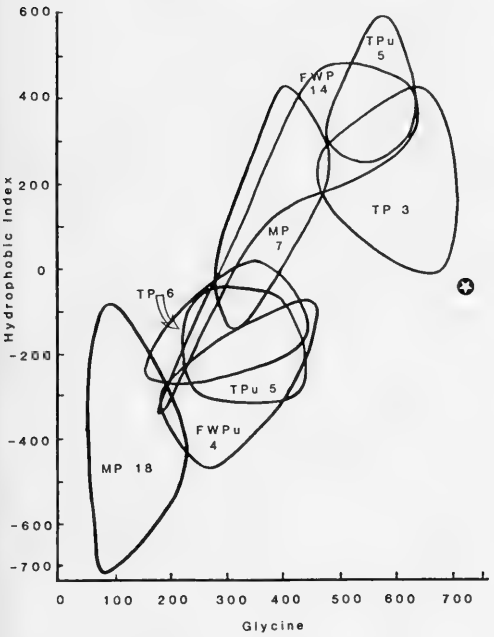

FIG. 12. The relationship between hydrophobic index and glycine content for gastropod periostraca. Hydrophobic index is defined in the footnote to Table 3. Because glycine has only a hydrogen in the side chain, it is assigned zero hydrophobicity (arbitrarily, as thermodynamically it will have a finite ΔG value for transfer between water and a less polar solvent) and is assumed to contribute neither net polar or apolar value. Designations, numerals and symbols have the same meanings as in Figure 11.

contents. That from *Bathymodiolus thermophilus* contains 85 residue percent though the few remaining amino acids give it more hydrophobic character (Hydrophobic index: +156) (Hunt, 1987).

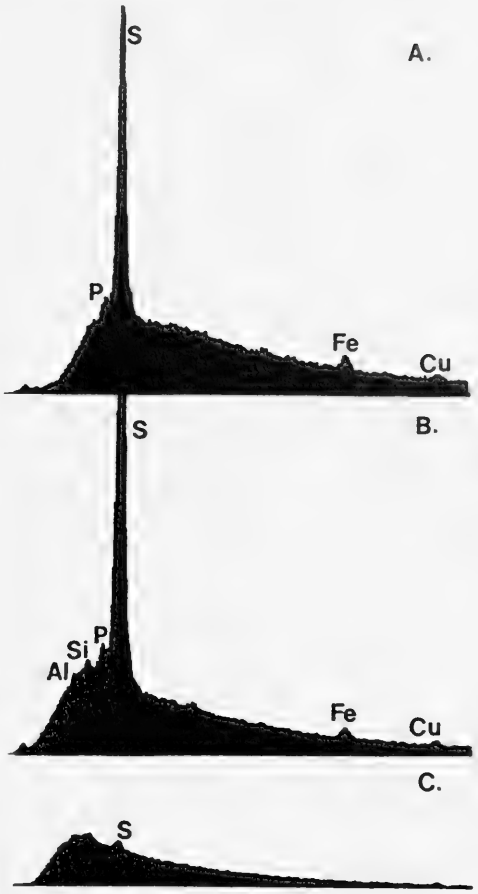

FIG. 13. Analysis of the periostracum by X-ray microprobe. A. Periostracum untreated other than by dilute acid decalcification to remove the shell. B. Periostracum extracted with carbon disulphide. C. The carbon disulphide extract dried onto the graphite stub.

TABLE 4. Elemental composition of the periostracum of *Lepetodrilus* determined by X-ray microprobe analysis. A. Untreated material removed from the shell with dilute acid. B. Another specimen after removal from the shell and extraction with carbon disulphide. C. The carbon disulphide extract concentrated by evaporation at room temperature and dried onto the graphite-coated stub. These compositions relate to Figure 13A–C. Traces of aluminium and silicon may originate from clay particles on the surface of the material. Low levels of material recovered by CS_2 extraction do not make count integration meaningful.

Element	Al	Si	P	S	Fe	Cu
Counts %total						
A	—	1.01	3.19	93.41	2.04	0.34
B	1.22	1.26	1.97	93.96	0.94	0.11
C	trace	trace	—	trace	—	trace

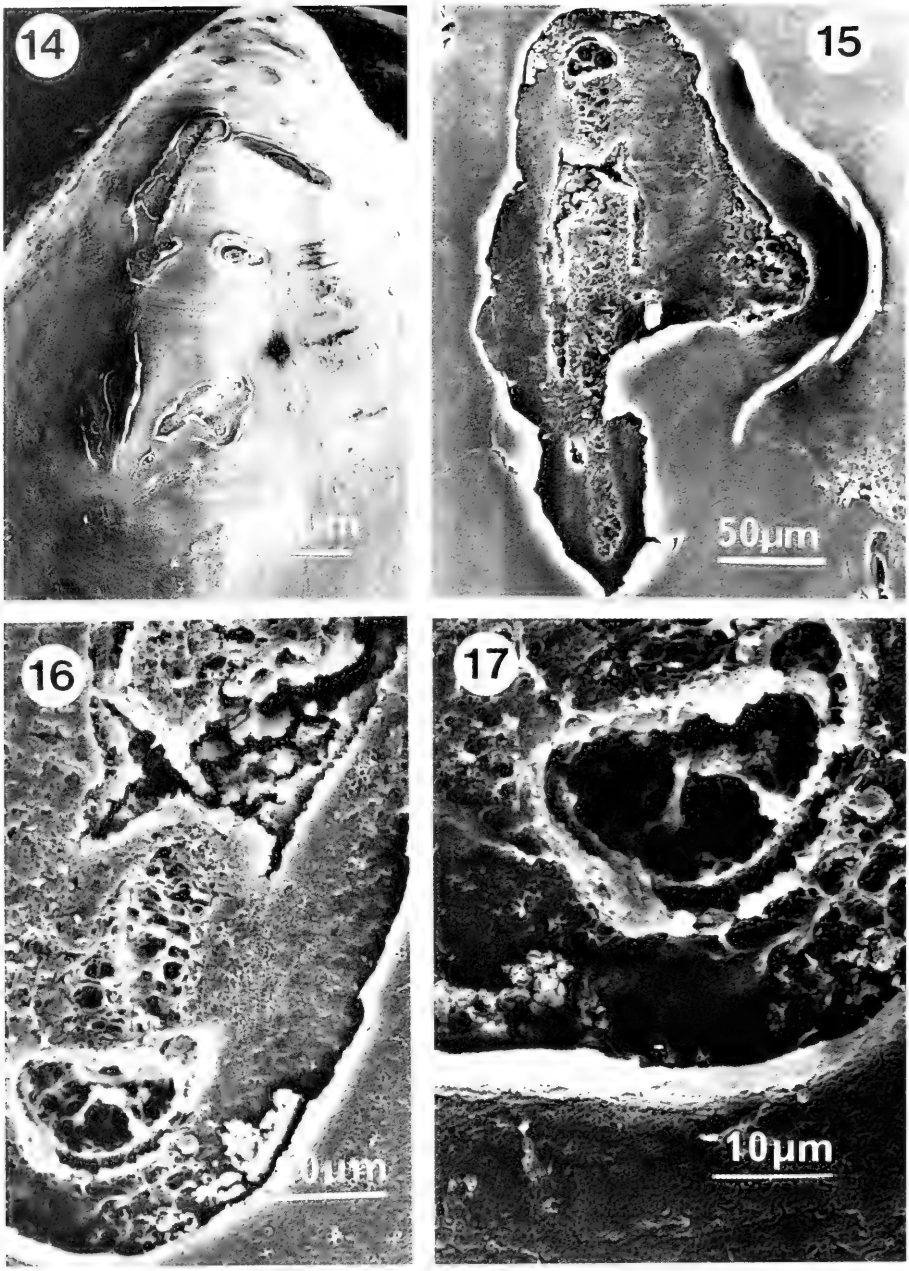

FIG. 14. Scanning electron micrograph of the shell surface in the apical region showing erosion pits penetrating the periostracum and the underlying calcified material.
FIG. 15. Detail of an erosion pit from the lower center of Figure 14. Note the cracking of the periostracum at the right which seems to follow the profile of the pit.
FIG. 16. Detail of the pit shown in Figure 15 which illustrates the stepped progression of erosion.
FIG. 17. Detail from Figure 16 illustrating what appears to be residual strands and sheets of organic matrix in and around the deepest pit.

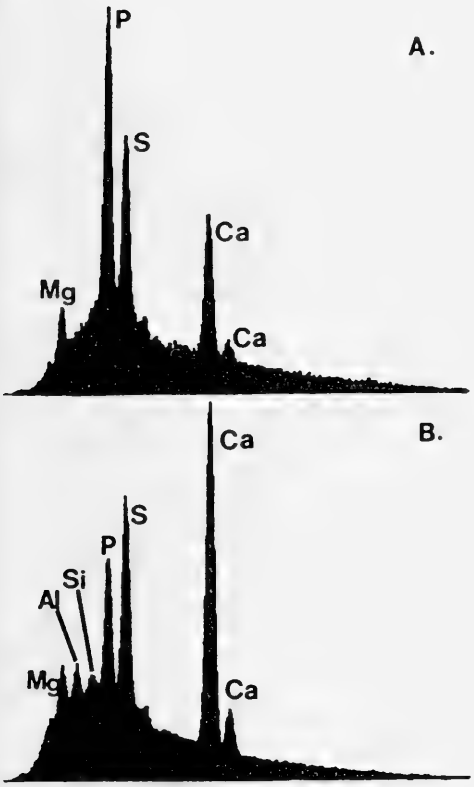

FIG. 18. Analysis of erosion pits by X-ray microprobe. A. Interior of a shell outside surface pit of the type shown in Figure 17. B. Interior of a pit that has penetrated the shell to the inside and probed from within the shell.

Most of the limpet shells are eroded by small pits showing that if the periostracum is penetrated the vulnerable aragonitic shell will be damaged. At 2000 m depth, wave action can hardly be the cause of periostracal damage. Most pits and periostracal cracks occur near the shell apex, where the protein sheet is oldest and curved more sharply to conform to the shell's contour. Aging, chemical deterioration, non-specific cross-linking could all contribute to progressive stiffening and brittleness causing cracking and porosity. Another possibility is biodegradation. Baross & Deming (1985) note extensive colonization of the limpets' shell surfaces by microorganisms. McLean (1988) remarks on heavy infestations by an unidentified sedentary organism forming globular irregularities on the shells of this species and the related *L. pustulosus*. These organisms may etch and damage the underlying periostracum. Herrera-Duvault & Roux (1986) have studied corrosion in mussel shells from the 13°N thermal vent site. After predator damage or microboring, bacterial activity destroys the organic matrix of the shell, making the dissolution of the aragonite layers easier.

High phosphorous and sulphur levels, found here in the erosion pits, are difficult to account for. The dark material seems to be organic, as the microprobe detects no metals other than calcium. Aragonite dissolution will leave behind shell matrix proteins. Possibly these are being secondarily tanned to form products interacting with sulphur and phosphorous-containing inorganic species in the water. Fibrous and sheet-like residues are visible in the pit shown in Figure 17. A more likely explanation is that pits provide a growth site for microorganisms. Accumulated bacterial material could be rich in sulphur and phosphorus as sulpho- and phospholipids and as the phosphate groups of nucleic acids and cell wall polymers.

ACKNOWLEDGEMENTS

I am indebted to Dr. Francoise Gaill for provision of specimens of *Lepetodrilus,* to Dr. K. Oates for assistance with X-ray microprobe analysis, and to Mr. Haydn Morris for carrying out amino acid analyses.

TABLE 5. Elemental composition of eroded pits in the shell of *Lepetodrilus* determined by X-ray microprobe analysis. A. Within a pit on the outside surface of the shell. B. Within a pitted area on the inside surface where erosion has penetrated the shell from the outside. These analyses relate to Figures 18A and 18B.

Element	Na	Mg	Al	Si	P	S	Cl	Ca
Counts %total								
A	0.36	3.58	—	—	39.08	28.33	1.07	25.57
B	0.35	2.11	2.57	1.27	13.94	27.06	0.84	51.87

LITERATURE CITED

ANDERSEN, S. O., 1979, Biochemistry of the insect cuticle. *Annual Review of Entomology,* 24: 29–61.

ANDERSON, S. O. & T. WEIS-FOGH, 1964, Resilin. A rubber-like protein in insect cuticle. *Advances in Protein Chemistry,* 2: 1–65.

BAROSS, J. A. & J. W. DEMING, 1985, The role of bacteria in the ecology of black-smoker environments. *Biological Society of Washington Bulletin,* 6: 355–371.

BEVELANDER, G. & H. NAKAHARA, 1970, An electron microscope study of the formation and structure of the periostracum of a gastropod *Littorina littorea. Calcified Tissue Research,* 1: 5–12.

CHOU, P. Y. & G. D. FASMAN, 1977, Secondary structural prediction of proteins from their amino acid sequence. *Trends in Biochemical Science,* 2: 128–131.

CRENSHAW, M. A. & J. M. NEFF, 1969, Decalcification at the mantle-shell interface in molluscs. *American Zoologist,* 9: 881–885.

CRENSHAW, M. A. & H. RISTEDT, 1976, Histochemical localization of reactive groups in septal nacre from *Nautilus pompilius* L. Pp. 355–367, in N. WATABE & K. M. WILBUR, eds., *The Mechanisms of mineralization in the invertebrates and plants,* Univ. of South Carolina Press.

DE BURGH, M. E. & C. L. SINGLA, 1984. Bacterial colonization and endocytosis on the gill of a new limpet species from a hydrothermal vent. *Marine Biology,* 84: 1–6.

DEGENS, E. T., D. W. SPENCER & R. H. PARKER, 1967, Paleobiochemistry of molluscan shell proteins. *Comparative Biochemistry and Physiology,* 20: 553–579.

FELBECK, H., M. A. POWELL, S. C. HAND & G. N. SOMERO, 1985, Metabolic adaptations of hydrothermal vent animals. *Biological Society of Washington Bulletin,* 6: 261–272.

FRETTER, V., 1988, New archaeogastropod limpets from hydrothermal vents; superfamily Lepetodrilacea II. Anatomy. *Philosophical Transactions of the Royal Society (London),* Series B, 319: 33–82.

HERRERA-DUVAULT, Y. & M. ROUX, 1986, Modalités et vitesse de dissolution de la coquille des modioles du site hydrothermal de 13°N sur la dorsale du Pacifique oriental. *Comptes Rendus de l'Académie de Science de Paris,* Série III, 302: 251–256.

HICKMAN, C. S., 1983, Radular patterns, systematics, diversity, and ecology of deep sea limpets. *Veliger,* 26: 73–92.

HUDDART, H. & S. HUNT, 1975, *Visceral muscle,* Blackie, Glasgow.

HUNT, S., 1987, Amino acid compositions of periostracal proteins from molluscs living in the vicinity of deep sea hydrothermal vents: an unusual methionine-rich structural protein. *Comparative Biochemistry and Physiology,* 88B: 1013–1021.

HUNT, S. & K. OATES, 1970, Fibrous protein ultrastructure of gastropod periostracum (*Buccinum undatum* L.). *Experientia,* 26: 1196–1197.

HUNT, S. & K. OATES, 1978, Fine structure and molecular organization of the periostracum in a gastropod mollusc *Buccinum undatum* L. and its relation to similar structural protein systems in other invertebrates. *Philosophical Transactions of the Royal Society (London),* Series B, 283: 414–459.

HUNT, S. & K. OATES, 1985, Helicoidal architecture in the periostracum of a terrestrial prosobranch *Pterocyclus latilabrum* Smith. *Journal of Molloscan Studies,* 51: 336–344.

JUNIPER, S. K., J. A. J. THOMPSON & S. E. CALVERT, 1986, Accumulation of minerals and trace elements in biogenic mucus at hydrothermal vents *Deep Sea Research,* 33A: 339–347.

LUTZ, R.A., 1982, Shell microstructure and mineralogy of two species of bivalves from deep-sea hydrothermal vents. *American Malacological Bulletin,* (1), Abstract, 101.

LUTZ, R. A. & D. C. RHOADS, 1980, Growth patterns within the molluscan shell: an overview. Pp. 203–254, in D. C. RHOADS & R. A. LUTZ, eds., *Skeletal growth of aquatic organisms,* Plenum Press.

MARSH, M. E. & R. L. SASS, 1983, Calcium-binding phosphoprotein particles in the extrapallial fluid and innermost shell lamella of clams. *Journal of Experimental Zoology,* 226: 193–203.

MCLEAN, J. H., 1985, Preliminary report of the limpets at hydrothermal vents. *Biological Society of Washington Bulletin,* 6: 159–166.

MCLEAN, J. H., 1988, New archaeogatropod limpets from hydrothermal vents; superfamily Lepetodrilacea I. Systematic descriptions. *Philosophical Transactions of the Royal Society (London),* Series B, 319: 1–32.

MELLOR, J. W., 1960, A comprehensive treatise on inorganic and theoretical chemistry, Volume 3: 824–827. Longmans, London.

MEENAKSHI, V. R., P. E. HARE, N. WATABE & K. M. WILBUR, 1969, The chemical composition of the periostracum of the molluscan shell. *Comparative Biochemistry and Physiology,* 29: 611–620.

PETIT, H., W. L. DAVIS, R. G. JONES & H. K. HAGLER, 1980, Morphological studies on the calcification process in the fresh-water mussel *Amblena. Tissue & Cell,* 12: 13–28.

REEKE, G. N., J. W. BECKER & G. M. EDELMAN, 1975, The covalent and three-dimensional structure of concanavalin A. *Journal of Biological Chemistry,* 250: 1525–1547.

ROUX, M., M. RIO & E. FATTON, 1985, Clam growth and thermal spring activity recorded by shells at 21°N. *Biological Society of Washington Bulletin,* 6: 211–221.

WALLER, T. R., 1983, Dahllite in the periostracum of *Lithophaga nigra* (Mollusca: Bivalvia) and its taxonomic and functional implications. *American Malacological Bulletin,* (1), Abstract, 101.

WANG, J. C., B. A. CUNNINGHAM & G. M. EDEL-

MAN, 1971, Unusual fragments in the subunit structure of concanavalin A. *Proceedings of the National Academy of Sciences of the USA,* 68: 1130–1134.

WILBUR, K. M. & A. S. M. SALEUDDIN, 1983, Shell formation. Pp. 235–287, in A. S. M. SALEUDDIN & K. M. WILBUR, eds., *The Mollusca,* 4(1). Academic Press.

Revised Ms accepted 3 February 1992

MALACOLOGIA, 1992, 34(1–2): 143–342

THE POMATIOPSIDAE OF HUNAN, CHINA (GASTROPODA: RISSOACEA)

George M. Davis[1], Cui-E Chen[2], Chun Wu[3] ,Tie-Fu Kuang[4], Xin-Guo Xing[5], Li Li[6], Wen-Jian Liu[7], Yu-Lun Yan[8]

ABSTRACT

This is a monograph involving the systematics of the 17 species of pomatiopsid snails thus far found in Hunan Province, the People's Republic of China. The Triculinae and Pseudobythinellini (new tribe) of the Pomatiopsinae dominate the pomatiopsid fauna. Four new species are described, three of *Neotricula* and one of *Tricula*. Detailed anatomical data are the basis for describing each species. The anatomies of "*Akiyoshia*" and *Lithoglyphopsis* are presented for the first time. *Guoia* is a new genus for some species previously considered to be *Lithoglyphus* (a strictly European hydrobiid genus) or *Lithoglyphopsis* (restricted to China). The anatomical data are the basis for phenetic and cladistic analyses to provide insight into those characters and character-states that serve to distinguish taxa, and to assess relationships among genera of the tribes Pachydrobiini (*Halewisia*, *Neotricula*, *Pachydrobia*, *Jinhongia*, *Robertsiella*, *Guoia*, *Wuconchona*, *Gammatricula*) and Triculini (*Tricula*, *Delavaya*, *Fenouilia*, *Lithoglyphopsis*, *Lacunopsis*). *Hubendickia* served as the outgroup genus of the remaining tribe of the Triculinae, the Jullieniini. Biogeographic deployment of the genera of all three tribes of the Triculinae is mapped on an area cladogram of relevant river systems. Genera of the Jullieniini dominate the lower Mekong River. *Tricula* extends from Northern India down the Yangtze and upper Mekong rivers. *Tricula* and *Neotricula* primarily flourish along the Yangtze River drainage. Four genera have shells that are so similar that shell characters cannot be used to distinguish among the genera: *Tricula*, *Neotricula*, *Jinhongia* and *Gammatricula*. Most of the species treated here are of medical importance because they either transmit or are suspected of transmitting lung flukes of the genus *Paragonimus*, or blood flukes of the genus *Schistosoma*.

Key words: Pomatiopsidae, biogeogrpahy, phenetics, cladistics, China, Hunan, *Schistosoma*, *Tricula*, *Neotricula*, *Paragoniumus*, Yangtze River

INTRODUCTION

This work is one of a series of papers dedicated to establishing the detailed anatomy and systematic relationships of genera of southeast Asian and Chinese freshwater prosobranch snails suspected of being members of the Pomatiopsidae as defined in Davis (1979, 1980). It is one more step in documenting the extensive speciation that has occurred within the tribes Triculini and Pachydrobiini of the Triculinae, which occur primarily throughout southern China, in contrast to the extensive Jullieniini adaptive radiation documented in the lower Mekong River in Thailand, Laos, and Cambodia (Davis, 1979).

In this work, *Guoia* is established as a new genus. The anatomies of "*Akiyoshia*" and *Lithoglyphopsis* are presented for the first time. Anatomical data are provided for clarification of the genus *Pseudobythinella*. Several nomenclatural problems are clarified or presented relative to necessary future work. Seventeen nominal species are treated.

Phenetic and cladistic analyses are done to provide insight into those characters and character-states that serve to distinguish taxa, and to assess relationships among genera of the tribes Pachydrobiini and Triculini,

[1]The Academy of Natural Sciences of Philadelphia, 1900 Benjamin Franklin Parkway, Philadelphia, Pennsylvania 19103-1195 U.S.A.
[2]Institute of Parasitic Diseases, Zhejiang Academy of Medical Sciences, Hangzhou, Zhejiang Province, People's Republic of China
[3]Hunan Medical University, Changsha, Hunan Province
[4]Hengshan County Anti-Epidemic Station, Hengshan, Hunan, People's Republic of China
[5]Anhua County Anti-Epidemic Station, Zhuzhou, Hunan, People's Republic of China
[6]Zhuzhou City Anti-Epidemic Station, Zhuzhou, Hunan, People's Republic of China
[7]Cili County Anti-Epidemic Station, Cili, Hunan, People's Republic of China
[8]Shimen County Anti-Epidemic Station, Shimen, Hunan, People's Republic of China

with one genus of the Jullieniini serving as the outgroup. Biogeographic deployment of the Triculinae is considered in conjunction with an assessment of the evolution of river systems in continental south Asia.

Most of the taxa treated here are of medical importance because they either transmit or are suspected of transmitting lung flukes of the genus *Paragonimus* or blood flukes of the genus *Schistosoma*.

MATERIAL AND METHODS

Localities are provided with the synonymy section for each species. Sites 1 to 12 are found on Figure 1. With reference to Figure 1, be aware that maps published at different times may provide different spellings for standard Chinese characters. Relevant here are: Hsiang = Xiang; Tzu = Zi; Lin = Li. The Yangtze River = the Chang Jiang (jiang = river; shui = river). Dong Ting Lake (Lake = Hu) = Tung t'ing Hu.

Abbreviations for institutions housing voucher species are: ANSP = Academy of Natural Sciences of Philadelphia (the A- number sequence indicates alcohol-preserved specimens); IZAS = Institute of Zoology, Academica Sinica; SMF = Senckenberg Museum, Frankfurt A.M. Germany; ZAMIP = Zhejiang Academy of Medical Sciences, Institute of Parasitic Diseases, Hangzhou, China. Voucher catalog numbers are provided in the synonymy section for each species.

Methods are those of Davis & Carney (1973), Davis et al. (1976), Davis (1979), and Davis & Greer (1980). All dissections were done with living material in Hunan, China using a Wild dissecting microscope and a Nikon high intensity lamp. Scanning electron microscopical analyses, photography of shells, radular preparations and computer analyses were done in Philadelphia.

Descriptions of taxa employ only those character and character-states useful to discriminate among species of Pomatiopsidae. Character-states common to all are not repeated here but are described elsewhere (Davis, 1979, 1980).

Relative sizes of organs or shells are defined by range in size (as in shells) or ratios to facilitate comparison among taxa using terms such as "small, " "elongate, " etc. This practice follows Davis et al. (1986) and all later papers in this series of studies. The sizes and ratio used are:

1. Shell length: large (≥ 5.0 mm), medium (4.0–4.9 mm), small (2.1–3.9 mm), minute (≤ 2.0 mm) (based on mean size of the mature size class with the greatest number of individuals, realizing that mature snails may occur with different numbers of whorls, e.g. 5.0, 5.5, 6.0 whorls).

2. Operculum attachment pad: width of attachment pad ÷ width of operculum: narrow (≤ 0.35), wide (0.36–0.55), very wide (≥ 0.56).

3. Osphradium length: length of osphradium ÷ length of gill (Davis et al. 1976, 1982, 1983): long (≥ 0.40), short (≤ 0.35).

4. Length of gill filament section Gf_2: length of Gf_2 ÷ length of Gf_1 and Gf_2: long (≥ 0.51), medium (=normal) (0.31–0.50), short (≤ 0.30).

5. Gill filament number: few (≤ 15), numerous moderate (16–25), numerous (≥ 26).

6. Bursa copulatrix length: length of bursa ÷ length of the pallial oviduct: long (≥ 0.40), short (≤ 0.38).

7. Albumen gland length: length of the albumen gland (Ppo) ÷ length of the entire pallial oviduct: standard (≥ 0.45), short (≤ 0.42).

8. Male gonad length: gonad length ÷ length of digestive gland: short (< 0.50), long (≥ 0.50).

9. Seminal receptacle duct length: very short or absent (≤ 0.02 mm), long (> 0.02 mm).

10. Radula length: short (≤ 0.40 mm), medium (0.41–0.59 mm), long (0.60–0.79), very long (≥ 0.80 mm).

11. Radula; mean rows of teeth: few (≤ 59), moderate (60–69), many (70–84), very many (≥ 85).

12. RPG ratio: length of the supraesophageal connective ÷ sum of the length of the right pleural ganglion, the supraesophageal connective, and the supraesophageal ganglion; concentrated (≤ 0.29), moderately concentrated (0.30–0.49), elongate (0.50–0.67), extremely elongate (≥ 0.68) (Davis et al. 1984, 1985).

13. Subesophageal connective length: usual or standard triculine (0.02–0.09 mm); none; long (≥ 0.10 mm) [based on average of several measurements].

Multivariate Analysis

Shell data were analyzed for populations of *Guoia*. The first data matrix involved 33 OTUs (operational taxonomic units) (individual shells) and 11 characters. The OTUs were:

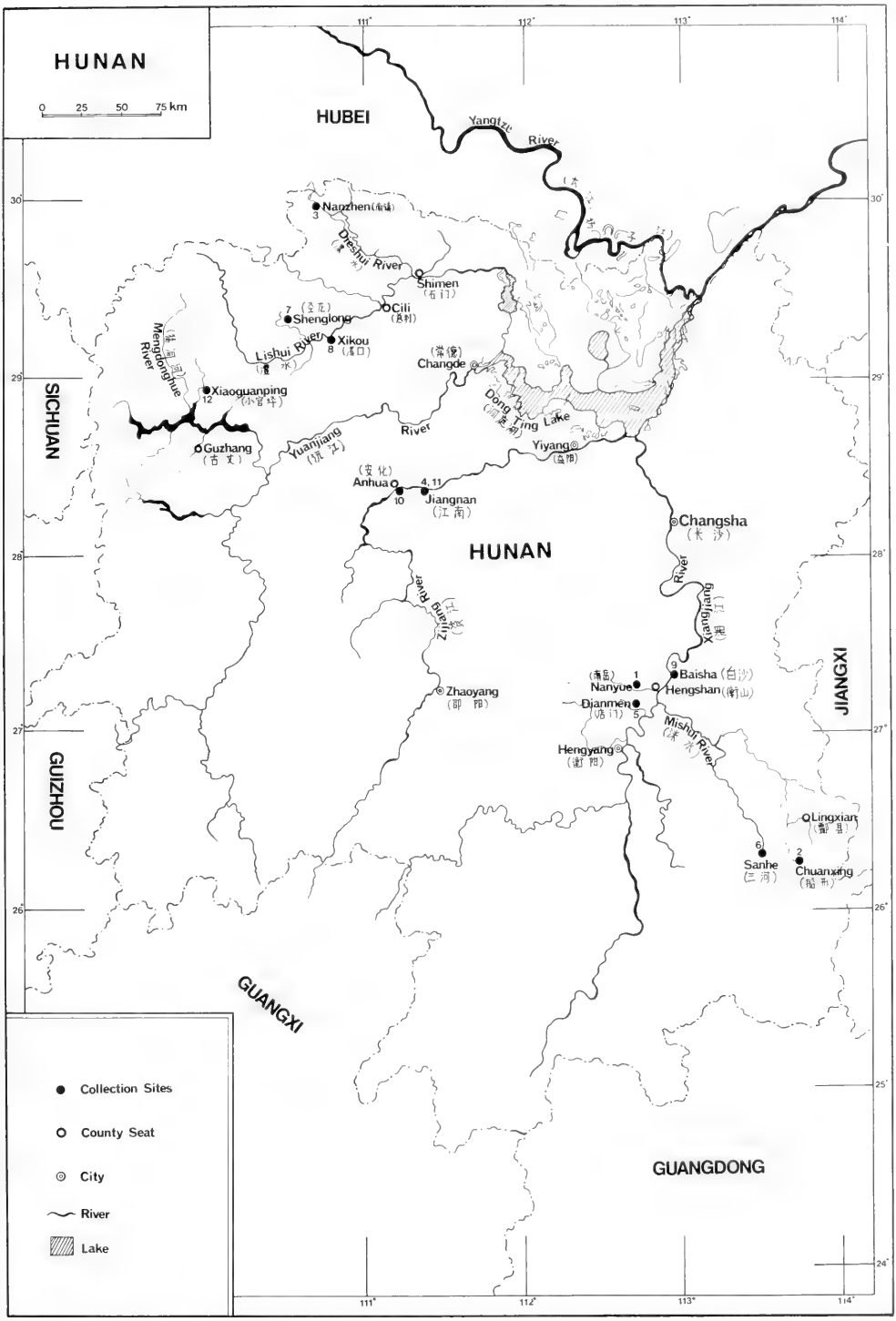

FIG. 1. Map of Hunan, China, showing localities from which specimens described in this monograph were collected.

Guoia viridulus, large class snails, males (1–7), females (8–12); ANSP cataloged specimens of *Guoia viridulus* collected over 90 years ago (18–21); small class snails, males (22–26), females (27–32). *Guoia fuchsianus* males (13, 14), females (15–17). ANSP cataloged historic *G. fuchsianus* (33).

The characters were:

1. Number of whorls
2. Length
3. Width
4. Length of body whorl
5. Length of penultimate whorl
6. Width of penultimate whorl
7. Width of 3rd whorl
8. Length of last three whorls
9. Length of aperture
10. Width of aperture
11. Width of columellar shelf

The second matrix included individuals of two populations from historic collections, *Guoia fuchsianus* cataloged in the ANSP collections: ANSP 98205 (34–38), ANSP 45961 (39–41). These OTUs were added to the OTUs of matrix one to give a total OTU count of 41. The character matrix was reduced because all OTUs 34–41 had eroded apices, thus characters 1, 2, 7, and 8 could not be measured for all individuals.

Computations were made using the 1974 version of NT-SYS (Rohlf et al., 1972). Characters were standardized (standard deviation and mean values). Similarity and distance coefficients were calculated and phenograms produced using UPGMA. Cophenetic correlations were calculated. Principal Component Analysis (PCA) was done with components extracted until eigenvalues became less than 1.0. A transposed matrix of the first three principal components with their character loading was postmultiplied by the standardized matrix to yield a matrix of OTU projections in the principal component space (Rohlf et al., 1972). The OTU locations in the three-dimensional space were used as the initial configuration for a nometric multidimensional scaling (MDS) placement of Q-mode taxonomic distances between OTUs (Kruskal, 1964). Ordination was done followed by a Prim Network (minimum Spanning Tree = MST). Subsequently a phenogram was produced based on MDS and the cophenetic correlation calculated.

A similar multivariate analysis was used to assess phenetic relationships among 30 OTUs on the basis of shell data. The OTUs involved species of *Tricula*, *Neotricula* or species the shells of which resembled those of species of *Tricula*. The analysis was done as an aid for distinguishing among species on the basis of shell characters.

Another similar multivariate analysis was done to assess phenetic relationships among the same species for which the shell analysis was done. However, this analysis involved 48 anatomical character-states.

Cladistic Analysis

Scorings were not done in binary alone but involved six multistate characters (Table 85). Analysis was first done using the computer-mediated program Hennig-86 (Farris, 1988). *Hubendickia* served as the outgroup. Options run were cc-. (character-states all unordered); ie; tplot; tsave; nelsen. A final non-computer-mediated cladogram was made after weighting one character following establishing the direction of evolution of its states.

Shell Characters

Shell character-states is illustrated in Figs. 2, 3. Aside from shell measurements there are a number of diagnostic qualitative character-states of use to discriminate among shells (Tables 1, 2).

Triculine shells have three predominant shapes (Fig. 2A): globose, ovate-conic, ovate-turreted. Many character-states involve the aperture. The adapical end may be regularly rounded or slightly constricted to form an adapical apertural notch (Adn, Fig. 3D). The constriction may be less pronounced (Fig. 3E). The adapical aperture and apertural notch may be extended to form the adapical apertural beak (Adb, Fig. 3A). The apertural notch may have a noticeable internal groove (Ngr, Fig. 3E) or lack a groove (Fig. 3A). The adapical apertural notch may be bounded by an adapical tooth or node on the inner lip (Adt, Fig. 3A, D); or the adapical inner lip may lack such a thickening (Fig. 3E, H).

The inner lip may (Ari, Fig. 3A) or may not be fused (Gap, Figs. 3D, E) to the body whorl. When separated from the body whorl the gap (Gap) may be narrow (Fig. 3E) or wide (Fig. 3D). The inner lip may be straight, arched (Fig. 3A), sigmoid or undulating (Fig. 3E), or angled (Fig. 3D). The adapical part of the inner lip may be thickened (Adil, Fig. 3D) or thin; the abapical part of the inner lip the

TABLE 1. Twenty-six shell character and character-states useful for describing shells of Triculinae as illustrated in Figures 2 and 3.

Abil	Abapical inner lip
Abs	Abapical spout
Adb	Adapical apertural beak
Adil	Adapical part of inner lip
Adt	Adapical tooth or node
Adn	Adapical apertural notch
Agp	Adapical apetural gap
Aol	Adapical outer lip angle
Aols	Adapical outer lip sinus
Ari	Arched inner lip
Cr	Crenulated suture
Ct	Columellar tooth
Gap	Gap between the body whorl and the inner lip
L	Length
Mln	Mid-lip notch
Nab	Normal adapical aperture
Ngr	Adapical notch groove
Ol	Outer lip
Sfo	Scooped forward
Sin	Sinuate outer lip
Stl	Straight lip
Umc	Umbilical chink
Var	Varix
W	Width
x	distance from base of body whorl to abapical end of aperture
y	distance from edge of outer lip to edge of body whorl

same. The inner lip may have a mid-lip notch (Mln, Fig. 3D).

The abapical end of the aperture may project noticeably beyond the base of the body whorl when the shell is viewed in apertural view (Fig. 3E); it may not (Fig. 3F). The abapical end of the aperture may be spout-like (Figs. 3D, E); it may not (Fig. 3A, F). The columella may have a tooth (Ct, Fig. 3F). It is necessary to break open the body whorl of some shells from a population to determine whether or not there is an internal columellar node, tooth, or keel.

The adapical end of the aperture may be pulled away from the body whorl leaving an adapical gap (Agp, Fig. 3D, F) or the adapical aperture may be fused to the body whorl (Fig. 3A).

In side view the outer lip may be straight (Stl, Fig. 3H) or sinuate (Sin, 3B). The outer lip may be aligned with the axis of coiling (Fig. 3C, H) or scooped forward (Sfo, Fig. 3B). In side view there may be an adapical depression or sinus in the outer lip (Aols, Fig. 3H) caused by an adapical apertural notch.

Rotating the shell from apertural view to the right (apex up) so that the inner lip is perpendicular to the horizontal, the abapical part of the inner lip may be deflected away from the columella causing a lip deflection angle (Fig. 3G, 2B). Such an angle may not occur.

Gill Filament Shape

Considering the longest (thus mid-gill) gill filaments, three shapes are found when the filaments are examined so as to see the entire leaflet (Fig. 4). The Gf_2 section may be flat, have a modest dome, or be high domed.

Vital Staining

Davis (1967) discussed using aqueous methylene blue and neutral red as vital stains. The exact methods are as follows: small quantities of powdered stain are dumped into a quantity of tap water (approximately 500 ml) and stirred until dissolved. Sufficient powder is added so that when the solution is placed before a light the solution is opaque. Wide-mouth jars are used, one each for the two stains. Wide mouth containers are specified because the stain is used over and over again. With the living animal pinned out on the black parafin-wax layer in a 9-cm Petri dish, the water covering the animal is poured off and the stain poured on to cover the animal. The stain is left on for 30 seconds to a minute, then poured back into the storage bottle. The animal is rinsed five to ten times to remove excess stain and then covered with water to continue the dissection.

Neutral red is used first to deliniate glandular tissue and the ducts of the female reproductive system. The two regions of the pallial oviduct are differentiated; the oviduct is stained as well as the gonad and oocytes.

Methylene blue is used next; it seems to harden and delineate the ducts of the female reproductive system. The slender duct of the seminal receptacle and the various other components of the bursa copulatrix complex of organs are made to stand out.

Bouins Solution

When all work with the living animal is finished, Bouins solution is most useful to eliminate problems caused by mucus, to delineate mantle cavity structures, such as the gill filaments, and to dissect the nervous system. The nerves and ganglia stain bright yellow enabling one to see them better and to differen-

TABLE 2. Shell character-states scored for 29 characters used for a multivariate analysis of phenetic relationships among 21 species of Triculinae, the shells of which either are classified as *Tricula* or *Neotricula* or resemble the shells of these two genera.

1. Size:	small (0), medium (1), minute (2), long (3)
2. Shape:	ovate-conic (0), ovate-turreted (1), turreted (2), cylindrical-conic (3), globose-conic (4)
3. Aperture shape:	ovate (0), pyriform (1), distorted (2)
4. Umbilicus:	none (0), chink (1), clearly open (2)
5. Whorl at suture:	smooth (0), crenulated (1)
6. Teleoconch sculpture:	none (0), spiral microsculpture at suture (1)
7. Spiral sculpture at mid body-whorl to shell base	none (0), with (1)
8. Protoconch whorls:	smooth (0), wrinkled (1), malleated and/or pitted (2)
9. Adapical aperture:	normal (0), with notch (1), with beak (2)
10. Adapical aperture:	normal (0), with internal groove (1)
11. Adapical aperture:	normal (0), with sinus (1)
12. Abapical aperture:	normal (0), with spout (1)
13. Inner lip:	straight (0), arched (1), sinuate (2), angled (3)
14. Outer lip-side view:	straight (0), sinuate (1)
15. Outer lip-side view:	parallel with axis of coiling (0), scooped forward (1), slanted back (2)
16. Inner lip:	no tooth (0), with tooth (1)
17. Inner lip:	no notch (0), with notch (1)
18. Base of inner lip, side view:	straight (0), angled to form lip deflection angle (1)
19. Inner lip:	thin (0), thick [≥ 0.10mm] (1), differentially thickened (2)
20. Inner lip:	fused to body whorl (0), partly separated (1), totally separated by narrow gap (2), widely separated (3)
21. Adapical aperture:	fused to body whorl (0), slightly separated (1), widely separated (2)
22. Columella within body whorl:	smooth (0), tooth or node (1), spiral keel (2), lamellae on aperture side of columella (3)
23. Varix:	none (0), slight (1), pronounced (2)
24. Adapical aperture:	normal (0), with beak tubercle (1)
25. Adapical outer lip angle:	none (0), slight (1), extended (2)
26. Base of body whorl:	normal (0), with keel spiraling down from umbilical area (1)
27. Base of shell at umbilicus:	normal (0), with wide columellar shelf (1)
28. Base of shell at abapical lip:	normal (0), with basal post (1)
29. Shell attains 7.0 whorls:	no (0), yes (1)

tiate nerves from muscle fibers. Bouins solution strengthens the nerves such that they can be handled better. Dissections of the head involving the buccal mass, salivary glands and associated nerves are facilitated.

Body Measurements

How the lengths of the gonad, digestive gland, and body are measured is illustrated in Davis & Carney (1973). Lengths of mantle cavity organs are measured with the mantle cut along the right side of the neck from the mantle edge to the rear of the mantle cavity. The mantle is then reflected to the left and pinned out as shown in Figure 5. How lengths of mantle cavity structures are measured is illustrated in Figure 5. The ocular micrometer is positioned and rotated along the dotted trajectory. As shown in Figure 5, not all gill filaments may be illustrated.

Abbreviations

a	line perpendicular to mid-line "x" at posterior edge of eye lobes
a'	Line perpendicular to mid-line "x" at the anterior edge of penial base
Adb	Adapical apertural beak
Ae	Abapical embayment
Af	Anterior foot;
Algo	Anterior lobes of gonad
Als	Adapical outer lip sinus
Apg	Anterior pedal glands.
Apo	Anterior pallial oviduct = capsule gland
Apo-1	Anterior pallial oviduct = capsule gland
Apo-2	Different tissue type anterior to capsule gland.
Ast	Anterior chamber of stomach
Au	Auricle
Bc	Basal crescent
Bg	Beak groove

Bm	Buccal mass
Bp	Base of penis
Bu	Bursa copulatrix
Cc	Cerebral commissure
Cl	Columellar muscle
Coi	Oviduct coil
Cr	Crescent ridge
Cs	Columellar shelf
Csd	Common sperm duct
Dbu	Duct of bursa
Di	Digestive gland
Dsr	Duct of seminal receptacle
Ebr	Eyebrow
Ebv	Efferent branchial vein
Edi	Anterior edge of digestive gland (Figs. 141, 142)
Edi	Dashed line indicates anterior limit of digestive gland
Ej	Ejaculatory duct
Emc	Posterior end of mantle cavity
Epr	Dashed line indicates posterior limit of prostate gland
Es	Esophagus
Ey	Eye
Eyb	Eyebrow
Fp	Fecal pellet
Gf_1	Thickened basal bar of gill filament
Gf_2	Slender terminal part of gill filament
Glo	Glandular lobe
Go	Gonad
Go-a	Section of gonad, the extent of which is indicated by the dashed line, removed to show seminal vesicle
Go-b	Gonad
Gr	Patch of white granules
Gra	Granules or glands, white to lemon yellow
Grv	Groove
Gs	Grey streak on Ast
Il	Inner lip
In	Intestine
In_1	Intestine looping around anterior end of style sac
In_2	Fecal pellet compressor section of intestine
In_3	Anterior intestine
Ki	Kidney
L	Length
Lap	Length of aperture
Lbw	Length of body whorl
LGf_1	Length of gill filament section Gf_1
LGf_2	Length of gill filament section Gf_2
LGi	Length of gill
LMa	Length (= width) of mantle collar anterior to gill
Lm	Dashed line is trajectory used to measure length of gill and length of mantle cavity
LofA	Length of shell with aperture pressed down on a horizontal surface
LOs	Length of osphradium
Lpl	Left pleural ganglion
Lpw	Length of penultimate whorl
Ma	Mantle collar
Ne	Neck
Ngr	Adapical notch groove
Odi	Opening from stomach to digestive gland
Oki	Opening of kidney into mantle cavity
Ol	Outer lip
Omc	Opening of spermathecal duct into mantle cavity
Omn	Osphradiomantle nerve
Ooc	Oocyte(s)
Oop	Opening into albumen gland (Ppo)
Oov	Opening of oviduct to albumen gland (enlarged in Fig. 10)
Ope	Opening for sperm entry to pericardium
Opo	Opening of oviduct into albumen gland
Opr	Opening to vas deferens
Os	Osphradium
Osd	Opening of spermathecal duct to mantle cavity (Figs. 11, 21)
Osd	Point where oviduct fuses to, and opens into pericardium
Osm	Osphradiomantle nerve
Osr	Oviducal seminal receptacle
Ov	Oviduct
Pa	Papilla
Pbu	Pericardial bursa
Pc	Pellet compressor (= In_2)
Per	Pericardium
Pe	Penis
Pf	Penial filament
Ppo	Posterior pallial oviduct = albumen gland
Pr	Prostate
Psc	Pleurosupraesophogeal connective
Pst	Posterior chamber of stomach
Rcg	Right cerebral ganglion
Ri	Yellow ridge
Rpl	Right pleural ganglion
Rs	Radular sac
Sd	Spermathecal duct
Sdo	Opening of oviduct into the pericardium
Sdu	Sperm duct
Sec	Pleurosupraesophageal connective
Seg	Supraesophageal ganglion
Sg	Salivary gland
Sn	Snout
Sr	Seminal receptacle
Sts	Style sac
Sty	Stylet
Suc	Pleurosubesophageal connective

Sug	Subesophageal ganglion
Sv	Seminal vesicle
Tn	Tentacle
Twv	Thin walled vestibule
Uc	Umbilical chink
Vd	Vas deferens
Vd_1	Posterior vas deferens
Vd_2	Anterior vas deferens
Ve	Vas efferens
Vei	Vein
Ven	Ventricle
W	Width (Fig. 110)
Wap	Width of aperature
Wgr	White granular inclusions
Wg	White granules
WofA	Width of shell with aperature pressed down on a horizontal surface
W	Wall of neck
x	Mid-line of snout-neck with snout anterior (up).
x	Marks the same point in Figs. 20, 21 A and B; 117A, 118
Yri	Yellow ridge along anterior and posterior ends of the Ast

SYSTEMATICS

Taxa Treated

POMATIOPSIDAE

Pomatiopsinae
  Pomatiopsini
    Oncomelania
      Oncomelania hupensis Gredler, 1881
  Pseudobythinellini, Davis & Chen new tribe
    Akioyshia
      "*Akiyoshia*" *chinensis* Liu, Zhang & Chen, 1982
    Pseudobythinella
      Pseudobythinella chinensis (Liu & Zhang, 1979)
      P. shimenensis Liu, Zhang & Chen, 1982
Triculinae
  Pachydrobiini
    ***Guoia* Davis & Chen gen. nov.**
      G. fuchsianus (Moellendorff, 1885)
      G. viridulus (Moellendorff, 1888)
    Neotricula
      N. cristella (Gredler, 1887)
      ***N. dianmenensis* Davis & Chen, sp. nov.**
      ***N. duplicata* Davis & Chen, sp. nov.**
      ***N. lilii* Chen & Davis, sp. nov.**
      N. minutoides (Gredler, 1885)

  Triculini
    Lithoglyphopsis
      L. modesta (Gredler, 1886)

    Tricula
      T. gredleri Kang, 1986
      ***T. maxidens* Chen & Davis, sp. nov.**
      T. odonta Liu, Zhang & Wang 1983a

Nomina nuda:
  Tricula gredleri
  Akiyoshia odonta

Nomina Nuda

Two names were introduced into the literature for presumed Pomatiopsidae from Hunan Province but without photographs, illustrations, designation of types, or descriptions that would permit one to identify the species in question. Accordingly these are nomina nuda. The nominal taxa involved are:

Tricula gredleri Feng et al., 1985 [Kang sp. nov.]
Tricula gredleri Feng et al., 1986 [Kang sp. nov.]
Akiyoshia (*Saganoa*) *odonta* Feng et al., 1985 [Kang sp. nov.]
Akiyoshia (*Saganoa*) *odonta* Feng et al., 1986 [Kang sp. nov.]

Higher Taxa Defined

The family Pomatiopsidae was differentiated from the Hydrobiidae in Davis (1979); two subfamilies were recognized, the Pomatiopsinae and Triculinae. Both subfamilies have a spermathecal duct, a pomatiopsid type central tooth (square to rectangular) with pronounced basal cusps arising from the face of the tooth (an exception includes the Pseudobythinellini discussed below), cover eggs (laid singly) with sand grains, and do not brood young. The penis is without complex glands or lobes. The differentiation of the pomatiopsid subfamilies from other higher taxa with spermathecal ducts was given in Davis et al.(1985: 74–75). These higher taxa are the Hydrobiidae: Littoridininae and Amnicolinae (also see Hershler & Thompson, 1988).

The Pomatiopsinae are Gondwanian in distribution. Pomatiopsinae snails have an elon-

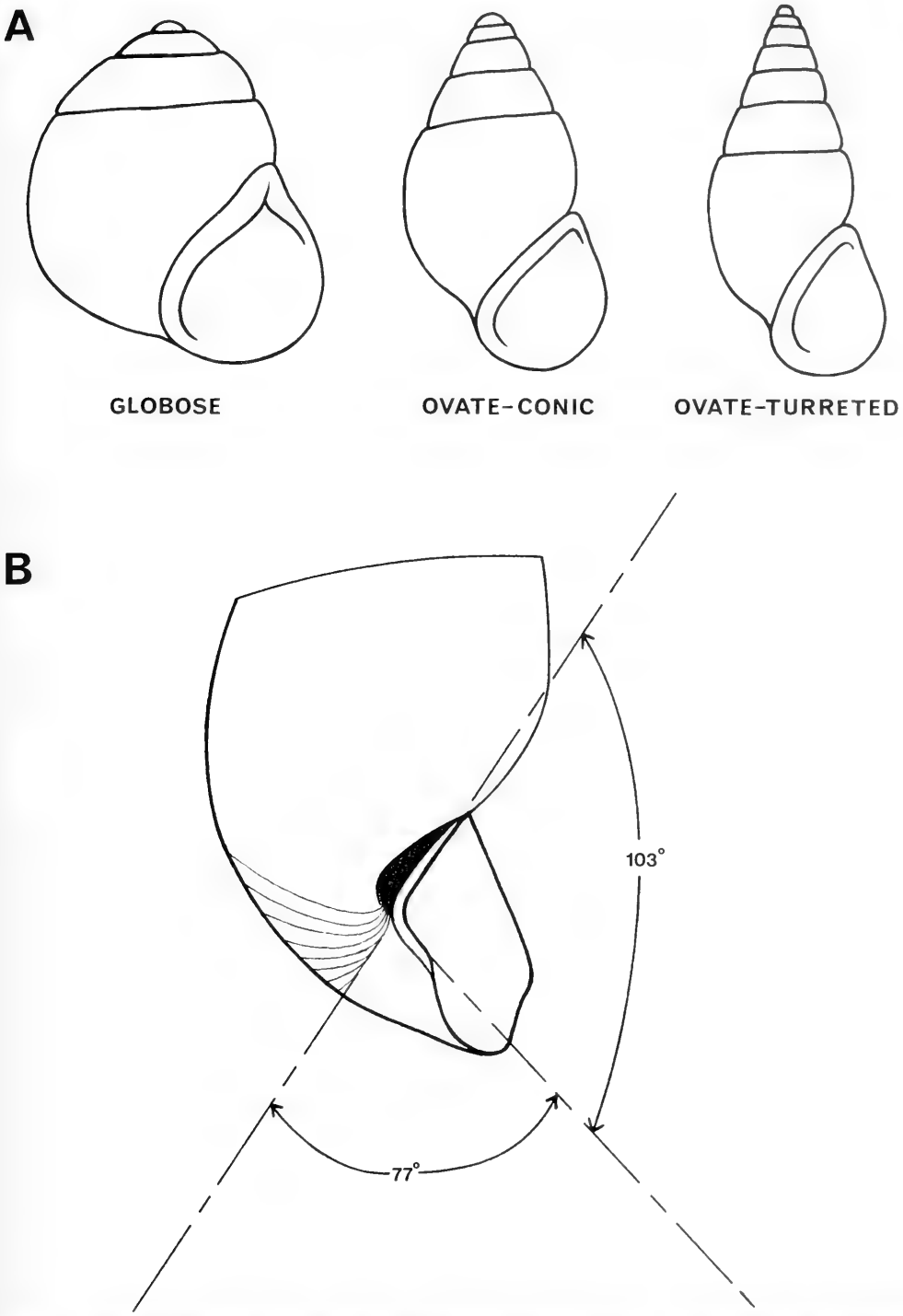

FIG. 2. Shell characters used in describing species of Hunan Triculinae. A. Three major shell shapes. B. Inner lip in side view showing a pronounced lip deflection angle.

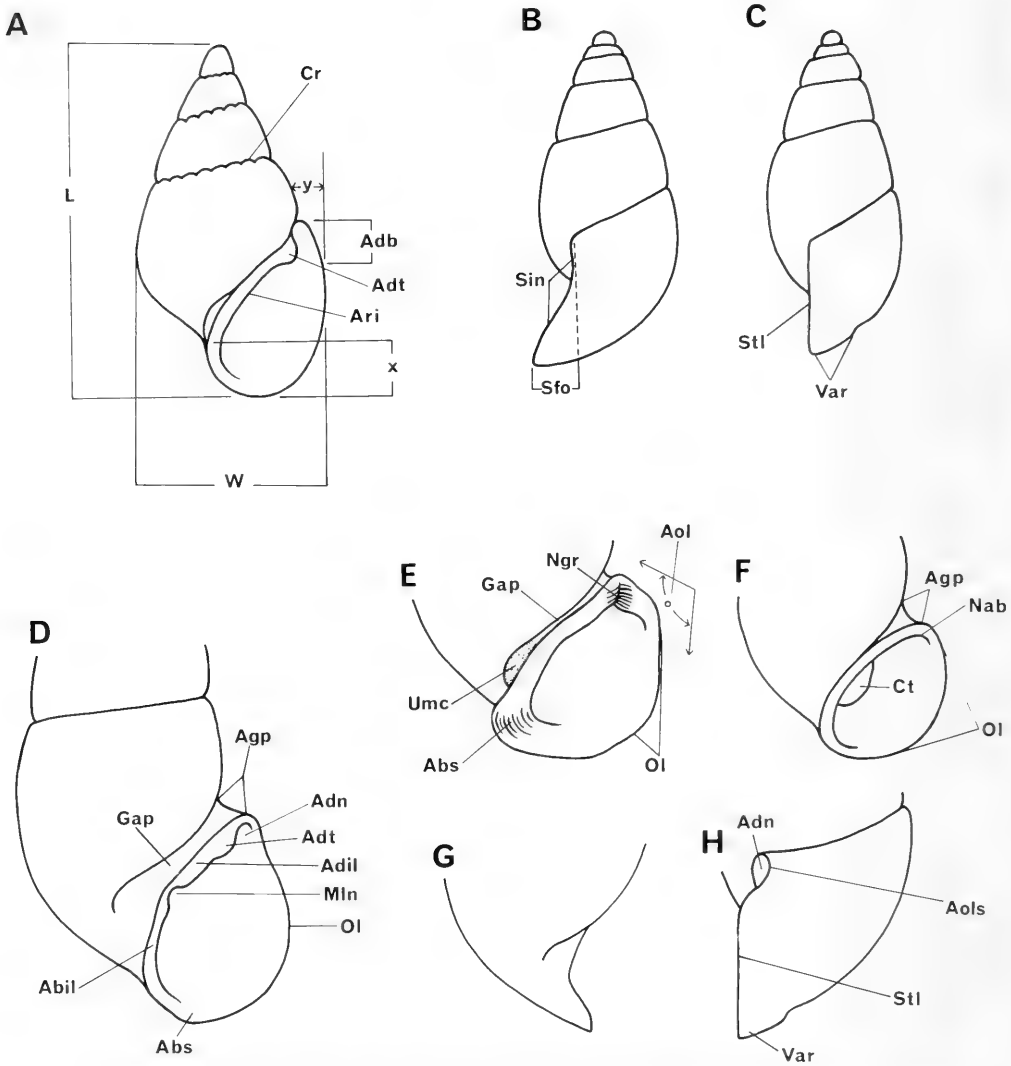

FIG. 3. Shell characters used in describing species of Hunan Triculinae. Labels are defined in Table 1.

gated spermathecal duct extending to the anterior end of the mantle cavity. In the tribe Pomatiopsini, the eyes are in pronounced bulges. These snails have a pedal crease, suprapedal fold and omniphoric groove. They move by a step-wise mode. They have evolved from freshwater to an amphibious mode of existence, and in Japan *Blanfordia* has become terrestrial (Davis, 1979, 1981). The tribe Pseudobythinellini is placed in the Pomatiopsinae because of the elongated spermathecal duct. The central tooth is of the *Hydrobia* type with a pair of cusps arising from the lateral angles. The eyes are not in pronounced eye lobes. There is no suprapedal fold, omniphoric groove or pedal crease. Animals move by ciliary glide. The penis of species classified here as Pseudobythinellini lacks a penial lobe with functioning duct (in addition to the vas deferens) that widens to form a wide coiled mass or penial gland in the cephalic haemocoel. The acces-

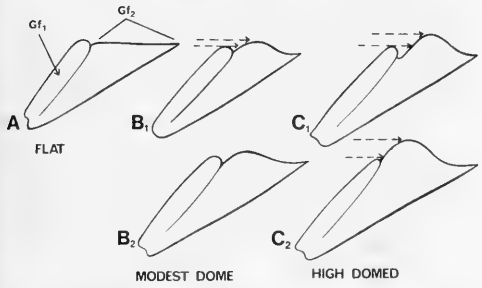

FIG. 4. Shapes of the Gf_2 segment of the largest gill filaments.

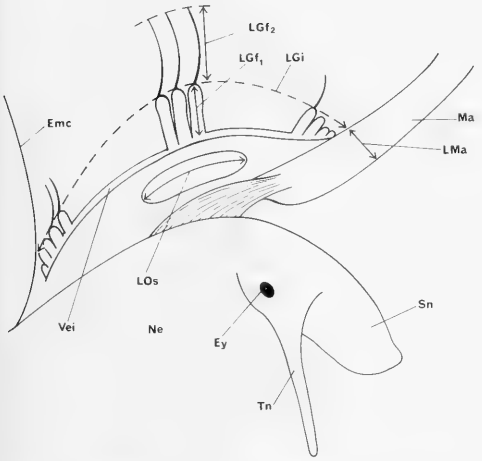

FIG. 5. Mantle reflected to reveal mantle cavity organs and how their lengths were measured. The dashed line is the trajectory for measuring the length of the gill. The length of the mantle cavity is measured from Emc along the LGi plus LMa.

sory penial lobe and penial gland are characteristic of the European genus *Bythinella* and North American genus *Amnicola* of the Hydrobiidae: Amnicolinae (Davis et al., 1985; Hershler & Thompson, (1988).

The Triculinae are Asian with a distribution from northern India throughout South China and southeast Asia. No Triculinae are found in Japan (Shikoku to Okinawa). Ioganzen & Starobogatov (1982) refer their new genus *Sibirobythinella* to the Triculidae. However, given the extensive convergences in structure such as the spermathecal duct and central tooth of the radula (reviewed in Davis et. al., 1985) it is not at all certain that taxa from Siberia or northeastern Russia relegated to the Triculidae by Russian workers are Triculinae sensu Davis (1979, 1980). *Sibirobythinella* is not, based on data provided, a triculine snail. The shell and radula might indicate placement in the Pseudobythinellini. Ioganzen & Starobogatov (1982) place their taxon in the family Triculidae apart from taxa they erected to family status such as Littoridinidae, Pomatiopsidae and Stenothyridae, all characterized by having a spermathecal duct running independently of the pallial oviduct from the mantle cavity to the bursa copulatrix. Unfortunately, they do not provide sufficient data to differentiate their taxon from European Hydrobiidae: Littoridininae, Amnicolinae, or Pomatiopsinae: Pseudobythinellini.

Triculinae snails have a short spermathecal duct opening to the posterior end of the mantle cavity. The snails are aquatic, do not have a suprapedal fold, pedal crease, or omniphoric groove. Only in a few derived genera are the eyes in pronounced lobes. Snails progress by ciliary glide.

Tribal, Generic and Species Descriptions

POMATIOPSINAE

Pomatiopsini

Type genus. Pomatiopsis Tryon 1862

Diagnosis. Ovate-conic to turreted shells. Shell length greater than 2.5 mm; most greater than 3.0 mm. Apical whorls are not flattened. Spermathecal duct runs from the bursa copulatrix to the anterior end of the mantle cavity. Spermathecal duct not tightly pressed to pallial oviduct. Sperm duct running posteriorly from oviduct to the bursa or the spermathecal duct at the bursa. Eyes are in pronounced eye lobes. There is a suprapedal fold, an omniphoric groove, and pedal crease. Basal cusps of the central tooth of the radula arise from the face of the tooth.

Oncomelania Gredler 1881

Type Species. Oncomelania hupensis Gredler 1881: 120-121; pl. 6, fig. 5

Type locality. U—tschang—fu, March 1879. [= Hubei Province; Wu—Tshan—fu; Yen, 1939].

Designation. By monotypy

Types. Bozen; lectotype and two paralectotypes

Bozen No. 89. No. types at SMF (Zilch, 1974: 197)

Oncomelania hupensis Gredler, 1881

No detailed study of this well-known species is presented here. This species is included for completeness sake in monographing the Pomatiopsidae of Hunan, China. This species is the vector for *Schistosoma japonicum* and abounds in the marshes around Dong Ting Lake and along the Yangtzee River (Fig. 1) (Lou et al., 1982; Liu et al., 1981). Detailed anatomical data for *Oncomelania* have been published elsewhere (Davis 1967, 1968a, 1969a; Davis & Carney 1973).

Pseudobythinellini Davis & Chen New Tribe

Type genus. Pseudobythinella Liu & Zhang 1979.

Diagnosis. Ovate shells less than 2.5 mm long, with flattened apical whorls. The sperm duct runs anteriorly from the oviduct to the spermathecal duct; it is so tightly pressed to the pallial oviduct that it is difficult to differentiate it. Unlike the Pomatiopsini, the sperm duct enters the spermathecal duct far anterior to the bursa copulatrix; the duct of the bursa is thus elongated (the continuation of the spermathecal duct to the bursa from the point of entry of the sperm duct). Eyes are not in pronounced eye lobes. There is no suprapedal fold, no omniphoric groove or pedal crease. Animals are aquatic and move by ciliary glide. Basal cusps of the central tooth of the radula arise from the lateral angles of the tooth.

Synonymy. Erhaiini Davis et al. 1985: 69.

Discussion. The genera included in this tribe are *Akiyoshia* and *Pseudobythinella* from China. Liu & Zhang, 1979, described certain species from China and classified them as *Bythinella* and *Pseudobythinella.* They provided no anatomical data aside from penis and radular illustrations. *Pseudobythinella* Liu & Zhang, 1979, was described as different from so-called *Bythinella* of China by (1) having a tooth or node on the inner lip, and (2) the central tooth having two pairs of basal cusps, those on each side on the same level (not *Hydrobia*-like).

The so-called *Bythinella* of China lack the complex male reproductive system characters that serve to define the Hydrobiidae: Amnicolinae of Europe and North America including genuine *Bythinella* (Europe) and *Amnicola* (North America). Because *Bythinella* does not occur in China, Davis & Kuo,[1] (in Davis et al., 1985) described the genus *Erhaia* to accommodate new species that Liu and Zhang would have considered to be *Bythinella.* Davis & Kuo (1985) raised the tribe Erhaiini to accommodate *Erhaia.*

As a result of this study, *Erhaia* is placed in the synonymy of *Pseudobythinella.* It is clear that at least one species described as *Bythinella* from China (*B. chinensis* Liu & Zhang, 1979) has a tooth on the columella; it is observed when the aperture is tilted. Upon breaking open the shell it is seen that this "tooth" is the terminus of a thick, glassy, spiral columellar shelf or ledge. In summary, there appears to be no basis for placing those taxa with an overall similar anatomical ground plan in separate genera on the basis of presence or absence of a tooth on the columella, or where the tooth is prominently seen in the aperture contrasted with the presence of a columellar thickening seen only upon breaking the shell. The type species of *Erhaia*, *E. daliensis* Davis & Kuo (in Davis et al., 1985) has no columellar "tooth" in evidence in the aperture even when the aperture is rotated to examine as deeply as possible into the shell. However, upon breaking open the body whorl, a pronounced thickened columellar ridge is seen. This glassy ridge is also found in *Erhaia kunmingensis* Davis & Kuo 1985, but it is not very pronounced and forms no node.

The same situation involves the basal cusps of the central tooth. The two basal cusps on a side being on the same level or one above the other is irrelevant to generic definition. Most species of *Pseudobythinella* (including the Chinese taxa described as *Bythinella*) have only one pair of basal cusps on the lateral angles.

The Pseudobythinellini are not classified as Hydrobiidae but are in the Pomatiopsidae for the following reasons: (1) There is evidence that the position of the basal cusps of the cen-

[1]Due to a change in China affecting the manner of spelling Chinese words in English, Dr. Y. H. Kuo in the literature until 1985 changed the spelling of his name to Y. H. Guo (see Davis et al., 1985, 1986).

tral tooth derived from the pomatiopsine condition, i.e. from the face of the tooth. In *Pseudobythinella kunmingensis* from Yunnan, China most central teeth of most snails had a single pair of basal cusps. However, some central teeth had two pairs (Davis et al., 1985: fig. 16F), the innermost arising from the face of the tooth and lower than the outermost pair arising from the laternal angle. This has not, to our knowledge, been seen in any taxon of Hydrobiidae that has a spermathecal duct. (2) The position of the connections of the spermathecal duct, duct of the bursa, and oviduct are unlike any seen in the Hydrobiidae. These Chinese species lack the complex penial lobes, three to four differentiated regions of the pallial oviduct, and tendency to brooding seen in the Hydrobiidae: Littoridininae. (3) There is the biogeographic overlap of these snails with at least one genus of the Pomatiopsini, more if *Akiyoshia*, originally described from Japan, is also a member of the *Pseudobythinella* clade.

Akiyoshia Kuroda & Habe 1954

Type Species. *Akiyoshia uenoi* Kuroda & Habe, 1954: 71–73, figs. 1–4

Type locality. Akiyoshi limestone cave, Yamaguchi Prefecture, Japan

Designation. By monotypy

Saganoa Kuroda, Habe & Tamu, 1957

Type species. *Akiyoshia* (*Saganoa*) *kishiiana* Kuroda, Habe & Tamu in Kuroda & Habe, 1957: 186–187, figs. 5–8.

Type locality. Saga (= Arashiyama), western foothills of Kyoto City, Japan

Designation. By original designation

Discussion. Species from China were described as *Akiyoshia* (*Saganoa*) by Liu et al. (1982). They were thus described because the shells of those species are minute, turreted, with roundish apertures, i.e. generally corresponded to the conchological descriptions given by Kuroda & Habe (1957). We doubt that the Chinese species are *Akiyoshia*, *s.s.*, or *Akiyoshia* (*Saganoa*) due to the distance and differences in geological events creating environments now inhabited by the Chinese and Japanese snails. We are reminded that species once described as *Tricula* from India, China, and the Ryukyu Archipelago are now classified in four genera on the basis of detailed anatomical data. We note that *Saganoa* species are blind cave- or well-dwelling snails; those collected from China are stream-dwelling and not blind. However, we will not describe a new genus until the relevant Japanese snails are studied and the data dictate such a course.

Akiyoshia (*Saganoa*) *chinensis* Liu et al., 1982

Holotype. IZAS, HN 798002; Liu, Zhang & Chen, 1982: 367, figs. 2–5 (in Liu et at. 1982).

Type Locality. Guzhang, Hunan Province, Sept. 1979

Assigned Species. China only: *Akiyoshia* (*Saganoa*) *chinensis* Liu, Zhang & Chen, 1982; *A.* (*S.*) *yunnanensis* Liu, Wang & Zhang, 1982. N = 2 (in Liu et at. 1982).

Habitat

Refer to *Tricula gredleri*, D87-3. This species was sympatric with *T. gredleri* and *T. maxidens*. Snails were collected from a village close to the type locality, approximately 5 km; the type locality is across the valley and on the opposite hillside from D87-3.

Depository

Specimens are catalogued into the collections of ZAMIP, M0010; ANSP 373142, A12658.

Description

Shell. Shells are minute, smooth, turreted with deep sutures and slightly convex whorls (Figs. 6A–E, 7A–E, 8). Shells of mature animals have 4.5–5.5 whorls; the majority are 5.0–5.5 whorls. Shell lengths of mature snails of 5.0 or more whorls range from 1.60–1.86 mm (Table 3). There is a slight umbilical chink. The aperture is sub-circular; there is a trace of a varix on some shells. In side view the outer lip is slightly sinuate (Fig. 7B). With the outer lip down (90° to the horizontal), the outer lip is either straight or angled. There are no apertural teeth or adapical notches.

Under SEM the following are observed: (1) Spiral microsculpture can be seen at the base of the shell (Fig. 7C), and on some whorls (Fig. 7D). (2) The protoconch is smooth (Fig. 7D, E). (3) Breaking open the body whorl reveals no internal columellar teeth or spiral ledges (Fig. 8A–E). The columella of the pen-

TABLE 3. Shell measurements (mm) of topotypical *Akioyshia chinensis*. Mean ± standard deviation (range). N = number measured.

	Large class		Small class		
	N = 3	N = 5	N = 1	N = 5	N = 1
No. Whorls	5.0–5.25	5.5	4.5	5.0	5.5
Length (L)	1.77±0.02 (1.76–1.80)	1.84±0.01 (1.82–1.86)	1.64	1.66±0.04 (1.60–1.68)	1.68
Width (W)	0.73±0.01 (0.72–0.74)	0.70±0.02 (0.68–0.74)	0.70	0.66±0.02 (0.64–0.68)	0.66
L last three whorls	1.53±0.02 (1.52–1.56)	1.51±0.03 (1.48–1.56)	1.44	1.44±0.02 (1.40–1.46)	1.40
L body whorl	0.91±0.03 (0.88–0.94)	0.88±0.03 (0.84–0.92)	0.86	0.85±0.02 (0.84–0.88)	0.80
L penultimate whorl	0.36 No. Var.	0.37±0.01 (0.36–0.38)	0.34	0.34±0.02 (0.32–0.36)	0.32
W penultimate whorl	0.59±0.01 (0.58–0.60)	0.58±0.01 (0.58–0.60)	0.58	0.56±0.01 (0.54–0.56)	0.54
W 3rd whorl	0.48±0.02 (0.46–0.50)	0.49±0.04 (0.44–0.54)	0.48	0.46 No Var.	0.46
L aperture	0.61±0.02 (0.60–0.64)	0.59±0.02 (0.56–0.60)	0.60	0.55±0.02 (0.52–0.58)	0.54
W aperture	0.49±0.01 (0.48–0.50)	0.46±0.04 (0.40–0.48)	0.46	0.31±0.01 (0.44–0.48)	0.44
x	0.20 No Var.	0.15±0.04 (0.10–0.22)	0.16	0.17±0.08 (0.16–0.24)	0.18
y	0.09±0.03 (0.06–0.12)	0.10±0.04 (0.04–0.14)	0.12	0.07±0.04 (0.06–0.08)	0.12

ultimate whorl has minute calcareous nodes (Fig. 8F). The inner edge of the inner lip has raised calcareous pitted nodes (Figs. 8G, H); the inner surface of the aperture is regularly pitted (Fig. 8G, I).

External features. The head is white; there are no white granules about the eye. There is no *Oncomelania*–type "eyebrow." The operculum is corneous and paucispiral (Fig. 7F.). The inner-lip edge is straight, i.e. the operculum shape is sub rectangular, not ovate. The inner muscle attachment callus is comparatively small and weakly developed, about 27% the diameter of the operculum.

Mantle cavity. Measurements and counts of mantle cavity organs are given in Table 4; see Figure 9. The gill is central in the mantle cavity and symmetrical about the osphradium. The osphradium is short in females, long in males relative to the length of gill. Being long in this case is an artifact of the much reduced gill. If the gill was the usual length, i.e. filling most the length of the mantle cavity, the osphradium would (and should) be classified as short.

There are only 11–14 gill filaments. Gf_2 is long in females, medium (or normal) in males. The total lengths of the longest gill filaments are 0.22 ± 0.03 mm. There is no patch of white granules anterior to the osphradium near to or partially on the mantle collar.

Female reproductive system. The body of an uncoiled female without head or kidney tissue is shown in Figure 10A. Measurements of relevant organs are given in Table 4. Important features are: (1) The gonad (Go) is a simple sac located posterior to the stomach. (2) The bursa copulatrix (Bu) is clearly seen posterior to the pallial oviduct (Ppo). It is small. (3) There are three histologically different sections to the pallial oviduct; the albumen gland (Ppo), capsule gland (Apo-1), and a dense white anterior region (Apo-2). These areas are clearly discernable in gross dissection of living animals. (4) The bursa complex of organs is shown in Figure 11 in the same relative position as in Figure 10. The usual pomatiopsid seminal receptacle is lost; the function of the seminal receptacle is relocated within a U-shaped bend or twist of the oviduct (Osr, Figs. 10, 11). (5) There is a pronounced, elongated sperm duct (Sdu) connecting the oviduct (Ov) to the spermathecal duct. The oviduct enters the albumen gland (Ppo) just posterior to the posterior end of the mantle cavity (Emc). (6) The spermathecal duct (Sd)

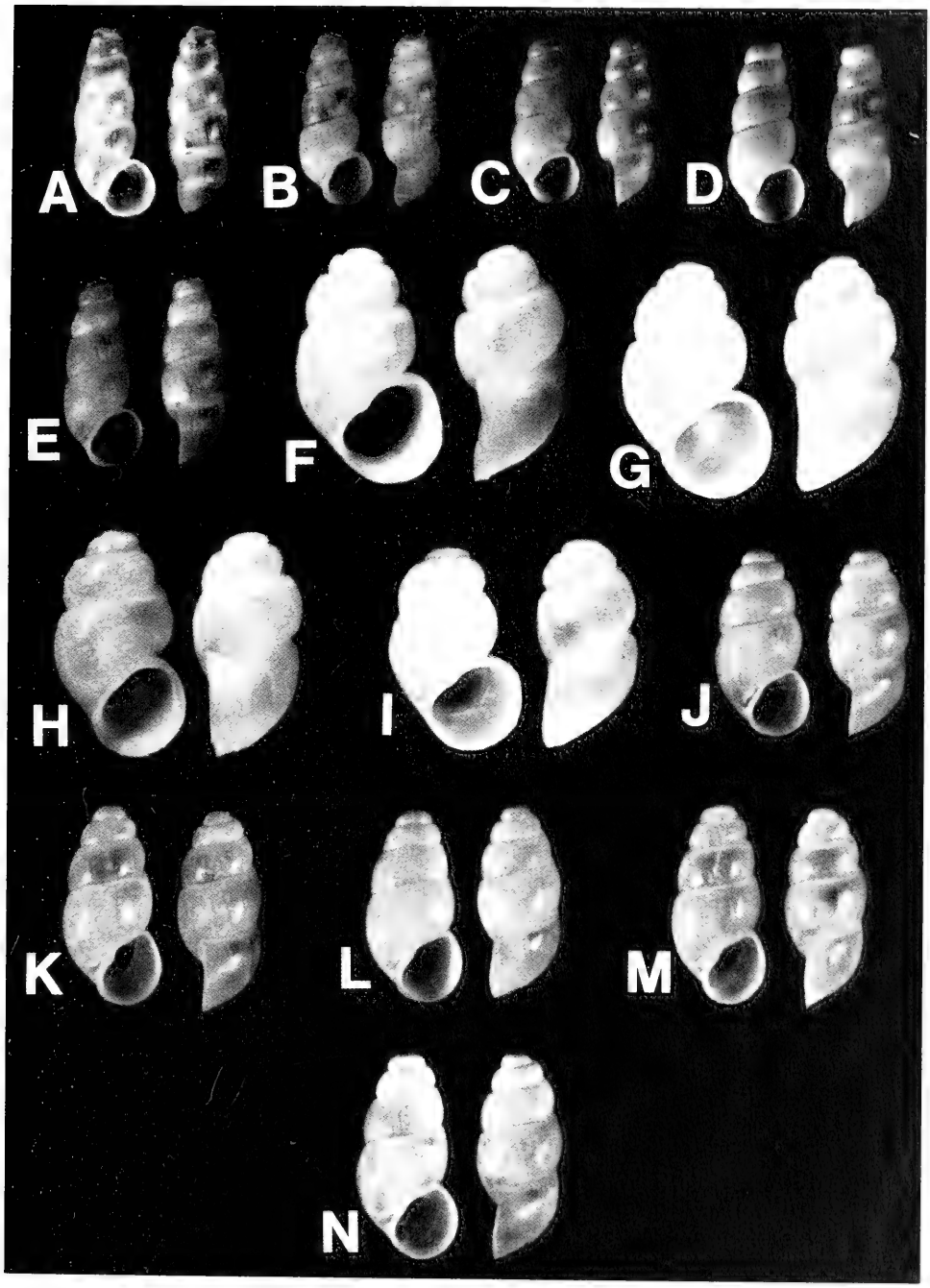

FIG. 6. Shells of *Akiyoshia chinensis* (A–E); *Pseudobythinella shimenensis* (F–I), and *P. chinensis* (J–N). The length of shell A is 1.77 mm; others are printed to same scale.

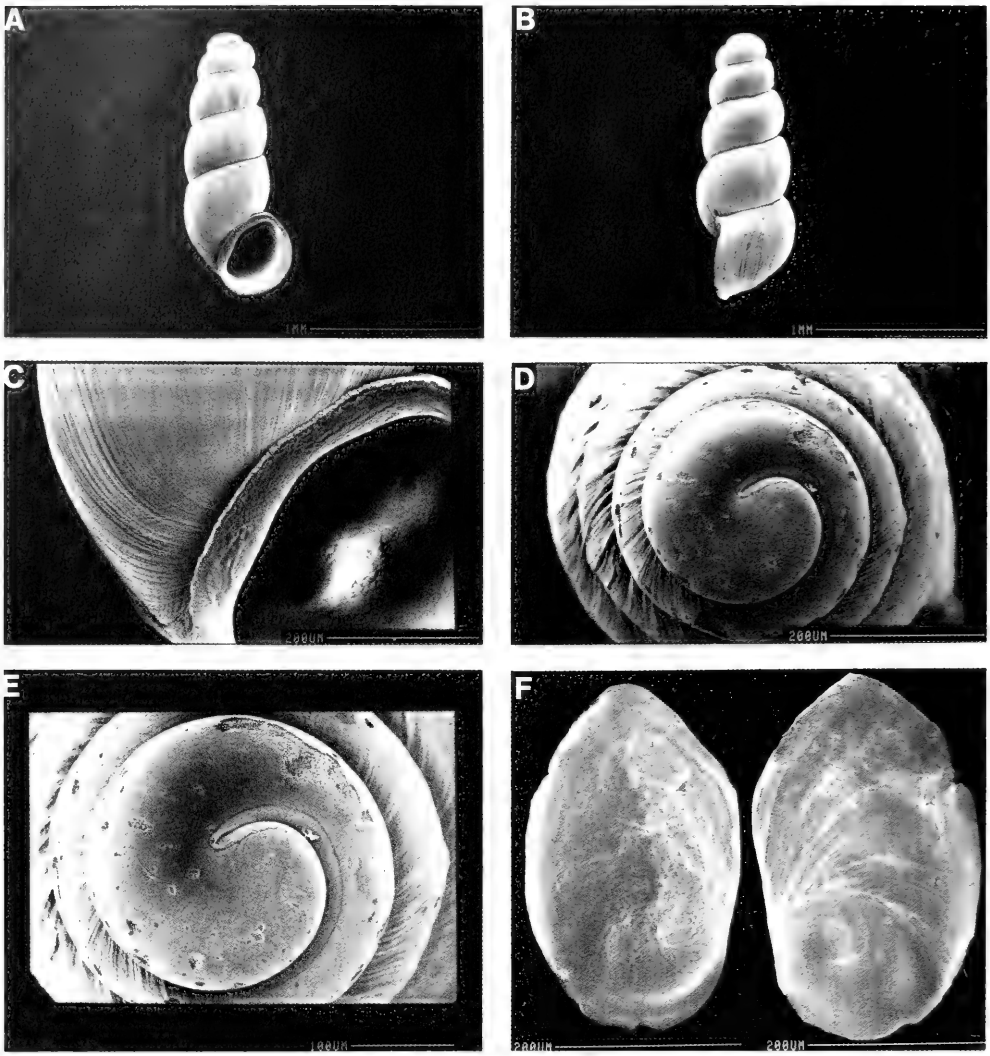

FIG. 7. SEM pictures of shell (A–E) and operculum (F) of *Akiyoshia chinensis*. C. Enlargement of base of shell showing rough growth lines crossed by fine spiral microsculpture. D, E. The apical whorls are smooth; teleoconch roughened sculpture starts at 1.5 whorls. Spiral microsculpture is seen at 1.5 to 1.75 whorls. F. Inner surface of operculum to left showing modestly developed attachment pad for muscles. Outer surface is to right showing paucispiral coil.

runs to the anterior end of the mantle cavity to open independently of the pallial oviduct.

Male reproductive system. An uncoiled male is shown in Figure 12 without head and with kidney tissue removed. Measurements of relevant organs are given in Table 4. Important features are: (1) The anterior lobes of the gonad (Go) are ventral to the posterior chamber of the stomach. (2) There are numerous lobes of the gonad that drain into a vas efferens (Ve). (3) The vas deferens leaves the vas efferens at mid-gonad to slightly posterior to

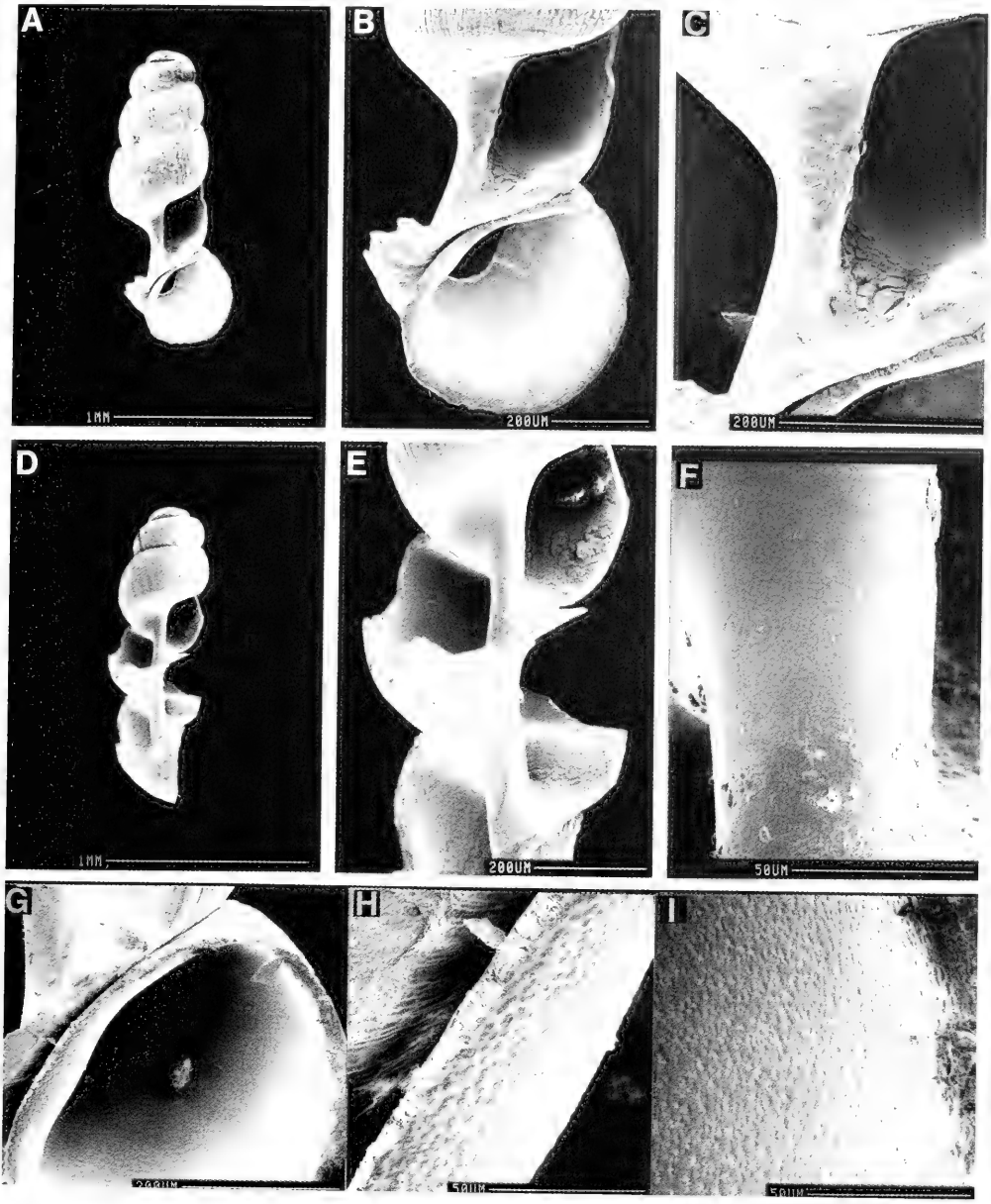

FIG. 8. SEM analysis of columella inside body whorl of *Akiyoshia chinensis* and sculptural attributes of columella and inner lip. See text for details.

mid-gonad to begin coiling as the seminal vesicle (Sv) dorsal to the gonad. (4) The prostate (Pr) overlies the posterior end of the mantle cavity. (5) The prostate consists of discernable lobes. (6) The anterior vas deferens (Vd_2) leaves the prostate close to mid-prostate. (7) The penis (Fig. 13 C) is simple with a long penial filament (Pf) and small papilla (Pa). A penial filament is defined as a terminal length of penis that is distinctly narrowed compared with the rest of the penis. This narrowing is not simply due to the gradual taper-

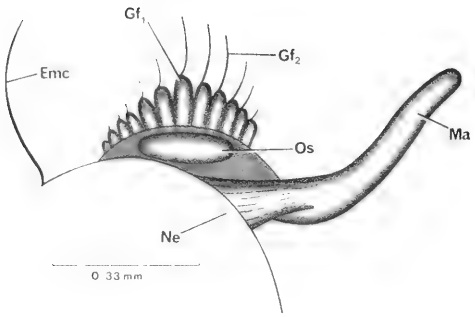

FIG. 9. Mantle cavity structures of *Akiyoshia chinensis*

ing of the penis. No ejaculatory duct was seen. An ejaculatory duct is a distinctly swollen muscle wrapped section of the vas deferens found in the base of the penis or neck. (8) The base of the penis (Bp) is to the right at the snout-neck mid-line (x, Fig. 13A, B) and oriented 65°–90° to the mid-line.

Digestive System. The digestive gland (Di) covers the posterior chamber of the stomach (Fig. 12). The stomach is shown in Figure 14 in the same relative position as in Figure 12. There is no caecal appendix; the style sac (including the intestinal loop) is 48% the length of the stomach.

Radular statistics are given in Tables 5 and 6. Refer to Figures 15, 16. The cusp formula most frequently encountered is

$$\frac{4(5)\text{-}1\text{-}(5)4;}{1(2)\text{-}1(2)}\ \ 4\text{-}1\text{-}4;\ 19\text{-}24;\ 16\text{-}21.$$

There are numerous cusps on the marginals but there are significantly more on the inner

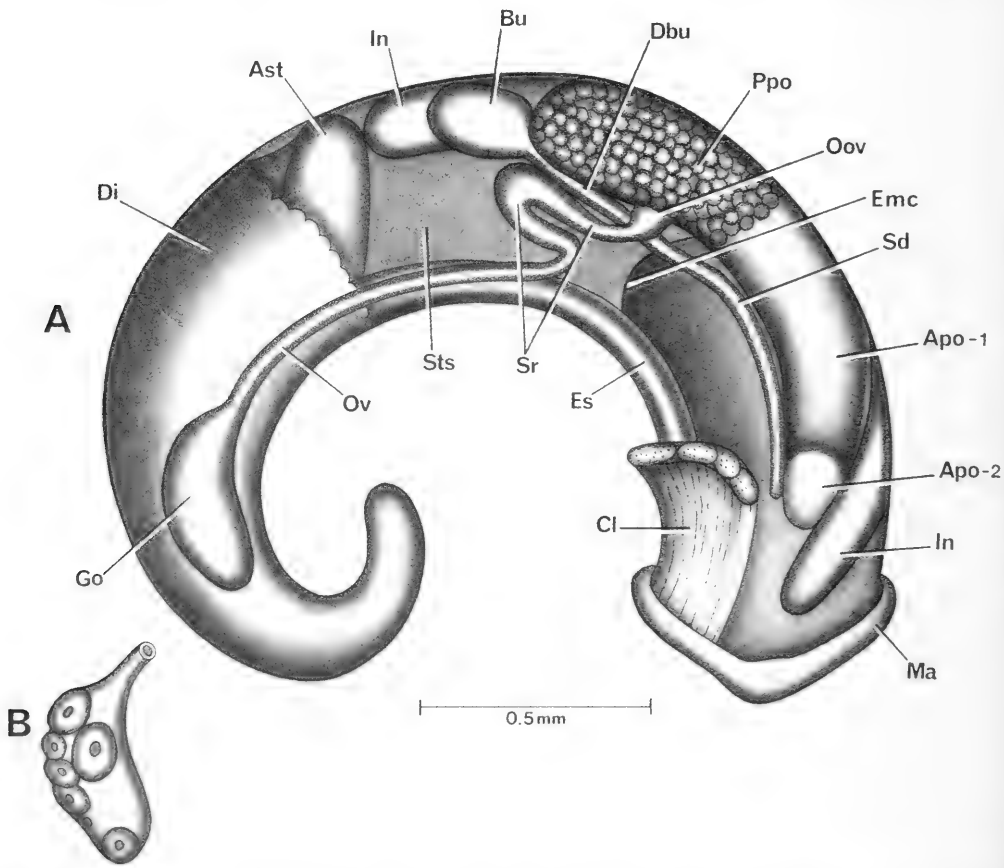

FIG. 10. Uncoiled female of *Akiyoshia chinensis* with head and kidney tissue removed (A) and gonad showing oocytes (B).

TABLE 4. Lengths (mm) or counts of non-neural organs and structures of *Akiyoshia chinensis*. N = number of snails used. Mean ± standard deviation (range).

	Females (N = 4)	Males (N = 2)
Body	3.27±0.20 (N = 3) (3.04–3.40)	3.06 (3.02, 3.10)
Gonad	0.40±0.11 (N = 3) (0.28–0.50)	1.36 (1.30, 1.42)
Digestive gland	1.59±0.19 (N = 3) (1.40–1.78)	0.80 (N = 1)
Posterior pallial oviduct (= albumen gland)	0.57±0.06 (N = 3) (0.50–0.60)	—
Anterior pallial oviduct (= capsule gland)	0.52±0.07 (N = 3) (0.46–0.60)	—
Total pallial oviduct = OV	1.09±0.10 (0.96–1.20)	—
Bursa copulatrix BU	0.24±0.03 (0.20–0.28)	—
Duct of BU	0.43±0.08 (0.32–0.50)	—
BU ÷ OV	0.22±0.02 (0.20–0.25)	—
Seminal receptacle	— —	—
Duct of seminal receptacle	— —	—
Mantle cavity	0.73±0.05 (0.70–0.80)	0.70 (0.60, 0.80)
Gill (G)	0.52±0.04 (0.50–0.58)	0.44 (0.40, 0.48)
Osphradium (OS)	0.17±0.04 (0.12–0.20)	0.21 0.20, 0.22
OS ÷ G	0.32±0.07 (0.25–0.39)	0.48 (0.42, 0.55)
No. of filaments	12±1.4 (11–14)	11.5 (11, 12)
Gf_2	0.11±0.03 (N = 5) M+F (0.08–0.12)	0.12 (0.10, 0.14)
Gf_1	0.10±0.02 (N = 5) M+F (0.08–0.14)	0.11 (0.10, 0.12)
Total Gf = TGF	0.22±0.03 (0.18–0.26)	0.23 (0.20, 0.26)
Gf_2 ÷ TGF	0.54±0.08 (0.46–0.67)	0.48 (0.46, 0.50)
Prostate	—	0.73 (0.70, 0.76)
Seminal vesicle	—	—
Penis	—	0.76 (N = 1)

marginals ($\bar{X}$ of 21.3 vs. 18.1 for the outer marginals). The central tooth is featured in Figure 15C, E, H. The central raised "tongue" running anterior—posterior on the face of the tooth is flanked by deep eye-socket-like depressions (contrast lack of such deep holes on each side of the "tongue" in *Pseudobythinella kunmingensis* and *P. daliensis* (Davis et al., 1985: figs. 9, 16). Whether one or two basal cusps, they arise from the lateral angle of the central tooth. The bases of the lateral angles are flared as in the above mentioned species of *Pseudobythinella*.

The shape of the lateral teeth is emphasized in Figure 15G, H. Marginals are featured in Figure 16. The outermost cusp of the outer marginal is extremely elongated, a unique feature (Fig. 16F–H).

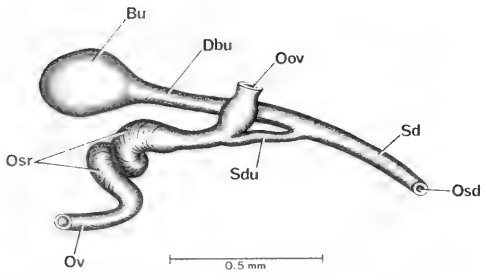

FIG. 11. Bursa copulatrix complex of organs of *Akiyoshia chinensis* positioned as in Figure 10.

Nervous system. No data.

Remarks

This species differs from those classified as *Pseudobythinella* by possessing a slender high-turreted shell without a trace of a tooth or node on the columella as examined in the aperture or within the body whorl. The standard seminal receptacle is lost; its function is moved into the oviduct. The bursa is a comparitively small sphere clearly visible posterior to the pallial oviduct in contrast to the elongated tubular bursa mostly, if not entirely, buried dorsal to the albumen gland in *Pseudobythinella*. The central tooth of the radula has deep-set socket-like depressions on either side of the "tongue" on the face of the tooth; these deep holes are lacking in *Pseudobythinella*.

Pseudobythinella Liu & Zhang, 1979

Synonymy. Erhaia Davis & Kuo, 1985.

Type species. Pseudobythinella jianouensis Liu & Zhang, 1979: 135-136, figs. 1–3.

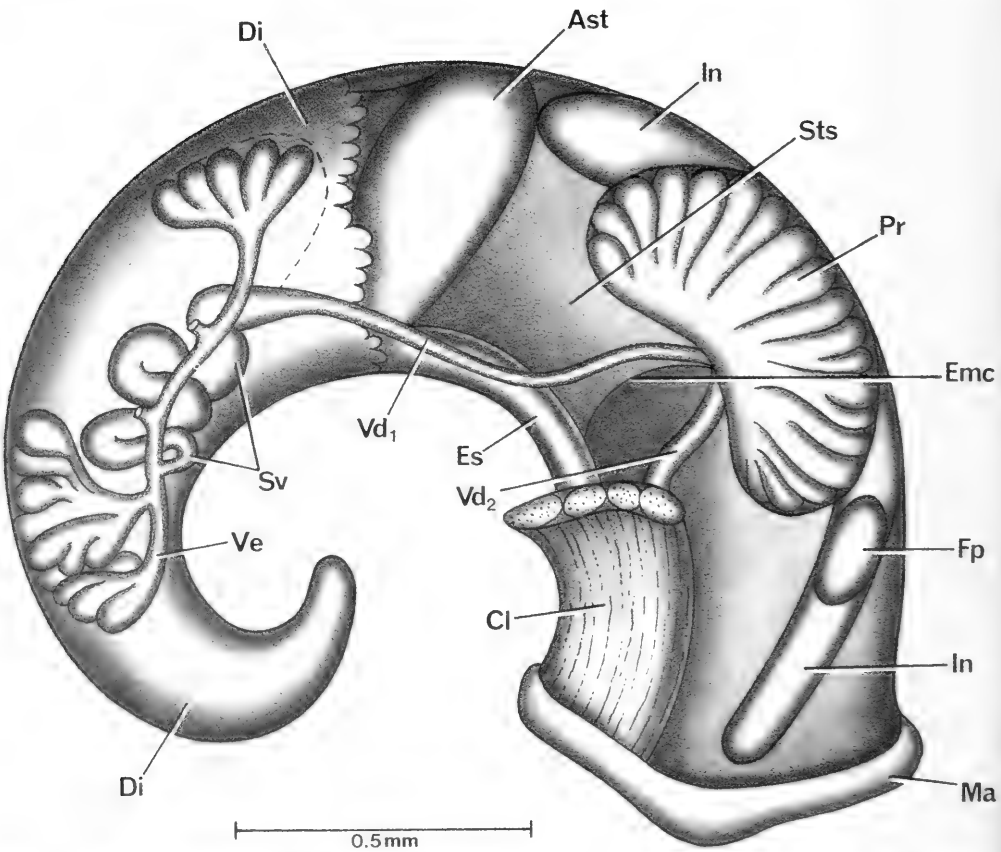

FIG. 12. Uncoiled male of *Akiyoshia chinensis* without head and kidney tissue removed. Some lobes of gonad are removed to reveal seminal vesicle (Sv). Dashed line shows contour of gonad.

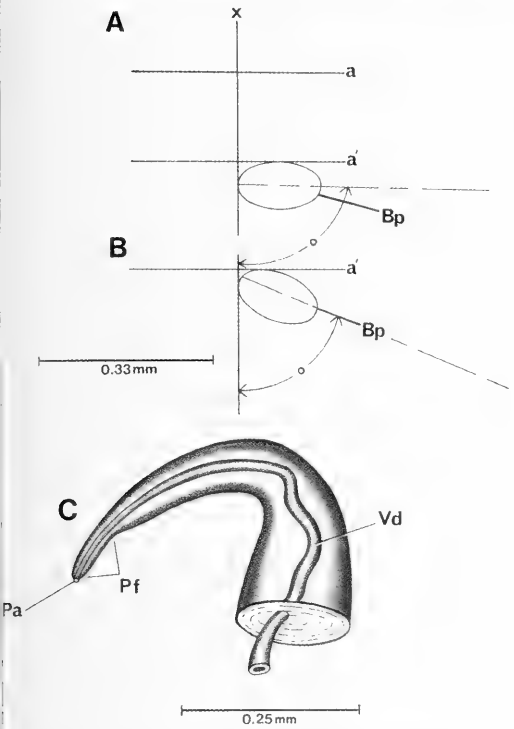

FIG. 13. Position of base of penis of *Akiyoshia chinensis* on neck (A, B) relative to snout-neck midline (x); penis (C).

Type locality. Jian'ou, Fujian Province, People's Republic of China.

Designation. By monotypy with designated type species.

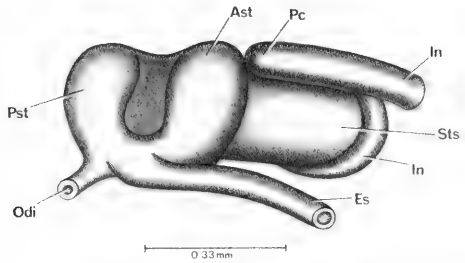

FIG. 14. Stomach of *Akiyoshia chinensis* positioned as in Figures 10 and 12.

Types. IZAS, FJ767701, holotype, plus paratypes.

Assigned Species. China only: *P. jianouensis* Liu & Zhang, 1979; *Bythinella chinensis* Liu & Zhang, 1979; *B. hubeiensis* Liu, Zhang & Wang, 1983b; *B. gongjianguoi* Kang, 1983b; *B. wufengensis* Kang, 1983a; *B. watanensis* Kang, 1983a; *P. liui* Kang, 1983b; *P. shimenensis* Liu, Zhang & Chen, 1982; *B. lii* Kang, 1985; *Erhaia daliensis* Davis & Kuo, 1985; *E. kunmingensis* Davis & Kuo, 1985. N = 11.

Diagnosis. Bythinella—like shell, minute, with smooth, flattened apical whorls. Apical whorls may have faint spiral microsculpture. Columella with spiral glassy thickening that may form a considerable keel or spiral ledge; the ledge may terminate in the aperture appearing as a "tooth" on the inner lip. Anatomical criteria are based on four species for which

TABLE 5. Radular statistics for *Akiyoshia chinensis*. Mean ± standard deviation (range). N = number used. In mm except for width of central tooth in μm.

	Females (N = 7)	Males (N = 4)
Shell length	1.71±0.09 (1.60–1.78)	—
Radular length	0.39±0.02 (0.36–0.42)	0.39±0.02 (0.37–0.40)
Radular width	0.04±0.003 (0.038–0.048)	0.04±0.005 (0.036–0.046)
Total rows of teeth	90.4±4.3 (84–96)	84.5±5.1 (81–92)
No. rows of teeth forming	33±1.6 (31–35)	31.3±1.3 (30–33)
Central tooth width	10.5±0.5 (N = 21) (9.5–10.7)	9.8±0.5 (N = 19) (8.9–10.2)

FIG. 15. Radula of *Akiyoshia chinensis*. A–E, males; F–H, females. C, E, H. features central teeth; G, H. Lateral teeth. D. features inner marginals.

FIG. 16. Radula of *Akiyoshia chinensis*. A, B, F = males; C–E, G, H = females. A. features inner marginals. B, D. Basal morphology of attachment zone of marginals. F–H. Outer marginals. See text for details.

TABLE 6. Cusp formulae for the radular teeth of *Akiyoshia chinensis* with the percent of radulae in which a given formula was found at least once.

Central Teeth		Lateral Teeth		Inner Marginal teeth		Outer Marginal teeth
4-1-4 / 1-1	57%	4-1-4	100%	14	—	14%
				15	—	14%
5-1-5 / 1-1	57%			16	—	29%
5-1-4 / 1-1	29%			17	—	71%
				18	14%	43%
5-1-5 / 2-2	29%			19	43%	71%
4-1-4 / 2-2	14%			20	71%	43%
				21	86%	29%
5-1-5 / 1-2	14%			22	71%	—
				23	86%	—
						—
				24	57%	—
				25	29%	
				$\bar{X}$ * = 21.3±1.8		18.1±1.7
				N = 70		N = 70

*Mean ± standard deviation of cusp number for all teeth counted.

TABLE 7. Shell measurements (mm) of *Pseudobythinella chinensis*. Mean ± standard deviation (range). Number measured = 5. All shells of mature animals had 4.5 whorls.

Length (L)	1.77±0.06 (1.68–1.84)
Width (W)	0.85±0.03 (0.83–0.90)
L last three whorls	1.64±0.06 (1.56–1.68)
L body whorl	1.07±0.06 (1.00–1.16)
L penultimate whorl	0.36±0.01 (0.34–0.36)
W penultimate whorl	0.69±0.07 (0.56–0.74)
L 3rd whorl	0.53±0.01 (0.52–0.54)
L aperture	0.70±0.03 (0.66–0.72)
W aperture	0.54±0.04 (0.52–0.60)
x	0.16±0.03 (0.12–0.20)
y	0.04±0.01 (0.02–0.06)

we have data; the two species of this study and *P. daliensis* and *P. kunmingensis* described in Davis et al. (1985). The female gonad is a simple tube or tube with low lobes. The oviduct has a wide 360° loop dorsal to the bursa copulatrix. There is the standard generalized seminal receptacle. Hydrobiid—type central tooth. The lateral tooth lacks a pronounced intermediate cusp. A lateral tooth has a pronounced curved process projecting posterior from the face of the tooth. The process is slight, or if large it is straight in *Akiyoshia chinensis*. Stomach without caecal appendix. There is a tendency for hypertrophy of the radular sac.

Pseudobythinella chinensis (Liu and Zhang)

Holotype. IZAS, HN766602, Liu & Zhang, 1979: fig. 4.

Type locality. Lengshuijiang, Xinhua, Hunan Province; July 1976. (approximately 27°4′N, 111°25′E)

Synonymy. *Bythinella chinensis* Liu & Zhang, 1979: 134, 136.
Erhaia chinensis, Davis et al., 1985
Pseudobythinella chinensis, this paper

Habitat

Snails were collected from Shen Keng Village, Sanhe Town, Lingxian County, Zhu Zhou Prefecture; 26°17′18″ N, 113°31′50″ E; Figure 1, site 6. The field collection number

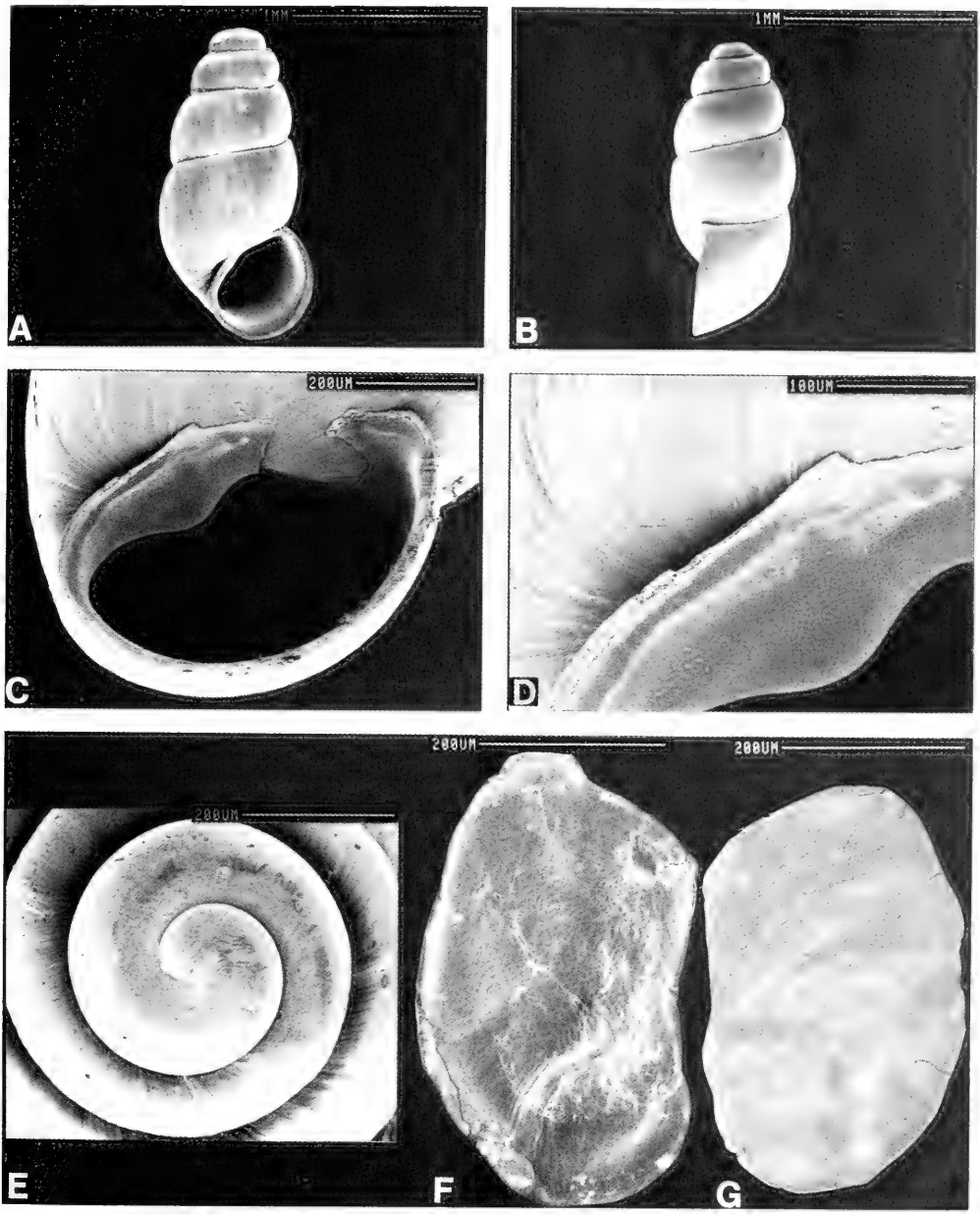

FIG. 17. SEM picture of shells (A–E) and opercula (F, G) of *Pseudobythinella chinensis*. Note that in A, no "tooth" is seen on columella. Tilting shell to look inside body whorl reveals a swelling or "tooth" on columella. C, D reveal no spiral microsculpture. See text for details. The apical whorls are smooth (E). Inner surface of operculum (F); outer surface (G).

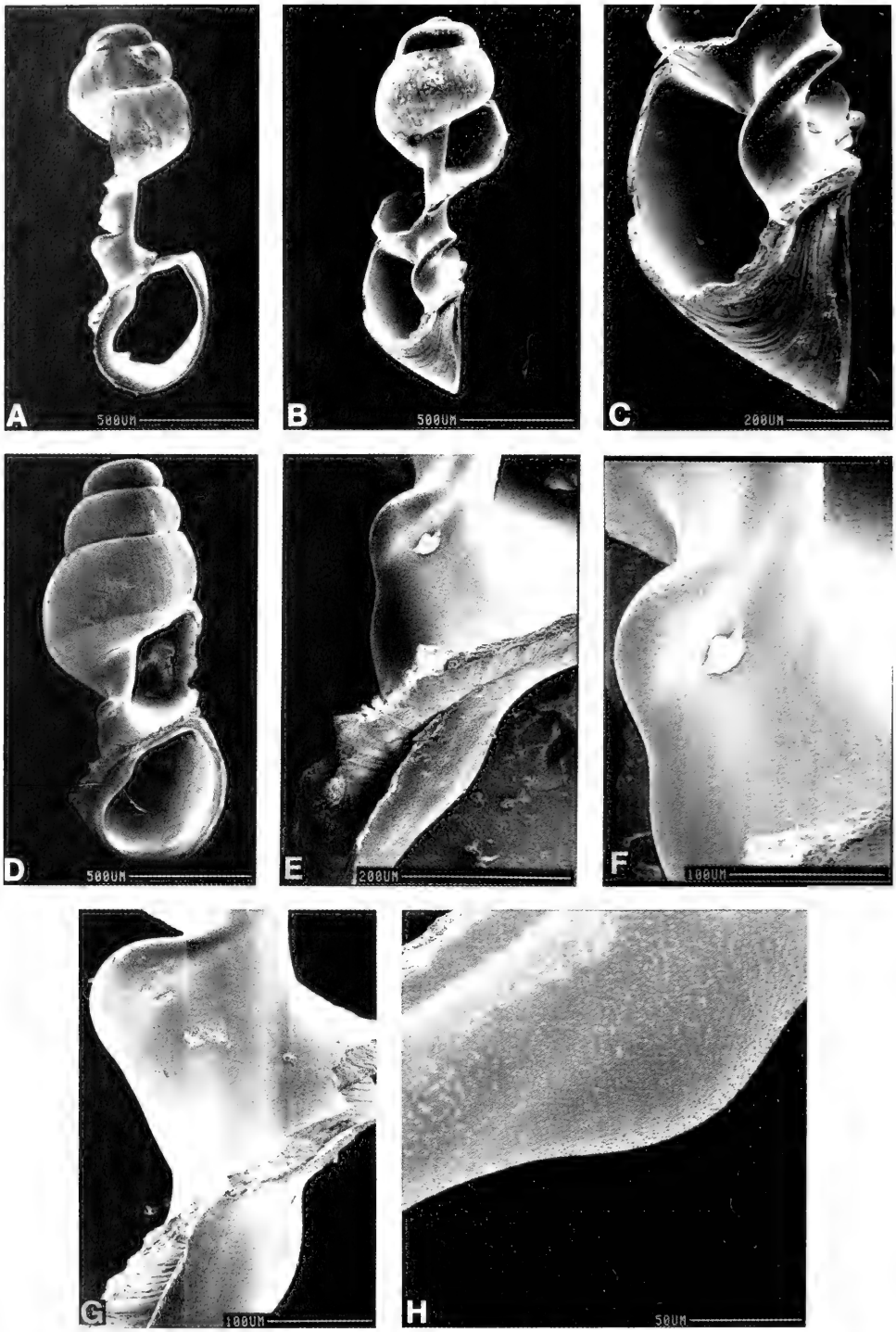

FIG. 18. SEM of shells of *Pseudobythinella chinensis* broken to show raised spiral ridge and "tooth" on columella inside body whorl. See text for discussion of sculpture on columella and inner lip.

TABLE 8. Lengths (mm) or counts of non-neural organs and structures of *Pseudobythinella chinensis*. N = number of snails used. Mean ± standard deviation (range).

	Females (N = 2)	Males (N = 1)
Body	3.68	3.28
	(3.42,3.94)	—
Gonad	0.32	0.90
	(0.30,0.34)	—
Digestive gland	1.72	1.80
	(1.70,1.74)	—
Posterior pallial oviduct (= albumen gland)	—	—
Anterior pallial oviduct (= capsule gland)	—	—
Total pallial oviduct = OV	1.20 (No. Var.)	—
Bursa copulatrix BU	0.38 (0.36,0.40)	—
Duct of BU	—	—
BU ÷ OV	0.32	—
	(0.30,0.33)	
Seminal receptacle	0.04(N=1)	—
Duct of seminal receptacle	0.12(N=1)	—
	—	
Mantle cavity	—	0.52
		—
Gill (G)	—	0.24
Osphradium (OS)	—	—
OS ÷ G	—	—
No. of filaments	—	12
Gf_2	—	0.10
Gf_1	—	0.10
Total Gf = TGF	—	0.20
Gf_2 ÷ TGF	—	0.50
Prostate	—	0.64
Seminal vesicle	—	0.40
Penis	—	0.52

assigned was D85-81. Snails came from a small stream that flowed between the peaks of big mountains; the elevation was 500 m. The stream was heavily shaded by vegetation lining the banks. The stream was 20–30 cm wide, 10–20 cm deep with a bottom paved with small rocks, leaves and mud.

Depository

Specimens are housed at ZAMIP, M0011; ANSP, 373139, A12655.

Description

Shells. Shells are minute, smooth, and conic-turreted (Figs. 6J–N; 17A–E; 18A–H). They are 4.5 whorls ranging in length from 1.68 to 1.84 mm (Table 7); they are umbilicate with a sub-ovate to sub-circular aperture. The sutures are moderately deep; whorls with slightly convex whorls. No tooth is visible in the aperture in 60% of the shells while a thickening on the columella is seen in the aperture of 40% of the shells. Tipping the aperture up, one can see a considerable tooth-like swelling on the columella, the terminus of the pronounced internal columellar keel. In side view the outer lip is straight to slightly sinuate; in the contrasting view the inner lip is straight (outer lip down, 90° to the horizontal).

SEM analyses show the apical whorls to be smooth (Fig. 17E). With the aperture tilted,

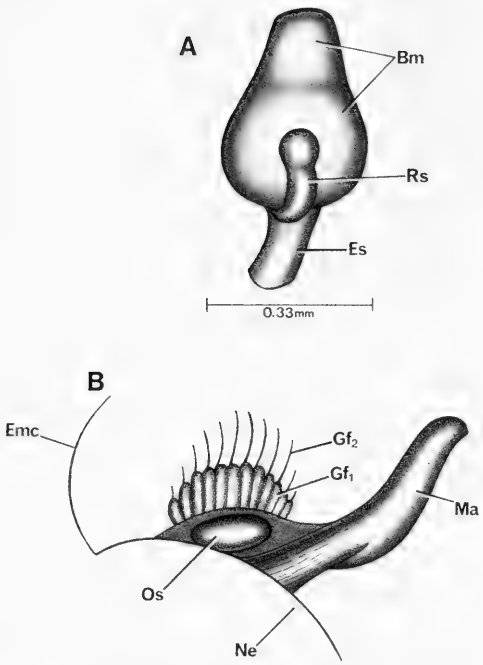

FIG. 19. The buccal mass of *Pseudobythinella chinensis* with pronounced radular sac (A) and reflected mantle showing mantle cavity organs (B).

the columeller "tooth" is seen (Fig. 17C, D); note the numerous calcareous pitted pustules on the columella and "tooth". With the shell broken open, it is seen that the "tooth" seen in the aperture is the terminus of a pronounced columellar keel starting at mid-body whorl and spiralling down to the aperture (Fig. 18A–E). An enlargement of the area of highest concentration of pitted calcareous pustules on the "tooth" (Fig. 18G) is given in Fig. 18H. The entire surface of the keel is roughened with calcareous pustules or micro-ridges.

External features. The head-neck is white; there are no white granules about the eyes. The operculum is corneous and paucispiral (Fig. 17F, G). The shape is sub-rectangular. The columeller edge is somewhat concave, especially where the operculum passes over the columeller "tooth" (Fig. 17C). The callus on the inner surface is weakly developed, but wide, 69% the width of the operculum (Fig. 17F).

Mantle cavity. The opened and reflected mantle cavity is shown in Figure 19B. Measurements and counts of relevant organs are given in Table 8. The gill is centrally located in the mantle cavity and the osphradium (Os) is centered against the gill. The osphradium by definition is long but this is an artifact of the much reduced size of the gill. The usual pomatiopsid gill nearly fills the length of the mantle cavity. On this criterion the osphradium is here considered short (circa 0.32 ratio). The Gf_2 is medium (= normal) length. The length of the longest gill filament is approximately 0.20 mm.

Female reproductive system. The body of an uncoiled female snail is shown in Figure 20 without head and with kidney tissue removed. Measurements of relevant organs are given in Table 8. Important features are: (1) The gonad (Go) is posterior to the stomach (Pst). (2) The gonad consists of a simple sac with four to five small undivided lobes protruding from the posterior end. (3) The bursa (Bu) is either completely covered by the albumen gland (Ppo) or only protrudes slightly posterior to the albumen gland (as in Fig. 20). (4) The oviduct (Ov) makes a pronounced bend pressing against the posterior edge of the bursa (Bu). (5) The spermathecal duct (Sd) runs to the anterior end of the mantle cavity to open independently of the pallial oviduct. (6) The sperm duct (Sdu) is unique in that it branches off the spermathecal duct near the anterior end of the spermathecal duct, far forward of the posterior end of the mantle cavity (Fig. 21). (7) The seminal receptacle (Sr) is unique in that it branches from the sperm duct (Sdu), not the oviduct, and in that it is entirely anterior to the posterior end of the mantle cavity (Fig. 21).

Male reproductive system. An uncoiled male is shown in Figure 22 without head or kidney tissue. Part of the gonad (Go) has been cut away to reveal the seminal vesicle (Sv) coiled dorsal to it. Measurements of relevant organs are given in Table 8. Important features are: (1) The gonad is posterior to the stomach. (2) There is no vas efferens in the usual sense. Thick lobes arise from a wide collecting gutter that functions as a vas efferens. (3) The seminal vesicle (Sv) arises from mid-gonad and makes a small knot dorsal to the gonad. (4) The posterior vas deferens (Vd_1) runs as a wide tube, swollen with sperm, from the seminal vesicle to become a slender duct only at the style sac. (5) The prostate overlies the

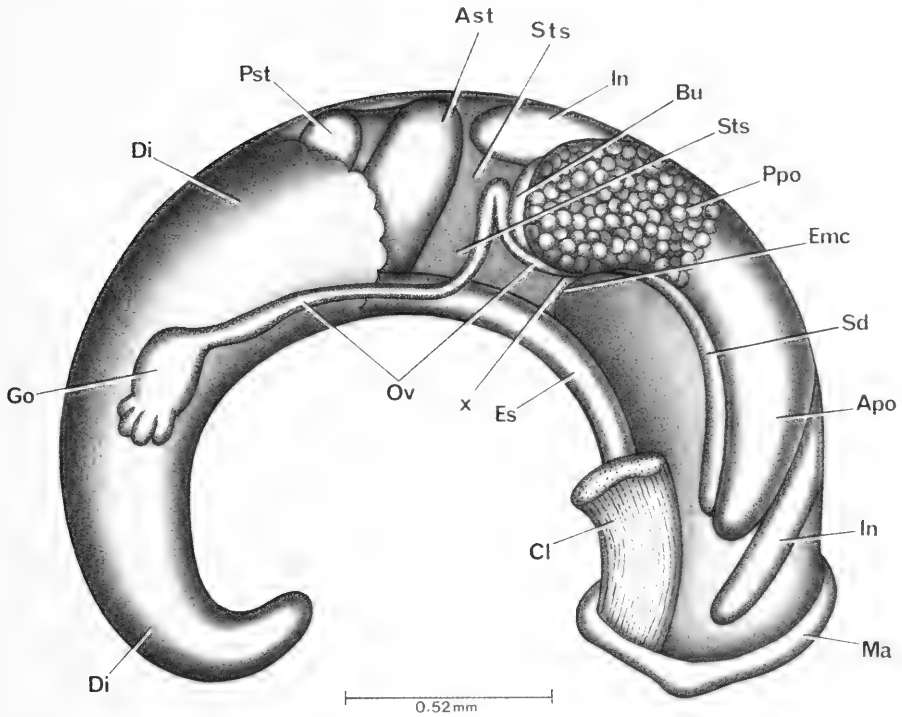

FIG. 20. Uncoiled female *Pseudobythinella chinensis* with head and kidney tissue removed.

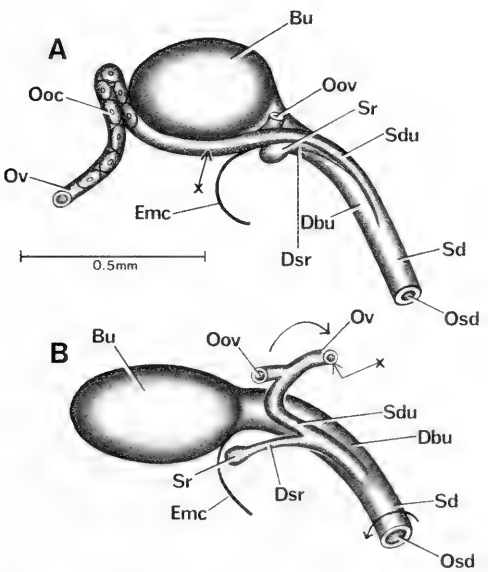

FIG. 21. Details and variation of bursa copulatrix complex of organs of *Pseudobythinella chinensis*. Figure 21A is in same orientation as in Figure 20. In B, oviduct cut and reflected in direction of arrow to show opening of oviduct (Oov) that attaches to albumen gland

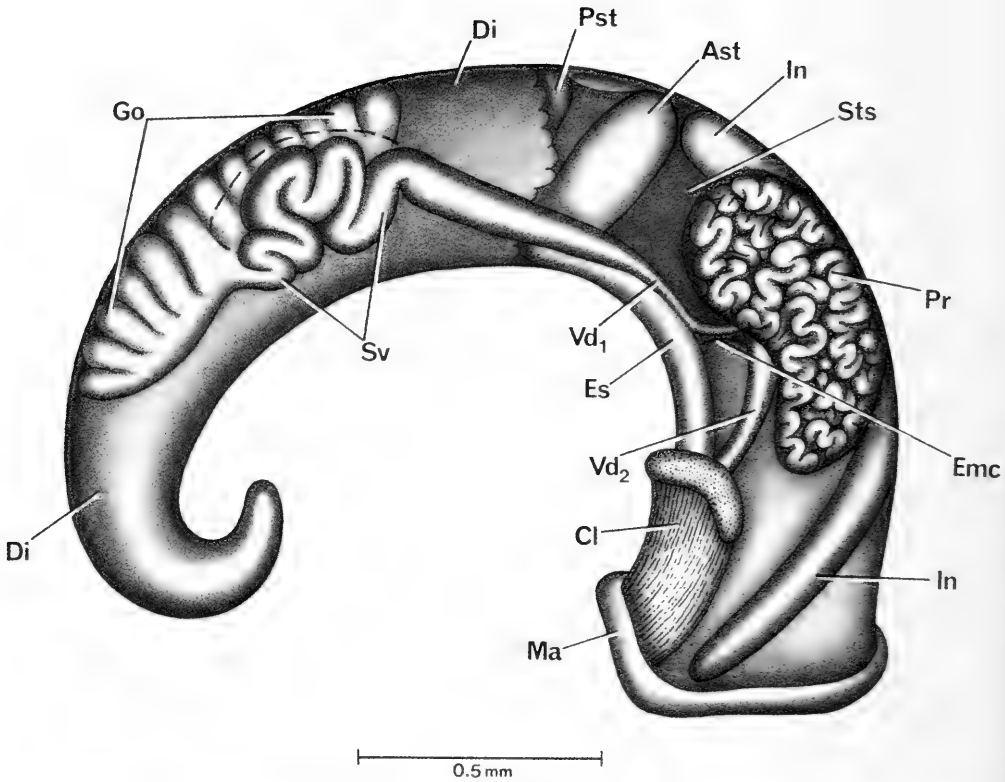

FIG. 22. Uncoiled male of *Pseudobythinella chinensis* without head or kidney tissue. Some of lobes of anterior gonad are cut away (- - -) to show knot of seminal vesicle (Sv) dorsal to gonad.

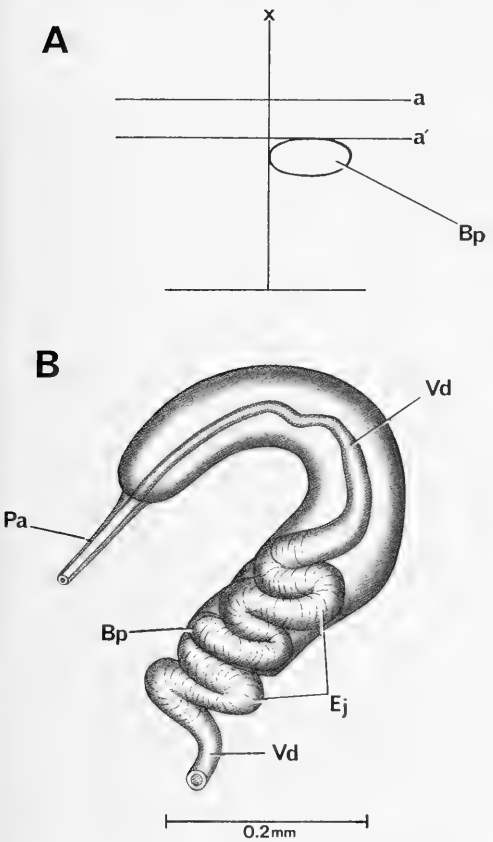

FIG. 23. A. The orientation of base of penis (Bp) of *Pseudobythinella chinensis* to snout-neck mid-line (x) and lobes of eyes (a). B. Penis.

posterior end of the mantle cavity. (6) The anterior vas deferens (Vd_2) separates from the prostate at mid-prostate. (7) The penis (Fig. 23B) has an enormous muscular ejaculatory duct (Ej) in the base that continues to coil for a short distance in the neck. (8) The penis has an enormously elongated papilla, a unique feature. (9) The base of the penis (Bp, Fig. 23A) arises to the right of the snout-neck mid-line x and at 90° to it.

Digestive system. The digestive gland (Di) covers the posterior chamber of the stomach (Pst, Figs. 20, 22). The radular sac (Rs) loops up over the buccal mass (Bm, Fig. 19 A). Radular statistics are given in Tables 9, 10. The radula is minute, with an extraordinary number of rows of teeth (97 per 0.48 mm)

TABLE 9. Radular statistics for *Pseudobythinella chinensis*. Mean ± standard deviation (range). N = number used. In mm except for width of central tooth in μm.

	Sex Unknown (N = 4)
Shell length	1.79±0.001
Radular length	0.48±0.01
Radular width	0.06±0.004
Total rows of teeth	97.3±6.7 (N = 3)
No. rows of teeth forming	10.3±4.0
Central tooth width	12.0±0.5 (N = 9)

(Fig. 24). The most commonly encountered cusp formula is $\frac{(4)5\text{-}1\text{-}5(4)}{1\text{-}1}$; 4(5)-1-(5, 6)4;

24-29; 17-22.

The inner marginal teeth have significantly more cusps(mean of 26) than do the outer marginals (mean of 20). The two outer cusps of the outer marginals are specialized to form a pincer-like process (Fig. 24G, H). The "tongue" on the face of the central tooth is broad and is not flanked by deep-set holes (Fig. 24A, B).

Nervous system. No data.

Remarks

This species differs from the other three for which we have anatomical data by the following: (1) The bursa may somewhat protrude posterior to the albumen gland. (2) the oviduct makes a pronounced bend near the bursa; the ascending and descending arms of the bend are pressed together (contrast the open 360° loops or complex oviduct loops of the other species). (3) The sperm duct is elongated and extends anterior to the posterior end of the mantle cavity to enter the spermathecal duct, a unique character-state. (4) The seminal receptacle branches off the sperm duct, not the oviduct, a unique character-state. (5) There is no vas efferens. (6) The penis has an extremely elongated papilla, a unique character-state.

Pseudobythinella shimenensis Liu, Zhang & Chen

Holotype. IZAS, HN797904; Liu et al., 1982: 254, 256, fig. 1.

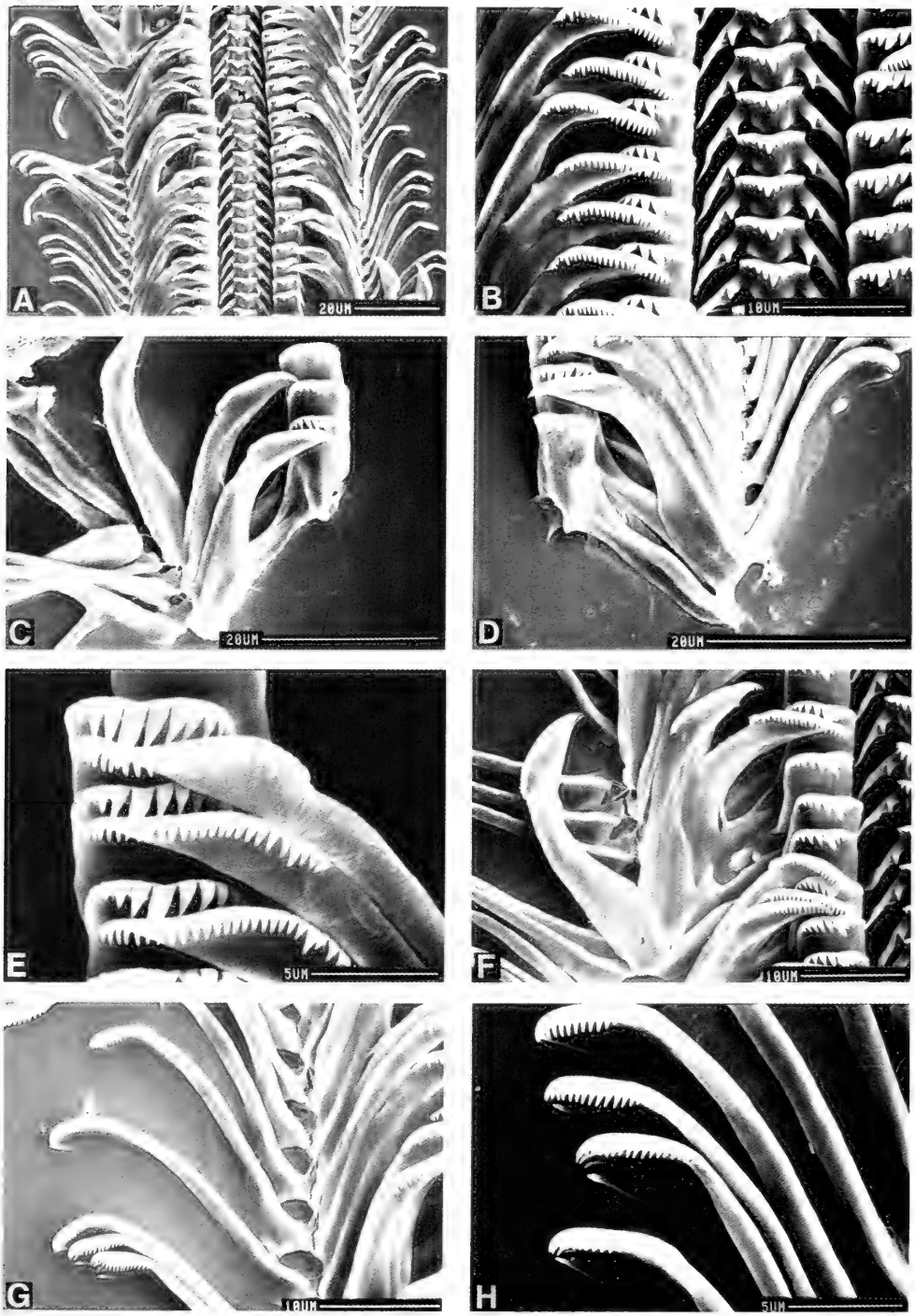

FIG. 24. Radula of *Pseudobythinella chinensis*. B. Central and inner marginal teeth emphasized. C, D. Details of morphology of lateral teeth. E, F. Inner marginals emphasized. G, H. Outer marginals. See text for details.

TABLE 10. Cusp formulae for the radular teeth of *Pseudobythinella chinensis* with the percent of the four radulae in which a given formula was found at least once.

Central Teeth		Lateral Teeth		Inner Marginal Teeth		Outer Marginal Teeth
5-1-5 / 1-1	75%	4-1-4	100%	17	—	75%
		5-1-5	75%	18	—	75%
5-1-4 / 1-1	50%					
		6-1-5	50%	19	—	75%
4-1-4 / 1-1	25%	4-1-5	50%	20	—	75%
		5-1-4	50%	21	—	50%
		6-1-4	25%	22	—	50%
				23	—	25%
				24	25%	25%
				25	100%	—
				26	100%	—
				27	75%	—
				28	25%	—
				29	25%	—
				$\bar{X}$ * = 26±1.0		20.0±2.1
				N = 40		N = 33

*Mean ± standard deviation of cusp number for all teeth counted.

Type locality. Shimen, Hunan Province, October 1979.

Synonymy. *Pseudobythinella shimenensis* Liu, Zhang & Chen, 1982: 254–256. *Pseudobythinella shimenensis* Davis et al., 1985: 68.

Habitat

Snails were collected from Qingguandu Village, Nanzhen Town, Shimen County, Changde Prefecture; 29°56′36″ N, 110°41′42″ E; Figure 1, site 3; topotypes. Snails were collected from under stones and leaves at the edge of a small pool of a stream. The water was clean, clear, cool.

Depository

Specimens are housed at ZAMIP, M0012, ANSP 373137, A12653.

TABLE 11. Shell measurements (mm) of *Pseudobythinella shimensis*. Mean ± standard deviation (range). Five shells measured, all 4.0 whorls.

Length (L)	1.98±0.04 (1.94–2.04)
Width (W)	1.17±0.02 (1.14–1.20)
L last three whorls	1.95±0.04 (1.92–2.02)
L body whorl	1.44±0.03 (1.41–1.48)
L penultimate whorl	0.38±0.01 (0.38–0.40)
W penultimate whorl	0.82±0.02 (0.80–0.84)
L 3rd whorl	0.48±0.02 (0.45–0.50)
L aperture	0.99±0.02 (0.96–1.00)
W aperture	0.76±0.03 (0.73–0.80)
x	0.24±0.12 (0.10–0.38)
y	0.07±0.04 (0.04–0.12)

Description

Shells. Shells are minute, smooth, ovate with flattened apex (Figs. 6F–I, 25, 26). Shell measurements are given in Table 11; shell lengths range from 1.94 to 2.04 mm for shells of 4.0

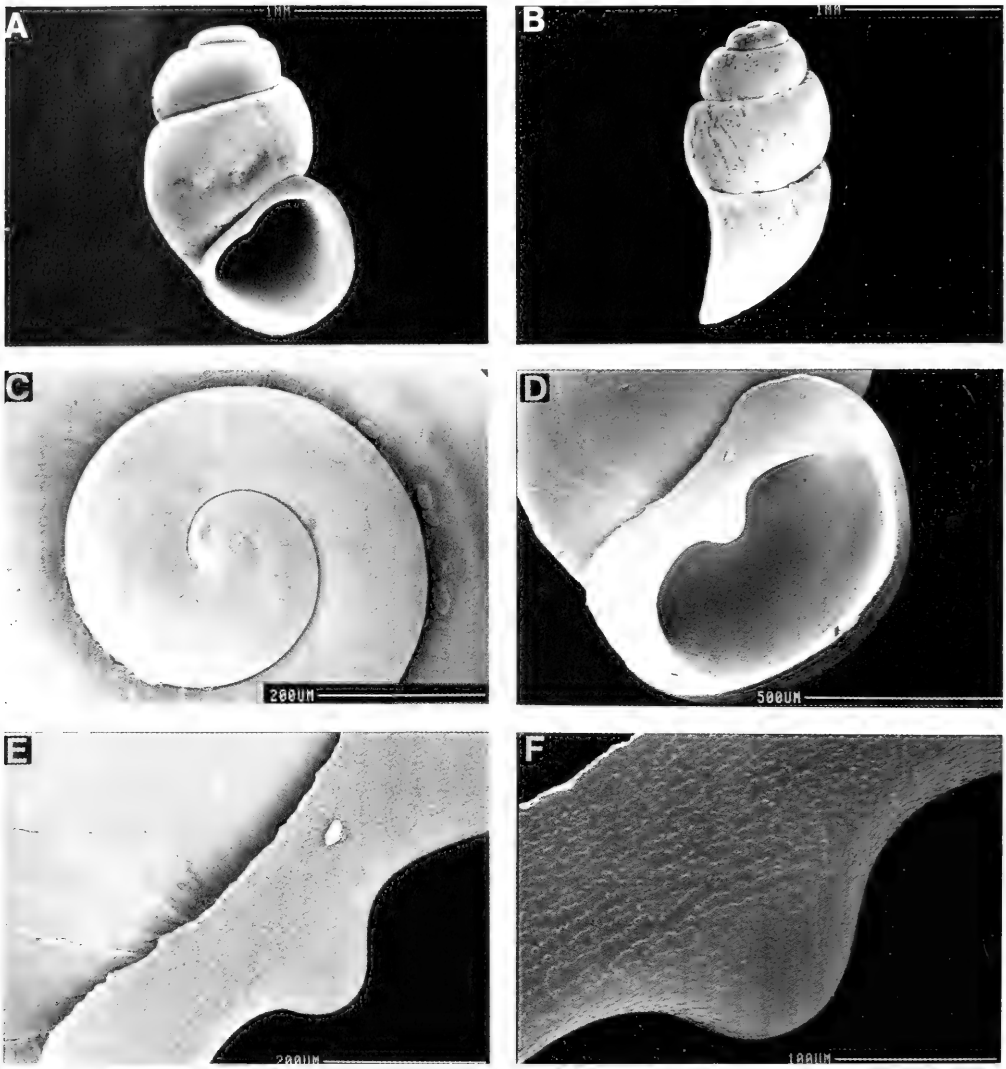

FIG. 25. SEM photographs of shells of *Pseudobythinella shimenensis*. A. Note slight swelling or tooth on columella. C. Apical whorls showing spiral microsculpture starting at 0.5 whorls. D. Aperture rotated to expose fully tooth on columella. E, F. Columella highly magnified to show sculpture pattern on inner lip, columella, and tooth.

whorls. The aperture is broadly ovate to subcircular. The sutures are deep and the whorls shouldered, convex. The inner lip is straight to saddle-shaped with a narrow umbilicus above the center of the saddle of 33%; no umbilicus, 66%. The columella has a tooth plainly in view in the aperture. The face of the body whorl is flattened in most specimens. The outer lip is straight to slightly arched (Fig. 25B). In side view, the adapical outer lip is fused to the body whorl in 40%; separated by 0.05 mm ± 0.03 mm (N = 5) from the body whorl in 60%.

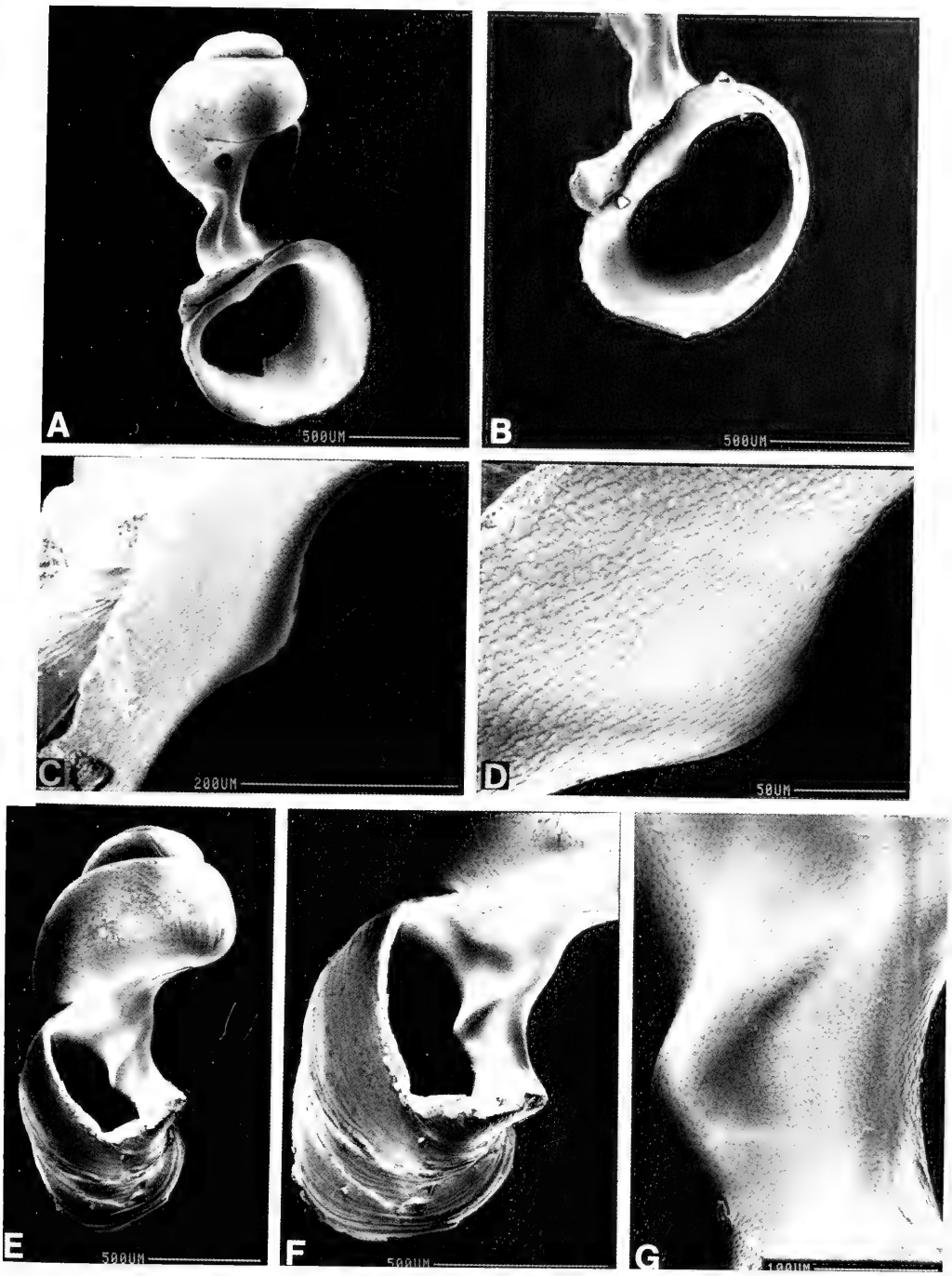

FIG. 26. SEM photographs of shells of *Pseudobythinella shimenensis* broken open to reveal raised spiral ridge on columella of body whorl that terminates as tooth. C, D. Large scale-like sculptural plates on columella at aperture contrast with thin line-like raised ridges on spiral ridge within body whorl (G).

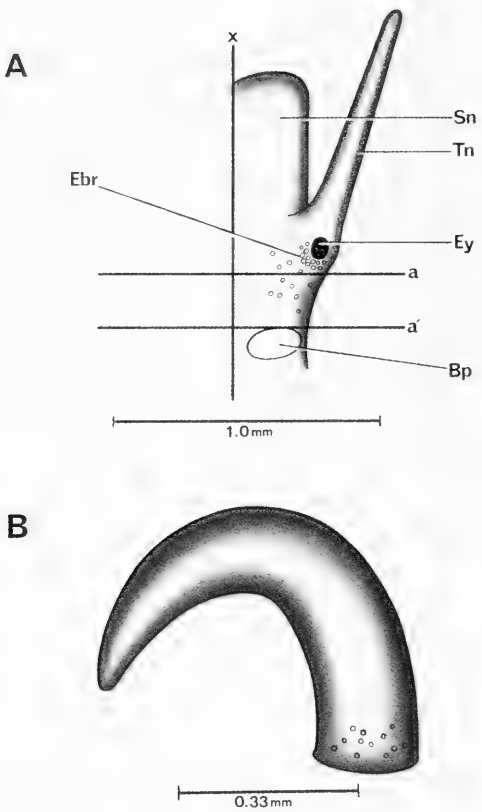

FIG. 27. Head (A) and penis (B) of *Pseudobythinella shimenensis*. A. Relationship of base of penis to mid-line of snout-neck (x) and to posterior end of eye lobes (a).

The inner lip is straight (outer lip down 90° to horizontal).

SEM examination shows that the tip of the apical whorl is smooth with fine spiral sculpture seen starting in less than half a whorl (Fig. 25C). Tilting the aperture somewhat, the columellar "tooth" is clearly seen (Fig. 25D–F). It is covered with raised calcareous lappets (Fig. 25E), contrasted with the pustules seen in *P. chinensis*. Upon breaking open several shells, it is seen that the "tooth" is the terminus of a columellar keel that starts mid-body whorl (Fig. 26A, B, E–G). The calcareous lappets begin on the columellar keel and extend to the aperture (Fig. 26D, G); above the keel there are minute raised calcareous ridges (Fig. 26G).

External features. The head is white with a small cluster of white granules about the medial edge of the eye, i.e. an "eyebrow" (Ebr, Fig. 27). There is a scattering of white granules posterior to the eyebrow at the side of the neck. The operculum is corneous, paucispiral and kidney-bean shaped with the columellar—side concavity corresponding to the tooth on the columella (Fig. 28). On the inner surface of the operculum the attachment pad for the muscle has a pronounced ridge (Fig. 28A, C). The pad is relatively narrow, some 40% the width of the operculum.

Mantle cavity. The reflected mantle showing mantle cavity organs is given in Figure 29; measurements and counts are given in Table 12. There are relatively few gill filaments (12–13) yet these take up 78% the length of the mantle cavity. The osphradium is mid-gill and is long. Gf_2 is long; the longest gill filaments are 0.36 mm long. There is no cluster of white granules just anterior to the osphradium close to the neck (Ne)—mantle collar (Ma) junction.

Female reproductive system. The body of an uncoiled female with head and kidney tissue removed is shown in Figure 30. Measurements and counts of organs are given in Table 12. Important features, to note are: (1) The gonad is located posterior to the stomach. It is a single small sac that has three or four small protruding lobes created by pressure of individual oocytes at the posterior end of the gonad. (2) The albumen gland (Ppo) covers most of the bursa copulatrix (Bu) and extends beyond the bursa to cover most of the style sac. The albumen gland curves around the bursa leaving the posterior end of the bursa exposed. Only in a few cases is the bursa completely covered by the albumen gland. (3) The spermathecal duct (Sd) is tightly pressed to the pallial oviduct and opens into the mantle cavity close to the anterior end of the capsule gland (Apo). (4) The bursa copulatrix complex of organs is shown in Figure 31 oriented in the same relative positions as in Figure 30. The bursa is short. (5) The oviduct enters (Oov) the albumen gland posterior to the posterior end of the mantle cavity (Emc). The sperm duct is short and branches off the spermathecal duct posterior to the posterior end of the mantle cavity. (6) The duct of the seminal receptacle (Dsr) branches off the oviduct posterior to the sperm duct (Fig. 31). The seminal receptacle

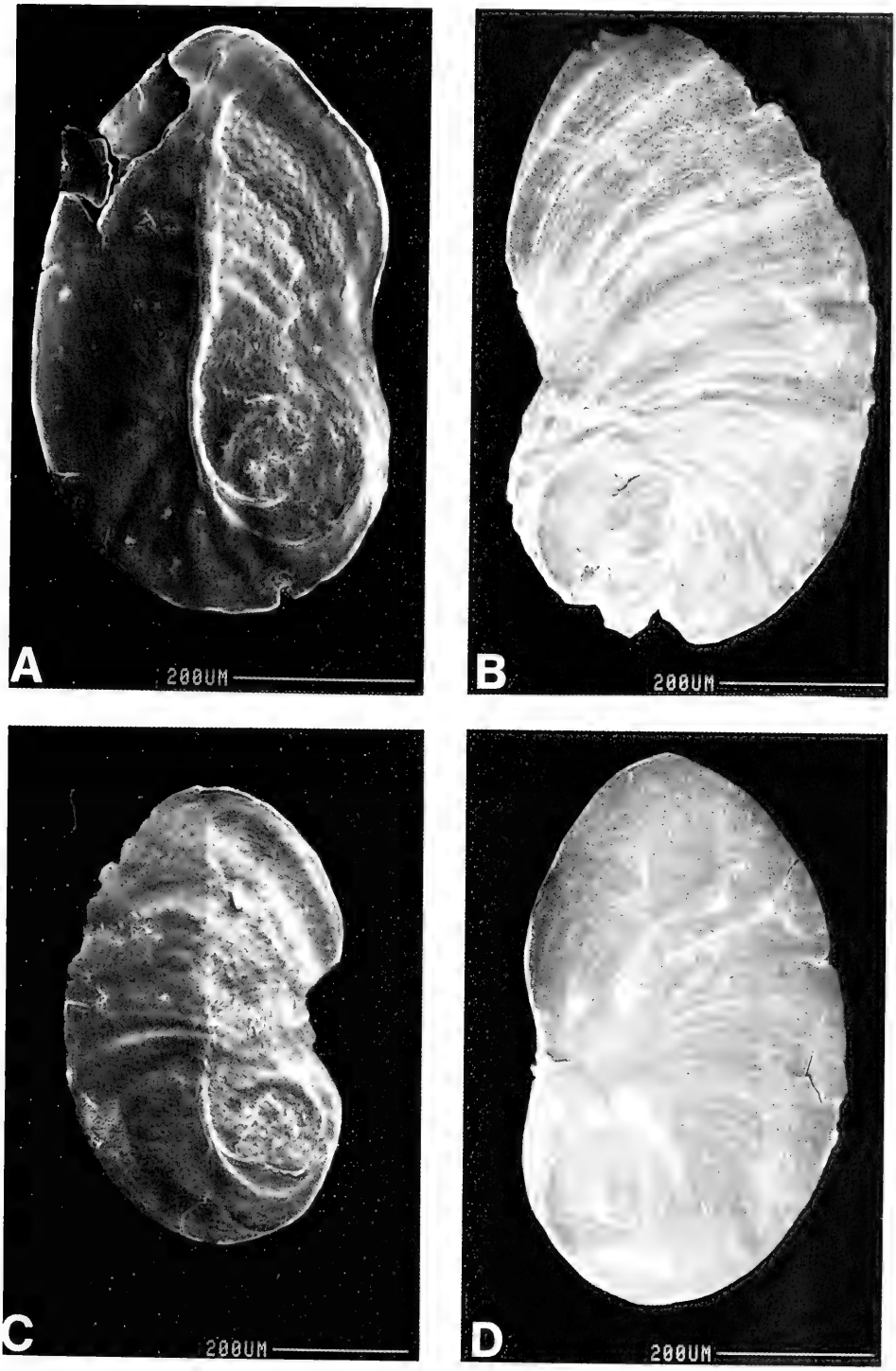

FIG. 28. Opercula of *Pseudobythinella shimenensis*. A, C. Inner surface. B, D. Outer surface. Note prominent ridge on inner surface running along inner edge of attachment pad.

TABLE 12. Lengths (mm) or counts of non-neural organs and structures of *Pseudobythinella shimenensis*. N = number of snails used. Mean ± standard deviation (range).

	Females (N = 5)	Males (N = 1)
Body	3.62±0.34 (3.26–4.04)	3.94
Gonad	0.47±0.09 (0.34–0.60)	2.00
Digestive gland	1.78±0.15 (1.68–2.04)	2.10
Posterior pallial oviduct (= albumen gland)	—	—
Anterior pallial oviduct (= capsule gland)	—	—
Total pallial oviduct = OV	1.52±0.09 (1.40–1.60) N = 4	—
Bursa copulatrix BU	0.49±0.11 (0.36–0.60) N = 4	—
Duct of BU	0.26 (N = 2) No. var.	
BU ÷ OV	0.33±0.08 (0.23–0.40) N = 4	—
Seminal receptacle	0.11±0.02 (0.08–0.13) N = 4	—
Duct of seminal receptacle	0.16±0.05 (0.10–0.22) N = 4	—
Buccal Mass	0.46 (N = 1)	—
Mantle cavity	0.98±0.11 (0.84–1.10) N = 4	.90
Gill (G)	0.76±0.07 (0.70–0.84) N = 4	.70
Osphradium (OS)	0.31±0.08 (0.20–0.40)	.28
OS ÷ G	0.40±0.08 (0.29–0.48) N = 4	.40
No. of filaments	12.3±0.5 (12–13)	.28
Gf_2	0.20 (N = 2)	—
Gf_1	0.16 (N = 2)	—
Total Gf = TGF	0.36 (N = 2)	—
Gf_2 ÷ TGF	0.55 (N = 2)	—
Prostate	—	1.00
Seminal vesicle	—	.80
Penis	—	.90

TABLE 13. Radular statistics for *Pseudobythinella shimenensis*. Mean ± standard deviation (range). N = number used. In mm except for width of central tooth in μm.

	Sex Unknown
Shell length	2.1±0.12 (1.9–2.2) N = 9
Radular length	0.79±0.46 (0.71–0.84) N = 5
Radular width	0.071±0.005 (0.064–0.076) N = 6
Total rows of teeth	113±1.7 (111–115)
No. rows of teeth forming	9±3 (6–14)
Central tooth width	14.1±0.82 (13.2–15.3) N = 13

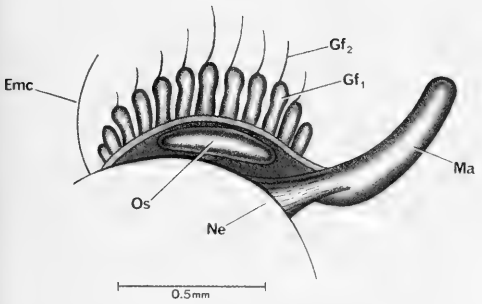

FIG. 29. Mantle cavity of *Pseudobythinella shimenensis*. Mantle cut and reflected to show mantle-cavity structures.

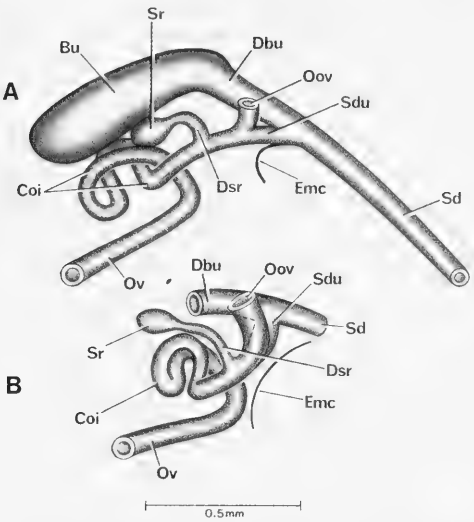

FIG. 31. Details and variation of bursa copulatrix complex of organs of *Pseudobythinella shimenensis*. Figure 31A is in same orientation as in Figure 30. B. Bursa cut away to show seminal receptacle (Sr) and oviduct coil (Coi).

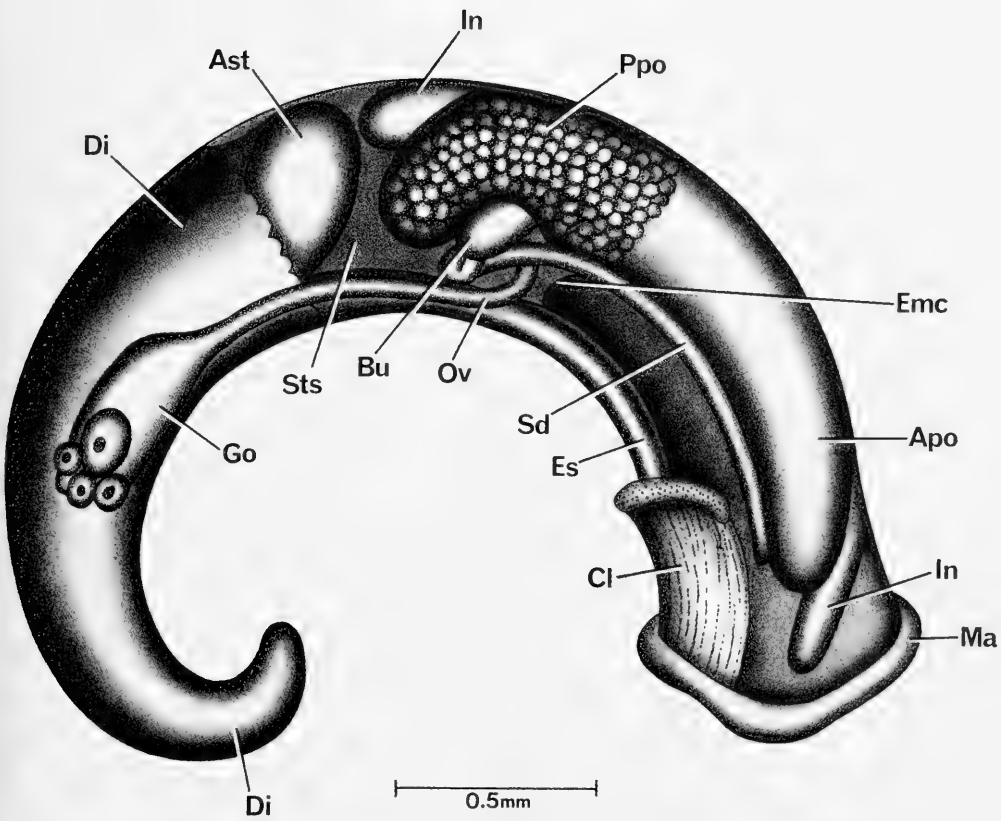

FIG. 30. Uncoiled female *Psuedobythinella shimenensis* with head and kidney tissue removed.

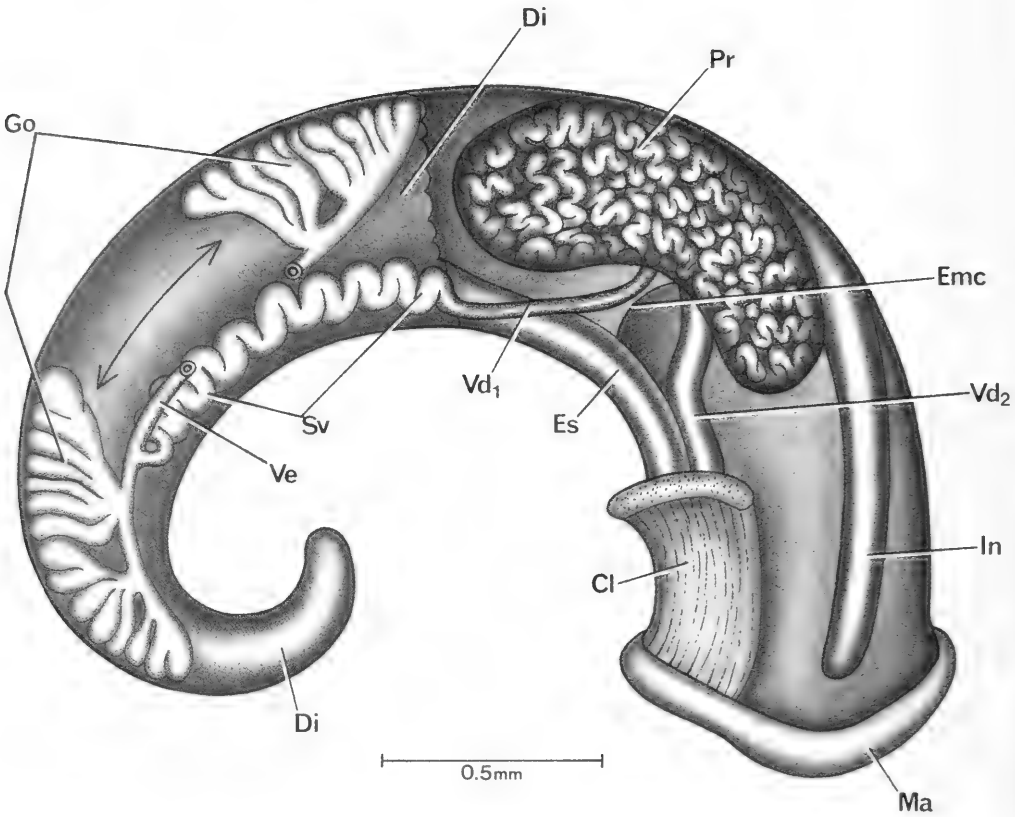

FIG. 32. Uncoiled male of *Pseudobythinella shimenensis* without head or kidney tissue. Some lobes of gonad removed (iine with arrows) to reveal seminal vesicle (Sv).

and the duct of the seminal receptacle are well developed. (7) Posterior to the duct of the seminal receptacle the oviduct makes an irregular loop or double coil that is dorsal to the bursa. In Figure 31A, the coil has been pulled out a little from beneath (dorsal to) the bursa to show the pattern of coiling. The coil is shown in actual position in Figure 30.

Male reproductive system. The body of an uncoiled male is shown in Figure 32 with head and kidney tissue removed. Measurements and counts of organs are given in Table 12. Important features to note are: (1) The gonad covers the stomach. (2) A portion of the gonadal lobes has been cut away to show the seminal vesicle (Sv) that coils regularly dorsal to the gonad. (3) There is a well-defined vas efferens (Ve) with the posterior vas deferens arising from the vas efferens at mid—to slightly posterior to mid-gonad. (4) There are a number of bundles of testicular lobes arising from the vas efferens. (5) The prostate overlies the posterior end of the mantle cavity (Emc). (6) The anterior vas deferens (Vd_2) leaves the prostate (Pr) close to the posterior end of the mantle cavity. (7) The penis is simple and without discernable papilla (Fig. 27B). (8) The base of the penis (Bp) arises from the neck to the right of the snout-neck mid-line (x) and at 90° to it (Fig. 27A). There is no discernable ejaculatory duct.

Digestive system. The digestive gland covers the posterior chamber of the stomach of females (Di, Fig. 30), and the entire stomach in males (Fig. 32). The radular sac (Rs, Fig. 33) is highly elongated, coiling dorsal to the buccal mass (Bm).

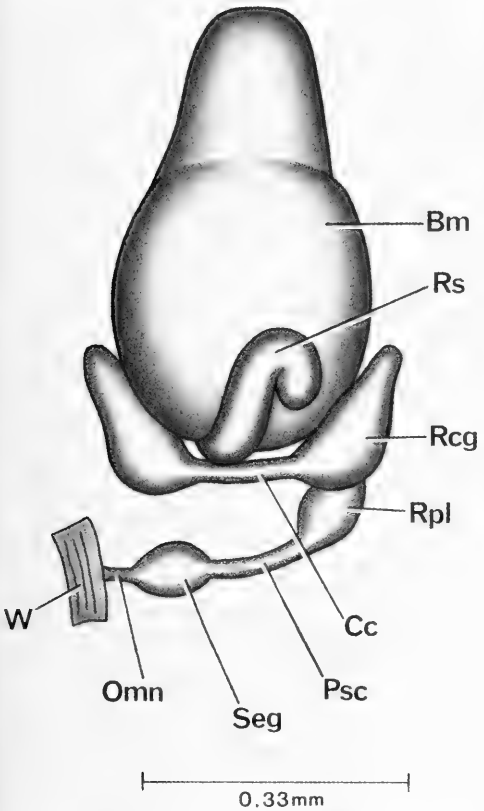

FIG. 33. Dorsal aspect of buccal mass of *Pseudobythinella shimenensis* with dorsal part of nerve ring. Note radular sac (Rs) coiling dorsally over buccal mass (Bm).

Radular statistics are given in Tables 13 and 14. The most commonly encountered cusp formula is

$$\frac{4(5)\text{-}1\text{-}(5)4}{1\text{-}1};\ 2(3)\text{-}1\text{-}\ 3(4);\ 17\text{-}20,\ 16\text{-}18.$$

There is a very large number of rows of teeth for the comparatively short length of radula (113 per 0.79 mm). The radula is illustrated in Figures 34, 35. Fig. 34B, D, E feature the central tooth. The face of the tooth is moderately raised as a tongue with a slight concavity on either side extending beneath the basal cusps. The lateral angles have the flared ends typical of *Pseudobythinella*.

The lateral teeth are featured in Figures 34C, D, F and 35A, B, E. Two points are important. (1) The basal process of the lateral tooth is prominent and curved towards midradula as also seen in *P. chinensis* but in contrast to the weak or slighly developed straight basal process seen in *Akiyoshia chinensis*. (2) As in the above mentioned taxa, there is a gradation in size of the cusps on the lateral tooth. The "1" of the 3-1-3 is not considerably larger than the flanking cusps. Inner marginal teeth (Figs. 34B, C, F; 35C, D, E, F) and outer marginals (Figs. 34C, E; 35C, G) have numerous small cusps. No one cusp is extra long (i.e. with derived specialization).

Nervous system. A segment of the nervous system is shown in Figure 33. The cerebral commissure (Cc) is elongated. The dorsal nerve ring is moderately concentrated (RPG of 0.38, Table 15). Otherwise the dorsal aspect of the nerve ring is typical for the Triculinae.

Remarks

This species differs from the others for which we have anatomical data as follows: (1) The glands about the eye form an "eyebrow". *Pseudobythinella chinensis* and *P. daliensis* lack any glands about the eyes; there is a scatter of glands in *P. kunmingensis*. (2) A tooth is clearly visible in the aperture of the shell. (3) The bursa is an elongated tube; it is an elongated ovoid sac in the other species. (4) The penis lacks an ejaculatory duct.

Pseudobythinella daliensis differs from the other three species by having a small, not minute shell. It does not have an elongated radular sac as do the others.

Pseudobythinella kunmingensis differs from the other three species by having a scatter of glands about the eyes. The spermathecal duct shares a common opening with the capsule gland (Apo) (not shown in Fig. 31 where the spermathecal duct is cut short).

TRICULINAE

Pachydrobiini Davis & Kang, 1990

Type genus. Pachydrobia Cross & Fischer, 1876

Diagnosis. Genera of Triculinae in which the spermathecal duct bypasses the pericardium and the oviduct does not make a closed 360° twist. With the exception of *Wuconchona*,

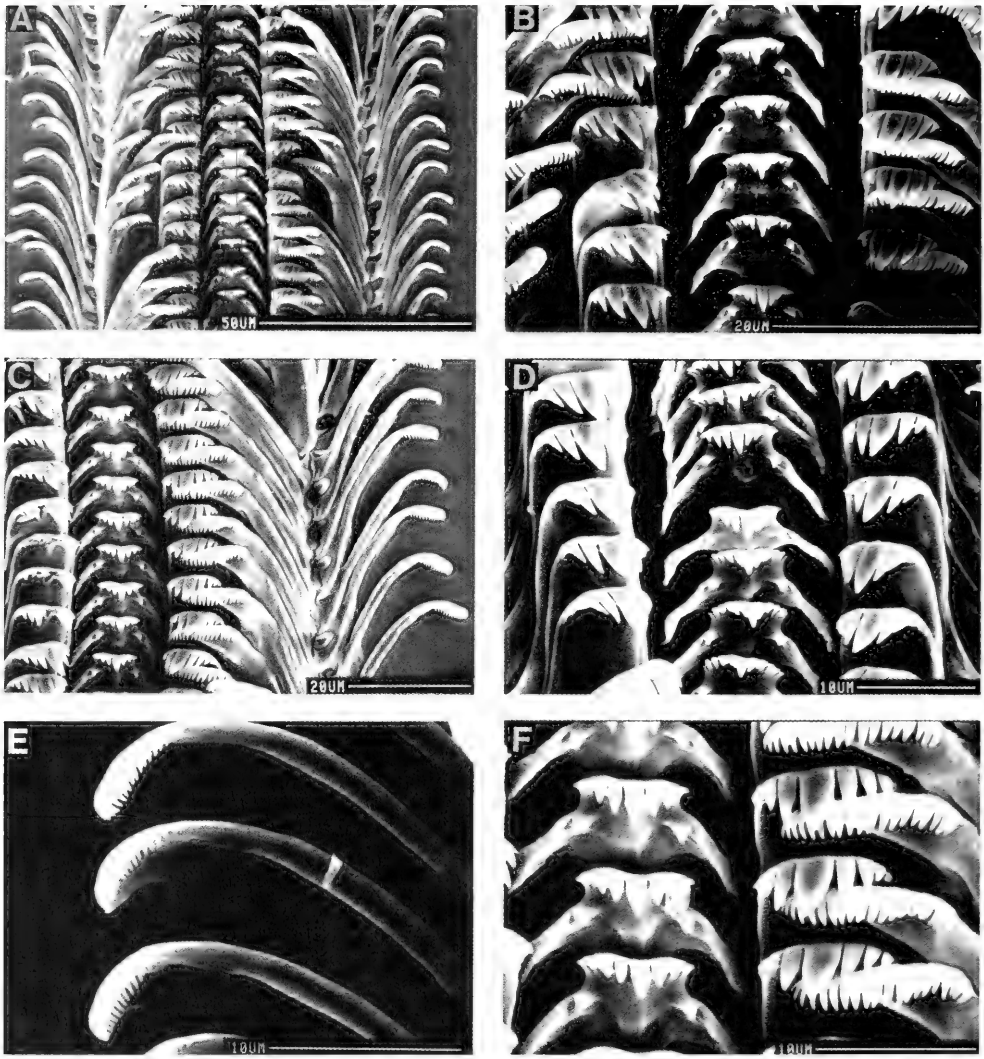

FIG. 34. Radula of *Pseudobythinella shimenensis* featuring central and lateral teeth (B–D, F) and outer marginal teeth (E).

there is a sperm duct. The seminal receptacle arises from the bursa or the duct of the bursa in the plesiomorphic state; the seminal receptacle is lost in the derived state and its function taken over by new structures.

Genera assigned. Guoia, *Halewisia*, *Neotricula*, *Pachydrobia*, *Robertsiella*, *Jinhongia*, *Gammatricula*, *Wuconchona* (N = 8).

The *Lithoglyphopsis* Problem

Considering all Asian genera of freshwater rissoacean snails, it has been especially important to locate and study the type species of *Lithoglyphopsis* for two reasons. (1) *Lithoglyphopsis* was the taxon that caused early European workers to include within the family Hydrobiidae those Asian taxa now known to

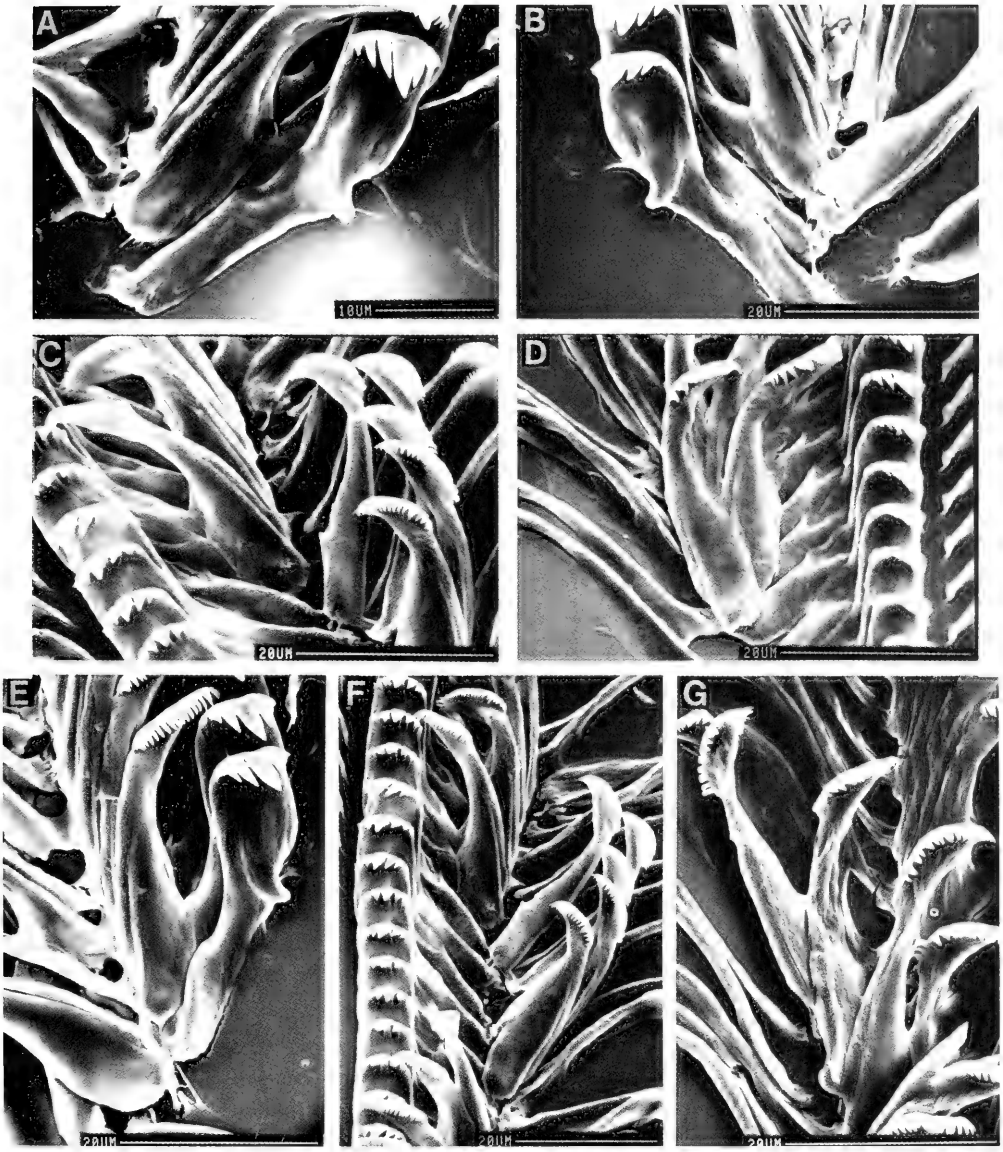

FIG. 35. Radula of *Pseudobythinella shimenensis* featuring entire lateral tooth (A, B, E), inner marginals (C–F), outer marginals (G).

be Pomatiopsidae: Triculinae. (2) The snail transmitting *Schistosoma mekongi* Voge et al., 1978, was originally described as *Lithoglyphopsis aperta* Temcharoen, 1971.

Considering the first, the shells of certain Chinese species from Hunan Province so much resembled shells of European *Lithoglyphus* that they were described as species of *Lithoglyphus* (Gredler, 1881, 1886; Moellendorff, 1888). Subsequently Thiele (1928) noted that the morphology of the central tooth of *L. modestus* differed slightly from that of European *Lithoglyphus* and he therefore established the genus *Lithoglyphopsis*, with *L. modestus* Gredler, 1886, as its type species by original designation. However, overall shell

TABLE 14. Cusp formulae for the radular teeth of *Pseudobythinella shinenensis* with the percent of the radulae in which a given formula was found at least once.

Central Teeth		Lateral Teeth		Inner Marginal Teeth		Outer Marginal Teeth
$\frac{4\text{-}1\text{-}4}{1\text{-}1}$	80%	2-1-3	60%	14	—	20%
$\frac{5\text{-}1\text{-}5}{1\text{-}1}$	40%	2-1-4	60%	15	—	40%
$\frac{5\text{-}1\text{-}4}{1\text{-}1}$	20%	3-1-3	60%	16	—	60%
$\frac{4\text{-}1\text{-}4}{1\text{-}1}$	20%	3-1-4	40%	17	80%	100%
				18	100%	80%
				19	100%	40%
				20	60%	20%
				21	40%	—
				$\bar{X}$ * = 18.7±1.2 N = 50		17.2±1.3 N = 49

*Mean ± standard deviation of cusp number for all teeth counted.

TABLE 15. Lengths of neural structures of *Pseudobythinella shimenensis*. The mean is given and with data when N = 2. N = number used.

Cerebral ganglion	0.20 (N = 2) (No. Var.)
Cerebral commissure	0.09 (N = 2) (0.08, 0.10)
Pleural ganglion	
Right (1)*	0.10 (N = 1)
Left	—
Pleuro-supraesophageal connective (2)*	0.12 (N = 1)
Pleuro-subesophageal connective	—
Supraesophageal ganglion (3)*	0.10 (N = 1)
Subesophageal ganglion	—
Osphradio-mantle nerve	0.04 (N = 1)
RPG ratio* = 2 ÷ 1+2+3	0.38 (N = 1)

and radular characters persuaded Thiele (1928) to include *Lithoglyphopsis* of the Hydrobiidae along with 12 other Asian Triculinae genera within the Tribe Lithoglypheae along with European *Lithoglyphus*. As late as 1974, Brandt included the Asian genera in question in the family Hydrobiidae, subfamilies Triculinae, Cohilopinae, Rehderiellinae, and Lithoglyphinae.

As for the second, Davis et al. (1976) studied this species and stated that it was most closely related to *Tricula*, especially *Tricula burchi* Davis, 1968b; they stated that *Tricula* might be a suitable genus for "*L.*" *aperta*. In 1980, Davis referred *L. aperta* to *Tricula*. Davis et al. (1976) pointed out that on the basis of both shell and radula, *Tricula aperta* could not be considered a species of *Lithoglyphopsis*. However, the questions have remained: What is *Lithoglyphopsis*? To which genera is *Lithoglyphopsis* most closely related? Can one establish once and for all that *Lithoglyphopsis* is a member of the Triculinae, not a member of the Hydrobiidae: Lithoglyphinae? What is the potential for species of *Lithoglyphopsis* to transmit a species of *Schistosoma*?

As a result of our studies in Hunan Province, it was clear that species historically considered to be *Lithoglyphus* in Hunan belong to two genera: *Lithoglyphopsis* and a new genus described here as *Guoia*.

Guoia Davis & Chen, genus nov.

Type Species. Lithoglyphus viridulus Moellendorff, 1888

Etymology. Named for Dr. Guo Yuan Hua, Institute of Parasitic Diseases, China National Center for Preventive Medicine, Shanghai, for his tireless efforts to discover and understand species of snails involved in disease transmission.

Diagnosis. Shells small (<3.6 mm long), and globose-conic. The spermathecal duct opens into the rear of the mantle cavity. A long, slender sperm duct connects the spermathecal duct (at a position close to the posterior end of the mantle cavity) to the oviduct close to where the oviduct opens into the albumen gland. Duct of the bursa is massive, running directly anterior from the large bursa to form the short spermathecal duct opening at the rear of the mantle cavity. There is no seminal receptacle; sperm are stored in a swelling of the oviduct just posterior to the juncture of the sperm duct and oviduct, or they are stored in an outpocketing of the sperm duct at the juncture to the oviduct. There is a thin corneous stylet at the tip of the penis. The penis has a glandular lobe. The ejaculatory duct is massive, extending posteriorly along the neck from the base of the penis. Radula *Tricula*-like.

Relationships. A member of the *Neotricula* clade by virtue of (1) the oviduct travels from gonad to albumen gland straight, without twist or coil (contrast the *Tricula* clade), and (2) the spermathecal duct does not enter the pericardium. The closest generic similarity is with *Robertsiella* of Malaysia in that (1) the penis of the males has a similar stylet, and (2) the spermathecal duct-duct of bursa-bursa connections and relative postitions are the same. There are differences. In *Robertsiella*, the seminal receptacle is encapsulated in the muscular wrapped duct of the bursa (*Guoia* lacks a seminal receptacle). A section of the oviduct of *Guoia* serves as a seminal receptacle. The shell of *Robertsiella* is ovate-conic, not globose-conic. The sperm duct of *Guoia* is elongated, twisting over the bursa; it is very short in *Robertsiella*. The duct of the bursa is very short in *Robertsiella*, elongated in *Guoia*.

Assigned Species.
Lithoglyphus fuchsianus Moellendorff, 1885
Lithoglyphus viridulus Moellendorff, 1888

Thiele (1928: 365) noted that of Asian species described as *Lithoglyphus*, *L. fuchsianus* and *L. viridulus*, had radulae that corresponded to the European *Lithoglyphus*, whereas the radulae of *L. modestus* and *L. tonkinianus* Bavay & Dautzenberg (a Vietnamese species) had an entirely different type of central tooth. He created the genus *Lithoglyphopsis* to include the latter two species and named "*L. modesta*" as the type species. Yen (1929) placed all Chinese taxa described as *Lithoglyphus* in the genus *Lithoglyphopsis* including *L. liliputanus* Gredler, 1881 from "Kwangtung" (= Guangdong). The shell of this last species is a miniature version of *L. modestus*. Until the anatomy is known its generic placement is *incertae sedis*.

Guoia viridulus (Moellendorff, 1888).

Lithoglyphus viridulus Moellendorff, 1888: 141, pl. 4, fig. 6, 6a-b
Lithoglyphus viridulus (Moellendorff, 1888). Thiele 1928
Lithoglyphopsis viridulus, Yen, 1939

Types: S.I.; Lectotype, 4129, fig. in Yen, 1939: pl. 4, fig. 9
Paralectotypes, 4130, figured here; Figure 36 A–C.
Type Locality: Hunan

Habitat

Anhua County, Anhua Town, Zijiang River; 28°23′46″ N, 111°12′41″ E., Figure 1, Site 10. Collected by Chen and Davis, 16 March 1987; field collection number D87-1. Catalog numbers are: large class, ANSP 373147, A12663; small class, ANSP 373148, A12664. D85-78, small class, ANSP 373149, A 12665; ZAMIP M0055. Snails were collected 1.6 km upstream from the town boat landing, along the shores of a small island in the middle of the river. Water flows through a stone breakwater at the upstream end of the island. Between the breakwater and the cobbles of the island was a protected area with water some 30 cm deep and with emergent vegetation. On the undersides of rocks at the breakwater on the protected side were numerous *Guoia viridulus* and *Lithoglyphopsis modesta*. Associated snail fauna included *Stenothyra hunanensis* (Davis et al. 1988), *Gyraulus* sp., *Radix* sp., *Semisulcospira* sp., and a viviparid.

Introduction

There were two size classes of fully mature snails living intermixed at the site (Fig. 37). Throughout the description these will be referred to as the large class and small-class snails. There are slight shape differences between the classes, yet we have felt it prudent not to consider them belonging to different

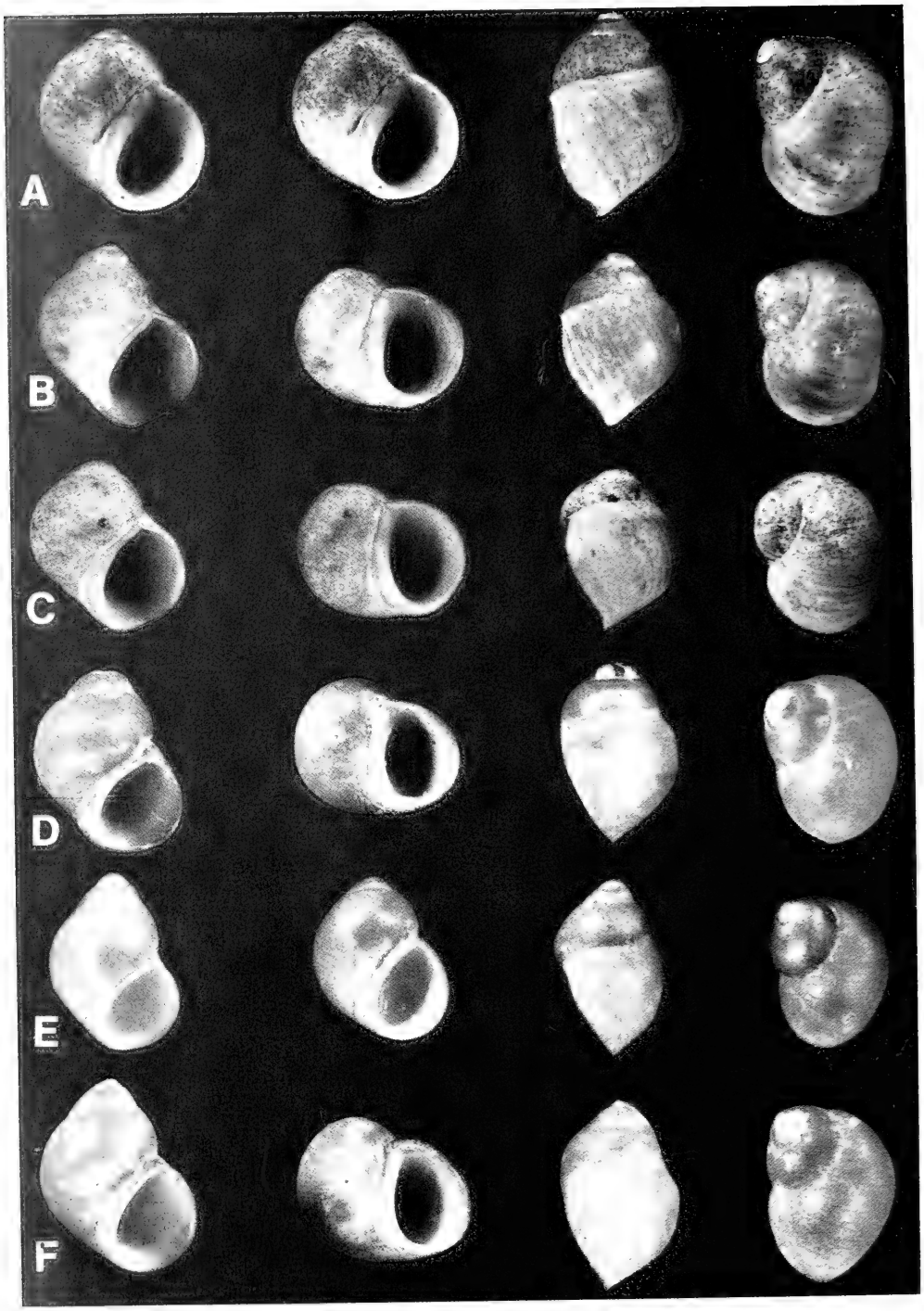

FIG. 36. Lectotype and paralectotypes of species of *Guoia*. A–C. Paralectotypes of *Guoia viridulus* (SMF 4130); A = 3.50 mm long. *Guoia fuchsianus*, D–F. D. Lectotype, L = 3.24 mm. E, F. Paralectotypes.

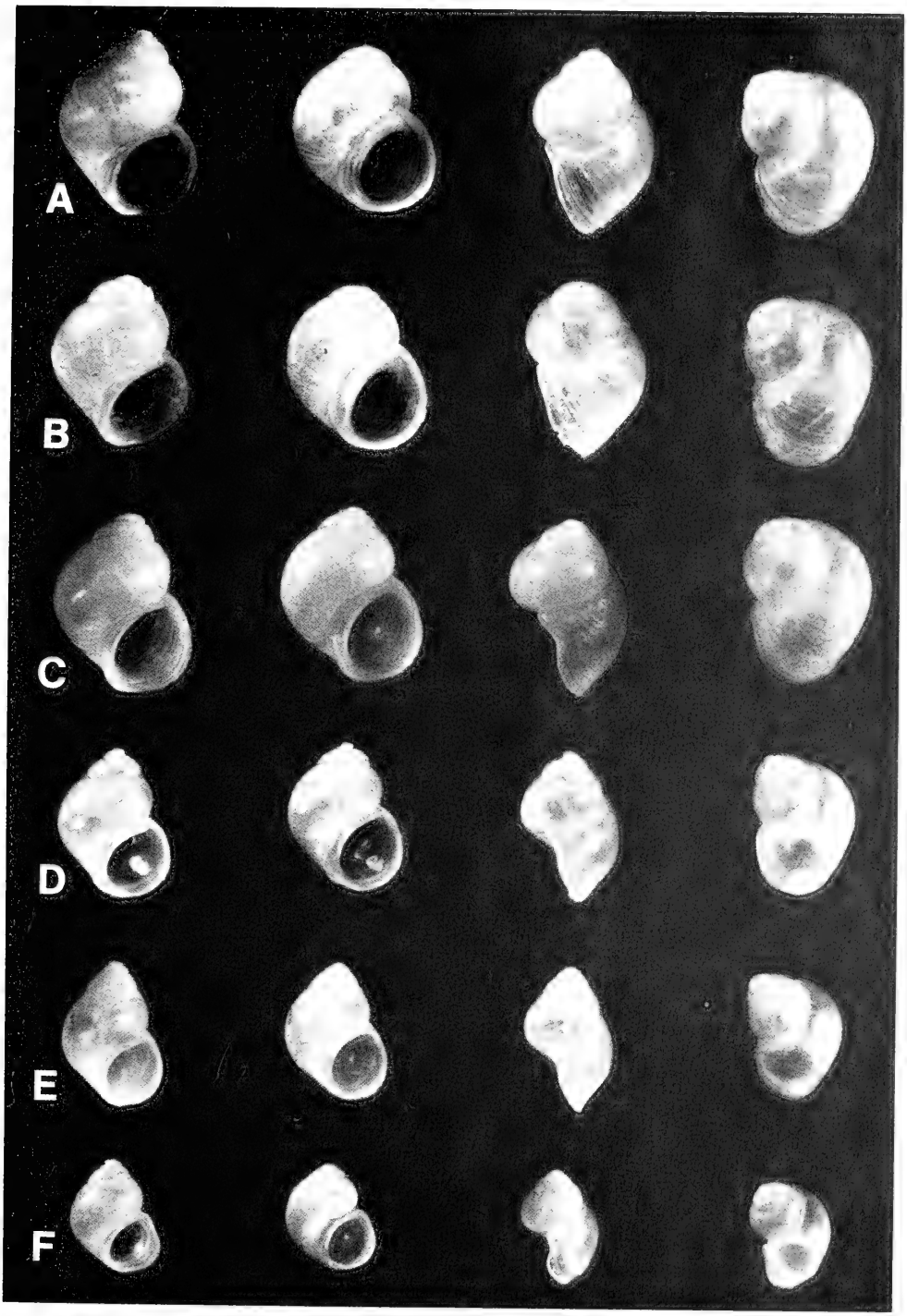

FIG. 37. Four aspects of each of six shells of *Guoia viridulus*. A–C. Large class; A = 3.6 mm long. D–F. Small class; D = 2.8 mm long. A, B, D, E = females; C, F = males.

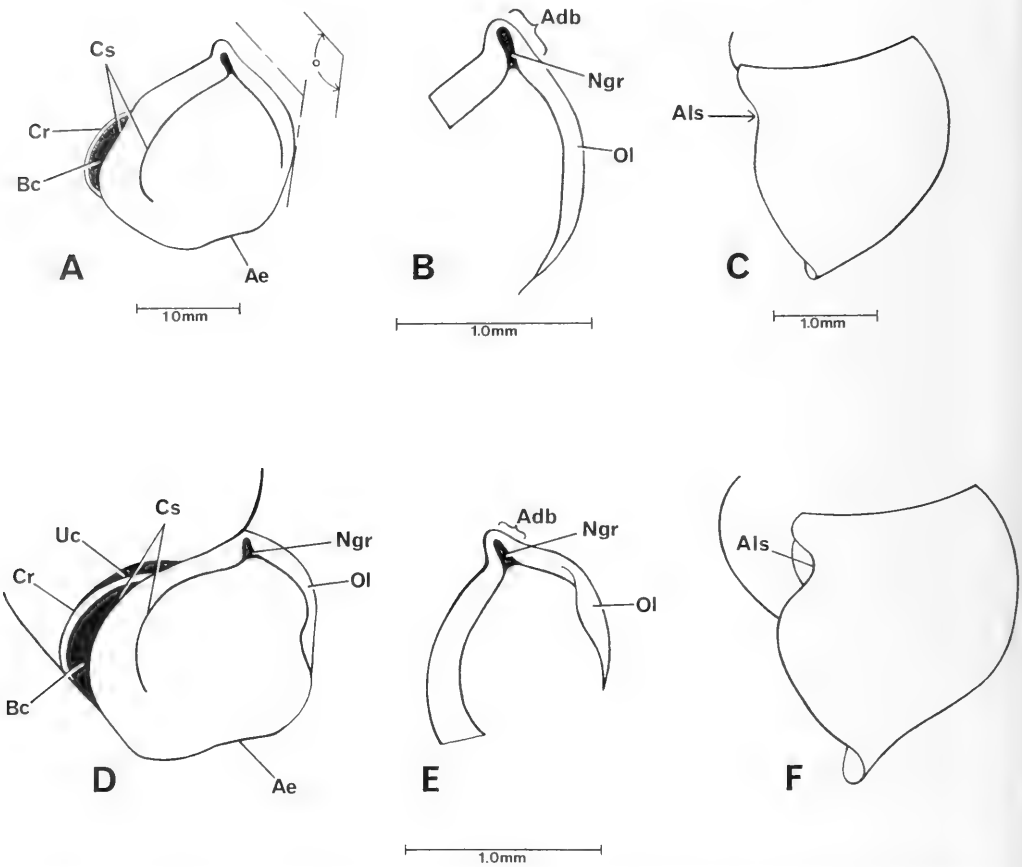

FIG. 38. Illustrated details of the apertural region of shells of *Guoia viridulus* characteristic of the species.

species as we could find no anatomical differences between them, and as they live in micro-sympatry. The greater amount of anatomical data was from the large-class snails based on living specimens. Subsequently, anatomical data were gathered in Philadelphia from alcohol-preserved small class snails.

As there is considerable similarity among shells of the two size classes of snails that we refer to as *G. viridulus*, as well as *G. fuchsianus*, we did a multivariate analysis of shell measurements of these taxa as well as older museum specimens of these species in order to attempt to assess differences among them. The following anatomical description is based on large class snails. Small class snails are contrasted with large class individuals in the remarks section for this species.

Description

Shells. Figures 36–39. Large-class (Figs. 37A–C, 39A–C). Shells small, globose-conic, 4.0–4.5 whorls, smooth but with rough growth lines. Aperture sub-circular with complete peristome, with pronounced apertural beak (Fig. 38, Adb) and a pronounced beak groove (Ngr). There is a wide columellar shelf (Cs), a small basal crescent (Bc) with crescent ridge (Cr). Some shells have an umbilical chink (Uc), others do not. The abapical lip has an embayment (Ae). The adapical outer lip is flared out making somewhat of an angle with the remaining outer lip. In side view, the lip is sinuate forming a slight sigmoid embayment (Als).

Females are larger than males (Table 16). Size ranges (lengths) are: males, 2.8 to 3.6

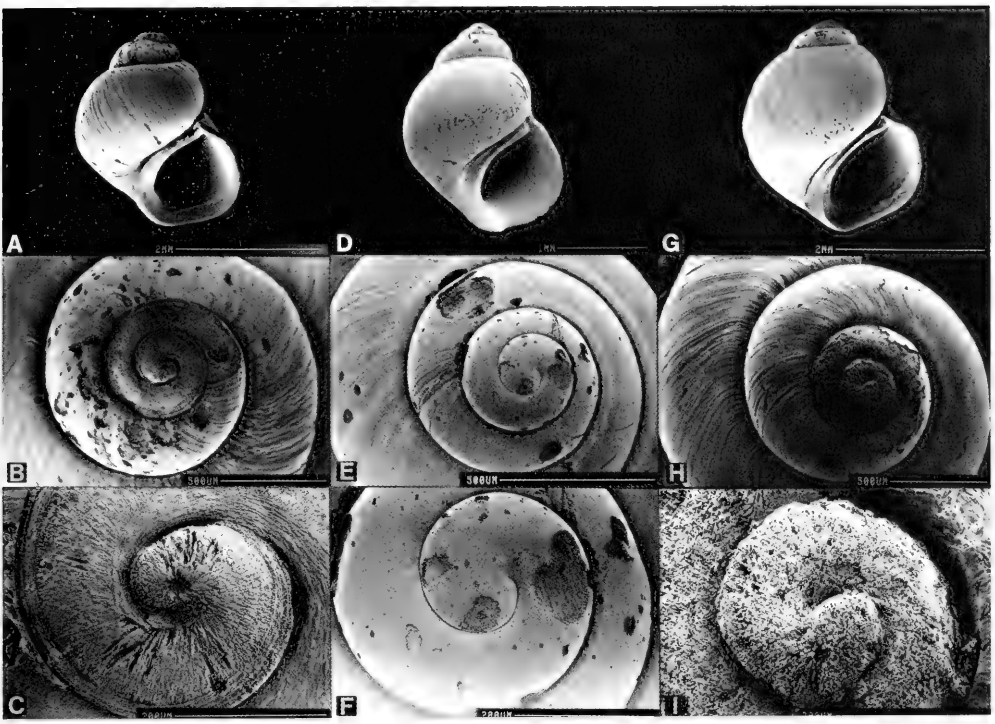

FIG. 39. SEM photos of shells of *Guoia viridulus* (A–F) and *G. fuchsianus* (G–I). A–C. Large form; D–F. Small form. B, C, E, F, H, I = enlargements of apical whorls.

mm; females, 2.8–3.8 mm. Our samples compare well with two lots of *G. viridulus* from the collections (Table 16, column 3). They compare well with paralectotypes (Figs. 36A–C compared with Fig. 37A–C).

Small-class (Figs. 37D–F). Shells as in the large class with the following differences. Length is substantially smaller (Table 16) with males 2.0–2.1 mm long, females 2.2–2.8 mm long. The small-class shells appear somewhat more conic than large class shells (compare Fig. 37E vs. 37A). However, the width to length ratio is not significantly different between classes; the length of the body whorl to total height is slightly greater in the large size class (0.84 ± 0.03, 0.84 ± 0.05 for large-class; 0.80 ± 0.02, 0.80 ± 0.03 for small class). The basal crescent and columellar shelf are deeply depressed in small class shells (Fig. 37D). The outer lip in side view has a deep sigmoid embayment (Fig. 38F).

SEM pictures of the apical whorls are shown in Figure 39B, C, E, F. The large class individuals inevitably had eroded apices; the small class shell apices were smooth. Some spiral microsculpture was noted at the shoulder of the body whorl of small class shells.

Multivariate analysis. The phenogram based on distance coefficients (cophenetic correlation 0.77) is given in Figure 40. Note the following: (1) Historic *G. viridulus* (nos. 18-21) form a discrete unit within the wider variance of 9 large-class Anhua *G. viridulus* collected by us. (2) One Anhua *G. viridulus* (no. 5) clusters with Baisha *G. fuchsianus* collected by us. (3) The one historic *G. fuchsianus* that had complete whorls so that it could be included in this analysis clusters in the middle of the *G. fuchsianus* variance. (4) Two small-class Anhua *G. viridulus* (nos. 27, 28) and two snails classified by us as large-class Anhua *G. viridulus*

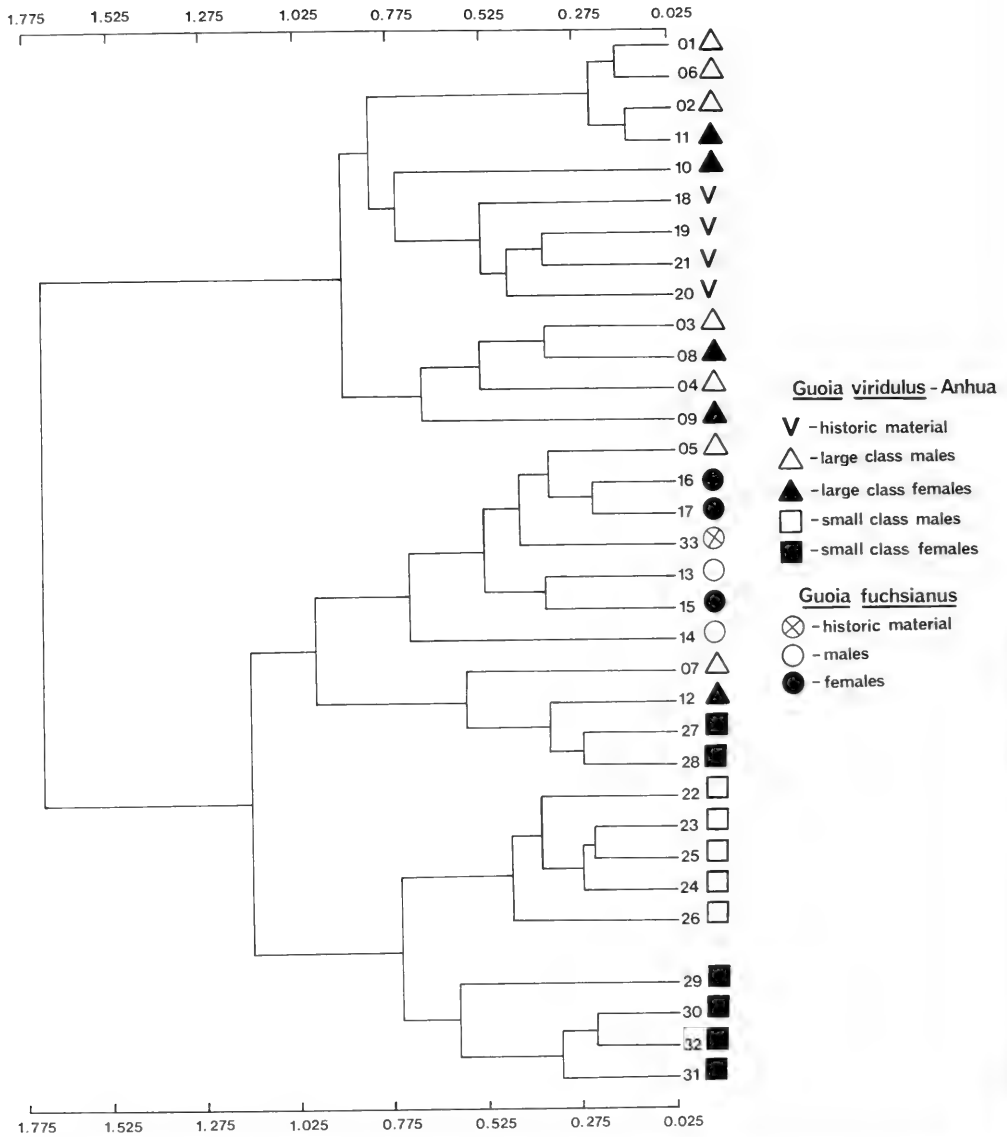

FIG. 40. UPGMA phenogram of distances for shell measurements of two species of *Guoia*. See text for details.

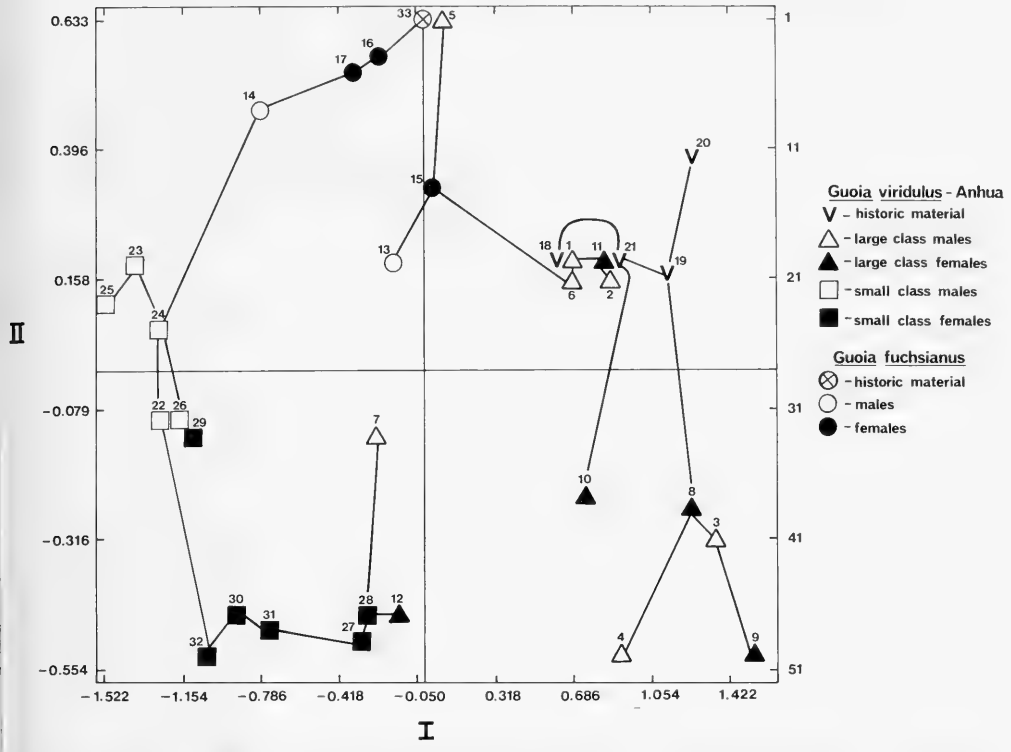

FIG. 41. Ordination diagram following three dimensional scaling. The first two principal components are given. Taxa are connected by a MST. See text for details.

(nos. 7, 12) form a sub cluster with *G. fuchsianus*. (5) Most (82%) of the small-class *G. viridulus* form a discrete cluster at the bottom.

In the PCA analysis, there were three significant components (Table 17); the first with 76.6% of the variance, the second with 13.49, the third with 5.69 (total of 95.8%). Character loadings showed the first component to be one of size (Table 18); characters loading heavily on the second component-axis are number of whorls and length of the penultimate whorl. Ordination on the first two PCA axes following MDS is given in Figure 41. The MST connects OTUs. Size increases from left to right. Along the second axis, relative to length, shells with more whorls, longer penultimate whorls, and wider 3rd whorls are to the bottom. Proportionally shorter penultimate whorls and narrower 3rd whorls are to the top. The second axis is one of changes in translation, whorl expansion, and whorl number. We deduce the following from the ordination diagram and table of character loadings. (1) We consider the small-class and large-class snails to belong to the same species, *G. viridulus*. With only two exceptions (nos. 5, 20) the variance along the second axis ranges from −0.554 to +0.182 for both size classes showing the same considerable variance in whorl translation and expansion. The only differences between the size classes are clear-cut differences in size, and the qualitative differences of deeper lip sinuation and depressed lip sinuation and depressed cres-

TABLE 16. Shell measurements for populations of *Guoia viridulis*.

	Large Class (D87-1)		ANSP 45501	Small Class (D87-1)	
	Males (N = 7)	Females (N = 5)	& 98206 (N = 4)	Males (N = 5)	Females (N = 6)
No. Whorls	4.0–4.5	4.0–4.5	4.5	4.0–4.25	4.5
Length (L)	3.21±0.28 (2.76–3.56)	3.36±0.38 (2.84–3.84)	3.44±0.16 (3.28–3.60)	2.12±0.06 (2.02–2.16)	2.48±0.24 (2.24–2.80)
Width (W)	2.57±0.16 (2.32–2.76)	2.61±0.29 (2.12–2.88)	2.89±0.19 (2.72–3.12)	1.66±0.08 (1.54–1.76)	1.86±0.14 (1.68–2.08)
L body whorl	2.69±0.28 (2.12–2.92)	2.82±0.31 (2.32–3.12)	2.99±0.11 (2.88–3.12)	1.70±0.06 (1.62–1.76)	1.99±0.22 (1.80–2.32)
L penultimate whorl	0.33±0.07 (0.20–0.38)	0.40±0.05 (0.36–0.48)	0.29±0.02 (0.28–0.32)	0.24±0.02 (0.22–0.28)	0.28±0.03 (0.24–0.32)
W penultimate whorl	1.16±0.13 (0.96–1.28)	1.22±0.13 (1.04–1.36)	1.11±0.04 (1.08–1.16)	0.80±0.04 (0.76–0.84)	0.90±0.10 (0.78–1.04)
W 3rd whorl	0.56±0.08 (0.48–0.68)	0.56±0.08 (0.48–0.68)	0.53±0.04 (0.48–0.56)	0.44±0.04 (0.40–0.50)	0.51±0.06 (0.40–0.56)
L last 3 whorls	3.15±0.26 (2.72–3.48)	3.28±0.34 (2.80–3.68)	3.38±0.17 (3.20–3.52)	2.05±0.06 (1.96–2.12)	2.41±0.23 (2.20–2.72)
L aperture	1.95±0.19 (1.56–2.12)	2.00±0.19 (1.68–2.20)	2.29±0.12 (2.16–2.44)	1.26±0.05 (1.20–1.32)	1.44±0.11 (1.32–1.60)
W aperture	1.56±0.17 (1.24–1.76)	1.62±0.22 (1.24–1.76)	1.83±0.12 (1.68–1.96)	0.94±0.05 (0.88–1.00)	1.10±0.09 (0.96–1.20)
W columellar shelf	0.33±0.04 (0.28–0.40)	0.31±0.10 (0.14–0.40)	0.33±0.05 (0.28–0.40)	0.13±0.02 (0.12–0.16)	0.11±0.03 (0.09–0.16)
W ÷ L	0.80±0.03 (0.77–0.84)	0.78±0.03 (0.75–0.81)	0.84±0.02 (0.82–0.87)	0.78±0.03 (0.76–0.82)	0.75±0.03 (0.71–0.79)

TABLE 17. Percent of variance accounted for by each principal component (PC).

PC	%	Accumulated %
1	76.6	76.6
2	13.5	90.1
3	5.7	95.8

cent-columellar callus in the small-class snails. Note that two shells (nos. 7, 12) where originally selected as large-class snails based on visual impression of shape and apertural characters, yet are clearly small-class snails when measured. The length variance for small-class shells was 2.02–2.84 mm, for

TABLE 18. Character loading on each PC axis.

	Components		
	1.	2.	3.
1. No. Whorls	0.293	−0.724	−0.624
2. Length	0.996	0.012	−0.015
3. Width	0.965	0.210	−0.092
4. Length of body whorl	0.970	0.192	−0.059
5. Length of penultimate whorl	0.700	−0.579	0.307
6. Width of penultimate whorl	0.944	−0.209	0.210
7. Width of 3rd whorl	0.745	−0.525	0.249
8. Length of last three whorls	0.994	0.054	−0.026
9. Length of aperture	0.994	0.271	−0.113
10. Width of aperture	0.949	0.270	−0.098
11. Width of columellar shelf	0.874	0.274	−0.034

TABLE 19. Lengths (mm) or counts of non-neural organs and structures of large-class *Guola viridulus*. Mean ± standard deviation (range). N = number of snails used.

	Females	Males (N = 1)
Body	5.69±1.29 (4.36–7.24) N = 4	6.0
Digestive gland	2.23±0.49 (1.80–2.9) N = 4	2.8
Gonad	0.89±0.46 (0.46–1.44)	1.4
Total pallial oviduct PO	2.09±0.21 (1.80–2.30) N = 4	—
Bursa copulatrix = Bu	0.61±0.11 (0.50–0.76) N = 4	—
Bu ÷ PO	0.29±0.03 (0.27–0.33) N = 4	—
Duct of bursa	0.12±0.06 (0.06–0.18) N = 3	—
Buccal mass	0.67±0.03 (0.64–0.70) N = 3	—
Mantle cavity	1.51±0.18 (1.30–1.66) N = 5	2.30
Osphradium = Os	0.53±0.09 (0.46–0.68) N = 5	1.00
Gill = G	1.35±0.17 (1.14–1.50) N = 5	2.00
Os ÷ G	0.40±0.05 (0.32–0.45) N = 5	0.50 (0.26–0.36)
No. gill filaments	24.4±2.1 (22–27) N = 5	25
Gf_2	0.25±0.09 (0.12–0.34) N = 8	male + female
Gf_1	0.37±0.07 (0.30–0.42) N = 8	male + female
Total Gf = TGF	0.57±0.17 (0.42–0.74) N = 8	male + female
Gf_2 ÷ TGF	0.39±0.08 (0.29–0.49)	male + female
Prostate	—	1.80
Seminal vesicle	—	1.20
Penis	—	3.33 (N = 2) (3.06–3.60)

large-class, 2.92-3.84 mm; thus for the species there is a 90% increase in size from shortest to longest mature specimen.

2) We consider the shells at the top of the ordination clustered around mid-axis 1 as belonging to *G. fuchsianus*. They differ considerably from *G. viridulus* in that all have 4.0 whorls, relatively narrower 3rd whorls and shorter penultimate whorls. Only 1 individual (no. 5) of *G. viridulus* (7%) grouped with shells of *G. fuchsianus*.

External features. The head is shown in Figure 42. The snout is transparent but flecked with spots of melanin pigment on the dorsal snout and bars of pigment along the tentacles. There is a small dense eyebrow (Eyb) about each eye comprised of yellow glands. The operculum is shown in Figures 43, 44C–F. It is ovate, paucispiral, with a modest internal attachment pad.

Mantle cavity. The reflected mantle is shown in Figure 45A. The mantle cavity structures are typical for taxa of the *Neotricula* clade. The opening of the spermathecal duct (Osd) is next to the pericardium (Pe). The osphradium (Os) is long and situated mid-gill. The terminal gill filaments (Gf_2) are normal length (Tables 19, 20). The length of the longest filaments is 0.57 ± 0.17 mm long. The filaments are not pleated and lack a pronounced crest (Fig. 45B).

TABLE 20. Lengths (mm) or counts of non-neural organs and structures of alcohol-preserved small-class *Guoia viridulus*. N = number of snails used.

	Females	Males (N = 1)
Body	6.3 (5.60, 6.98) N = 2	—
Digestive gland	2.75 (2.4, 3.1) N = 2	—
Gonad	1.10 (N = 1)	—
Posterior pallial oviduct (= albumen gland)	1.2 (1.1, 1.3) N = 2	—
Anterior pallial oviduct (= capsule gland)	1.3 (1.2, 1.34) N = 2	—
Total pallial oviduct	2.28±0.33 (1.9–2.5) N = 3	—
Bursa copulatrix	0.43±0.16 (0.25–0.56) N = 3	—
Mantle cavity	1.81 (1.62, 2.00) N = 2	1.50
Osphradium = Os	0.67 (0.58, 0.76) N = 2	0.62
Gill = G	1.61 (1.42, 1.80) N = 2	1.24
Os ÷ G	0.41 (0.41, 0.42) N = 2	0.41
No. gill filaments	22 (21, 23) N = 2	19
Gf_2	0.23±0.07 (0.16–0.30) N = 3	male & female
Gf_1	0.30±0.08 (0.24–0.36) N = 3	male & female
Total Gf = TGF	0.53±0.13 (0.40–0.66) N = 3	male & female
Gf_2 ÷ TGF	0.43±0.03 (0.40–0.46) N = 3	male & female
Prostate	—	1.04
Penis	—	2.24

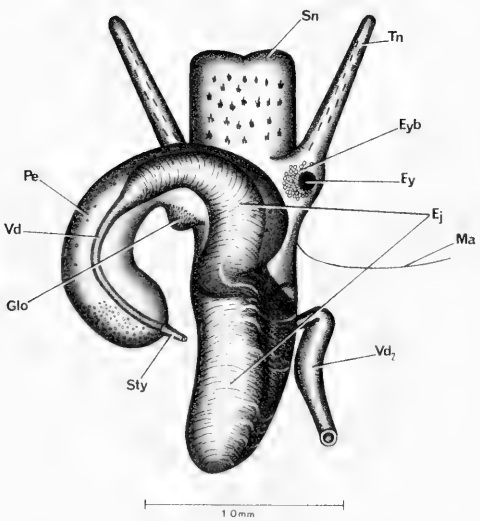

FIG. 42. Head and penis of *Guoia viridulus*.

Female reproductive system. The body of an uncoiled female without head and with kidney tissues removed is shown in Figure 46A. Measurements of relevant organs are given in Tables 19, 20. Important features to note are: (1) The body is not squat, but regularly tubular (contrast *Lithoglyphopsis modesta*). (2) The posterior pallial oviduct (Ppo) does not bend over the style sac (contrast *L. modesta*). (3) The gonad (Go) is posterior to the stomach. (4) Sperm enter the system at the rear of the mantle cavity (Emc) through the opening of the spermathecal duct. The spermathecal duct does not enter the pericardium (contrast taxa of the *Tricula* clade). (5) The pericardium does not swell out into the mantle cavity. The bursa copulatrix complex of organs is shown in Figure 47. (6) The terminal end of the muscular spermathecal duct (Sd) is a thin walled vestibule (Twv). The spermathecal duct is short or long; it is that section of duct between

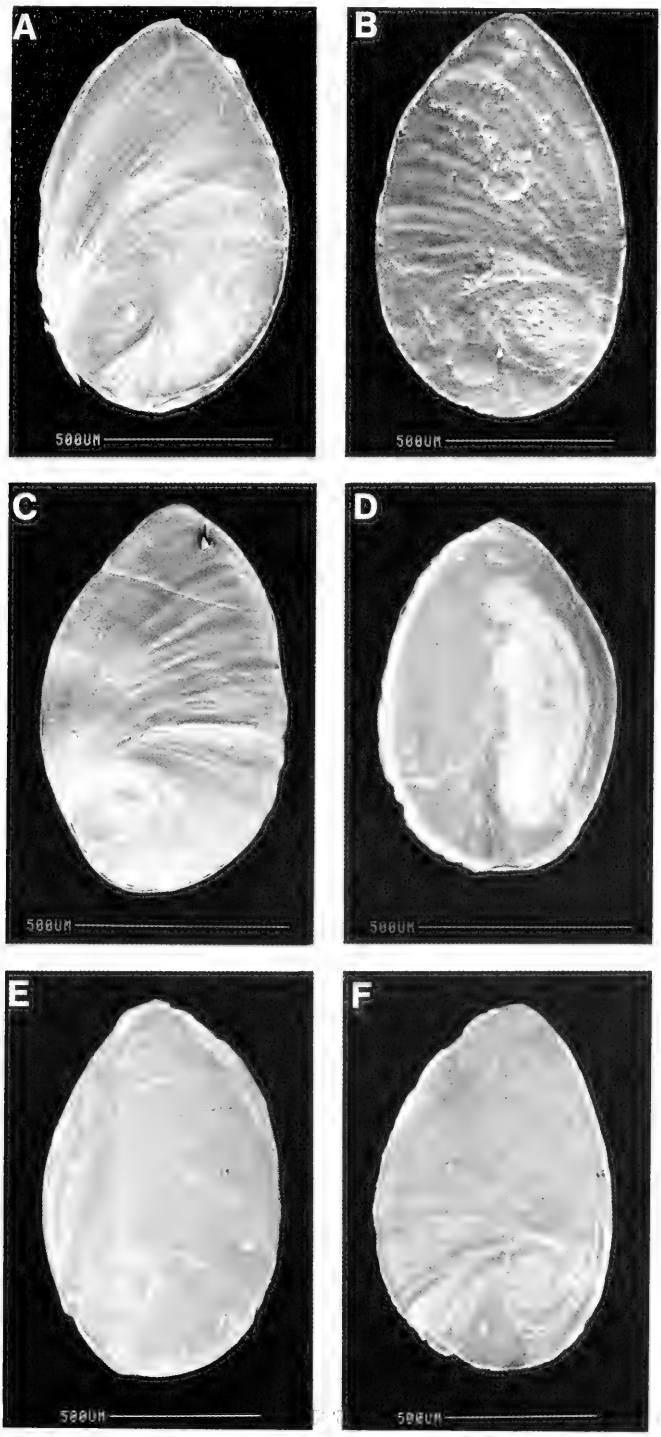

FIG. 43. Opercula of *Guoia viridulus* (A–D) and *Guoia fuchsianus* (E, F). A, B from large-class specimens; C, D from small-class specimens. A, C, E. Outer surfaces; B, D, F. Inner surfaces.

TABLE 21. Radular statistics for *Guoia viridulus* snails. Mean ± standard deviation (range). In mm except for width of central tooth in μm.

	Large Class	
	Females (N = 4)	Males (N = 3)
Radular length	0.96±0.11 (0.84–1.08)	0.94±0.02 (0.92–0.96)
Radular width	0.12±0.01 (0.104–0.132)	0.12±0.01 (0.112–0.128)
Total rows of teeth	70±4 (66–75)	71.7±2.5 (69–74)
Rows of teeth forming	10±1.8 (8–12)	9.7±0.06 (9–10)
Central tooth width	27±3.5 (24–32)	26±2 (24–28)
	Small Class	
Radular length	0.67±0.05 (0.64–0.72)	0.61±0.05 (0.60–0.62)
Radular width	0.09±0.01 (0.08–0.10)	0.08±0.01 (0.07–0.09)
Total rows of teeth	69±3.6 (66–73)	69.7±6.7 (64–77)
Rows of teeth forming	7.5±0.6 (7–8)	8.7±0.6 (8–9)
Central tooth width	18±1.6 (16–20)	17.3±1.2 (16–18)

the end of the mantle cavity (Emc) and the point where the sperm duct (Sdu) arises from the spermathecal duct. (7) The spermathecal duct runs directly posterior from the mantle cavity to become the duct of the bursa (Dbu) directly posterior to which the thin-walled bursa copulatrix (Bu) swells as a large oval sac. (8) The sperm duct (Sdu) is a long convoluted duct transporting sperm from the spermathecal duct to the oviduct close to where the latter (Opo) enters the albumen gland (Ppo). (9) The usual seminal receptacle has been lost. When dissecting living specimens one often observes a bright pink sheen or glittering within a section of the oviduct (Ov) just posterior to the juncture of the sperm duct (Sdu) and oviduct (Osr, Fig. 47). This section of oviduct assumes the function of the seminal receptacle and is called the oviducal seminal receptacle (Osr). The duct may be considerably swollen with sperm (Fig. 47D, E). (10) Posterior to the sperm storage area (Osr) the oviduct is convoluted (Fig. 47B). (11) The bursa is posterior to the posterior pallial oviduct (Bu, Fig. 46). (12) The bursa is short.

Male reproductive system. The body of an uncoiled male is shown in Figure 48 without head but with kidney tissue (Ki) left in place. Measurements of relevant organs are given in Tables 19, 20. Important features are: (1) The gonad consists of relatively large lobes draining into a vas efferens (Ve, Fig. 49). (2) The seminal vesicle arises from the vas efferens (Ve) approximately one third of the way posterior from the anterior end of the gonad (Fig. 49). The juncture of the vas efferens and the beginning seminal vesicle may be swollen (Fig. 48). The coils of the seminal vesicle may be ventral to or dorsal to the lobes of the gonad. (3) The gonad is posterior to the stomach. (4) The prostate (Pr) overlaps the posterior end of the mantle cavity (Emc). (5) The penis has a glandular lobe (Fig. 42 Glo) on the concave edge near the base. (6) The penis has a stylet (Sty, Fig. 42).

The stylet requires some comment. It is very much like the stylet observed in *Robertsiella* (Davis & Greer, 1980). It is corneous and very fragile. In the living-moving male, it is very obvious at 50X, projecting from the tip of the penis (Fig. 42). However, in relaxed and fixed specimens it is not in evidence. Rarely at 50X one observed a pin-prick of light reflecting from the tip of the stylet mostly retracted into the penis. To observe the stylet in preserved specimens, the penis is cut from

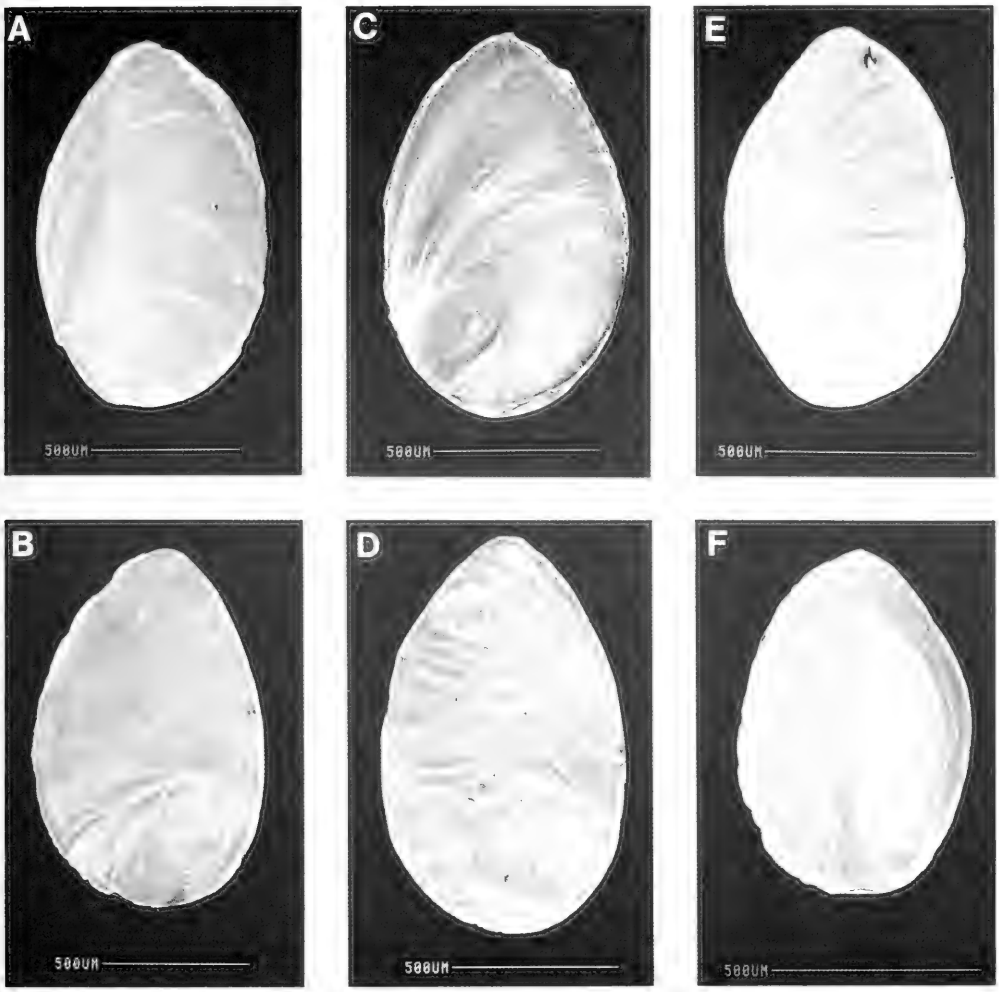

FIG. 44. Opercula of *Guoia viridulus* (C–F) and *G. fuchsianus* (A, B). C, D from large-class snails; E, F from small-class snails. A, C, E. Outer surfaces; B, D, F. Inner surfaces.

the animal, mounted in water on a slide with cover slip, and examined at 400 X (Fig. 50). The stylet is quickly dissolved when the penis is placed in Clorox (0.5% Na hypochlorite). Thus the stylets of *Robertsiella* and *Guoia* are not robust as those found in *Stenothyra* (Davis et al. 1986, 1988).

(7) The ejaculatory duct is massive and highly muscularized (Ej, Figs. 42, 51). It extends out of the base of the penis and from the posterior penis along the entire length of the dorsal neck. The circular ejaculatory duct is slightly left (Fig. 52), central, or to the right of the snout-neck mid-line (Fig. 51).

Digestive system. The digestive gland covers the posterior chamber of the stomach. The paired salivary glands are the standard triculine type. The radular sac does not coil up over the buccal mass.

The radulae of large-class snails are shown in Figures 53E–H and 54A–H. Teeth counts and statistics are given in Tables 21, 22. The most frequently encountered formula is:

$$\frac{3\text{-}1\text{-}3}{3\text{-}3};\ 3(4)\text{-}1[2]\text{-}3(4);\ 10\text{-}13;\ 8\text{-}10.$$

The inner pair of basal cusps of the central tooth are comparatively enormous. The cen-

TABLE 22. Cusp formulae for the radular teeth of *Guoia viridulus* with the percent of the radulae in which a given formula was found at least once.

Central Teeth		Lateral Teeth		Inner Marginal Teeth		Outer Marginal Teeth	
Large Class (N = 5 radulae)							
3-1-3 / 3-3	60%	3-1[2]-4	60%	8		8	40%
3-1-3 / 4-3	20%	4-1[2]-3	60%	9	20%	9	60%
3-1-4 / 4-4	20%	3-1[2]-3	40%	10	60%	10	40%
4-1-3 / 3-3	20%	3-1[2]-5	20%	11	80%	11	20%
4-1-4 / 3-3	20%	4-1[2]-4	10%	12	60%	12	0
5-1-5 / 3-3	20%			13	40%	13	20%
5-1-4 / 3-3	20%			14	20%	14	20%
5-1-5 / 3-3	20%			$\bar{X}$ = * 1.5±1.6 N = 50		10.4±2.3	
Small Class (N = 5 radulae)							
4-1-4 / 3-3	40%	4-2-3	100%	11	20%	11	0
4-1-3 / 4-3	40%	3-2-4	80%	12	60%	12	40%
4-1-5 / 3-3	40%	4-2-4	60%	13	80%	13	80%
3-1-5 / 4-4	40%	5-2-3	60%	14	100%	14	100%
3-1-3 / 4-3	20%	5-2-4	60%	15	80%	15	60%
3-1-4 / 4-4	20%	3-2-3	40%	16	60%	16	0
3-1-3 / 4-4	20%	4-2-4	40%				
4-1-4 / 4-4	20%	4-2-5	20%	$\bar{X}$ = *7.40±0.9 N = 30		6.3±0.6 N = 30	
4-1-3 / 3-4	20%						
4-1-4 / 4-3	20%						

*Mean ± standard deviation of cusp number for all teeth counted.

tral cusp at the anterior edge of the central tooth is frequently grooved or split.

The radulae of small-class snails are shown in Figures 54E–H and 55. Teeth counts and statistics are given in Tables 21, 22. The most frequently encountered formula is:

3(4)-1-(4)3; 3(4)-1[2]-3(4); 12-16; 12-15.
3-3

Comparing both size classes, as one would expect, the small-class has a smaller radula except for total rows of teeth, which are not significantly different between classes. The

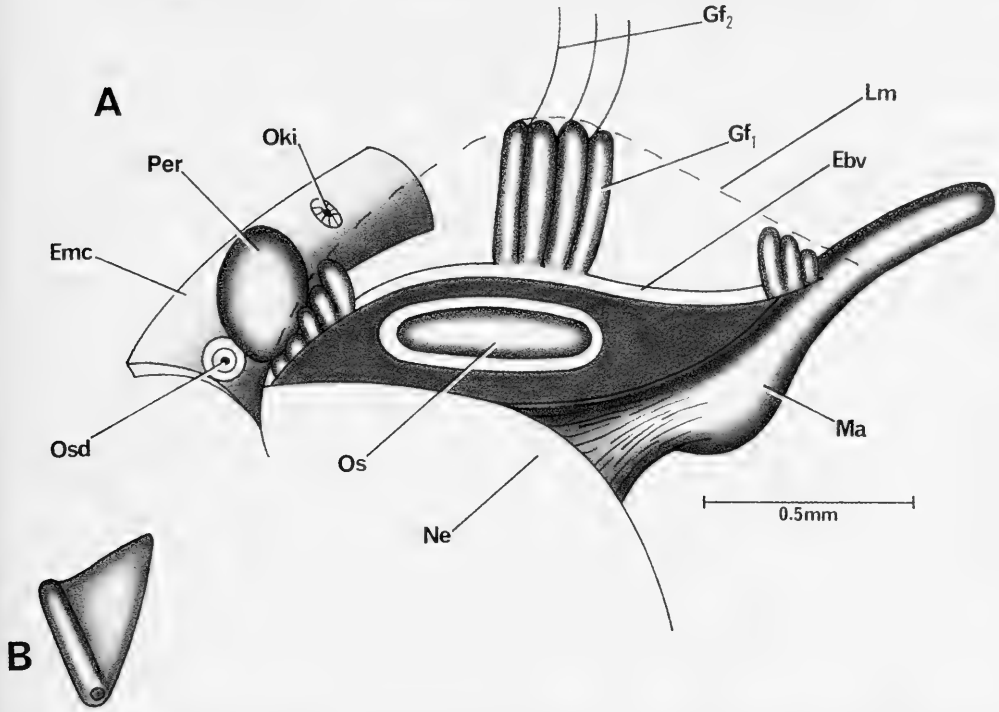

FIG. 45. Cut and reflected mantle to show mantle cavity organs of *Guoia viridulus* (A). Not all gill filaments are shown. B. Single gill filament.

morphologies of the teeth of both size classes are the same.

Nervous system. Measurements are given in Table 23. The RPG ratio is 0.229 ± 0.11, that is, the pleuro-supraesophageal connective is concentrated. The pleuro-subesophageal connective is lost in the fusion of ganglia. The osphradio-mantle nerve is elongated (>0.12 mm) thus compensating for the low RPG ratio.

Remarks

In comparing small- and large-class snails, no qualitative anatomical differences were found. The sizes of the bodies and organs were not significantly different. However, the small class animals were relaxed with sodium nembutol prior to fixing in 8% formalin and grading up to 70% ethyl alcohol. Presumably, the extended fixed bodies would measure longer than animals removed living from the shells and pinned out in a contracted state. Because the animals of the two size classes do not differ in details of anatomy, and because they live in microsympatry, they are considered the same species.

While the shells are significantly different in size, the range of variance along the second principal component is the same for both size classes indicating that the substantive difference is only one of size. What could account for this? Has this phenomenon been seen before? A similar situation was reported for *Tricula xianfengensis* Davis & Guo, 1986, in which large and small class mature snails with the same anatomy and shell shape were found in a narrow ditch alongside a kitchen garden in Xiaguan City, Yunnan Province. In both of these cases, we suspect that the size classes resulted from two different cohorts when egg laying occurred at different seasons. It is possible that eggs laid late in the season with growth extending into the cold weather months resulted in a small size class due to stunting caused by decreased rate of growth in the fall and winter. Presumably egg laying and growth in the late spring and summer would result in optimal growth. A comparative molecular genetic analysis of these size classes would be most instructive and desirable.

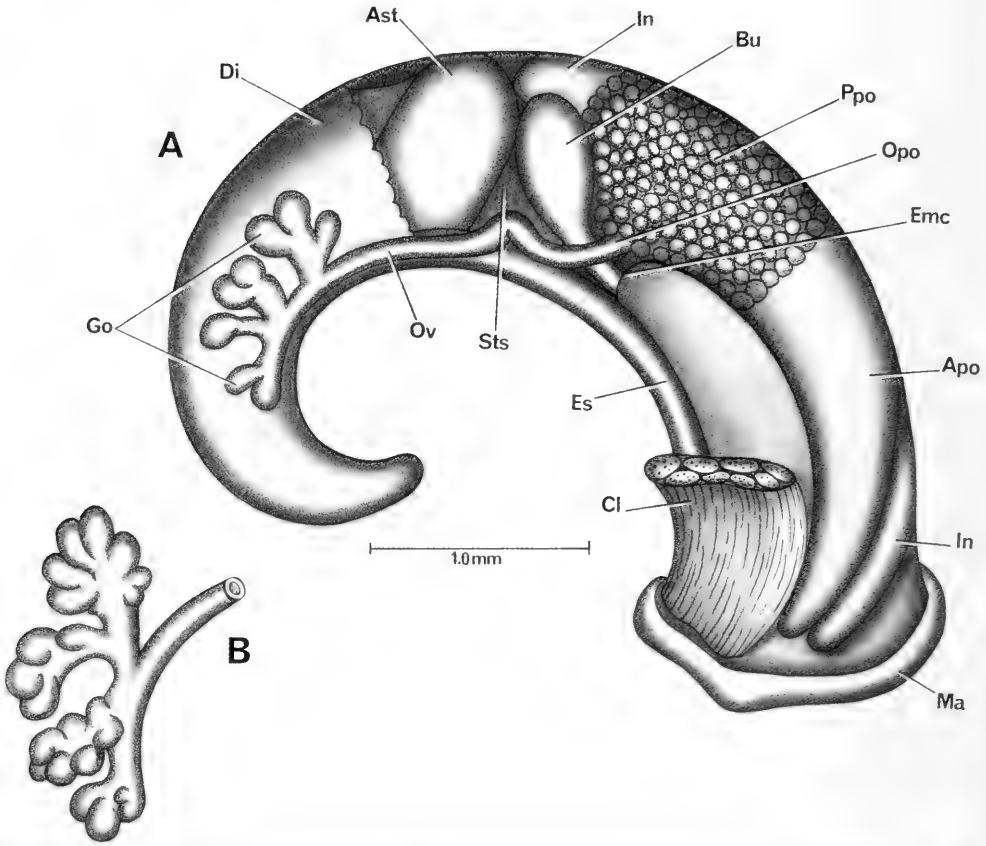

FIG. 46. Uncoiled female of *Guoia viridulus* with head and kidney tissue removed (A). B. Variation in gonad morphology.

TABLE 23. Lengths of neural structures from four individuals of large class *Guoia viridulus*. Mean ± standard deviation (range).

Cerebral ganglion	0.31±0.03	(0.26–0.32)
Cerebral commissure	0.07±0.02	(0.06–0.10)
Pleural ganglion		
Right (1)	0.15±0.04	(0.10–0.12)
Left	0.11±0.01	(0.10–0.12)
Pleuro-supraesophageal connective (2)	0.08±0.04	(0.04–0.14)
Pleuro-subesophageal connective	0	0
Supraesophageal ganglion (3)	0.12±0.02	(0.10–0.14)
Subesophageal ganglion	0.12±0.02	(0.10–0.14)
Osphradio-mantle nerve	0.15±0.03	(0.12–0.18)

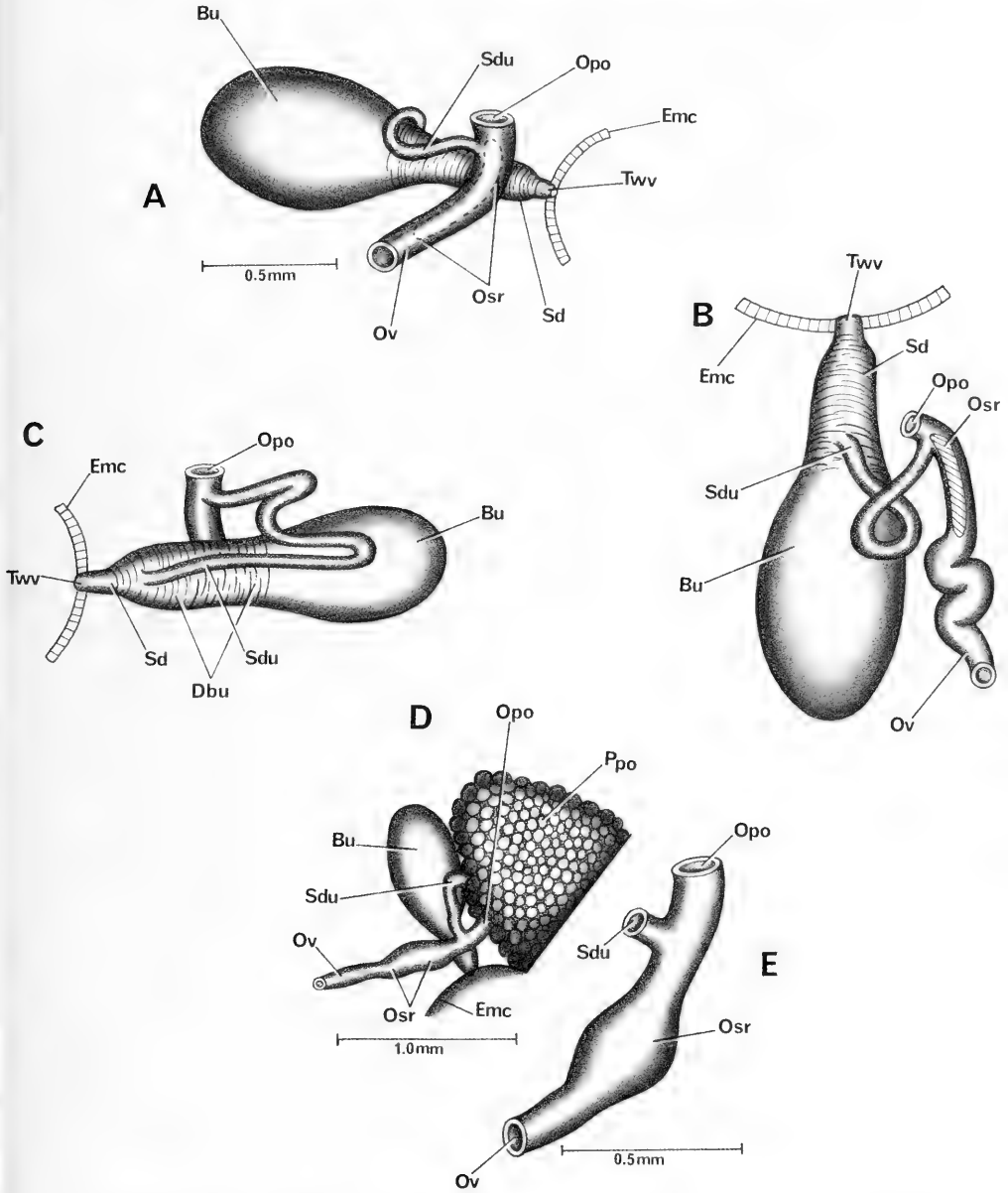

FIG. 47. Bursa copulatrix complex of organs of *Guoia viridulus*. Organs in A are in same orientation as in Figure 46. Figures B, C shows bursa flipped over to show dorsal aspect to reveal origin of elongated and twisting sperm duct (Sdu). Figure D most closely approximates organ position in Figure 46 but with tissue cleared away to show relationships of ducts relative to end of mantle cavity (Emc) and albumen gland (Ppo). E. Blown up section of oviduct within which sperm are stored (Osr).

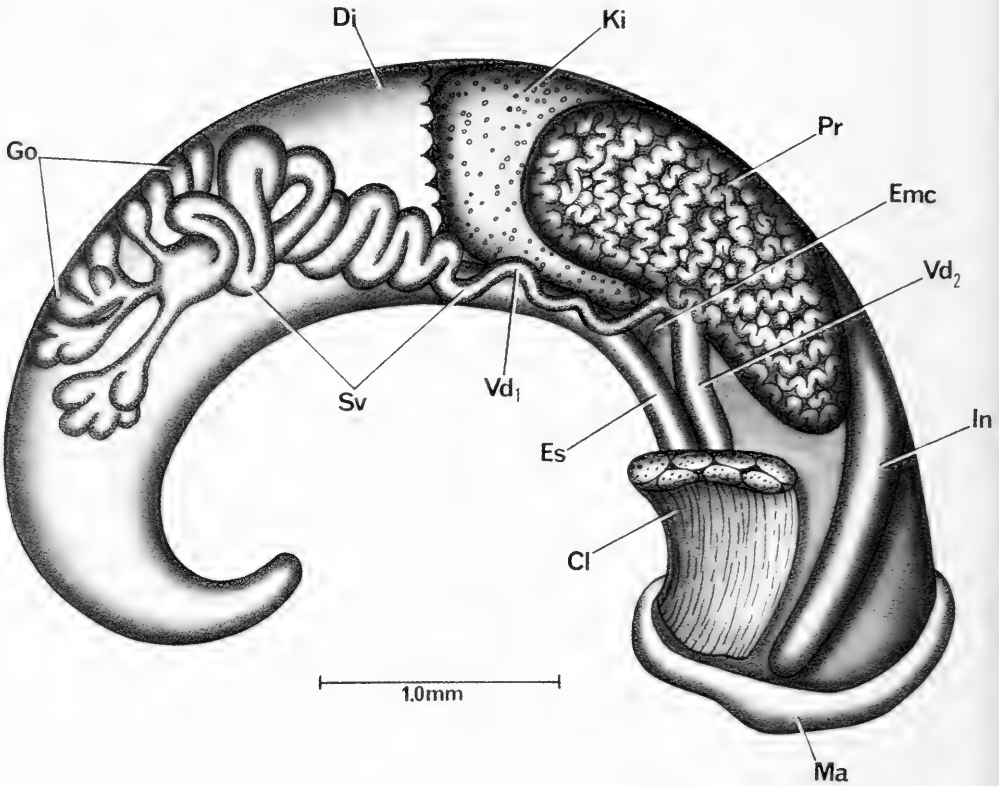

FIG. 48. Uncoiled male of *Guoia viridulus* with head removed.

Guoia fuchsianus (Moellendorff, 1885)

Lithoglyphus fuchsianus Moellendorff, 1885: 169, 170
Lithoglyphus, fuchsianus, Moellendorff, 1888: 140. pl. 4, fig. 5, 5a–b.
Lithoglyphus fuchsianus, Thiele, 1928
Lithoglyphopsis fuchsianus, Yen, 1939

Type locality. Moellendorff, 1885: Hsiang-tan provinciae sinensis Hunan.
Moellendorff, 1888: Hsiangtan and Hêngshan-hsien; Hunan.
Yen, 1929: Heng-dshou-fu, Hunan

Types. Lectoype: SI, 4127. Figured by Yen (1939: pl. 4, fig. 10); paralectotypes: SMF, 4128. Figured here, Figure 36E, F.

Habitat

Xiangjiang River at Baisha, Hengshan County, 25°58′22″N, 112°45′55″E. Figure 1,

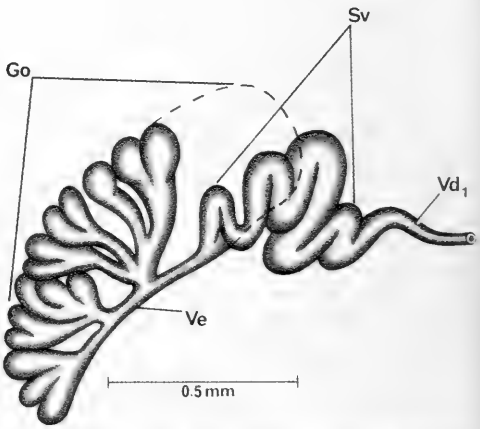

FIG. 49. Male gonad with anterior lobes cut away to show origin of vas deferens from vas efferens (Ve), and seminal vesicle (Sv) that lies dorsal to gonad. Dashed line indicates extent of gonad cut away.

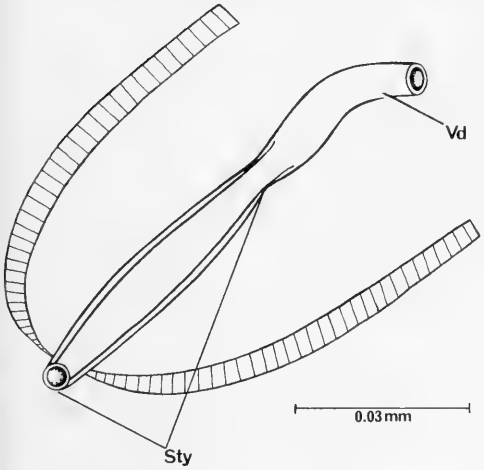

FIG. 50. Tip of penis of preserved *Guoia viridulus* as observed under compound microscope at 400X. Sty, Stylet; Vd, Vas deferens.

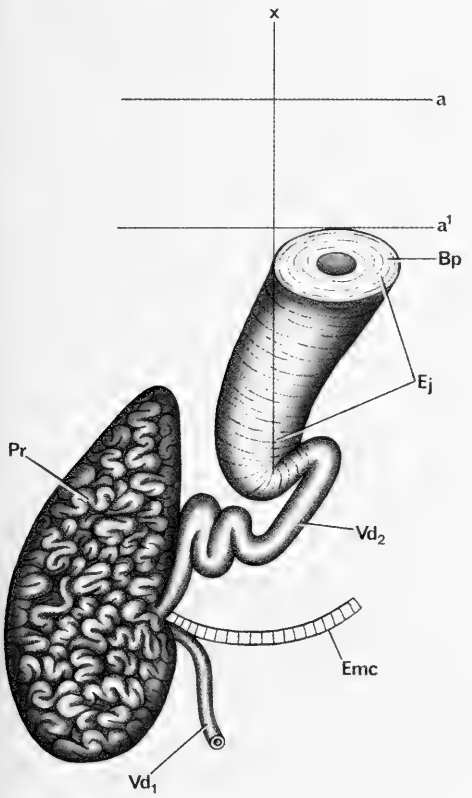

FIG. 51. Relationship of ejaculatory duct to mid-line (x) of snout-neck of *Guoia viridulus* (from small-class specimen).

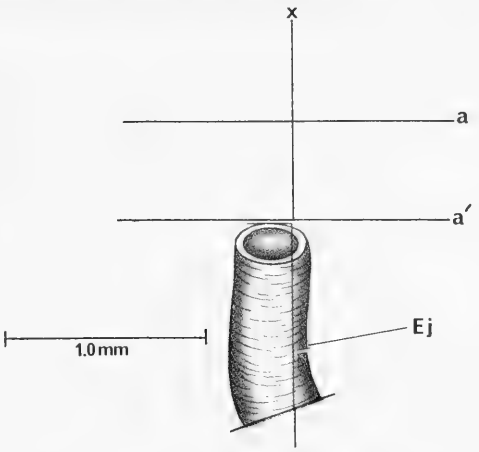

FIG. 52. Ejaculatory duct of *Guoia viridulus* slightly to left of snout-neck mid-line.

locality 9. Collected by Davis, Chen, & Wu, October 1985, field number D85-75; by Chen & Wu, 1986. Snails sympatric with *Lithoglyphopsis modesta* on stones at the bottom of the river in 2.0–2.5 m depth. Catalog numbers are: D86-B, ANSP 373145; A12661. D85-75, ANSP 373146; A12662.

Description

Shell. Shells (Figs. 36D–F, 39G–I, 56C–F, 57, 58) are small (Table 24), and generally as described for large class *L. viridulus* with the following differences. The outer lip of *G. fuchsianus* is only slightly sinuate. There is a more pronounced umbilical depression. The inner lip is separated slightly from the body whorl by a narrow depressed groove, the basal crescent (Fig. 57, Bc) paved with shell growth increments from body whorl to the inner lip (Figs. 57, 58). The penultimate whorl of the species is proportionally shorter than that of *G. viridulus* and the third whorl less wide.

Overall, however, the shells have such intrapopulation variance that the species are difficult to differentiate on the basis of shells alone. Some 10% of the shells from one population are virtually indistinguishable from shells of the other. An example of variance in shape for *G. fuchsianus* is shown in Figure 58A–D, in which camera lucida drawings of two shells from collection D86-B are illustrated with two shells from historic ANSP 98205. Because most of the historic *G. fuch-*

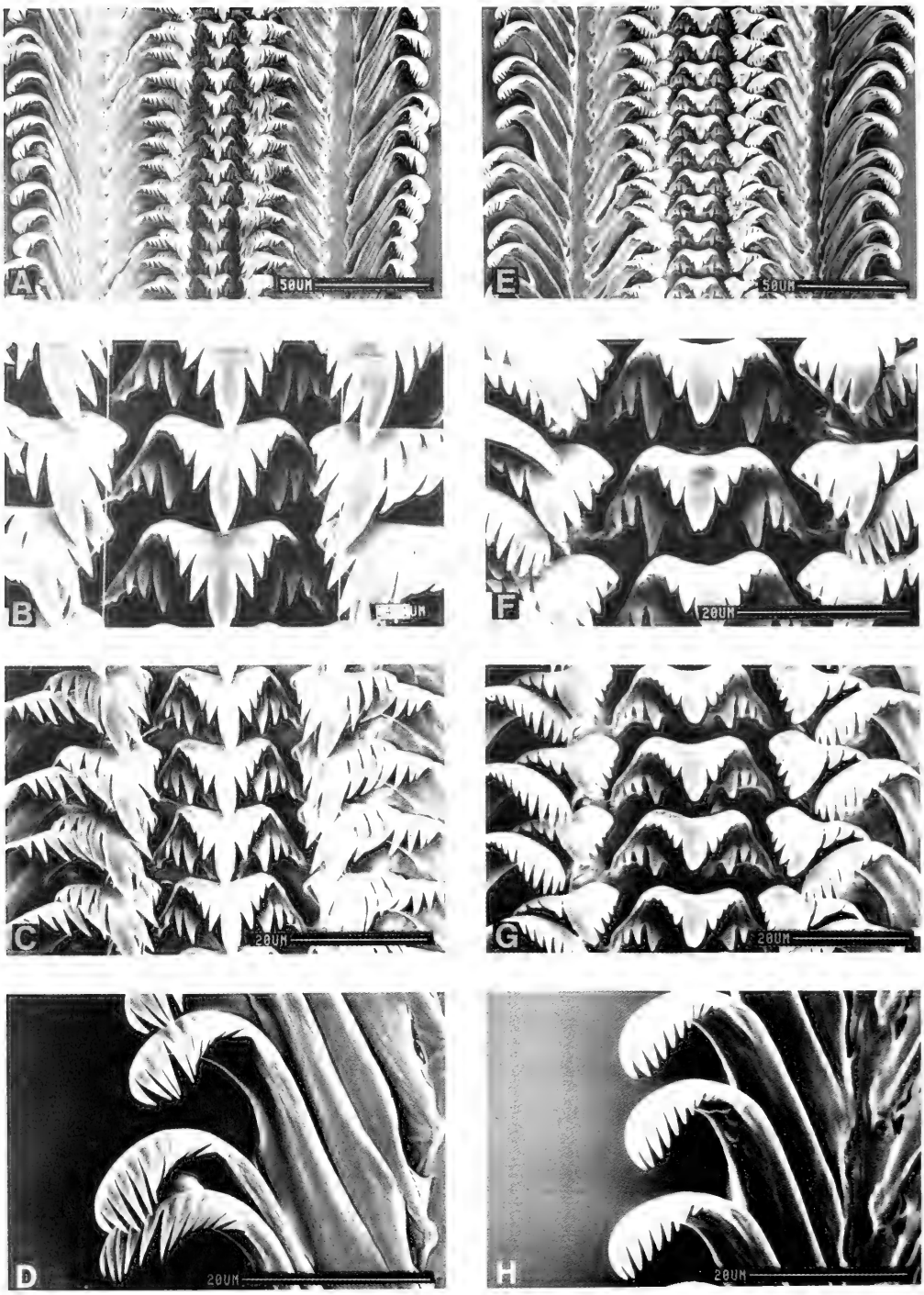

FIG. 53. Radulae of large size-class *Guoia viridulus* (E–H) and *G. fuchsianus* (A–D). A, E. = portions of radulae. B–C, F–G. Central, lateral and inner marginal teeth; D, H. Outer marginal teeth.

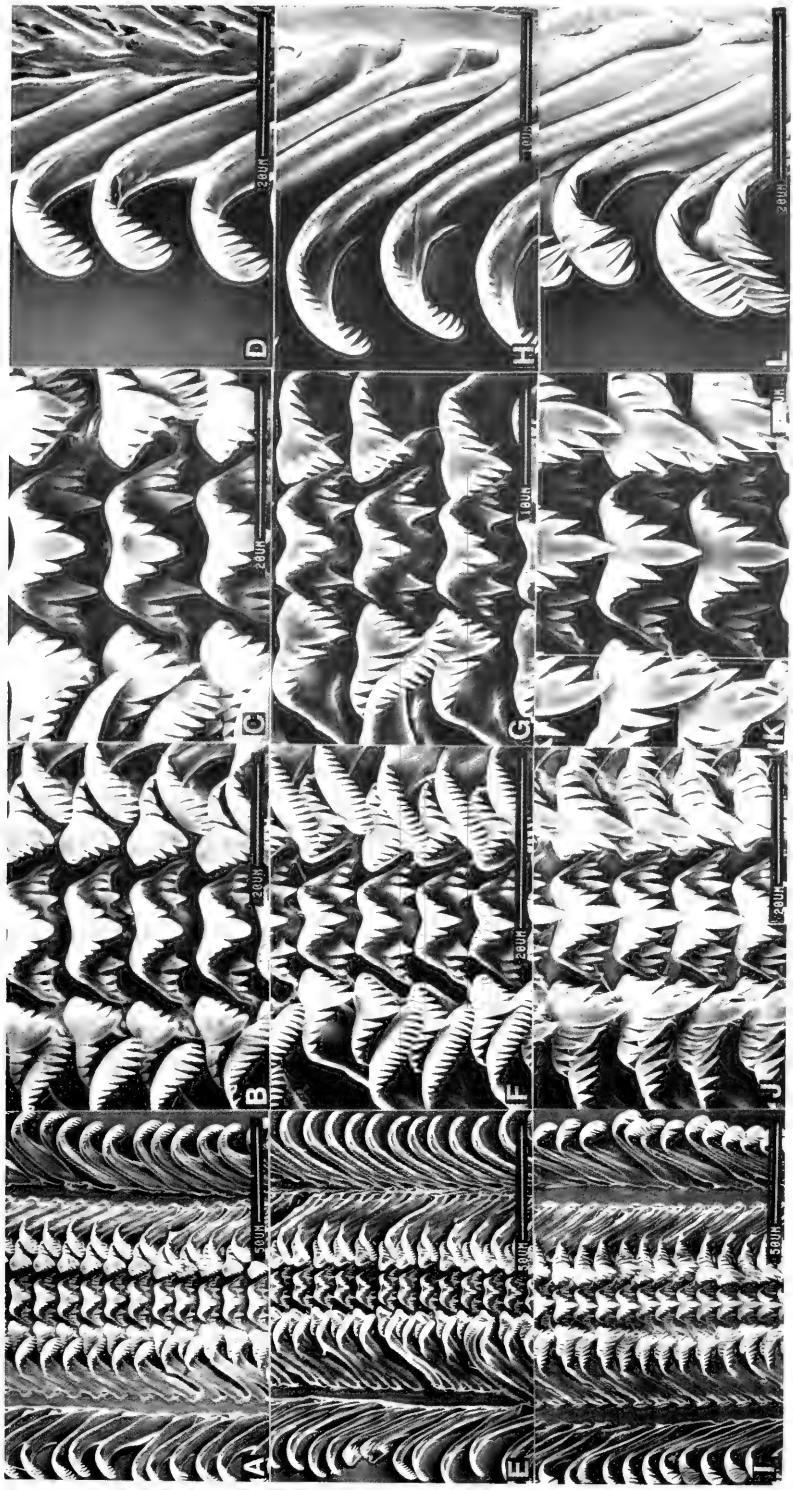

FIG. 54. Radulae of large size-class (A–E) and small size-class (E–H) *Guoia viridulus*; and *Guoia fuchsianus* (I–L). A, E, I. Segments of radulae; B, C, F, G, J, K. Central, lateral and inner marginal teeth; D, H, L. Outer marginal teeth.

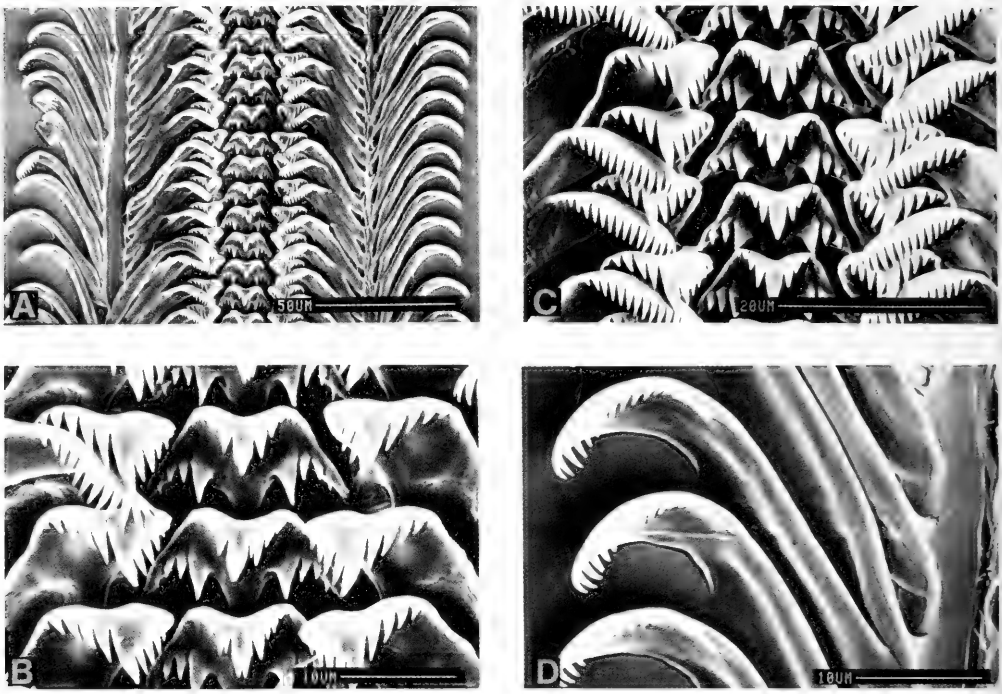

FIG. 55. Radula of small size-class *Guoia viridulus*. A. Segment of radula; B, C. Central, lateral and inner marginal teeth; D. Outer marginal teeth.

sianus had eroded shells so that characters 1, 7, and 8 could not be measured, the multivariate analyses involving all populations of *G. viridulus* and *G. fuchsianus* without these three characters did not provide differentiation of species or populations. Individuals were simply spread out along a size gradient. The historic *G. fuchsianus* specimens are larger than field-collected specimens. Still, basing size on the length of body whorl and width, this species is somewhat smaller than *G. viridulus* (compare Tables 24 and 16).

Anatomy. In 1985, most of the snails were sexually immature so that complete anatomical data could not be gathered. Organ measurements and counts that could be made are presented in Table 25. Sufficient observations were made to demonstrate that *Guoia fuchsianus* is a distinct species, not to be confused with *G. viridulus*. Only anatomical features unique to this species will be presented here.

(1) The duct of the bursa (Dbu, Fig. 59B) is a considerably swollen duct that narrows before opening into the capacious bursa (Bu). (2) The duct of the bursa is comparatively long: 0.35 mm for *G. fuchsianus*, 0.12 for *G. viridulus*. (3) The sperm storage area (Sr) is a swelling that bulges out of the sperm duct (Sdu) where the sperm duct opens into the oviduct (Ov, Fig. 59). (4) The buccal mass is longer (0.64–0.70 mm for *G. viridulus*, 0.70–0.72 for *G. fuchsianus*). (5) The central anterior cusp of the central tooth of the radula and flanking cusps are considerably more posteriorly projecting than those of *G. viridulus* (compare Fig. 54C, G, K). The anterior cusp support and cusps of *G. fuchsianus* form a prominent triangular-shaped projection posteriorly. This, coupled with the elongated central cusp, causes the tip of the central cusp to overlap the tooth immediately posterior. A ratio will demonstrate the difference between taxa. The length from anterior central edge to posterior tip of the central cusp divided by width of the anterior central cusp yields 0.75–0.88 for *G. fuchsianus* and 0.57–0.71 for *G. viridulus*. (See Tables 26, 27 for radular statistics.) (6) Measurements of neural structures are given in Table 28. The RPG ratio is 0.42, that is, the pleuro-supraesophageal

connective is moderately concentrated (contrast the concentrated condition in *G. viridulus*, RPG ratio = 0.23).

The penis of two individuals had a well-developed stylet but no glandular lobe or pronounced ejaculatory duct. The prostate was fully developed and penis length was 1.5–1.6 mm long. Because the penis of *G. viridulus* with a pronounced glandular lobe exceeded 3.0 mm in length, it is possible that the ones we observed for *G. fuchsianus* were immature, underdeveloped, or, conversely, atrophied. We are not convinced that the penis of *G. fuchsianus* lacks a glandular lobe or ejaculatory duct.

Remarks

Conchological characters that separate this species from *G. fuchsianus* are few and discussed above. Refer also to the multivariate analysis presented under *G. viridulus*.

Whereas it is clearly desirable to have more anatomical data, the available data substantiate the placement of this species in the genus *Guoia*. The six anatomical differences provided above convince us that we are dealing with a distinct species. The penial data are not of sufficient quality to permit us to make a definitive comment except that a stylet is definitely present.

Neotricula Davis, 1986

Type Species. Lithoglyphopsis aperta Temcharoen, 1971: 103–104, pl. 7, fig. 14.

Tricula aperta (Temcharoen), Davis 1979, 1980.

Type locality. Mekong River at Ban Na on Khong Island, Laos

Assigned Species. N. aperta (type for genus assigned in Davis et al., 1986a); *N. burchi* (Davis, 1968) [Thailand]; *N. cristella* (Gredler, 1887); *N. dianmenensis* Davis & Chen, sp. nov.; *N. duplicata* Davis & Chen, sp. nov.; *N. lilii* Chen & Davis, sp. nov.; *N. minutoides* (Gredler, 1885); N = 7.

Diagnosis. Shells small to medium sized, ovate conic, smooth. Central tooth of radula with several anterior cusps (contrast single triangular blade as in *Delavaya*). The oviduct runs from the gonad to the pallial oviduct without making a loop or twist. The spermathecal duct does not enter the pericardium but opens into the posterior mantle cavity; it is a narrow duct throughout. The duct of the bursa enters a U-shaped bend to run into a discrete sem-

TABLE 24. Shell measurements (mm) for populations of *Guoia fuschianus*. Mean ± standard deviation (range).

	Baisha		ANSP: 98205, 45961	
	Males (N = 2)	Females (N = 3)	Whole Shell (N = 1)	Eroded Shell (N = 8)
1. No. Whorls	4.0	4.0	4.0	—
2. Length (L)	2.26 (2.48, 2.76)	2.79±0.12 (2.72–2.79)	2.96	—
3. Width (W)	2.20 (2.08, 2.32)	2.36±0.07 (2.32–2.44)	2.32	2.44±0.12 (2.28–2.60)
4. L body whorl	2.26 (2.16, 2.36)	2.45±0.02 (2.44–2.48)	2.60	2.70±0.12 (2.56–2.88)
5. L penultimate whorl	0.24 (0.20, 0.28)	0.23±0.05 (0.20–0.28)	0.24	0.30±0.04 (0.24–0.36)
6. W penultimate whorl	0.90 (0.80, 1.00)	0.92±0.07 (0.88–1.00)	0.86	1.01±0.08 (0.92–1.12)
7. W 3rd whorl	0.46 (0.40, 0.52)	0.47±0.02 (0.44–0.48)	0.40	—
8. L last three whorls	2.60 (2.48, 2.72)	2.77±0.09 (2.72–2.88)	2.92	—
9. L aperture	1.68 (1.56, 1.80)	1.85±0.08 (1.76–1.92)	2.00	1.93±0.08 (1.80–2.04)
10. W aperture	1.38 (1.28, 1.48)	1.45±0.02 (1.44–1.48)	1.52	1.54±0.08 (1.40–1.60)
11. W columellar shelf	0.18 (0.16, 0.20)	0.25±0.02 (0.24–0.28)	0.28	0.28±0.04 (0.20–0.32)
W ÷ L	0.84 No var.	0.85±0.01 (0.84–0.85)	0.78	—

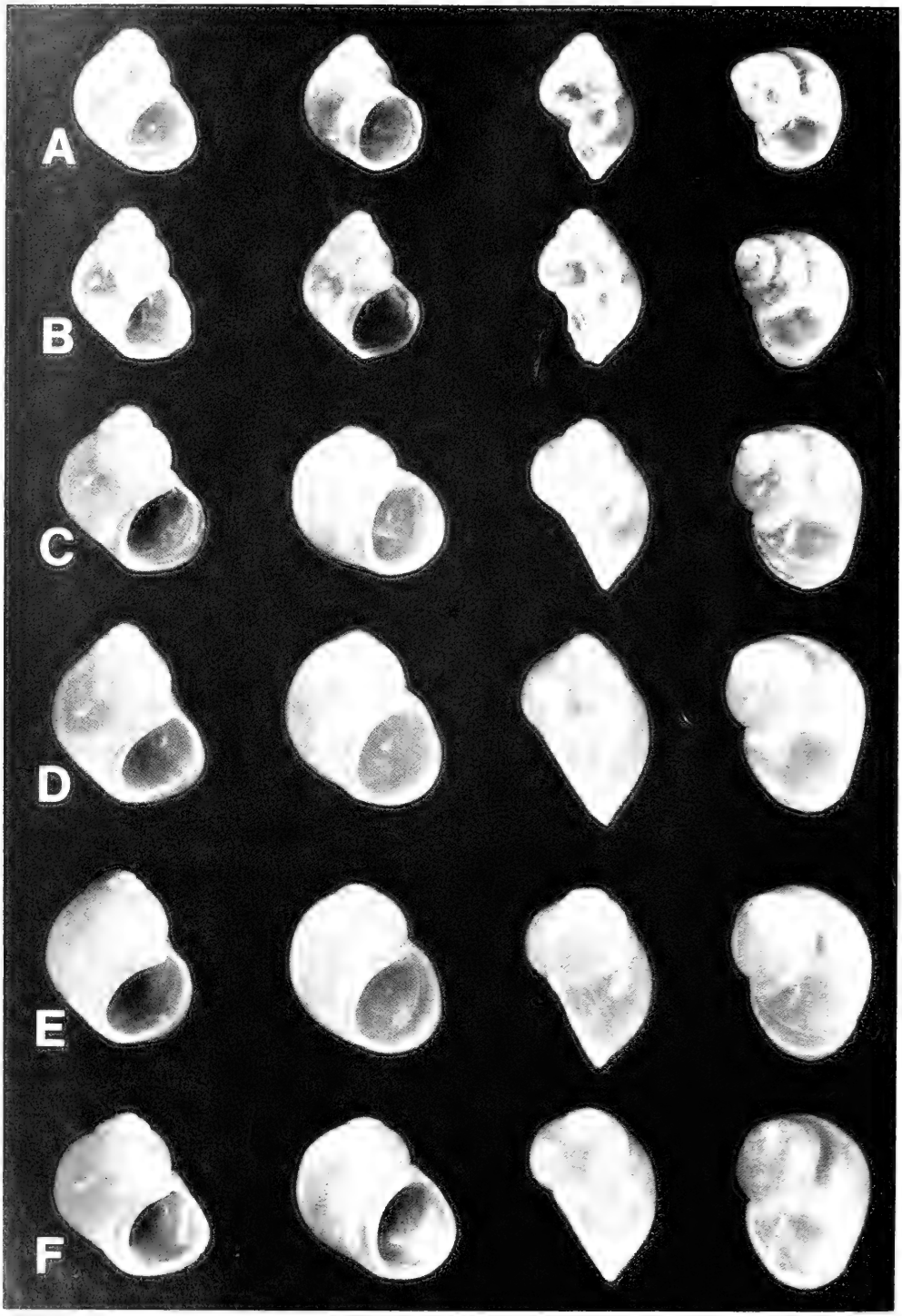

FIG. 56. Shells of small-class *Guoia viridulus* (A, B) for comparison with shells of *G. fuchsianus* (C–F). Shell A is 2.36 mm long; others printed at same scale. All are from females except E, which is from a male.

TABLE 25. Lengths (mm) or counts of non-neural organs of female *Guoia fuschianus*.

	1.	2.	3.	$\bar{X}$.
Body	4.9			
Digestive gland	2.1			
Bursa copulatrix	0.68	0.54		0.61
Duct of bursa	0.34	0.36		0.35
Buccal mass	0.70	0.72		0.71
Mantle cavity	2.0	1.70	2.20	1.97±0.25
Gill	1.8	1.50	2.00	1.77±0.25
Osphradium	0.9	0.7	0.84	0.81±0.10
Osphradium ÷ gill	0.50	0.47		0.48
No. gill filaments	25	22	25	24.0±1.7
Gf_2	0.16	0.22		0.19
Gf_1	0.48	0.46		0.47
Total Gf	0.64	0.68		0.66

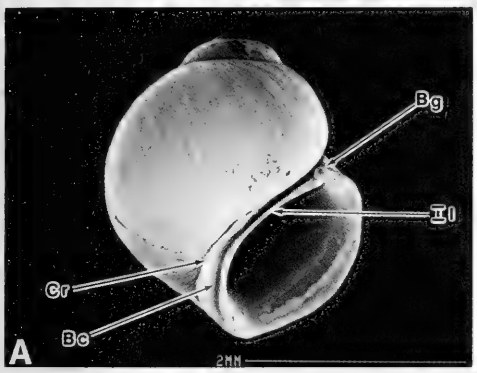

FIG. 57. SEM photograph of a shell of *Guoia fuchsianus*.

inal receptacle in most species. The duct of the seminal receptacle may shorten or become lost. The spermathecal duct joins the duct of the bursa (contrast joining the bursa as in *Halewisia*). A slender duct, the sperm duct, connects the U-shaped duct to the oviduct.

Neotricula cristella (Gredler, 1887)

Paralectotypes. SMF 4242; plate 4, fig. 3, in Yen, 1939

Type locality. Kiangshi Province, "in Quellwasser."

Synonymy. Hydrobia cristella Gredler, 1887
Tricula cristella, Yen, 1939
Neotricula cristella, this paper

Habitat

Material for this paper was collected from Mojingtai, Hengshan Mountain, Nanyue Town, Hengshan County, Hengyang Prefecture; 27°15′N, 112°39′13″E; Figure 1 site 1. Snails came from a small stream 0.4 km down the mountain road from the Mojingtai Hotel towards the Banshan Ting Temple. Collections number = D85-73; the collection was made by Dr. Chen Cui—E, 28 Sept. 1985.

Depository

Specimens are deposited in ZAMIP, M0001; in ANSP 368774 and A12146.

Description

Shell. Shells are small, narrowly ovate-conic, of 5.0 to 5.5 whorls (Figs. 60H–L, 61A–D). Lengths range from 2.40 to 2.84 mm (Table 29). The aperture is ovate; there is no umbilicus. The whorls at the suture are smooth (not crenulated). SEM analyses reveals a faint trace of spiral microsculpture on the adapical surface of the whorls at the suture. The inner lip is arched and widely separated from the body whorl, the distance increasing from abapical to adapical. Thus, the adaptical end of the aperture is widely separated from the body whorl. The adapical end of the aperture has a wide notch; there is no internal notch groove; there is no sinus. There is no abapical spout. In side view, the outer lip is slightly sinuate; it is not scooped forward. The inner lip lacks nodes, teeth or notches. The inner lip is thin throughout. In side view, the inner lip is straight on some shells, angled to form a deflection angle in others. Within the

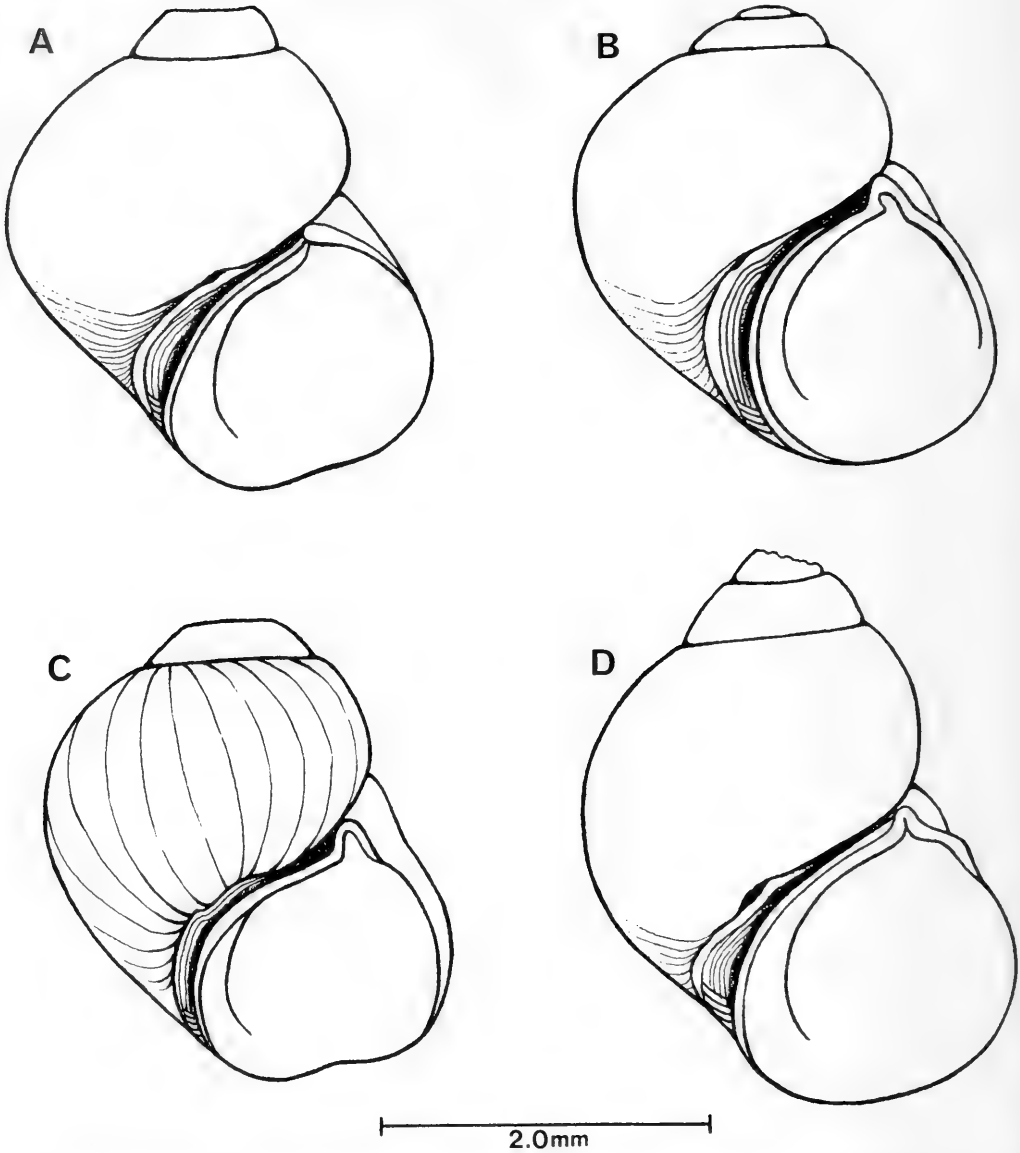

FIG. 58. Illustration of four shells of *Guoia fuchsianus* aided by camera lucida. Shells A, D from ANSP 98205 (historic collections); shells B, C from D86-B.

body whorl, the columella is smooth. There is a slight varix on some shells, no varix on others. In apertural view, the lip projects beyond the base of the shell 0.34 ± 0.06 mm. SEM analysis shows the protoconch to be slightly wrinkled (Fig. 61C, D).

External features. The head is not pigmented. There are no granules about the eyes (Fig. 62). There is a patch of white granules where the mantle margin meets the neck. The operculum is corneous, paucispiral and appears to have two layers, a larger outer layer and a

TABLE 26. Radular measurements (mm) and counts for *Guoia fuchsianus.* Mean ± standard deviation (range). In mm except for width of central tooth in μm.

	Female (N = 5)	Male (N = 2)
Radular length	0.90±0.05 (0.84–0.98)	0.80 (no variation)
Radular width	0.11±0.003 (0.11–0.12)	0.11 (0.10–0.11)
Total rows of teeth	72.6±4.3 (66–78)	68.5 (68–69)
No. rows of teeth forming	23.8±1.1 (23–25)	22.5 (22–23)
Central tooth width	23.2±2.3 (22–26)	22 (no variation)

TABLE 27. Cusp formulae for the radular teeth of *Guoia fuschianus* with the percent of radulae in which a given formula was found at least once. N = 3 radulae.

Central Teeth		Lateral Teeth		Inner Marginal Teeth		Outer Marginal Teeth	
4-1-4 / 2-2	66%	3-1[2]-4	100%	10	33%	10	33%
		4-1[2]-3	66%	11	66%	11	66%
3-1-3 / 3-3	33%	3-1[2]-3	66%	12	100%	12	100%
		4-1[2]-4	33%			13	33%
		2-1[2]-4	33%	$\bar{X}$=* 11.4±0.7 N = 26		11.3±0.8 N = 30	

*Mean ± standard deviation of cusp number for all teeth counted.

TABLE 28. Lengths (mm) of neural structures of *Guoia fuchsianus.* Mean (data). N = 2

Cerebral ganglion	0.29 (0.28, 0.30)
Cerebral commissure	0.12 (no variation)
Pleural ganglia	
Right (1)	0.11 (0.10, 0.12)
Left	0.10 (no variation)
Supraesophageal connective (2)	0.16 (0.12, 0.20)
Subesophageal connective	0
Supraesophageal ganglion (3)	0.11 (0.10, 0.12)
Subesophageal ganglion	0.10 (no variation)
Osphradio-mantle nerve	0.12 (0.10, 0.14)
RPG ratio (2 ÷ 1+2+3)	0.42 (0.38, 0.46)

narrower inner layer (Fig. 61E, F). The internal attachment pad is prominent but only 40 to 50% the width of the operculum.

Mantle cavity. Mantle cavity organs are shown in Figure 63A. Organ measurements and counts are given in Table 30. The osphradium is slightly anterior to mid-gill; it is oval and small. There are 13 to 15 gill filaments, of which only seven or eight are fully developed, that is, with both Gf_1, and Gf_2 elements prominent. The anterior five filaments are widely separated and without the Gf_2 part. Gf_2 is long. The longest gill filaments are 0.38 ± 0.09 mm long. The largest gill filaments in lateral view are modestly domed (Fig. 63B). The pericardium (Pe), opening of the kidney into the mantle cavity (Oki) and the opening of the spermathecal duct (Sd) into the mantle cavity are shown in relationship to each other (Fig. 63A).

Female reproductive system. An uncoiled female without head and with kidney tissue removed is shown in Figure 64. Measurements of organs are given in Table 30. Important features are: (1) The gonad (Go) is posterior to the stomach, is small and consists of few lobes. (2) The bursa copulatrix (Bu) is round and situated directly posterior to the albumen gland (Ppo). (3) The albumen gland is of normal size. (4) The bursa copulatrix complex of organs is shown in Figure 65. Organs in Figure 65A have the same orientation as in Figure 64. The bursa is short. (5) The duct of the seminal receptacle (Dsr) is a U-shaped con-

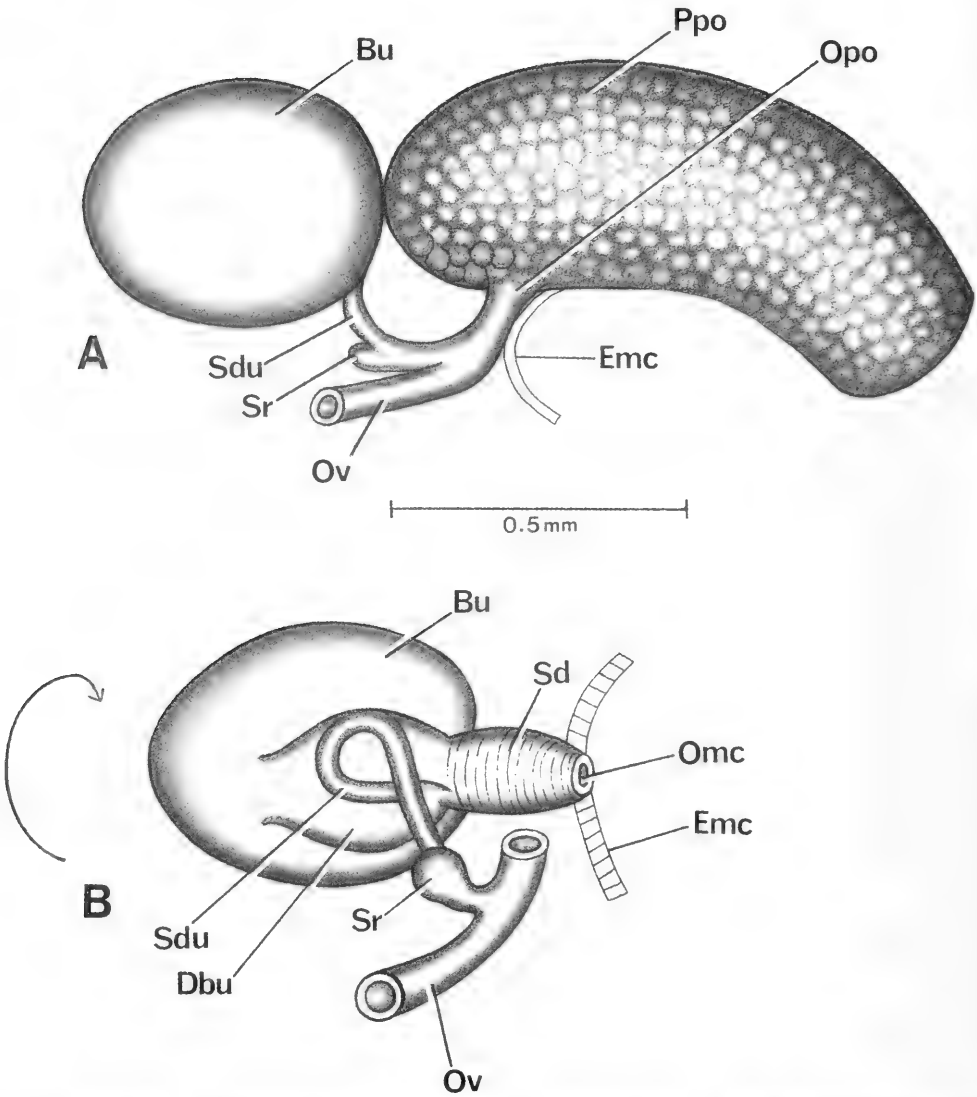

FIG. 59. Aspects of female reproductive system of *Guoia fuchsianus*. A. Female reproductive system oriented in same position as in Figure 46A. Anterior pallial oviduct not shown. B. Bursa of A turned 180° over, as indicated by the arrow, to show the relationships of ducts attaching to the bursa (Bu) and oviduct (Ov).

tinuation of the duct of the bursa (Fig. 65B, C). It turns to the right side and tucks dorsal to the bursa. (6) The duct of the seminal receptacle (Dsr) is long. The seminal receptacle (Sr) is a comparatively minute bulb. (7) The spermathecal duct (Sd) is short and opens into the posterior end of the mantle cavity (Emc). (8) The spermathecal duct opens into the bottom of the U-shaped bend formed by the duct of the bursa at a point opposite the opening of the duct of the seminal receptacle (Fig. 65A, B).

Male reproductive system. An uncoiled male snail without head and with kidney tissue removed is shown in Figure 66. Measurements of organs are given in Table 30. Important

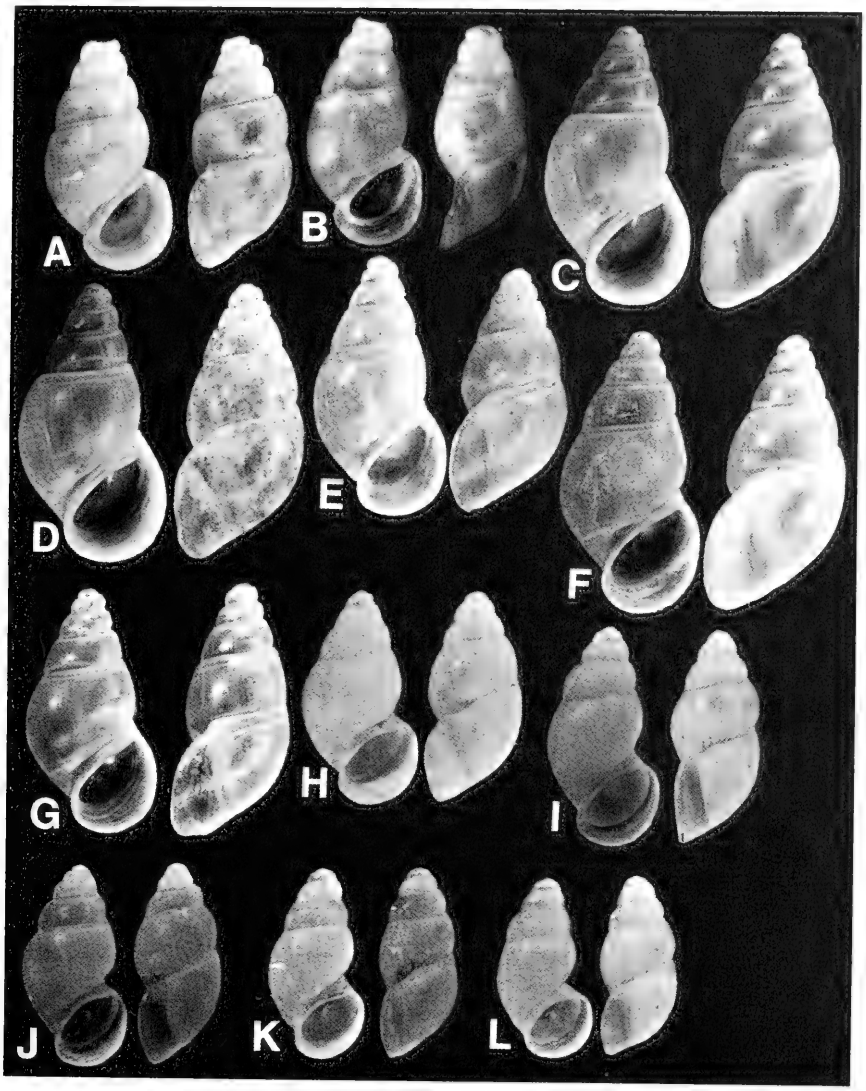

FIG. 60. Shells: *Neotricula lilii*, A, B. Paratypes. *N. minutoides*, C–G. *N. cristella*, H–L. Length of shell A is 3.12 mm; others printed to same scale.

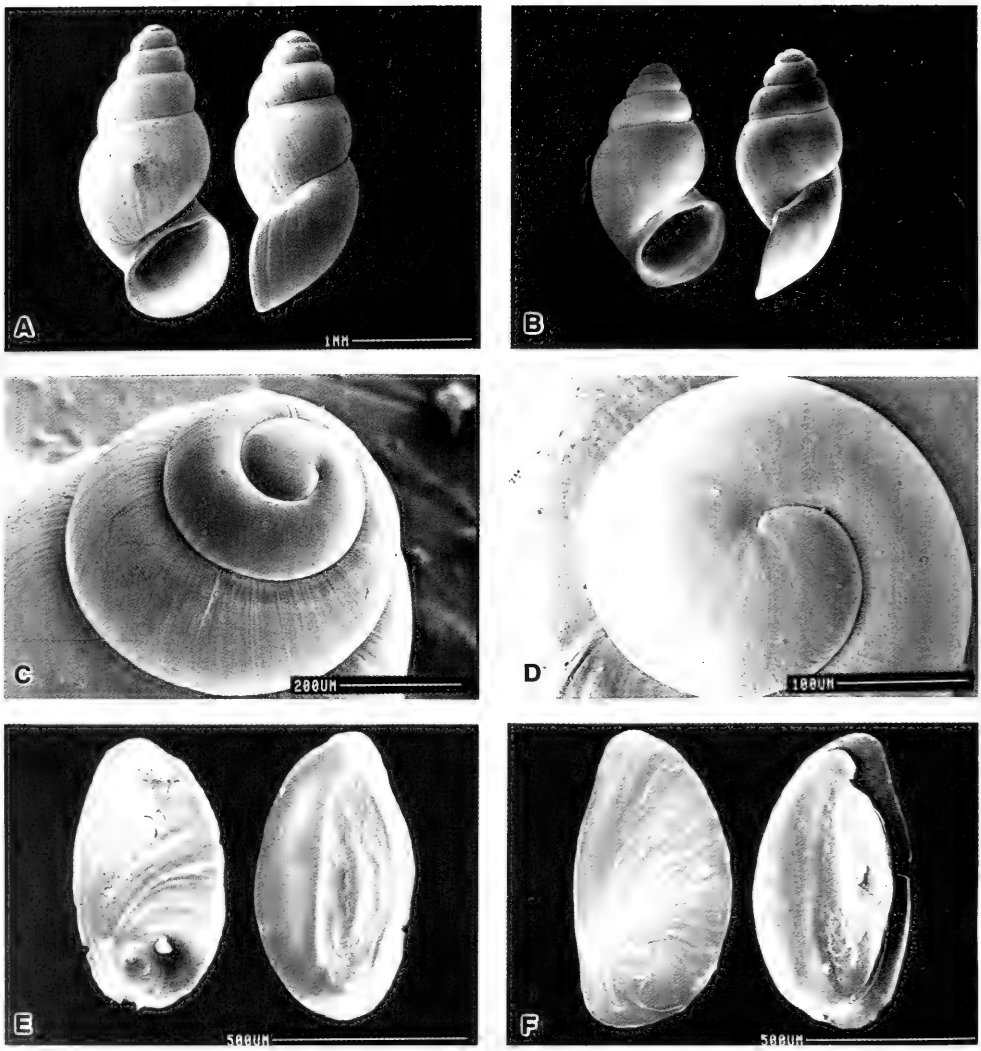

FIG. 61. SEM photographs of shells (A–D) and *opercula* (E, F) of *Neotricula cristella*. C, D. Details of apical whorls. In E, F, inside surface of opercula shown on right side.

TABLE 29. Shell measurements (mm) for male and female *Neotricula cristella*. Mean ± standard deviation (range). N = number measured.

	Females		Males
Whorls	5.0–5.25 (N = 4)	5.5 (N = 2)	5.0 (N = 3)
Length (L)	2.64±0.10	2.78	2.37±0.02
	(2.52–2.76)	(2.72–2.84)	(2.36–2.40)
Width (W)	1.33±0.09	1.38	1.21±0.08
	(1.24–1.44)	(1.36–1.40)	(1.12–1.28)
L body whorl	1.85±0.11	1.86	1.61±0.02
	(1.76–2.00)	(1.84–1.88)	(1.60–1.64)
L penultimate whorl	0.40±0.01	0.45	0.36±0.03
	(0.38–0.40)	(0.40–0.50)	(0.34–0.40)
W penultimate whorl	0.90±0.02	0.94	0.83±0.03
	(0.88–0.92)	(0.88–2.00)	(0.80–0.86)
L last three whorls	2.46±0.11	2.56	2.20±0
	(2.36–2.60)	(2.52–2.60)	—
L aperture	1.21±0.08	1.14	1.07±0.06
	(1.16–1.32)	(1.12–1.16)	(1.00–1.12)
W aperture	0.81±0.05	0.80	0.69±0.02
	(0.76–0.88)	—	(0.68–0.72)
Tip apical whorl (W)	0.14±0.02	—	—
	(0.12–0.16) N = 6*	—	—
Diameter 1st whorl	0.28±0.02	—	(0.26–0.30) N = 6*
x**	0.37±0.02	0.34±0.06	
	(0.36–0.40) N = 3*	(0.28–0.40)	

* all whorl classes
**distance from base of body whorl to abapical tip of aperture

features are: (1) The gonad (Go) is posterior to the stomach. (2) The prostate (Pr) overlaps the posterior end of the mantle cavity (Emc). (3) The seminal vesicle (Sv) arises from the vas efferens (Ve) about mid-gonad. (4) The seminal vesicle is coiled lateral to the gonad, like a spring or coils in a knot dorsal to the gonad posterior to the stomach. It does not continue onto the stomach. (5) The anterior vas deferens (Vd_2) leaves the prostate at the posterior end of the mantle cavity. (6) The penis is simple but with a very elongated penial filament. (Pf, Fig. 67). (7) The vas deferens is highly coiled passing through the center of the penis. There is no ejaculatory duct in the base of the penis or in the neck. (8) The orientation of the base of the penis (Bp) to the snout-neck midline (x) and the posterior edge of the eye bulges is shown in Figure 62. The long axis of the penial base varies from 70° to 90° from "x" as shown.

Digestive system. The digestive gland covers the posterior chamber of the stomach of females but is posterior to the stomach of males. Radular statistics are given in Tables 31 and 32. There are 99 ± 3.4 rows of teeth along a radula 0.54 mm long. The most frequently encountered formula is

$$\frac{3(2)\text{-}1\text{-}(2)3}{3(2)\text{-}(2)3};\ 3\text{-}1[2]\text{-}3(4);\ 14\text{-}17;\ 12\text{-}15.$$

SEM photographs of radulae and teeth are given in Figures 68, 69. Central teeth are featured in Figure 68C–F; they are typical of the generalized triculine type. The morphology of the entire lateral tooth is shown in Figure 68A, B. The one unusual feature seen in the radula of this species involves the dominant cusp of the lateral tooth, the "1" of the 3-1-3; it is deeply divided, almost forming two cusps. (Fig. 68A–F, 69A–C).

Nervous system. Measurements are given in Table 33. The RPG ratio of 0.36 shows that the dorsal nerve ring is moderately concentrated.

Remarks

Conchologically, this species differs from all other *Neotricula* by having a shell with (1)

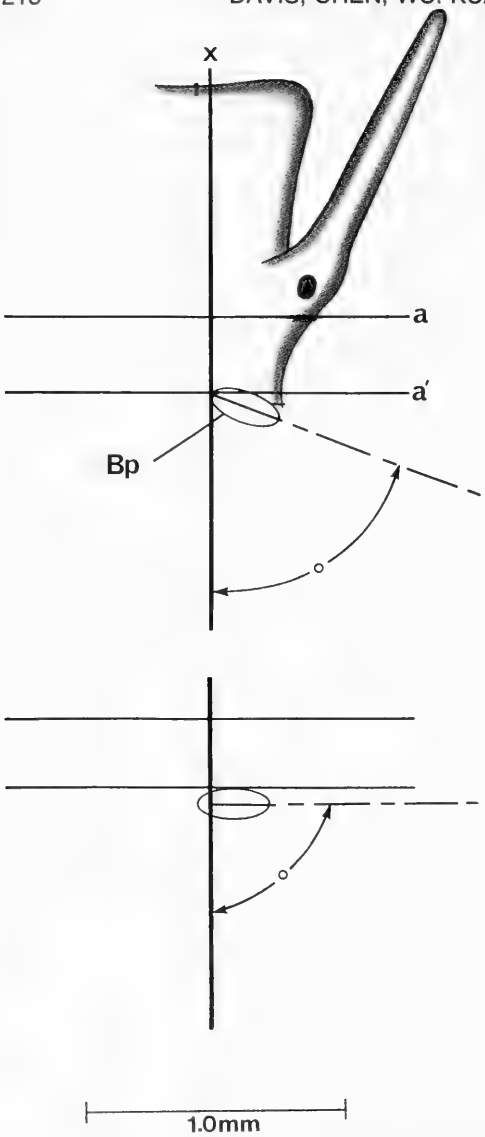

FIG. 62. Head of a male snail of *Neotricula cristella* showing the orientation of long axis of the penial base (Bp) to snout-neck mid-line x.

the inner lip widely separated from the body whorl, and (2) the adapical end of the aperture widely separated from the body whorl.

The multivariate analysis involving all species of Triculinae with shells closely resembling those of *Tricula* or *Neotricula* indicates different affinities depending on the analysis used. The phenogram based on distance coefficients (Fig. 153) shows linkage with *Gammatricula chinensis*. The differences are: (1) The sutures of *N. cristella* are smooth; those of *G. chinensis* are crenulated. (2) The adapical aperture of the former has a notch; of the latter, no notch. (3) The inner lip of the former is thin, of the latter, thick. (4) The inner lip of the former is widely separated from the body whorl, of the latter, narrowly separated. (5) The adapical end of the aperture of the former is widely separated from the body whorl, of the latter, slightly separated. (6) There is no abapical outer lip deflection angle in the former, a slight one in the latter.

The minimum spanning tree (Fig. 154) based on distance coefficients yields a different closest relationship, one with *Tricula hudiequanensis*. However, (1) *T. hudiequanensis* has a medium length shell (*N. cristella* has a small shell). (2) The adapical aperture of the former does not have a notch. (3) The outer lip of the former, in side view, is scooped forward; it is straight in the latter. (4) The inner lip of the former is thick; it is thin in the latter. (5) The inner lip and adapical aperture are not as greatly separated from the body whorl in the former as in the latter.

The most distinguishing anatomical character (considering only species of *Neotricula*) is the long penial filament. This species shares with *N. lilii* the character-state of having very many rows of teeth on the radula; with *N. minima*, the state that the digestive gland covers the posterior chamber of the stomach. The U-shaped continuation of the duct of the bursa into the duct of the seminal receptacle is shared with *N. burchi* of northwest Thailand and *N. aperta* of the lower Mekong River.

Neotricula dianmenensis Davis & Chen, sp. nov.

Holotype: ZAMIP-M0034, Figure 70A.
Paratypes: ANSP 373143, A12659; ZAMIP MOO04. Figure 70B–D; Figure 71A, B.

Type Locality: Jiepai Village, Dianmen Town, Hengshan County, Hengyang Prefecture. 27°15′16″N, 112°33′31″E. Figure 1, Site 5. Field collection D85-80.

Collection Date: October 1985.

Etymology: Named for the town of Dianmen.

Habitat

300 m above sea level. Snails were collected from a small stream 20–25 cm wide and

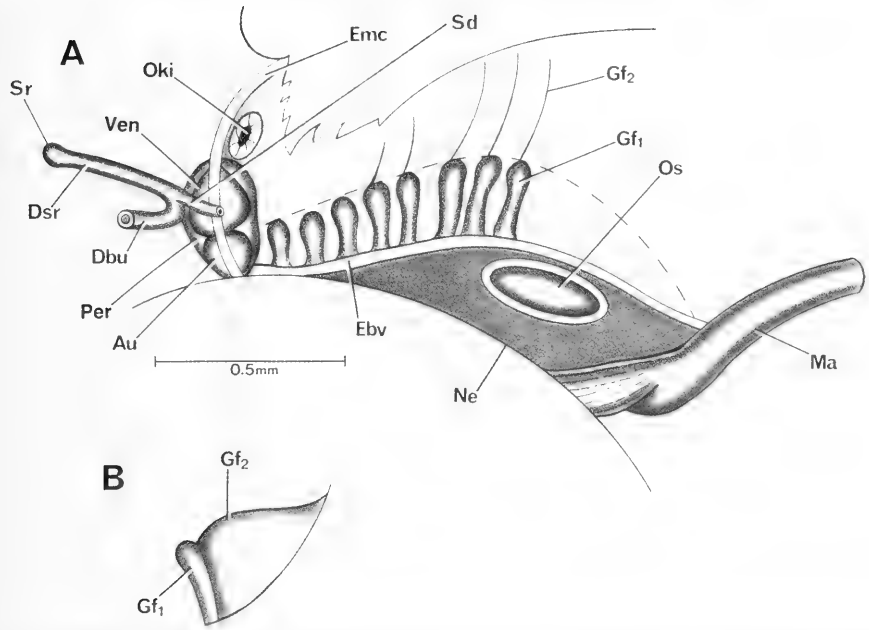

FIG. 63. A. Mantle cavity structures of *Neotricula cristella* showing the relationship of the gill to pericardium (Pe) and openings of the kidney (Oki) and spermathical duct (Sd). B. Single gill filament

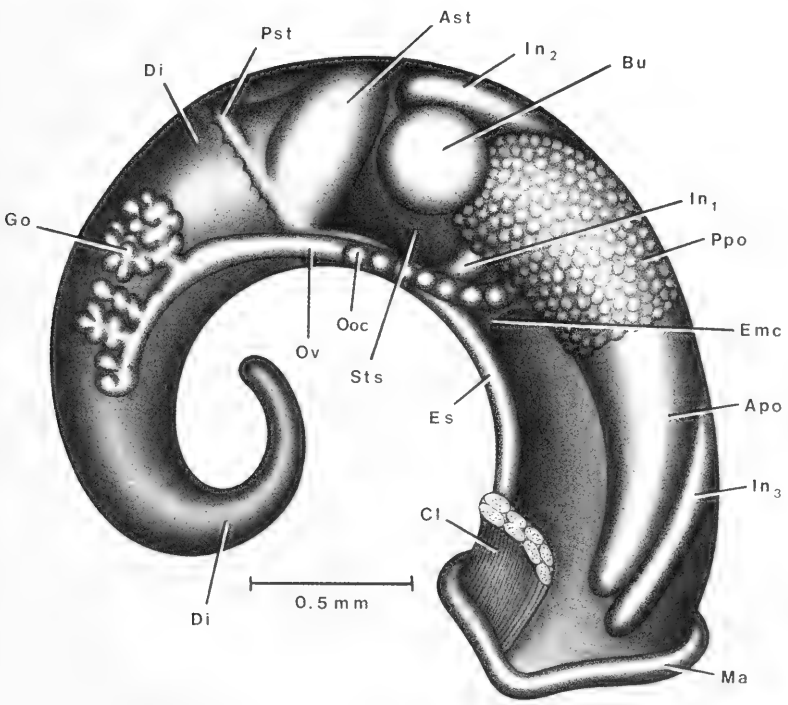

FIG. 64. Uncoiled female *Neotricula cristella* with head and kidney tissue removed.

TABLE 30. Lengths (mm) or counts of non-neural organs and structures of *Neotricula cristella*. Mean ± standard deviation, (range).

	Females (N = 5)	Males (N = 3)
Body	4.60±0.17 (4.34–4.76)	4.17±0.32 (3.80–4.36)
Gonad	0.62±0.08 (0.54–0.70)	1.03±0.21 (0.80–1.20)
Digestive gland	2.06±0.17 (1.90–2.30)	1.93±0.31 (1.60–2.20)
Posterior pallial oviduct (= albumen gland)	0.86±0.06 (0.76–0.90)	—
Anterior pallial oviduct (= capsule gland)	0.96±0.09 (0.90–1.10)	—
Total pallial oviduct = OV	1.82±0.13 (1.66–2.00)	—
Bursa copulatrix = BU	0.38±0.05 (0.34–0.46)	—
Duct of BU	0.19±0.05 (0.14–0.26)	—
BU ÷ OV	0.21±0.04 (0.17–0.20)	—
Seminal receptacle	0.10±0.02 (0.08–0.12)	—
Duct of seminal receptacle	0.19±0.04 (0.16–0.24)	—
Mantle cavity	1.11±0.28 (0.76–1.44)	1.00±0.07 (0.96–1.08)
Gill (G)	0.92±0.28 (0.60–1.28)	0.85±0.05 (0.80–0.90)
Osphradium (OS)	0.23±0.08 (0.16–0.36)	0.24±0.02 (0.22–0.26)
OS ÷ G	0.26±0.08 (0.18–0.37)	0.29±0.03 (0.26–0.33)
No. of filaments	13.6±0.9 (13–15)	13.3±1.2 (12–14)
Gf_2	0.23±0.06 (0.16–0.30)	—
Gf_1	0.16±0.03 (0.12–0.20)	—
Total Gf = TGF	0.38±0.09 (0.26–0.50)	—
Gf_2 ÷ TGF	0.61±0.04 (0.56–0.65)	—
Prostate	—	0.81±0.02 (0.80–0.90)
Seminal vesicle	—	0.38±0.07 (0.40–0.44)
Penis	—	1.53±0.18 (1.40–1.74)
Buccal mass	0.50±0.06 (0.44–0.56)	—

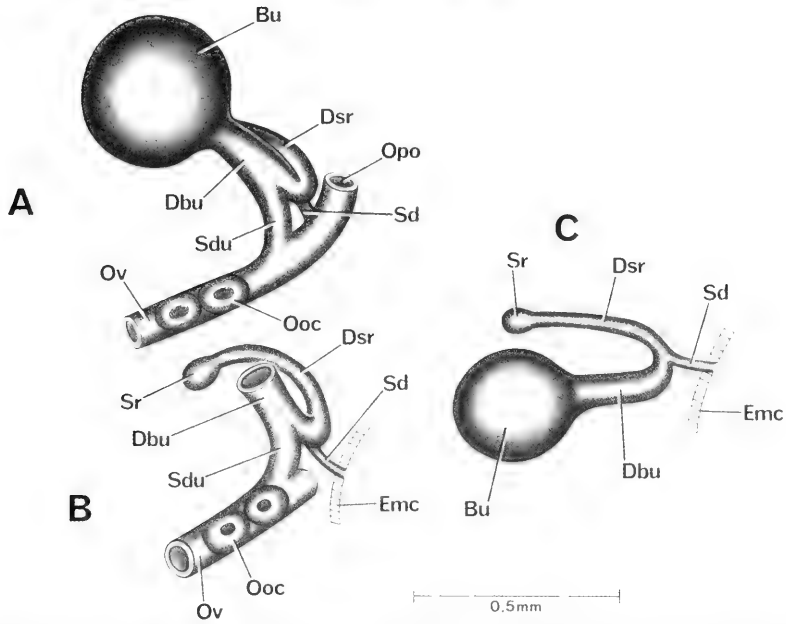

FIG. 65. Details and variation of bursa copulatrix complex of organs of *Neotricula cristella*. Figure A is in same orientation as in Figure 64. B. Bursa removed to show entire seminal receptacle (Sr) and duct (Dsr). C. Bursa rotated to show interconnection of Dbu, Dsr and the spermathical duct (Sd).

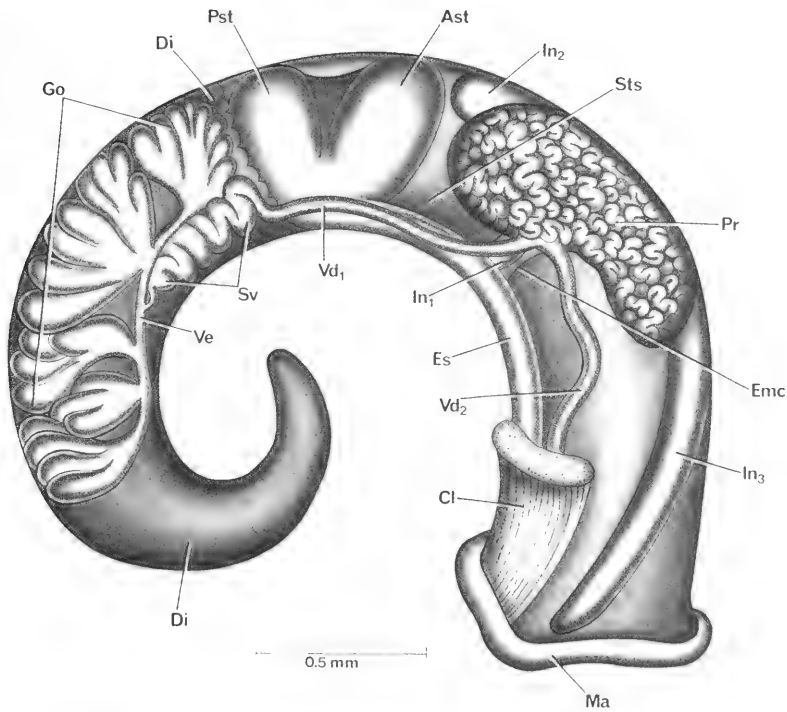

FIG. 66. Uncoiled male of *Neotricula cristella* without head or kidney tissue.

TABLE 31. Radular statistics for *Neotricula cristella*. Mean ± standard deviation (range). N = number used. In mm except for width of central tooth in μm.

	Males and females (N = 4)
Shell length	2.58±0.30 (2.16–2.88)
Radular length	0.54±0.05 (0.48–0.59)
Radular width	0.06±0.002 (0.056–0.060)
Total rows of teeth	99±3.4 (95–103)
No. rows of teeth forming	23±6.9 (16–32)
Central tooth width	12.9±0.8 (12.3–14)

TABLE 33. Lengths (mm) of neural structures of *Neotricula cristella*. Mean ± standard deviation (range). N = 3.

Cerebral ganglion	0.23±0.06 (0.16–0.28)
Cerbral commissure	0.05±0.01 (0.04–0.06)
Pleural ganglion	
Right (1)*	0.08±0.02 (0.06–0.10)
Left	0.10±0.04 (0.06–0.14)
Pleuro-supraesophageal connective (2)*	0.11±0.01 (0.10–0.12)
Pleuro-subesophageal connective	0.09±0.06 (0.02–0.14)
Supraesophageal ganglion (3)*	0.11±0.01 (0.10–0.12)
Subesophageal ganglion	0.11±0.01 (0.10–0.12)
Osphradio-mantle nerve	0.05±0.03 (0.02–0.08)
RPG ratio* = 2 ÷ 1+2+3	0.36±0.01 (0.36–0.38)

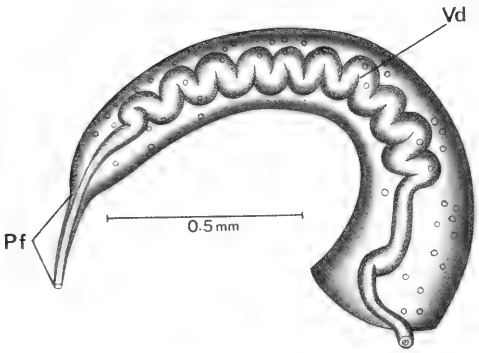

FIG. 67. Penis of *Neotricula cristella*.

10–15 cm deep. The flow was slow; the water was clean and cool. The stream flows down from Nanyue Mountain. The bottom of the stream was paved with small rocks, sand, and leaves. At stream side was short, scrubby vegetation. There were some 50 snails per stone.

Description

Shell. The shells are small, ovate-conic, of 5.0 to 5.5 whorls (Figs. 70A–D, 71A, B). Because the apices of most mature snails are eroded, it is not possible to be precise about lengths;

TABLE 32. Cusp formulae for the radular teeth of *Neotricula cristella* with the percent of radulae in which a given formula was found at least once.

Central Teeth		Lateral Teeth		Inner Marginal Teeth		Outer Marginal Teeth
3-1-3 / 3-3	93%	3-1[2]-3	79%	11	—	7%
		3-1[2]-4	21%	12	—	21%
2-1-2 / 2-2	21%			13	14%	71%
		4-1[2]-3	14%	14	43%	79%
4-1-4 / 3-3	9%	4-1[2]-4	7%	15	71%	50%
				16	71%	—
				17	50%	—
				18	21%	—
				$\bar{X}$ * = 15.1±2.7 N = 138		13.6±1.2 N = 127

*Mean ± standard deviation of cusp number for all teeth counted.

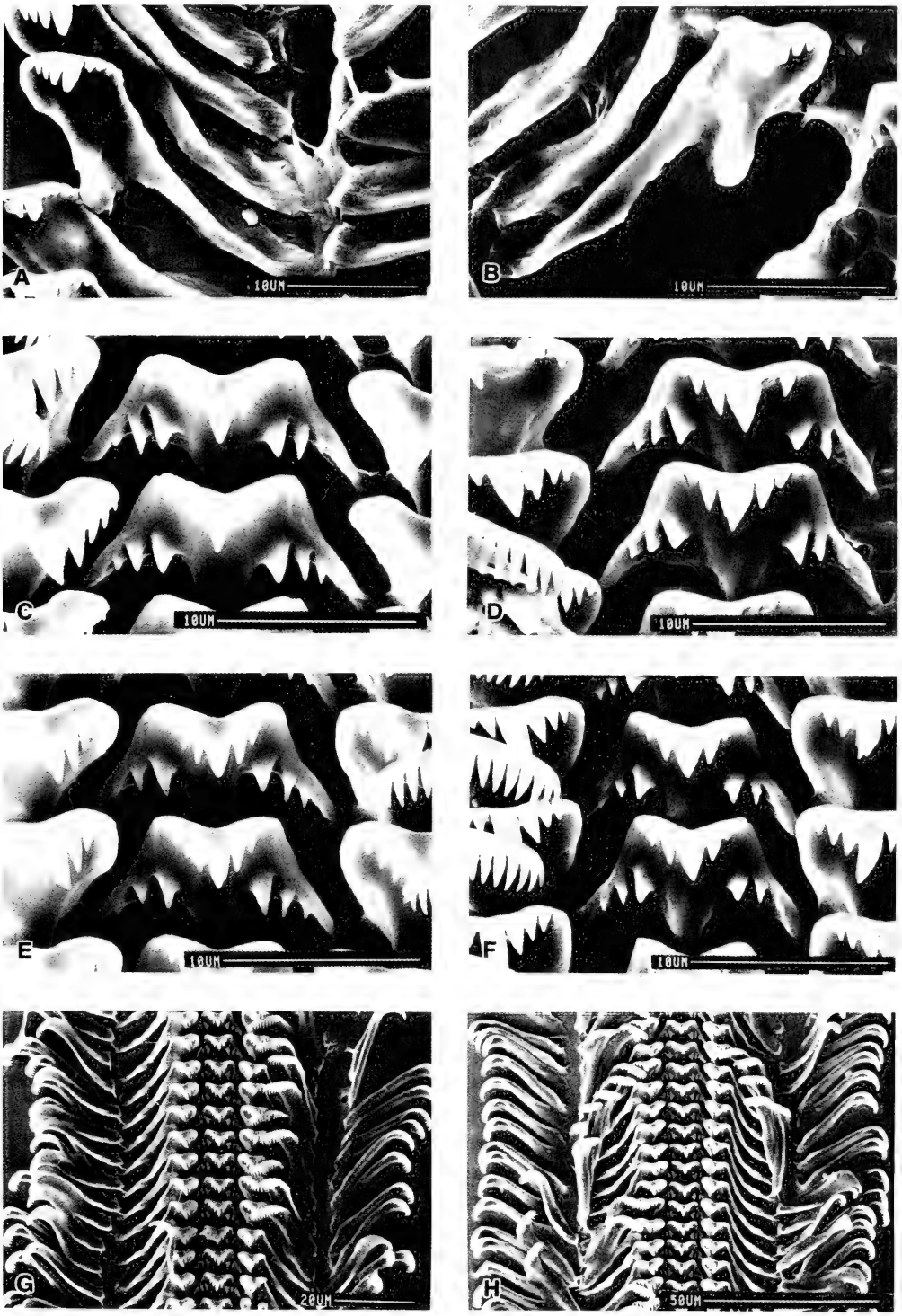

FIG. 68. Radula of *Neotricula cristella*. See text for details.

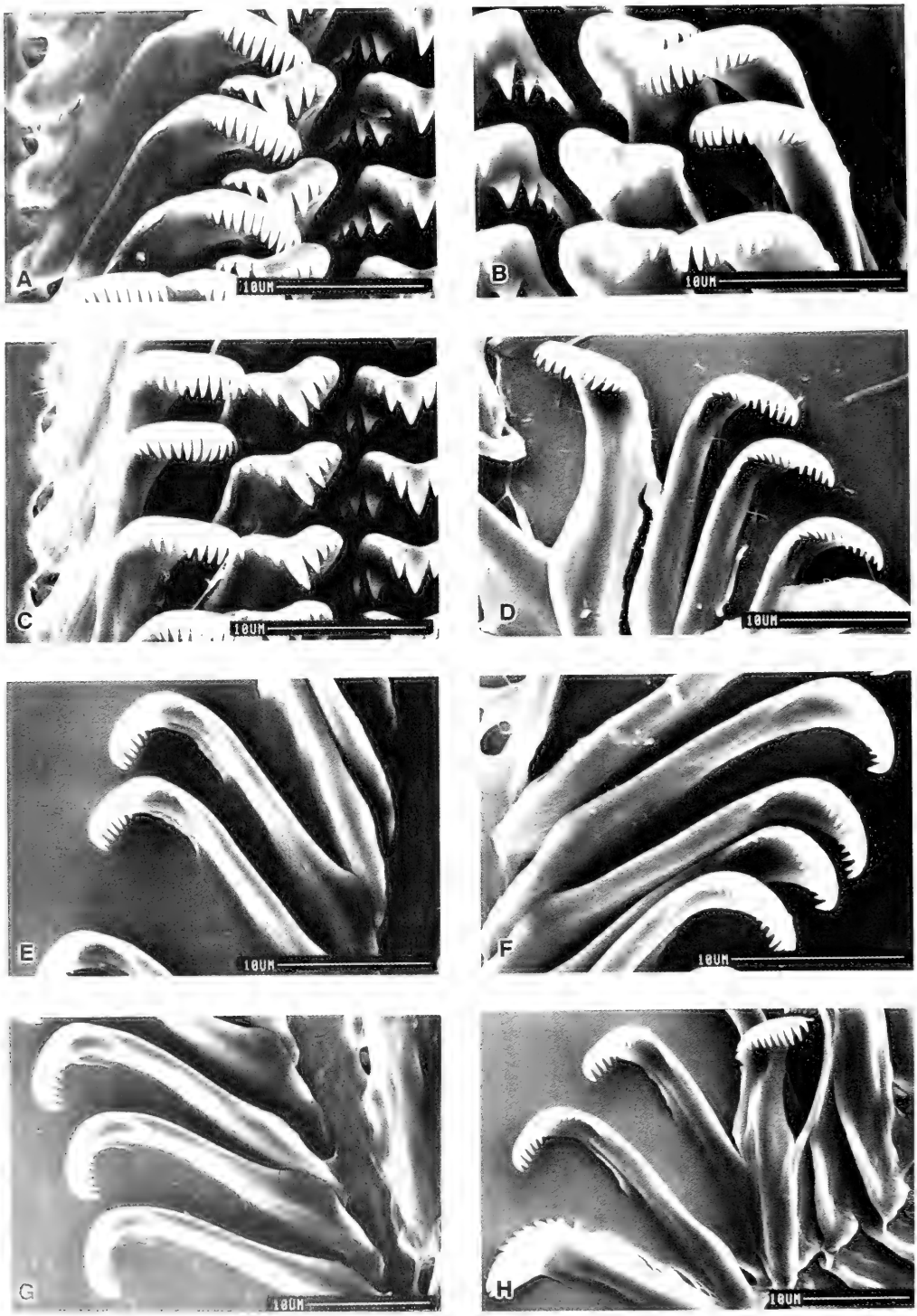

FIG. 69. Radula of *Neotricula cristella*. See text for details.

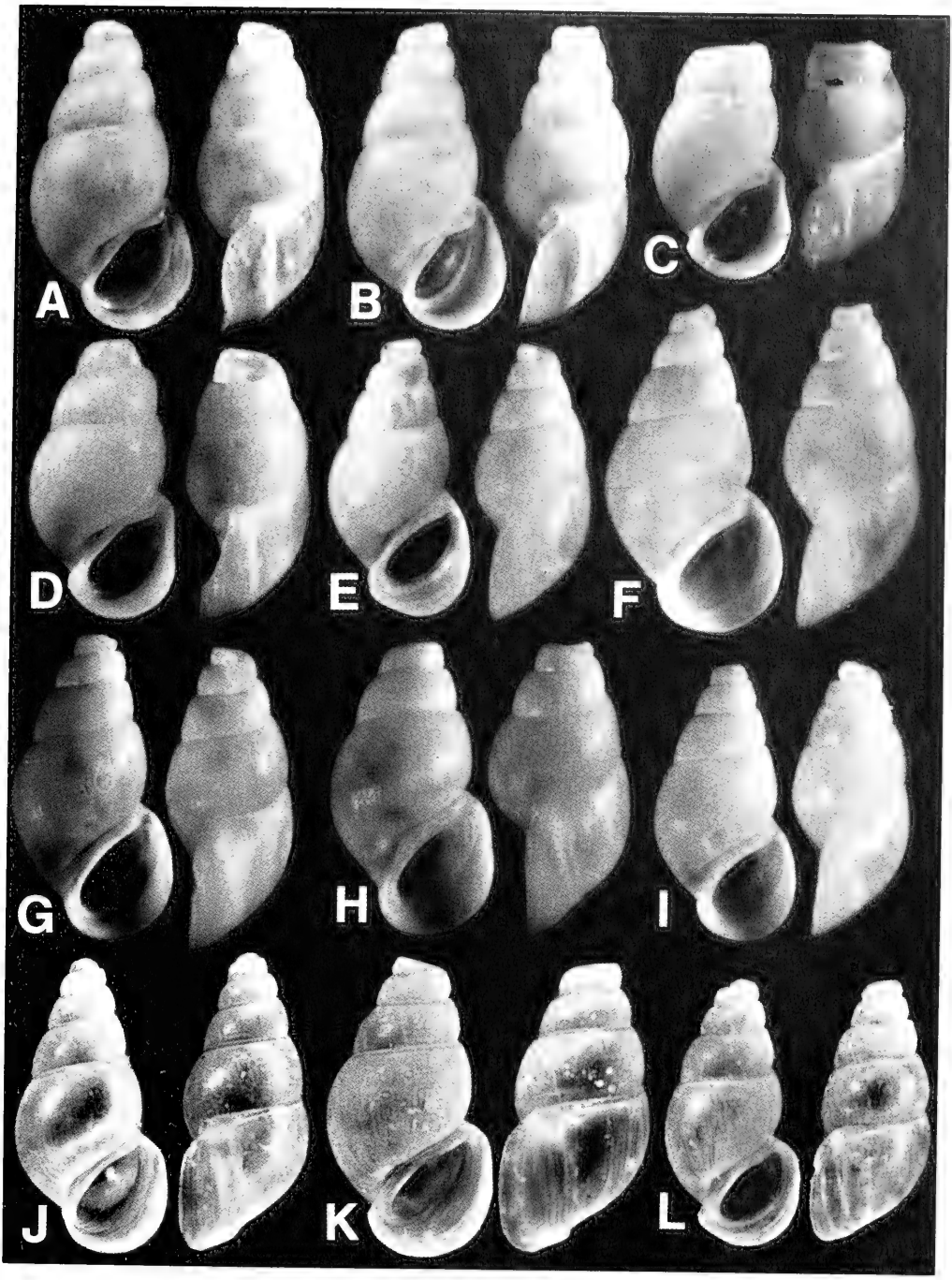

FIG. 70. Shells of: *Neotricula dianmenensis* A–D. A. Holotype. *Neotricula duplicata* E–I from D85 collections. F. Holotype. *Neotricula lilii* J–L. J. Holotype. A = 3.32 mm; other shells printed at same scale. Shells not designated as holotypes are paratypes.

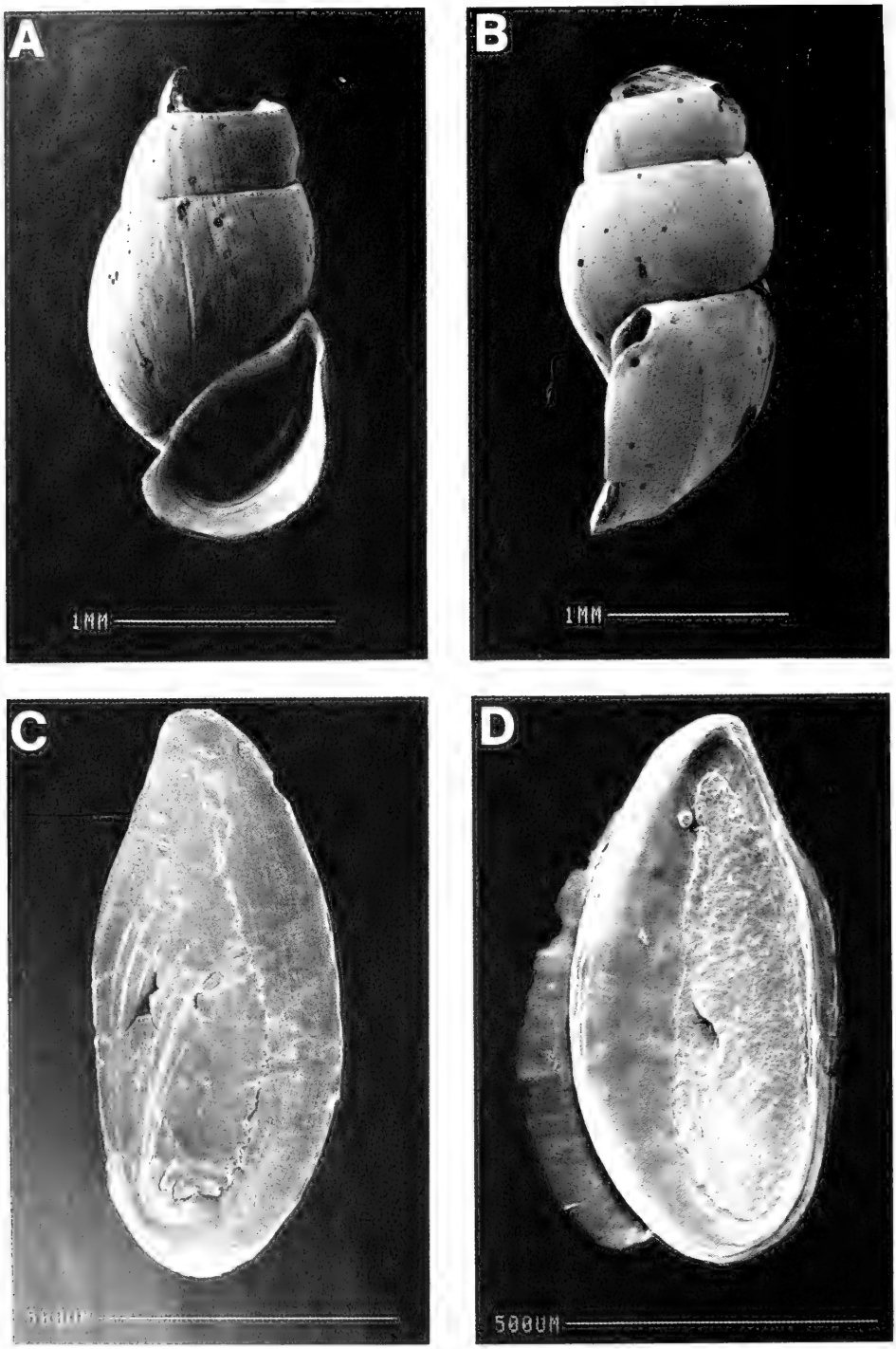

FIG. 71. SEM photographs of shells (A, B) and opercula (C, D) of *Neotricula dianmenensis*. D. Inner surface.

TABLE 34. Shell measurements (mm) for *Neotricula dianmenensis*. Mean ± standard deviation (range). All except two shells were eroded, therefore lengths are less than for entire specimens. e = eroded. *, probably a male.

	Shells used for dissections		Types		
	Females (3)	Males (1)	Holotype	Paratypes (5)	*Small Paratype (1)
No. Whorls	3e	5.5	4e	2.0–4.0e	5.0
Length (L)	2.90±0.20 (2.76–3.12)	2.72	3.32	2.89±0.25 (2.64–3.20)	2.76
Width (W)	1.50±0.08 (1.44–1.60)	1.36	1.64	1.50±0.06 (1.44–1.56)	1.28
L body whorl	2.02±0.12 (1.92–2.16)	1.76	2.20	1.96±0.08 (1.84–2.04)	1.68
L penultimate whorl	0.54±0.10 (0.48–0.62)	0.40	0.52	0.52±0.05 (0.46–0.56)	0.44
W penultimate whorl	1.10±0.10 (1.04–1.20)	0.96	1.16	1.08±0.06 (1.00–1.16)	0.96
W 3rd whorl	—	—	0.80	0.77±0.05 (0.72–0.80) N = 3	0.68
	—	—			
L last three whorls	2.90±0.20 (2.76–3.12)	2.72	3.12	2.85±0.19 (2.64–2.96) N = 3	2.40
L aperture	1.47±0.08 (1.40–1.56)	1.24	1.56	1.43±0.08 (1.32–1.52)	1.26
W aperture	0.91±0.02 (0.88–0.92)	0.80	0.96	0.91±0.03 (0.88–0.94)	0.80
x	0.42±0.05 (0.40–0.48)	0.40	0.50	0.43±0.08 (0.32–0.52)	0.36
y	—	—	0.16	0.09±0.05 (0.04–0.16)	0.08

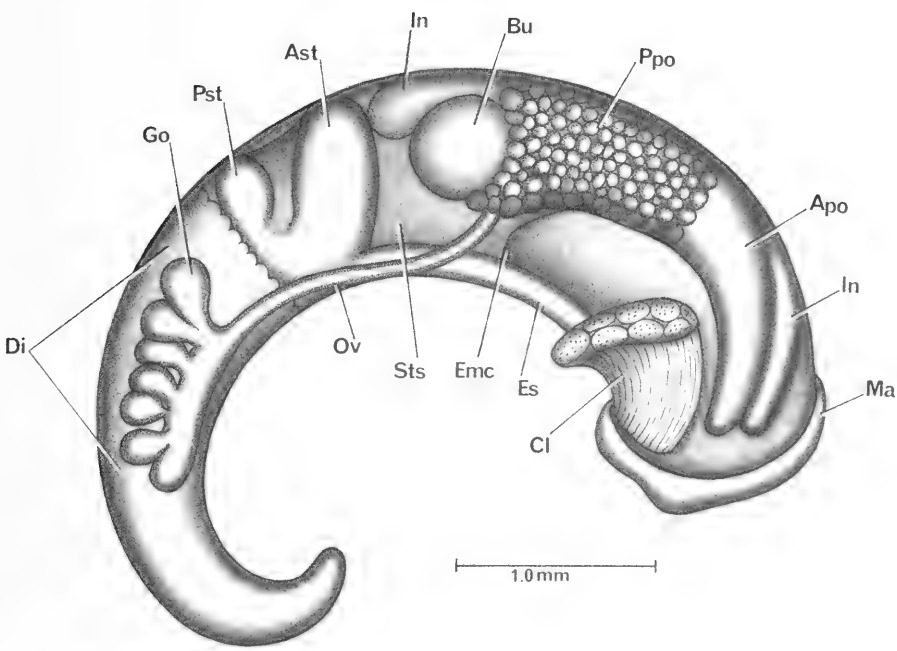

FIG. 72. Uncoiled female *Neotricula dianmenensis* with head and kidney tissue removed.

TABLE 35. Dimensions (mm) or counts of non-neural organs and structures of *Neotricula dianmenensis*. N = number of snails used. L = length. Mean ± standard deviation (range).

	Females (N = 3)	Males (N = 1)
Body L.	4.9±0.53 (4.4–5.4)	3.9
Digestive gland L	1.99±0.36 (1.76–2.4)	1.9
Gonad L.	0.75±0.08 (0.70–0.84)	1.1
Pallial oviduct L. = PO	1.58±0.16 (0.44–0.56)	—
Bursa copulatrix L. = BU	0.50±0.06 (0.44–0.56)	—
Duct of bursa L.	0.18 (0.16, 0.20) N = 2	—
BU ÷ PO	0.32±0.07 (0.26–0.40)	—
Seminal receptacle L.	0.15±0.01 (0.14–0.16)	—
Duct of seminal receptacle L. (see text)	0 to 0.12	—
Buccal mass L.	0.55±0.04 (0.52–0.60)	
Mantle cavity L.	1.41±0.20 (1.20–1.60)	1.26
Osphradium L. = Os	0.35±0.05 (0.30–0.40)	0.34
Gill L. = G	1.23±0.21 (1.00–1.40)	1.06
Os ÷ G	0.29±0.03 (0.26–0.32) N = 4	—
No. filaments	18.3±1.5 (17–20)	17
Gf_2 L	0.25 (0.20, 0.30) N = 2	(males & females)
Gf_1 L.	0.21 N = 2	(males & females)
Total Gf L. = TGF	0.46 N = 2 no variation	
Gf_2 ÷ TGF	0.54 (0.44, 0.65) N = 2	(males & females)
Prostate L.	—	1.0
Seminal vesicle L.	—	0.70
Penis L.	—	1.54

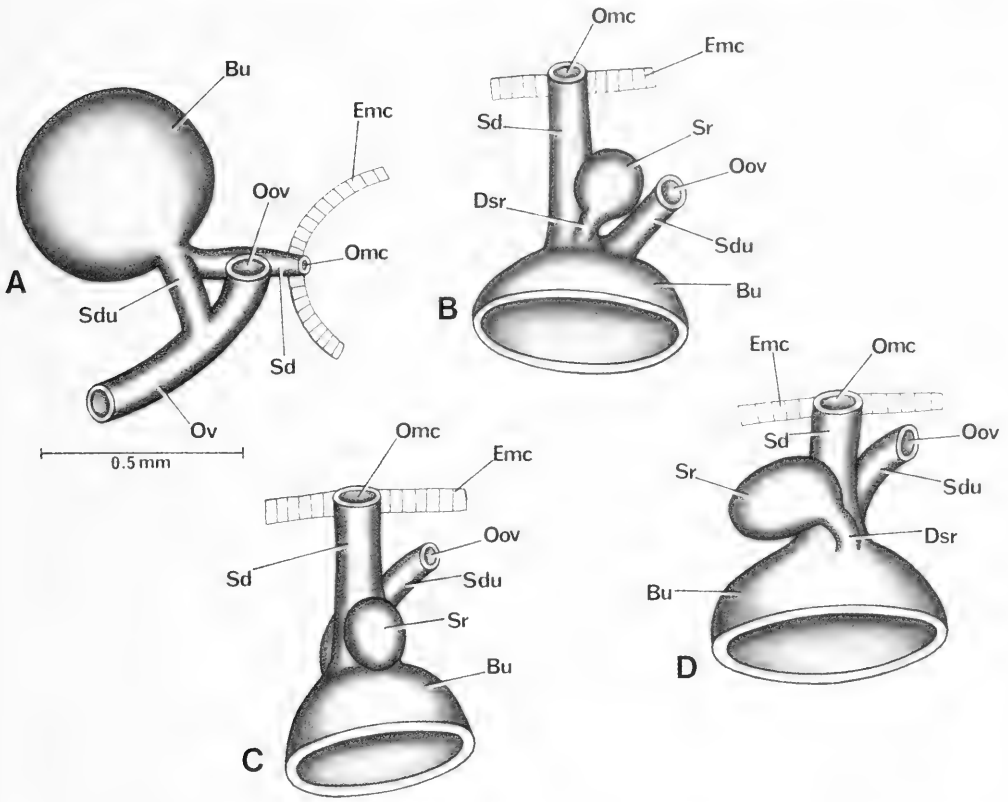

FIG. 73. Details and variation of bursa copulatrix complex of organs of *Neotricula dianmenensis*. A, same orientation as in Figure 72. B–D. Bursa complex flipped over to show where seminal receptacle enters the base of bursa, and variation.

we can give no data on apical whorl characters. Lengths probably range from 2.76 to 3.44 mm (Table 34). There is possibly sexual dimorphism, with the males smaller. The aperture shape is distorted due to the pronounced aperture beak. There is a narrow but pronounced umbilicus. The whorls at the suture are smooth (not crenulated). SEM analysis reveals a trace of spiral microsculpture below the sutures (also seen at 50X). There is an angulation of the inner lip just abapical to the pronounced beak tubercle. The inner lip is fused to the body whorl (most shells). The inner lip is slightly separated from the body whorl opposite the beak tubercle (some shells). The adapical end of the aperture is fused to the body whorl; there is a pronounced apertural beak some 0.26 mm long with a wide opening into the interior (0.12–0.16 mm wide gap); there is no internal notch groove. There is an apertural sinus. In side view, the outer lip is straight; it is slightly scooped forward. Facing the inner lip in side view, there is a strong lip deflection angle. There is no varix. In apertural view, the abapical lip extends beyond the base of the shell 0.43 ± 0.08 mm.

The whorls are slightly convex and the sutures sharply defined but shallow.

External features. Details of the head are not available. The operculum (Fig. 71C,D) is distinctive for its long, thin shape. The width to length ratio is 0.44 ± 0.03. As seen in Figure 71D, there may be an easily detached external layer. The internal attachment pad is pro-

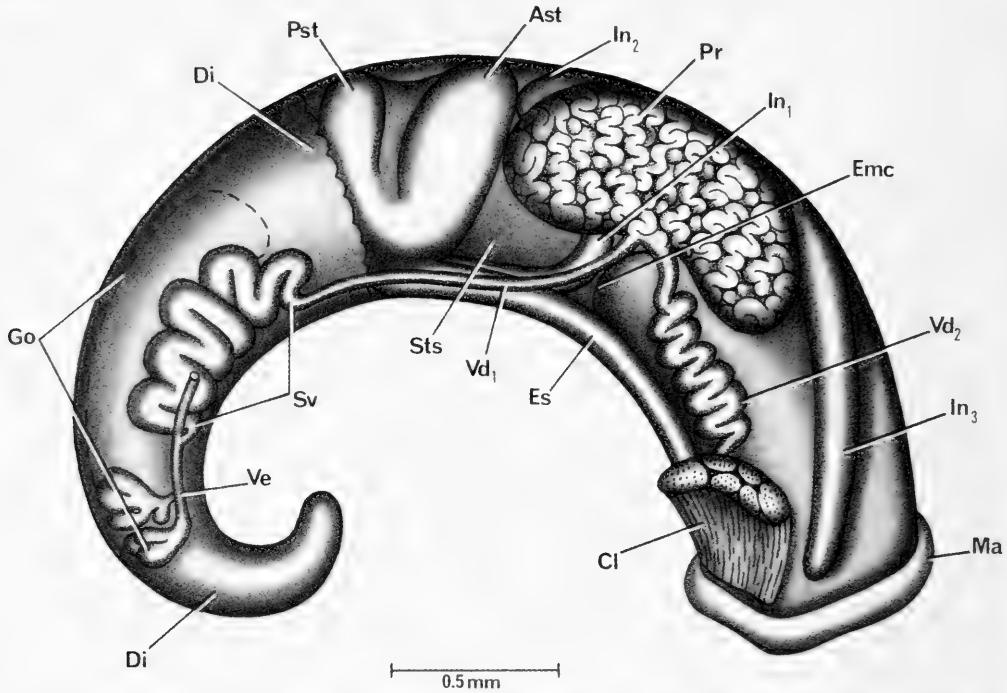

FIG. 74. Uncoiled male of *Neotricula dianmenensis* without head or kidney tissue. Some lobes of gonad cut away to show seminal vesicle that coils dorsal to gonad. Dashed line shows anterior limit of gonadal lobes.

nounced (Fig. 71D). The shape of the operculum reflects the inner lip angulation.

Mantle cavity. Measurements and statistics are given in Table 35. Mantle cavity structures and relationships are normal for those of *Neotricula*. The osphradium is mid-gill; it is short. Gill filaments are normally developed; Gf_2 is normal length. Gf_2 does not have a pronounced crest.

Female reproductive system. The body of an uncoiled female without head and with kidney tissue removed is shown in Figure 72. Measurements of organs are given in Table 35. Important features are: (1) The gonad is posterior to the stomach; it consists of few lobes. (2) The bursa (Bu) is clearly seen posterior to the posterior pallial oviduct (Ppo). (3) Sperm enter the system at the posterior end of the mantle cavity (Emc) by passing into the spermathecal duct (Sd) that bypasses the pericardium. The spermathecal duct runs a short distance to open into the bursa (Bu, Fig. 73A) dorsal to the duct of the bursa (Dbu). (4) The sperm duct (Sdu) runs from the bursa (Bu) to the oviduct (Ov); there is no duct of the bursa. (5) The seminal receptacle (Sr) arises from the spermathecal duct where the latter joins the bursa (Fig. 73B–D). (6) The duct of the seminal receptacle varies in length from 0 (Sr fused to the spermathecal duct, Fig. 73C) to moderately long (Fig. 73D). (7) The oviduct runs from gonad to pallial oviduct without making a loop or twist. (8) The oviduct opens into the pallial oviduct close to the posterior end of the pallial oviduct. (9) The bursa copulatrix is round and short. (10) The length of the albumen gland is standard (based on one individual for which this could be discerned, ratio of 0.47).

Male reproductive system. The body of an uncoiled male is shown in Figure 74 without head and with kidney tissue removed. The anterior lobes of the gonad were removed to reveal the seminal vesicle. Measurements are given in Table 35. Important features are: (1) The gonad consists of numbers of finely divided lobes that drain into a vas efferens

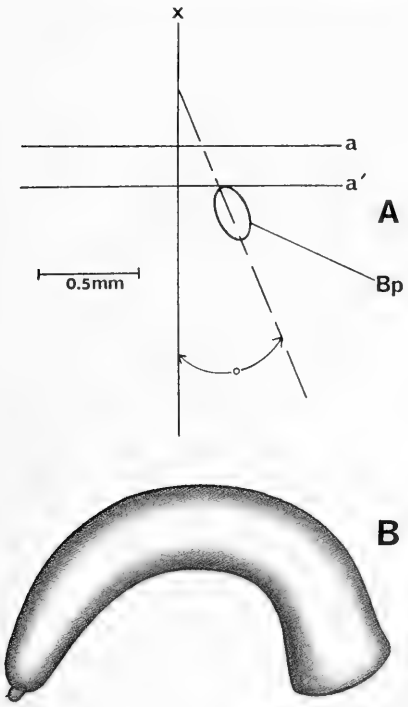

FIG. 75. The penis (B). (A), orientation of the base of the penis (Bp) of *Neotricula dianmenensis* to the snout-neck mid-line (x).

TABLE 36. Radula statistics for *Neotricula dianmenensis*. Mean ± standard deviation (range). In mm except the central tooth width in μm. N = 4. Shell lengths not available.

Radular length	0.45±0.06	(0.36–0.48)
Radular width	0.08±0.002	(0.76–0.080)
Total rows of teeth	58.8±4.2	(56–65)
No. rows of teeth forming	1.90±3.6	(14–22)
Central tooth width	14.1±0.6	(13.4–14.9) N = 11

(Ve, Fig. 74). (2) The posterior vas deferens arises from the vas efferens posterior to mid-gonad and immediately coils as the seminal vesicle (Sv) that is dorsal to the lobes of the gonad. (3) The seminal vesicle coils posterior to the stomach. (4) The gonad is entirely posterior to the stomach. (5) The prostate is massive; it overlaps the posterior end of the mantle cavity. The posterior prostate overlaps the entire style sac (Sts). (6) The penis is simple, without lobes; it has a papilla (Fig. 75B). (7) No ejaculatory duct was found. (8) The shaft of the penis arises from the neck to the right of the snout-neck mid-line (x, Fig. 75A) at an angle of 22°–23°.

Digestive system. The digestive gland is posterior to the stomach (only slight overlap on the posterior chamber (Figs. 72, 74). The rad-

TABLE 37. Cusp formulae for the radular teeth of *Neotricula dianmenensis* with the percent of radulae (N = 4) in which a given formula was found at least once.

Central Teeth		Lateral Teeth		Inner Marginal Teeth		Outer Marginal Teeth (N = 3)	
2-1-2 / 2-2	50%	3-1-4	75%	7	25%	7	0
		4-1-3	50%	8	25%	8	0
3-1-3 / 2-3	25%	4-1-2	25%	9	25%	9	33%
		2-1-3	25%	10	25%	10	33%
3-1-3 / 2-2	25%	2-1[2]-2	25%	11	100%	11	66%
2-1-3 / 2-2	25%	3-1-2	25%	12	100%	12	100%
		3-1-3	25%	13	75%	13	66%
		3-1-4	25%	14	25%	14	0
				$\bar{X}$* = 11.5±1.7 N = 38		11.6±1.2 30	

*Mean ± standard deviation of cusp number for all teeth counted.

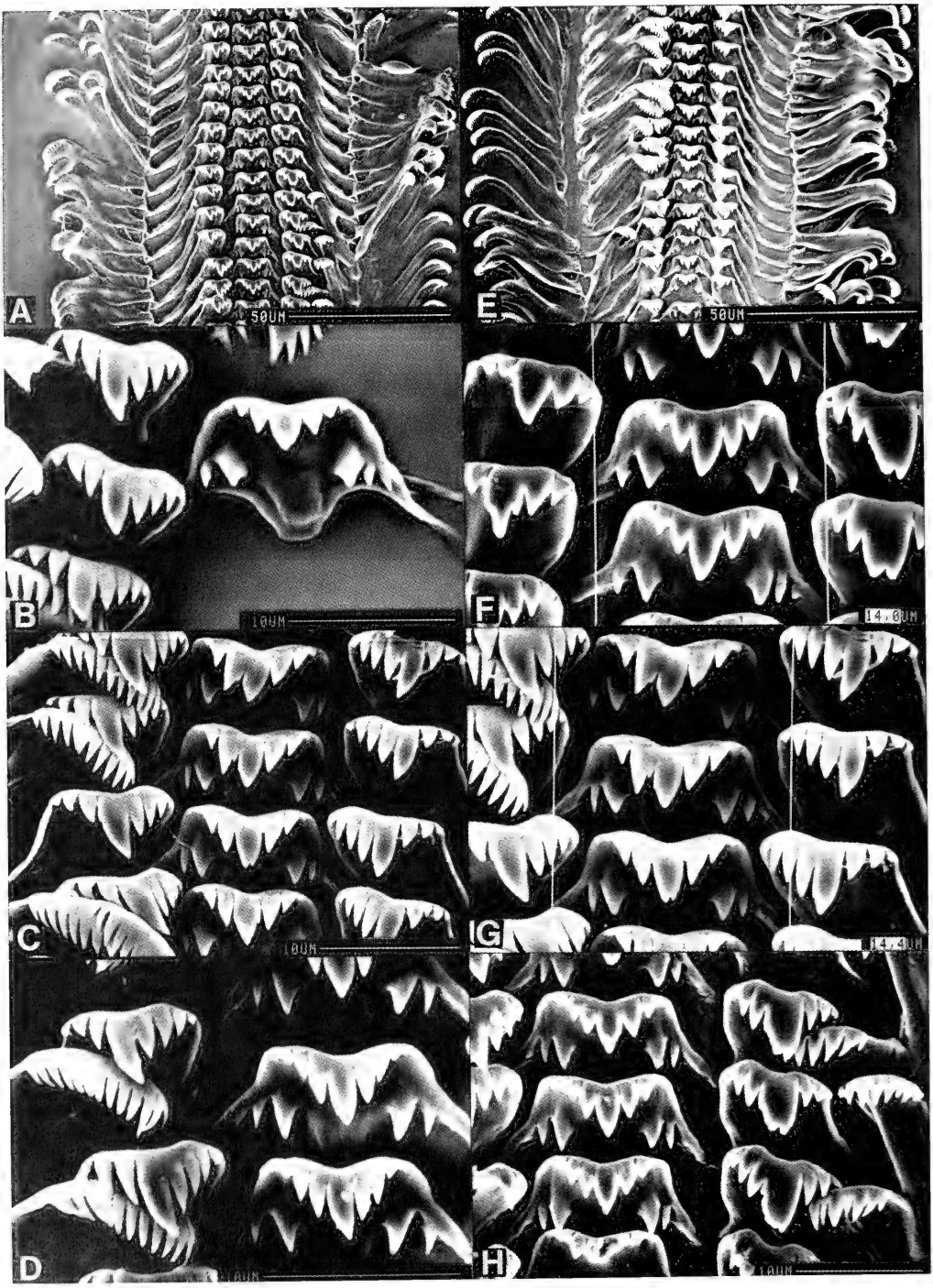

FIG. 76. Radula of *Neotricula dianmenensis*. A, E. Segments of the radula. B–D, F–H. Central, lateral and inner marginal (C, D, H) teeth. See text for details.

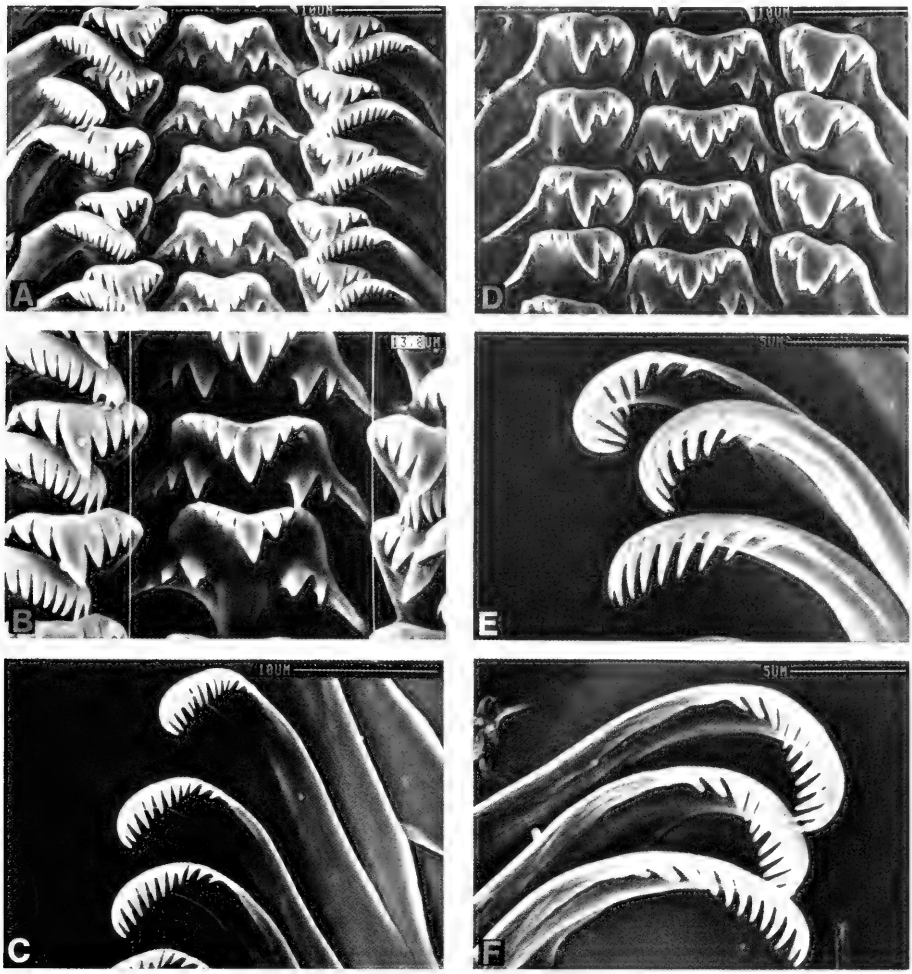

FIG. 77. Radula of *Neotricula dianmenensis*. Outer marginals are featured in C, E, F. Dominant cusp of lateral tooth (i.e. the "1" of the 3-1-2) is either massive (D) or bifurcated (B).

TABLE 38. Lengths (mm) of neural structures of *Neotricula dianmenensis*. Mean ± standard deviation (range). N = 4.

Cerebral ganglion	0.23±0.01	
Cerebral commissure	0.07±0.01	
Pleural ganglia		
Right (1)	0.13±0.01	
Left	0.12–	(no variation)
Pleuro-supraesophageal connective (2)	0.13±0.04	(0.10–0.18)
Pleuro-subesophageal connective	0.08 N = 2	(0.06–0.10)
Supraesophageal ganglion (3)	0.11±0.01	(0.10–0.12)
Subesophageal ganglion	0.12–	
Osphradio-mantle nerve	0.04±0.01	(0.02–0.04)
RPG ratio = 2 ÷ 1+2+3	0.35±0.01	(0.34–0.36)

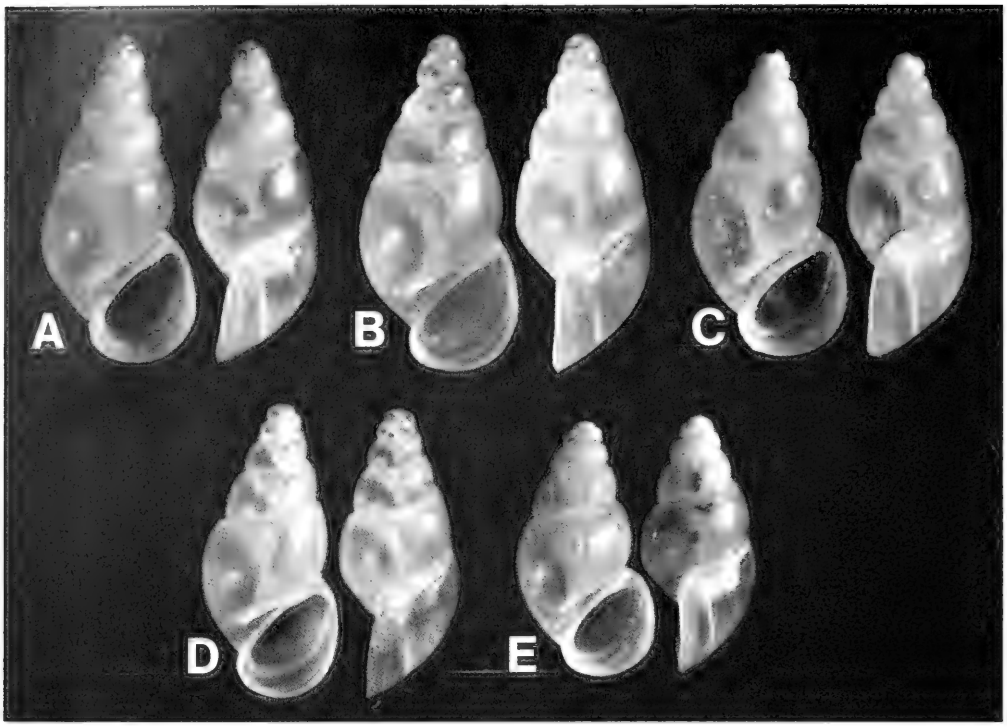

FIG. 78. Paratypes of *Neotricula duplicata* from D87-2. Shell in Figure A is 3.52 mm long; other shells printed at same scale.

ula sac does not coil dorsal to the nerve ring. The radula is shown in Figures 76, 77; radular statistics are given in Tables 36 and 37. The radula is typical Triculini. The enlarged cusp of the lateral tooth (the "1" of 3-1-2, etc.) is frequently bifid or massive (Figs. 77A, B, D). The typical radular formula is:

$$\frac{2(3)\text{-}1\text{-}(3)2}{2\text{-}2}, \quad 3(4)\text{-}1[2]\text{-}2 \text{ to } 4,\ 10\text{-}13,\ 10\text{-}13.$$

Nervous system. Standard Triculinae. Measurements are given in Table 38. The RPG ratio shows the supraesophageal connective to be moderately concentrated.

Remarks

Conchologically, *N. dianmenensis* is most similar to *N. duplicata* and *N. lilii* (Figs. 153, 154). However, it differs from the other two by having a distorted aperture shape (Table 2, char. 3), an angled inner lip (char. 13), and a pronounced beak tubercle (char. 24). Additionally, it differs from *N. duplicata* by having a clearly open umbilicus (char. 4), an adapical apertural sinus (char. 11), a sinuate outer lip (char. 14), and a thin inner lip (char. 19).

Anatomically the greatest similarity is to *N. duplicata* (Fig. 157), but it differs from that species in seven characters (15% of the 46 comparable characters, Table 80). *Neotricula. dianmenensis* has few rows of teeth whereas *N. duplicata* has many (char. 42). The gonad of the former is posterior to the stomach; it overlaps the stomach in the latter. The spermathecal duct is comparatively long in the former, short in the latter (char. 19). There is no duct of the bursa in the former; it is long in the latter (char. 16). The osphradium is long in the former, short in the latter (char. 9).

***Neotricula duplicata* Davis & Chen sp. nov.**

Holotype. ZAMIP-M0035, Figure 70A.

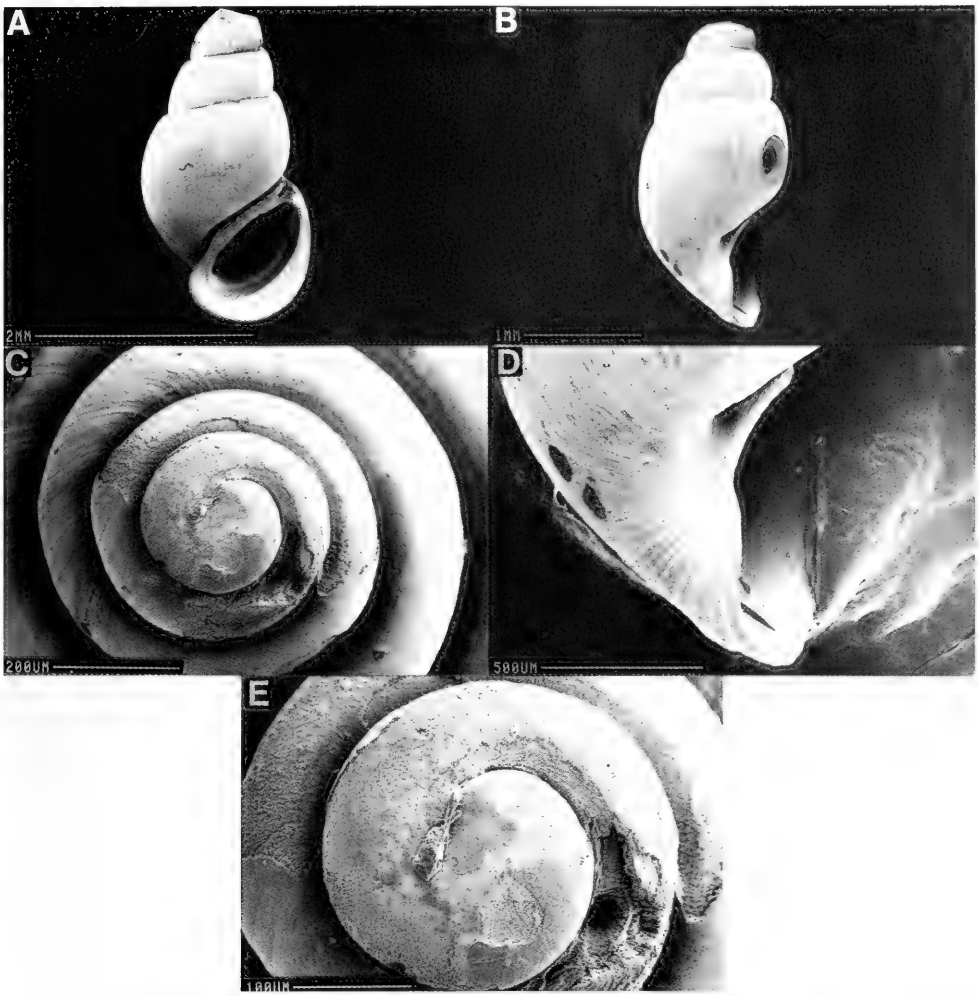

FIG. 79. SEM photographs of shells of *Neotricula duplicata* from D85-79. B, D show the abapical lip deflection. C, E. Enlargements of apical whorls.

Paratypes. ANSP 373152, A12668; 373151, A12667; ZAMIP M0003; Figure 70E, G–I; Figure 78B–E.

Type Locality. Huang-sha-ping Village, Jiangnan Town, Anhua County, Yiyang Prefecture. 28°21′24″E, 110°15′11″N. Figure 1, site 4. Collection numbers D85-79, 5 October 1985, Davis, Hoagland & Chen; D87-2, 18 March 1987, Davis & Chen.

Etymology. Named for the duplication of anatomical research effort on specimens collected from this population in both 1985 and 1987, not realizing in 1987 that the population had been dissected and analyzed in 1985.

Habitat

Some 400 m from Zijiang River, a small stream flowed from a hill through rice fields. The stream was about 10 cm deep, 14 cm wide with a mud substratum. Snails were collected in the upper narrow shaded part of the stream from under stones. Associated molluscan fauna: *Gyraulus* sp.

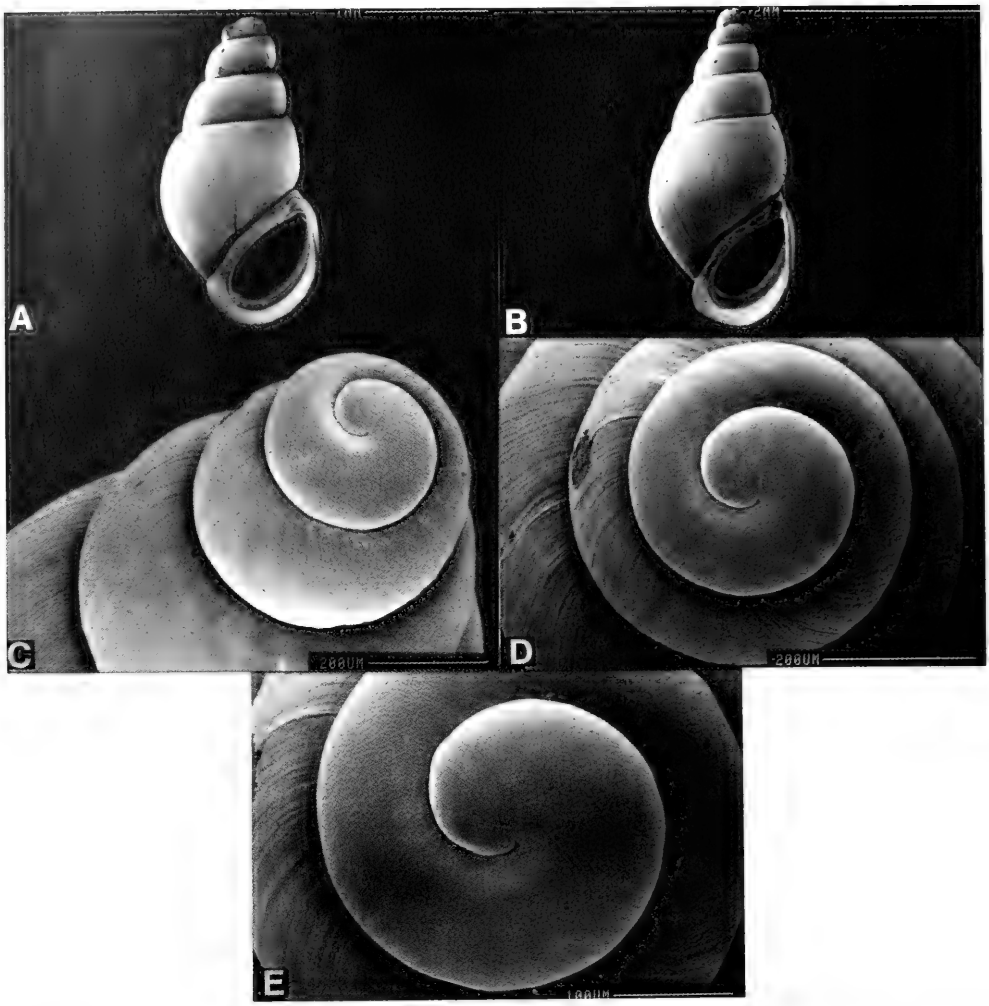

FIG. 80. SEM photographs of shells of *Neotricula duplicata* from D87-2. C–E. Enlargements of apical whorls.

Description

Shell. Shells are illustrated in Figures 70E–I, 78A–E, 79, 80. They are small, ovate-conic (Tables 39–41). Because most snails are eroded, it is difficult to analyze size classes based on whorl numbers. It is clear that there are two size classes of mature snails (Table 39); females are larger than males (Table 41). Additionally, there appear to be two size classes within each sex (Table 41). The size range based on uneroded shells is 2.72–3.88 mm. The aperture is pyriform. Adapically there is a strong apertural beak; there is no beak tubercle. There may or may not be an internal notch groove.

The whorls at the suture are smooth (not crenulated). There is an umbilical chink. SEM analysis reveals faint spiral microsculpture at the shoulders of the whorls after the second whorl (Fig. 80D, E).

The inner lip is straight to arched, narrowly separated from the body whorl, and uniformly thick. The adapical end of the aperture is only

TABLE 39. Measurements in mm of D85-79 shells of *Neotricula duplicata*. Mean ± standard deviation (range). e = eroded apical whorls; ( ) = number measured. Sex unknown.

	Holotype	Paratypes	
	large class	large class	small class
No. Whorls	4e	3e–4e (3)	3e–5e (5)
Length (L)	3.44	3.03±0.06 (3.00–3.10)	2.87±0.10e (2.72–3.00)
Width (W)	1.72	1.57±0.10 (1.50–1.68)	1.46±0.04 (1.44–1.48)
L last three whorls	3.12	2.91±0.16 (2.80–3.10)	2.67±0.06 (2.56–2.72)
L body whorl	2.24	2.12±0.14 (2.04–2.28)	1.94±0.02 (1.92–2.96)
L penultimate whorl	0.52	0.45±0.02 (0.44–0.52)	0.47±0.02 (0.44–0.48)
W penultimate whorl	1.10	0.99±0.07 (0.92–1.06)	0.97±0.02 (0.96–1.00)
W 3rd whorl	0.76	0.66±0.05 (0.60–0.70)	0.65±0.02 (0.64–0.68)
L aperture	1.60	1.51±0.12 (1.44–1.64)	1.36±0.04 (1.32–1.40)
W aperture	1.08	0.95±0.08 (0.88–1.04)	0.86±0.04 (0.80–0.88)
x	0.48	0.48±0.07 (0.40–0.52)	0.44±0.06 (0.36–0.52)
y	0.20	0.15±0.06 (0.08–0.16)	0.15±0.04 (0.10–0.20)

TABLE 40 Measurements in mm of paratype shells of *Neotricula duplicata* from D87-2. Mean ± standard deviation (range). e = eroded apical whorls; ( ) = number measured. Sex unknown.

No. Whorls	5e	5.5 (3)	6.0 (2)
Length (L) of eroded shell	3.44		
Length of uneroded shells		2.89±0.20 (2.72–3.12)	3.53 (3.46,3.60)
Width (W)	1.60	1.37±0.09 (1.32–1.48)	1.61 (1.60,1.62)
L last three whorls	2.92	2.59±0.15 (2.48–2.76)	3.10 (3.00,3.20)
L body whorl	2.08	1.87±0.08 (1.80–1.96)	2.18 (2.08,2.28)
L penultimate whorl	0.56	0.45±0.03 (0.42–0.48)	0.54 (0.52,0.56)
W penultimate whorl	1.06	0.91±0.05 (0.88–0.96)	1.10 (1.08,1.12)
W 3rd whorl	0.72	0.62±0.05 (0.58–0.68)	0.72 No variation
L aperture	1.52	1.33±0.09 (1.28–1.44)	1.52 (1.44,1.60)
W aperture	1.00	0.85±0.06 (0.84–0.92)	0.96 No variation
x	0.52	0.37±0.05 (0.32–0.40)	0.42 (0.40,0.44)
y	0.16	0.10±0.02 (0.08–0.12)	0.14 (0.12,0.16)

TABLE 41. Measurements (mm) of shells of *Neotricula duplicata* from both collections where animals were used for dissections. Mean ± standard deviation (range). All except two shells were eroded, therefore lengths are less than for entire specimens. e = eroded. *, probably a male. ( ) = number measured.

	Females			Males		
No. Whorls	2e–5e (3)	5.5 (1)	6.0 (1)	4e–5e (2)	5.0(1)*	5.5 (2)
Length (L) of eroded shells	3.31±0.45e (2.80–3.68)			3.22 (3.12, 3.32)		
Length of uneroded shells		3.60	3.88		2.88	3.12 No var.
Width (W)	1.77±0.08 (1.68–1.84)	1.76	1.76	1.57 (1.56, 1.58)	1.48	1.56 No var.
L last three whorls	3.24 (N = 2) No var.	3.20	3.36	2.88 (2.76, 3.00)	2.62	2.76 (2.72, 2.80)
L body whorl	2.36±0.08 (2.28–2.44)	2.36	2.36	2.10 (2.08, 2.12)	1.96	1.96 (1.92, 2.00)
L penultimate whorl	0.69±0.34 (0.48–1.08)	0.52	0.62	0.49 (0.42, 0.56)	0.40	0.46 (0.44, 0.48)
W penultimate whorl	1.12±0.04 (1.08–1.16)	1.12	1.16	1.05 (1.02, 1.08)	0.96	1.01 (1.00, 1.02)
W 3rd whorl	0.64 (N = 2) (0.56, 0.72)	0.78	0.82	2.88 (2.76, 3.00)	2.62	2.76 (2.72, 2.80)
L aperture	1.60±0.06 (1.56–1.68)	1.60	1.64	1.46 (1.42, 1.48)	1.32	1.38 (1.36, 1.40)
W aperture	1.07±0.08 (0.88–0.92)	1.08	1.06	0.92 No var.	0.88	0.94 (0.92, 0.96)

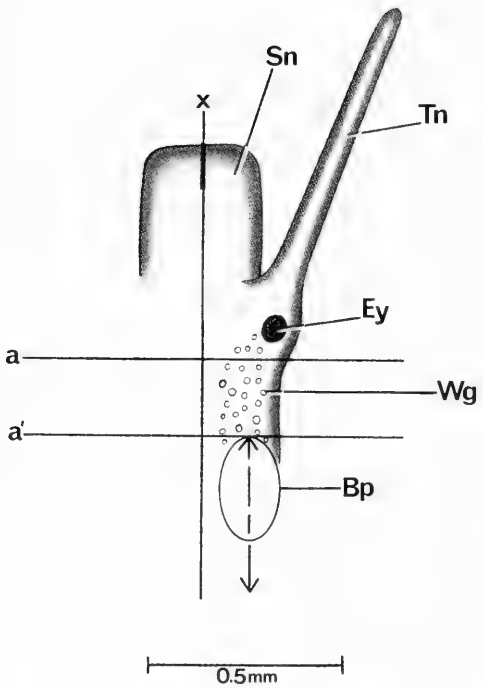

FIG. 81. Head of a male *Neotricula duplicata* from D85-72 showing the relationship of the base of the penis (Bp) to the mid-line of the snout-neck (x).

slightly separated from the body whorl. There is no apertural sinus. In side view, the outer lip is straight; the outer lip is slightly scooped forward. In side view, the inner lip has a strong deflection angle, some 140°. There is no varix. The abapical lip just beyond the base of the shell 0.48 ± 0.07 mm; the abapical lip has a spout.

SEM examinations of the apical whorls (Figs. 79C–E; 80C–E) show that the tip of the apical whorl is smooth, but that just beyond the tip the shell is minutely wrinkled. Coarse growth lines begin just before 1.75 whorls.

External features. The head is dark grey to black. There may or may not be white granules close to the eyes extending posteriorly back along the neck (Wg, Fig. 81). When granules occur, they do not form a dense lunate mass or "eyebrow."

Opercula from both collections are shown in Figures 82, 83. They are elongate-ovoid and are composed of discernable flaky layers. The muscular attachment pad (Fig. 82B, D) is pronounced and wide (66% width of the operculum).

Mantle cavity. Mantle cavity organs are shown in Figure 84; not all gill filaments are

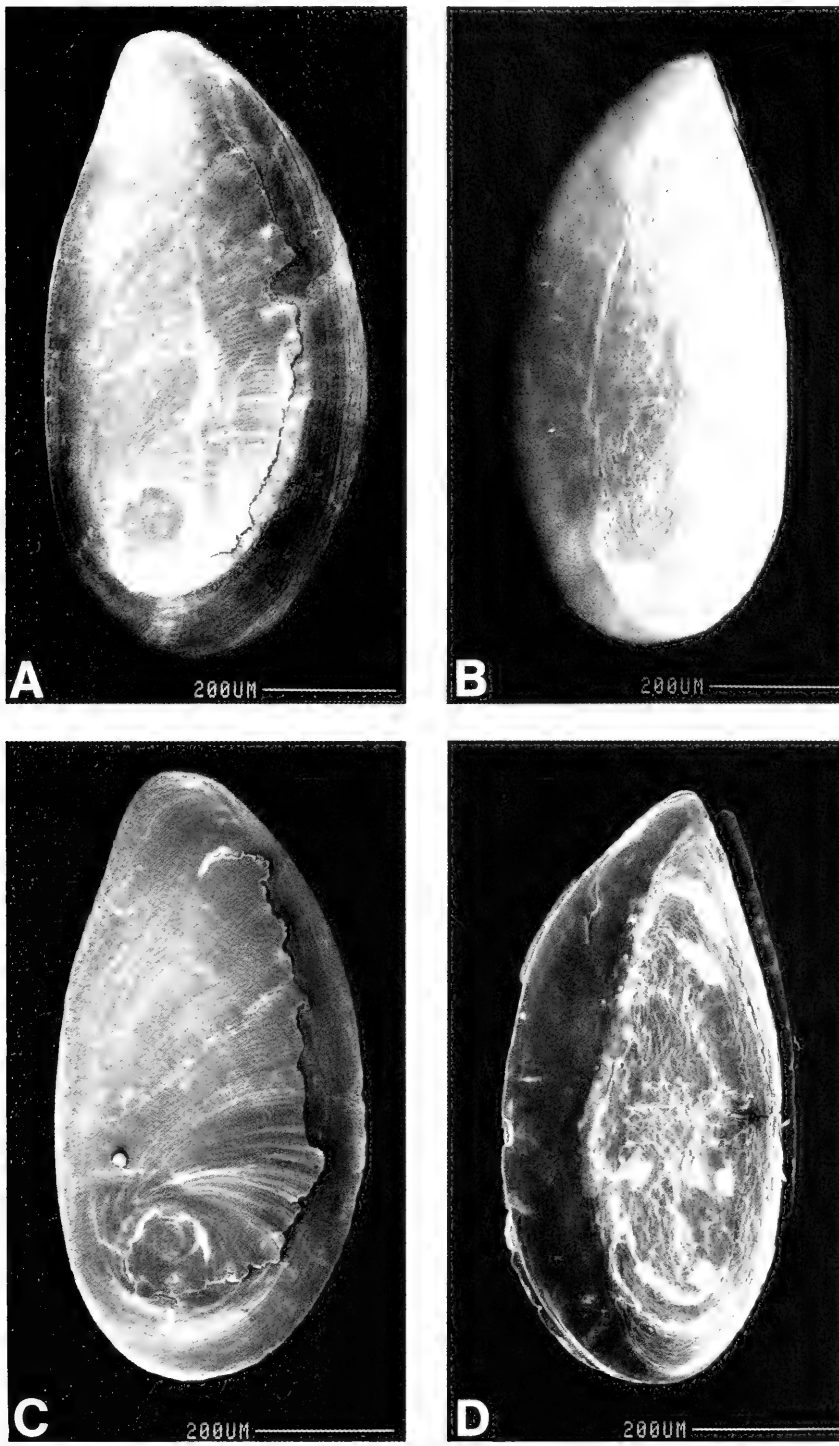

FIG. 82. Opercula of *Neotricula duplicata* from D85-79. A, C. Outer surface; B, D. Inner surface. Note the external loose, flaky layer (A, C, D).

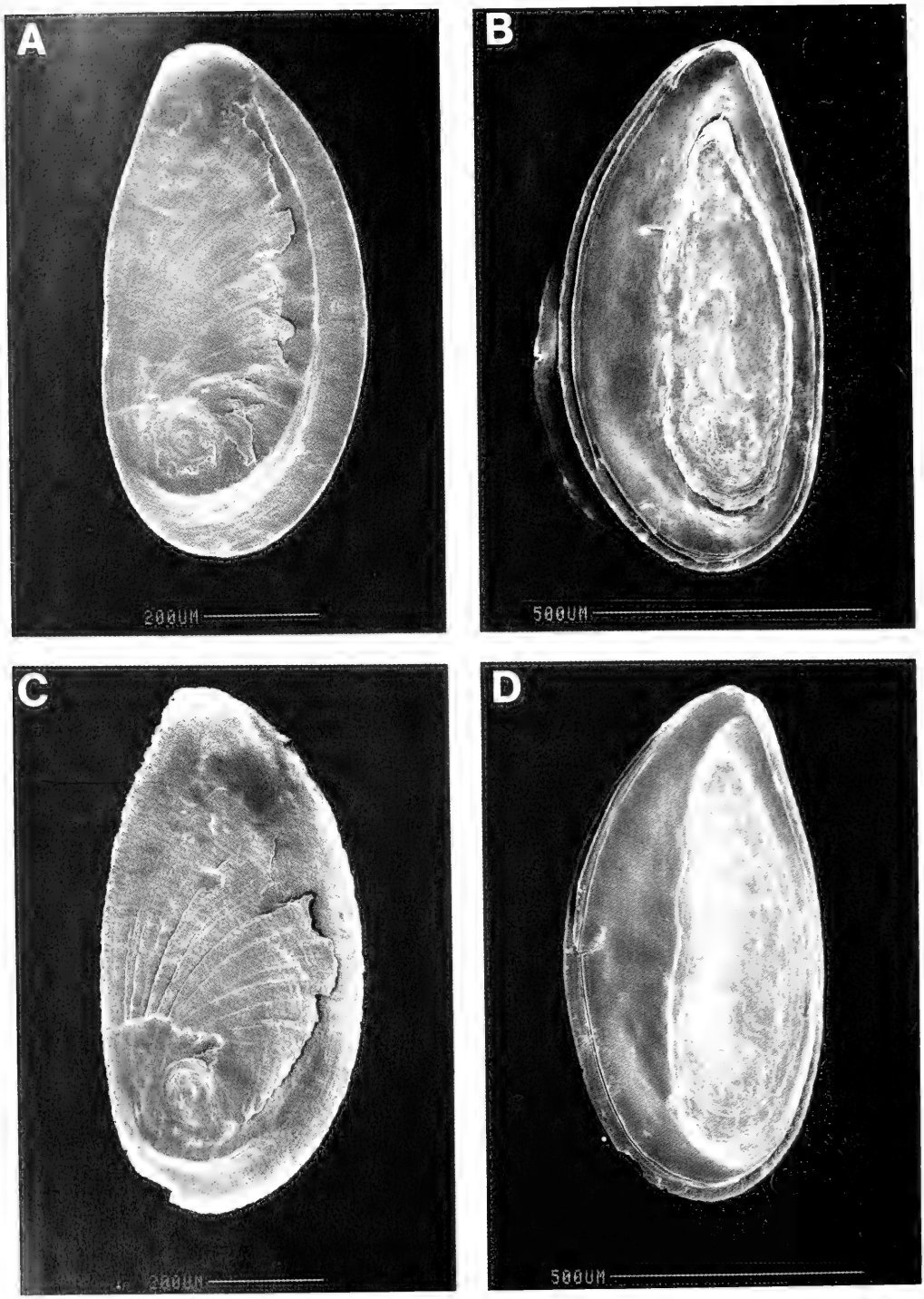

FIG. 83. Opercula of *Neotricula duplicata* from D87-2.

TABLE 42. Lengths (mm) or counts of non-neural organs of *Neotricula duplicata*. Mean ± standard deviation (range). For D87-2 snails, N = 5 for females, N = 4 for males; for D85-79 snails, N = 5 for females, N = 3 for males unless stated otherwise.

	Females		Males	
	D87-2	D85-79	D87-2	D5-79
Body	4.99±0.45 (4.46–5.70)	4.90±0.51 (4.20–5.46)	4.43±0.14 (4.30–4.56)	4.31±0.02 (4.30–4.34)
Digestive gland	1.95±0.46 (1.30–2.50)	2.03±0.20 (1.74–2.30)	2.02±0.14 (1.86–2.20)	1.92±0.14 (1.76–2.00)
Gonad	0.61±0.13 (0.48–0.74) N = 4	0.75±0.05 (0.70–0.80)	1.50±0.38 (1.20–2.10)	1.23 N = 2 (1.16, 1.30)
Total pallial oviduct (= TPO)	1.70±0.20 (1.50–1.90) N = 3	2.04±0.34 (1.78–2.50) N = 4	—	—
Bursa copulatrix (= Bu)	0.47±0.12 (0.30–0.60) N = 4	0.48±0.05 (0.44–0.56)	—	—
Duct of bursa	0.17±0.06 (0.10–0.20) N = 3	0.10 No var. N = 2	—	—
Bu ÷ TPO	0.32±0.12 (0.20–0.43) N = 3	0.23±0.04 (0.18–0.30)	—	—
Seminal receptacle	0.21±0.07 (0.16–0.30)	0.25±0.05 (0.18–0.26)	—	—
Duct of seminal receptacle	0.06 No var. N = 2	0.06 N = 1	—	—
Mantle cavity	1.51±0.18 (1.26–1.70)	1.48±0.07 (1.40–1.56) N = 4	1.33±0.04 (1.30–1.38)	1.35±0.19 (1.14–1.52)
Ctenidium (= CT)	1.27±0.19 (1.00–1.50)	1.28±0.09 (1.20–1.36) N = 4	1.07±0.09 (1.00–1.20)	1.15±0.19 (0.94–1.30)
Osphradium (= OS)	0.37±0.13 (0.20–0.48)	0.37±0.03 (0.34–0.40) N = 3	0.35±0.06 (0.28–0.36)	0.36±0.13 (0.24–0.50)
No. gill filaments	19.3±1.7 (17–21)	18.0±1.4 (16–19) N = 4	17.0±1.2 (16–18)	23.6±7.1 (16–30)
OS ÷ CT	0.30±0.11 (0.17–0.44)	0.29±0.04 (0.23–0.28) N = 3	0.33±0.07 (0.23–0.40)	0.32±0.10 (0.20–0.38)
Gf_1	0.20±0.09 (0.12–0.34) N = 8	0.28±0.05 (0.24–0.36) N = 4	—	—
Gf_2	0.24±0.07 (0.20–0.30) N = 8	0.23±0.03 (0.20–0.26) N = 4	—	—
Total Gf	0.46±0.08 (0.32–0.56) N = 8	0.50±0.05 (0.44–0.50) N = 4	—	—
$Gf_2 \div Gf_1 + Gf_2$	0.43±0.15 (0.25–0.63)	0.54±0.07 (0.48–0.64) N = 4	—	—
Prostate	—	—	0.85±0.13 (0.70–1.00)	0.87±0.06 (0.80–0.90)
Seminal vesicle	—	—	0.53±0.22 (0.20–0.70)	0.45±0.09 (0.40–0.56)
Penis	—	—	1.16±0.27 (0.90–1.54)	1.51±0.22 (1.36–1.76)

illustrated. Measurements and counts are given in Table 42. The osphradium is approximately mid-gill; it is short (ratio of 0.29). The shape of the osphradium is lunate, not oval. The number of gills ranges from 17 to 30. Gill filament section Gf_2 is normal; the length of the longer gill filaments is 0.46 to 0.50 mm long. The shape of the gill leaflet in side view is moderate to high domed. There is no circular patch of white or yellowish granules just

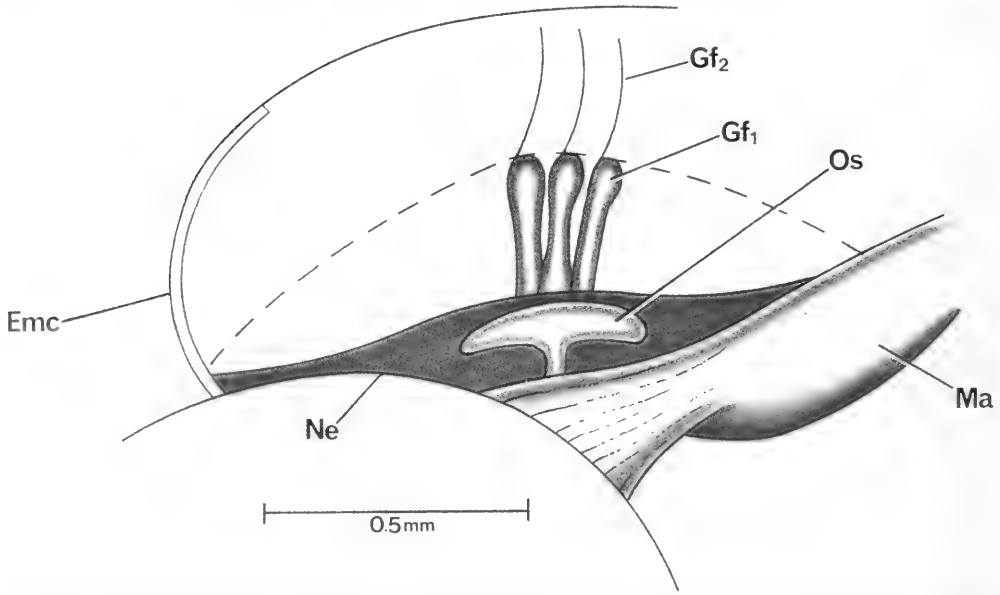

FIG. 84. Mantle cavity organs of *Neotricula duplicata* from D89-79. Dashed line is the trajectory for measuring length of gill and mantle cavity. Only three central gill filaments are illustrated.

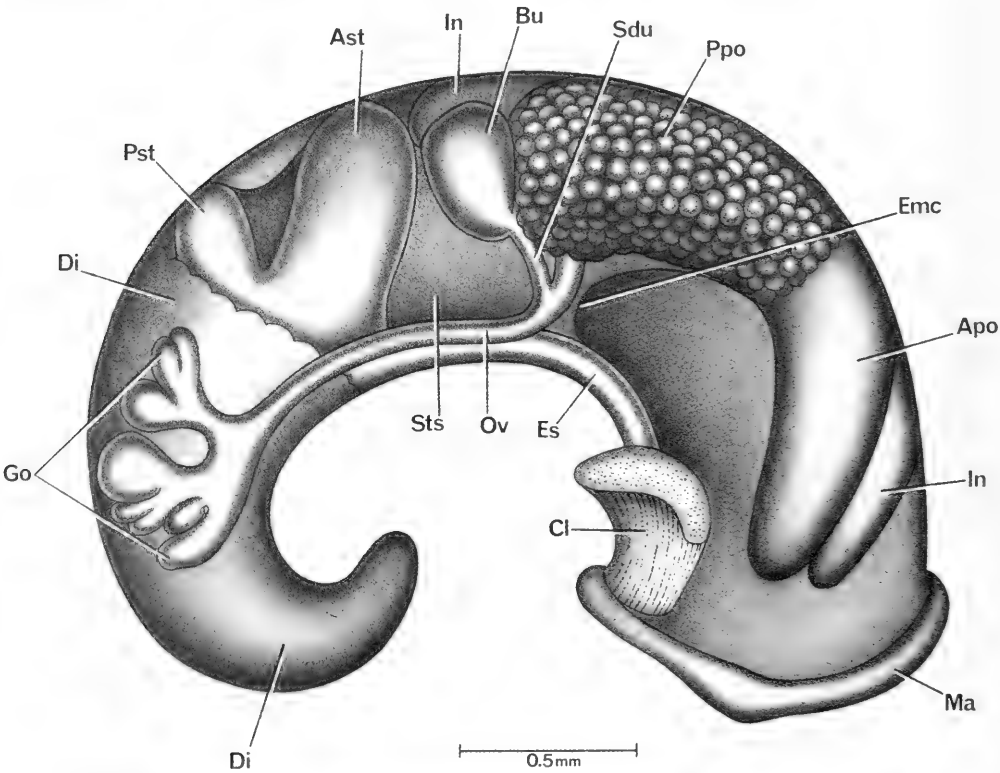

FIG. 85. Uncoiled female *Neotricula duplicata* with head and kidney tissue removed; from D85-79.

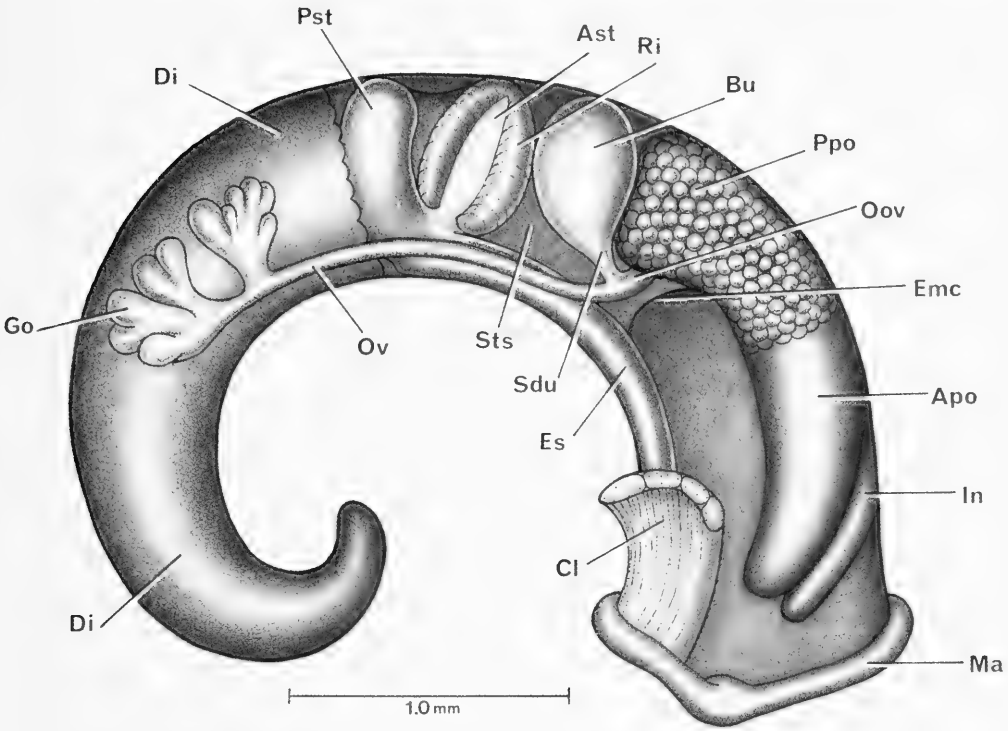

FIG. 86. Uncoiled female *Neotricula duplicata* with head and kidney tissue removed from D87-2.

anterior to the osphradium next to the neck-mantle collar (Ma) juncture.

Female reproductive system. The bodies of uncoiled females without head or kidney tissue are shown in Figures 85, 86. Organ measurements are given in Table 42. Important features are: (1) The gonad is posterior to the stomach; it is relatively short and of few lobes. (2) The albumen gland (Ppo) is of normal length. (3) The bursa copulatrix (Bu) is clearly visible posterior to the albumen gland; the bursa is small and round to oval. (4) The oviduct runs from the gonad to the albumen gland without coiling. (5) The bursa copulatrix complex of organs is shown in Figures 87, 88. Figure 87A is positioned exactly as in Figures 85, 86. The spermathecal duct (Sd) opens into the posterior mantle cavity; it is short and swollen in most specimens. (6) The seminal receptacle (Sr) arises from the dorsal surface at the juncture of the duct of the bursa and the spermathecal duct. (7) The duct of the seminal receptacle (Dsr) slowly increases in diameter to form a club-shaped (not spherical) storage sac that lies dorsal to the bursa copulatrix. In some specimens, it is clear that the seminal receptacle is a U-shaped continuation of the duct of the bursa and that the spermathecal duct attaches at the bottom of the "U" (Fig. 88C). (8) The sperm duct (Sdu) arises from the duct of the bursa on the ventral side just posterior to the duct of the seminal receptacle.

Male reproductive system. The posterior section of an uncoiled male with kidney tissue removed is shown in Figure 89. It is the same in specimens from both D85 and D87 collections. The outline of the gonad (Go) is shown (dashed line) but most of the lobes of the gonad are removed to show the seminal vesicle (Sv) coiled dorsal to the gonad. Measurements of organs are given in Table 42. Important features are: (1) The gonad overlaps the posterior part of the posterior chamber of the stomach (Pst). (2) The prostate (Pr) overlaps the posterior end of the mantle cavity (Emc) and covers the style sac. (3) The seminal vesicle, while coiling dorsal to the gonad, does not extend over the stomach. (4) The anterior vas deferens leaves the prostate (Pr) close to

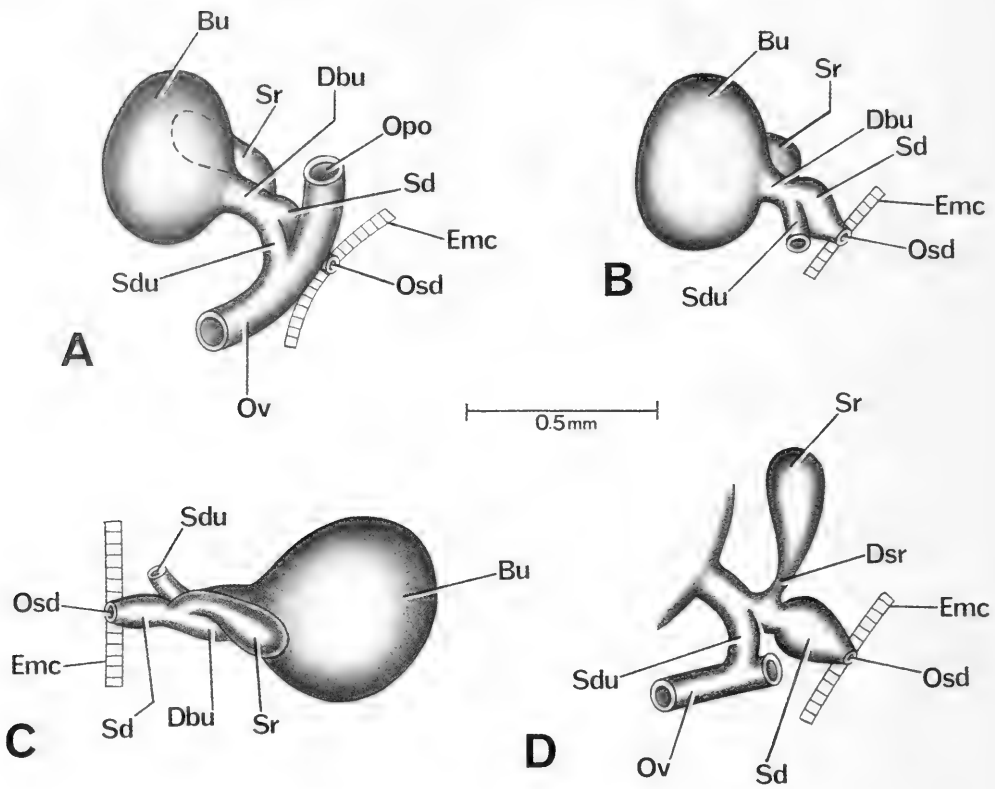

FIG. 87. Details and variation of bursa copulatrix complex of organs of *Neotricula duplicata* from D85-79. Figure A is in same orientation as in Figures 85 and 86. B. Swelling of spermathecal duct (Sd) seen in most individuals. C. Bursa complex seen in B flipped over 180° so that Emc is to left; this view shows juncture of duct of the bursa (Dbu), seminal receptacle (Sr) and spermathecal duct (Sd). D. As in A, but with oviduct (Ov) pulled to left to show the juncture of Dsr and Sd with duct of bursa.

TABLE 43. Radular statistics for *Neotricula duplicata.* Mean ± standard deviation (range). In mm except for the width of the central tooth in μm. N = number counted.

	D85-77	D87-2
Shell length (not eroded)	3.20±0.26 (2.84–3.60) N = 8	3.43±0.21 (4.44–5.20)
Radula length	0.55±0.04 (0.66–0.60) N = 11	0.57±0.04 (0.52–0.62) N = 10
Radula width	0.08±0.004 (0.072–0.088) N = 11	0.08±0.006 (0.078–0.092) N = 10
Total rows of teeth	70.4±4.1 (61–74) N = 8	60.1±8.0 (46–69) N = 10
No. rows of teeth forming	9.0±2.1 (7–13) N = 8	10.3±3.3 (6–15) N = 10
Central tooth width	15.5±0.8 (14.6–16.8) N = 9	17.1±1.5 (15.8–19.0) N = 7

the posterior end of the mantle cavity (Emc). (5) The penis is simple, with a small evertible papilla (Fig. 90B). In some specimens, the papilla is withdrawn and cannot be seen (living tissue, fresh microscope mount). In others, only the tip of the papilla can be seen being

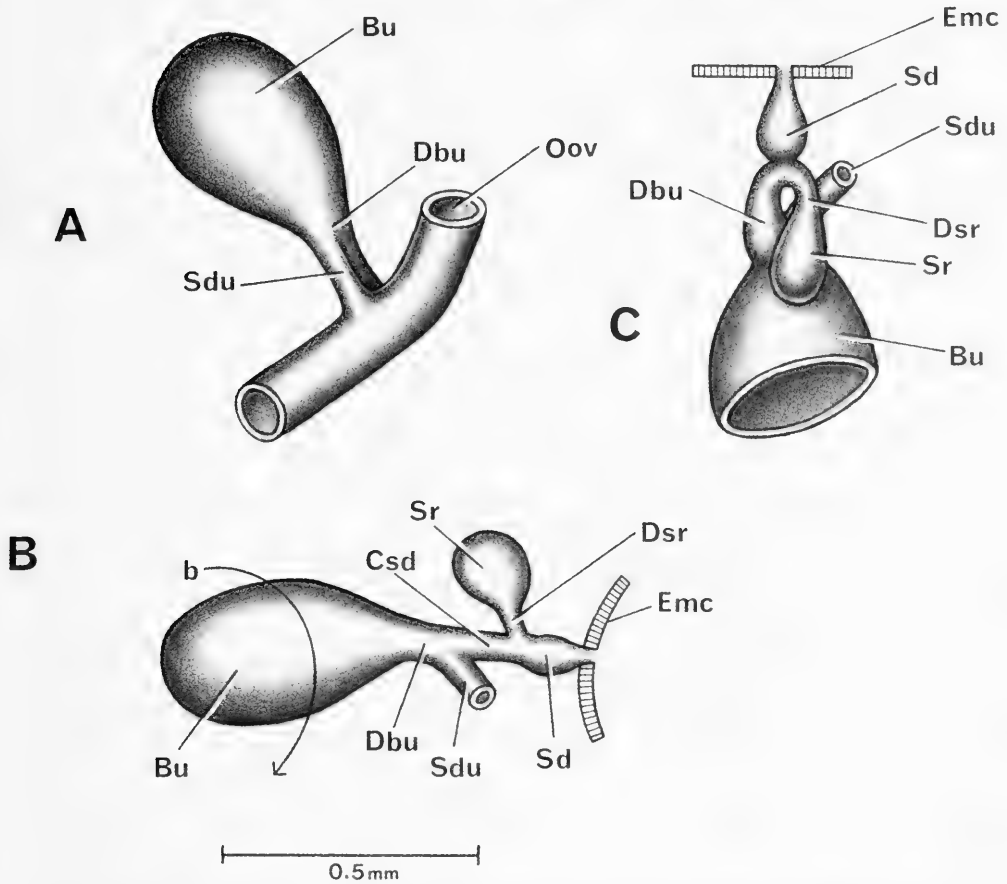

FIG. 88. Details and variation of bursa copulatrix complex of organs of *Neotricula duplicata* from D87-2. Figure A is in same orientation as in Figures 85 and 86. B–C. Variation in configuration of seminal receptacle (Sr). B. Bursa complex rotated in the direction of arrow to show interconnections of Dbu, Csd, Sr and Sd. C. Dorsal side of bursa complex to show that duct of bursa (Dbu) makes a U-shaped bend into duct of seminal receptacle (Dsr). Swollen short spermathecal duct (Sd) enters bottom of U-shaped bend. Note: Common sperm duct (Csd) is that portion of duct extending from duct of bursa between Sdu and Sd. Duct of bursa is defined in all papers as that duct extending from bursa copulatrix (Bu) anteriorly to point where another sperm duct connects to it, e.g. the Sdu.

pushed out and then withdrawn. (6) The base of the penis (Bp, Figs. 81, 90A) is oriented on the neck in diverse ways. The angle of the long axis of attachment varies from parallel to the mid-line of the snout-neck (x) through 90°. The base may overlap the mid-line or be to the right of mid-line. (7) No ejaculatory duct is seen in the base of the penis or in the neck.

Digestive system. The digestive gland is posterior to the stomach in both sexes. However, in some males of the D87-2 collection both digestive gland and gonad covered the posterior chamber of the stomach.

Radular statistics are given in Tables 43 and 44. The most commonly encountered formula in the D85-79 collection was:

$$\frac{2\text{-}1\text{-}2}{2(3)\text{-}(3)2};\ 3\text{-}1[2]\text{-}3(2);\ 12\text{-}15;\ 11\text{-}14;$$

in the D87 2 collection it was:

$$\frac{3(2)\text{-}1\text{-}(2)3}{3(2)\text{-}(2)3};\ 3(4)\text{-}1\text{-}3;\ 12\text{-}14;\ 11\text{-}13.$$

SEM photographs of radulae from snails of both collections are given in Figures 91–94 No significant differences occur between the

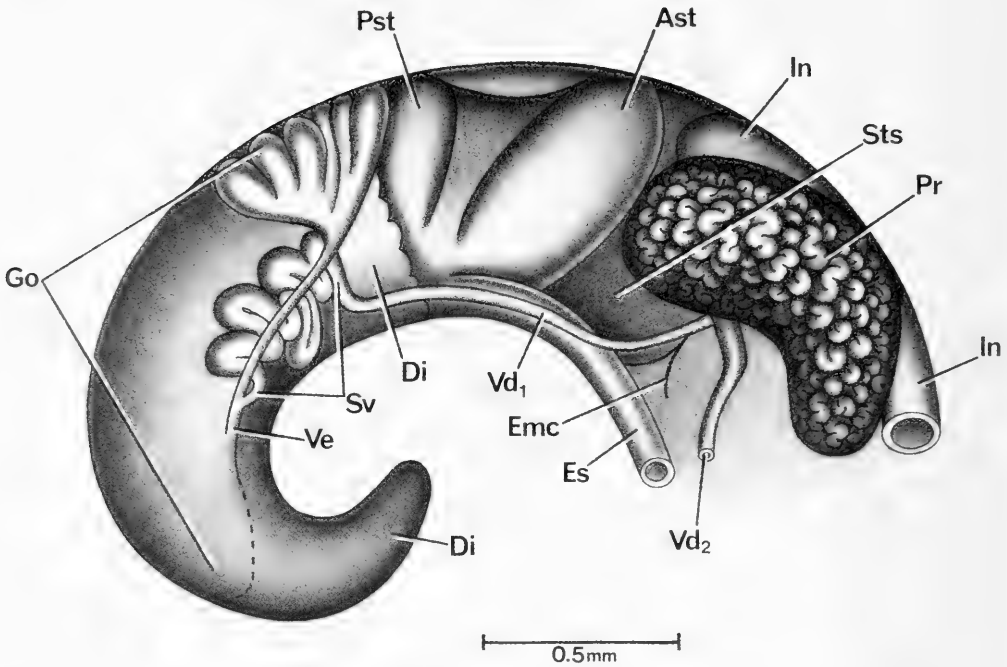

FIG. 89. Uncoiled male of *Neotricula duplicata* from D85-79. Anterior part of mantle cavity omitted. Posterior lobes of the gonad (Go) removed to show coiled seminal vesicle (Sv) dorsal to gonad. Dashed line indicates extent of gonad.

snails of the two collections; the tooth morphologies are the same and are typical of the generalized triculine type. Of note is the split or fork in the dominant central cusp of the lateral tooth (i.e. the "1" of the 3-1-3) (Fig. 91C, 92C, D, 93G, 94C).

The stomach has a noteworthy character. The anterior chamber of the stomach (Ast, Fig. 95) has at the anterior and posterior edges prominent yellow ridges (Yri).

Nervous system. Measurements of neural structures are given in Table 45. The RPG ratio indicates a moderately concentrated dorsal aspect of the nerve ring.

Remarks

These detailed anatomical studies of a single population collected two years apart provide a unique opportunity to assess (1) how well methods provide an adequate assessment of qualitative and quantitative characterstokes. The 1987 study is a control for the 1985 study, particularly as it was not remembered in 1987 that the 1985 assessment had been made. (2) Variation due to sampling (in part) and actual quantitative changes that could have occurred in two years. This is the first time that we have obtained an indication of the amount of variation that might be expected in such a study. This is of considerable help in assessing how much difference may actually exist when comparing two populations, each studied only once, e.g. between *N. cristella* and *N. dianmenensis* of this monograph.

Overall, there was excellent agreement in qualitative anatomy when comparing the two year classes. There was significant variation in cusp counts between year classes, particularly involving the marginal teeth. More variation occurred in central tooth cusp numbers in the 1987 year class.

Conchologically, *N. duplicata* is most similar to *N. dianmenensis*, *N. lilii*, and *Tricula gredleri* (Figs. 153, 154). Differences from *N. dianmenensis* are given on page 234. *Neotricula duplicata* differs from *T. gredleri* in three characters (10%). The former has spiral microsculpture lacking in the latter (char. 6). The former has an abapical spout lacking in the

TABLE 44. Cusp formulae for the radular teeth of *Neotricula duplicata* with the percent of radulae in which a given formula was found at least once.

Central Teeth (N = 10)		Lateral Teeth		Inner Marginal Teeth		Outer Marginal Teeth	
			D85-79				
2-1-2 / 3-3	70%	3-1[2]-3	100%	9	—	9	10%
2-1-2 / 2-2	30%	3-1[2]-2	50%	10	10%	10	20%
2-1-2 / 3-2	30%	4-1[2]-3	30%	11	20%	11	60%
2-1-2 / 2-3	20%	2-1[2]-3	20%	12	50%	12	70%
3-1-3 / 2-2	10%			13	100%	13	60%
3-1-2 / 2-2	10%			14	90%	14	40%
				15	50%	15	—
				16	30%	16	—
				17	20%	17	—
				$\bar{X}$* = 13.6±1.5 N = 108		12.0±1.1 120	
			D87-2				
3-1-3 / 3-3	60%	3-1[2]-3	100%	11	—	11	40%
2-1-2 / 3-3	50%	4-1[2]-3	40%	12	70%	12	90%
2-1-2 / 2-3	40%	3-1[2]-4	30%	13	80%	13	30%
3-1-3 / 2-2	30%	2-1[2]-3	10%	14	60%	14	20%
2-1-2 / 3-2	20%	3-1[2]-2	10%	15	20%	15	—
2-1-2 / 2-2	10%			$\bar{X}$ = 12.9±0.7 N = 100		12.1±1.3 N = 100	
3-1-3 / 2-3	10%						
3-1-2 / 3-3	10%						
2-1-2 / 3-2	10%						
2-1-3 / 3-3	10%						

*Mean ± standard deviation of cusp number for all teeth counted.

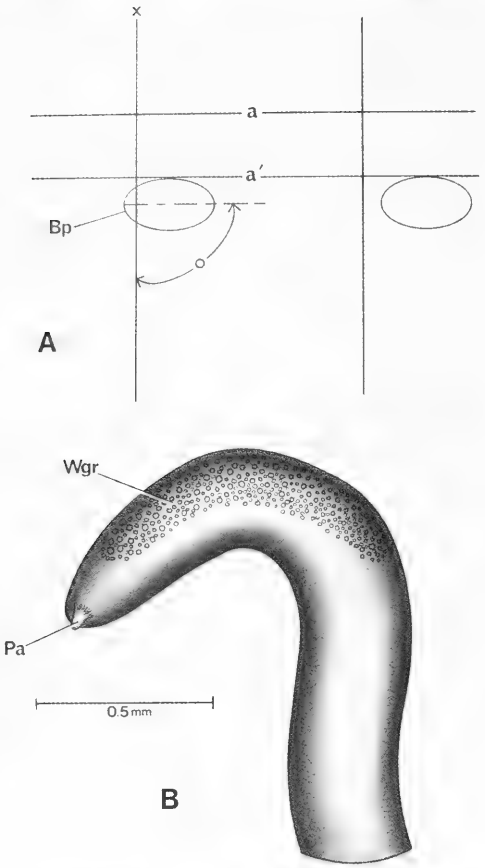

FIG. 90. A. The position of base of the penis of *Neotricula duplicata* relative to the snout-neck mid-line (x). B. Penis.

latter (char. 12). The latter has an adapical beak tubercle lacking in the former (char. 24). Anatomical differences are considerable, those used to define the genera among others (Fig. 157).

Conchologically, *N. duplicata* differs from *N. lilii* by having a wrinkled protoconch, not a smooth one (char. 8); having an adapical beak instead of a notch (char. 9); having a straight to arched inner lip, not a sinuate one (char. 13); having a thick inner lip, not a thin one (char. 19); by lacking a slight varix found in the latter (char. 23); and by lacking an adapical outer lip angle seen in the latter (char. 25). Anatomically, these species differ in nine characters (19%) (Figs. 157, 158). The differences are: The former has an elongated oval operculum with two or more layers (chars. 2, 3); the latter has an ovate operculum with one layer. The opercular attachment pad is very wide in the former, wide in the latter (char. 4). Gill filament section Gf_2 is of medium length in the former, long in the latter (char. 8). The bursa shape is ovoid in the former, round in the latter (char. 15). The spermathecal duct is short in the former, long in the latter (char. 19). The spermathecal duct runs directly anterior from the duct of the bursa to the mantle cavity in the former; it slants away at an angle in the latter (char. 20). The vas deferens bends away from the prostate at the posterior end of the mantle cavity in the former, at mid-prostate in the latter (char. 31). *Neotricula lilii* has very many rows of teeth on the radula; *N. duplicata* has many (char. 42).

***Neotricula lilii* Chen & Davis, sp. nov.**

Holotype. ZAMIP-M0002, Figure 70J.

Paratypes. ANSP 373138, A12654, Figure 70 K, L Figure 96A-D.

Type Locality. Chang Wang Village, Chuanxing Town, Lingxian County, Zhuzhou Prefecture. 26°17′18″N, 113°41′3″E. Figure 1, Site 2.

Etymology. Named for Dr. Li Li, Zhuzhou Prefectural Epidemic station, who collected this species.

Habitat

The assigned field collection number was D85-74. Snails came from a mountain stream 550 m above sea level. The stream was 10 to 15 cm deep, with small rocks, leaves and mud. There was low vegetation beside the stream.

Description

Shell. The shells are small, ovate-conic, with 5.5 to 6.0 whorls (Figs. 60A–B, 70J–L, 96A–B). Measurements are given in Tables 46, 47. Limited data suggest that females are larger than males (Table 47) with the lengths of the last three whorls of females ranging from 2.98–3.28; those for males, 2.72–2.80. The aperture is pyriform. Adapically there is a wide apertural notch; there is no beak tubercle.

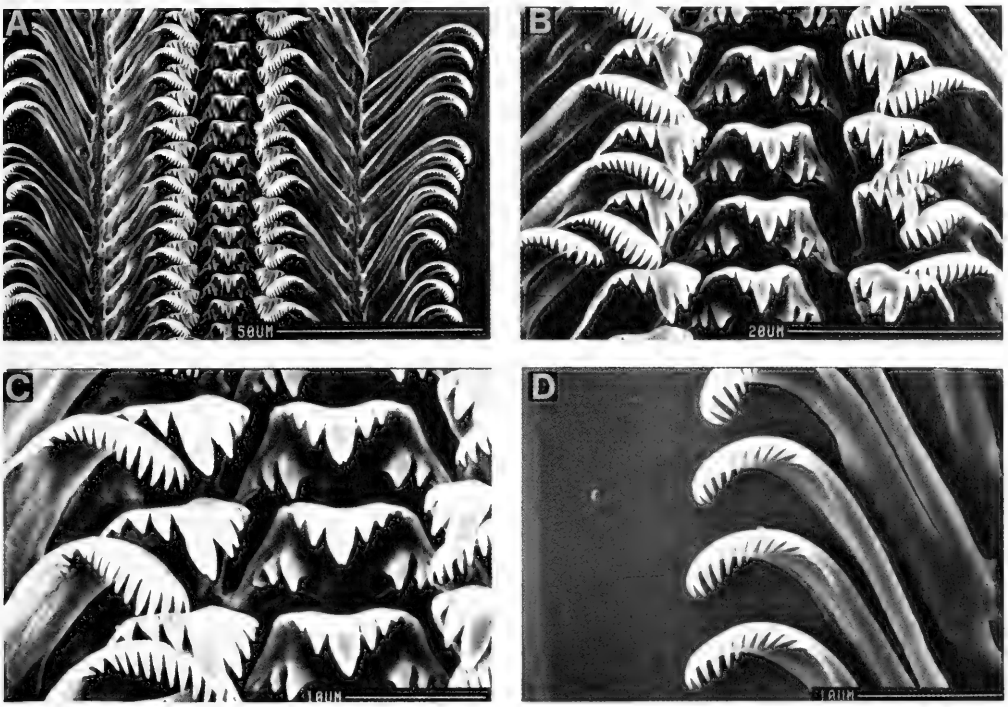

FIG. 91. Radula of *Neotricula duplicata* from D85-79. Centrals, laterals and inner marginals featured in B, C. D. Outer marginals.

TABLE 45. Lengths (mm) of neural structures of *Neotricula duplicata.* Mean ± standard deviation (range). * = neural elements measured to calculate the RPG ratio. N = number measured.

	D85-79 (N = 4)	D87-2 (N = 5)
Cerebral ganglion	0.26±0.03	0.24±0.03
	(0.22–0.30)	(0.24–0.26)
Cerebral commissure	0.05±0.02	0.04±0.01
	(0.02–0.06)	(0.03–0.06)
Pleural ganglion		
Right (1)*	0.14±0.03	0.13±0.02
	(0.10–0.16)	(0.10–0.16)
Left	0.12±0.03	0.12±0.01
	(0.08–0.14)	(0.10–0.12)
Pleuro-supraesophageal	0.14±0.04	0.11±0.02
connective (2)*	(0.10–0.18)	(0.10–0.14)
Pleuro-subesophageal	0.06±0.05	0.06±0.02
connective	(0.00–0.10)	(0.03–0.08) N = 4
Supraesophageal	0.13±0.02	0.12±0.02
ganglion (3)*	(0.10–0.14)	(0.10–0.14)
Subesophageal	0.11±0.02	0.11±0.01
ganglion	(0.10–0.12)	(0.10–0.12) N = 4
Osphradio-mantle nerve	0.08±0.01	0.08±0.04
	(0.06–0.08)	(0.00–0.12)
RPG ratio (2 ÷ 1+2+3)*	0.34±0.08	0.31±0.03
	(0.26–0.45)	(0.28–0.35)

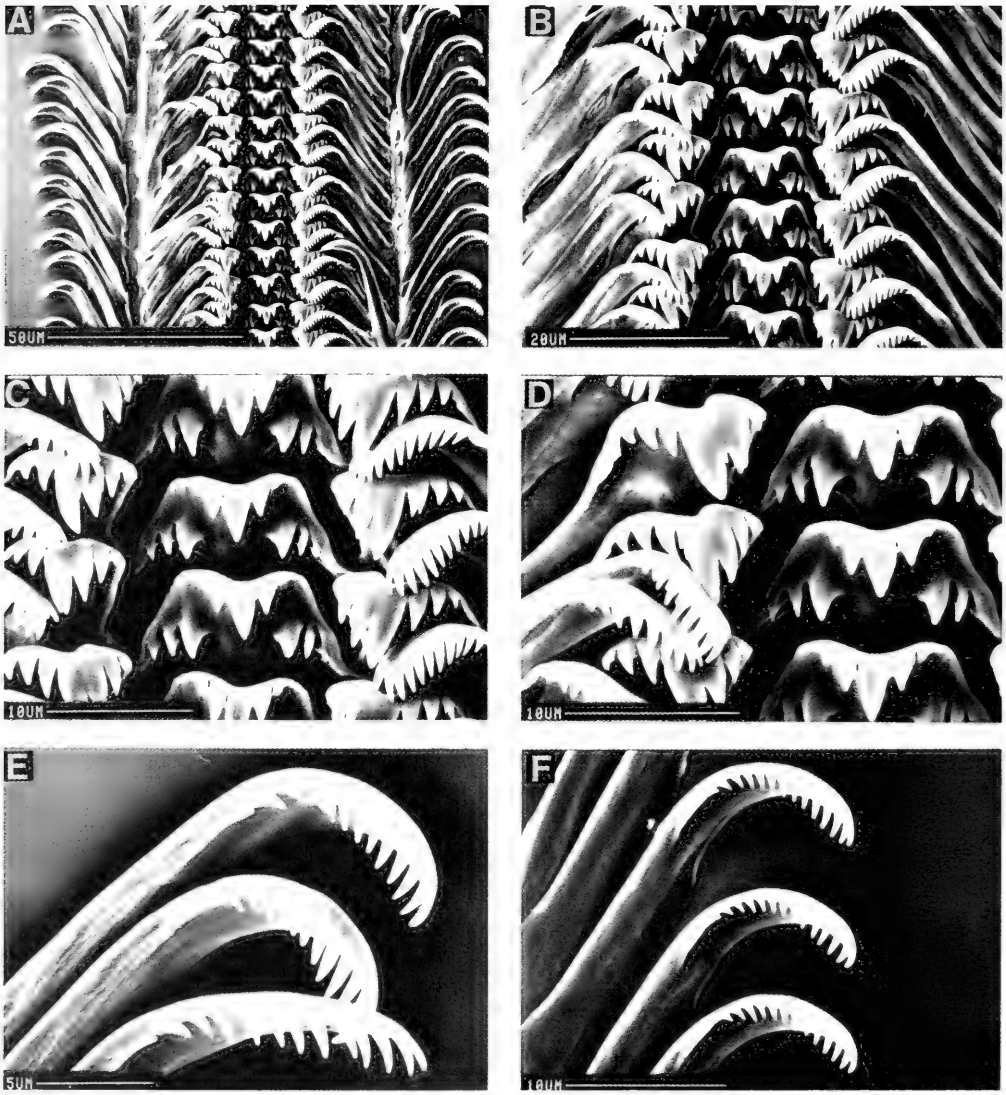

FIG. 92. Radula of *Neotricula duplicata* from D85-79. Centrals, laterals and inner marginals featured in B–D. E, F. Outer marginals.

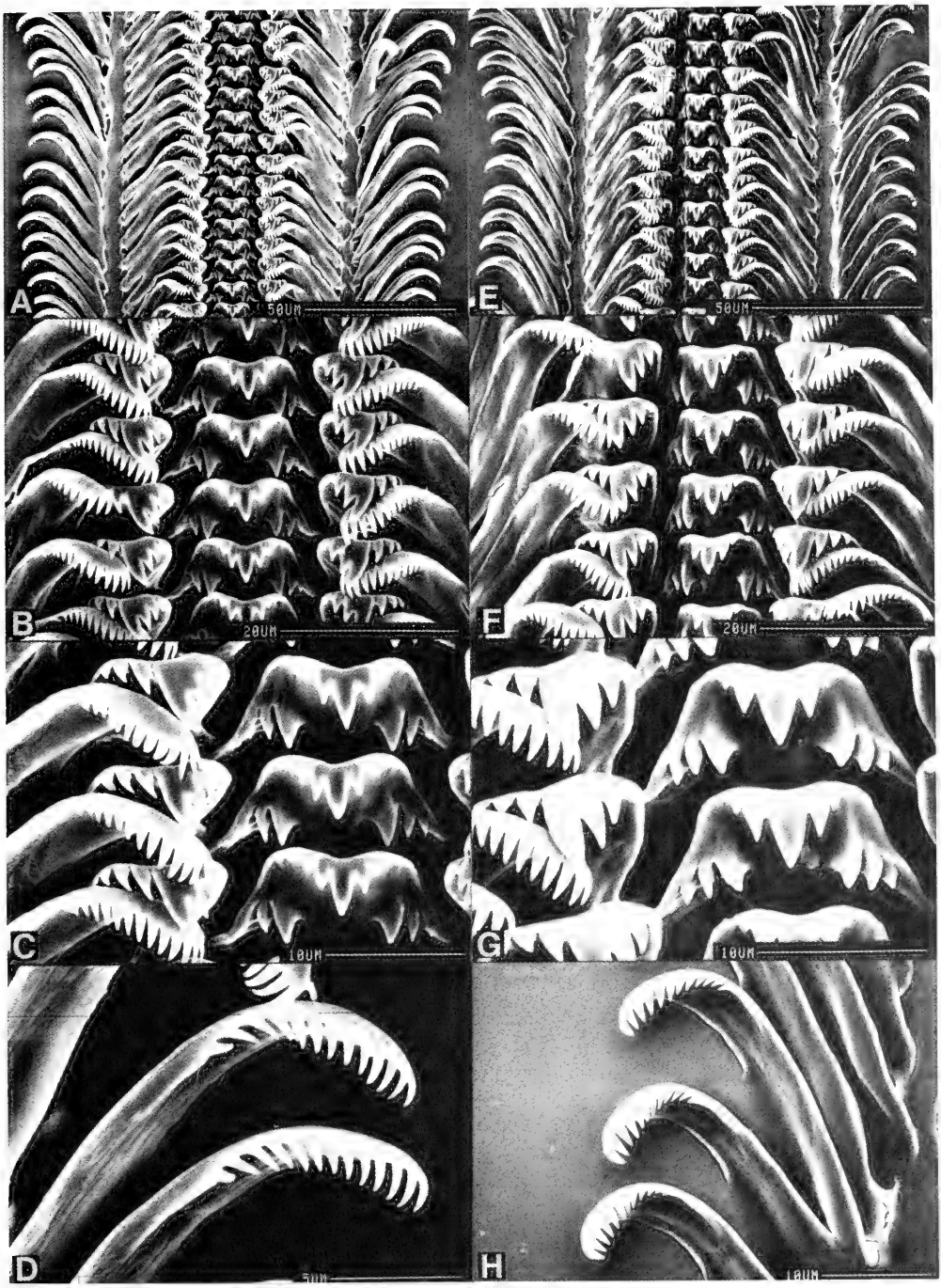

FIG. 93. Radula of *Neotricula duplicata* from D87-2. Centrals, laterals and inner marginals featured in B, C, E, G. D, H = outer marginals. A–D = males; E–H = females.

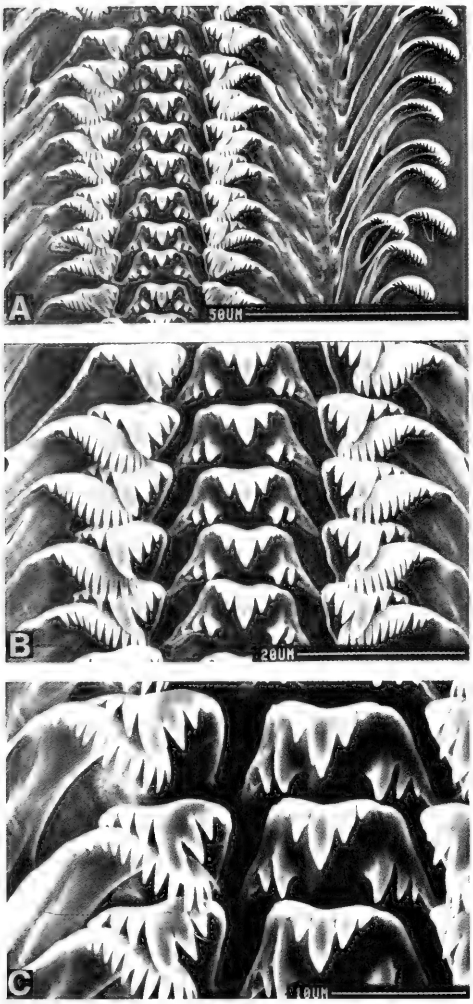

FIG. 94. Radula of female *Neotricula duplicata* from D87-2.

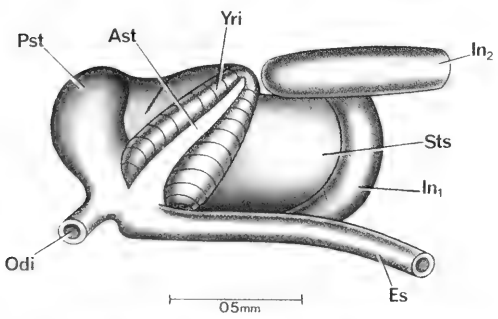

FIG. 95. Ventral aspect of the stomach of *Neotricula duplicata* in same orientation as in Figures 85, 86.

There is no internal notch groove. There is a pronounced adapical outer lip angle.

The whorls at the sutures are smooth (not crenulated). There is an umbilicus. SEM analysis reveals faint spiral microsculpture at the shoulders of the whorls after 1.75 whorls (Fig. 96A, C).

The inner lip is slightly sinuate and clearly separated from the body whorl in most specimens; it is uniformly thickened. In some (< 20%), the adapical inner lip is fused to the body whorl. The adapical end of the aperture is only slightly separated from the body wall. An apertural sinus is apparent examining the outer lip in side view. In side view, the outer lip, abapical to the sinus, is straight. The outer lip is slightly scooped forward. In side view, the inner lip has a strong deflection angle. There is a slight varix. There is an abapical spout. The abapical lip projects beyond the base of the shell 0.50 ± 0.05. SEM examination of the shell reveals that the apical whorl is smooth. (Fig. 96D).

External features. The head is grey. There are no granules about the eyes and no "eyebrow." The operculum is corneous and paucispiral. The inner lip edge is straight abapically and slightly sinuate towards the apertural beak end (adapically). The muscle attachment callus is pronounced and narrow, only 40% of the operculum width. A porous, regularly pitted surface of the callus was found in most specimens (75%) (Fig. 96E–H).

Mantle cavity. Measurements and counts of mantle cavity structures are given in Table 48. The ovoid osphradium is mid-gill; it is short. There are 20–24 gill filaments. Gf_2 is long. The length of the longest filament is 0.51 mm. The larger gill filaments are moderately domed. There is no spherical patch of white granules anterior to the osphradium where the mantle collar joins the neck.

Female reproductive system. The body of an uncoiled female without head or kidney tissue is shown in Figure 97. Organ measurements are given in Table 48. Important features are: (1) The gonad (Go) is posterior to the stomach; it is short and consists of few groups or bundles of lobes. (2) The bursa copulatrix (Bu) is spherical and prominent posterior to the albumen gland (Ppo). (3) The bursa is short. (4) The albumen gland is standard (= normal) length. (5) The bursa copulatrix complex of organs is shown in Figure 98A, B in the same orientation as in Figure 97. The nar-

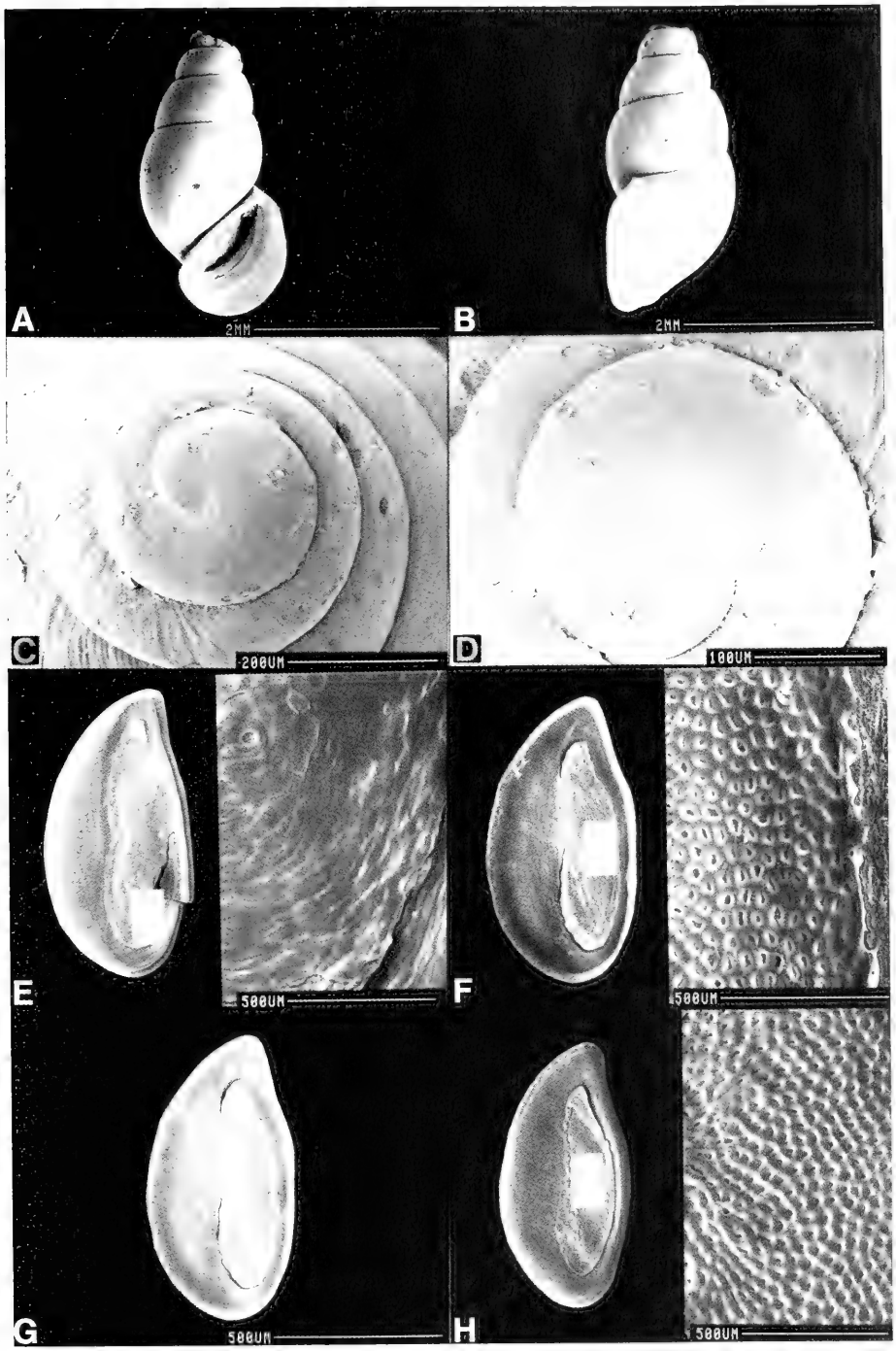

FIG. 96. SEM photographs of shells and operculum of *Neotricula lilii*. C, D. Enlargements of apical whorls. E–H. Inner surfaces of four opercula; insets provide enlargements of attachment pads to reveal microstucture.

TABLE 46. Shell measurements (mm) for the types of *Neotricula lilii*. Mean ± standard deviation (range). e = eroded apical whorls. N = number measured.

		Paratypes	
	Holotype	Larger (N = 1)	Smaller (N = 4)
No. Whorls	5.5	4e	4e to 5.5
Length (L)	3.20	3.20	2.98±0.18 (2.76–3.20)
Width (W)	1.52	1.68	1.51±0.10 (1.38–1.62)
L last three whorls	2.76	3.00	2.70±0.11 (2.54–2.80)
L body whorl	1.96	2.20	1.90±0.09 (1.76–1.96)
L penultimate whorl	0.48	0.48	0.49±0.02 (0.48–0.52)
W penultimate whorl	0.98	1.12	1.03±0.05 (0.96–1.08)
W 3rd whorl	0.72	0.80	0.72±0.04 (0.68–0.76)
L aperture	1.40	1.60	1.39±0.10 (1.24–1.48)
W aperture	0.92	1.04	0.93±0.06 (0.86–1.00)
x	0.52	0.56	0.50±0.05 (0.44–0.56)
y	0.12	0.20	0.15±0.04 (0.12–0.20)

TABLE 47. Shell measurements (mm) for *Neotricula lilii* used for anatomical work. Mean ± standard deviation (range). e = eroded apical whorls. N = number measured.

	Females		Males
	Larger Size Class (N = 3)	Small Size Class (N = 1)	(N = 3)
No. Whorls	4e–6.0	5.75	3e–4e
Length (L)	3.43±0.19 (3.20–3.56)	3.12	2.89±0.12 (2.76–3.00)
Width (W)	1.63±0.08 (1.56–1.72)	1.48	1.47±0.06 (1.40–1.52)
L last three whorls	3.11±0.15 (2.98–3.28)	2.72	2.76±0.04 (2.72–2.80)
L body whorl	2.21±0.12 (2.08–2.28)	1.92	1.95±0.06 (1.88–2.00)
L penultimate whorl	0.55±0.04 (0.52–0.60)	0.48	0.49±0.04 (0.44–0.52)
W penultimate whorl	1.13±0.06 (1.08–1.20)	1.00	1.03±0.04 (1.00–1.08)
W 3rd whorl	—	—	—
L aperture	1.59±0.10 (1.48–1.68)	1.32	1.35±0.08 (1.28–1.44)
W aperture	0.99±0.02 (0.96–1.00)	0.96	0.89±0.02 (0.88–0.92)
x	0.52±0.06 (0.44–0.56)	0.52	0.45±0.02 (0.44–0.48)

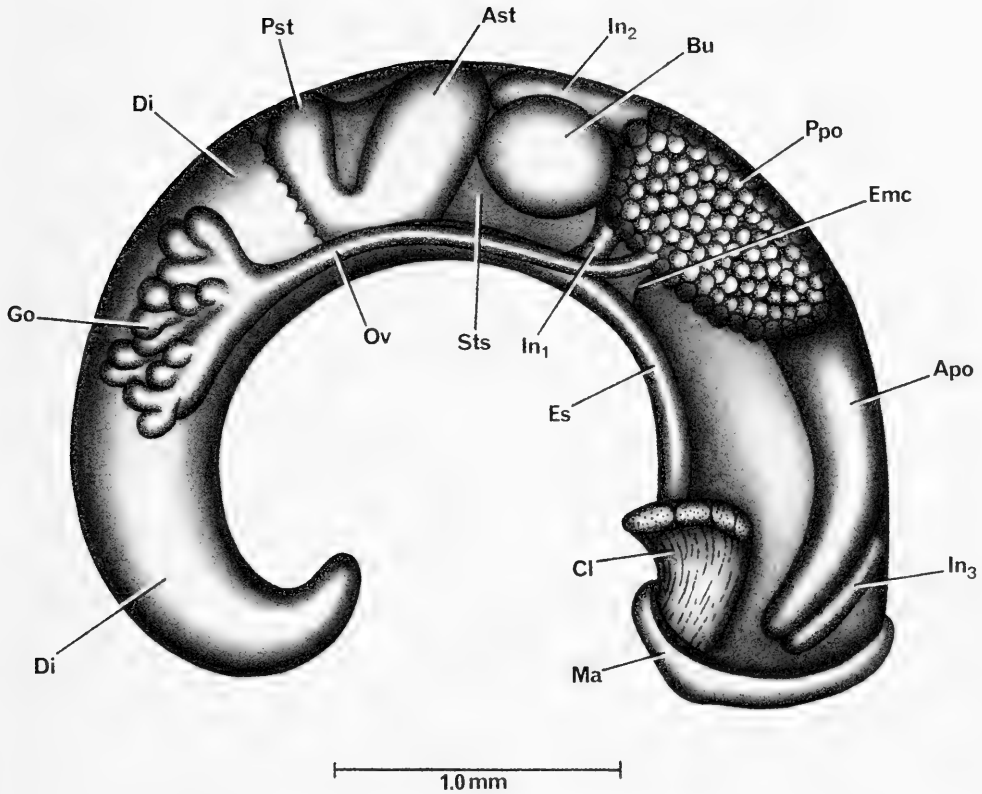

FIG. 97. Uncoiled female *Neotricula lilii* with head and kidney tissue removed.

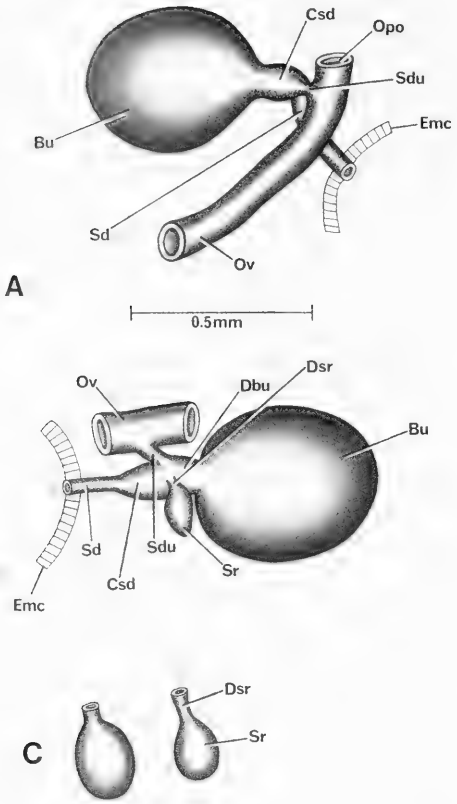

FIG. 98. Details and variation of bursa copulatrix complex of organs of *Neotricula lilii*. Figure A is in same orientation as in Figure 97. B. Bursa flipped over to show place where seminal receptacle (Sr) enters common sperm duct (Csd). C. Variation in size and shape of seminal receptacle.

row spermathecal duct dilates to form the common sperm duct (Csd) from which opens the sperm duct (Sdu) and the seminal receptacle (Sr) (Fig. 98 B). (6) The sperm duct is very short and to the left of the common sperm duct. (7) The seminal receptacle arises some 45° from the opening of the sperm duct; it arises from the right dorso-lateral side of the sperm duct. (8) The seminal receptacle varies in shape from elliptical to sub-spherical (Fig. 98C); it has a very short duct (Dsr). (9) The duct of the bursa (from the bursa to openings of Dsr and Sdu) is extremely short. (10) The distance from the posterior end of the mantle cavity (Emc) to the bursa is short, only 0.16 mm to 0.32 mm. The spermathecal duct—common sperm duct run straight posteriorly from the end of the mantle cavity to the bursa.

Male reproductive system. A section of an uncoiled male without kidney tissue is shown in Figure 99. The anterior gonadal lobes are removed to show the seminal vesicle (Sv). Organ measurements are given in Table 48. Important features are: (1) The gonad (Go) slightly overlaps the posterior chamber of the stomach. (2) The seminal vesicle (Sv) arises from the vas efferens (Ve) at mid-gonad to slightly posterior to mid-gonad. (3) The prostate (Pr) overlaps the posterior end of the mantle cavity and covers half the style sac (Sts). (4) The anterior vas deferens (Vd_2) diverges from the prostate slightly anterior to the posterior end of the the mantle cavity. (5) The penis is simple with a papilla (Pa) that everts (Fig. 100B). There is a massive concentration of white granules along the anterior convex edge. (6) The penis arises to the right of the snout-neck mid-line (Fig. 100A). The long axis of the penial base (Bp) is swollen at its base increasing the diameter from 0.14 mm to 0.22 mm. (7) No ejaculatory duct is seen in the penial base or neck.

Digestive system. The digestive gland is posterior to the stomachs of both males and females. Radular statistics are given in Tables 49 and 50. The radula is illustrated in Figures 101, 102. The central tooth is the generalized triculine type (Fig. 101B, E). The dominant cusp of the lateral tooth (the "1" of the 3-1-3) is almost always bifurcated (Fig. 101). The most commonly encountered cusp formula is

$$\frac{3(2)\text{-}1\text{-}(2)3}{2\text{-}2};\ 3\text{-}[2]\text{-}3(4);\ 13\text{-}15;\ 12\text{-}14.$$

Nervous system. It is standard triculine. Measurements are given in Table 51. The RPG ratio of 0.44 indicates that the dorsal nerve ring is moderately concentrated.

Remarks

Conchologically, *N. lilii* is most similar to *N. duplicata* and *N. dianmenensis* (Figs. 153–155). The comparison of these three species is given in the remarks section for the two previously treated species. Anatomically, *N. lilii* is most similar to *N. cristella*, a species that has a very different shell (Figs. 154, 156–158). There are five differences (Tables 80, 81) (10%): *N. lilii* has an operculum with a single layer whereas the operculum of *N. cristella*'s has two or more layers (char. 3). The former

TABLE 48. Lengths (mm) or counts of non-neural organs and structures of *Neotricula lilii*. N = number of snails used. Mean ± standard deviation (range).

	Females (N = 4)	Males (N = 3)
Body	4.96±0.82 (3.92–5.86)	4.27±0.08 (4.64–4.80)
Gonad	0.80±0.12 (0.70–0.96)	1.42±0.07 (1.36–1.50)
Digestive gland	2.03±0.23 (1.80–2.30)	2.13±0.19 (2.00–2.34)
Posterior pallial oviduct (= albumen gland)	1.00±0.08 (0.96–1.10) N = 3	—
Anterior pallial oviduct (= capsule gland)	1.14±0.16 (0.96–1.26) N = 3	—
Total pallial oviduct = OV	2.15±0.22 (1.92–2.36) N = 3	—
Bursa copulatrix = BU	0.52±0.04 (0.50–0.56) N = 3	—
Duct of BU	0.10 (N = 1)	—
BU ÷ OV	0.24±0.02 (0.23–0.26)	—
Seminal receptacle	0.19±0.02 (0.16–0.20)	—
Duct of seminal receptacle	0.04±0.02 (0.02–0.06)	—
Mantle cavity	1.54±0.20 (1.20–1.56)	1.37±0.07 (1.30–1.44)
Gill (G)	1.19±0.15 (1.0–1.36)	1.22±0.07 (1.16–1.30)
Osphradium (OS)	0.32±0.05 (0.28–0.38)	0.38±0.02 (0.36–0.40)
OS ÷ G	0.27±0.07 (0.22–0.38)	0.31±0.02 (0.28–0.33)
No. of filaments	21.8±1.7 (20–24)	21.4±0.6 (21–22)
Gf_2	0.32±0.03 (0.28–0.36) N = 6	Males & Females
Gf_1	0.19±0.03 (0.16–0.20) N = 6	Males & Females
Total Gf = TGF	0.51±0.05 (0.46–0.58) N = 6	Males & Females
Gf_2 ÷ TGF	0.63±0.04 (0.58–0.69) N = 6	Males & Females
Prostate	—	1.02±0.13 (0.90–1.16)
Seminal vesicle	—	1.00±0.20 (0.80–1.20)
Penis	—	1.15±0.01 (1.50–1.52)

TABLE 49. Radular statistics for *Neotricula lilii*. Mean ± standard deviation (range). N = 4. In mm except for width of central tooth in μm.

Shell length	3.00±0.17 (2.80–3.16)
Radular length	0.58±0.01 (0.57–0.60)
Radular width	0.08 (0.072–0.080)
Total rows of teeth	87 (84, 90) (N = 2)
No. rows of teeth forming	19 (16, 22) (N = 2)
Central tooth width	17.2 (16.2–17.9) N = 3

has a moderate number of gill filaments whilst the latter has few (char. 6). The male gonad overlaps the stomach of the former; it is posterior to the stomach in the latter (char. 27). The anterior vas deferens leaves the prostate at mid-prostate in the former; from the prostate at the posterior end of the mantle cavity in the latter (char. 31). The penial tip of the former has a papilla; that of the latter a long penial filament.

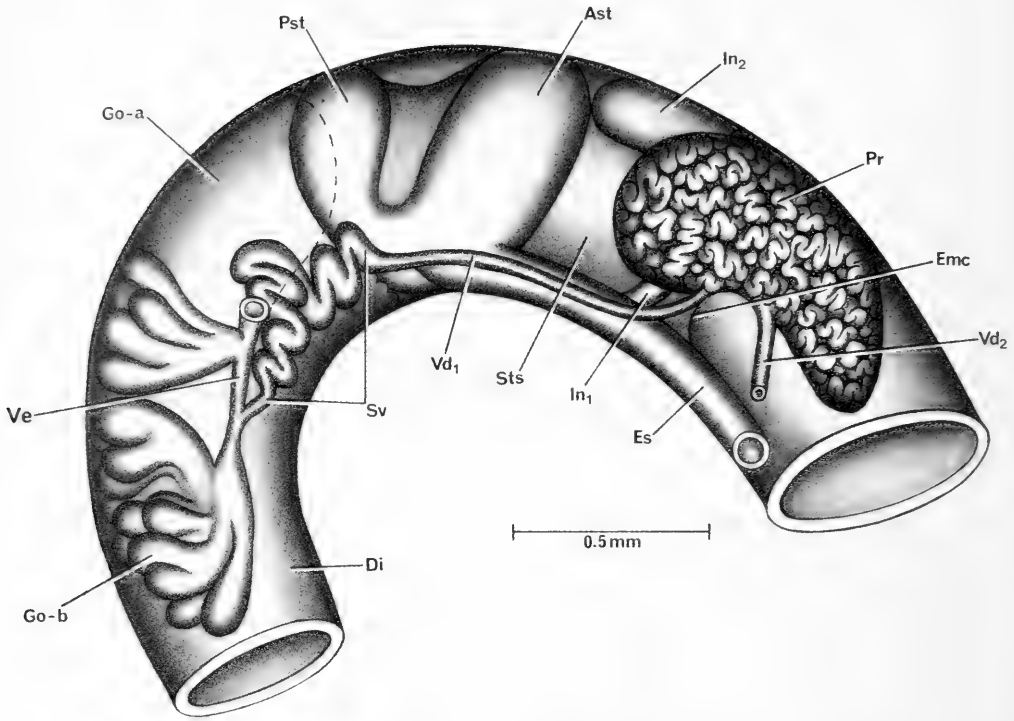

FIG. 99. Uncoiled male of *Neotricula lilii* without head or kidney tissue. Anterior part of mantle cavity omitted as is posterior end of digestive gland.

TABLE 50. Cusp formulae for the radular teeth of *Neotricula lilii* with the percent of the three radulae in which a given formula was found at least once.

Central Teeth		Lateral Teeth		Inner Marginal Teeth		Outer Marginal Teeth
$\frac{3\text{-}1\text{-}3}{2\text{-}2}$	66%	3-1[2]-3	100%	12	—	33%
$\frac{2\text{-}1\text{-}2}{2\text{-}2}$	33%	3-1-3	66%	13	100%	66%
$\frac{3\text{-}1\text{-}3}{2\text{-}3}$	33%	4-1[2]-3	33%	14	100%	100%
		3-1-4	33%	15	66%	33%
				16	33%	—
				$\bar{X}$ * 14.2±0.9 N = 30		13.8±1.0 N = 30

*Mean ± standard deviation of cusp number for all teeth counted.

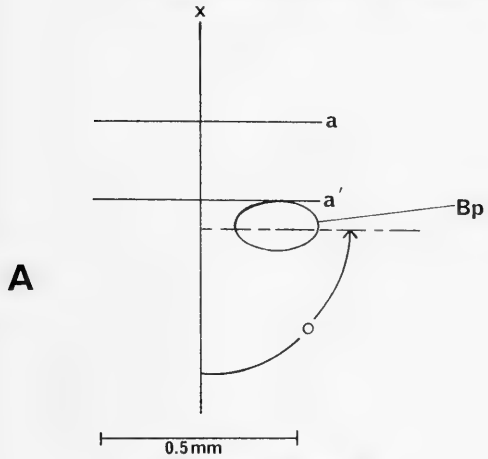

FIG. 100. A. Relationship of base of the penis of *Neotricula lilii* to mid-line of snout-neck (x) and to posterior end of eye lobes (a). B. Penis.

Neotricula minutoides (Gredler, 1885)

Paralectotypes. SMF 4155; pl. 4, fig. 1, in Yen, 1939.

Type locality. "Aus Quellen bei Hensan"; Heng-shan-hsien, Hunan (Yen, 1939). Near site 1, fig. 1 (Hengshan)

Synonymy. Bithynia minutoides Gredler, 1885
Hydrobia minutoides (Gredler, 1887)
Tricula minutoides, Yen, 1939
Neotricula minutoides, this paper

Habitat

Specimens collected for this paper came from Tong Meng Village, Xikou town, Cili County, Changde Prefecture; 29°13′58″N, 110°44′12″E; Figure 1 site 8. The field collection number was D85-83 on 7 October 1985. Specimens were collected from Tong meng village, Xikou Tow, Cili County, Changde Prefecture; 29°13′58″N, 110°44′12″E; Figure 1 site 8. The assigned collection number was D85-83. The habitat was a small perrenial stream 15–25 cm wide and 5–10 cm deep at an altitude of 550 m above sea level. The stream was shaded; the flow was slow. The bottom of the stream was paved with small stones in mud. The water was clean and cool. The sides of the stream had weeds and short shrubery.

TABLE 51. Lengths of neural structures of *Neotricula lilii.* Mean ± standard deviation (range). N = 4. * = neural elements measured to calculate the RPG ratio.

Cerebral ganglion	0.25±0.01 (0.24–0.26)
Cerebral commissure	0.09±0.05 (0.04–0.16)
Pleural ganglion	
Right (1)*	0.11±0.01 (0.10–0.12)
Left	0.10 (N = 3) No var.
Pleuro-supraesophageal connective (2)*	0.17±0.03 (0.12–0.18)
Pleuro-subesophageal connective	0.08±0.03 (0.04–0.10) N = 3
Supraesophageal ganglion (3)*	0.11±0.03 (0.10–0.14)
Subesophageal ganglion	0.08±0.04 (0.10–0.12) N = 3
Osphradio-mantle nerve	0.02 (0, 0.04) N = 2
RPG ratio* = 2 ÷ 1+2+3	0.44±0.08 (0.33–0.50)

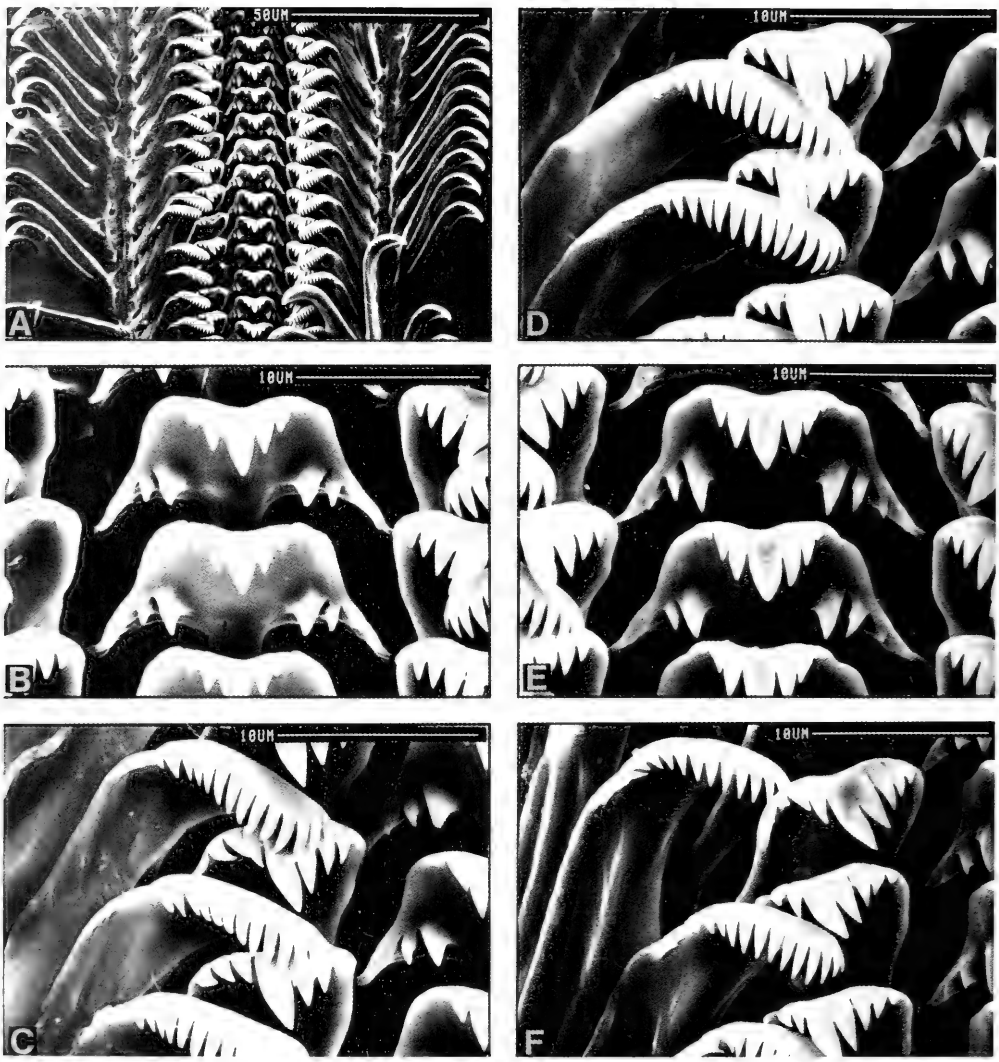

FIG. 101. Radula of *Neotricula lilii*. A. Segment of radula. B, E. Central teeth. C, D, F. Lateral and inner marginal teeth.

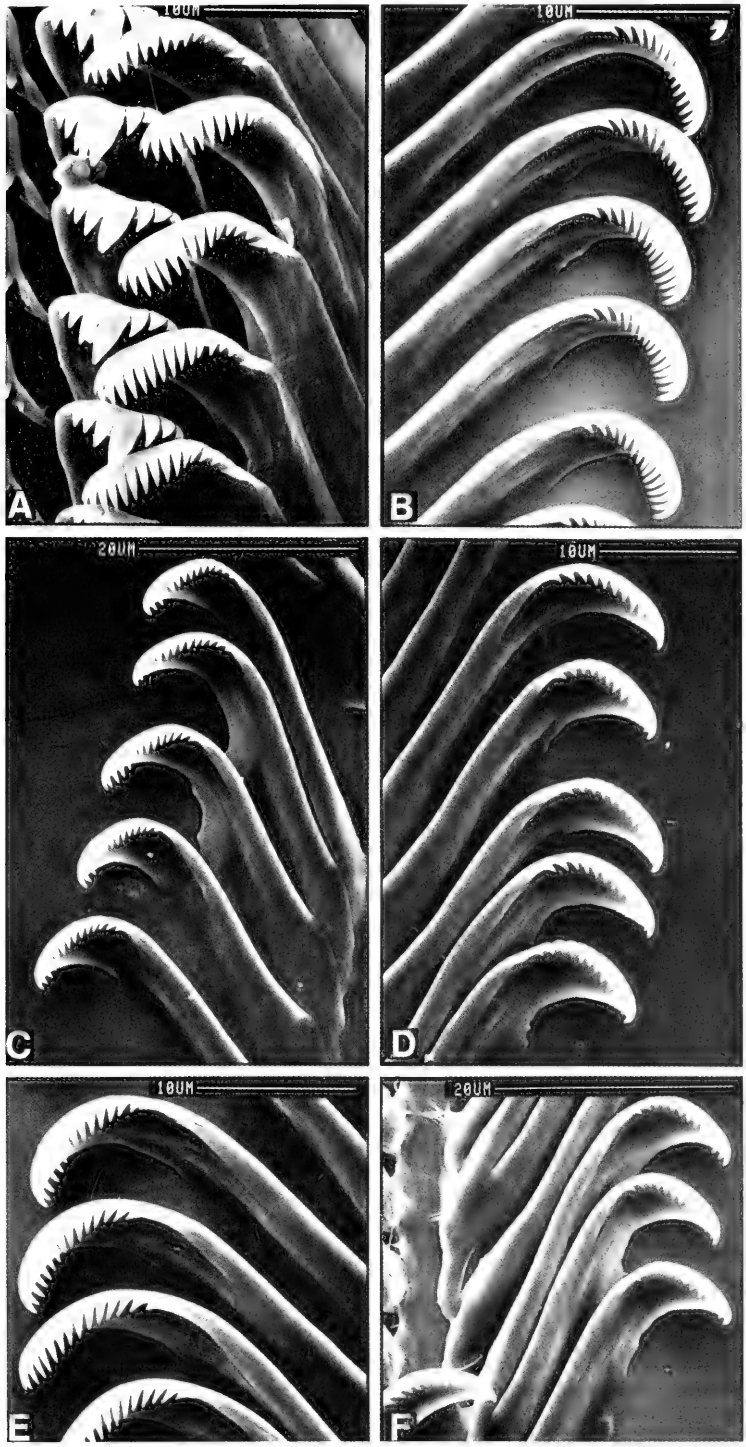

FIG. 102. Radula of *Neotricula lilii*. A. Right lateral and inner marginal teeth. B–F. Outer marginal teeth; B, D, F = right; C, E = left outer marginal teeth.

TABLE 52. Shell measurements (mm) of *Neotricula minutoides*. Mean ± standard deviation (range). N = 5; all shells 5.5 whorls.

Length (L)	3.41±0.20 (3.14–3.60)
Width (W)	1.68±0.09 (1.60–1.80)
L last three whorls	3.07±0.18 (2.84–3.28)
L body whorl	2.28±0.15 (2.12–2.48)
L penultimate whorl	0.50±0.04 (0.44–0.56)
W penultimate whorl	1.09±0.05 (1.04–1.16)
W 3rd whorl	0.72±0.03 (0.68–0.76)
L aperture	1.53±0.13 (1.40–1.70)
W aperture	1.02±0.07 (0.96–1.12)
x	0.44±0.05 (0.40–0.52)
y	0.18±0.05 (0.12–0.24)

Depository

Specimens are deposited in ZAMIP, M0006; ANSP, 373136, A12652.

Description

Shells. The shells are small, ovate-conic with 5.5 whorls (Figs. 60C–G, 103A–E). Lengths range from 3.14–3.60 mm (Table 52). The aperture is pyriform. Adapically there is no notch or beak, nor is there an internal notch groove. There is no adapical outer lip angle.

The whorls at the suture are smooth (not crenulated). There is a pronounced umbilicus. SEM analysis reveals faint traces of spiral microsculpture on the adapical part of the whorls of the teleoconch.

The inner lip is thick and arched. It is clearly separated from the body whorl by a narrow gap. The adapical apertural lip is pulled away from the body whorl but the interspace is filled with shell layers (as is the inner side of the inner lip). There is no apertural sinus. In side view, the outer lip is straight and slightly scooped forward. In side view, the inner lip is straight. There are no apertural teeth or notches, no varix, no spout. The abapical lip projects beyond the base of the shell 0.44 ± 0.05 mm.

As seen with SEM, the protoconch is minutely wrinkled (Fig. 103C–E). Growth lines begin on the teleconch at 2.0 whorls.

External Features. The head is dark grey, with few or no white granules about the eyes. The operculum is corneous and paucispiral (Fig. 103F). It appears to grow in layers. The internal attachment pad is prominent, some 49% the width of the operculum.

Mantle cavity. Mantle cavity structures are typically triculine. Organ measurements are given in Table 53. The osphradium is located mid-gill; it is small. Only one gill filament was measured; it was 0.58 mm long. For this filament Gf_2 was long.

Female reproductive system. An uncoiled female without head and with kidney tissue removed is shown in Figure 104. Measurements of organs are given in Table 53. Important features are: (1) The gonad is posterior to the stomach, is small, and consists of one or two bundles of lobes. (2) The bursa copulatrix (Bu) is round, small and situated directly posterior to the albumen gland (Ppo). It is not occluded by the posterior part of the albumen gland. (3) The albumen gland is short. (4) The bursa copulatrix complex of organs is shown in Figure 105. The orientation of organs in Figure 105A is the same as that in Figure 104. The bursa (Bu) is short. (5) The seminal receptacle (Sr) is spherical; it may or may not have a duct. In either case, it opens into the base of the duct of the bursa where the latter runs into the spermathecal duct (Sd) and also receives the sperm duct (Sdu). This opening for the seminal receptacle is on the dorso-lateral side of the bursa complex (Fig. 105C). (6) When there is a discernable duct of the seminal receptacle, it is extremely short, about 0.02 mm. (7) The spermathecal duct is short and swollen; it is nearly a straight, as well as a direct continuation of the duct of the bursa; it opens into the posterior end of the mantle cavity (Emc).

Male reproductive system. The posterior half of an uncoiled male with kidney tissue removed is shown in Figure 106. Measurements of organs are given in Table 53. Important features are: (1) The gonad (Go) is posterior to the stomach. It consists of several bundles of lobes (removed in Figure 106 to reveal the seminal vesicle) arising from the vas efferens. (2) The prostate (Pr) overlaps the posterior end of the mantle cavity (Emc.) (3) The seminal vesicle (Sv) arises from mid-vas efferens. (4) The seminal vesicle forms a small knot of ducts dorsal to the gonad; it does not continue onto the stomach. (5) The anterior vas deferens (Vd_2) leaves the prostate near the posterior end of the mantle cavity (Emc). (6) The penis (Figure 107B) is simple, slender and differs from that of any other Hunan species by being highly extensible. (7) The penis has no papilla nor was an ejaculatory duct found at the base of the penis or in the neck. (8) The orientation of the base of the penis on the neck is shown in Figure 107A. It slightly overlaps the snout-neck mid-line; it is

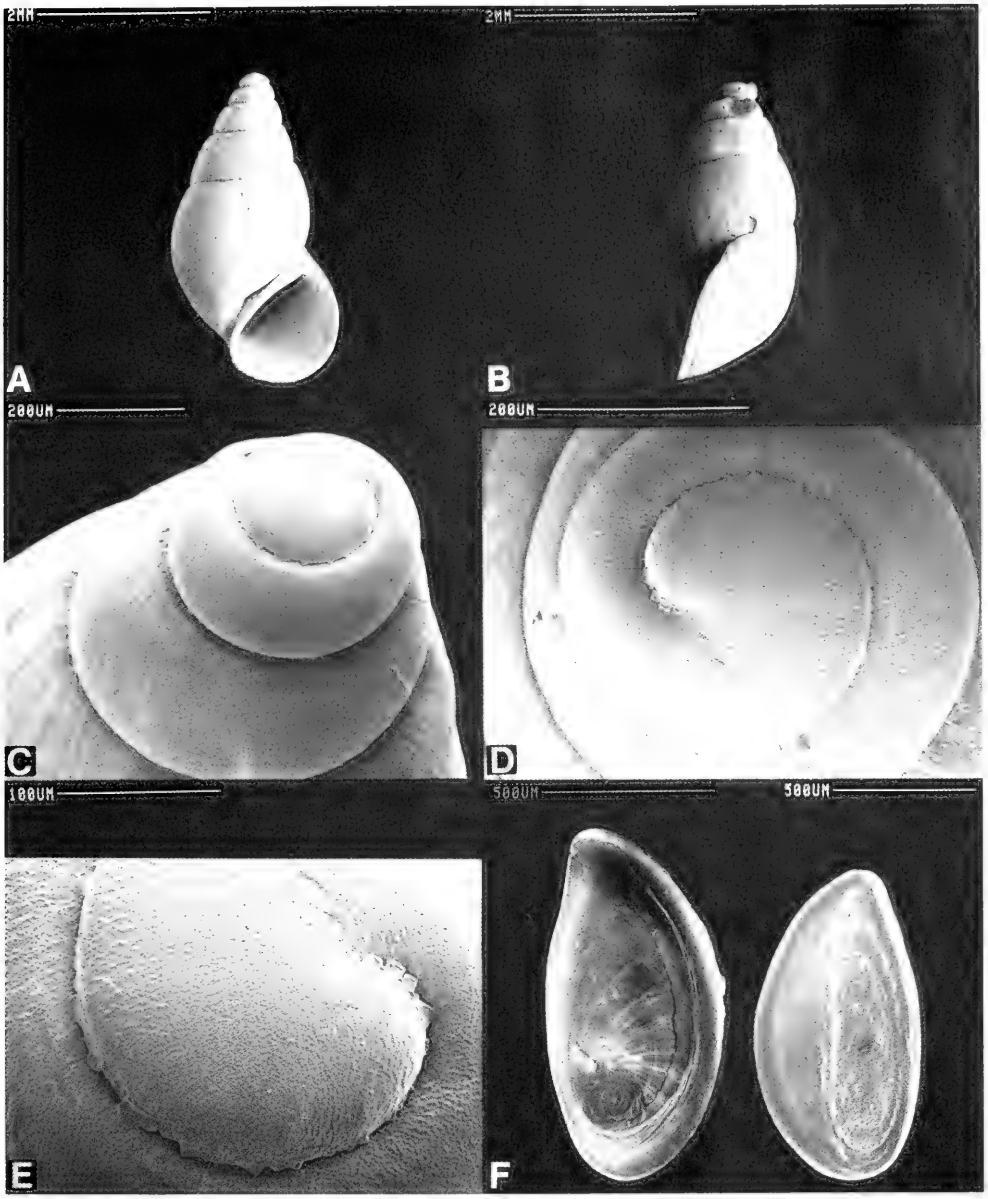

FIG. 103. SEM photographs of shells and opercula of *Neotricula minutoides*. Note in B that the outer lip is slanted. C–E. Details of protoconch and in C, beginning teleconch. F. Opercula with outer surface (left) and inner surface (right).

orientated at an angle of 40° to the snout-neck mid-line (x).

Digestive system. The digestive gland covers the posterior chamber of the stomach of both sexes. Radular statistics are given in Tables 54 and 55. There are 56.4 ± 4.8 rows of teeth along a radula of 0.51 mm length. The most frequently encountered formula is

$$\frac{(2)3\text{-}1\text{-}3(2)}{2\text{-}2};\ 2 \text{ to } 4\text{-}[2]\text{-}2(3);\ 12\text{-}14;\ 11\text{-}14.$$

TABLE 53. Lengths (mm) or counts of non-neural organs and structures of *Neotricula minutoides*. N = number of snails used. Mean ± standard deviation (range).

	Females (N = 5)	Males (N = 1)
Body	5.02±0.13 (4.90–5.16)	4.40
Gonad	0.83±0.15 (0.70–1.00)	1.28
Digestive gland	2.10±0.28 (1.80–2.36)	1.90
Posterior pallial oviduct (= albumen gland)	0.80 (0.60, 1.00) N = 2	—
Anterior pallial oviduct (= capsule gland)	1.28 (1.16, 1.40) N = 2	—
Total pallial oviduct = OV	2.02±0.34 (1.76–2.40)	—
Bursa copulatrix = BU	0.55±0.14 (0.40–0.66)	—
Duct of BU	—	—
BU ÷ OV	0.28±0.10 (0.17–0.35)	—
Seminal receptacle	0.10 (no var.) N = 2	—
Duct of Seminal receptacle	—	—
Mantle cavity	1.56 (1.36, 1.76) N = 2	1.40
Gill (G)	1.40 (1.20, 1.60) N = 2	1.24
Osphradium (OS)	0.41 (0.36, 0.46) N = 2	0.44
OS ÷ G	0.29 (0.29, 0.30) N = 2	0.35
No. of filaments	17 (13, 21) N = 2	18
Gf_2	0.36 N = 1	—
Gf_1	0.22 N = 1	—
Total Gf = TGF	0.58 N = 1	—
Gf_2 ÷ TGF	0.62 N = 1	—
Buccal mass	0.57 N = 1	—
Prostate	—	1.10
Seminal vesicle	—	0.48
Penis	—	2.60

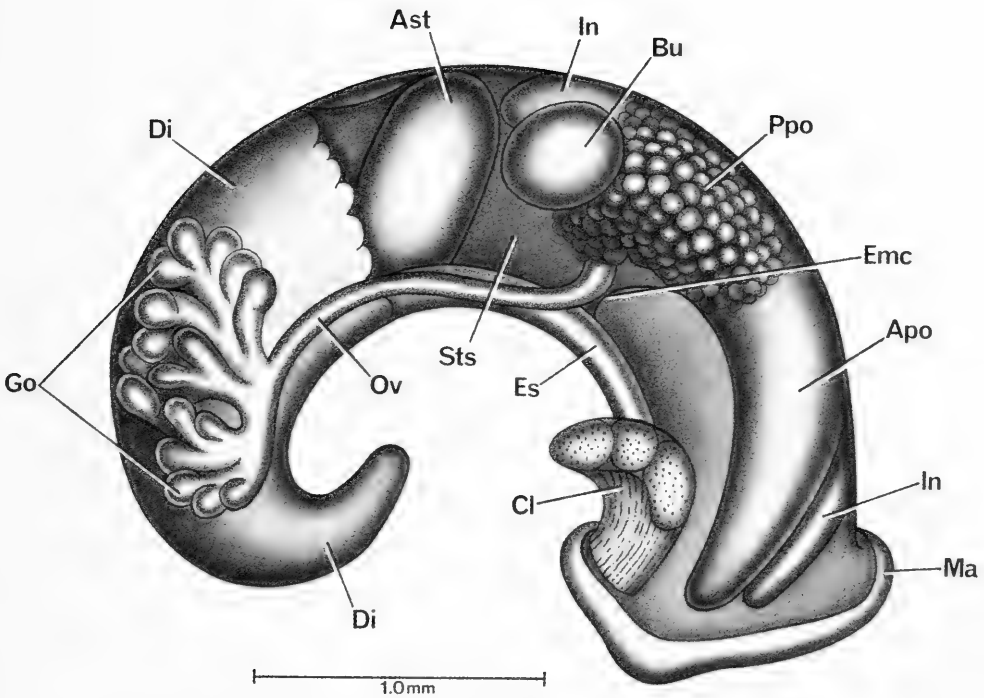

FIG. 104. Uncoiled female *Neotricula minutoides* with head and kidney tissue removed.

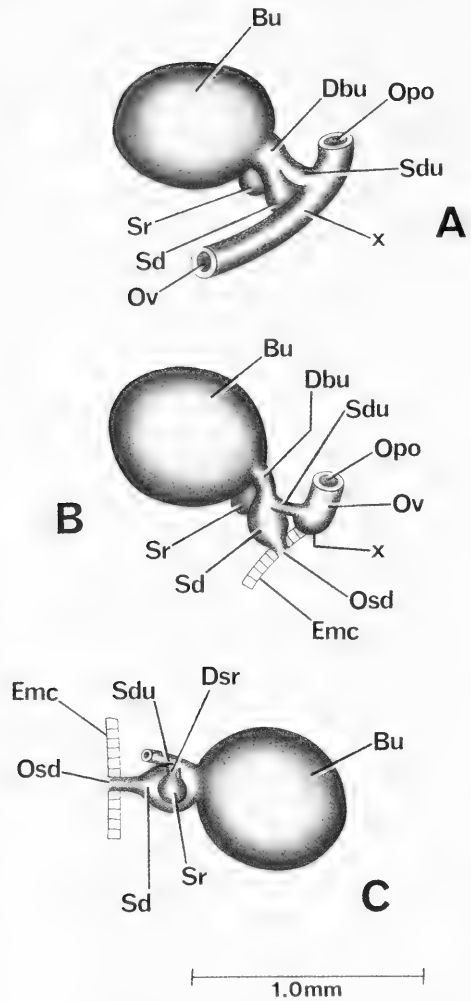

FIG. 105. Details and variation of the bursa copulatrix complex of organs of *Neotricula minutoides*. Figure A is in the same orientation as in Figure 104. B. Section of oviduct cut away at "x" to show continuation of duct of bursa (Dbu) into spermathecal duct (Sd) with latter opening (Osd) into posterior end of mantle cavity. C. Bursa complex flipped over to show relationships of seminal receptacle to sperm duct (Sdu), spermathecal duct (Sd) and duct of bursa.

The radula is shown in Figure 108. A pronounced bifurcation of the blade of the primary cusp of the lateral tooth may be found (Fig. 108C, D, E). Otherwise tooth morphologies are standard triculine.

TABLE 54. Radular statistics for *Neotricula minutoides*. Mean ± standard deviation (range). N = number used. In mm except for width of central tooth in μm.

	Females (N = 6)
Shell length	3.67±0.30 (3.40–4.00)
Radular length	0.51±0.06 (0.44–0.57)
Total rows of teeth	56.4±4.8 (50–60) N = 7
No. rows of teeth forming	10.9±6.3 (5–21) N = 8
Central tooth width	15.1±1.1 (13.4–16.8) N = 13

Nervous system. Measurements are given in Table 56. The RPG ratio is 0.45; the dorsal nerve ring is thus moderately concentrated.

Remarks

Conchologically, this species most closely resembles *Tricula bambooensis* (Figs. 153–155). *Neotricula minutoides* has a proportionally much wider shell (compare illustrations here with Davis et al., 1986: fig. 20A–E). Additionally, the outer lip of the former, in side view, is scooped forward; it is parallel with the axis of coiling in the latter (char. 15). The adapical aperture of the former is fused to the body whorl; it is slightly separated from the body whorl in the latter (char. 21). The aperture of the former is pyriform; it is oval in the latter (char. 3).

The most prominent anatomical differences are those that separate the two genera.

TRICULINI Davis, 1979

Type genus. *Tricula* Benson, 1843

Diagnosis. Those genera of Triculinae in which the spermathecal duct enters the pericardium. The oviduct makes a 360° closed twist. In the plesiomorphic state, the seminal receptacle arises from the oviduct; in the derived state, the seminal receptacle is lost and its function taken over by derived structures attaching to the oviduct-spermathecal duct juncture. There is no sperm duct.

Genera assigned. *Delavaya*, *Fenouilia*, *Lacunopsis*, *Lithoglyphopsis*, *Tricula*. (N=5).

Lithoglyphopsis Thiele, 1928

Type species. *Lithoglyphus modestus* Gredler, 1886 [1887]

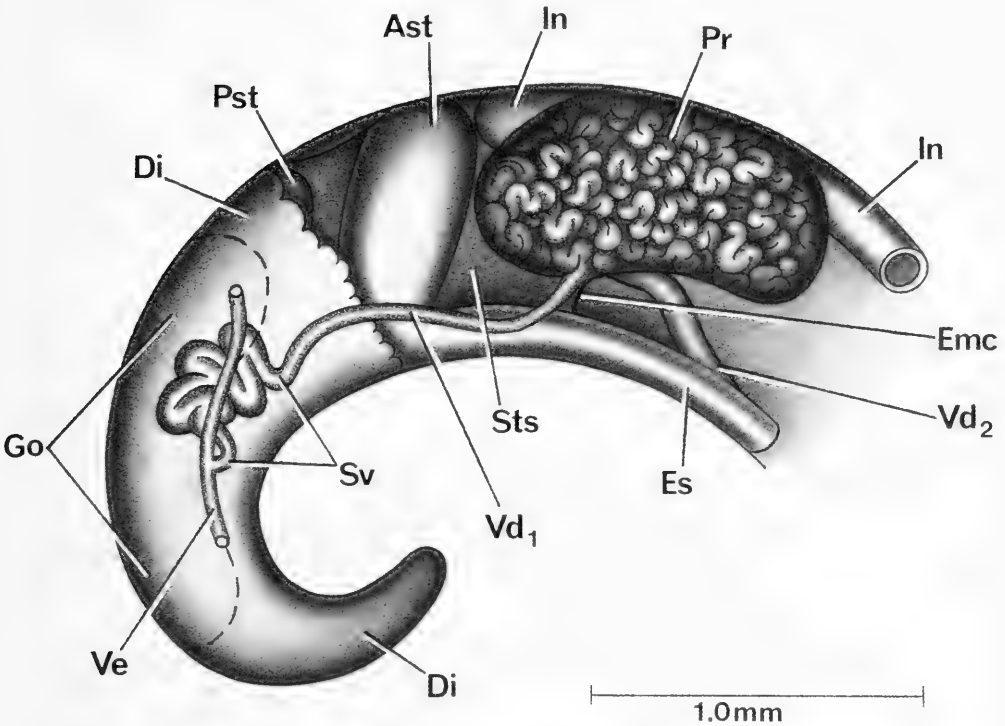

FIG. 106. Uncoiled male of *Neotricula minutoides* without head or kidney tissue. Anterior part of mantle cavity omitted. Outline of gonad (Go) represented by a dashed line; lobes of gonad removed to show knot of tubes of seminal vesicle (Sv).

TABLE 55. Cusp formulae for the radular teeth of *Neotricula minutoides* with the percent of radulae in which a given formula was found at least once. N = 7 radulae. [ ] indicates one cusp support with a split blade.

Central Teeth		Lateral Teeth		Inner Marginal Teeth		Outer Marginal Teeth	
3-1-3 / 2-2	71%	3-[2]-2	57%	11	29%	11	100%
2-1-2 / 2-2	57%	2-[2]-3	29%	12	71%	12	71%
3-1-3 / 3-2	29%	4-1-3	29%	13	86%	13	71%
		4-[2]-3	29%	14	71%	14	43%
3-1-3 / 2-3	14%	3-1-2	14%	$\bar{X}$ * = 12.5±1.9		12.1±1.6	
2-1-3 / 2-2	14%	3-1-3	14%	N = 64		N = 64	
		4-[2]-2	14%				

*Mean ± standard deviation of cusp number for all teeth counted. N = number of teeth counted on 7 radulae.

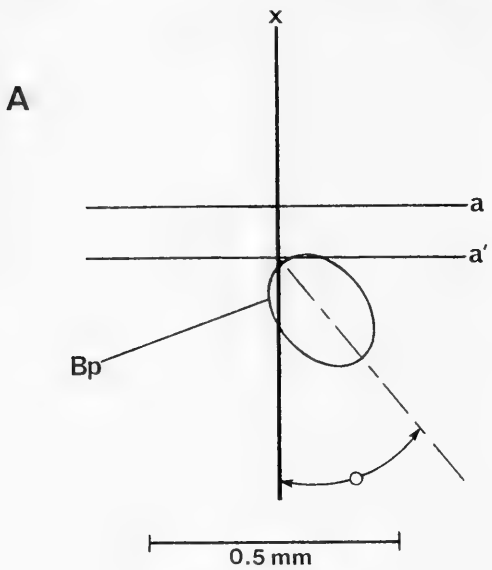

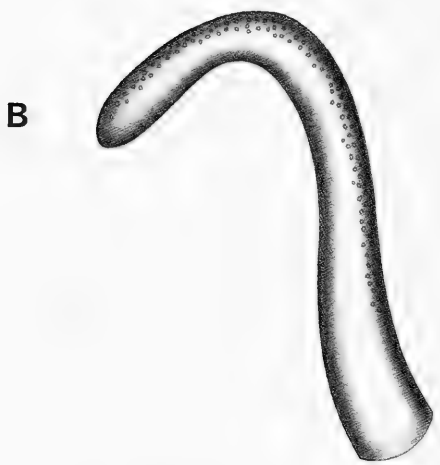

FIG. 107. A. Relationship of base of the penis of *Neotricula minutoides* to mid-line of the snout-neck (x) and to posterior end of the eye lobes (a). B. Penis.

TABLE 56. Lengths (mm) of neural structures of *Neotricula minutoides*. Mean ± standard deviation (range). N = number used = 2. * = neural elements measured to calculate the RPG ratio.

Cerebral ganglion	0.28 (0.26, 0.30)
Cerebral commissure	0.06 (0.5, 0.6)
Pleural ganglion	
Right (1)*	0.13 (0.12, 0.14)
Left	0.11 (0.10, 0.12)
Pleuro-supraesophageal connective (2)*	0.20 (no var.)
Pleuro-subesophageal connective	0.07 (0.04, 0.10)
Supraesophageal ganglion (3)*	0.11 (0.10, 0.12)
Subesophageal ganglion	0.11 (0.10, 0.12)
Osphradio-mantle nerve	0.05 (0.04, 0.06)
RPG ratio* = 2 ÷ 1+2+3	0.45 (no var.)

Lithoglyphopsis modesta (Gredler)

Types. Paralectotypes SMF 4214a. Figure 109A = specimen figured by Yen (1939). Figure 109B-D = additional type specimens.

Type locality. See above

Synonymy. Lithoglyphus modestus Gredler, 1886
Lithoglyphopsis modesta, Thiele, 1928
Lithoglyphopsis modesta, Wenz, 1939: 580, Figure 1581
Lithoglyphopsis, *modestus* Yen, 1939: 43, pl. 4, Figure 7.

Habitat

The type locality is today known as Baisha, Hengshan County from the Xiangjiang River; 25°58′22″N, 112°45′55″E, Figure 1, locality 9. Snails were collected by diving to obtain stones from the river bottom at a depth of about 2.0–2.5 m. Collected by Chen and Wu in 1986, collection number 86-B, ANSP 373144, A12660, ZAMIP M00054.

The locality from which snails were used for most of the dissections was Anhua town, Anhua County, Zijiang River; 28°23′46″N, 111°,12′41″E, Figure 1, locality 10. The collection number was D87-1, by Davis, Chen and Xing on 16 March 1987, ANSP 373150, A12666. Snails were collected 1.6 km upstream from the town boat landing. Collections came from the shores of a small island in the middle of the river. Water flows through a stone breakwater at the upstream end of the

Type locality. Hen-Kiou-fee bis Pe-shang (Gredler, 1886), = Heng-dshou-fu bis Pe-shang, Hunan (Yen, 1939).

Designation. By Thiele, 1928

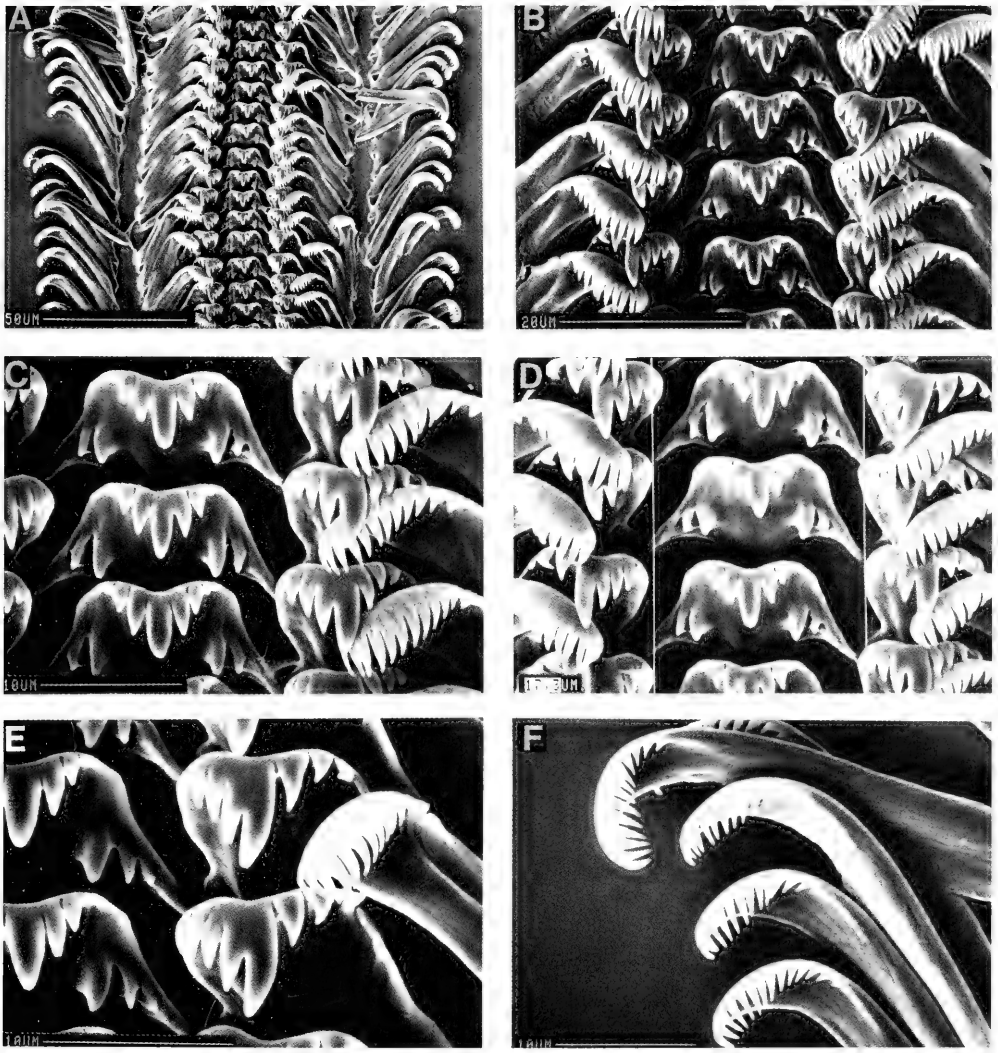

FIG. 108. Radula of *Neotricula minutoides*. A. Section of radula. B–E. Central, lateral and inner marginal teeth. F. Outer marginal teeth.

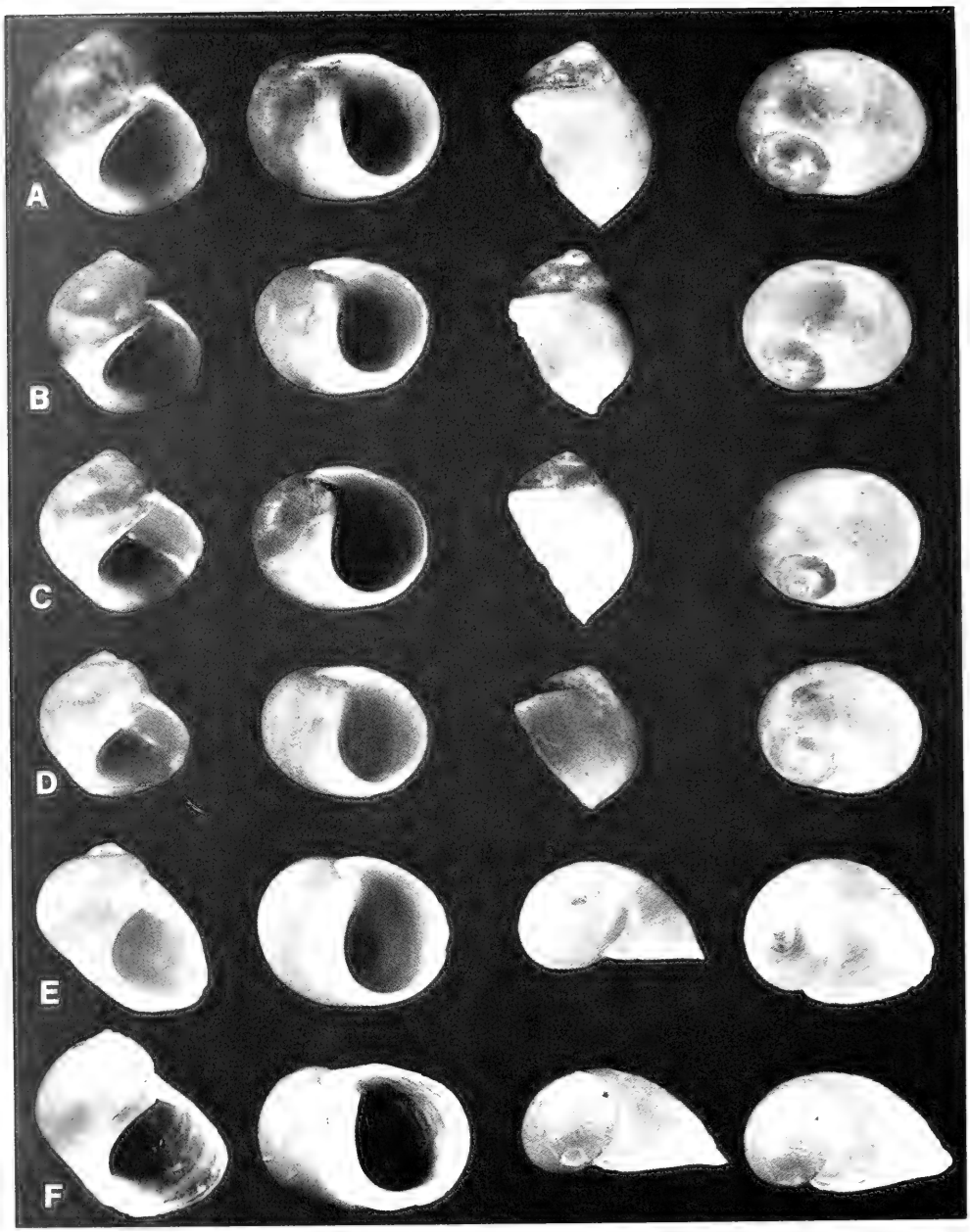

FIG. 109. Shells of *Lithoglyphopsis modesta*. A–D, paralectotypes, SMF; A. specimen figured by Yen (1939). E, F. Specimens from Anhua, D87-1. A = 4.56 mm long; other shells printed at same scale.

TABLE 57. Shell measurements (mm) of Anhua and Baisha populations of *Lithoglyphopsis modesta*. Mean ± standard deviation (range). N = numbered measured.

	Anhua		Baisha	
	Female (N = 5)	Male (N = 6)	Female (N = 5)	Male (N = 5)
No. Whorls	3.0–3.5	3.0–3.5	3.0–4.0	3.5–4.0
Length (L)	5.18±0.04 (4.58–5.57)	5.10±0.60 (4.16–5.66) N = 5	4.53±0.27 (4.16–4.91)	4.46±0.31 (4.15–4.90)
Width (W)	4.87±0.33 (4.74–4.99)	4.68±0.42 (3.91–5.16)	4.49±0.23 (4.24–4.83)	4.58±0.32 (4.23–4.98)
L body whorl	4.91±0.40 (4.37–5.41)	4.76±0.54 (3.91–5.24)	4.27±0.22 (4.07–4.65)	4.19±0.32 (3.90–4.65)
L penultimate whorl	0.15±0.04 (0.08–0.17)	0.21– No. var.	0.20±0.05 (0.17–0.25)	0.252– No. var.
W penultimate whorl	1.12±0.15 (0.99–1.33)	1.06±0.10 (0.99–1.25) N = 5	1.00±0.09 (0.91–1.04)	1.04±0.11 (0.91–1.16)
W 3rd whorl	0.44±0.04 (0.42–0.50) N = 3	0.42±0.06 (0.33–0.50) N = 4	0.44±0.04 (0.42–0.50)	0.46±0.50 (0.42–0.50)
L aperture	4.43±0.19 (4.16–4.66)	4.20±0.31 (3.66–4.58)	4.05±0.17 (3.90–4.07)	4.03±0.20 (3.90–4.32)
W aperture	3.62±0.23 (3.24–3.83)	3.52±0.31 (3.00–3.83)	3.29±0.15 (3.15–3.49)	3.32±0.30) (3.07–3.74)
L crescent	2.31±0.19 (2.08–2.50)	2.25±0.35 (1.83–2.58)	2.04±0.19 (1.83–2.32)	2.20±0.35 (1.83–2.57)
W crescent	0.42±0.06 (0.33–0.50)	0.35±0.06 (0.25–0.42)	0.38±0.09 (0.25–0.50)	0.58±0.17 (0.49–0.83)
W columellar plate	0.73±0.06 (0.67–0.83)	0.77±0.17 (0.50–1.00)	0.68±0.07 (0.58–0.75)	0.72±0.08 (0.66–0.83)
L "A"	5.53±0.25 (5.16–5.74)	5.26±0.44 (4.58–5.66)	4.95±0.22 (4.73–5.23)	5.08±0.30 (4.81–5.48)
W "A"	4.20±0.27 (3.91–4.58)	4.08±0.33 (3.58–4.49)	3.64±0.22 (3.49–3.94)	3.74±0.26 (3.49–4.07)

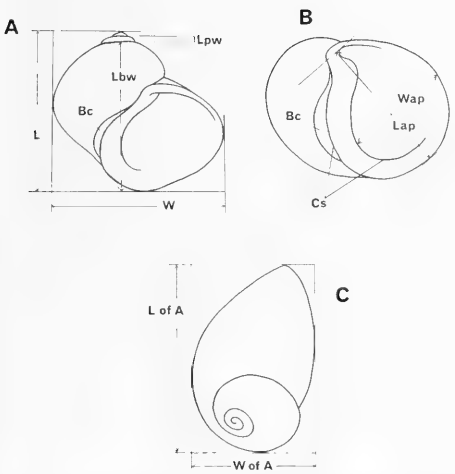

FIG. 110. Illustration to show three shell orientations for measurements.

island. Snails were collected from the bottom surface of stones along the protected inner edge of the breakwater where there was an expansive shallow water area some 30 cm deep and with emergent vegetation. Associated fauna included: *Stenothyra hunanensis*, *Semisulcospira* sp, a species of Viviparidae, a planorbid, and *Radix* sp.

Description

Shells. Shells measurements are given in Table 57 for the two populations. Shells are illustrated in Figures 109–113. How measurements are made for these globose shells is given in Figure 110. Shells are medium to long in length. They are nearly round in outline with the apex to base alignment as in Figure 110C; they are globose and smooth. The shell is dominated by the body-whorl.

FIG. 111. Shells of *Lithoglyphopsis modesta* from Anhua (D87-1) A–C; "*L.*" *liliputinus*, D; and *Guoia viridulus*, paralectotypes, E, F. Shell A is 4.72 mm long; other shells printed at same scale.

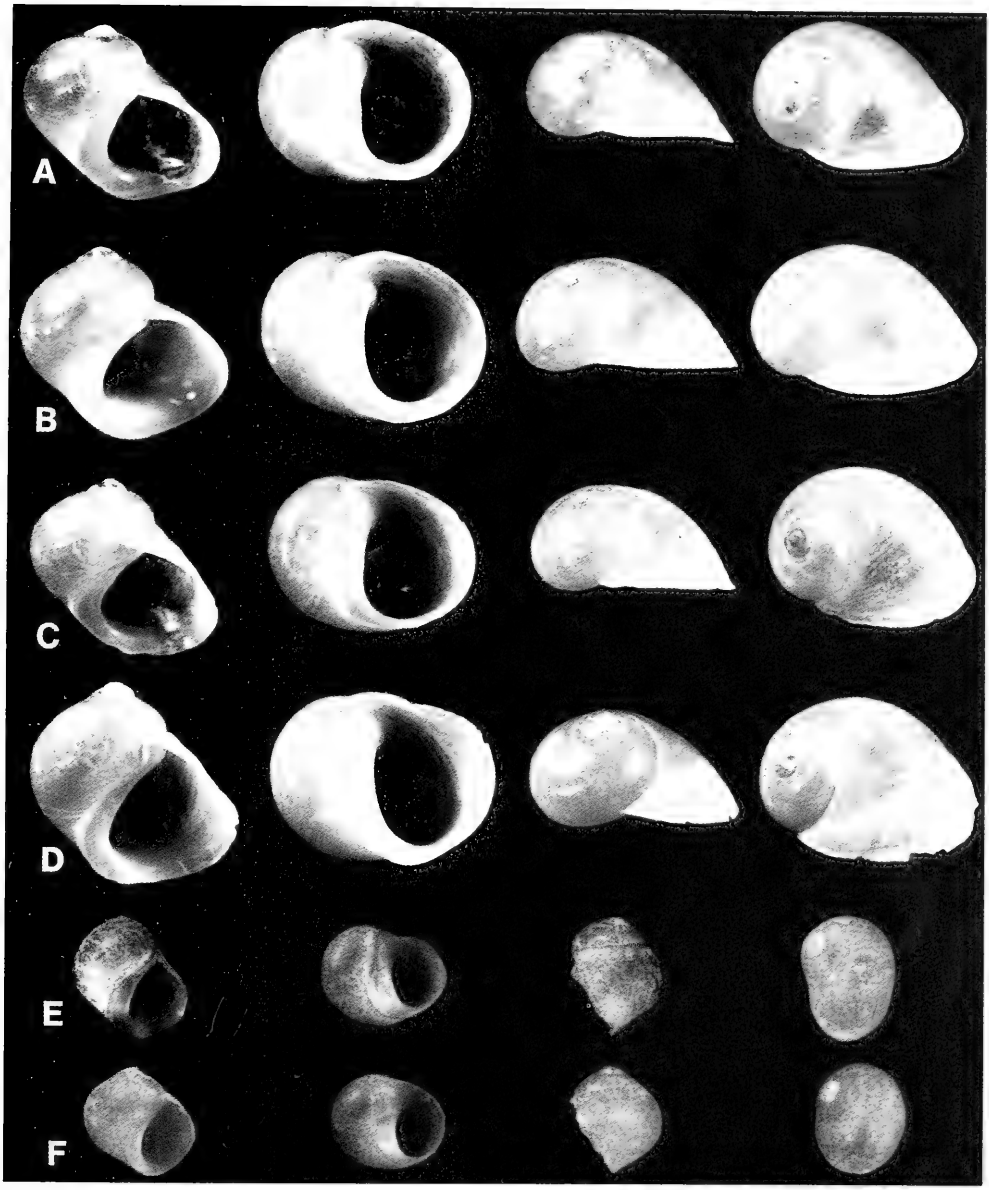

FIG. 112. Shells of *Lithoglyphopsis modesta* from Baisha (86-B), A–D. A, B = males; C, D = females. "*L.*" *liliputinus*, E, F. A = 4.72 mm; other shells printed to same scale.

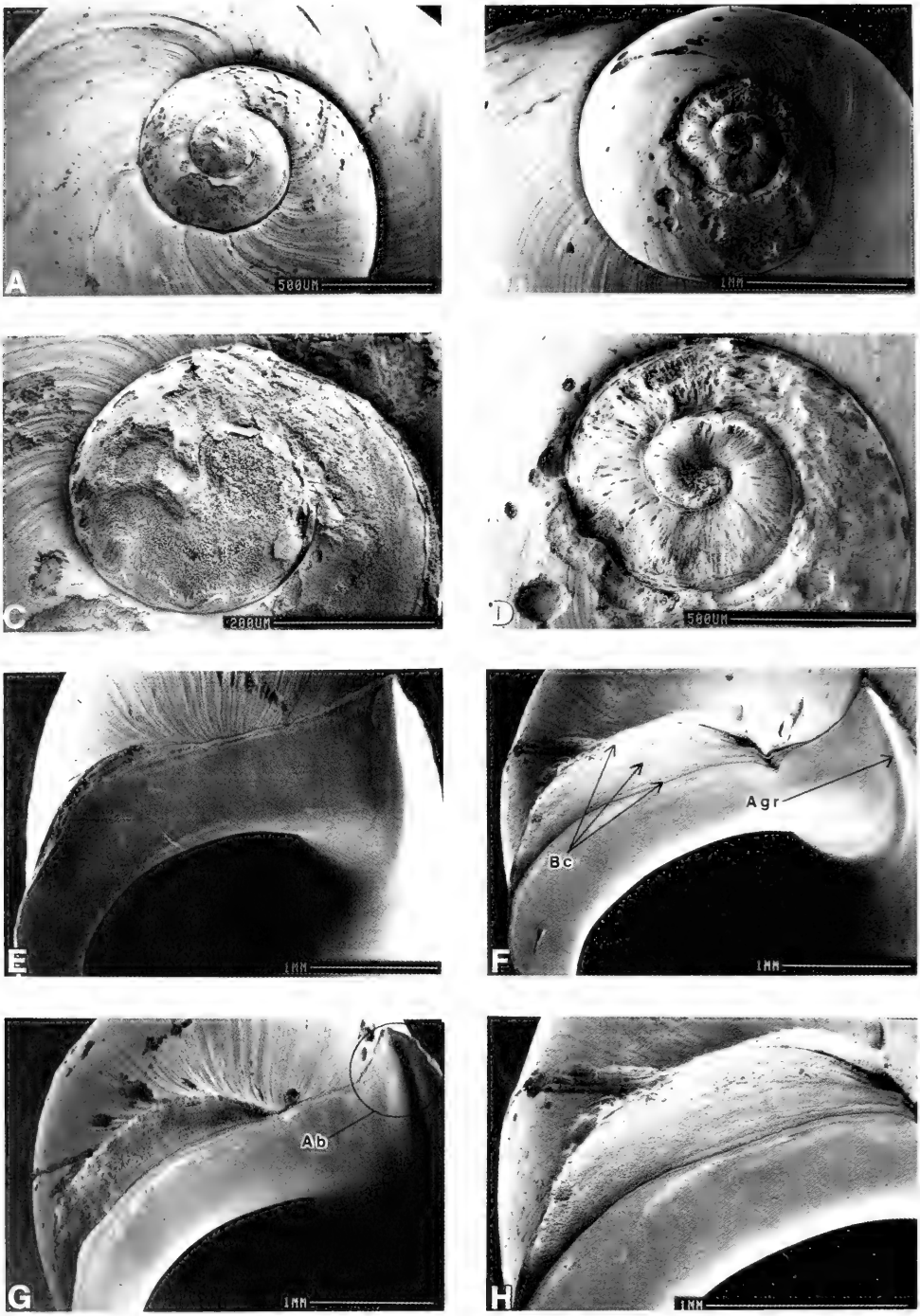

FIG. 113. SEM photographs of shells of *Lithoglyphopsis modesta*. A–C. Enlargements of apical whorls. Spiral microsculpture is seen on second and third whorls. E–H. Enlargement of apertural areas showing basal crescent (Bc), apertural beak (Ab), and beak or adapical apertural groove (Agr).

TABLE 58. Lengths (mm) or counts of non-neural organs and structures of *Lithoglyphopsis modesta*. Mean ± standard deviation (range). N = number of snails used. *See text for discussion of pallial oviduct length.

	Females	Males (N = 2)
Body	7.52±1.52 (4.96–9.40) N = 6	7.85 (7.50, 8.20)
Digestive gland	3.01±0.60 (2.16–4.0) N = 6	3.65 (3.10, 4.20)
Gonad	1.96±0.21 (1.10–2.20) N = 6	3.35 (2.70, 4.00)
Posterior pallial oviduct (= albumen gland)	1.43±0.06 (1.40–1.50) N = 6	—
Anterior pallial oviduct (= capsule gland)	2.89 N=1	—
Total pallial oviduct = PO	4.23±0.33 (3.70–4.60)	—
Bursa copulatrix	0.87 (0.80, 0.94) N = 2	—
Duct of bursa	0.31±0.09 (0.22–0.40) N = 3	—
Bu ÷ PO	0.22 (0.18–0.25) N = 2	—
Seminal receptacle	0.19 (0.18, 0.20) N = 2	—
Duct of seminal receptacle	0.33±0.04 (0.30–0.38) N = 3	—
Buccal mass	1.60±0.13 (1.50–1.78) N = 4	—
Mantle cavity	4.57±0.26 (4.28–4.86) N = 5	4.08 (3.96, 4.20)
Osphradium = Os	1.94±0.22 (1.76–2.30)	1.15 (1.0, 1.30)
Gill = G	4.20±0.26 (4.28–4.86)	3.70 (3.60, 3.80)
Os ÷ G	0.47±0.05 (0.39–0.48)	0.31 (0.26, 0.36)
No. filaments	39±2 (38–41) N = 4	41 no variation
Gf_2	0.43±0.19 (0.20–0.80) N = 16	male + female
Gf_1	1.04±0.14 (0.70–1.30) N = 16	male + female
Total Gf = TGF	1.48±0.21 (1.06–1.90) N = 15	male + female
Gf_2 ÷ TGF	0.29±0.12 (0.13–0.41) N = 16	male + female
Prostate	—	2.52 (1.84, 3.20)
Seminal vesicle	—	1.60 no variation
Penis	—	3.67 (3.60, 3.74)

TABLE 59. Radula statistics for *Lithoglyphopsis modesta*. Mean ± standard deviation (range). In mm except for the width of the central tooth in μm. N = number measured.

	Females (N = 10)	Males (N = 7)
	Anhua Population (D87−1)	
Greatest shell dimension	4.92±0.47 (4.00−5.36)	4.91±0.26 (4.44−5.20)
Radular length	2.52±0.20 (2.26−2.90)	2.44±0.16 (2.20−2.66)
Radular width	0.23±0.02 (0.20−0.27)	0.23±0.01 (0.22−0.24)
Total rows of teeth	69±5 (62−77)	66±3 (61−70)
No. rows of teeth forming	31±4 (25−36)	25±5 (19−32)
Central tooth width	55±4 (48−58)	55±1 (54−56)
	Baisha Population (1986)	
Greatest shell dimension	4.79±0.25 (4.60−5.16)	4.77±0.32 (4.28−5.12)
Radular length	2.60±0.36 (2.10−2.96)	2.78±0.13 (2.10−3.00)
Radular width	0.21±0.01 (0.20−0.22)	0.21±0.01 (0.20−0.22)
Total rows of teeth	66±8 (55−77)	74±3 (71−80)
No. rows of teeth forming	34±7 (23−40)	37±2 (35−39)
Central tooth width	51±5 (48−60)	49±2 (48−52)

TABLE 60. Cusp formulae or the radular teeth of *Lithoglyphopsis modesta* with the percent of radulae in which a given formula was found at least once. N = number used and/or counted.

Central Teeth		Lateral Teeth		Inner Marginal Teeth		Outer Marginal Teeth	
			Anhua Population (N = 10)				
$\frac{1}{2\text{-}2}$	60%	0-1-3	80%	6	30%	6	20%
$\frac{1}{3\text{-}3}$	50%	2-1-0	70%	7	90%	7	90%
$\frac{1}{3\text{-}2}$	40%	3-1-0	60%	8	90%	8	70%
$\frac{1}{2\text{-}3}$	10%	0-1-2	40%	9	30%	9	20%
		4-1-0	10%	10	0	10	10%
				$\tilde{X}^*$ = 7.4±0.8 N = 100		7.5±0.9	
			Baisha Population (N = 3)				
$\frac{1}{2\text{-}2}$	67%	0-1-3	100%	5	—	5	33%
		2-1-0	67%	6	33%	6	100%
$\frac{1}{2\text{-}3}$	67%	0-1-2	67%	7	67%	7	100%
$\frac{1}{3\text{-}2}$	33%	3-1-0	33%	8	67%	8	33%
				$\tilde{X}^*$ = 7.40±0.9 N = 30		6.3±0.6	

*Mean ± standard deviation of cusp number for all teeth counted.

TABLE 61. Dimensions of neural structures from five individuals of *Lithoglyphopsis modesta*. Mean ± standard deviation (range). In mm; L = length. * = neural elements measured to calculate the RPG ratio.

Cerebral ganglion L	0.55±0.07	(0.46–0.64)
Pleural ganglion L		
Right (1)*	0.26±0.04	(0.20–0.30)
Left	0.18±0.02	(0.16–0.20)
Cerebral commissure L	0.30±0.07	(0.20–0.38)
Pleuro-supraesophageal connective L (2)*	0.19±0.03	(0.16–0.24)
Pleuro-subesophageal connective L	0.02	(n variation)
Supraesophageal ganglion L (3)*	0.29±0.03	(0.24–0.32)
Subesophageal ganglion L	0.20±0.03	(0.18–0.24)
Osphradio-mantle nerve L	0.27±0.08	(0.20–0.30)
Pedal commissure L	0.23±0.11	(0.10–0.30)
RPG ratio* (2 ÷ 1+2+3)	0.26±0.03	(0.23–0.30)

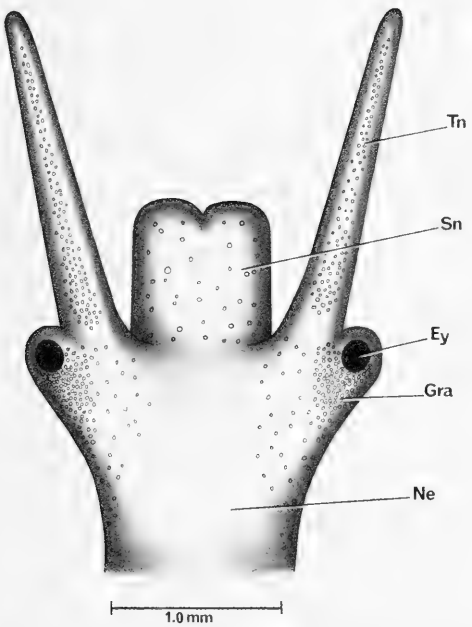

FIG. 114. Head of *Lithoglyphopsis modesta* from a snail collected from D87-1.

The apex is a protruding nipple, a scant 7 to 8% of the overall shell length. In side view, with axis of coiling vertical, the outer lip is straight and slanted back (to the right) 35° to the axis of coiling (Fig. 109, column 3). The shell length (L) is always with the axis of coiling vertical. Greatest overall length (L of A) is with the shell resting on the aperture (Fig. 110C). The aperture is measured by tilting the axis of coiling so that the plane of the aperture is horizontal (Lap, Fig. 110B). There is a wide columellar shelf 0.32 to 0.36 mm wide (Cs, Fig. 110B); the edge at the aperture is straight to slightly arched. There is a pronounced crescent-shaped ridge to the left of the columellar shelf with a somewhat depressed concavity, the basal crescent (Bc), between the ridge and the columella. The peristome is complete. There is no umbilicus. The adapical end of the aperture is produced into a beak-like projection (Ab, Fig. 113G). The aperture shape is round to broadly pyriform. The apex of some individuals may have a reddish color; the cleaned shell is horn yellow.

The SEM pictures of varied aspects of the shell are shown in Figure 113. The apical whorls are shown in Figure 113A–D. They are invariably eroded. Spiral microsculpture is evident (Fig. 113A, B, D). Figure 113E–H shows variation in the size of the basal crescent (Bc). The apertural beak (Ab) is featured in Figure 113F–G showing the groove (Agr) running inside it.

External features. The head is shown in Figure 114; it is broad and squat; there are pronounced bulging eye lobes at the base of each tentacle. In these character-states the head is similar to those of *Fenouilia* and *La-*

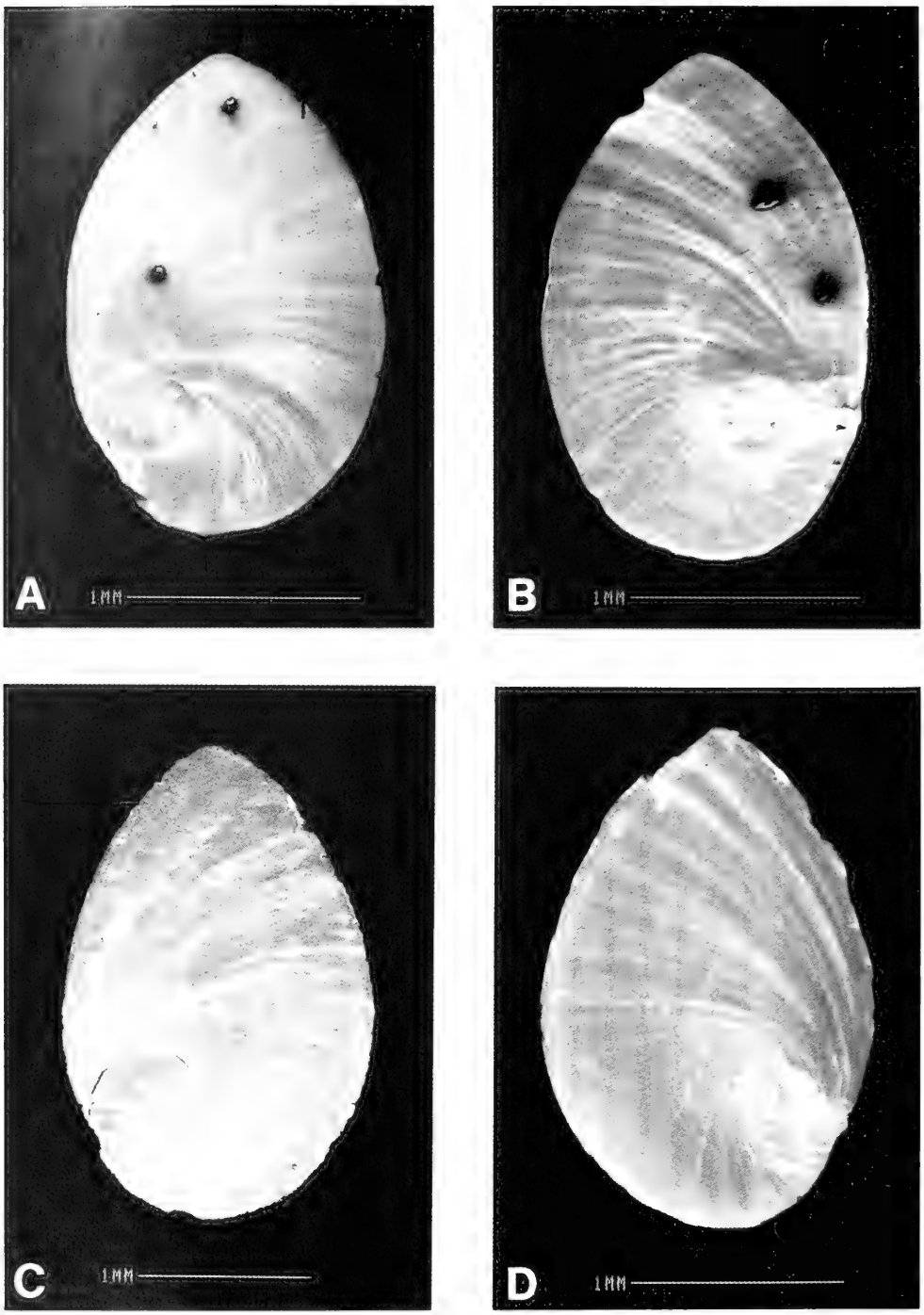

FIG. 115. Opercula of *Lithoglyphopsis modesta*. A, B from Baisha snails; C, D from Anhua snails. A, C. External surfaces; B, D. Internal surfaces.

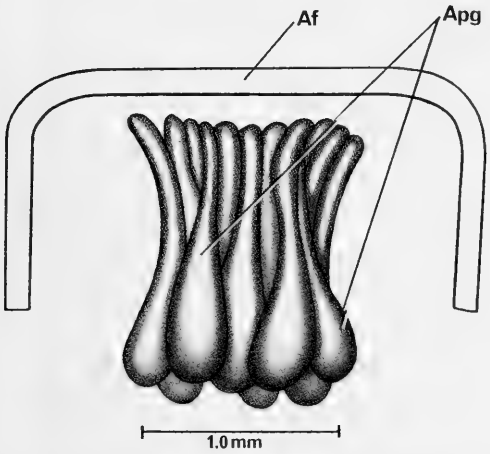

FIG. 116. Masses of anterior pedal glands (Apg) in anterior foot seen through dorsal surface.

cunopsis. The granules shown on the head vary in color from bright lemon yellow to light yellow to white. There is a pronounced omniphoric groove; no suprapedal fold. The operculum is shown in Figure 115; it is regularly ovate, corneous, paucispiral without discernable internal pad; without ridges. The attachment area is barely distinguishable.

Opening the anterior foot dorsally and removing the buccal mass and supporting muscle bands, one sees a mass of tubular anterior pedal glands (Figure 116). These come up as a bunch over the elongated pedal commissure.

Mantle cavity. The reflected mantle is shown in Figure 117A. The mantle cavity is typical for those of species of Triculini in which the spermathecal duct (Sd) enters the pericardium and the pericardium (Pe) swells out into the mantle cavity. Organ measurements and statistics are given in Table 58.

The osphradium (Os) is long; the posterior end may be considerably narrowed (Figs. 117, 119C). Variation in osphradial shape is shown in Figure 119C. The terminal gill filament Gf_2 is short, that is the ratio is 0.29 ± 0.12 (Table 58). The length of the longest filaments is 1.48 ± 0.21 mm. In lateral view the filament is pleated and Gf_2 has a pronounced dome (Fig. 117B).

The pericardium bulges out into the mantle cavity and the opening into the pericardium for sperm entry is clearly observable (Ope, Fig. 117A). The mantle cavity organs and arrangement is typical of the taxa of the *Tricula* clade of Triculini.

Female reproductive system. The body of an uncoiled female without head and with kidney tissue removed is shown in Figure 118. Measurements of the relevant organ systems are given in Table 58. Important features to note are: (1) The body is squat and fat as would be expected from shell shape. (2) The dorsal surface is densely pigmented with melanin. (3) The posterior pallial oviduct (Ppo) makes a pronounced bend over the style sac. (4) The gonad covers the stomach. (5) The sperm enter the system at the rear of the mantle cavity through the pericardium (Ope, Fig. 117A). The pericardium swells out into the mantle cavity. The spermathecal duct (Sd) is a short tube running from the pericardium to the swollen section of the oviduct (Fig. 119A). (6) The oviduct makes a tight twist or coil dorsal to the bursa copulatrix. (7) The seminal receptacle (Dsr) arises from the oviduct posterior to the duct of the bursa (Dbu, Fig. 119A). (8) The bursa complex is dorsal to the posterior pallial oviduct (= albumen gland). (9) The oviduct opens into the pallial oviduct close to the posterior end of the mantle cavity, i.e. not into the posterior end of the pallial oviduct. (10) The bursa is short. (11) The albumen gland length is short if the albumen gland is measured from the posterior edge on the stomach thereby not including the bend over the style sac (ratio of 0.35 ± 0.02). However, measuring along the bend the actual length (functional length) averages 1.83 mm and this divided by that pallial oviduct length averages 0.45 ± 0.03, i.e. the functional length is standard.

Character-states 5–7 are the same as those found in *Tricula*, *Fenouilia*, and *Delavaya*.

Male reproductive system. The body of an uncoiled male is shown in Figure 120 without head and with kidney tissue removed. Measurements of relevant organs are given in Table 58. Important features are: (1) The gonad consists of moderately large lobes draining into a vas efferens (Ve). (2) The posterior vas deferens arises from the vas efferens at mid-gonad or slightly posterior to mid-gonad and

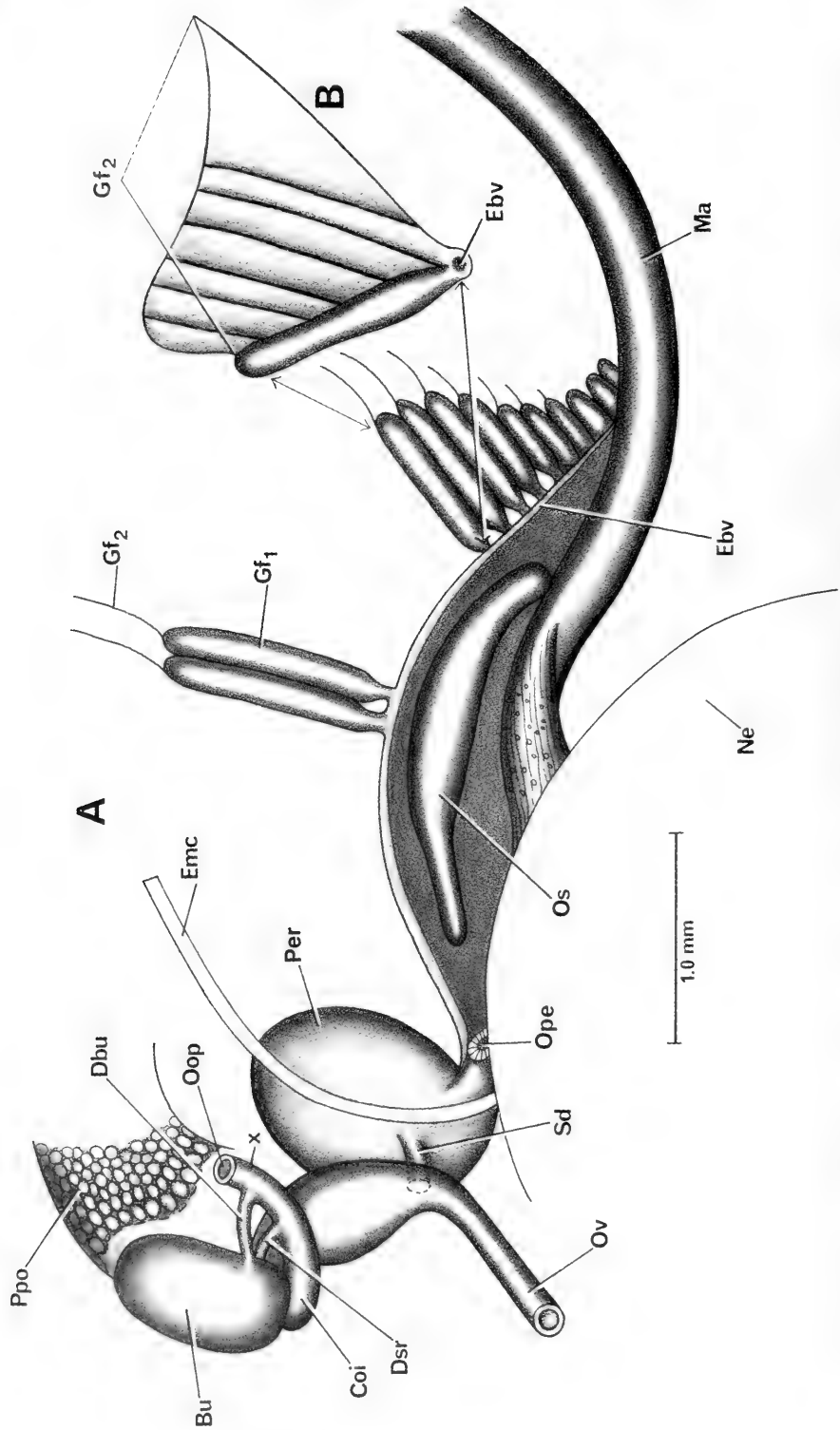

FIG. 117. Cut and reflected mantle (A) showing mantle cavity structures and their relationship to posterior end of mantle cavity (Emc), pericardium (Pe) and bursa copulatrix (Bu) complex of organs. Not all gill filaments (Gf_2 & Gf_1) are shown. B. A single gill filament.

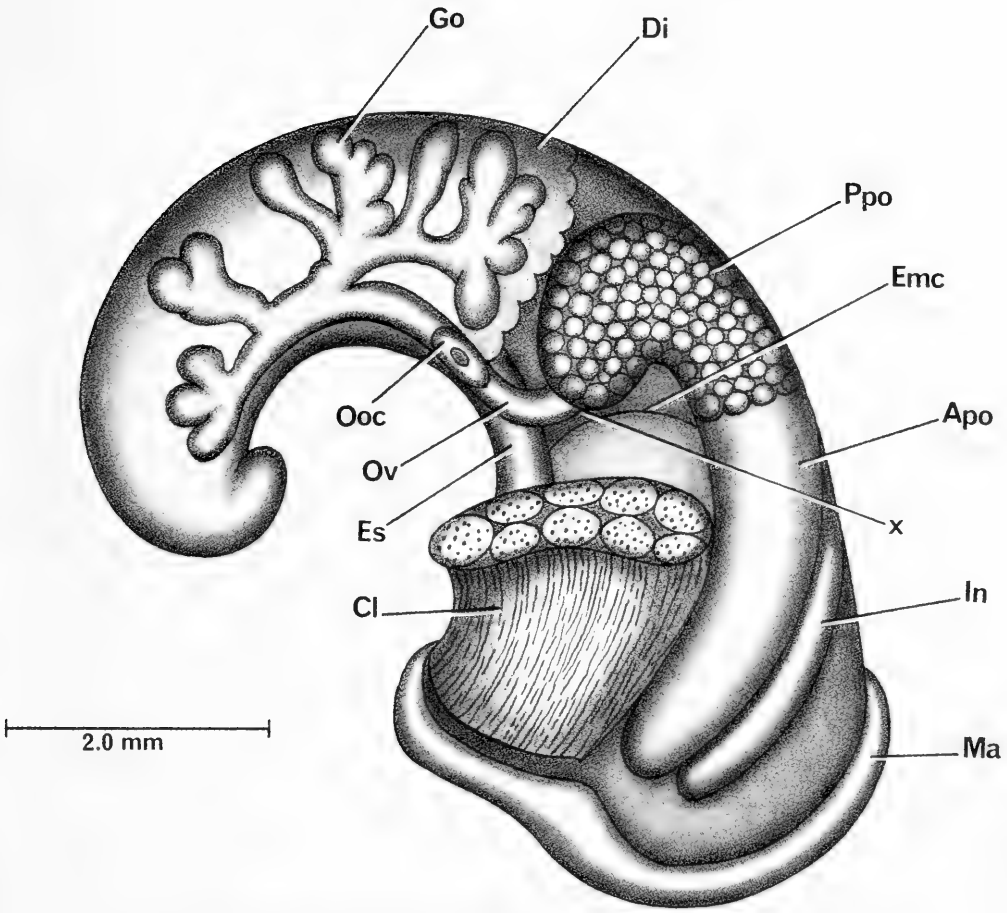

FIG. 118. Uncoiled female *Lithoglyphopsis modesta* with head and kidney tissue removed.

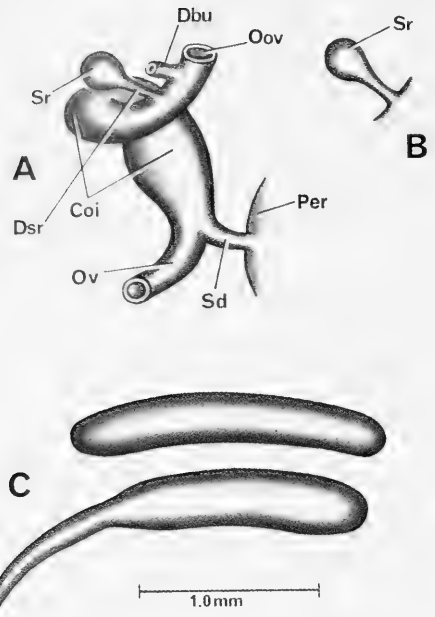

FIG. 119. Bursa copulatrix complex of organs; A, B. Variation in shape of the *osphradium*, C; refer also to Os, Figure 117A. In Figure A, organs are in the same orientation as in Figures 117 and 118. However, here the bursa copulatrix is cut away to show the oviduct coil (Coi) and the seminal receptacle (Sr) where it attaches to oviduct. B. Variation in the shape of seminal receptacle.

forms a loosely coiled seminal vesicle (Sv) visible to the left side of the gonad. (3) The gonad covers the stomach (is ventro-lateral to it). (4) The prostate is comparatively massive, covering the style sac and part of the anterior chamber of the stomach. (5) The penis is simple, without lobes (Fig. 121B). The anterior end is extremely slender, that is, a long penial filament (Pf). There is no papilla. (6) There is a slender muscular ejaculatory duct (Ej) beneath the base of the penis in the neck. (7) The shaft of the penis arises to the right of the snout-neck mid-line (x, Fig. 121A at an angle of 30° ± 10°).

Digestive system. The digestive gland covers the posterior chamber and most of the anterior chamber of the stomach (Figs. 118, 120) in males and females. The buccal mass and salivary glands are shown in Figure 122A. The paired salivary glands (Sg) are massive and run posteriorly over the nerve ring. The radular sac (Rs) is extremely elongate and coils up dorsally along the buccal mass (Bm) between the buccal mass and the right cerebral ganglion (Rcg, Fig. 122B).

The radula is shown in Figure 123. Teeth counts and statistics are given in Tables 59 and 60. Diagnostic features are (1) the large, singular triangular anterior cusp of the central tooth, (2) the massive basal cusps on the face of the central tooth, and (3) the massive dominant cusp on the lateral tooth.

The stomach (Fig. 124) has a relatively slender posterior chamber (Pst) that is slanted from ventral to dorsal along its whole length and is buried dorsal to the digestive gland. The digestive gland covers part of the anterior chamber (Ast) as does the prostate. There is no caecal appendix.

Nervous system. There are several noteworthy features of the nervous system (Fig. 122B). (1) The RPG ratio has a mean of 0.26 (Table 61); the pleuro-supraesopheageal connective is short. (2) The cerebral commissure is elongate (exceeds 0.12 mm). (3) The cerebral ganglion have melanin splotches (Fig. 122B). (4) The pedal commissure is elongate (exceeds 0.12 mm). (5) The osphradio-mantle nerve is elongate (exceeds 0.12 mm).

Remarks

Lithoglyphopsis modesta could only be confused with various species of *Lacunopsis* on the basis of shell. Anatomically they differ as the latter has several accessory seminal receptacles; the generalized seminal receptacle is lost.

Liu et al. (1980) described *Lithoglyphopsis ovatus*, *L. grandis*, *Lacunopsis yunnanensis* and *L. auris* as new species from Yunnan, China. On the basis of the shell illustrations given, and in the absence of anatomical data, it is not possible to ascertain generic status or discuss relationships. *Lacunopsis yunnanensis* has a shell with a pronounced keel. That together with the central tooth morphology given indicates a possibility that a species of *Fenouilia* is involved.

The shells of *Lythoglyphopsis liliputanus* (Gredler, 1881) look like a miniature *L. modesta* (Figs. 111D, 112E, F). Nothing is known

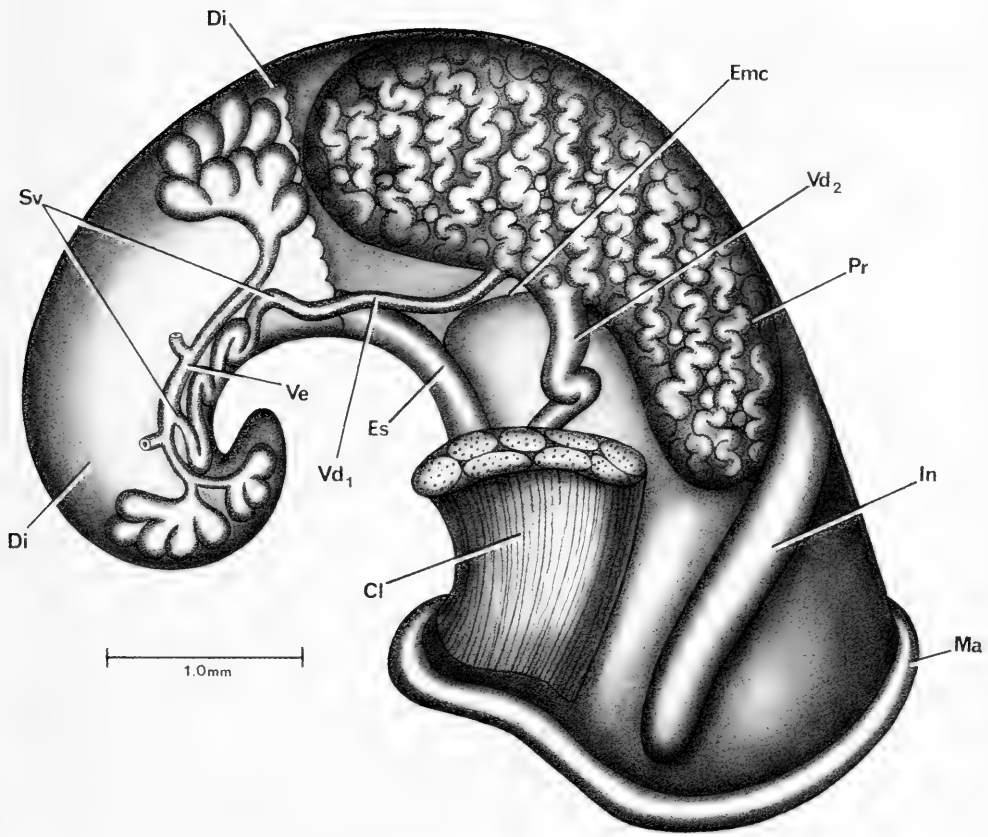

FIG. 120. Uncoiled male *Lithoglyphopsis modesta* without head and with kidney tissue removed. Two bundles of gonadal lobes were cut away.

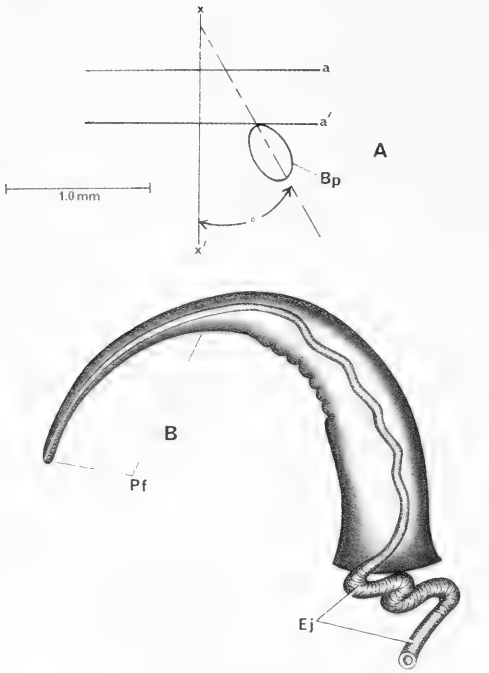

FIG. 121. A. Relationship of base of penis (Bp) of *Lithoglyphopsis modesta* to snout-neck mid-line (x). B. Penis

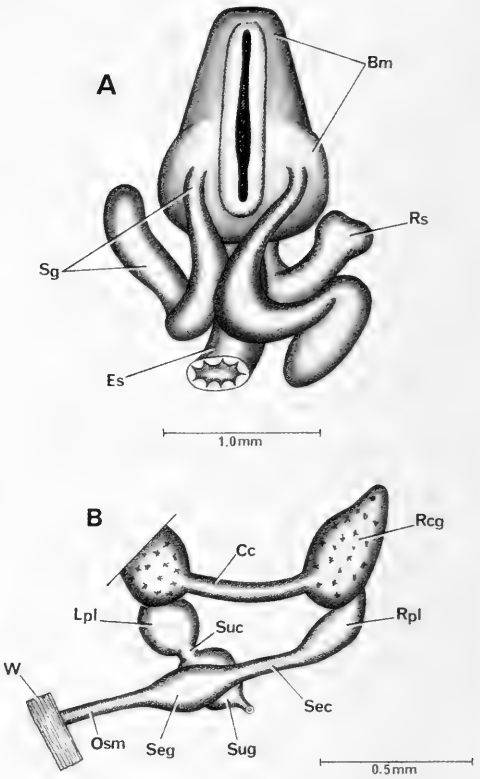

FIG. 122. A. Dorsal aspect of the buccal mass of *Lithoglyphopsis modesta*. B. Dorsal aspect of nerve ring.

of this species except for the shells. The type locality is Lien-dshou-ho in Kwangtung [= Guangdong Province], immediately south of Hunan (Yen, 1939). The lectotype and paralectotypes are in the Bozen Museum, No. 109 (Zilch, 1974).

It is probable that there are additional species of *Lythoglyphopsis*. The closest relationship of *L. modesta* to any other Triculinae thus far studied is with *Fenouilia kreitneri* (see Davis et al. 1983). Both species have a fat body, thus fitting a shell shape that is globose or rather trochoid. The shells are quite different. *Lythoglyphopsis modesta* has a globoseconic shell where as *Fenouilia* has a trochoid to trochoid-ovate shape. The shell of the former is smooth, that of the latter has keels. The characters of the head are the same. The female reproductive system is virtually the same except for two substantive differences. One is the very short spermathecal duct of the former bridging the oviduct to the pericardium where the oviduct turns towards the bursa complex. The spermathecal duct is elongated in the latter. The other is the bending around of the posterior pallial oviduct thus covering the bursa complex of organs (in the former). In the latter, the pallial oviduct does not bend; the bursa is posterior to the pallial oviduct. The male reproductive system is the same in both taxa with one substantive difference; the penis of the former has a long penial filament lacking in the latter. The radular sac is extremely elongated and coils up dorsally along the buccal mass; it is short, that is, generalized in length in the latter (as also in *Lacunopsis*). The cerebral commissure of the former, is over double that of the latter. The gill filaments are different. In the former they are of moderate length with a short section of Gf_2 clearly seen. In the later, the gill filament Gf_1 is elongated; Gf_2 is not visible with the mantle reflected.

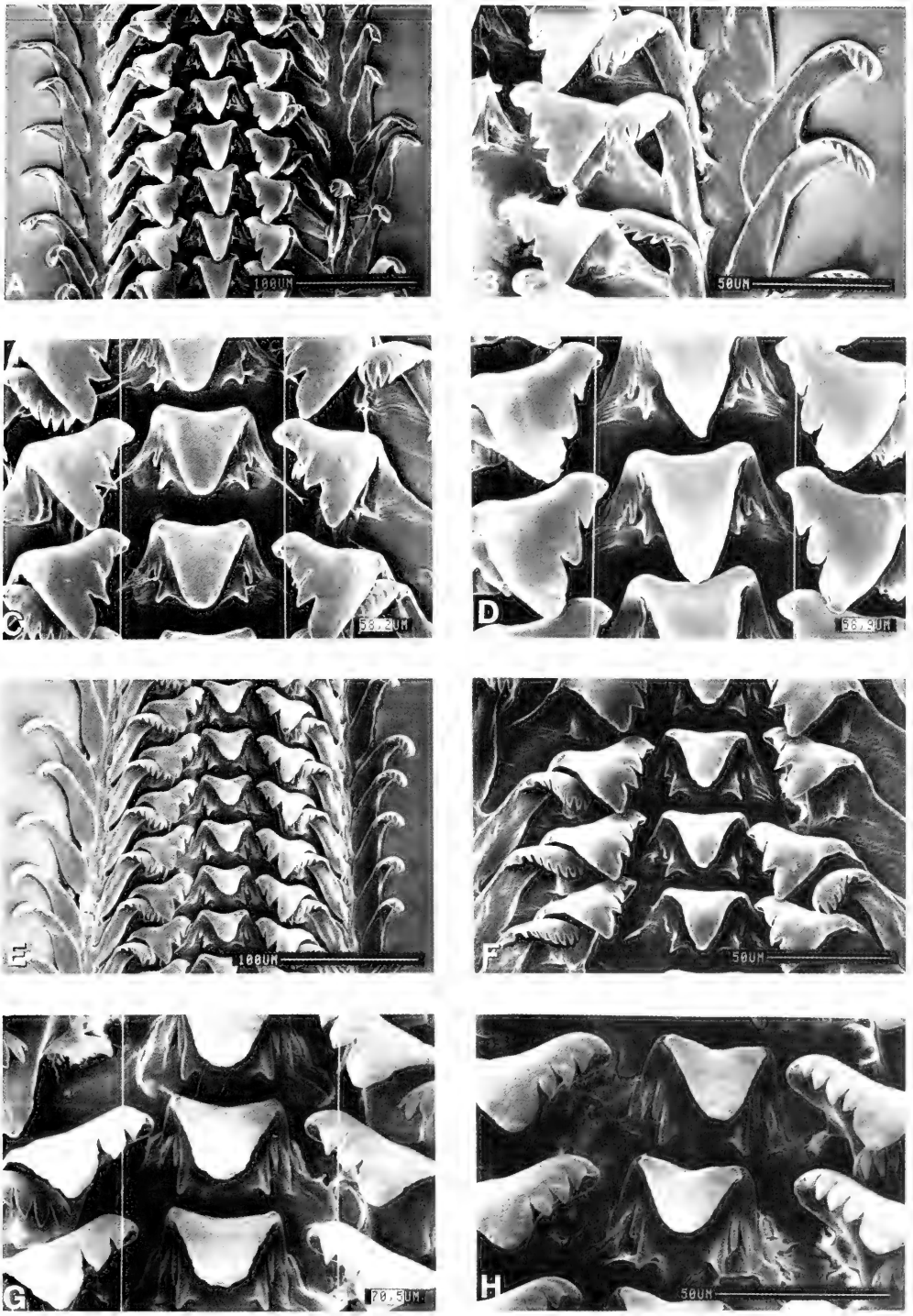

FIG. 123. Radula of *Lithoglyphopsis modesta*. A, E segments of radula. C, D, G, H. Central and lateral teeth. B, E, F. Lateral, inner and outer marginal teeth.

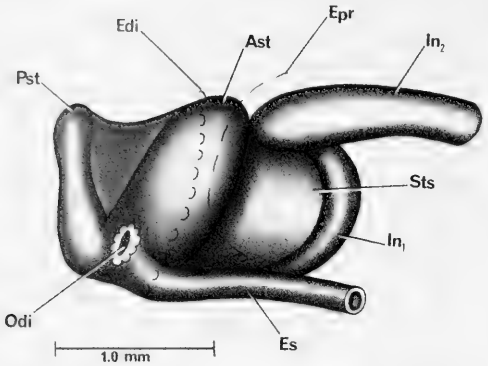

FIG. 124. Ventral aspect of the stomach of *Lithoglyphopsis modesta*.

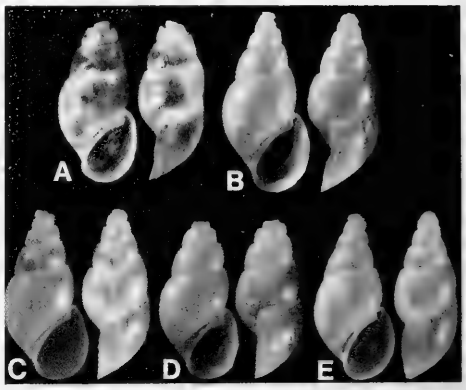

FIG. 125. Shells of *Tricula gredleri*. Figure A is 3.2 mm long; other shells are printed at same scale.

However, given this series of differences between the two taxa, without more data for more species, it is not possible to define generic limits clearly.

Tricula Benson, 1843

Type Species. *Tricula montana* Benson, 1843: 465

Type locality. Bhimtal, N. India

Designation. By monotypy

Assigned species. Based on anatomical study; type species and Chinese species only. *T. montana* Benson, 1843; *T. bambooensis* Davis & Zheng, 1986 (in Davis et al., 1986b); *T. bollingi* Davis, 1968; *T. gregoriana* Annandale, 1924; *T. hudiequanensis* Davis & Guo, 1986 (in Davis et al., 1986b); *T. ludongbini* Davis & Guo, 1986; *T. xianfengensis* Davis & Guo, 1986; *T. xiaolongmenensis* Davis & Guo, 1986. *T. gredleri* Kang, 1986; *T. maxidens* Chen & Davis, sp. nov; *T. odonta* Liu, Zhang & Wang, 1983a. N = 11.

Diagnosis. Shells small to medium, ovate-conic. Central tooth as in *Neotricula*. The oviduct makes a tight 360° twist dorsal to the bursa. The spermathecal duct enters the pericardium; the spermathecal duct starts as a wide duct when diverging from the oviduct and narrows to a slender duct at the pericardium. The duct of the seminal receptacle arises from the oviduct, from the base of the duct of the bursa, or from the duct of the bursa. The duct of the bursa runs undiminished in diameter into the oviduct close to the opening of the oviduct into the albumen gland. Some species of *Tricula* have a pericardial bursa (Davis et al., 1986b: 515, fig. 40). The type species has a pericardial bursa (Davis et al., 1986a: 434, fig. 6A).

Tricula gredleri Kang, 1986

Syntypes. Hubei Medical College, Department of Parasitology, Wuhan City, Hubei Province, People's Republic of China. Figured in Kang (1986: pl.1, fig. 2). Holotype not segregated in Kang's collection. SMF 305653–305654

Type locality. Maluxi, "(28°56′N, 109°92′E)", Orientalis Commune, Guzhang County, Hunan Province. Collected 18 Oct. 1983.

Etymology. Named for Vincent Gredler, the German malacologist who first described Chinese *Tricula* from Hunan Province.

Habitat

Specimens studied for this paper were collected from a small stream at Yantuo Village, Xiaoguanping Town, Guzhang County, Xiangxi Prefecture; 28°42′7″N, 110°0′37″E (Fig. 1, site 12), 20 May 1987, Li Chi-Jian. The habitat was 700 m at the edge of the stream shaded by short shrubs. The name of the stream is You Shui He (he = small stream). The field number is D87-3.

Depository

Specimens are catalogued into the collections of ZAMIP, M0008; ANSP 373141, A12657.

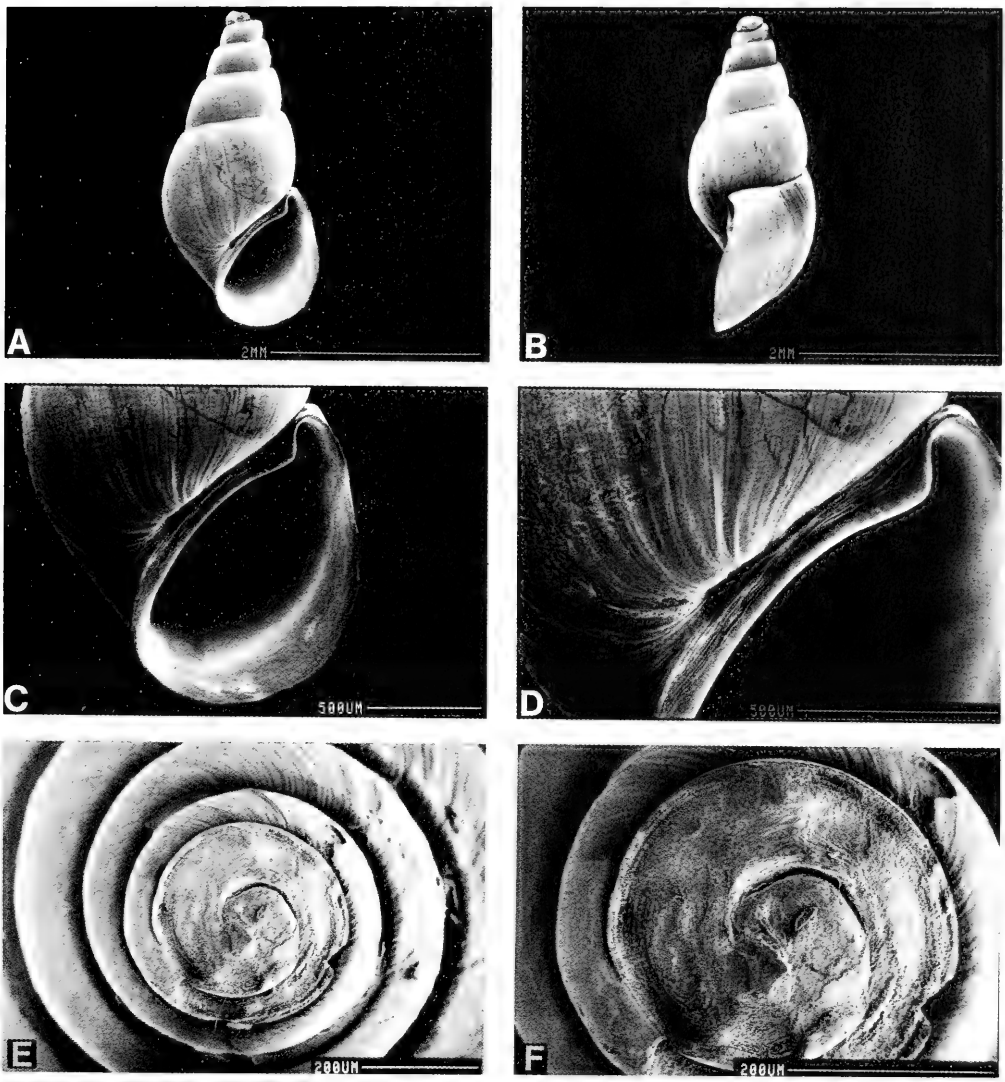

FIG. 126. SEM photographs of shells of *Tricula gredleri*. A, B. Whole shells of mature individuals; C–D. Magnified view of the aperture showing small but deep umbilicus and pronounced apertural notch. E, F. Eroded protoconchs; teleoconch begins at 1.75 whorls.

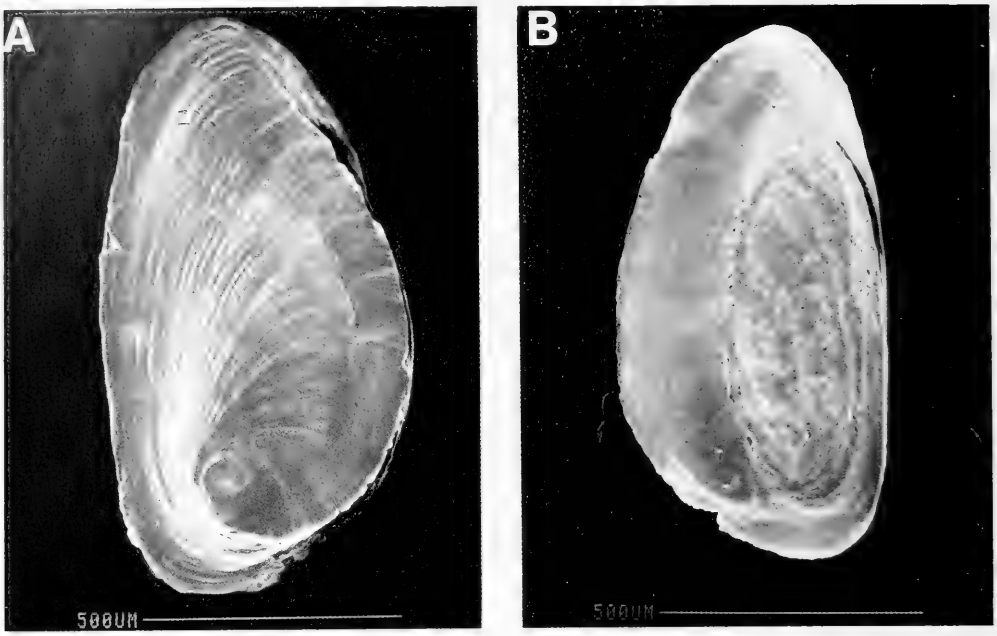

FIG. 127. Opercula of *Tricula gredleri*. Outer surface at left (A); inner surface to the right (B).

Description

Shell. Shells are small, ovate-conic, and smooth (Figs. 125, 126). Virtually all shells are eroded at the apices so that a true understanding of length is not possible. Lengths do exceed 3.30 mm (Table 62). The aperture is pyriform. Adapically there is a pronounced apertural beak with beak tubercle. There is no internal notch groove. There is no adapical outer lip angle.

The whorls at the suture are smooth (not crenulated). There is an umbilical chink. The inner lip is straight abapical to the beak tubercle; it is separated from the body whorl. Adapically shell material may be layered between the lip and the body whorl to the point of fusion. The inner lip is uniformly thin. An apertural sinus is seen when the outer lip is seen in side view. Abapical to the sinus the lip is straight to slightly scooped forward. In side view, the inner lip is straight; there is no spout, no varix.

The abapical lip projects beyond the base of the shell 0.38 ± 0.02 mm.

External features. The head is translucent; there is no deposition of melanin pigment. There are no white or yellow granules about the eyes. The operculum (Fig. 127) is corneous and paucispiral. It is unique in being especially thickened abapically and sitting cap-like on the foot. The attachment pad is prominent, some 56% the width of the operculum.

Mantle cavity. Mantle cavity organs are shown in Figure 128. Organ measurements and counts are given in Table 63. The osphradium is positioned slightly anterior to mid-gill; it is elliptical and short. There are 13 to 19 gill filaments with both Gf_1 and Gf_2 elements prominent. The longest gill filaments are 0.48 ± 0.09 mm long. Gill filament section Gf_2 is long. In side view, the largest gill filaments are moderately domed.

The portal for sperm entry into the pericardium (Ope) is shown. The pericardium (Pe) is considerably swollen and there is an enormous pericardial bursa (Pbu) pushing the lining of the mantle cavity far forward into the mantle cavity.

Female reproductive system. An uncoiled female without head and with kidney tissue removed is shown in Figure 129. Measurements of organs are given in Table 63. Important features are: (1) The gonad is posterior to the stomach. It is small and consists

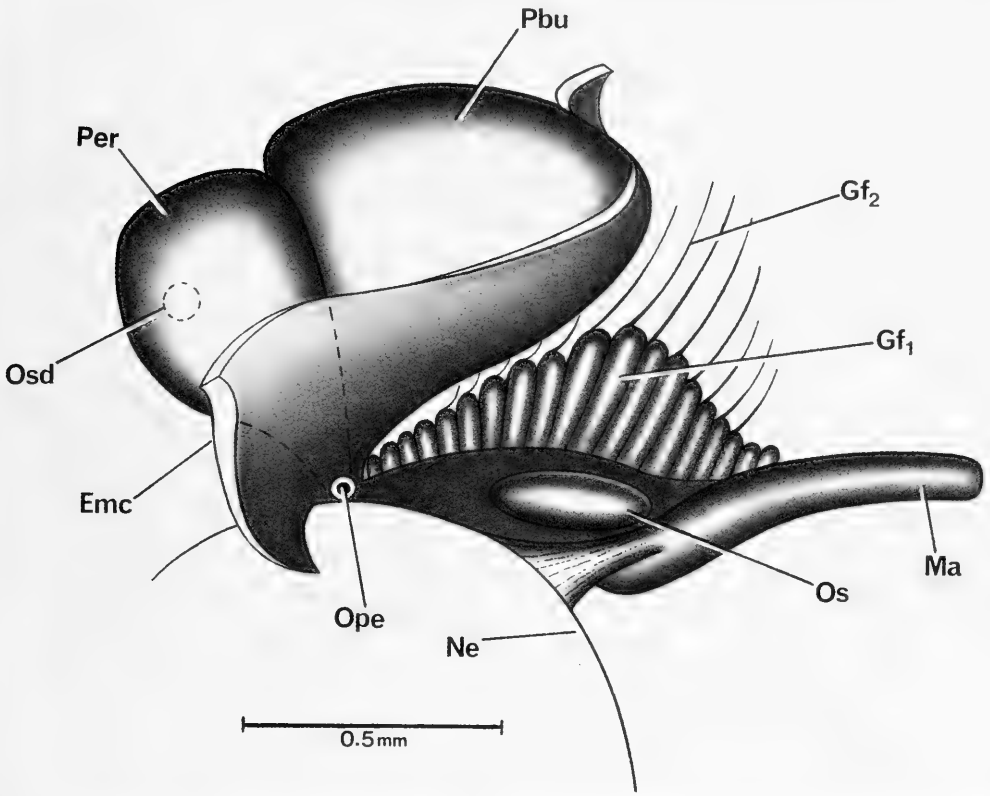

FIG. 128. Mantle cavity of *Tricula gredleri* showing the enormous pericardial bursa (Pbu) bulging into mantle cavity.

TABLE 62. Shell measurements (mm) of *Tricula gredleri* syntypes and of shells of snails used for dissections. All shells that had eroded apices = e. Mean ± standard deviation (range). N = number measured. M = male, F = female.

	Syntypes (N = 2)		For Anatomy (N = 5)
	1.	2.	
No. Whorls	4e	5e	3e–4e
Length (L)	3.08e	3.12e	3.16 (4e,M); 3.32 (4e,F)
Width (W)	1.40	1.36	1.52±0.11 (1.36–1.64)
L last three whorls	2.80	2.76	3.01±0.11 (2.84–3.16)
L body whorl	2.04	2.08	2.20±0.11 (2.12–2.36)
L penultimate whorl	0.44	0.40	0.54±0.02 (0.52–0.56)
W penultimate whorl	0.92	0.96	1.06±0.05 (1.00–1.12)
W 3rd whorl	0.64	0.60	0.71±0.04 (0.68–0.76)
L aperture	1.48	1.48	1.50±0.08 (1.40–1.56)
W aperture	0.80	0.88	0.99±0.05 (0.92–1.04)
x			0.38±0.02 (0.36–0.40)
y			0.18±0.06 (0.10–0.24)

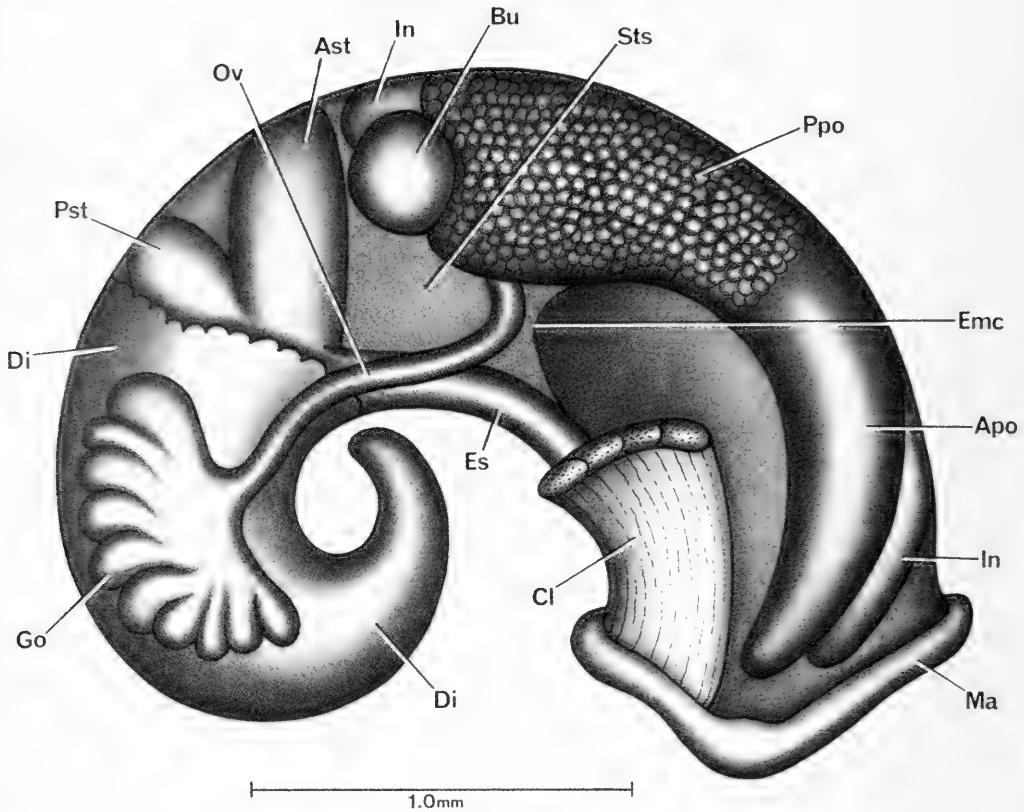

FIG. 129. Uncoiled female *Tricula gredleri* with head and kidney tissue removed.

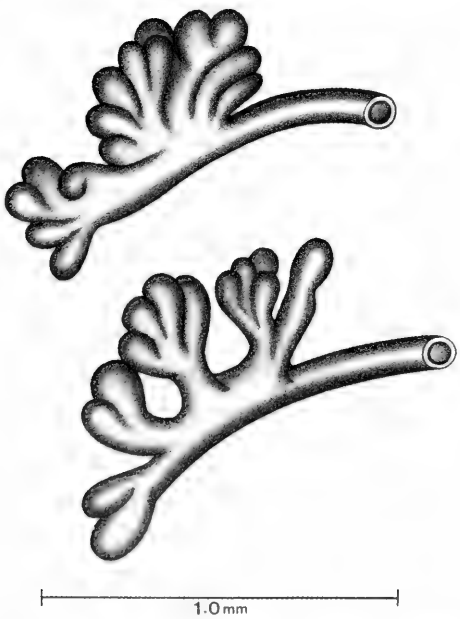

FIG. 130. Variation in gonad structure of female *Tricula gredleri*.

of one to four bundles of lobes Figures 129, 130. (2) The bursa copulatrix (Bu) is round to sub-triangular, minute, and clearly visible posterior to the albumen gland (Ppo). (3) The albumen gland is of normal size. (4) The bursa copulatrix complex of organs is shown in Figures 131, 132. In Figure 131 the orientation of the bursa complex is the same as in Figure 129. The 360° twist of the oviduct (Ov) and the duct of the bursa arising from the oviduct are seen in Figure 131; these two character-states are seen in all genera of the tribe Triculini. (5) The species is unique in having such an enlarged pericardial bursa (Pbu). (6) In Figure 132A and B, it is shown that the duct of the seminal receptacle arises from the oviduct slightly posterior to the opening of the duct of the bursa either slightly offset dorsolaterally, or directly in line with the opening of the duct of the bursa (Fig. 132 C). (7) The seminal receptacle (Sr) is a small sphere. (8) There is no spermathecal duct, or, at best, a minute one; the oviduct appears, in gross dissection, to be fused to the pericardium (Sdo,

TABLE 63. Lengths (mm) or counts of non-neural organs and structures of *Tricula gredleri*. N = number of snails used. Mean ± standard deviation (range).

	Females (N = 5)	Males (N = 2)
Body	4.96±0.45 (4.30–5.44)	4.80 (4.60, 5.00)
Gonad	0.85±0.11 (0.70–1.00)	2.60 (2.40, 2.80)
Digestive gland	2.17±0.32 (1.70–2.50)	1.97 (1.92, 2.02)
Posterior pallial oviduct (= albumen gland)	1.05±0.19 (0.80–1.20) N = 4	—
Anterior pallial oviduct (= capsule gland)	1.13±0.15 (1.00–1.30) N = 4	—
Total pallial oviduct = OV	2.14±0.17 (2.00–2.40)	—
Bursa copulatrix = BU	0.31±0.01 (0.31–0.32)	—
Duct of BU	0.17±0.01 (0.16–0.18) N = 3	—
BU ÷ OV	0.14±0.01 (0.13–0.16)	—
Seminal receptacle	0.17±0.01 (0.16–0.18) N = 4	—
Duct of seminal receptacle	0.08±0.02 (0.06–0.10) N = 4	—
Mantle cavity	1.42±0.13 (1.30–1.60)	1.55 (1.50, 1.60)
Gill (G)	1.07±0.17 (1.30–1.60)	1.11 (1.10, 1.12)
Osphradium (OS)	0.35±0.08 (0.30–0.46) N = 4	0.31 (0.24, 0.38)
Os ÷ G	0.35±0.09 (0.25–0.46) N = 4	.28 (0.22, 0.34)
No. of filaments	16.8±2.3 (13–19)	16.0 (No var.)
Buccal mass	0.58±0.09 (0.50–0.68)	—
Gf_2	0.26±0.06* (0.20–0.36) N = 6	—
Gf_1	0.22±0.08* (0.18–0.26) N = 6	—
Total Gf = TGF	0.48±0.09* (0.38–0.62) N = 6	—
Gf_2 ÷ TGF	0.54±0.03* (0.50–0.58) N = 6	—
Prostate	—	0.93 (0.86, 1.00)
Seminal vesicle	—	0.70 (0.60, 0.80)
Penis	—	2.60 (2.00, 3.20)

*males and females

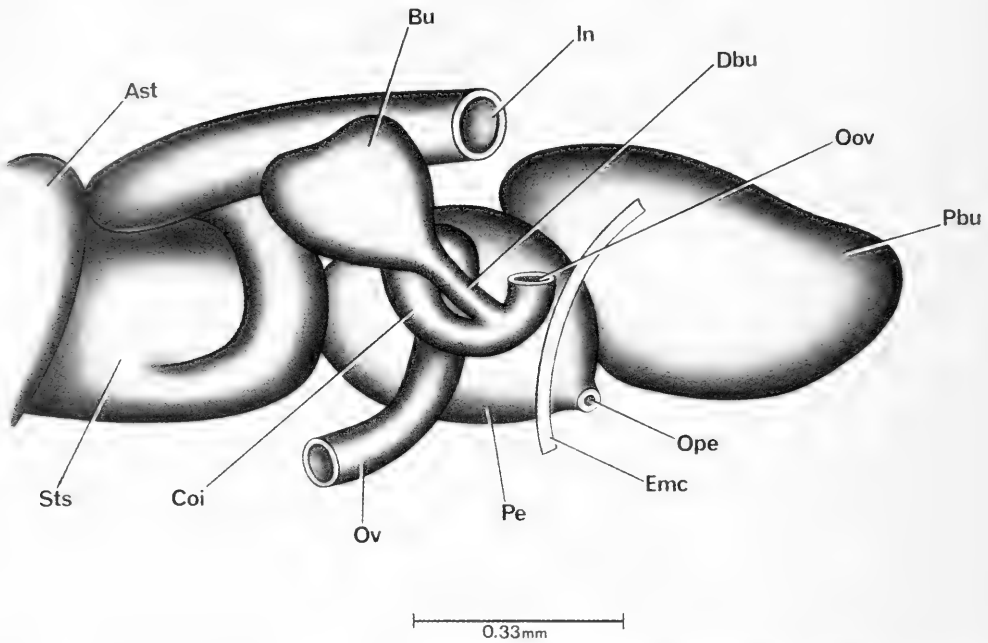

FIG. 131. Details and variation of bursa copulatrix complex of organs relative to style sac (Sts), pericardium (Pe) and posterior end of mantle cavity (Emc).

TABLE 64. Radular statistics for *Tricula gredleri*. Mean ± standard deviation (range). N = number used. In mm except for width of central tooth in μm.

	Females (N = 3)	Males (N = 4)
Shell length	3.41±0.17 (3.28–3.60)	3.30 (3.10, 3.40) N = 2
Radular length	0.49±0.10 (0.39–0.60)	0.51±0.03 (0.47–0.54)
Radular width	0.07±0.002 (0.072–0.076)	0.07±0.01 (0.060–0.072)
Total rows of teeth	56±4.4 (53–61)	63.4±4.2 (61–70)
No. rows of teeth forming	16.0±2.0 (14–18)	16.3±1.5 (15–18)
Central tooth width	13.7±1.0 (12.8–15.0) N = 8	15.1±1.4 (13.1–17.1) N = 17

Fig. 132B). (9) Sperm enter the female system from the mantle cavity into the pericardium hence to the oviduct.

Male reproductive system. An uncoiled male without head and with kidney tissue removed is shown in Figure 133. Two bundles of gonadal lobes are cut away to show the seminal vesicle (Sv). Measurements are given in Table 63. Important features are: (1) The gonad fills the digestive gland (Di) and covers the posterior and anterior chambers of the stomach. (2) The prostate (Pr) overlaps the posterior end of the mantle cavity (Emc). (3) The seminal vesicle (Sv) arises from the vas efferens (Ve) about mid-gonad. (4) The seminal

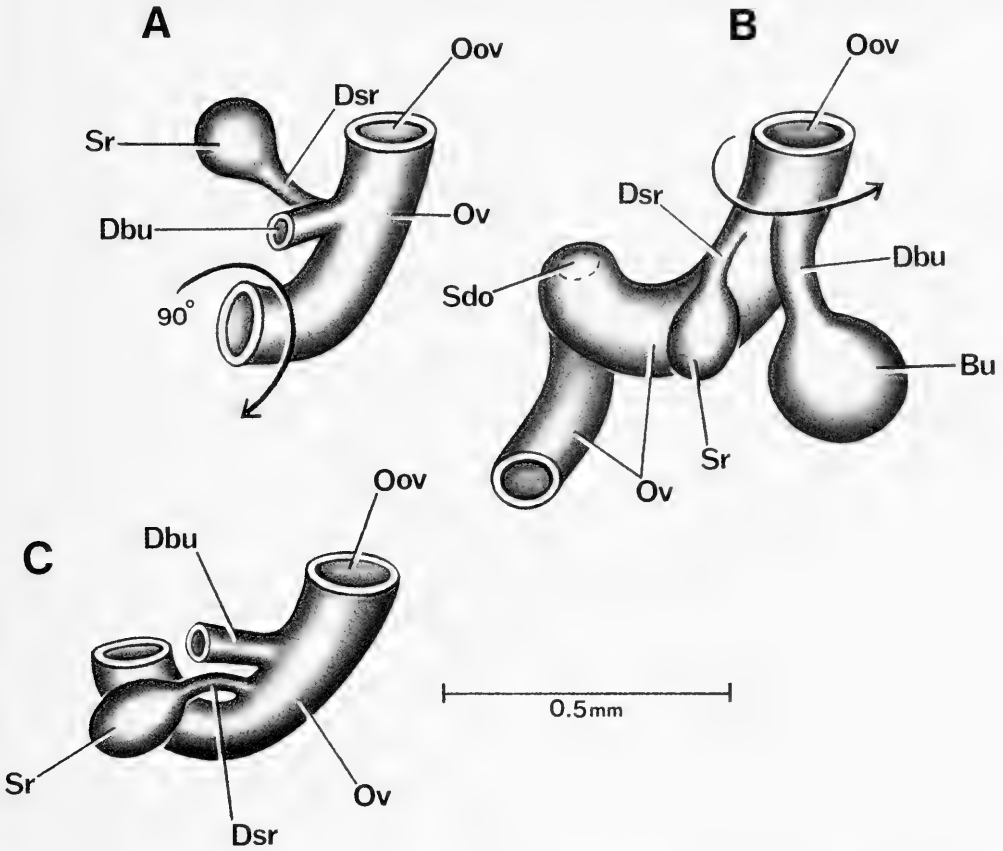

FIG. 132. Details and variation of bursa copulatrix complex of organs of *Tricula gredleri*. A. Compared with Figure 131, bursa copulatrix cut off and duct system rotated 90° to show position of seminal receptacle (Sr) and its duct (Dsr). Complex in A is further rotated in B to show where duct of seminal receptacle (Dsr) opens into oviduct (Ov). C. Section of oviduct oriented as in Figure 131 showing a variation in position of opening of duct of seminal receptacle into oviduct, the usual *Tricula* position.

TABLE 65. Cusp formulae for the radular teeth of *Tricula gredleri* with the percent of the seven radulae in which a given formula was found at least once.

Central Teeth		Lateral Teeth		Inner Marginal Teeth		Outer Marginal Teeth	
$\frac{3\text{-}1\text{-}3}{2\text{-}2}$	71%	2-[2]-3	86%	8	29%	8	14%
$\frac{3\text{-}1\text{-}3}{3\text{-}3}$	14%	3-[2]-2	86%	9	57%	9	71%
$\frac{3\text{-}1\text{-}2}{2\text{-}2}$	14%	2-[2]-4	43%	10	71%	10	57%
$\frac{2\text{-}1\text{-}2}{2\text{-}2}$	14%	4-[2]-2	14%	11	57%	11	71%
$\frac{4\text{-}1\text{-}3}{3\text{-}2}$	14%						
				$\bar{X}$ * = 9.69±2.01 N = 70		9.0±3.1 N = 70	

*Mean ± standard deviation of cusp number for all teeth counted.
[ ] = blade bifurcates thus resembling two cusps.

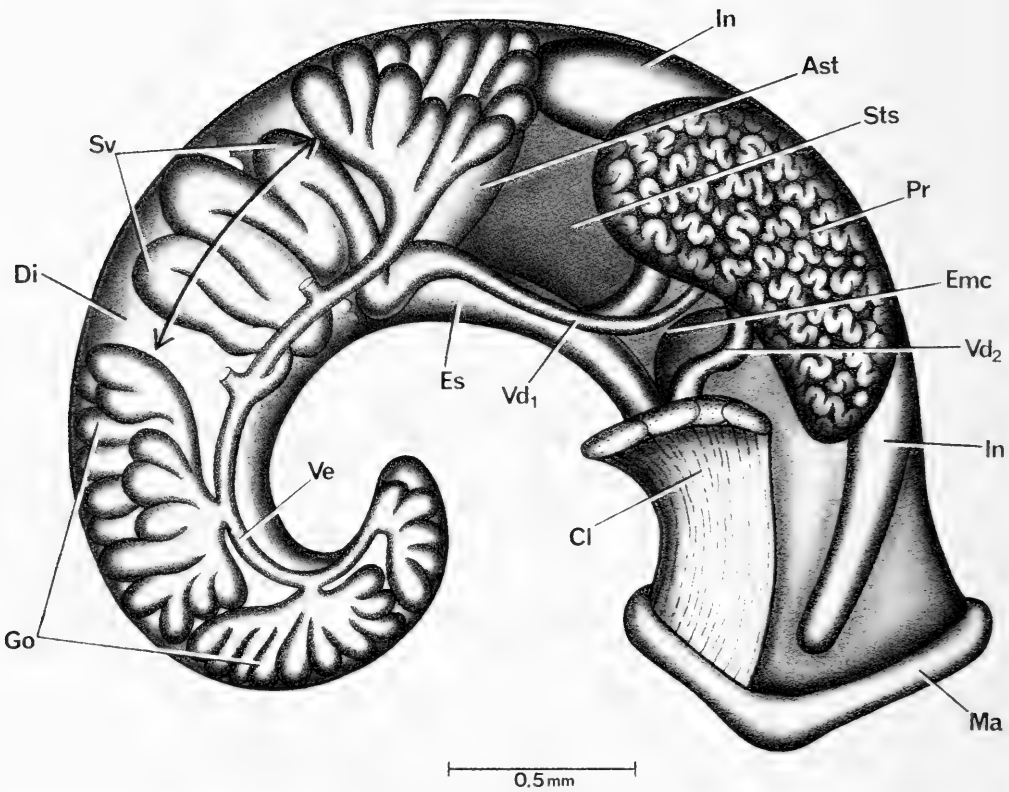

FIG. 133. Uncoiled male of *Tricula gredleri* without head or kidney tissue. Two sections of gonadal lobes removed to reveal seminal vesicle coiled dorsal to gonad.

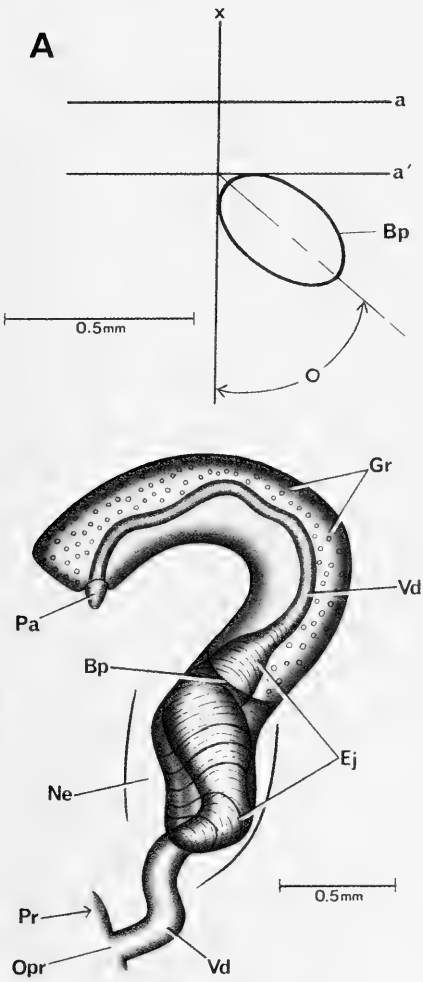

FIG. 134. A. Relationship of base of penis of *Tricula gredleri* to mid-line of snout-neck (x) and to posterior end of eye lobes (a). B. Penis.

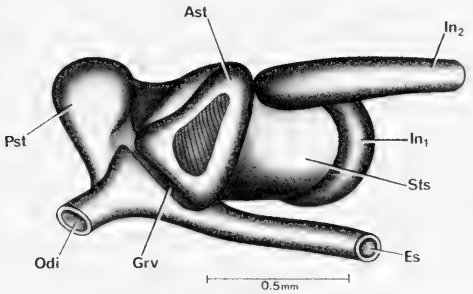

FIG. 135. Stomach of *Tricula gredleri* oriented exactly as in Figures 129, 131, and 133.

TABLE 66. Lengths of neural structures of *Tricula gredleri*. Mean ± standard deviation (range). N = number used = 5. * - neural elements measured to obtain the RPG ratio.

Cerebral ganglion	0.24±0.02 (0.22–0.26)
Cerebral commissare	0.04±0.02 (0.02–0.06)
Pleural ganglion Right (1)*	0.12±0.02 (0.10–0.14)
Left	0.12±0.02 (0.10–0.14)
Pleuro-supraesophageal connective (2)*	0.14±0.02 (0.12–0.16)
Pleuro-subesophageal connective	0.14±0.03 (0.10–0.16)
Supraesophageal ganglion (3)*	0.12±0.02 (0.10–0.14)
Subesophageal ganglion	0.12±0.02 (0.10–0.14)
Osphradio-mantle nerve	0.07±0.03 (0.04–0.12)
RPG ratio* = 2 ÷ 1+2+3	0.37±0.04 (0.33–0.41)

vesicle coils dorsal to the gonad from mid-gonad anterior to cover the posterior chamber of the stomach. (5) The anterior vas deferens (Vd_2) leaves the prostate near the posterior end of the mantle cavity (Emc). (6) The penis is unique among triculine taxa (Figure 134B). The anterior end is blunt with a protudable papilla (Pa) emerging from the edge of the square penial tip at the concave side of the penis. (7) The ejaculatory duct is massive and extends as a wide muscular duct from the base of the penis along the dorsal aspect of the neck to the end of the neck. (8) The orientation of the base of the penis to the snout-neck mid-line is shown in Figure 134A. It is to the right of the mid-line ("x"), and at an angle of 45°–50° to it.

Digestive system. The digestive gland is posterior to the stomach of both sexes. The stomach is shown in Figure 135. Two features of note are: (1) there is a groove (Gr) or crease between the anterior chamber of the stomach (Ast) and the section of stomach receiving the esophagus (Es) and duct of the digestive gland (Odi). (2) The anterior chamber (Ast) is yellow with a centrally positioned grey area.

Radular statistics are given in Tables 64 and 65. There appears to be sexual dimorphism in the number of rows of teeth on the

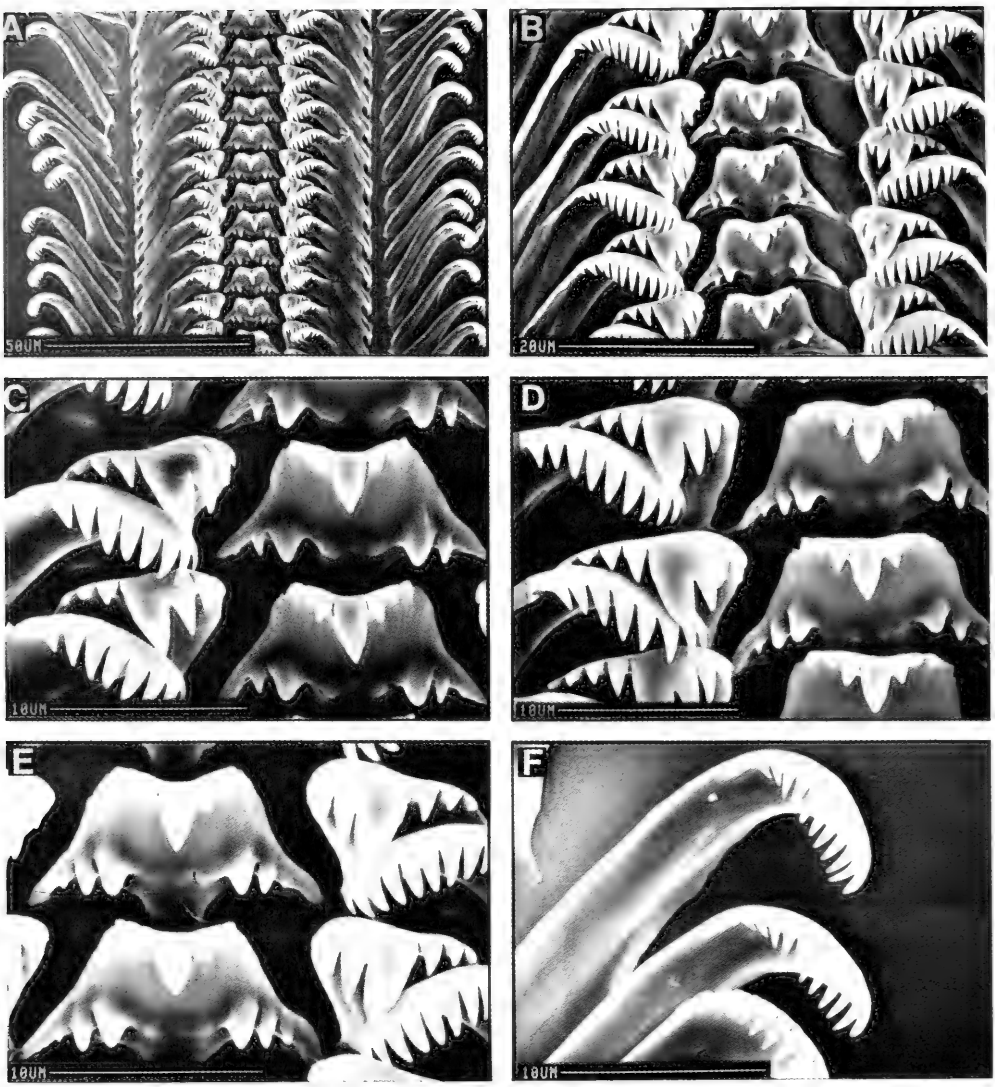

FIG. 136. Radula of *Tricula gredleri*. A. Section of radular ribbon. B-E. Central, lateral and inner marginal teeth. F. Outer marginal teeth. Note pronounced bifurcation of the blade of the major cusp of lateral tooth (especially in Figs. C–E).

radular ribbon; males have more (61 to 70 on a radula 3.30 mm long). However, the sample size is small. The most frequently encountered formula is

$$\frac{3\text{-}1\text{-}3}{(3)2\text{-}2(3)};\ 2(3)\text{-}[2]\text{-}2(3);\ 9\text{-}11;\ 9\text{-}11.$$

SEM photographs of radulae are shown in Figure 136. The dominant cusp of the lateral tooth (Fig. 136B–E) has a blade that bifurcates. Otherwise the tooth morphologies are standard triculine.

Nervous system. Measurements are given in Table 66. The RPG ratio of 0.37 indicates that the dorsal nerve ring is moderately concentrated. The pleuro-subesophagal connective of this species is unusual for its length, equal to that of the pleuro-supraesophageal connective.

Remarks

Conchologically, *Tricula gredleri* is most similar to *N. duplicata* (Figs. 153–155). Conchological comparison with *N. duplicata* is given in the remarks section for that species. Anatomically, *T. gredleri* has the generic-level character-states that serve to differentiate it from *N. duplicata*.

Tricula gredleri has seven *unique* anatomical character-states (Tables 80, 81). The operculum is cap-like, not a flat sheet (char. 2). The oviduct is fused to the pericardium; there is no discernable length of spermathecal duct (chars. 19,20). The penial opening of this species arises form the concave edge of a blunt tip (char. 34). The anterior chamber of the stomach is lemon yellow (char. 40). The pleuro-subesophageal connective is long (char. 48).

Tricula gredleri belongs to the species group within *Tricula* that has a pericardial bursa *T. montana*, *T. gredleri*, *T. gregoriana* and *T. maxidens*. Its closest relationship anatomically is with *T. odonta*.

***Tricula maxidens* Chen & Davis, sp. nov.**

Holotype. ZAMIP, M0009, Figure 137A.

Paratypes. ANSP 373140, A12656, Figure 137B–E.

Type locality. Yantuo Village, Xiaoguanping Town, Guzhang County, Xiangxi Prefecture; 28°42′7″N, 110°0′37″E. Figure 1, site 12.

Etymology. contraction from the Latin maximum (the greatest) and dens (tooth).

Habitat

These snails were collected in sympatry with *Tricula gredleri* and *Akiyoshia chinensis* from a small mountain stream at an altitude of 700 m. The field number assigned was D87-3.

Description

Shell. Shells are small, smooth, and cylindrical-conic (Figs. 137A–E; 138A–D, F). They mature at 5.5 whorls with the largest size class ranging in length from 2.08–2.24 mm (Table 67). The sutures are deep and the whorls are slightly convex. Cleaned shells are glassy; there is no umbilicus. The aperture is semi-circular with the inner lip a flat-straight edge. The inner lip is fused to the body whorl. The outer lip in side view, is straight, without notch or sinuation. With the outer lip down and 90° to the horizontal, the inner lip is seen in side view with a slight angulation. The most prominent feature is the relatively gigantic columellar tooth seen in the aperture (Fig. 138B) that continues inside the shell wrapping the columella adapically. SEM analyses of the apical whorls indicates that they are minutely malleated to smooth (Fig. 138D, F).

External Features. The head is devoid of melanin pigment. There are no white or yellow granules or glands around the eyes. The operculum (Fig. 138E) is corneous, paucispiral and kidney-bean shaped. The embayment on the columellar side corresponds to the large tooth on the columella. The attachment pad is narrow (33% of operculum width) and moderately prominent.

Mantle cavity. Mantle cavity organs are shown in Figure 139A. Organ measurements and counts are given in Table 68. The osphradium (Os) is mid-gill, and long. There are 10 to 15 well developed gill filaments. The longest gill filament are 0.27 ± 0.01 mm long. The Gf_2 part of the gill is long. Sperm enter the pericardium at the rear of the mantle cavity (Ope). The pericardium (Pe) is moderately swollen and bulges out into the mantle cavity. A discrete but small and delicate pericardial bursa (Fig. 139D) was seen in two individuals, it measured 0.30 x 0.14 mm.

Female reproductive system. An uncoiled female without head and with kidney tissue removed is shown in Figure 140. Measurements of organs are given in Table 68. Important features are: (1) The gonad (Go) is posterior to the stomach; it is small and with bundles of lobes. (2) The bursa copulatrix is round and small; half the bursa is dorsal to the posterior end of the albumen gland (Ppo). (3) The albumen gland is of standard length. (4) The bursa copulatrix complex of organs is shown in Figure 139. The orientation in Figure 139A is the same as that in Figure 140. The bursa copulatrix (Bu) is short. (5) The seminal receptacle (Sr) is spherical; it has a short duct (Dsr) opening into the right ventro-lateral edge of the oviduct (Ov) just posterior to the opening of the duct of the bursa (Dbu) into the oviduct. (6) The spermathecal duct (Sd) is moderately long; it runs to open into the pericardium (Pe). (7) The pericardium is swollen with sperm and distends into the posterior mantle cavity. In some specimens, a minute

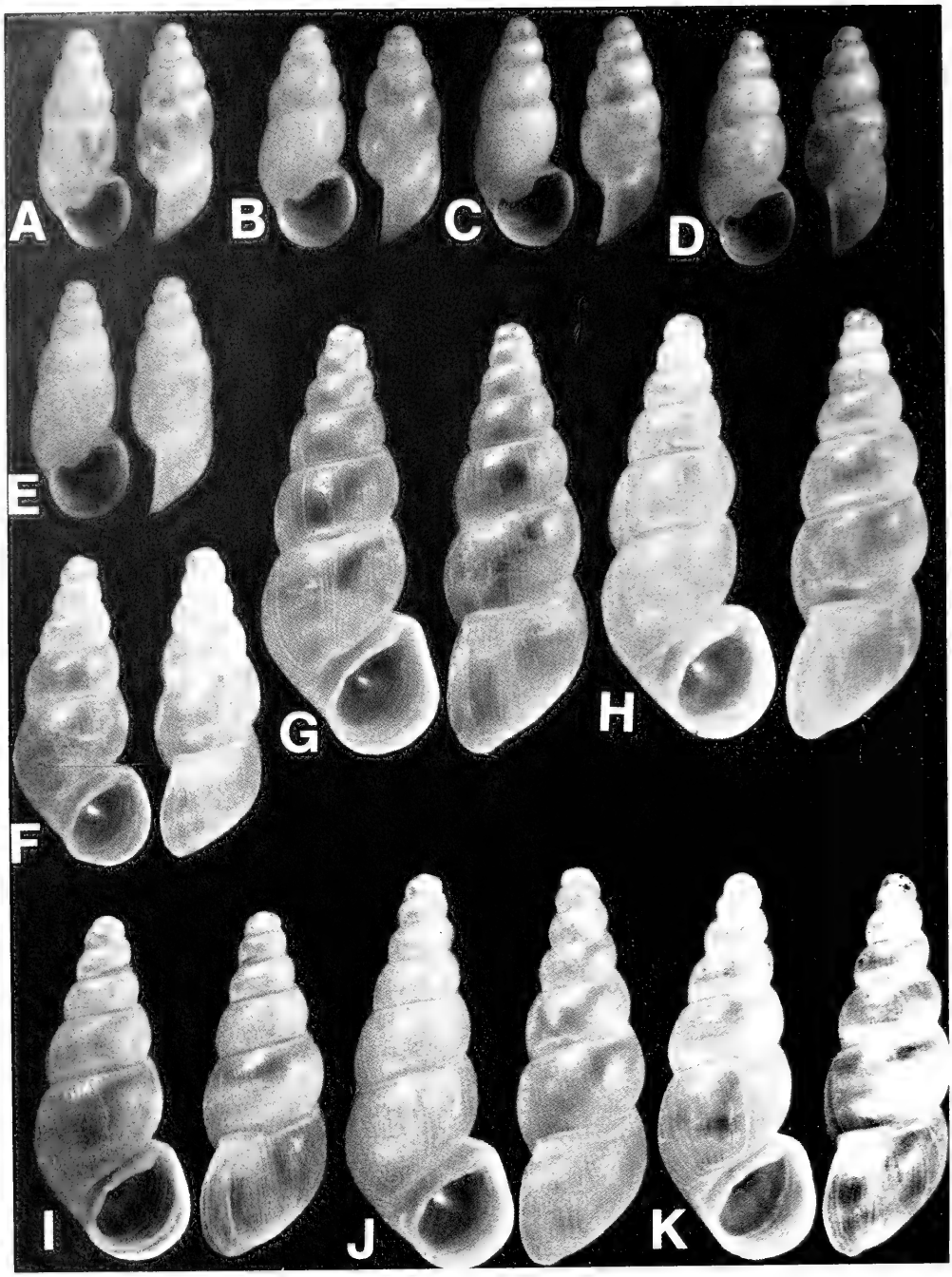

FIG. 137. Shells of *Tricula maxidens*, A–E; *Tricula odonta*, F–K. A. Holotype; B–E. Paratypes. Length of A = 1.94 mm; other shells printed to same scale.

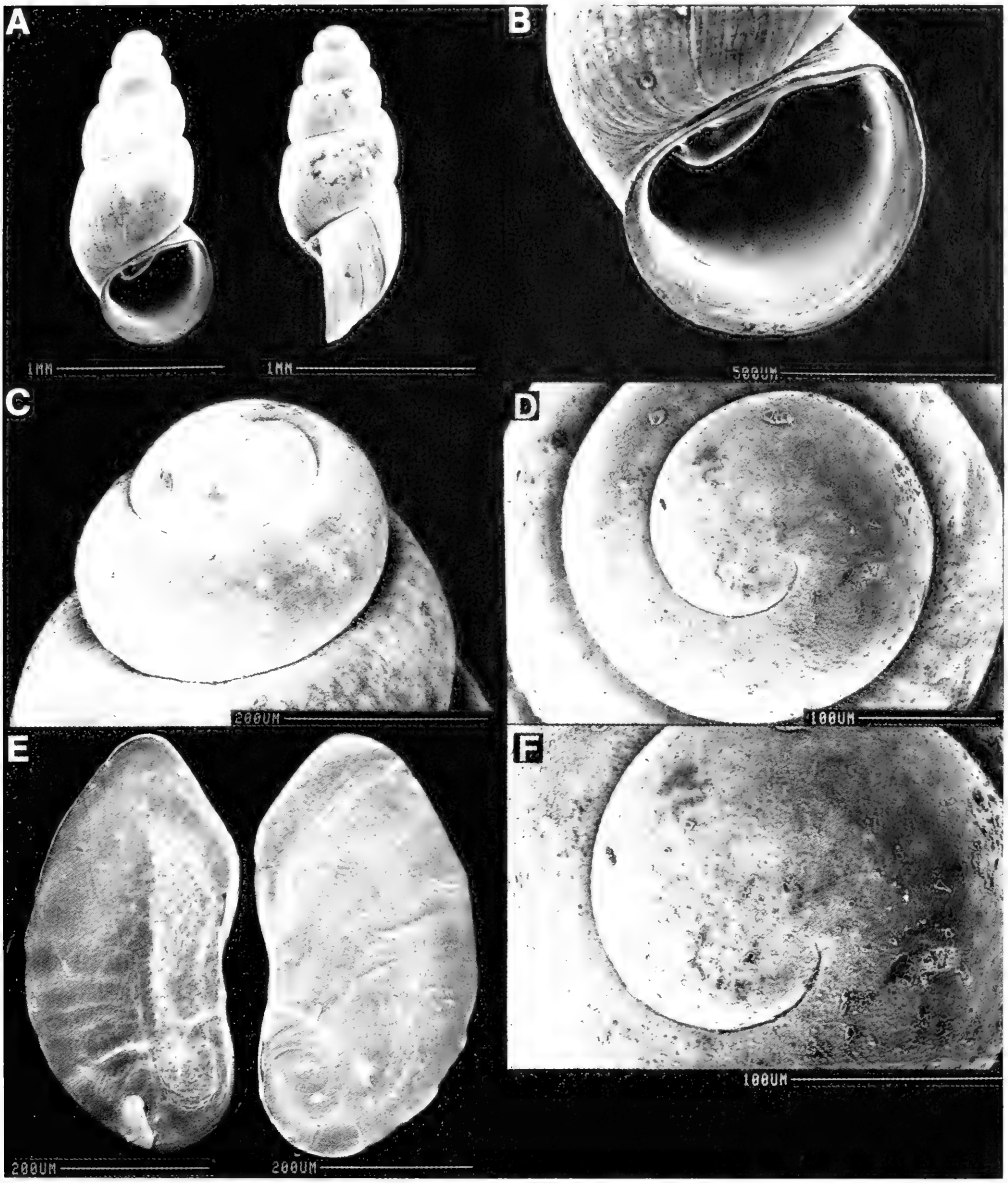

FIG. 138. SEM photographs of shells and opercula of *Tricula maxidens*. A. Shells of mature individuals. Note straight outer lip (right photo) and prominent columellar tooth. B. Enlargement of aperture showing columellar tooth. C, D, F. Protoconch. Although encrusted, protoconch is seen to be vaguely malleated. E. Opercula: right operculum shows outer surface with paucispiral growth line; left operculum shows inner surface with narrow attachment pad.

TABLE 67. Shell measurements (mm) of *Tricula maxidens*. Mean ± standard deviation (range). b = broken apical whorls. N = number measured.

		Paratypes	
	Holotype	Large class (N = 5)	Small Class (N = 3)
No. Whorls	5.5	5.5	5.5
Length (L)	1.94	2.17±0.06 (2.08–2.24)	1.97±0.06 (1.92–2.04)
Width (W)	0.86	0.92±0.03 (0.90–0.96)	0.82±0.03 (0.80–0.86)
L last three whorls	1.82	1.95±0.03 (1.92–2.00)	1.73±0.08 (1.68–1.82)
L body whorl	1.24	1.34±0.04 (1.28–1.36)	1.16±0.10 (1.08–1.28)
L penultimate whorl	0.40	0.40±0.03 (0.36–0.44)	0.35±0.02 (0.32–0.36)
W penultimate whorl	0.68	0.71±0.01 (0.70–0.72)	0.62±0.02 (0.60–0.64)
W 3rd whorl	0.48	0.50±0.01 (0.48–0.52)	0.46±0.02 (0.44–0.48)
L aperture	0.76	0.86±0.02 (0.84–0.90)	0.73±0.06 (0.68–0.80)
W aperture	0.58	0.62±0.02 (0.60–0.64)	0.55±0.05 (0.52–0.60)
x	0.30	0.34±0.02 (0.32–0.36)	0.32 no variation
y	0.08	0.08±0.01 (0.06–0.10)	0.07±0.03 (0.04–0.10)

pericardial bursa was observed (Fig. 139D, Pbu).

Male reproductive system. An uncoiled male with head and kidney tissue removed is shown in Figure 141. Lengths of non-neural organs are given in Table 68. Important features are: (1) The gonad (Go) covers the posterior chamber of the stomach and most of anterior chamber (Ast). (2) The prostate (Pr) is relatively massive and overlaps the posterior end of the mantle cavity (Emc); it covers half the style sac. (3) The vas deferens arises from mid-gonad to slightly anterior to mid-gonad (Fig. 142). (4) The seminal vesicle forms a short coil of tubes dorsal to the gonad and posterior to the stomach. (5) The anterior vas deferens (Vd_2) leaves the prostate slightly posterior to the anterior end of the prostate (Fig. 141). (6) The penis is simple, without papilla; it is slender (Fig. 143B). (7) There is a pronounced ejaculatory duct (Ej) in the base of the penis. (8) The orientation of the long axis of the penial base (Bp) to the snout-neck mid-line (x) is shown in Fig. 143A. The penial base is to the right of the mid-line and at an angle of 40°.

Digestive system. The digestive gland is posterior to the stomach in both sexes. Radular statistics are given in Tables 69 and 70. There are 59.8 ± 6.4 rows of teeth along a radula of 0.29 ± 0.04 mm (= equivalent of 207 teeth per mm). The most frequently encountered formula is

$$\frac{3\text{-}1\text{-}3;\ 3(4)\text{-}1\text{-}4;\ 12\text{–}14;\ 13\text{–}14.}{2\text{-}2}$$

The radula is shown in Figure 144; radula morphology is of the generalized *Tricula* type. The central anterior cusp of the central tooth is long and dagger-like. The dominant cusp of the lateral tooth is slender and dagger-like.

The stomach (Fig. 145) is the usual type but with a diagnostic grey streak (Gs) running across the ventral surface of the anterior chamber (Ast).

Nervous system. Measurements not taken.

Remarks

Conchologically, among species of Triculinae, *T. maxidens* is unique and clearly separated from all other species (Figs. 153–155). Unique character-states (Tables 2, 76) are the cylindrical-conic shape (char. 2) and the massive tooth nearly filling the aperture (char. 16). The columella within the body whorl has

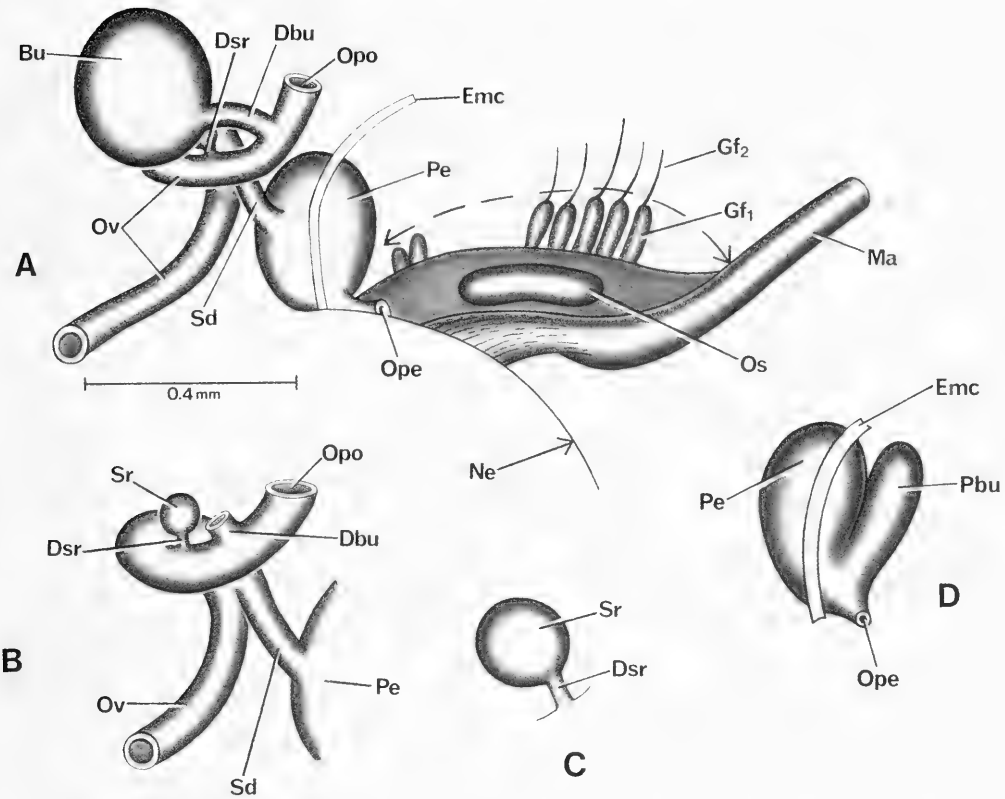

FIG. 139. Details and variation of bursa copulatrix of organs of *Tricula maxidens*. Figs. A and B in the same orientation as in Figure 140. C. Enlarged seminal receptacle. D. Pericardium with minute pericardial bursa (Pbu).

a raised spiral keel. The shell seems more similar to *Pseudobythinella* than to *Tricula*.

Anatomically, this species is most closely allied phenetically to *T. xiaolongmenensis* (Figs. 156–158). It differs from that species in 11 character-states (26%); see Tables 80, 81. Some of these differences are: In *T. maxidens* the bursa is covered by the albumen gland; in *T. xiaolongmenensis* the bursa is posterior to the albumen gland (char. 14). In the former, the duct of the seminal receptacle arises from the inside edge of the oviduct; it arises from the outside edge in the latter (char. 24). The former has a slight pericardial bursa; the latter has no pericardial bursa (char. 25). The radula is short in the former, of medium length in the latter (char. 41). The central anterior cusp of the central tooth is long and dagger-like in the former, the standard type in the latter (char. 44).

Tricula odonta Liu, Zhang & Wang, 1983a

Holotype. SX 788104 (= IZAS; Beijing, People's Republic of China). Figure 1.

Type locality Shangnan, Shaanxi Province. 24 October 1978

Distribution. Shangnan, Shangxian, Zhenping, Tongguan, Ningqiang and Yuanqu of Shanxi Province; Xingshan and Wufeng of Hubei Province; Henan Province

TABLE 68. Lengths (mm) or counts of non-neural organs and structures of *Tricula maxidens*. N = number of snails used. Mean ± standard deviation (range).

	Females (N = 5)	Males (N = 2)
Body	3.30±0.33 (2.90−3.68)	3.24 (3.22, 3.26)
Gonad	0.47±0.09 (0.36−0.60)	1.31 (0.90, 1.72)
Digestive gland	1.32±0.19 (1.00−1.48)	1.41 (1.40, 1.42)
Posterior pallial oviduct (= albumen gland)	0.58±0.11 (0.54−0.70) N = 3	—
Anterior pallial oviduct (= capsule gland)	0.67±0.15 0.50−0.80) N = 3	—
Total pallial oviduct = OV	1.23±0.23 (1.00−.150)	—
Bursa copulatrix = BU	0.24±0.05 (0.22−0.30)	—
Duct of BU	0.09±0.01 (0.08−0.10) N = 4	—
BU ÷ OV	0.20±0.06 (0.16−0.30)	—
Seminal receptacle	0.07±0.01 (0.06−0.08) N = 3	—
Duct of seminal receptacle	0.02 N=1	—
Mantle cavity	0.81±0.08 (0.74−0.90) N = 3	0.82 N = 1
Gill (G)	0.66±0.13 (0.54−0.80) N = 3	0.70 N = 1
Osphradium (OS)	0.28 (0.24, 0.32) N = 2	0.26 N = 1
OS ÷ G	0.39 (0.38, 0.40) N = 2	0.37 N = 1
No. filaments	12.7±2.5 (10−15)	14 N = 1
Gf_2	0.17±0.01 (0.16−0.18)	—
Gf_1	0.11±0.01 (0.10−0.12)	—
Total Gf = TGF	0.27±0.01	—
Gf_2 ÷ TGF	0.61±0.04 (0.57−0.64)	—
Prostate	—	0.75 (0.70, 0.80)
Seminal vesicle	—	0.65 (0.40, 0.90)
Penis	—	0.64 (0.52, 0.76)

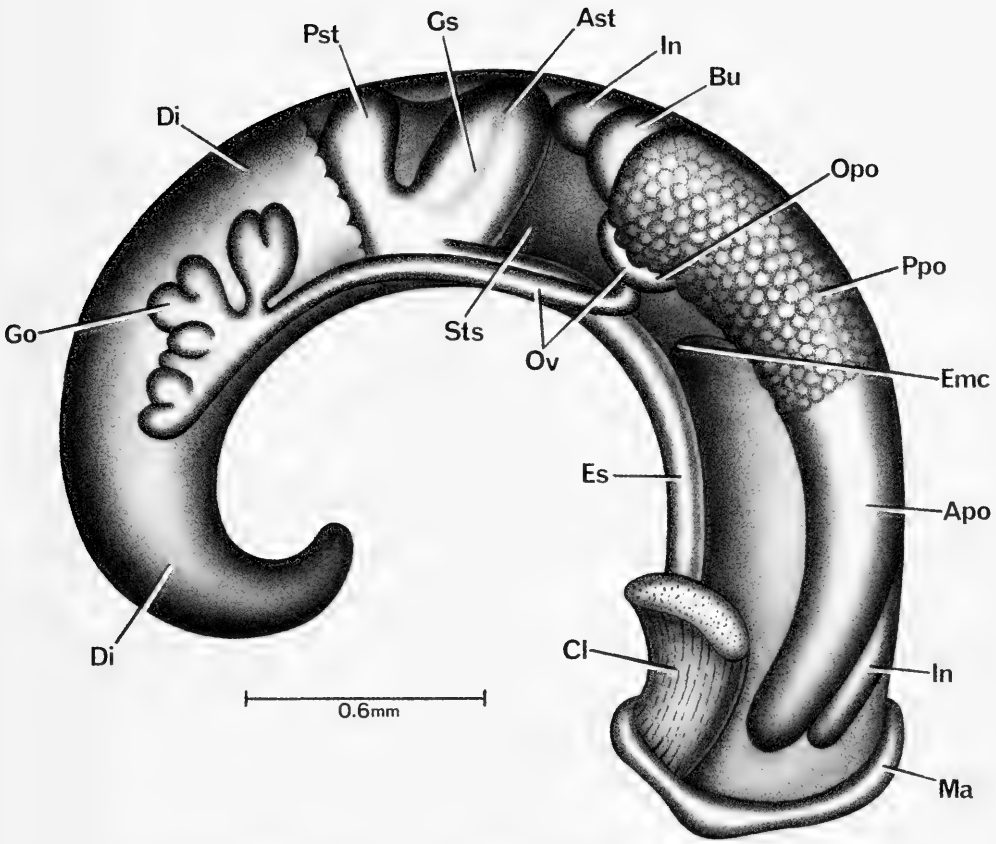

FIG. 140. Uncoiled female *Tricula maxidens* with head and kidney tissue removed.

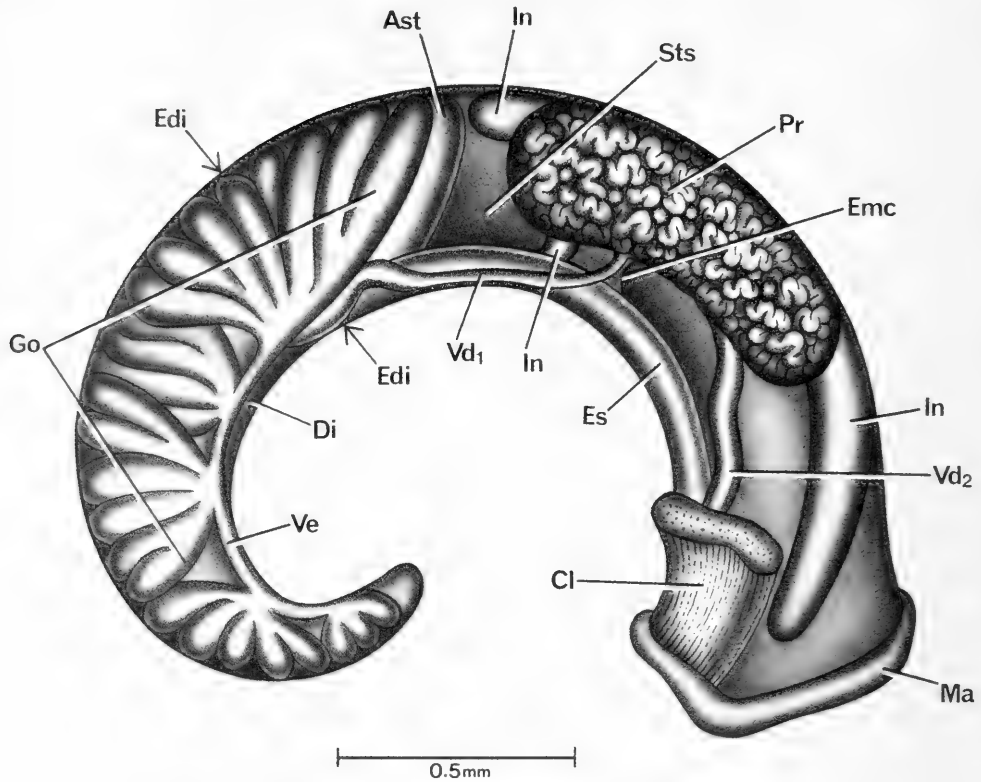

FIG. 141. Uncoiled male of *Tricula maxidens* without head or kidney tissue.

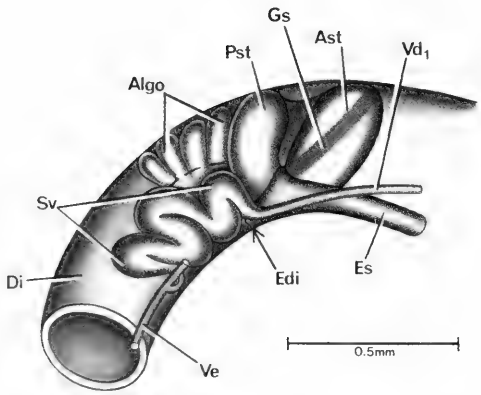

FIG. 142. A. Figure to show seminal vesicle (Sv) of *Tricula maxidens* in relationship to stomach. Most of gonad and vas efferens cut away.

TABLE 69. Radular statistics for *Tricula maxidens*. Mean ± standard deviation (range). N = number used. In mm except for width of central tooth in μm.

	Females (N = 4)
Shell length	2.19±0.08 (2.08–2.24)
Radular length	0.29±0.04 (0.240–0.204)
Radular width	0.03±0.01 (0.028–0.040)
Total rows of teeth	59.8±6.4 (55–69)
No. rows of teeth forming	11.3±1.5 (9–12)
Central tooth width (N = 18)	9.6±0.3 (9.0–10.1)

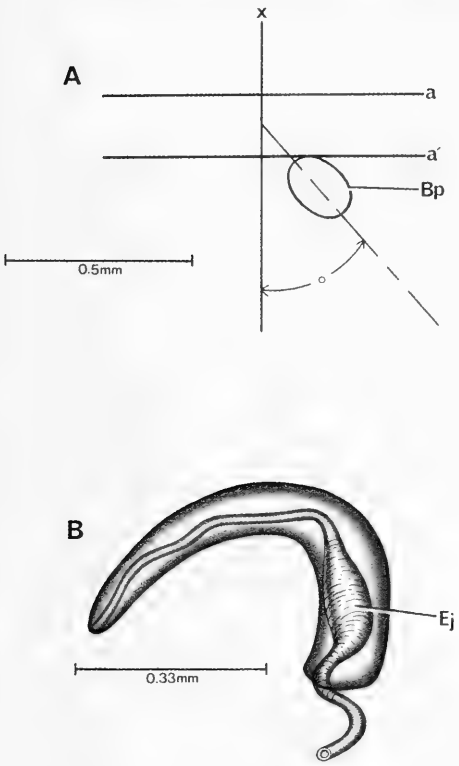

FIG. 143. *Tricula maxidens*: A. Relationship of base of penis to mid-line of snout-neck (x) and to posterior end of eye lobes (a). B. Penis.

Habitat

Material for this study was collected on 7 October 1985 from Shenglong Village, Sanhuokou Town, Cili County, Changde Prefecture; 29°38′35″N, 110°39′12″E; Figure 1, site 7. The field collection number assigned was D85-82. Specimens came from a small stream flowing to the Lishui River. The collector was Dr. Liu Wen Jian of Cili County Public Health Station.

Depository

Specimens for this study were deposited in ZAMIP, M0005; ANSP, 368773, A12145.

Description

Shell. Shell measurements are given in Table 71; See Figures 137F–K, 146. Mature males and females are primarily 7.0 whorls; relatively few are 6.0 or 6.5 whorls (Table 71). Only one specimen of 7.5 whorls was ever seen (within the size range of 7.0 whorls snails of Table 71). Shells are medium sized with a length range of 3.76 to 4.36 mm for shells of 7.0 whorls (the dominant size class). Shells are ovate-turretted. The whorls are slightly convex; the sutures are deep. The peristome is complete; the inner lip is widely separated from the body whorl along its entire length (0.08 ± 0.02 mm, range 0.06–0.10;

TABLE 70. Cusp formulae for the radular teeth of *Tricula maxidens* with the percent of the seven radulae in which a given formula was found at least once.

Central Teeth		Lateral Teeth		Inner Marginal Teeth		Outer Marginal Teeth	
3-1-3 / 2-2	100%	3-1-4	75%	12	75%	12	25%
		4-1-4	75%	13	100%	13	75%
4-1-4 / 2-2	25%	2-1-3	25%	14	100%	14	100%
4-1-3 / 2-2	25%	5-1-4	25%	15	25%	15	25%
				16	25%	16	25%
3-1-4 / 2-2	25%						
2-1-3 / 2-2	25%			$\bar{X}$ * = 13.4±0.9 N = 40		13.9±0.9 N = 40	
3-1-3 / 2-3	25%						

* Mean ± standard deviation of cusp number for all teeth counted.

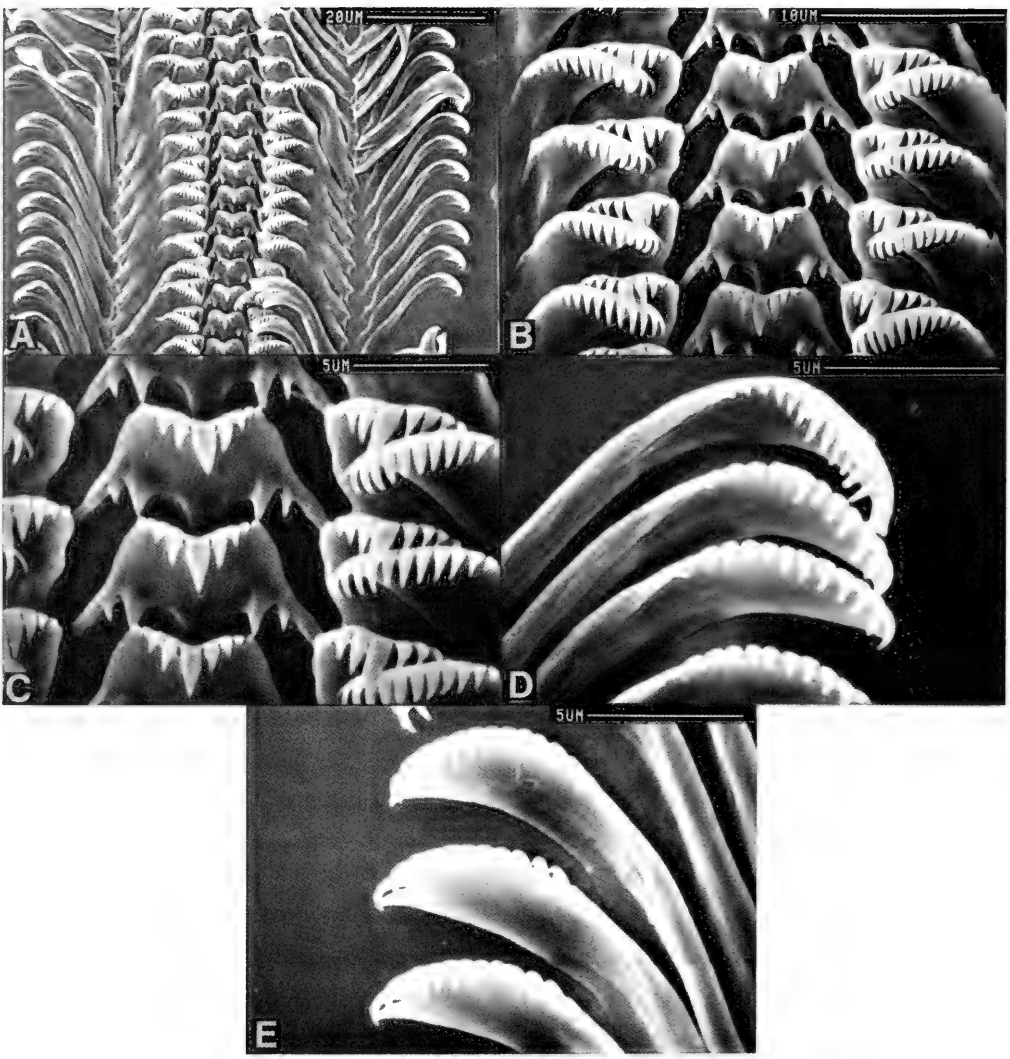

FIG. 144. Radula of *Tricula maxidens*. A. Part of radular ribbon. B, C. Central, lateral and inner marginal teeth. D, E. Outer marginal teeth.

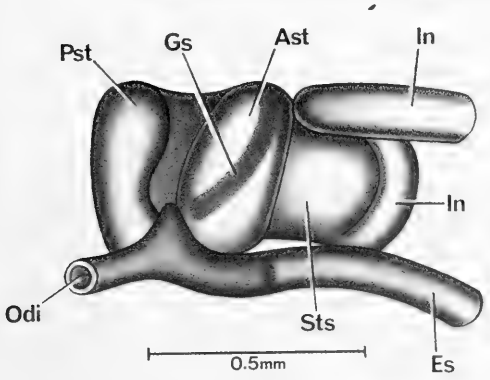

FIG. 145. Stomach of *Tricula maxidens*.

N = 5). The aperture is pyriform. The adapical end of the inner lip has a tooth-like swelling; this, plus the thickening of the outer lip opposite the swelling, enclose an adapical notch. Mid-columella there is a marked indentation. Although the inner lip is separated from the body whorl, there is no umbilicus in some individuals; there is one in some. Facing the aperture of the shell the adapical outer lip may be sinuate (16%); in side view, the outer lip is scooped forward (83%) or straight (17%). When the outer lip is scooped forward there is an adapical sinuation or notch. There is no basal post (see Davis et al., 1986). The cleaned shell is glistening, glassy.

The nuclear whorls (Fig. 146) have a rough, wrinkled surface. There are 1.5 nuclear whorls. The roughened surface may not be discerned at magnifications less than 200 or 300X. The aperture has six diagnostic features: (1) There is an adapical notch or beak bounded by (2) a thickening or node on the inner lip; (3) The inner lip has an angulation located some 60% of the length of the inner lip abapically from the adapical end of the aperture. The inner lip is thickened noticeably from the fulcrum of the angle to the apertural notch. (4) There is an indentation at the fulcrum of the angle. Abapical to the fulcrum of the angle the inner lip edge is thin. (5) In side view, the adapical end of the outer lip is slightly sinuate, the remaining lip is straight. (6) With the outer lip down, 90° to the horizontal, the inner lip has a slight sinuation that corresponds to a slight trough seen on the abapical end of the inner lip in apertural view.

External features. The head of this species is dark gray. No cluster of white granules or glands about the eyes were observed.

The operculum is corneous. The typical paucispiral growth line is not seen; the nucleus is prominent (Fig. 147E–G). The operculum has an odd irregular shape reflecting

TABLE 71. Shell measurements (mm) of mixed males and females of *Tricula odonta*. Mean ± standard deviation (range). N = number measured.

No. specimens (N)	N = 7	N = 2	N = 1
No. Whorls	7.0	6.5	6.0
Length (L)	4.09±0.22	3.40	3.00
	(3.76–4.36)	(3.32, 3.48)	—
Width (W)	1.52 ±0.10	1.40	1.28
	(1.48–1.60) N = 5	—	—
L body whorl	2.09±0.09	1.86	—
	(1.96–2.24)	(1.84, 1.88)	—
L penultimate	0.69±0.06	0.58	0.56
whorl	(1.16–1.26) N = 5	(1.02, 1.08)	—
W penultimate	1.20±0.05	1.06	0.98
whorl	(1.16–1.26) N = 5	(1.02, 1.08)	—
L last three whorls	3.25±0.17	2.78	2.48
	(3.04–3.48)	(1.71, 2.84)	—
L apertue	1.34±0.05	1.20	1.04
	(1.28–1.40) N = 5	—	—
W aperture	0.89±0.02	0.85	0.76
	(0.88–0.92) N = 5	(0.84, 0.86)	—
x	0.37±0.08		
	(0.28–0.48) N = 4		
y	0.19±0.07		
	(0.12–0.28) N = 4		

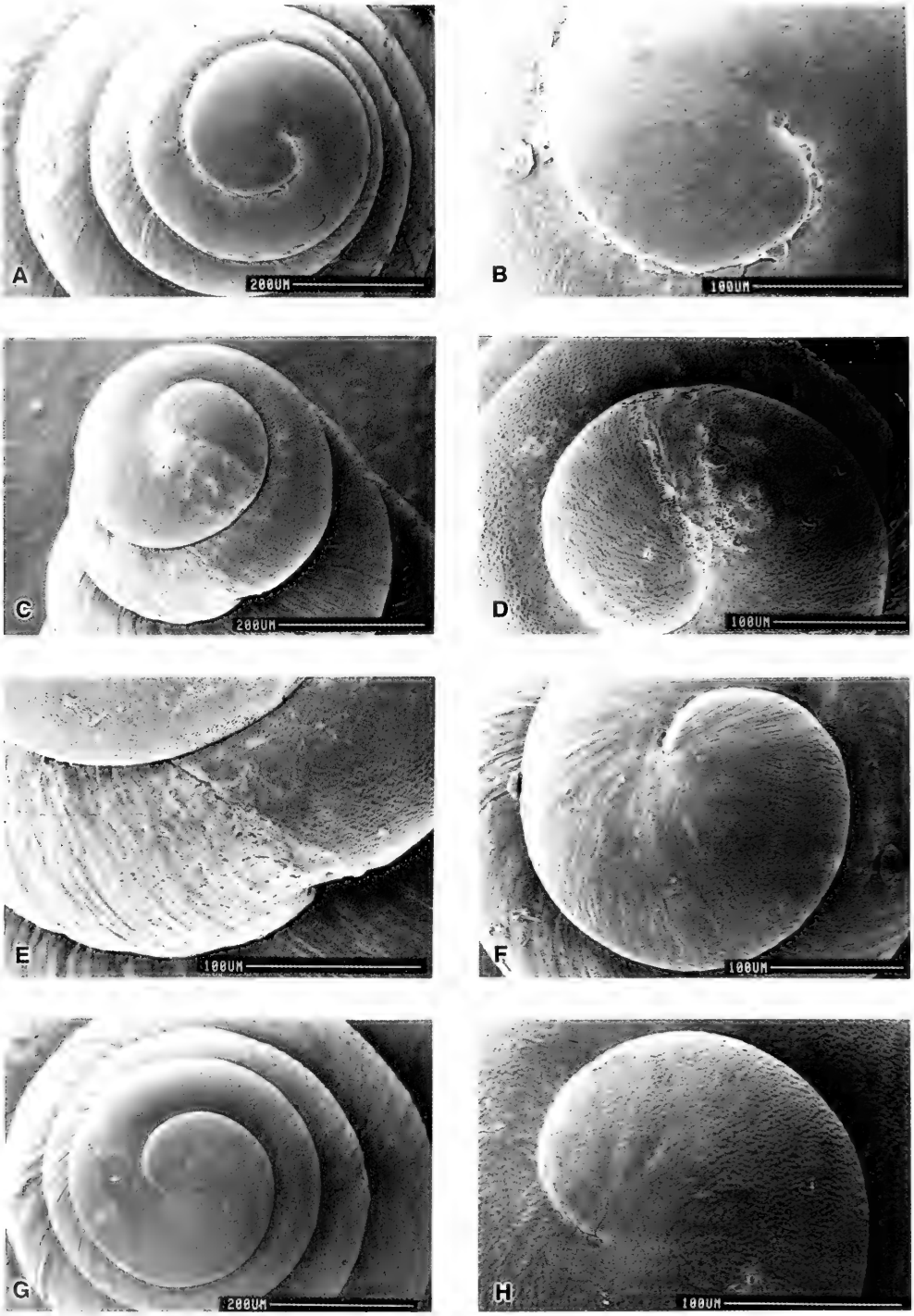

FIG. 146. SEM photos of shell apical whorls of *Tricula odonta*. Teleoconch begins at about 1.50 to 2.0 whorls (A, C, G). The protoconch is heavily wrinkled (B, D, F, H).

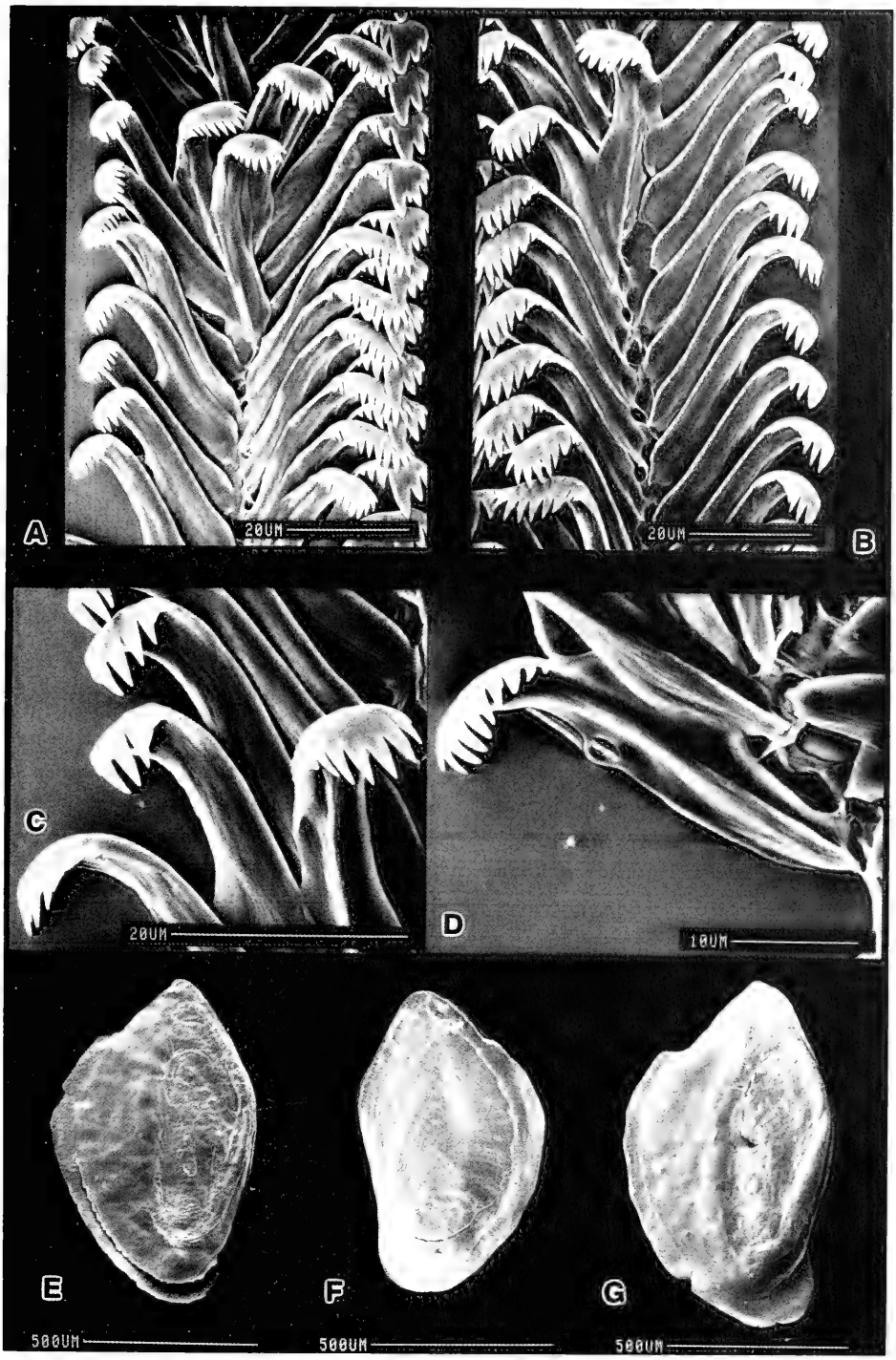

FIG. 147. Radula (A–D) and opercula (E–G) of *Tricula odonta*. A. Left lateral, inner and outer marginal teeth. B–D. Marginal teeth. E, G. Inner surfaces. Note irregular shape of opercula and thickened ridge along columellar edge of operculum in G. F. Outer surface. All three opercula show the double layers (see text).

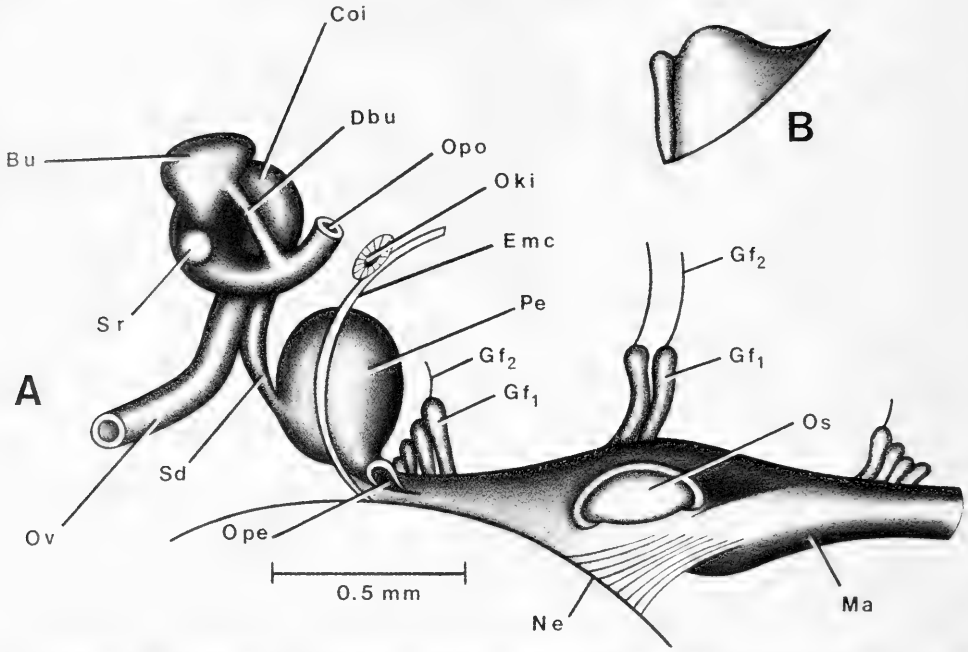

FIG. 148. Details and variation of bursa copulatrix complex of organs and mantle cavity structures of *Tricula odonta*. A in same orientation as in Figure 149. Not all gill filaments shown. B. Single gill filament.

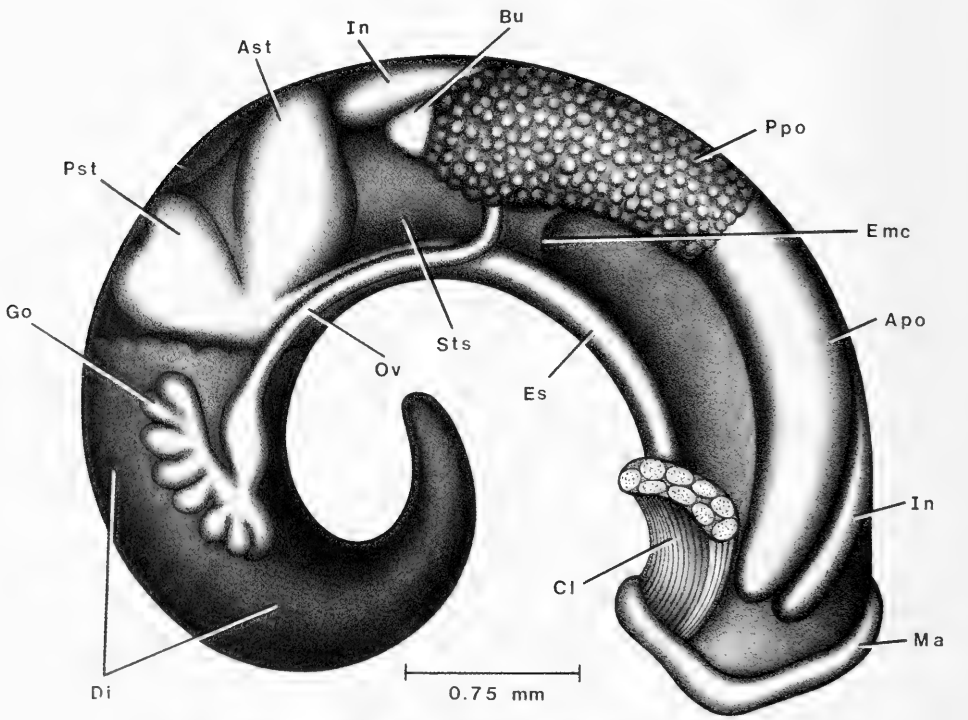

FIG. 149. Uncoiled female *Tricula odonta* with head and kidney tissue removed.

TABLE 72. Lengths (mm) or counts of non-neural organs and structures of *Tricula odonta*. Mean ± standard deviation (range). N = number measured.

	Females (N = 3)	Males (N = 2)
Body	5.83±0.36 (5.60–6.24)	4.74 (4.7, 4.78)
Gonad	0.74±0.15 (0.60–0.90)	1.55 (1.50, 1.60)
Digestive gland	2.45±0.19 (2.24–2.60)	2.04 (2.00, 2.08)
Mantle cavity	1.83±0.15 (1.80–2.00)	1.53 (1.50, 1.60)
Osphradium	0.34±0.05 (0.30–0.40)	0.33 (0.30, 0.36)
Ctenidium = Gill	1.63±0.15 (1.50–1.80)	1.38 (1.36, 1.40)
OS ÷ G	0.21±0.04 (0.17–0.25)	0.24 (0.22, 0.26)
Gill filament No.	29.7±1.5 (28–31)	25.5 (24, 27)
Buccal mass (males + females; N = 3)	0.57±0.06 (0.50–0.62)	—
Posterior pallial oviduct (= albumen gland)	0.92 (0.64, 1.20) N = 2	—
Anterior pallial oviduct (= capsule gland)	1.12 (1.0, 1.24) (N = 2)	—
Total pallial oviduct = OV	2.04 (1.64, 2.44) N = 2	—
Bursa copulatrix = BU	0.28±0.03 (0.24–0.30)	—
Duct of BU	0.21±0.04 (0.16–0.24)	—
BU ÷ OV	0.14	
Seminal receptacle	0.11±0.03 (0.08–0.14)	—
Gf_2	0.26±0.02* (0.24–0.28)	—
Gf_1	0.23±0.02* (0.20–0.24)	—
Total Gf = TGF	0.49±0.01* (0.48–0.50)	—
Gf_2 ÷ TGF	0.53±0.04* (0.50–0.58)	
Prostate	—	0.75 (0.70, 0.80)
Seminal vesicle	—	0.66 N = 1
Penis	—	1.62 (1.40, 1.84)

*males and females

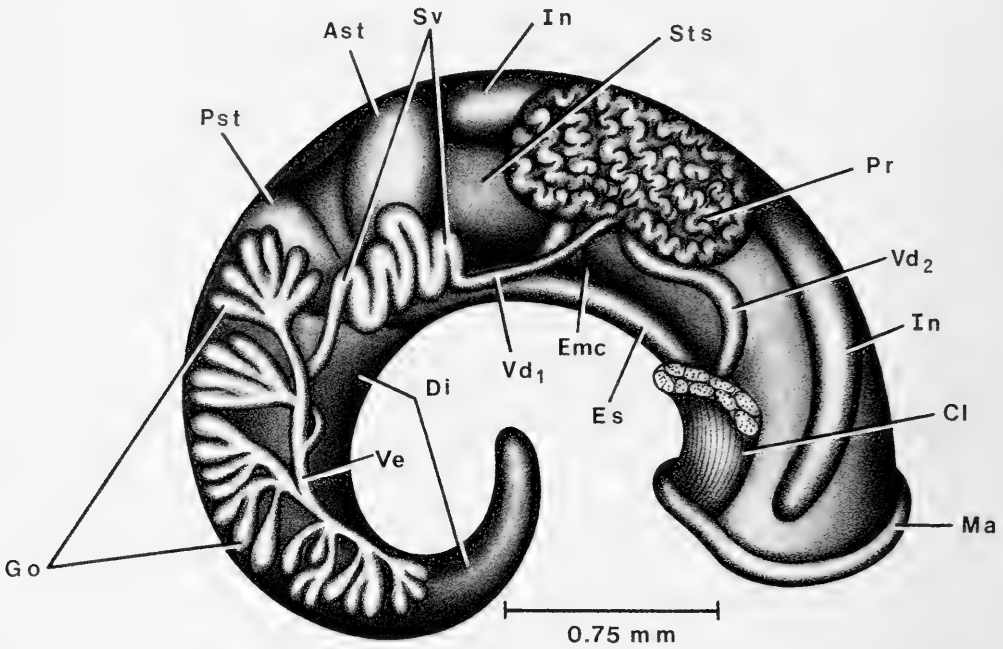

FIG. 150. Uncoiled male of *Tricula odonta* without head or kidney tissue.

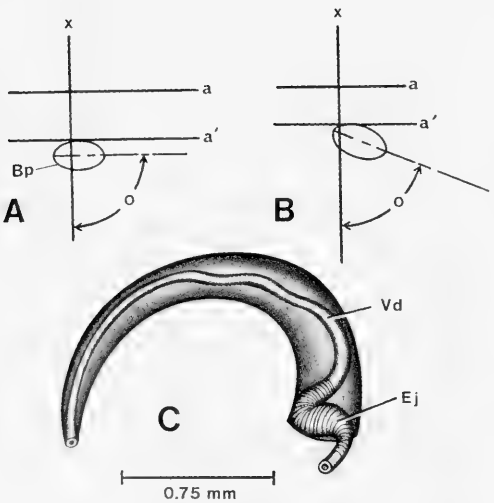

FIG. 151. A, B. Relationship of base of penis to mid-line of snout-neck (x) and to posterior end of eye lobes (a) of *Tricula odonta*; C. Penis.

TABLE 73. Radular statistics for males and females of *Tricula odonta*. Mean ± standard deviation (range). N = 5. In mm except for width of central tooth in μm.

Shell length:	No shell measurements; radulae came from heads of snails used in dissections.
Radular length	0.54±0.04 (0.52–0.62)
Radular width	0.08±0.004 (0.08–0.09)
Total rows of teeth	61.3±4.4 (56–69)
No. rows of teeth forming	7±1.7 (5–10)
Central tooth width	19.8±2.9 (18.1–23.6)

the pyriform shape of the aperture and the mid-inner lip indentation. It is particularly narrow at the abapical end, not broadly or regularly rounded as in those species with an oval operculum. The operculum consists of two layers that are readily separated if the oper-

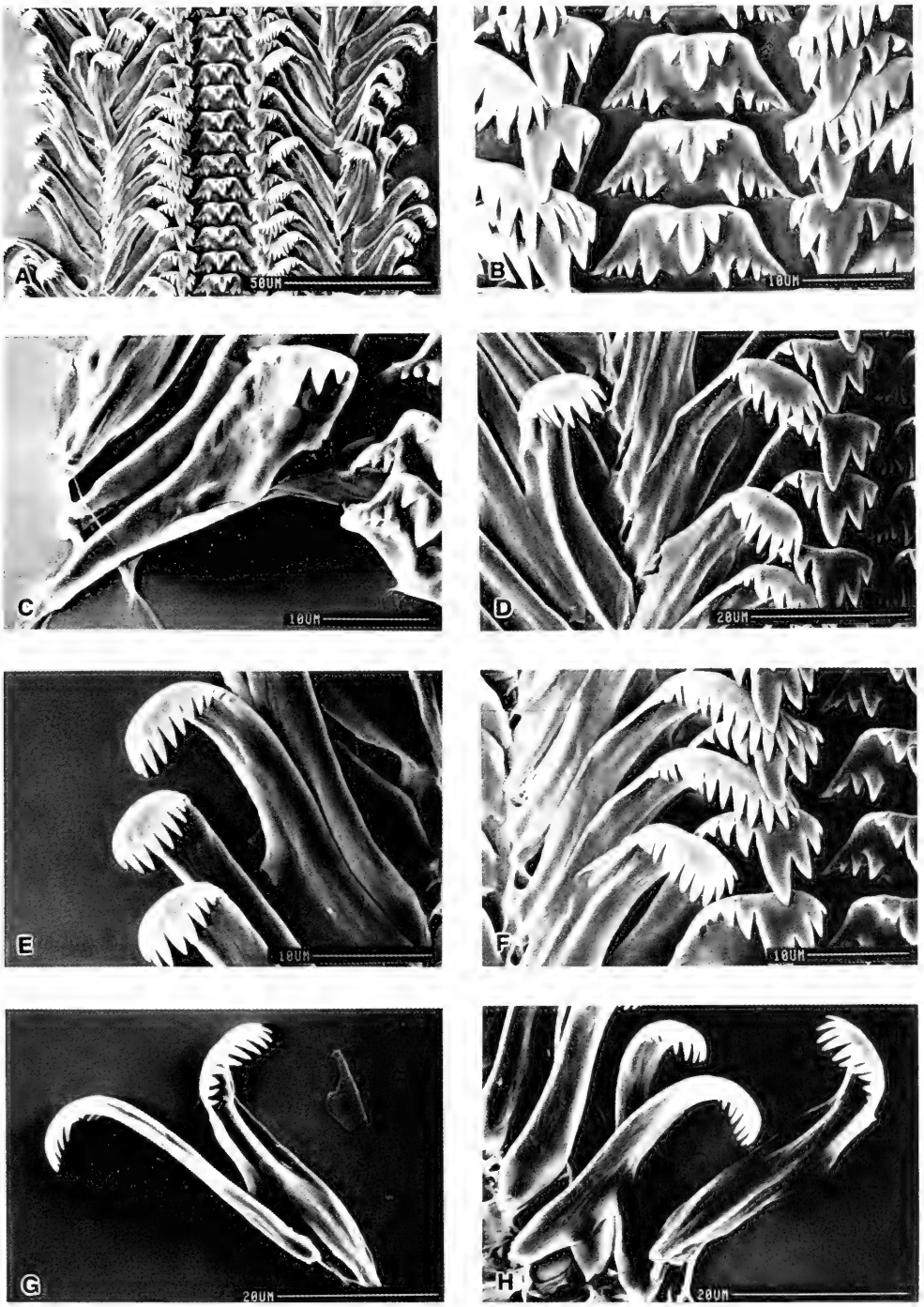

FIG. 152. Radula of *Tricula odonta*. A. Part of a radular ribbon. B. Central tooth. C. Left lateral tooth. D, F. Left lateral and marginal teeth. Note pronounced bifurcation of the major cusp of lateral tooth. E, G, H. Marginal teeth.

TABLE 74. Cusp formulae for the radular teeth of *Tricula odonta* with the percent of the radulae in which a given formula was found at least once. N = number of radulae used.

Central Teeth N = 6		Lateral Teeth N = 6		Inner Marginal Teeth (N = 3)		Outer Marginal Teeth (N = 4)	
3-1-3 / 3-3	50%	2-1[2]-3	83%	7	—	7	25%
		3-1-3	33%	8	—	8	50%
3-1-3 / 2-2	33%	2-1-2	17%	9	33%	9	25%
2-1-2 / 3-3	33%	1-1[2]-2	17%	10	66%	10	50%
2-1-2 / 4-4	17%			11	33%	11	25%
				12	66%	12	50%
3-1-3 / 4-4	17%			13	66%	13	25%
				14	33%	14	25%
						15	25%
				$\bar{X}$ * = 11.5±1.6 N = 30		9.2±1.7 N = 40	

*Mean ± standard deviation of cusp number for all teeth counted.

TABLE 75. Lengths of neural structures of four individuals of *Tricula odonta*. Mean ± standard deviation (range). * = neural elements measured to attain the RPG ratio.

Cerebral ganglion	0.24±0.03 (0.20−0.26)
Cerebral commissure	0.03±0.02 (0.02−0.06)
Pleural ganglion	
Right (1)*	0.12±0.02 (0.10−0.14)
Left	0.12±0.02 (0.10−0.14)
Pleuro-supraesophageal connective (2)*	0.20±0.07 (0.12−0.24)
Pleuro-subesophageal connective	0.05±0.04 (0.02−0.10)
Supraesophageal ganglion (3)*	0.12±0.01 0.10−0.12)
Subesophageal ganglion	0.09±0.03 (0.06−0.12)
Osphradio-mantle nerve	0.05±0.02 (0.02−0.06)
RPG ratio* = 2 ÷ 1+2+3	0.45±0.10 (0.32−0.55)

culum is left too long in dilute Clorox used for digesting and clearing away tissue fused to the operculum There is an inner thickened ridge on the columellar side. The attachment callus is 54.5 ± 3.5% of the width of the operculum; it is prominent and much thickened in some specimens.

Mantle cavity. Measurements and counts of mantle cavity structures are given in Table 72. See Figure 148A. The osphradium is short (mean ratio 0.22 ± 0.04; N = 5). The position of the osphradium is approximately mid-gill (Fig. 148A). The slender aspect of the gill filament (Gf_2) is long (mean ratio 0.53 ± 0.04; N = 3). The length of the longest gill filament is 0.49 ± 0.01 mm long (N = 3). The shape of the filaments is shown in Figure 148B. It is high domed.

Female reproductive system. The body of an uncoiled female with head and kidney tissue removed is illustrated (Fig. 149). Measurements of the relevant organs are given in Table 72. Diagnostic features are: (1) The gonad is posterior to the stomach. (2) The bursa copulatrix (Bu) is posterior to the pallial oviduct (Ppo) at mid-ventrolateral surface as shown. (3) The bursa copulatrix complex of organs is the same as seen in T. *bollingi* (Davis, 1968) in that the oviduct makes a tight loop (twist of 360°) dorsal to the bursa (Fig. 148A). (4) The seminal receptacle is spherical, posterior to the duct of the bursa (Dbu) and fused to the surface of the oviduct on the mid-ventral surface, not from the inner curvature as seen in other species. (5) The spermathecal duct enters the pericardium; the

pericardium is swollen with sperm. (6) Sperm enter the pericardium at the posterior end of the mantle cavity (Ope, Fig. 148A) (7) The bursa copulatrix is minute (mean ratio, 0.15 ± 0.04; N = 3). (8) The length of the posterior pallial oviduct is standard.

Male reproductive system. The body of an uncoiled male with head and kidney tissue removed is shown (Fig. 150). Lengths of relevant organs are given in Table 72. Important features are: (1) The gonad either overlaps the posterior chamber of the stomach or is posterior to the stomach. (2) The prostate overlaps the posterior end of the mantle cavity and covers the anterior half of the style sac. (3) The vas deferens arises from mid-vas efferens to slightly anterior to mid-gonad. (4) The seminal vesicle coils on the stomach; in some individuals, the posterior vas deferens was not swollen to form the seminal vesicle (presumable immature, just pre-sperm production individual). (5) The anterior vas deferens (Vd_2) leaves the prostate slightly anterior to mid-prostate. (6) The penis is simple, without papilla (Fig. 151C). The opening of the vas deferens is comparatively large and pronounced. (7) The base of the penis is 0.18 ± 0.03 mm posterior to the eye-lobes (Fig. 151A, B). Variation in the position of the base of the penis to the snout-neck mid-line (x) is shown in Figure 151 A, B. A part of the penial base is to the left of the mid-line. The long axis of the penial base varies from 65° to 90° to the snout-neck mid-line. (8) There is a large ejaculatory duct (Ej) in the base of the penis (Fig. 151C).

Digestive System. The digestive gland is posterior to the stomach. Radular statistics are given in Tables 73 and 74. Radular morphology is the generalized *Tricula* type (Figs. 147A–D, 152). There are 61 rows of teeth per radula length of 0.54 mm. The major cusp of the lateral teeth is massive and split thus giving the appearance of being two cusps. The most commonly encountered formula is

$$\frac{3(2)\text{-}1\text{-}(2)3;}{3(2)\text{-}(2)3}\quad 2(3)\text{-}[2]\text{-}3;\ 9\text{-}14;\ 7\text{-}14.$$

Nervous System. Lengths of neural structures are given in Table 75. The RPG ratio of 0.45 shows the dorsal nerve ring to be moderately concentrated.

Remarks

Conchologically, aside from *Neotricula aperta*, *T. odonta* has the most distinctive shell (Fig. 153) in that it attains 7.0 whorls (Tables 2, 76) (char. 29). It has a beak tubercle (char. 24) as do two other species: *Tricula gredleri* and *N. dianmenensis*. The adapical aperture is widely separated from the body whorl as is seen in *N. cristella* (char. 21). The inner lip is widely separated from the body whorl as it is in *N. cristella* (char. 20). A unique state, the inner lip is differentially thickened (char. 19). Another unique state, the inner lip has a notch (char. 17). Among species of *Tricula*, only this species of those thus far studied, has an abapical apertural spout (char. 12), an angled inner lip (char. 13), and an abapical lip deflection angle. (char. 18).

Anatomically, *Tricula odonta* stands apart from other species of *Tricula* (Tables 80, 81), but is most similar to *T. xianfengensis* (Figs. 156–158). *Tricula odonta* differs from the latter in 17 characters (37%). Most notable are the difference in operculum shape that reflects differences in shell apertural shape (char. 2), the differences in Gf_2 length (char. 8), female gonad length (char. 12) and seminal receptacle duct length (char. 23). *Tricula odonta* has a large ejaculatory duct; the latter does not have an ejaculatory duct (chars. 36, 37). The radula of the former is of medium length, of the latter, long (char. 41). The dorsal nerve ring is moderately concentrated in the former, elongated in the latter (char. 42).

MULTIVARIATE RELATIONSHIPS

Shells

The 29 shell characters scored are given in Table 2, the actual scores in Table 76. All species of *Tricula* and *Neotricula,* as well as other species having shells resembling those of *Tricula* or *Neotricula* and for which anatomical data are available, were included. The sources for data for species not treated in this paper are listed in Appendix I. The phenogram based on UPGMA treatment of distance coefficients is given in Figure 153. Distance coefficients were used because the cophenetic correlation (phenogram to orignal matrix) was r = 0.928 for distances; r = 0.725 using similarities.

It is clear that one cannot sort species to genus on the basis of shell characters. Additionally, of the 21 species, four (19%) could not be clearly distinguished on the basis of the shell characters used; *Tricula bollingi* phenotypes 1 and 3 clustered with *T. ludongbini*,

TABLE 76. Scoring of 44 OTUs for 29 shell characters listed in Table 2. Shells from the same population of some species varied for some characters. Such a species was divided into as many as three OTUs, e.g. xin-1, xin-2, xin-3. All species for which there were adequate anatomical data were used. Abbreviations are : ape, *N. aperta;* bur, *N. burchi;* cri, *N. cristella;* dia, *N. dianmenenensis;* dup, *N. duplicata;* lil, *N. lilii;* min, *N. minutoides;* bam, *T. bambooensis;* boll, *T. bollingi;* grd, *T. gredleri;* grg, *T. gregoriana;* hud, *T. hudiequanensis;* lud, *T. ludongbini;* max, *T. maxidens;* mon, *T. montana;* odn, *T. odonta;* xin, *T. xianfengensis;* xia, *T. xiaolongmensis;* chi, *G. chinensis;* jin, *J. jinghongensis;* niz, *W. niuzhuangensis.*

	Neotricula													*Tricula* (N = 11)								
	1	2	3	4	5	6	7	8	9	10	11	12	13	14	15	16	17	18	19	20	21	22
	ape	bur-1	bur-2	cri-1	cri-2	dia-1	dia-2	dup-1	dup-2	lil-1	lil-2	min-1	min-2	bam-1	bam-2	bol-1	bol-2	bol-3	grd-1	grd-2	grg-1	grg-2
1	1	0	0	0	0	0	0	0	0	0	0	0	0	0	0	0	0	0	0	0	1	1
2	4	1	1	0	0	0	0	0	0	0	0	0	0	0	1	0	0	0	0	0	0	0
3	1	0	0	0	0	2	2	1	1	1	1	1	1	0	0	0	1	0	1	1	1	1
4	0	0	1	0	0	2	2	1	1	2	2	2	2	2	2	0	1	2	1	1	1	2
5	0	1	1	0	0	0	0	0	0	0	0	0	0	0	0	0	0	0	0	0	0	0
6	0	1	1	1	1	1	1	1	1	1	1	0	1	0	0	0	0	0	0	0	0	0
7	0	0	0	0	0	0	0	0	0	0	0	0	0	0	0	0	0	0	0	0	0	0
8	2	0	0	1	1	0	0	1	1	0	0	1	1	1	2	3	3	3	1	1	0	0
9	2	0	0	1	1	2	2	2	2	1	1	0	0	0	0	0	0	0	2	2	0	1
10	1	0	0	0	0	0	0	1	0	0	0	0	0	0	0	0	0	0	0	0	0	0
11	0	0	0	0	0	1	1	0	0	1	1	0	0	0	0	0	0	0	1	1	0	0
12	0	1	0	0	0	1	1	1	1	1	1	0	0	0	0	0	0	0	0	0	0	0
13	1	1	1	1	1	3	3	0	1	2	2	1	1	1	1	1	1	1	0	0	1	1
14	0	1	1	1	1	1	1	0	0	0	0	0	0	0	0	0	1	0	0	0	1	1
15	2	1	1	0	0	0	1	1	1	1	1	1	1	2	2	0	1	0	0	1	0	0
16	0	0	0	0	0	0	0	0	0	0	0	0	0	0	0	0	0	0	0	0	0	0
17	0	0	0	0	0	0	0	0	0	0	0	0	0	0	0	0	0	0	0	0	0	0
18	0	0	0	1	0	1	1	1	1	1	1	0	0	0	0	0	0	0	0	0	0	0
19	0	0	0	0	0	0	0	1	1	0	0	1	1	1	1	0	0	0	1	1	0	0
20	0	0	0	3	3	1	0	2	2	2	1	2	2	2	2	0	1	0	2	2	0	0
21	0	0	0	2	2	0	1	1	1	0	1	0	0	1	1	0	1	0	1	1	0	0
22	0	0	0	0	0	0	0	0	0	0	0	0	0	0	0	0	0	0	0	0	0	0
23	0	0	0	1	1	0	0	0	0	1	1	0	0	0	1	0	0	0	0	0	0	0
24	0	0	0	0	0	1	1	0	0	0	0	0	0	0	0	0	0	0	1	1	0	0
25	0	0	0	0	0	0	0	0	0	1	1	0	0	0	0	0	0	0	0	0	0	0
26	1	0	0	0	0	0	0	0	0	0	0	0	0	0	0	0	0	0	0	0	0	0
27	1	0	0	0	0	0	0	0	0	0	0	0	0	0	0	0	0	0	0	0	0	0
28	0	0	0	0	0	0	0	0	0	0	0	0	0	0	0	0	0	0	0	0	0	0
29	0	0	0	0	0	0	0	0	0	0	0	0	0	0	0	0	0	0	0	0	0	0

whereas phenotype 2 clustered with *T. xiaolongmenensis* phenotype 1. *Tricula xiaolongmenensis* phenotype 2 did not have close affinity to any other species in the upper half of the phenogram. *Tricula montana* phenotype 3 clustered with *T. gregoriana*, not with phenotypes 1 and 2 of *Tricula montana*. *Tricula xianfengensis* phenotype 2 did not have close affinity with any other species in the upper half of the phenogram. While most shells can be classified readily on the basis of the characters used (exact measurements and whorl numbers would allow further discrimination), four of the 44 OTUs (only 9%) do not cleanly segregate with their other conspecific OTUs.

It is useful to compare the phenogram with a plot of the Prim Network (Minimum Spanning Tree [MST]) (Fig. 154) based on the distance coefficients (drawn to scale of actual pathway distances). The two are useful in assessing those species most closely resembling a species of immediate concern. For example, what species might be conchologically confused with *Tricula gredleri*? An examination of Figures 153 and 154 indicates that *N. duplicata* is the most closely allied phenetically. The several differences are then readily found in Tables 2 and 76. With MST, only two OTUs of different species do not link with other conspecific OTUs (i.e. *T. montana* phenotype 3; *T. bollingi* phenotype 2). Thus, only 5% of the OTUs do not segregate cleanly. Table 77 provides a ranking of species by a

TABLE 76. (Continued)

	Tricula (N = 11)				*Tricula*												*Gamma-tricula*		*Jinhongia*		*Wucon-chona*	
	23	24	25	26	27	28	28	30	31	32	33	34	35	36	37	38	39	40	41	42	43	44
	hud-1	hud-2	lud-1	lud-2	max-1	max-2	mon-1	mon-2	mon-3	odn-1	odn-2	xin-1	xin-2	xin-3	xio-1	xio-2	chi-1	chi-2	jin-1	jin-2	niz-1	niz-2
1	1	1	0	0	0	0	0	0	0	1	1	1	2	1	0	0	0	0	0	0	0	0
2	0	1	0	0	3	3	1	2	1	1	1	0	1	2	1	1	0	0	0	1	0	0
3	0	0	0	0	0	0	0	1	1	1	1	0	0	0	1	1	0	0	0	0	1	1
4	1	2	2	2	0	0	0	1	2	2	2	1	1	1	0	1	1	2	0	1	0	1
5	0	0	0	0	0	0	0	0	0	0	0	0	0	0	0	0	1	1	1	1	0	0
6	0	0	0	0	0	0	0	0	0	0	0	0	0	0	0	0	0	1	1	1	1	1
7	0	0	0	0	0	2	0	0	0	0	0	0	0	0	0	0	0	0	1	1	0	0
8	1	2	1	2	0	0	0	0	0	1	1	2	2	2	2	2	0	0	0	1	0	1
9	0	0	0	0	0	0	0	0	0	1	1	0	1	0	0	1	0	0	0	0	1	1
10	0	0	0	0	0	0	0	0	0	0	0	0	0	0	0	0	0	0	0	0	0	0
11	0	0	0	0	0	0	0	0	0	1	1	0	0	0	0	0	0	0	0	0	0	0
12	0	0	0	0	0	0	0	0	0	1	1	0	0	0	0	0	0	0	1	1	0	0
13	1	1	1	1	0	0	0	1	0	3	3	0	0	0	0	0	1	1	1	1	2	2
14	1	1	0	0	0	0	0	0	1	0	0	0	0	1	1	0	1	1	1	0	0	0
15	1	1	0	1	0	0	0	1	0	0	1	0	0	0	0	0	0	1	1	1	0	1
16	0	0	0	0	1	1	0	0	0	0	0	0	0	0	0	0	0	0	0	0	0	0
17	0	0	0	0	0	0	0	0	0	1	1	0	0	0	0	0	0	0	0	0	0	0
18	0	0	0	0	0	0	0	0	0	1	1	0	0	0	0	0	0	0	0	1	1	1
19	1	1	0	0	0	0	0	0	0	2	2	0	0	0	0	0	1	1	0	0	0	0
20	2	2	0	0	0	0	0	0	0	3	3	0	0	0	0	0	2	2	0	0	0	0
21	1	1	1	1	1	1	1	1	1	2	2	0	0	0	1	1	1	1	0	0	0	0
22	0	0	0	0	2	2	0	0	0	0	0	0	0	0	1	1	0	0	0	0	2	2
23	0	0	0	0	0	0	0	0	0	0	0	0	0	0	0	1	1	1	0	1	0	0
24	0	0	0	0	0	0	0	0	0	1	1	0	0	0	0	0	0	0	0	0	0	0
25	0	0	0	0	0	0	0	0	0	0	0	0	1	0	0	0	1	1	0	0	0	0
26	0	0	0	0	0	0	0	0	0	0	0	0	0	0	0	0	0	0	0	0	0	0
27	0	0	0	0	0	0	0	0	0	0	0	0	0	0	0	0	0	0	0	1	0	0
28	0	0	0	0	0	0	0	0	0	0	0	0	0	0	0	0	0	0	1	1	0	0
29	0	0	0	0	0	0	0	0	0	1	1	0	0	0	0	0	0	0	0	0	0	0

TABLE 77. Ranking species on a consistency index for shell characters. The index = 1.0−[number of character state differences between phenotypes in a population ÷ 29 characters]. Numbers in ( ) = number of phenotypes.

N. aperta (1)	1.0	*T. ludongbini* (2)	0.93
N. cristella (2)	0.97	*N. dianmenensis* (2)	0.90
N. minima (2)	0.97	*T. bambooensis* (2)	0.90
T. gredleri (2)	0.97	*T. hudiequanensis* (2)	0.90
T. maxidens (2)	0.97	*G. chinensis* (2)	0.90
T. odonta (2)	0.97	*W. niuzhuangensis* (2)	0.90
N. burchi (2)	0.93	*T. xiaolongmenensis* (2)	0.86
N. duplicata (2)	0.93	*T. xianfengensis* (3)	0.83
N. lilii (2)	0.93	*T. bollingi* (3)	0.79
T. gregoriana (2)	0.93	*T. montana* (3)	0.79
		J. jinhongensis (2)	0.76

consistency index based on the character-state differences between OTUs of the same species (1.0 = no differences). This table helps clarify the problems of why *T. montana* and *T. bollingi* do not cleanly link with conspecific OTUs (i.e. three classes of phenotype varying over six character-states).

Principal Component Analysis (PCA) was done. There are ten components that account for 84.6% of the vaiance (Table 78). The first three components account for only 45% of the variance. Factor loading of characters for the first ten PCs are given in Appendix II. Ordination diagrams are not provided because: (1)

TABLE 78. Principal component analysis of shell data: First ten principal components are listed with the percentage of variance loading on each component.

Components	Eigenvalue	Percent	Cumulative
1	6.16870	21.27	21.27
2	3.56713	12.30	33.57
3	3.27486	11.29	44.86
4	2.59528	8.45	53.81
5	2.45005	8.45	62.26
6	1.76301	6.08	68.34
7	1.38014	4.76	73.10
8	1.30153	4.49	77.59
9	1.10735	3.82	81.41
10	0.93280	3.22	84.62

most taxa cluster too close together at the center of the plots; (2) the MST results (Fig. 155) are much less satisfactory than those given in Figure 154; there are 14 mismatches of phenotypes (i.e. 32%). Three dimensional scaling produced even less acceptable results.

PCA analysis is useful in demonstrating the utility of shell characters used for discriminating among species. The first component (Table 79) is not one of size but involves ten apertural characters that are most useful in distinguishing among species. As examples: (1) only four species (*N. dianmenensis*, *N. lilii*, *T. gredleri*, *T. odonta*) have a pronounced adapical apertural sinus; (2) only three species have an adapical apertural beak tubercle (*T. dianmenensis*, *T. gredleri*, *T. odonta*); (3) only *T. odonta* has a mid-lip inner lip notch and a shell of 7.0 whorls.

The second component is defined on the basis of seven components that include sculpture, size, varix formation, and shell base characters. The third component involves three (shape, columellar and apertural groove) characters, while the fourth is defined by four characters, with teeth and internal keels as well as sculpture and outer lip orientation.

The *Neotricula duplicata* cluster of five taxa (*N. duplicata*, *N. lilii*, *N. odonta*, *N. dianmenensis*, *N. gredleri*), best seen in Figures 153 and 154, have four to seven of the following seven character states: an outer lip sinus, adapertural beak or notch, abapical spout, a beak tubercle, a thickened inner lip, the inner lip completely separated from the body whorl, and an angled or sinuate inner lip.

All species of *Neotricula* thus far examined, except the alpha race of *N. aperta*, have spiral microsculpture on the shoulders of the teleoconch whorls; not so for species of *Tricula*. *Neotricula aperta* is unique for its globoseconic shape, wide columellar shelf, and keel on the base of the body whorl bordering the wide columellar shelf. Only *T. maxidens* has a cylindrical-conic shell and a large columellar tooth clearly visible in the aperture. Only *J. jinghongensis* has spiral microsculpture at the base of the body whorl and a basal post. Only *T. xiaolongmenensis* has a domed tooth on the *columella* inside the body whorl. Only *W. niuzhuangensis* has a spiral keel on the columella inside the body whorl that does not extend basally so as to be seen as a tooth in the aperture (in contrast to *T. maxidens*). Only three species have crenulated whorls at the suture: *N. burchi*, *G. chinensis*, *J. jinghongensis*.

Anatomy

Thirty OTUs were scored for 48 character states (Tables 80, 81). A UPGMA phenogram based on distance coefficient is given (Fig. 156). Distances were used as the cophenetic correlation because r = 0.960 is superior to that using similarity coefficients (r = 0.865). In this phenetic treatment, species do not group neatly into well-defined generic clusters. However, by eliminating characters with missing data and using the Prim Network (MST) (Fig. 157), well-defined generic groupings resulted.

In the PCA analysis, ten components were extracted before eigenvalues dropped below 1.0; these components accounted for 89.8% of the variance (Table 82). Factor loadings of characters on each of the ten components are given in Appendix III. Ordination on the first two PC axes is given (Fig. 158) with OTUs connected by the MST based on the original distance matrix (with characters involving missing data removed) (Fig. 157). The spe-

TABLE 79. Shell characters highly correlated on each of nine principal components. * = also loads ≥ 0.440 on another axis.

Characters	Loading	COMPONENTS I. APERTURAL/WHORLS
11	−0.849	sinus—adaptical aperture
24	−0.733	beak tubercle—adaptical aperture
13	−0.715	inner lip shape
18	−0.696	lip deflection angle
17	−0.665	notch, inner lip
29	−0.665	shell has 7.0 whorls
12	−0.653	abapical spout
20	−0.636	inner lip separated from body whorl
19	−0.632	inner lip thickness
9	−0.606	adapical notch, beak
3	−0.582	apertural shape
		II. SIZE, SCULTPURE, VARIX, SHELL BASE
6	+0.812	spiral microsculpture
5	+0.653	whorl at suture crenulated
28	+0.596	basal post
12*	+0.497	abapical spout
1	−0.461	size
8	−0.461	protoconch sculpture
23	+0.458	varix
		III. SHAPE, KEEL, COLUMELLAR SHELF: *N. APERTA* AXIS
26	+0.810	keel at external base of shell
27	+0.751	columellar shelf
10	+0.728	inner adapical apertural groove
2	+0.645	shape
		IV. STRUCTURE ON COLUMBELLA INSIDE OR OUTSIDE SHELL; OUTER LIP
16	−0.715	inner lip tooth
7	−0.611	spiral sculpture at shell base
22	−0.585	internal columellar keel
15	+0.443	outer lip scooped forward
		V. APERTURE, WHORL CRENULATION
3*	+0.574	apertural shape
5*	−0.499	crenulated suture
19*	−0.459	inner lip thickened
9*	+0.450	adaptical apertural notch, beak
		VI. VARIX, LIP SEPARATION
23*	−0.553	varix
21	−0.496	adaptical aperture separated from body whorl
20*	−0.444	inner lip separated from body whorl
		VII. LIP ANGLE, SIZE
25	−0.696	lip angle
1*	−0.570	aize
		VIII. LIP SINUATION
14	+0.734	lip sinuation
		IX. PROTOCONCH SCULPTURE
8*	−0.494	protoconch sculpture

cies fall cleanly into generic clusters on the ordination diagram. Through use of Figures 157 and 158, it is clear which species pairs are most similar anatomically; e.g., *Tricula montana* is most similar to *T. gregoriana*.

The ordination diagram and an assessment of anatomical characters with high loadings on each of the ten principal components are useful for assessing OTU relationships. The first and second components clearly separate genera (Table 83). Characters 17, 18, 24, 21 clearly serve to separate generic clusters. Species with the 360° open oviduct circle complex of organs with the spermathecal duct entering the pericardium are to the left upper and lower quadrants. Species that have lost

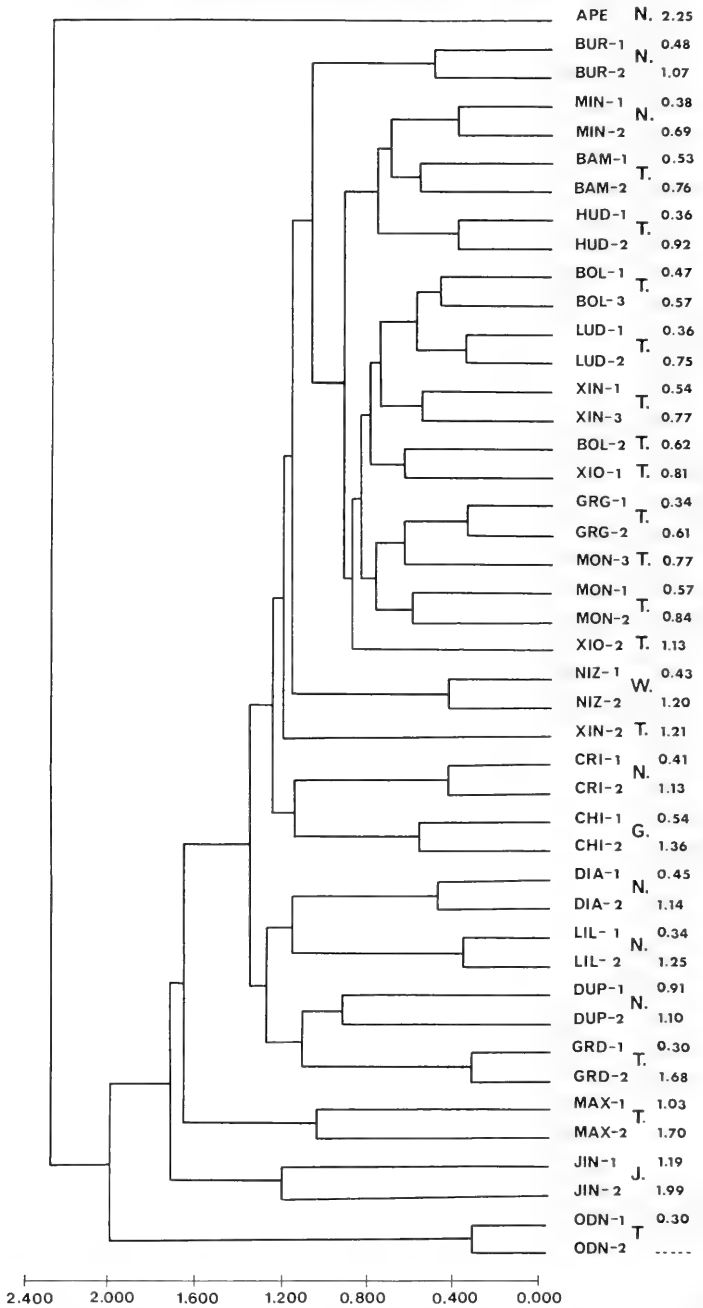

FIG. 153. Phenogram based on UPGMA treatment of distance coefficients involving shell characters from phenotypes (1–3) of 21 species (Tables 76, 77). G, *Gammatricula*; J, *Jinhongia*; N, *Neotricula*; T, *Tricula*; W, *Wuconchona*. APE, *N. aperta*; BUR, *N. burchi*; BAM, *T. bambooensis*; BOL, *T. bollingi*; CRI, *N. cristella*; CHI, *G. chinensis*; DIA, *N. dianmenensis*; DUP, *N. duplicata*; GRD, *T. gredleri*; GRG, *T. gregoriana*; HUD, *T. hudiequanensis*; JIN, *J. jinhongensis*; LIL, *N. lilii*; LUD, *T. ludongbini*; MAX, *T. maxidens*; MIN, *N. minutoides*; MON, *T. montana*; NIZ, *W. niuzhuangensis*; ODN, *T. odonta*; XIO, *T. xiaolongmenensis*; XIN, *T. xianfengensis*.

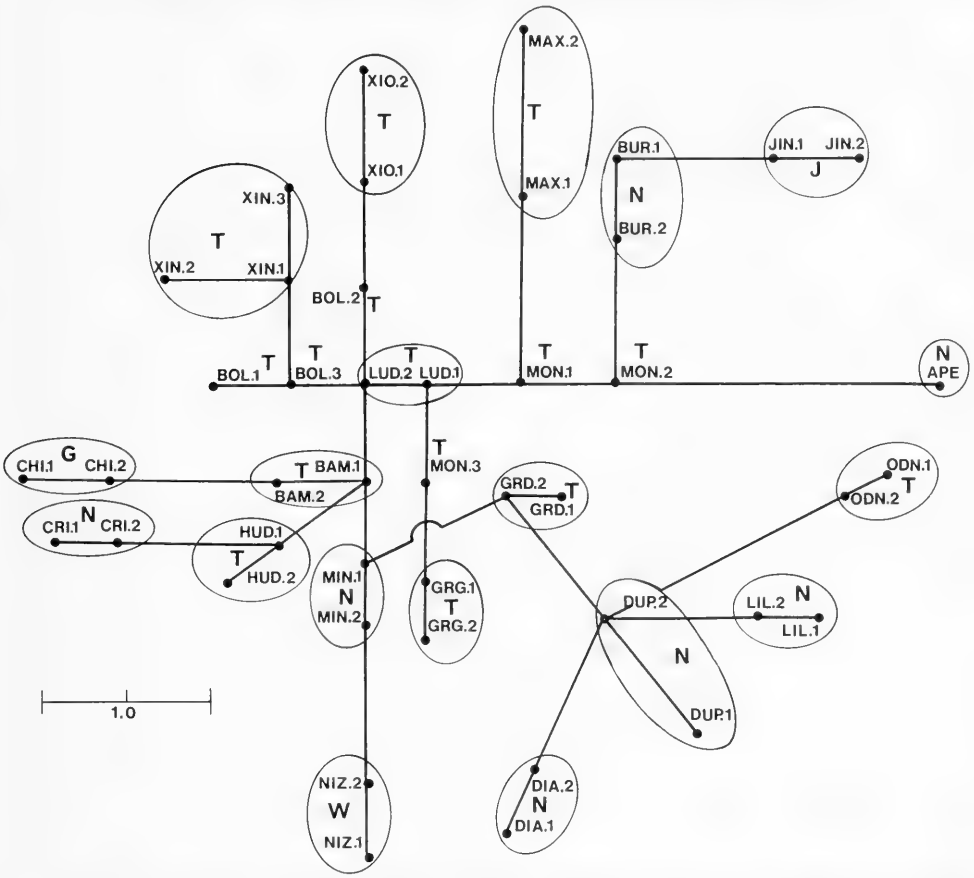

FIG. 154. Minimum spanning tree (MST) based on distance coefficients involving shell characters treated in Tables 2 and 76. The tree is drawn to scale using inter-taxon distances. See caption for Figure 153 for defining abbreviations.

the seminal recepatacle and have the spermathecal duct opening into the mantle cavity are in the upper right quadrant.

While major groupings along the 1st component are established by the four highly correlated characters given above, species placements are dictated by the 14 other characters with loadings ≤ 0.678. *Tricula gredleri* is far to the left because of character 37; it alone, of all the OTUs, has a massive ejaculatory duct. *Wuconchona niuzhuangensis* is far to the right because it shares with *Gammatricula chinensis* character states for characters 21 and 35; the function of the seminal receptacle is moved to the inside of the oviduct, and the concave edge of the penis has a white muscular zone. *Wuconchona* is displaced to the right of *Gammatricula* due to characters 17, 28, and 29. *Wuconchona* is unique in having a discrete U-shaped bend of the oviduct, a very short male gonad, and no vas efferens.

Distribution along the second principal component is due to the interaction of 12 characters. *Tricula gredleri*, *Neotricula dianmenensis*, and *N. minutoides* are at the bottom of the ordination diagram because of characters 2, 19, 20, 34, and 40. Unique to *T. gredleri* are operculum shape, fusion of the oviduct to the pericardium, the lemon color of

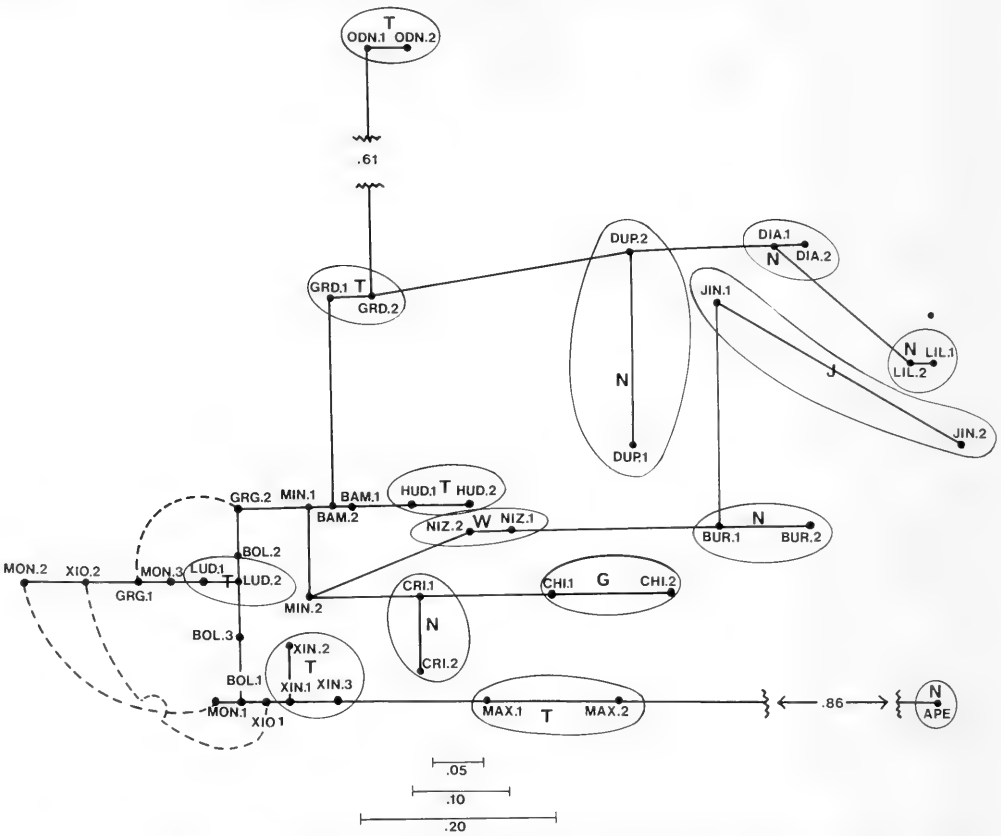

FIG. 155. MST based on shell distance coefficients following PCA analysis. Abbreviations are defined in caption for Figure 153. See text for details.

the anterior chamber of the stomach, and the position of the penial opening. *Neotricula dianmenensis* and *N. minutoides* have few rows of teeth per radula. *Tricula minutoids* has a highly extensible penis. *Jinhongia*, *Wuconchona* and *Gammatricula* are at the top because of the loss of the seminal receptacle (and duct).

Comparing Figures 156–158, it is seen which species are most similar anatomically and the affect of intrapopulation variation on distance measures. Linkages at a value $\leq$ 0.40 (distance coefficients) clearly involve population variation. Linkages $\geq$ 0.67 involve discrete species.

There are species clusters of phenetically closely related species. The biggest cluster, one that has the least distances among species, involves the *Tricula bollingi* complex: *T. bollingi*, *T. bambooensis*, *T. hudiequanensis* and *T. ludongbini*. These species occur in Yunnan, China. Within this complex, *T. hudiequanensis* is unique in that it has a scatter of a few white glands about the eyes (char. 1). The attachment pad of the operculum is very wide (char. 4). The shell is most similar to that of *T. bambooensis* (Figs. 153–155). However, there is a 12.5% difference between *T. hudiequanensis* and *T. bambooensis* (chars. 1, 4, 6, 8, 14, 37). Within the *T. bollingi* complex, *T. bollingi* is unique in that the female gonad is posterior to the stomach (char. 11), the radula is of medium length, not short (char. 41), and the radula has a moderate number of rows of teeth, not few (char. 42). The shell of *T. bollingi* is most similar to that of *T. ludongbini*.

A closely allied species pair involves *T. montana* from India and *T. gregoriana* from

TABLE 80. Anatomical characters and character-states (n = 48) showing one or more differences among 20 species belonging to the genera *Tricula* or *Neotricula,* or where the shells indicate affinity to these two genera.

	External Features (N = 5, 10%)
1. Glands about the eyes	no glands (0), scatter of a few glands (1), dense concentration of glands (2)
2. Operculum shape:	ovate (0), mid-columellar indentation (1), elongate-oval (2), irregular shape (3), cap-like (4)
3. Operculum:	single layer (0), two or more layers (1)
4. Operculum attachment pad:	wide (0), narrow (1), very wide (2)
5. Operculum; thick internal ridge:	none (0), has (1)
	Mantle Cavity (N = 5, 10%)
6. Gill filament number:	few (0), moderate (1), many (2)
7. Gill filament shape:	flat (0), moderate dome (1), high domed (2)
8. Gf_2 length:	long (0), medium (1), short (2)
9. Osphradium length:	long (0), short (1)
10. Circular grandular mass anterior to osphradium:	none (0), has (1)
	Female Reproductive System (N = 16, 33%)
11. Gonad:	behind stomach (0), overlaps stomach (1)
12. Gonad:	long (0), short (1), very short (2)
13. Bursa:	short (0), long (1), minute (2)
14. Bursa:	posterior to pallial oviduct [Ppo] (0), covered wholly or considerably by Ppo (1), ventral to Ppo (2), postero-lateral to Ppo (3)
15. Bursa:	round (0), triangular to subtriangular (1), ovoid (2)
16. Bursa; duct:	≥ 0.04 mm long (0), none (1)
17. Oviduct at bursa:	makes 360° tight twist (0), runs to Ppo without twist or bend (1), no twist but has discrete bend (2)
18. Spermathecal duct:	enters pricardium (0), enters mantle cavity (1)
19. Spermathecal duct:	long (0), short (1), none, fused to pericardium (2)
20. Spermathecal duct:	slants at an angle from duct of bursa or oviduct to mantle cavity, or at an angle from anterior-posterior axis (0), runs directly anterior from duct of bursa to mantle cavity (1), none, oviduct fused to pericardium (2)
21. Seminal receptacle:	arises from oviduct or duct of bursa (0), lost, function removed to inside swelling between duct of bursa and spermathecal duct (1), lost, function removed to inside oviduct (2)
22. Seminal receptacle duct:	U-shaped continuation of duct of bursa (0), arises from oviduct (1), from juncture of duct of bursa and oviduct (2), from duct or bursa (3), lost (4)
23. Seminal receptacle duct:	≥ 0.02 mm long (0), very short to ductless (1), seminal receptacle and duct lost (2)
24. Seminal receptacle arises from:	inside edg of oviduct in coil (0), outside edge of oviduct coil (1), from duct of bursa (2), seminal receptacle lost (3)
25. Pericardial bursa:	none (0), slight (1), large (2), extremely enlarged (3)
26. Albumen bland:	normal (0), short (1)
	Male Reproductive System (N = 11, 23%)
27. Gonad:	posterior to stomach (0), overlaps stomach (1)
28. Gonad:	long (0), short (1)
29. Vas efferens:	has (0), does not have (1)
30. Seminal vesicle:	coils posterior to stomach (0), coils also on stomach (1), coils only on stomach (2)
31. Vas deferens—2:	leaves prostate at Emc (0), leaves prostate at mid-prostate (1)
32. Penial tip:	no papilla (0), has papilla (1), long penial filament (2)
33. Penis:	normal (0), highly extensible (1)
34. Penial opening:	center of penial tip (0), from concave edge of blunt penial tip (1)

(*continued*)

TABLE 80. (Continued).

	External Features (N = 5, 10%)
35. Penis:	no white muscular zone on concave edge (0), has such zone (1)
36. Ejaculatory duct:	none (0), in base of penis (1), extends from penial base into the neck (2), only in neck (3)
37. Ejaculatory duct:	none (0), slight (1), large/prominent (2), massive (3)
	Digestive System (N = 9, 19%)
38. Digestive bland:	posterior to stomach (0), covers Pst (1)
39. Anterior chamber of stomach [Ast]:	no streak (0), with grey-melanin streak (1)
40. Ast lemon yellow color:	no (0), yes (1)
41. Radula:	short (0), medium length (1), long (2), very long (3)
42. Radula:	no. rows teeth: few (0), moderate no. (1), many (2)
43. Radula central tooth:	has paired swellings at posterior face of tooth between innermost basal cusps (1), lacks (0)
44. Radula central tooth:	central cusp: generalized type (0), long and dagger-like (1)
45. Lateral tooth major cusp:	1 (0), 1 [2] = (1)
46. Lateral tooth major cusp:	normal (0), displaced towards outer edge (1)
47. RPG ratio:	moderately concentrated (0), elongated (1), concentrated (2)
48. Length pleuro-subesophageal connective:	usual (0), none (1), long (2)

Yunnan, China. They are similar anatomically (Fig. 157) and conchologically (Figs. 153, 154). They differ in seven anatomical characters (15%).

PHYLOGENETIC RELATIONSHIPS

Phylogenies involving 19 genera of the three tribes of Triculinae were recently published (Davis et al. 1990; Davis & Kang, 1990; Davis, 1992). To these are now added the two additional genera (*Guoia*, *Lithoglyphopsis*), additions made possible because of this study. In this analysis, only one genus of the Jullieniini is used (outgroup), and the 13 genera grouped in the Triculini and Pachydrobiini. The characters and character-states used are listed in Table 84. There are 17 characters listed under synapomorphies, an additional 14 as autapomorphies. Scores are tabulated in Table 85. The result of the Hennig-86 analysis was 20 equally parsimonious trees with a length of 37, a consistency index of 86 and an ri (retention index; Farris, 1989) index of 91. Four of the trees and the Nelsen consensus tree are given (Figs. 159–163). All show the separation of the three tribes with the same genera assigned to each of the tribes. The only difference among the 20 trees for genera of the Triculini was the tricotomy of *Fenouilia*, *Lacunopsis*, *Lithoglyphopsis* or, alternatively, the divergence of *Fenouilia* from *Lacunopsis* and *Lithoglyphopsis*. The separation ((*Fenouilia*) (*Lacunopsis*, *Lithoglyphopsis*)) is warranted as *Fenouilia* has a trochoid shell, and the other two genera have globose shells.

The greatest shifting about involves genera of the Pachydrobiini. The consensus tree reduces the shifting to produce a polycotomy for *Neotricula*, *Halewisia*, *Pachydrobia*, and *Jinhongia*. In all trees, *Gammatricula* and *Wuconchona* diverge from the same node separated from the node that supports the subcluster of ((*Robertsiella*) (*Guoia*-a, *Guoia*-b)).

A single tree resolves with the ordering of character-states involving (1) the position of the seminal receptacle and its duct, (2) the loss of the seminal receptacle and the direction of evolution of the location of the structures functionally replacing the seminal receptacle, and (3) an analysis of homoplasies (Fig. 164). The generalized position of the seminal receptacle is a branch off the oviduct posterior to the duct of the bursa and anterior to a coiling of the oviduct between the gonopericardial duct and the bursa copulatrix (outgroups *Hydrobia*, Hydrobiidae; *Pomatiopsis*, Pomatiopsinae: Pomatiopsini). This position is seen in the genera of the tribe Triculini. In the Triculini and Pachydrobiini, the position of

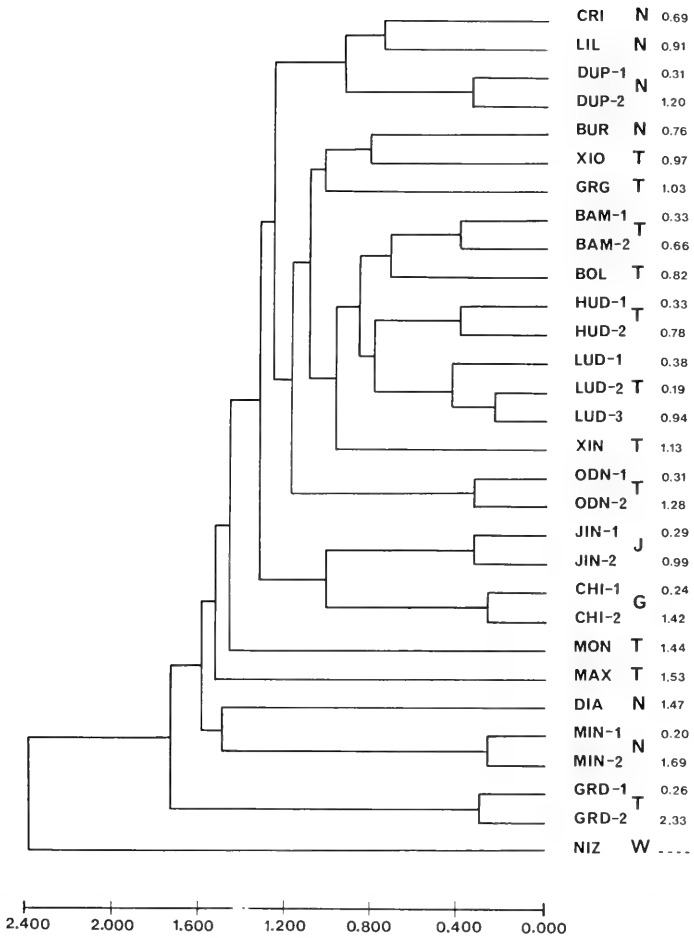

FIG. 156. Phenogram based an UPGMA treatment of distances based on all 48 anatomical characters from 1 to 2 phenotypes of 20 species. See Tables 80, 81. Abbreviations are defined in the caption for Figure 153.

TABLE 81. Scoring of 30 OTUs for 48 character-states listed in Table 80: bur-1, bur-2, etc. indicates that shells of *Neotricula burchi* exhibit more than one character-state for one or more characters. bur, *burchi*; cri, *cristella*; dia, *dianmenesis*; dup, *duplicata*; lil, *lilli*; min, *minutoides*; bam, *bambooensis*; bol, *bollingi*; grd, *gredleri*; grg, *gregoriana*; hud, *hudiequanensis*; lud, *ludongbini*; max, *maxidens*; mon, *montana*; odo, *odonta*; xian, *xianfengensis*; xio, *xiaolongmenensis*; chi, *chinensis*; jin, *jinhongensis*; niz, *niuzhuangensis*. NC = missing data.

	1	2	3	4	5	6	7	8	9	10	11	12	13	14	15
	N.cri	N.dia	N.dup1	N.dup2	N.lil	N.min1	N.min2	N.bur	T.mon	T.bam1	Tbam2	Tboll	Tgred1	Tgred2	Tgreg
1	0	NC	0	1	0	0	1	2	1	0	0	0	0	0	2
2	0	2	2	2	0	0	0	0	0	0	0	0	4	4	0
3	1	1	1	1	0	1	1	0	0	0	0	0	0	0	0
4	0	0	2	2	0	0	0	NC	0	0	0	0	0	0	0
5	0	0	0	0	0	0	0	0	0	0	2	0	0	0	0
6	0	1	1	1	1	1	1	1	1	2	2	1	1	1	2
7	1	NC	1	2	1	NC	NC	NC	1	2	1	2	1	1	NC
8	0	1	1	1	0	0	0	NC	0	1	1	1	0	0	0
9	1	0	1	1	1	1	1	1	1	1	0	1	1	1	1
10	0	0	0	0	0	0	0	0	1	0	1	0	0	0	0
11	0	0	0	0	0	0	0	0	0	0	1	0	0	0	0
12	1	1	1	1	1	1	1	1	1	1	2	0	1	1	1
13	0	0	0	0	0	0	0	0	0	2	2	2	2	2	0
14	0	0	0	0	0	0	0	3	0	2	2	2	2	2	0
15	0	0	2	2	0	0	0	2	2	2	0	2	0	1	2
16	0	1	0	0	0	0	0	0	0	0	0	0	0	0	0
17	1	1	1	1	1	1	1	1	0	0	0	0	0	0	0
18	1	1	1	1	1	1	1	1	0	0	0	0	0	0	0
19	0	0	1	1	0	1	1	0	0	0	0	0	2	2	0
20	0	1	1	1	0	1	1	0	0	0	0	0	2	2	0
21	0	0	0	0	0	0	0	0	0	0	1	0	0	0	0
22	0	0	0	0	0	0	0	0	3	1	0	1	1	1	3
23	0	0	0	0	0	1	1	0	0	0	0	0	0	0	0
24	2	2	2	2	2	2	2	2	2	0	0	0	0	0	2
25	0	0	0	0	0	0	0	0	2	0	0	0	3	3	2
26	0	0	0	0	0	1	1	0	0	0	0	0	0	0	0
27	0	0	1	1	1	0	0	0	1	1	1	1	1	1	1
28	0	0	0	0	0	0	0	0	0	0	0	0	0	0	0
29	0	0	0	0	0	0	0	0	0	0	0	0	0	0	0
30	0	0	0	0	0	0	0	0	1	1	1	1	1	1	1
31	0	0	0	0	1	0	0	1	1	1	1	1	0	0	1
32	2	1	1	1	1	0	1	0	1	0	0	1	1	1	1
33	0	0	0	0	0	1	0	0	0	0	0	0	0	0	0
34	0	0	0	0	0	0	0	0	0	0	0	0	1	1	0
35	0	0	0	0	0	0	0	0	0	0	0	0	0	0	0
36	0	0	0	0	0	0	0	1	2	1	1	1	2	2	3
37	0	0	0	0	0	0	1	1	2	1	1	1	3	3	2
38	1	0	0	0	0	1	1	0	0	0	0	1	0	0	0
39	0	0	0	0	0	1	0	0	0	0	0	0	0	0	0
40	0	0	0	0	0	0	1	0	0	0	0	0	1	1	0
41	1	1	1	1	1	1	0	1	2	2	2	1	1	1	1
42	3	0	2	2	3	0	0	1	2	2	2	1	1	2	2
43	0	0	0	0	0	0	0	0	1	0	0	0	0	0	0
44	0	0	0	0	0	0	1	0	0	0	0	0	0	0	0
45	1	1	1	1	1	1	0	0	1	0	0	0	1	1	0
46	0	0	0	0	0	0	0	0	0	0	0	0	0	0	0
47	0	0	0	0	0	0	0	NC	0	0	0	0	0	0	0
48	0	0	0	0	0	0	0	NC	NC	0	0	0	2	2	0

TABLE 81. (Continued)

	16 Thud1	17 Thud2	18 Tlud1	19 Tlud2	20 Tlud3	21 Tmax	22 Todol	23 Todo20	24 Txian	25 Txiao	26 Jjin1	27 Jjin2	28 Wniz	29 Gchi1	30 Gchi2
1	1	1	0	0	0	0	0	3	1	2	1	1	2	1	1
2	0	0	0	0	0	1	3	1	0	0	0	0	2	0	0
3	0	0	1	1	1	0	1	0	1	0	1	1	0	1	1
4	2	2	0	0	0	1	0	1	2	1	0	0	2	0	0
5	0	0	0	0	0	0	1	2	0	0	0	0	1	0	0
6	1	1	2	2	2	0	2	2	2	1	1	1	0	1	1
7	2	2	2	2	2	NC	2	0	NC	NC	NC	NC	NC	0	1
8	0	0	0	0	0	0	0	1	1	0	1	1	0	0	0
9	1	1	1	1	1	0	1	0	1	1	1	1	1	1	1
10	0	0	0	0	0	0	0	0	0	0	0	0	1	0	0
11	1	1	1	1	1	0	0	1	1	NC	0	0	0	0	0
12	1	1	0	0	0	1	1	2	0	1	0	1	2	0	0
13	2	2	2	2	2	0	2	0	2	0	0	0	1	1	1
14	0	0	0	0	0	1	0	1	0	0	2	2	0	0	0
15	2	2	1	1	1	0	1	0	2	2	2	2	2	2	2
16	0	0	0	0	0	0	0	0	0	0	0	0	0	0	0
17	0	0	0	0	0	0	0	0	0	0	1	1	2	1	1
18	0	0	0	0	0	0	0	0	0	0	1	1	1	1	1
19	0	0	0	0	0	0	0	0	0	0	0	0	1	0	0
20	0	0	0	0	0	0	0	0	0	0	0	0	0	0	0
21	0	0	0	0	0	0	0	1	0	0	1	1	2	2	2
22	1	2	1	3	2	1	1	1	1	1	4	4	4	4	4
23	0	0	0	0	0	0	1	0	0	0	2	2	2	2	2
24	0	0	0	2	2	0	0	0	0	1	3	3	3	3	3
25	0	0	0	0	0	1	0	0	0	0	0	0	0	0	0
26	0	0	0	0	0	0	0	0	1	0	0	0	1	0	0
27	1	1	1	1	1	1	0	1	1	NC	1	1	0	0	0
28	0	0	0	0	0	0	0	0	0	0	0	0	1	0	0
29	0	0	0	0	0	0	0	0	0	0	0	0	1	0	0
30	1	1	1	1	1	0	2	2	1	0	0	0	1	0	0
31	1	1	1	1	1	1	0	0	1	1	1	1	1	1	1
32	1	1	0	0	0	0	0	0	0	0	1	1	2	1	1
33	0	0	0	0	0	0	0	0	0	0	0	0	0	0	0
34	0	0	0	0	0	0	0	0	0	0	0	0	0	0	0
35	0	0	0	0	0	0	0	0	0	0	0	0	1	1	1
36	1	3	1	2	3	1	1	1	0	1	1	1	0	1	1
37	2	2	2	2	2	2	2	2	0	1	2	2	0	1	1
38	0	0	0	0	0	1	0	0	0	0	1	1	1	0	0
39	0	0	0	0	0	1	0	0	0	0	0	0	0	0	0
40	0	0	0	0	0	0	0	0	0	0	0	0	0	0	0
41	3	3	2	2	2	0	1	1	2	1	1	1	1	1	1
42	2	2	2	2	2	2	2	2	2	2	2	2	2	2	2
43	0	0	0	0	0	0	0	0	0	0	0	0	0	0	0
44	0	0	0	0	0	1	0	0	0	0	1	1	0	0	0
45	0	0	0	0	0	0	1	1	0	0	0	0	0	0	0
46	0	0	0	0	0	0	0	0	0	0	0	0	1	0	0
47	0	0	0	0	0	NC	0	0	1	1	0	0	2	0	0
48	0	0	0	0	0	NC	0	0	0	2	0	0	1	0	0

the opening into the duct of the seminal receptacle shifts as follows: along the oviduct to the base of the duct of the bursa (one species of Tricula); → to stem off the duct of the bursa (one species of *Tricula*, nearly all *Neotricula*, *Halewisia*); → to stem off the sperm duct (*Pachydrobia*). The presumption is that no large scale rearangements of ducts were made in a single step. To obtain the uncoiled oviduct seen in *Neotricula* (contrast Triculini), first the duct of the seminal receptacle, then the spermathecal duct would have had to migrate along the oviduct to move onto the duct of the bursa. With this accomplished, the

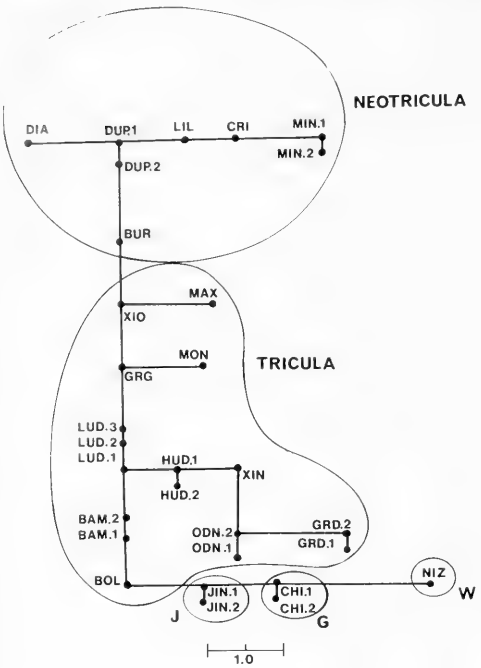

FIG. 157. MST based on distance coefficients involving all anatomical characters treated in Tables 80 and 81. The tree is drawn to scale using intertaxon distances. See caption for Figure 153 for defining abbreviations. Generic groupings have been circled.

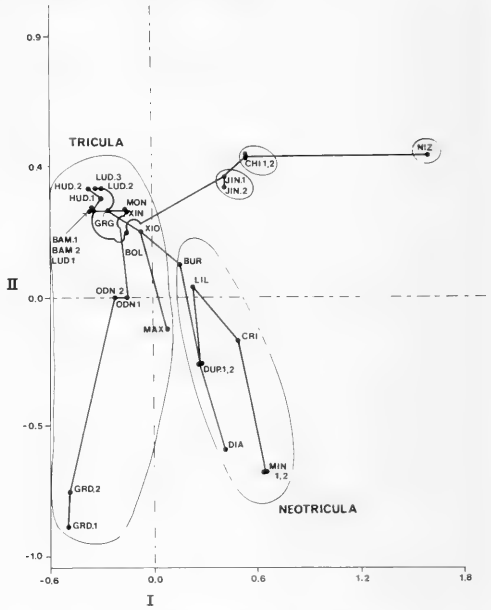

FIG. 158. Ordination diagram following PCA and MST seen in Figure 157. All characters scored in Table 81 as NC were removed in this analysis to permit the PCA treatment. The ordination is on the first two PCA axes. Generic groupings have been circled. See text for details. See caption for Figure 153 for defining abbreviations.

TABLE 82. Principal Component Analysis of anatomical data (matrix of 41 × 30). The first ten principal components are listed with the percentage of variance loading on each component.

Component	Eigenvalue	Percent	Cumulative
1	8.87575	21.65	21.65
2	6.86082	16.73	38.38
3	5.58656	13.63	52.01
4	3.54706	8.65	60.66
5	2.70292	6.59	67.25
6	2.60035	6.34	73.59
7	2.12427	5.18	78.77
8	1.83148	4.47	83.24
9	1.61804	3.95	87.19
10	1.05972	2.58	89.77

proximal section of the duct of the bursa (as seen in *Tricula*) would become the sperm duct, linking the new bursa complex to the oviduct to facilitate fertilization. In no case is a species of Pachydrobiini seen with the seminal receptacle arising from the oviduct! The most probable sequence is the move of the seminal receptacle from the oviduct to the duct of the bursa (situation seen in *Tricula* species b). Then the spermathecal duct mi-

TABLE 83. Characters with high loadings, that define each of ten components. **High loading on more than one axis (above).

Characters	Loadings	COMPONENT
		I. GENERIC ORGANIZERS*, N = 18
17*	+0.934	oviduct 360° circle
18*	+0.838	spermathecal duct enters pericardium
24*	+0.734	origin of seminal receptacle
27	−0.678	male gonad overlaps stomach
23	+0.658	seminal receptacle duct length
21*	+0.649	seminal receptacle lost
37	−0.644	ejaculatory duct prominence
36	−0.623	position of ejaculatory duct
6	−0.616	gill filament number
28	+0.610	male gonad length
29	+0.610	presence of vas efferens
46	+0.610	position of lateral tooth major cusp
35	+0.599	white muscular zone on penis
13	−0.580	bursa size
38	+0.579	digestive gland covers Pst
30	−0.546	poisition of seminal vesicle
41	−0.460	radula length
26	+0.519	albumen gland length
		II. SPERMATHECAL DUCT, RADULA, PENIS, STOMACH, N = 12
20	−0.871	orientation spermathecal duct
31	+0.847	where vas efferens leaves prostate
45	−0.784	major cusp of lateral tooth
19	−0.723	length spermathecal duct
15	+0.696	bursa shape
22	+0.665	configuration duct of seminal receptacle
2	−0.601	operculum shape
34	−0.575	position of penial opening
40	−0.575	color of Ast
42	+0.522	number of rows of teeth
39	−0.449	melanin streak on Ast
33	−0.471	penis highly extensible
		III. MALE REPRODUCTIVE, RADULA, OPERCULUM, STOMACH, N = 14
46**	+0.632	poisition major cusp lateral tooth
28**	+0.632	male gonad length
29**	+0.632	has/has not: vas efferens
2**	+0.596	operculum shape
40**	+0.589	Ast color
34**	+0.589	position penial opening
10	+0.573	gland mass anterior to osphradium
25	+0.570	pericardial bursa
19**	+0.514	length spermathecal duct
30**	+0.485	position serminal receptacle
5	+0.469	ridge on operculum
45**	+0.447	lateral tooth major cusp
3	−0.446	opercular layers
32	+0.446	penial tip
		IV. RADULA, OPERCULUM, REPRODUCTIVE, N = 5
44	−0.631	central cusp, central tooth
5**	+0.545	opercular ridge
30**	+0.529	position, seminal vesicle
14	−0.502	bursa position
26**	+0.470	albumen gland length
		V. OPERCULUM, FEMALE REPRODUCTIVE, MANTLE CAVITY, N = 4
3**	+0.646	opercular layers
12	−0.484	female gonad length

(*continued*)

TABLE 83. (Continued).

Characters	Loadings	COMPONENT
23**	+0.424	length duct seminal receptacle
10*	−0.421	gland mass anterior to osphradium
		VI. STOMACH, PENIS, FEMALE REPRODUCTIVE, N = 6
39**	+0.583	melanin streak on Ast
33**	+0.530	highly extensible penis
26**	+0.482	albumen bland length
38**	+0.475	digestive bland covers Pst
32**	−0.455	penis tip
16	−0.435	duct of bursa
		VII. CENTRAL TOOTH, OSPHRADIUM, OPERCULUM, N = 4
9	+0.617	osphradium length
43	+0.465	swelling on face of central tooth
5**	−0.443	opercular ridge
44*	−0.417	central cusp of central tooth
		VIII. CENTRAL TOOTH, N = 1
43**	−0.610	swellings on face of central tooth
		IX. BURSA, TEETH, N = 2
16**	−0.611	duct of bursa
42**	+0.523	rows of teeth: number
		X. BURSA, N = 1
14**	+0.538	position of bursa

grates along the oviduct to the duct of the bursa, with subsequent shift of the spermathecal duct from opening into the pericardium to opening into the posterior end of the mantle cavity next to the pericardium, and the uncoiling of the oviduct (as seen in *Neotricula* species of type a, and b). Subsequently, either the duct of the seminal receptacle migrates onto the sperm duct, or the point where the spermathecal duct joins the duct of the bursa moves distally towards the bursa leaving anterior to it that proximal piece of duct that once was the duct of the bursa, with the seminal receptacle attached to it (as seen in *Pachydrobia*). In this scenario, both *Halewisia* and *Pachydrobia* evolved from progenators resembling *Neotricula* species of type a (e.g. *N. aperta*, *N. cristella*). In *Halewisia* the spermathecal duct migrated to open into the bursa copulatrix. The shell is a derived type (Davis, 1979: 111). *Pachydrobia* has evolved a large first-order adaptive radiation (Davis, 1992) of greater than 14 species in which the shell has modified from the generalized *Tricula* type variously: larger, thick shells with thick lips; tendency to have pronounced macrosculpture (nodes, spines); tendency to shell assymetry.

There is parallel evolution in the Triculini and Pachydrobiini involving loss of the seminal receptacle and duct with new structures arising in different locations to accomodate the functions of the seminal receptacle. The solution to this loss is quite different in the two tribes, hence, no difficulty arises regarding correct tribal classification or assessment of intergeneric relationships. The tendency towards loss is minor in the Triculini, involving only one genus, *Lacunopsis*; it is major development in the Pachydrobiini involving the majority of genera (five of eight). In *Lacunopsis*, two or more accessary seminal receptacles arise to the exterior of the juncture of the oviduct and spermathecal duct. In the Pachydrobiini, solutions to the loss of the seminal receptacle are all within the relevant ducts (duct of the bursa, sperm duct, oviduct). The most parsimonious direction of evolution is as follows: the duct of the seminal receptacle is lost, the seminal receptacle becomes fused to the duct of the bursa close to or at the bursa (as in *N. dianmenensis*); → The seminal receptacle is replaced by an outpocketing within the encapsulated duct of the bursa (as in *Robertsiella*); → the sperm storage area shifts anteriorly to a swelling at the juncture of the duct of the bursa, spermathecal duct and sperm duct (as in *Jinhongia*); → the next shift is into the sperm duct (*Guoia*-a), and finally the oviduct (*Guoia*-b) → and farther posterior within the oviduct (*Wuconchona* and *Gammatricula*).

TABLE 84. Characters and character-states used for the cladistic analysis.

SYNAPOMORPHIES

1. Spermathecal duct opens to pericardium: (a) (0); (b) to posterior mantle cavity (1).
2. Oviduct makes: (a) a closed, tight 360° twist posterior to duct of the bursa (0); (b) an open 360° circle (1); (c) does not have the 360° twist or circle (2).
3. Sperm duct: (a) absent (0); (b) present and short (1); (c) present and elongated (2).
4. Spermathecal duct: (a) has primitive position between pericardium and oviduct as seen in *Pomatiopsis* (Pomatiopsinae) (0); (b) joins oviduct before oviduct twist (1); (c) joins oviduct 180° or more into oviduct circle (2); (d) joins duct of bursa, or common sperm duct (3); (e) joins bursa (4).
5. Seminal receptacle: (a) arises from primitive condition from oviduct posterior to the duct of the bursa (as in *Pomatiopsis*) (0); (b) from left side of the oviduct and pressed to the contour of the oviduct circle complex (1); (c) joins duct of bursa or common sperm duct (2); (d) joins the sperm duct (3); is lost; function replaced by: (e) an outpocketing of the encapsulated duct of the bursa (4); (f) an internal duct swelling at the juncture of bursa and spermathecal duct (5); (g) an outpocketing of sperm duct or swelling of sperm duct at juncture of sperm duct and oviduct (6); (h) within the oviduct (7); (i) two or more seminal receptacles arise from the oviduct (outside the duct) at the juncture of the oviduct with the spermathecal duct (8).
6. Duct of serminal receptacle(s): (a) short (0); (b) long (1); (c) lost due to fusion of the seminal receptacle to the duct of the bursa (2); (d) lost as the usual seminal receptacle is lost (3).
7. Gonad 1 or 2, or 3 finger-like tubes: (a) (0); (b) (1).
8. Vas deferens runs to style sac, turns posteriorly to form seminal vesicle: (a) (0); (b) (1).
9. Central tooth: (a) anterior cusps 5 or more (0); (b) only one large triangular blade (1)
10. Foot shape, power: (a) slender, weak (0); (b) wide, powerful (1)
11. Head shape: (a) standard (0); (b) wide, squat head; eyes in pronounced lobes (1)
12. Shell shape: (a) ovate-conic (0); (b) globose (1); (c) trochoid (2)
13. Shell size (a) small, thin (0); (b) increased length, thickness (1)
14. Penis with chitenous stylet: (a) (0); (b) (1).
15. Spermathecal duct with vaginal section: (a) (0); (b) (1).
16. Bursa copulatrix elongated relative to length of albumen gland: (a) (0); (b) (1).
17. Penis has a strongly developed muscular white zone at concave edge: (a) (0); (b) (1).

AUTAPOMORPHIES

Fenouilia

18. Gill filament section Gf_1 extremely elongated (1)

Lithoglyphopsis

19. Radular sac extremely elongated (1).
20. Posterior pallial oviduct bends 180° around (1).
21. Extremely long cerebral commissure (1).

Jinhongia

5f (above). Function of the seminal receptacle within an internal swelling at the juncture of the bursa and spermathecal duct (1).

Robertsiella

5e (above). Function of the seminal receptacle within a cavitation of the duct of the bursa (1).

22. Common sperm duct, duct of the bursa encapsulated (1).

Guoia

23. The penis has a glandular lobe (1).
24. The sperm duct is not only much elongated, it coils (1).

Wuconchona

25. The columella of the shell within the body whorl has a raised spiral ridge (1).
26. The spermathecal duct is short (1).
27. The male gonad is a wide sac, few lobes, floor of sac opens to a vas deferens, i.e. no vas efferens (1).
28. The dominant cusp of the lateral tooth is displaced towards the outside edge of the tooth (1).
29. The oviduct makes a U-shaped bend (1).

(*continued*)

TABLE 84. (Continued).

Gammatricula

30. The posterior half or third of the prostate is smooth (1).

Pachydrobia

31. The shell lip is especially thickened (1).
5d (above). The seminal receptacle arises from the sperm duct.

Halewisia

4e (above). The spermathecal duct joins the bursa copulatrix.

TABLE 85. Scoring 18 OTUs for synapomorphies listed in Table 84. Hub, *Hubendickia* (outgroup of Jullieniini); Tr-a, *Tricula* species a, Tr-b, species b; *Delavaya;* Fen, *Fenouilia; Lac, Lacunopsis;* Lit, *Lithoglyphopsis;* Ne-a, *Neotricula* species a, Ne-b, species b, Ne-c, species c; Hal, *Halewisia;* Pac, *Pachydrobia;* Gu-a, *Guoia* species a, Gu-b, species b; Rob, *Robertsiella;* Jin, *Jinhongia;* Wuc, *Wuconchona;* Gam, *Gammatricula.*

	1 Hub	2 Tr-a	3 Tr-b	4 Del	5 Fen	6 Lac	7 Lit	8 Ne-a	9 Ne-b	10 Ne-c	11 Hal	12 Pac	13 Gu-a	14 Gu-b	15 Rob	16 Jin	17 Wuc	18 Gam
1	0	0	0	0	0	0	0	1	1	1	1	1	1	1	1	1	1	1
2	1	0	0	0	0	0	0	2	2	2	2	2	2	2	2	2	2	2
3	0	0	0	0	0	0	0	1	1	1	2	1	2	2	1	1	0	1
4	2	1	1	1	1	1	1	3	3	3	4	3	3	3	3	3	0	3
5	1	0	2	0	0	8	0	2	2	2	2	3	6	7	4	5	7	7
6	1	0	0	0	0	0	0	0	1	2	1	1	3	3	3	3	3	3
7	1	0	0	0	0	0	0	0	0	0	0	0	0	0	0	0	0	0
8	1	0	0	0	0	0	0	0	0	0	0	0	0	0	0	0	0	0
9	0	0	0	1	1	1	1	0	0	0	0	0	0	0	0	0	0	0
10	0	0	0	0	1	1	1	0	0	0	0	0	0	0	0	0	0	0
11	0	0	0	0	1	1	1	0	0	0	0	0	0	0	0	0	0	0
12	0	0	0	0	2	1	1	0	0	0	0	0	0	0	0	0	0	0
13	0	0	0	1	1	1	1	0	0	0	0	1	0	0	0	0	0	0
14	0	0	0	0	0	0	0	0	0	0	0	0	1	1	1	0	0	0
15	0	0	0	0	0	0	0	0	0	0	0	0	1	1	1	0	0	0
16	0	0	0	0	0	0	0	1	0	0	1	0	0	0	0	0	1	1
17	0	0	0	0	0	0	0	0	0	0	0	0	0	0	0	0	1	1

There is clear-cut parallelism in the intraductal shifting of sperm storage. The *Robertsiella-Guoia* clade has highly derived character-states: the chitenous sheath on the penial papilla, the vaginal section of the spermathecal duct, the thick, straight and relatively short continuous duct running from the end of the mantle cavity into the bursa, and the loss of the seminal receptacle. The clade is relatively old within the 12 ± 4 million years in which the triculine macro adaptive radiation (Davis, 1992) has been evolving. The presence of *Robertsiella* in Malaysia and *Guoia* in Hunan, China, indicate both the age of the clade in and its origin in northern Burma or Yunnan, China. Three character-states involving the sperm storage location are found within this one clade: (1) within an outpocketing of the encapsulated duct of the bursa (*Robertsiella*), (2) within the sperm duct next to the oviduct (*Guoia*-a), (3) within the proximal oviduct (*Guoia*-b). The parallel situation is seen in the genera *Wuconchona* and *Gammatricula* that are found only (thus far) in southeastern China. In these genera, the simplified gonad, penial-characters (but lacking the chitenous penial stylet), and sperm storage in a more distal section of oviduct indicate a clade of derived taxa clearly divergent from the *Robertsiella-Guoia* clade.

Other parallelisms are simply partitioned and understood. In each second order radiation (Davis, 1980, 1992) there are trends for increasing size (seen in shell length), increasing complexity in sculpture (from smooth → ribs → reticulate sculpture, spiral cords, spines or nodes), and changes in shape (ovate-conic to turreted, globose, assymetry

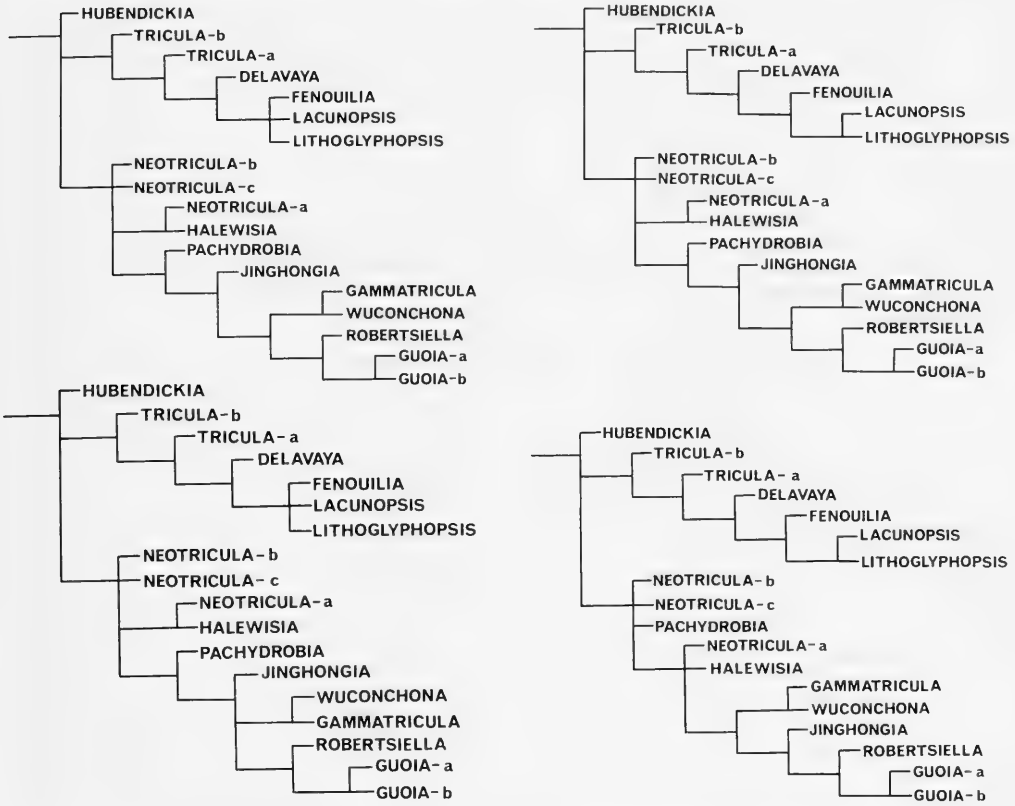

FIGS. 159–162 Four representatives of the 20 computer-generated cladograms following the Hennig-86 treatment of data given in Tables 85 and 86. See text for details.

(see Davis, 1979). The primitive small ovate-conic shell seen in *Tricula*, *Neotricula*, *Jinhongia* and *Gammatricula* is the basic platform from which splendid first order adaptive radiations arose, most with distinctive patterns of shell development (e.g. *Pachydrobia*, *Julliena*, *Hubendickia*, *Lacunopsis*. However, while one can discern the shells of *Lacunopsis* from those of *Hubendickia* or *Pachydrobia*, there is convergence in the globose shell types such that the shell character-states of *Guoia*, *Lithoglyphopsis* and *Lacunopsis* merge. Fortunately, there is extreme anatomical divergence between *Guoia*, *Lacunopsis* and *Lithoglyphopsis*; accordingly these genera are readily classified in one or the other of the relevant second order radiations.

The length of the duct of the seminal receptacle increases with increasing anatomical complexity in the Jullieniini and Triculini. The trend is particularly pronounced in the Jullieniini (Davis, 1979; 1991). There is a parallel increase in the length of the sperm duct involving some derived genera of the Triculini and Pachydrobiini; it is particularly evident in *Guoia*.

OLD PROBLEMS RESOLVED

Two unsolved questions of a decade ago can now be answered. (1) What is *Lithoglyphopsis* and its relationship to *Lithoglyphopsis aperta* Temcharoen, 1971? (2) Given the impact of the Himalayan orogeny as a driving force of the spectacular triculine radiation, too few species of *Tricula* or species morphologically close to *Tricula* had been found a decade ago (Davis, 1980). There were numerous species of *Pachydrobia*, *Lacunopsis*, *Hubendickia*, etc. known a decade ago, but only three species of *Tricula*, *sensu* Davis,

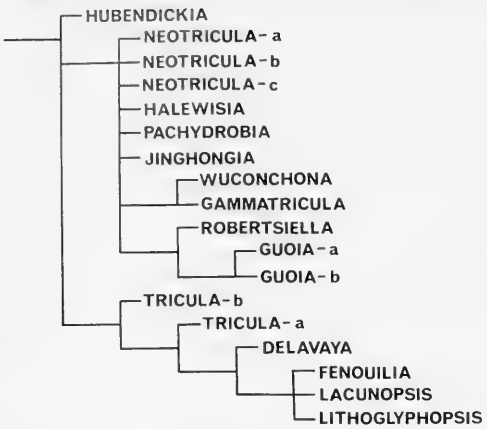

FIG. 163. The nelsen consensus tree resolving the 20 trees generated following the Hennig-88 treatment of data given in Tables 85 and 86.

1979, had been found in Southeast Asia. A few species from Burma had been described as *Tricula* on the basis of shells (reviewed in Davis, 1980). It was predicted that more would be found (Davis, 1980). How extensive was the *Tricula* radiation?

Concerning the first question, it is evident that *Lithoglyphopsis* is most closely related to *Fenouilia* and *Delavaya* anatomically and to *Lacunopsis* conchologically. *Lithoglyphopsis* is a derived genus in the tribe Triculini. *Lithoglyphopsis aperta*, the snail host for *Schistosoma mekongi*, is the type species for the genus *Neotricula* (Davis et al., 1986a). *Neotricula* is an anatomically generalized genus in the tribe Pachydrobiini. Thus, while *Lithoglyphopsis* and *Neotricula* are members of the same subfamily, they are highly divergent genera within the Triculinae.

The second issue is now resolved. With research initiated in Yunnan, China, in 1983 (Davis et al., 1986b) and with this and other ongoing research, it is clear that *Tricula, sensu* Davis, 1979, comprises an extremely large radiation primarily located in southern China. The concept of *Tricula sensu* Davis, 1979, has changed. The anatomical data support four genera with a *Tricula*-type shell: *Tricula*, *Neotricula*, *Gammatricula*, and *Jinhongia*. Anatomical data have been published for seven species of *Neotricula*, eleven species of *Tricula* and one each for *Jinhongia* and *Gammatricula*. These 20 species are one third of the estimated 60 species (conservative estimate) with *Tricula*-like shells that we think occur throughout southern China, Burma and northern Vietnam (Davis, 1992).

BIOGEOGRAPHY

Biogeography at a glance is provided in Figure 165. An area cladogram for river evolution is given with the number of species of each genus for which we have anatomical data listed for each region of river. Overall Triculinae biogeography has been reviewed recently (Davis, 1992). Only a few points need to be emphasized here. (1) Thus far, *Neotricula* has its greatest deployment in the mid to lower Yangtze River, whereas *Tricula* has more species in the upper Yangtze River. (2) The distribution of *Guoia*, *Robertsiella*, *Tricula* and *Neotricula* show that the major innovative anatomical developments in the Triculini and Pachydrobiini had occurred before the Yangtze-Mekong river drainages were completely separated.

(3) The tribes Triculini and the derivative Pachydrobiini dominate the Yangtze River drainage; no Jullieniini have been found, thus far, in the mid or lower Yangtze River drainages. Conversely, the Jullieniini dominate the Mekong River drainage with their greatest radiation in the lower Mekong River. (4) Only *Pacydrobia* of the Pachydrobiini and *Lacunopsis* of the Triculini have undergone explosive adaptive radiations (considering all genera of the Triculini and Pachydrobiini); this has occurred in the lower Mekong River. (5) The most derived anatomical character-states are found in the lower river systems.

(6) There are considerable ecological differences among tribes. With the exception of *Kunmingia* living in the shallow basin of a limestone spring, the other genera of the Jullieniini live in a large river environment. Considering the Triculini and Pachydrobiini, only *Lacunopsis*, *Lithoglyphopsis*, *Guoia*, *Halewisia* and *Pachydrobia* live in large rivers. *Fenouilia* lives on the bottom of a large lake, as did *Parapyrgula* (presumed extinct). *Tricula*, *Neotricula*, *Jinhongia* and *Gammatricula* live in upland shaded small streamlets of pure, cold water. Only *Neotricula aperta* has adjusted to living in a large river environment.

There are numerous species of *Neotricula* and *Tricula* in Hubei Province and provinces to the east, species that are in the process of being studied. We have seen at least one additional species of *Gammatricula*. The proven distribution of *Tricula* is from northern India to

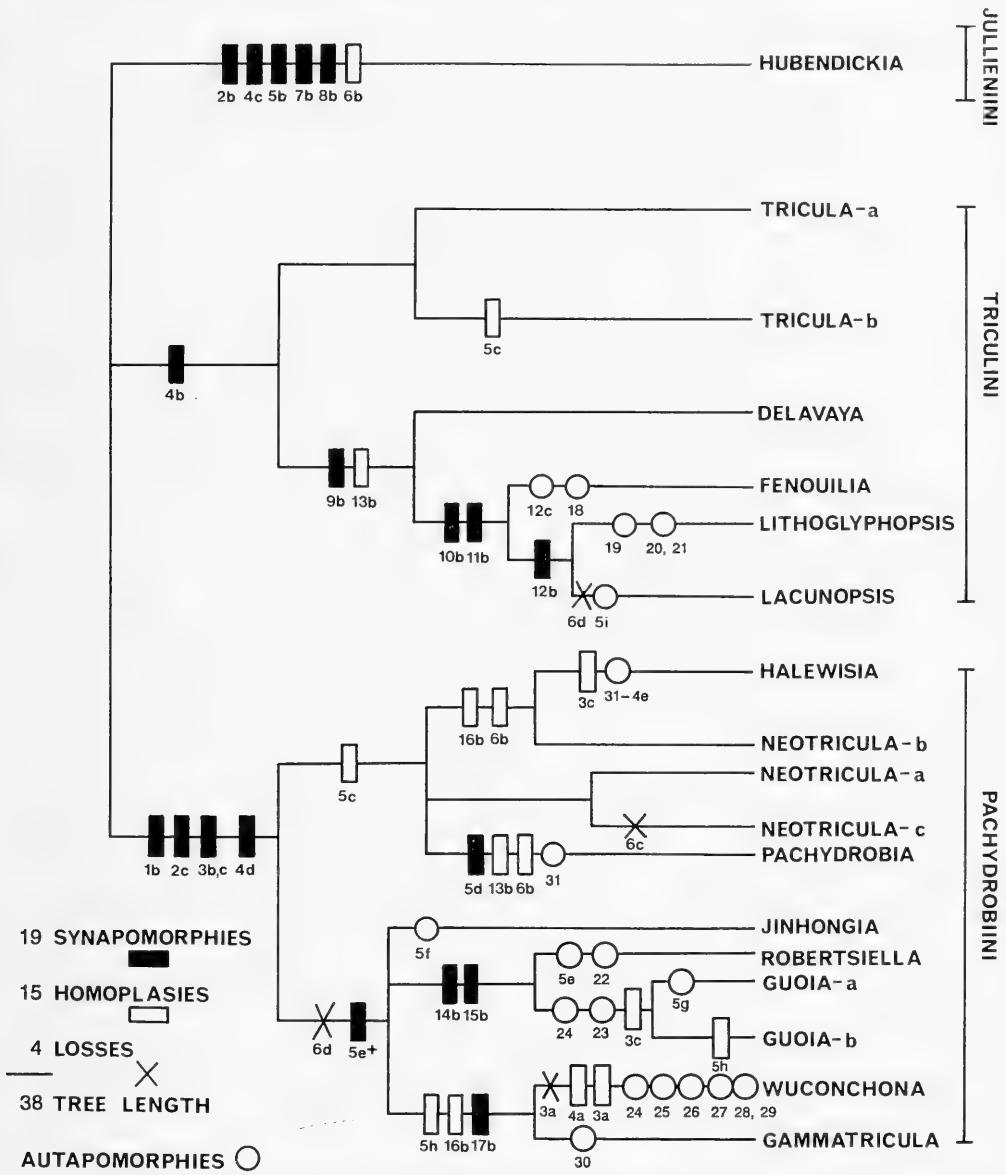

FIG. 164. The cladogram resulting from weighting one character in particular, the seminal receptacle, and the direction of evolution of character states with the primitive condition being 5a (= score 0) (see Table 85) (all Triculini except *Lacunopsis*); the shift of the duct of the seminal receptacle to the duct of the bursa (5c = score 2); the loss of the seminal receptacle, its function transferred into the duct of the bursa ($5e^+$ and 5e on the cladogram); the move within the duct system to the juncture of duct of the bursa, sperm duct and spermathecal duct (5f) → to the sperm duct (5g) → to the oviduct (5h). Parallelisms are accounted for; see text for details.

the East China Sea. As discussed in Davis (1992), there are numerous diverse Triculinae in Yunnan that have not yet been studied. It is highly probable that species of *Neotricula* will be found among them in the upper Yangtze River drainage. While this study has done

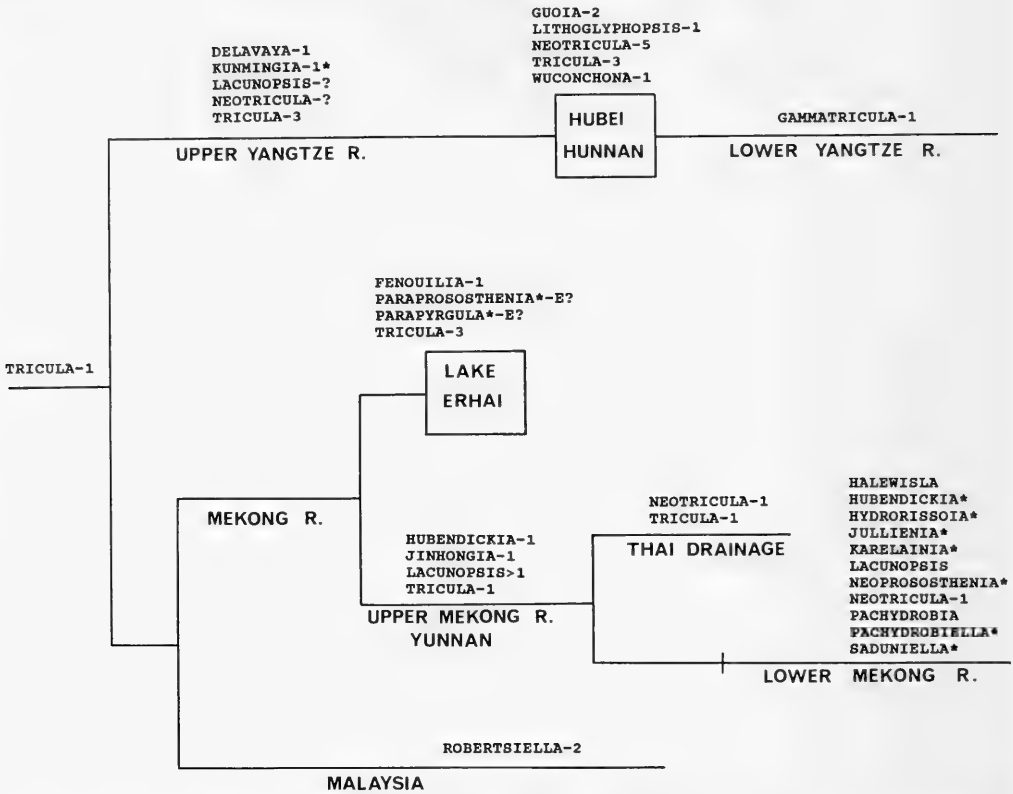

FIG. 165. An area cladogram for rivers showing the location of triculine genera. Those genera with the asterisk belong to the tribe Jullieniini. The question mark indicates the possibility that the genus might be found there. E? indicates probable extinction. With the exception of *Pachydrobia* and *Lacunopsis* in the lower Mekong River, each with more than ten species, the number of species of each genus of the Triculini and Pachydrobiini studied anatomically is given at each location along the drainage systems. *Tricula*-1 is *Tricula montana* of northern India. See text for further details.

much to reduce the probability that new genera of Triculinae will be found (we would expect one or two more, especially in Yunnan), there is considerably more to be learned concerning species of *Tricula* and *Neotricula* and their patterns of distribution.

ACKNOWLEDGEMENTS

Use of the facilities of Hunan Medical College and the Zhejiang Academy of Medical Sciences is gratefully acknowledged. The drawings were made by Davis with renderings by Elizabeth Carrossa and Susan Trammell. Scanning electron microscope work was done by Dr. Chen Cui-E and Caryl Hesterman. Photographs of the shells were taken and printed by Dr. Chen and Caryl Hesterman. Graphics were done by Susan Trammell. Dr. John Hendrickson is thanked for his help in executing the NTSYS programs. The work was supported by the National Natural Science Foundation of China award No. 3860607 to Dr. Chen, and N.I.H. award A1 11373 to Dr. Davis.

LITERATURE CITED

ANNANDALE, N., 1924, The molluscan hosts of the human blood fluke in China and Japan, and species liable to be confused with them. In E. C. FAUST, and H. E. MELENEY, Studies on schistosomiasis japonica. *American Journal of Hygiene Monographic Series*, No.3: 269–294, 1 pl.

BENSON, W. H., 1843, Description of *Camptoceras*, a new genus of the Lymnaeidae, allied to *Ancylus*, and of *Tricula*, a new type of form allied to *Melania*. *Calcutta Journal of Natural History*, 3(12): 465–468.

BRANDT, R. M., 1974, The non-marine aquatic Mollusca of Thailand. *Archiv für Molluskenkunde*, 105: 1–423.

CROSSE, H. & P. FISCHER, 1876, Mollusques fluviatiles, recueillis au Cambodge, par la Mission scientifique francaise de 1873. *Journal de Conchyliologie*, 24: 313–342, pls. 10–11.

DAVIS, G. M., 1967, The systematic relationship of *Pomatiopsis lapidaria* and *Oncomelania hupensis formosana* (Prosobranchia: Hydrobiidae). *Malacologia,* 6(1–2): 1–143.

DAVIS, G. M., 1968a, A systematic study of *Oncomelania hupensis chiui. Malacologia*, 7(1): 17–70.

DAVIS, G. M., 1968b, New *Tricula* from Thailand. *Archiv für Molluskenkunde*, 98: 291–317.

DAVIS, G. M., 1969a, Reproductive, neural and other anatomical aspects of *Oncomelania minima* (Prosobranchia: Hydrobiidae). *Venus, Japanese Journal of Malacology*, 28(1): 1–36.

DAVIS, G. M., 1969b, *Oncomelania* and the transmission of *Schistosoma japonicum*: a brief review. In HARINASUTA, C., ed., *Proceedings of the Fourth Asian seminar on parasitology and tropical medicine, schistosomiasis and other snail-transmitted helminthiasis*, 24–27 February, Manila. pp. 93–103.

DAVIS, G. M., 1979, The origin and evolution of the gastropod family Pomatiopsidae, with emphasis on the Mekong River Triculinae. *Monograph of the Academy of Natural Sciences of Philadelphia* No. 20: 1–120.

DAVIS, G. M., 1980, Snail hosts of Asian *Schistomosoma* infecting man: origin and coevolution. In J. I. BRUCE, et al., eds., *The Mekong schistosome, Malacological Review, Supplement* 2: 195–238.

DAVIS, G. M., 1981, Different modes of evolution and adaptive radiation in the Pomatiopsidae (Prosobranchia: Mesogastropoda). *Malacologia*, 21(1/2): 209–262.

DAVIS, G. M., 1992, Evolution of prosobranch snails transmitting Asian *Schistosoma*; coevolution with *Schistosoma*: a review. *Progress in Clinical Parasitology*, in press.

DAVIS, G. M. & P. CARNEY, 1973, Description of *Oncomelania hupenis lindoensis*, first intermediate host of *Schistosoma japonicum* in Sulawesi (Celebes). *Proceedings of the Academy of Natural Sciences of Philadelphia*, 124(1): 1–34.

DAVIS G. M. & G. GREER, 1980, A new genus and two new species of Triculinae (Gastropoda: Prosobranchia) and the transmission of a Malaysian mammalian *Schistosoma* sp. *Proceedings of the Academy of Natural Sciences of Philadelphia*, 132: 245–276.

DAVIS, G. M. & Z. B. KANG, 1990, The genus *Wuconchona* of China (Gastropoda: Pomatiopsidae: Triculinae): anatomy, systematics, cladistics, and transmission of *Schistosoma. Proceedings of the Academy of Natural Sciences of Philadelphia*, 142: 119–142.

DAVIS, G. M., C. E. CHEN, X. G. XING & C. WU, 1988, The Stenothyridae of China, No. 2: *Stenothyra hunanensis. Proceedings of the Academy of Natural Sciences of Philadelphia*, 140(2): 247–266.

DAVIS, G. M., V. KITIKOON & P. TEMCHAROEN, 1976, Monograph on "*Lithoglyphopsis*" *aperta*, the snail host of Mekong River schistosomiasis. *Malacologia*, 15(2): 241–287.

DAVIS, G. M., Y. H. KUO, K. E. HOAGLAND, P. L. CHEN, H. M. YANG, & D. J. CHEN, 1984, *Kunmingia*, a new genus of Triculinae from China: phenetic and cladistic relationships. *Proceedings of the Academiy of Natural Sciences of Philadelphia*, 136: 165–193.

DAVIS, G. M., Y. H. GUO, K. E. HOAGLAND, P. L. CHEN, L. C. ZHENG, H. M. YANG, D. J. CHEN & Y. F. ZHOU, 1986b, Anatomy and systematics of triculine (Prosobranchia: Pomatiopsidae: Triculinae) freshwater snails from Yunnan, China, with descriptions of new species. *Proceedings of the Academy of Natural Sciences of Philadelphia*, 138(2): 466–575.

DAVIS, G. M., Y. H. KUO, K. E. HOAGLAND, P. L. CHEN, H. M. YANG & D. J. CHEN, 1983, Advances in the Systematics of the Triculinae (Gastropoda: Prosobranchia): the genus *Fenouilia* of Yunnan, China. *Proceedings of the Academy of Natural Sciences of Philadelphia* 135: 177–199.

DAVIS, G. M., Y. H. KUO, K. E. HOAGLAND, P. L. CHEN, H. M. YANG & D. J. CHEN, 1985, *Erhaia*, a new genus and new species of Pomatiopsidae from China (Gastropoda: Rissoacea). *Proceedings of the Academy of Natural Sciences of Philadelphia*, 137: 48–78.

DAVIS, G. M., Y. Y. LIU & Y. G. CHEN, 1990, New Genus of Triculinae (Prosobranchia: Pomatiopsidae) from China: Phylogenetic Relationships. *Proceedings of the Academy of Natural Sciences of Philadelphia*, 142: 143–165.

DAVIS, G. M., N. V. S. RAO & K. E. HOAGLAND, 1986a, In search of *Tricula* (Gastropoda: Prosobranchia): *Tricula* defined, and a new genus described. *Proceedings of the Academy of Natural Sciences of Philadelphia*, 138(2): 426–442.

FARRIS, J. S., 1988, *Hennig 86, Version 1.5.* Stony Brook, N.Y. 18 pp.

FARRIS, J. S., 1989, The retention index and the rescaled consistency index. *Cladistics* 5: 412–419.

FENG, X. C., F. H. ZHOU & S. J. ZHANG, 1985, New discovery of first intermediate hosts of *Paragonimus skrjabini—Tricula gredleri* Kang sp. nov. and *Akiyoshia (Saganoa) odonta* Kang sp. nov. *Hunan Medicine*, 2(4): 65.

FENG, X. C., F. H. ZHOU & S. J. ZHANG, 1986, Discovery of new snails, first intermediate hosts, transmitting *Paragonimus* in Guzhang County. *Chinese Public Health*, 5(5): 38–39.

GREDLER, P. V., 1881, Zur Concylien-Fauna von China. III. Stück. *Jahrbücher der Deutschen Malakozoologischen Gesellschaft*, 8: 110–132.

GREDLER, P. V., 1885, Zur Concylien-Fauna von China. VIII. S.1–19. Selbstverlag, Bozen.

GREDLER, P. V., 1886, Zur Concylien-Fauna von China. IX. *Malakozoologische Blätter* (n.s.) 9: 1–20. Cassel.

GREDLER, P. V., 1887, Zur Conchylien-Fauna von China. XII. Stuck. *Nachrictsblatt der Deutschen Malakozoologische Gesellschaft*, No. 19 (11 u.12): 168–178.

GUO, Y. H. & J. R. GU, 1985, Studies on the intermediate host of *Schistosoma* and *Paragonimus*: 1. *Tricula jinhongensis*, a new species of *Tricula* from Yunnan Province. (Gastropoda: Hydrobiidae). *Acta Zootaxonomica Sinica*, 10(3): 250–252.

HERSHLER, R. & F. G. THOMPSON, 1988, Notes on morphology of *Amnicola limosa* (Say, 1817) (Gastropoda: Hydrobiidae) with comments on status of the subfamily Amnicolinae. *Malacological Review*, 21: 81–92.

IOGANZEN, B. G. & Y. A. STAROBOGATOV, 1982, A finding of a freshwater mollusk of the family Triculidae (Gastropoda: Prosobranchia) in Siberia. *Zoologichesky* Zhurnal, 61(8): 1141–1147.

KANG, Z. B., 1983a (Sept.), A new genus and three new speices of the family Hydrobiidae (Gastropoda: Prosobranchia) from Hubei Province, China. *Oceanologia et Limnologia Sinica*, 14(5): 499–505.

KANG, Z. B., 1983b (Nov.), Two new molluscan hosts for *Paragonimus skrjabini*. *Oceanologia et Limnologia Sinica*, 14(6): 536–541.

KANG, Z. B., 1985, Descriptions of a new species of *Bythinella* from China. *Acta Hydrobiologica Sinica*, 9(1): 84–88.

KANG, Z. B., 1986, Descriptions of eight new minute freshwater snails and a new and rare species of land snail from China (Prosobranchia: Pomatiopsidae, Hydrobiidae; Hydrocenidae). *Archiv für Molluskenkunde*, 117: 73–91.

KRUSKAL, J. B., 1964, Multidimensional scaling by optimizing goodness of fit to a nonmetric hypothesis. *Psychometrika*, 29: 1–27.

KURODA, T. & T. HABE, 1954, New aquatic gastropods from Japan. *Venus*, 18(2): 71–78.

KURODA, T. & T. HABE, 1957, Trolobiontic aquatic snails from Japan. *Venus,* 19: 183–196.

LIU, Y. Y., T. K. LOU, Y. X. WANG & W. Z. ZHANG, 1981, Subspecific differentiation of oncomelaniid snails. *Acta Zootaxonomica Sinica*, 6(3): 253–266

LIU, Y. Y., Y. X. WANG & W. Z. ZHANG, 1980, On new species and new records of freshwater snails of the family Hydrobiidae from Yunnan, China. *Acta Zootaxonomica Sinica*, 5(4): 358–368.

LIU, Y. Y. & W. Z. ZHANG, 1979, On new genus and species of freshwater snails harbouring cercariae of lung flukes from China. *Acta Zootaxonomica Sinica*, 4(2): 132–136.

LIU, Y. Y., W. Z. ZHANG & C. E. CHEN, 1982, *Pseudobythinella shimenensis*, sp. nov., a new aquatic *Paragonimus* cercariae carrying snail from Hunan Province. *Acta Zootaxonomica Sinica*, 7(3): 254–256.

LIU, Y. Y., W. Z. ZHANG, Y. X. WANG, C. E. CHEN & S. Z. CHEN, 1982, Discovery of *Akiyoshia* Kuroda et Habe (Hydrobiidae: Mollusca) from China with descriptions of two new species. *Acta Zootaxonomica Sinica*, 7(4): 364–367.

LIU, Y. Y., W. Z. ZHANG, & Y. X. WANG, 1983a, Studies on *Tricula* (Prosobranchia: Hydrobiidae) from China. *Acta Zootaxonomica Sinica*, 8(2): 135–139.

LIU, Y. Y., W. Z. ZHANG & Y. X. WANG, 1983b, Three new species of Hydrobiidae (Gastropoda: Prosobranchia) from China. *Acta Zootaxonomica Sinica*, 8(4): 366–369.

LOU, T. K., Y. Y. LIU, W. Z. ZHANG & Y. X. WANG, 1982, A discussion on the classification of *Oncomelania* (Mollusca). *Sinozoologica*, 2: 97–117.

MOELLENDORFF, O.F. VON, 1885, Diagnoses specierum novarum sinensium. *Nachrichtsblatt der deutschen Malakozoologischen Gesellschaft*, 11(u.12): 161–170.

MOELLENDORFF, O.F. VON, 1888, Materialien zur Fauna von China. *Malakozoologische Blätter* (n.f.) 10: 132–163, pl. 4.

ROHLF, F. J., J. KISHPAUGH & D. KIRK, 1972, *NT-SYS: Numerical taxonomy system of multivariate statistical programs.* Technical Report, State University of New York, Stony Brook, NY.

TEMCHAROEN, P., 1971, New aquatic mollusks from Laos. *Archiv. für Molluskenkunde*, 102: 91–109.

TRYON, G. W., 1862, Notes on American fresh water snails, with descriptions of two new species. *Proceedings of the Academy of Natural Sciences of Philadelphia*, 14: 451–452.

THIELE, J., 1928, Revision des systems der Hydrobiiden und Melaniiden. *Abteilung für Systematik, Ökologie und Geographie der Tiere*, 55: 351–402.

VOGE, M., D. BRUCKNER & J. I. BRUCE, 1978, *Schistosoma mekongi* sp. n. from man and animals, compared with four geographic strains of *Schistosoma japonicum*. *Journal of Parasitology*, 64(4): 577–584.

WENZ, W., 1939, Gastropoda, Part 3, Prosobranchia. Pp. 555–581 in O. H. SCHINDEWOLF, ed., *Handbuch der Paläozoologie,* Berlin (Borntraeger).

YEN, T. C., 1939, Die chinesischen Land-und Süsswasser—Gastropoden des Naturmuseums Senckenberg. *Abhandlungen der Senckenbergischen Naturforschenden Gesellschaft*, 444: 1–234.

ZILCH, A., 1974, Vinzenz Gredler und die Erforchung der Weichtiere Chinas durch Franzikaner aus Tirol. *Archiv für Molluskenkunde*, 104: 171–228.

Revised Ms. accepted 16 December 1991

APPENDIX 1. Sources of data for species of Triculinae used in the multivariate analyses (excluding species treated in this paper).

Neotricula aperta (Temcharoen, 1971): in Davis et al., 1976 [Type species of genus; designated in Davis et al., 1986a].
Neotricula burchi (Davis, 1968)
Tricula montana Benson, 1843: in Davis et al., 1986a [Type species of genus]
T. bambooensis Davis & Zheng, 1986: in Davis et al. 1986b
T. bollingi Davis, 1968
T. gregoriana Annandale, 1924: in Davis et al., 1986b
T. hudiequanensis Davis & Guo, 1986: in Davis et al., 1986b
T. ludongdini Davis & Guo, 1986: in Davis et al., 1986b
T. xianfengensis Davis & Guo, 1986: in Davis et al., 1986b
T. xiaolongmenensis Davis & Guo, 1986: in Davis et al., 1986b
Jinhongia jinhongensis (Guo & Gu, 1985): in Davis et al., 1986b [Type species of genus]
Gammatricula chinensis Davis, Liu & Chen, 1990: in Davis et al., 1990 [Type species of genus]
Wuconchona niuzhuangensis Kang, 1983: in Davis & Kang, 1990a [Type species of genus]

APPENDIX 2. Factor loading of characters for the ten principal components that collectively account for 85% of the variation in this study of shell characters.

	PRINCIPLE COMPONENTS				
	I.	II.	III.	IV.	V.
1.	−0.0410545	−0.4614740	0.1951133	0.1102495	−0.1964896
2.	0.3371738	−0.2702949	0.6452890	−0.2870722	−0.2273258
3.	−0.5820084	0.0153342	0.2508085	0.0428066	0.5737585
4.	−0.4883084	−0.0937884	−0.3041671	0.3050418	−0.0443432
5.	0.1598786	0.6532829	−0.1058710	−0.0463305	−0.4989291
6.	−0.2746159	0.8122425	0.0071554	−0.0500111	0.1822269
7.	0.2803561	0.2844659	0.2436223	−0.6108634	−0.2804339
8.	0.1706873	−0.4612060	0.0912007	0.4000807	−0.1060740
9.	−0.6064097	0.0550309	0.4268830	0.0825438	0.4504842
10.	−0.0511060	−0.0086817	0.7289513	0.3538858	0.0138379
11.	−0.8494929	0.0619407	0.1342359	−0.1052565	0.2478488
12.	−0.6526540	0.4972618	0.2145493	−0.2189934	−0.0605389
13.	−0.7146944	0.2136463	0.0176418	−0.0641302	0.0094302
14.	0.1056108	0.2477635	−0.3376958	0.0983843	−0.0247723
15.	−0.1938874	0.2239324	0.2971711	0.4426535	−0.3136139
16.	0.3325563	−0.1555008	0.1835824	−0.7154313	0.0046761
17.	−0.6648433	−0.3846053	0.0730909	−0.3156229	−0.4205736
18.	−0.6955758	0.3660246	0.1990413	−0.2286217	0.2015936
19.	−0.6319250	−0.3369728	−0.1161682	0.0574202	−0.4591451
20.	−0.6360441	−0.1127735	−0.2589680	0.1512705	−0.3323932
21.	−0.4095072	−0.3166545	−0.2127306	−0.1982544	−0.2723410
22.	0.3875425	−0.1664845	0.1605595	−0.5852705	0.3093103
23.	−0.0710536	0.4584002	−0.2259200	0.1122301	−0.2893657
24.	−0.7326382	−0.1977977	0.0873077	−0.2158382	0.1143209
25.	−0.0983867	0.3013054	−0.2336317	0.1312115	−0.1079600
26.	0.0980229	−0.0845837	0.8104326	0.3794045	−0.1045079
27.	0.1178917	0.2651106	0.7510733	0.1976523	−0.3326711
28.	0.1214556	0.5956626	0.1896647	−0.1906758	−0.4167448
29.	−0.6648433	−0.3846053	0.0730909	−0.3156229	−0.4205736
	VI.	VII.	VIII.	IX.	X.
1.	0.3384070	−0.5698774	0.0460096	−0.1038296	−0.2015172
2.	−0.1341500	−0.1682082	0.1296563	0.2262901	0.1179613
3.	0.1338242	0.0179137	0.0716831	0.1584757	0.0337647
4.	0.1847772	−0.0621649	−0.3912900	0.3915480	−0.0423710
5.	0.1626572	−0.0789925	0.2185103	0.1225756	−0.0940029
6.	−0.1021466	0.0043270	0.0444586	−0.0901887	0.2147945
7.	−0.0002180	0.1959912	−0.1031375	0.0608091	−0.2179681
8.	0.0615272	0.1587772	−0.2981737	−0.4940681	−0.0164338
9.	−0.2213138	−0.0213113	0.1639645	−0.1460116	−0.2374873
10.	−0.2431751	0.0326452	0.1561172	0.0089133	−0.0482282
11.	−0.1235609	0.0485087	−0.0126241	0.0552378	−0.3203997
12.	0.1602039	0.0045610	−0.0563521	−0.0245823	−0.0996069
13.	0.2771966	−0.1739794	−0.0983610	0.0695070	0.4416130
14.	0.2559430	−0.1571185	0.7337301	0.0273879	0.1133017
15.	−0.0909669	0.2889332	−0.2158527	0.4116663	0.2163310
16.	−0.3295022	0.0224967	−0.0264935	0.2984503	0.0080422
17.	0.1965575	−0.1292952	−0.0028319	−0.0987587	0.1400116
18.	−0.0673200	−0.1059933	−0.1987022	−0.2522537	0.2059356
19.	−0.1305618	0.1619921	−0.0220588	0.1714101	−0.1204920
20.	−0.4444652	0.1209360	0.1189897	−0.0587002	−0.0058012
21.	−0.4959528	0.1709711	0.2976215	−0.1487671	0.1337223
22.	−0.1349609	−0.2227013	−0.2268552	−0.0828126	0.1662128
23.	−0.5534215	−0.2637156	−0.0907283	−0.2368980	0.0500118
24.	0.1807102	0.1188745	0.2030360	0.0449544	−0.2547120
25.	−0.3337661	−0.6962163	−0.1929729	0.1613878	−0.2710739
26.	−0.0871736	−0.1570683	0.1745502	0.0772054	0.1175377
27.	0.0513585	−0.0302295	−0.0577648	−0.1412964	−0.0056331
28.	0.3292032	0.2276822	−0.1024080	−0.2274468	−0.2240125
29.	0.1965575	−0.1292952	−0.0028319	−0.0987587	0.1400116

APPENDIX 3. Factor loading of characters for the ten principal components that collectively account for 90% of the variation in this study of anatomical characters. Only 41 characters are used as no missing data were allowed in the PCA analysis.

	PRINCIPLE COMPONENTS				
	I.	II.	III.	IV.	V.
2.	−0.0971430	−0.6013535	0.5959546	0.0668697	0.2552416
3.	0.2857560	−0.0616901	−0.4464561	0.1288039	0.6460538
5.	0.2334109	0.0746406	0.4689891	0.5445427	0.1455881
6.	−0.6159816	0.2368112	−0.1616069	0.3824686	0.3790016
9.	−0.1030642	0.2758602	0.2265553	0.1676757	0.3476608
10.	0.3783801	0.2220442	0.5730512	0.1711390	−0.4213342
12.	0.2808698	−0.3578114	0.3977414	0.2035502	−0.4838175
13.	−0.5800852	0.2057583	0.3564111	0.3719478	0.3222399
14.	−0.2141655	−0.0802545	0.1442952	−0.5024069	−0.1107264
15.	−0.0625617	0.6955844	0.1884190	−0.0751765	0.0585363
16.	0.1441796	−0.2877685	−0.1940611	0.0395566	0.0007327
17.	0.9340978	−0.0764409	−0.0112246	−0.1052855	0.1197626
18.	0.8379920	−0.1581357	−0.2415173	−0.2205638	0.2052664
19.	0.0948649	−0.7225091	0.5135236	−0.0776931	0.1336098
20.	−0.0477885	−0.8711195	0.2605822	−0.1511693	0.1926126
21.	0.6492946	0.4411572	0.2990977	−0.2707346	0.3700605
22.	0.2164818	0.6650421	0.3564631	−0.3670552	0.2019860
23.	0.6580347	0.2659786	0.1374653	−0.1748385	0.4240264
24.	0.7339792	0.1832732	−0.1162168	−0.3264529	0.1854340
25.	−0.3732890	−0.4181728	0.5697897	−0.3883381	−0.1400759
26.	0.5188465	−0.1851264	0.0220450	0.4697214	−0.1053183
27.	−0.6784778	0.1793504	0.0918947	−0.1980585	−0.2374376
28.	0.6098325	0.1973294	0.6315968	0.2793996	−0.1918658
29.	0.6098325	0.1973294	0.6315968	0.2793996	−0.1918658
30.	−0.5456913	0.1716460	0.4846009	0.5285202	0.0935103
31.	−0.0988049	0.8467538	−0.0251339	−0.2078032	−0.2906712
32.	0.4414210	0.0242099	0.4463780	−0.3216799	−0.0195030
33.	0.3388348	−0.4707434	−0.3449156	0.2567195	−0.0462704
34.	−0.3332398	−0.5745382	0.5893458	−0.3239226	0.1852541
35.	0.5994937	0.3691855	0.3543632	−0.0498222	0.3475240
36.	−0.6232941	0.2722790	0.2957349	−0.2475745	0.0005819
37.	−0.6437625	0.1028952	0.3961242	−0.3618655	0.0745969
38.	0.5793707	−0.1093442	−0.1040323	−0.1968725	−0.3085475
39.	0.2811599	−0.4485988	−0.3590495	0.0503694	−0.3279842
40.	−0.3332398	−0.5745382	0.5893458	−0.3239226	0.1852541
41.	−0.4597675	0.4187379	0.0153485	0.3484048	−0.0427419
42.	−0.1782957	0.5215056	0.2159982	−0.1292289	0.0143310
43.	−0.0840292	0.1112269	0.1647247	−0.0415819	−0.3936273
44.	0.1616456	0.1293033	−0.1539454	−0.6310220	−0.2087496
45.	0.0864995	−0.7839667	0.0446516	0.1787427	0.0927740
46.	0.6098325	0.1973294	0.6315968	0.2793996	−0.1918658
	VI.	VII.	VIII.	IX.	X.
2.	−0.1394164	−0.3474175	−0.0792670	0.1056858	0.0854577
3.	0.0093270	−0.0592813	−0.2851638	0.1587237	−0.0517160
5.	0.0449117	−0.4425233	−0.2218537	0.3159829	0.1471501
6.	0.1163917	0.0395406	−0.1044403	−0.0334291	0.2700133
9.	0.1417184	0.6167990	0.2681562	0.4167362	0.1386042
10.	−0.1248724	0.2536923	−0.3529955	−0.0161008	0.1129820
12.	−0.1854555	−0.0913738	0.0851108	0.1708288	0.1926282
13.	0.2550922	−0.1352908	0.1456703	−0.1650157	−0.1249281
14.	0.2836786	−0.1617582	0.3841972	−0.0299036	0.5384613
15.	−0.0788765	0.2099368	0.2237864	0.0080864	0.3954614
16.	−0.4354456	−0.3648156	−0.2176404	−0.6109018	0.1593562
17.	−0.1534960	0.0609385	0.1527720	0.0182737	0.1012241
18.	−0.1997098	0.1097419	0.1298337	0.0507008	0.1254707

(*continued*)

APPENDIX 3. (Continued)

	PRINCIPLE COMPONENTS				
	VI.	VII.	VIII.	IX.	X.
19.	0.1677881	0.2533934	0.1785646	0.0104447	−0.0195058
20.	0.0126496	0.1760192	0.0752291	−0.1513470	0.0383810
21.	0.1104381	−0.0205072	−0.0538776	−0.1350167	−0.0573354
22.	0.2026985	0.0578036	−0.3427233	−0.0726498	−0.0024815
23.	0.3357801	−0.0910891	−0.2196621	0.1255442	0.1376799
24.	−0.1652149	0.2716005	−0.1927697	−0.0061319	0.0910426
25.	0.0315530	0.1971248	−0.2439671	−0.0636229	−0.0579249
26.	0.4822483	0.2524238	0.0512107	−0.0957911	−0.0476433
27.	−0.0037041	0.0253443	0.1257655	0.2416408	−0.0378403
28.	0.0709616	−0.1122485	0.1196700	−0.0827769	−0.0295994
29.	0.0709616	−0.1122485	0.1196700	−0.0827769	−0.0295994
30.	0.1328322	−0.1671411	−0.2060764	0.1016164	0.0785346
31.	0.1569631	0.0579261	0.1100781	−0.2140089	−0.0485999
32.	−0.4554683	0.1161356	0.0894265	0.0458263	−0.2058747
33.	0.5295037	0.3717229	−0.1185204	−0.0160033	0.0198906
34.	0.1115931	0.0793780	0.1069966	−0.0967904	−0.0698220
35.	0.0258687	0.0397086	−0.0296042	−0.2666091	−0.2045914
36.	0.1449843	0.1298960	−0.2864864	−0.1526312	−0.0600707
37.	0.2668363	−0.1405495	−0.3199402	0.0507502	0.0056072
38.	0.4748601	−0.1419334	0.0072793	0.2376274	−0.0643782
39.	0.5829850	0.0145123	−0.1912881	0.0057201	−0.1940589
40.	0.1115931	0.0793780	0.1069966	−0.0967904	−0.0698220
41.	−0.0477399	0.3526877	0.0829260	−0.2145180	−0.0505431
42.	−0.3470802	−0.0603708	0.1326352	0.5233748	−0.3710022
43.	−0.2444863	0.4647836	−0.6101984	0.0604030	0.1866010
44.	0.3225032	−0.4169769	−0.1464836	0.2691902	0.0783850
45.	−0.3467677	0.1343245	−0.2636901	0.3034776	0.0343297
46.	0.0709616	−0.1122485	0.1196700	−0.0827769	−0.0295994

MALACOLOGIA, 1992, 34(1–2): 343–354

CROP EPITHELIUM OF NORMAL FED, STARVED AND HIBERNATED SNAILS *HELIX LUCORUM:* A FINE STRUCTURAL-CYTOCHEMICAL STUDY

V. K. Dimitriadis, D. Hondros & A. Pirpasopoulou

Department of Genetics, Development and Molecular Biology, School of Biology, Aristotle University of Thessaloniki, Thessaloniki, 54006, Greece

ABSTRACT

The crop epithelium of the snail *Helix lucorum* consists of four cell types: ciliated and unciliated columnar cells, mucous cells, and basal cells. The morphologic features of the epithelium show that the digestive activities in the crop lumen are probably mediated by digestive enzymes regurgitated from the digestive gland and the stomach, rather than secreted by the crop cells themselves. On the other hand, the crop epithelium is probably responsible for the absorption of nutrients from the crop lumen. The mucous cells secrete a periodate-reactive, non-sulfated and non-carboxylated material, whereas the dense bodies observed in the columnar cells show a positive reaction for acid phosphatases, as well as for periodate-reactive, sulfated and carboxylated glycoconjugates and possibly are of lysosomal origin. Thirty seven days of hibernation increased the number of mucous cells and the number of the dense bodies in the columnar cells, while the amount of glycogen particles and lipid inclusion drastically decreased in non-mucous cells compared to controls. Hibernation did not alter the carbohydrate content of mucous cells. In addition, hibernation caused increased appearance of extrusion of cytoplasmic regions into the crop lumen, as well as lysis of certain columnar cells compared to controls. Forty days of starvation induced similar but less intense phenomena in the crop epithelium.

Key words: *Helix lucorum,* snail, crop, fine structure, hibernation, starvation, cytochemistry.

INTRODUCTION

The crop of Pulmonata consists of a thin tube connected to the oesophagus and followed by the main stomach. There are few data about the structure and function of the cells that constitute the pulmonate crop, which is regarded as a region where food is stored for certain periods (Runham, 1975). Furthermore, there is little available information on the morphology and function of these cells at the ultrastructural level (Roldan, 1987; Roldan & Garcia-Corrales, 1988). As far as the digestive enzymes of the digestive tube of molluscs are concerned, there are contradictory views about their origin, for example whether they are of exogenous or endogenous origin or both (Fretter, 1952; Jeuniaux, 1954; Owen, 1966; Charrier, 1990).

In addition, little is known about the biochemistry, physiology and fine structural cell morphology of snails exposed to such conditions as hibernation and starvation, and that literature mainly refers to the digestive gland epithelium (Sumner, 1965; Oxford & Fish, 1979; Janssen, 1985; Dimitriadis & Hondros, in press). To our knowledge, the only related information at the ultrastructural level comes from the snail *Theba pisana*, in which starvation resulted in the disappearance of lipid droplets and glycogen particles in the columnar crop cells (Roldan, 1987).

The present study was designed: (1) to examine the fine structural features of the crop epithelium of the snail *Helix lucorum;* (2) to cytochemically characterize the crop cells; and (3) to study the effect of starvation and hibernation on crop cell morphology. One further question was also addressed: is the carbohydrate content of the mucous cells altered in starved and hibernated snails compared to controls?

MATERIALS AND METHODS

Adult *Helix lucorum* (Gastropoda, Pulmonata, Helicidae) were collected from Edessa, northern Greece. The largest shell diameter of the snails used in the present study varied from 41 to 43 mm, and the body weight was between 19 and 21.5 g.

The effect of hibernation on crop cells was examined in snails kept in a cold room at 4±1°C under a photoperiod of 9 h light : 15 h dark (Lazaridou-Dimitriadou & Saunders,

1986), for 37 days. Starved snails were kept at 19±1°C and a photoperiod of 13L : 11D for 40 days. Control fed snails were kept at 19 ± 1°C and a photoperiod 13L : 11D.

The tissues were fixed in Karnovsky's fixative (Karnovsky, 1965), postfixed in 2% osmium tetroxide, dehydrated, and embedded in Spurr's resin. Sections were cut using a Reichert OmU3 ultramicrotome, post-stained with uranyl acetate and lead citrate, and examined under a JEOL 100B electron microscope operating at 80 KV. For light microscopic observations, thick sections were stained with 1% toluidine blue.

For carbohydrate cytochemistry, finely minced pieces of crop were incubated overnight in low iron diamine (LID) (Takagi et al., 1982) or in high iron diamine (HID) (Spicer et al., 1978; Sannes et al., 1979), treated with osmium tetroxide and embedded in Spurr's resin. Thin sections of these specimens were stained with the thiocarbohydrazide-silver proteinate (TCH-SP) sequence. Control tissues were exposed in 1 M $MgCl_2$ in place of LID or HID. Specimens without osmium tetroxide treatment were used for the postembedding periodate-thiocarbohydrazide-silver proteinate (PA-TCH-SP) method (Thiéry, 1967). Control sections were stained without the periodate treatment. Thin sections of buffer- and osmium tetroxide-treated tissues post-stained with uranyl acetate and lead citrate were used to characterize normal crop epithelial ultrastructure.

To demonstrate acid phosphatase activity, a modified method similar to that proposed by Barka & Anderson (1962) was applied. Tissues sections approximately 1 mm in thickness were fixed in glutaraldehyde and then incubated in a medium containing 0.2 M tris/maleate (pH 5) as a buffer an 0.1 M β-glycerophosphate as substrate at 37° for 15–30 min. Control sections were incubated in the absence of substrate.

Morphometric evaluation was performed according to the methods described by Weibel (1979) and Steer (1981). Samples of five cells were analysed from each crop section of four different snails. The volume density of the dense bodies and of the lipid inclusions in the supranuclear cytoplasm of the columnar cells was determined from point counting stereology, using a test square lattice with a period d = 10 mm, equivalent to 1 μm on the specimen. A minimum of 480 points were counted per cell. The distribution of columnar and mucous cells within the crop epithelium were determined by measuring nucleated cells of both types on light microscope micrographs at a final magnification of ×500. Mean values and standard deviations of the morphometric parameters were calculated and statistically compared using Student's t-test, significant level $P<0.05$.

RESULTS

Morphology of the Crop Epithelium

The light and electron microscope examinations of the crop epithelium of *Helix lucorum* revealed that it is surrounded by connective tissue, muscular layers and a system of haemocoelic spaces surrounded by amoebocytes. The crop epithelium consists of four cell types: ciliated and unciliated columnar cells, mucous cells, and basal cells (Fig. 1).

The ciliated and unciliated cells are columnar epithelial cells displaying similar morphology to each other. Ciliated cells are the most frequent cell type observed in the crop epithelium. As far as the electron microscope techniques permit, it is found that the ciliated and unciliated cells are gathered in groups or irregularly dispersed in the crop epithelium.

The nucleus of both ciliated and unciliated cell types is usually in the middle portion of the cells (Figs. 1, 2). Their cytoplasm contains small quantities of rough endoplasmic reticulum and a small number of Golgi complexes usually located in the supranuclear cytoplasm. Numerous mitochondria are predominantly in the apex of the cells (Fig. 2). The apical plasma membrane of the ciliated cells forms well-developed microvilli, and long cilia, displaying the "9+2" system of microtubules, are regularly dispersed among the microvilli (Figs. 2, 6). A well-developed microvillar border, similar to that observed in the ciliated cells is also present in the unciliated cells (Figs. 1, 2). Both ciliated and unciliated cells possess moderate quantities of glycogen particles, lipid inclusions, and electron-dense bodies in cytoplasmic areas adjacent to the nuclei.

In certain cases, columnar cells showing similar morphologic characteristics but presenting a cytoplasm with a lower electron density than the adjacent ciliated and unciliated cells are apparent in crop epithelium.

A characteristic feature of columnar cells is the presence of many electron-dense bodies in cytoplasmic areas adjacent to their nuclei

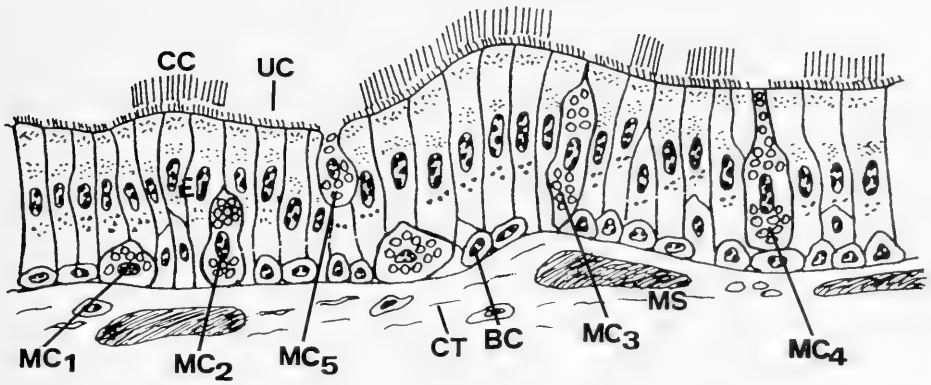

FIG. 1. Drawing of the various cell types observed in the crop epithelium of *Helix lucorum*. BC, basal cell; CC, ciliated cell; CT, connective tissue; MC_{1-5}, mucous cell in various stages of their development; MS, muscles; UC, unciliated cell.

(Figs. 2, 17). The dense bodies react positively for periodate-reactive, sulfated and carboxylated glycoconjugates when the PA.TCH.SP, HID.TCH.SP and LID.TCH.SP cytochemical sequences are applied, respectively (Figs. 3, 4). Columnar cells display large numbers of glycogen particles that react strongly to periodate-reactive polysaccharides by the PA.TCH.SP technique (Fig. 3); they also contain lipid inclusions, usually located in the middle and basal portion of the cells, as well as a few infoldings of the basal plasma membrane.

The third cell type, mucous cells, show a cytoplasm that is largely composed of mucous secretory granules (Figs. 1, 7). Mitochondria and rough endoplasmic reticulum are dispersed throughout the remaining cytoplasm, and numerous Golgi complexes (Fig. 9) are frequently observed with their trans face in opposition to a mucous granule. The nucleus of these cells is usually situated in their middle portions. In many cases, the rough endoplasmic reticulum appears swollen and contains crystalline-like material (Fig. 8). Mucous granules are usually spherical in shape, are 1–2 μm in diameter, and contain a fibrillar matrix without cores (Figs. 7, 8).

Mucous cells are irregularly located across the epithelium. Mucous cells of different sizes and epithelial orientations from each other are observed in transverse sections of the crop epithelium (Fig. 1). The development of mucous cells seems to occur in following stages: (1) Spheroid or ovoidal mucous cell appear in the base of the epithelium via differentiation of basal cells. (2) The mucous cells increase in size and extend their dorsal side towards the apex of the epithelium. (3) The mucous cells further increase in size; their dorsal side is in close attachment to the luminal surface of the epithelium. (4) The mucous cells are transepithelially oriented. Their luminal surface is limited and their apical region is narrow. (5) The mucous cells are finally secreted into the crop lumen.

At the same time, mucous cells showing all the above-mentioned morphologic stages are present in transverse sections of the crop epithelium. Mucous cells displaying a nontransepithelial orientation are also presented in the apex of crop epithelium.

Mucous cells react positively to the PA.TCH.SP cytochemical method indicating a content rich in periodate-reactive polysaccharides (Figs. 9, 10). Most of the reaction products are observed in a weblike structure within the matrix of the secretory granules. A strong PA.TCH.SP positive reaction is also found in the Golgi complexes and glycogen particles of the mucous cells (Fig. 9). The crystalline-like material inside the rough endoplasmic reticulum lack PA.TCH.SP reaction product (Fig. 10). Often, mucous cells located near the apex of the epithelium display a large cisterna in their apical portion (Fig. 11); this cisterna displays a negative reaction for carbohydrate and acid phosphatase (Fig. 11).

Mucous granules react negatively to the HID.TCH.SP and LID.TCH.SP sequences

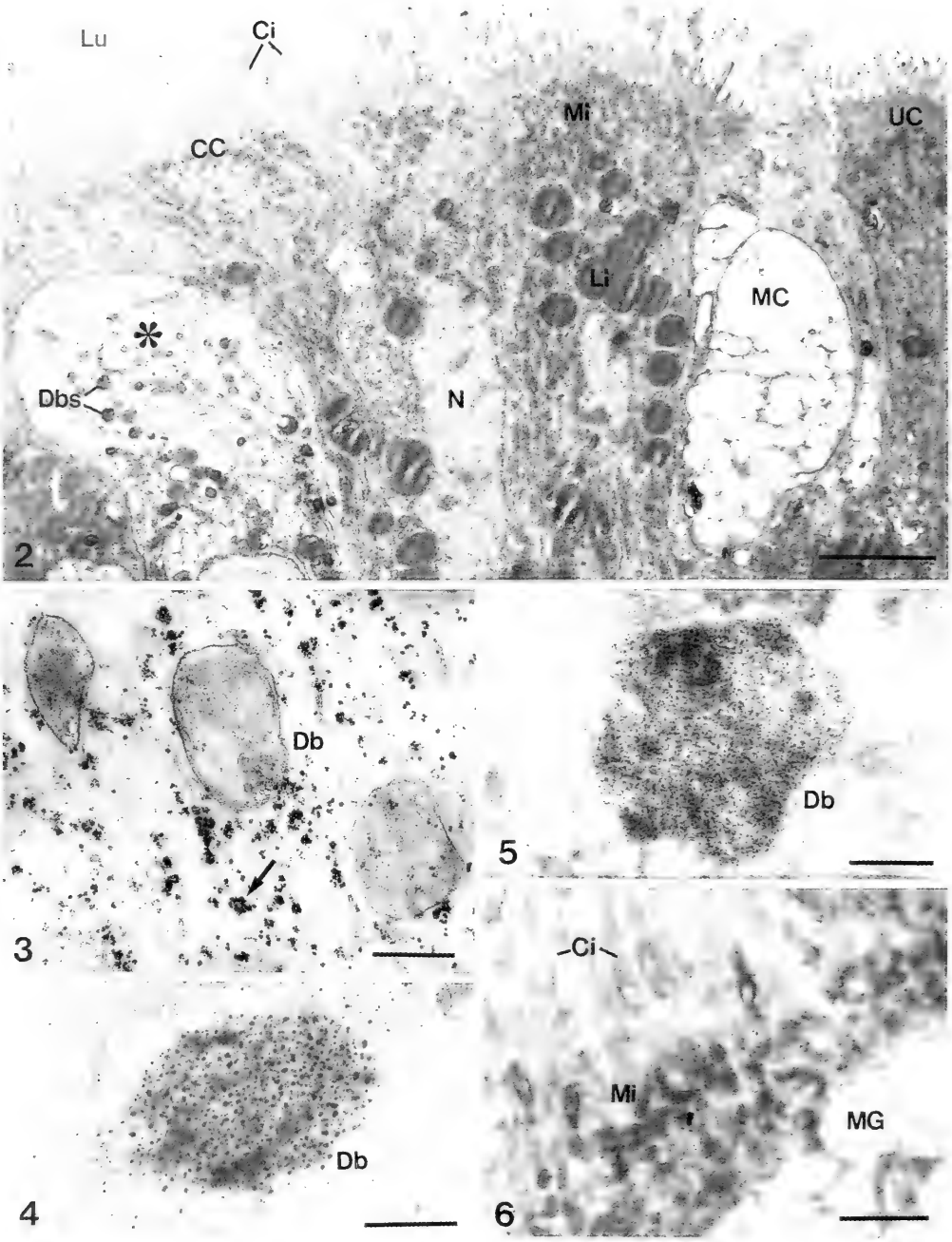
Lu
Ci
CC
Mi
UC
Li
MC
Dbs
N
2
Db
3
Db
5
Ci
Mi
MG
6
Db
4

(Fig. 6), indicating absence of sulfated and carboxylated glycoconjugates.

Finally, the fourth cell type, basal cells, are elongated to oval, and their ventral surfaces are attached to the basement membrane. Few mitochondria and little rough endoplasmic reticulum are found in these cells.

Control sections of all the cytochemical techniques used showed negative reactivity.

Morphology of the Crop Epithelium of Starved and Hibernated Snails

Snails starved for 40 days or hibernated for 37 days presented large regions of crop epithelium where ciliated and unciliated cells were morphologically similar to those of controls. In the latter cells, however, a significant increase in the volume density of dense bodies in the hibernated snails (Fig. 13), as well as a significant decrease in the volume density of lipid inclusions in both starved and hibernated snails was noted. The presence also of glycogen particles was less apparent in the experimental snails than in controls.

The application of the PA.TCH.SP, HID.TCH.SP and LID.TCH.SP techniques in the starved and hibernated snails indicated a carbohydrate content of mucous cells similar to that identified in controls, that is, the presence of periodate-reactive, non-sulfated and non-carboxylated polysaccharides was apparent in both experimental and control snails.

Mucous cells in starved and hibernated snails significantly increased in numbers (Fig. 12). In the experimental snails, the number of the luminal surface-oriented mucous cells was increased, while the mucous cells located at the base of the epithelium was decreased compared to controls. In many cases, mucous cells were smaller in size compared to controls and were positioned in the apex of the epithelium, displaying a non-transepithelial orientation. The latter was more apparent in the hibernated snails.

In the starved and hibernated snails, there were also other crop epithelial regions where increased lytic phenomena compared to controls were observed. The latter phenomena included lysis of certain cells (Fig. 15), as well as disorganization of apical cell regions (Fig. 16) and extrusion of cytoplasmic regions into the crop lumen (Fig. 17). The lytic phenomena were more intense in the hibernated than in the starved snails.

DISCUSSION

The available data concerning the role of the crop epithelium in Pulmonata is inconsistent. According to Owen (1966), the crop is implicated in food storage and enzyme secretion. In addition, van Weel (1961) suggested the existence of extracellular digestion in the crop lumen by enzyme activity of variable origin.

It is not clear, however, whether the enzymes are secreted by the crop wall cells (Owen, 1966), transferred from the digestive gland (Hirsch, 1917; Fretter, 1952), or produced by bacteria in the crop lumen (Jeuniaux, 1954). In the present study, the columnar cells of the snail *Helix lucorum* did not show morphological features that support their extensive secretory function. Such characteristics would be, for example, large amounts of rough endoplasmic reticulum, as well as large number of Golgi complexes and secretory granules produced by the Golgi complexes. Therefore, the results of the

FIG. 2. Transverse view of crop epithelium. In the apical portion of the ciliated (CC) and unciliated cells (UC) there are numerous mitochondria (Mi), while in their middle portion there are abundant lipid inclusions (Li). Note the similarity in the morphology of ciliated and unciliated cell. The asterisk shows a columnar cell presented less electron dense cytoplasm compared to the adjacent cells. Ci, cilia; Dbs, dense bodies; Lu, crop lumen; MC, mucous cell; N, nucleus. Bar = 3 μm.

FIG. 3. Detection of periodate-reactive polysaccharides (PA.TCH.SP technique). A positive PA.TCH.SP reaction is shown in the dense bodies (Db) and glycogen particles (arrow) in a columnar cell. Un-counterstained section. Bar = 0.4 μm.

FIG. 4. Detection of sulfated polysaccharides (HID.TCH.SP technique). A positive HID.TCH.SP reaction is shown in a dense body (Db) in a columnar cell. Un-counterstained section. Bar = 0.3 μm.

FIG. 5. Detection of acid phosphatase. A positive reaction for acid phosphatase indicates a dense body (Db) in a columnar cell. Un-counterstained section. Bar = 0.35 μm.

FIG. 6. Detection of carboxylated polysaccharides (LID.TCH.SP technique). A negative LID.TCH.SP reaction is noticed in the mucous granules (MG) of a mucous cell. Note the adequate ability of the technique to stain the mitochondria (Mi) and the cilia (Ci) of a ciliated cell. Un-counterstained section. Bar = 1.5 μm.

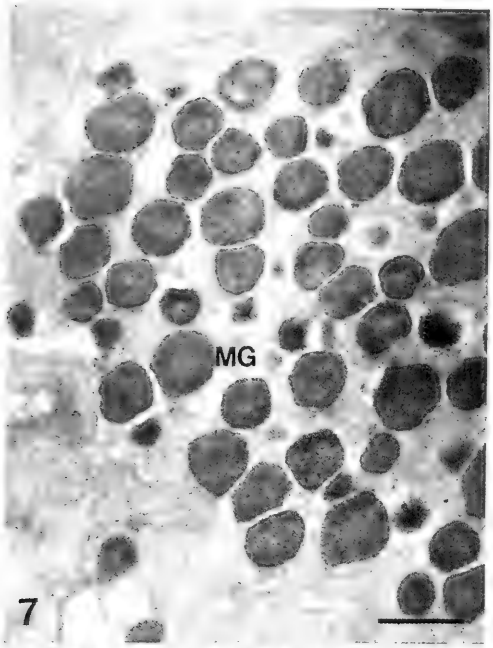
MG
7

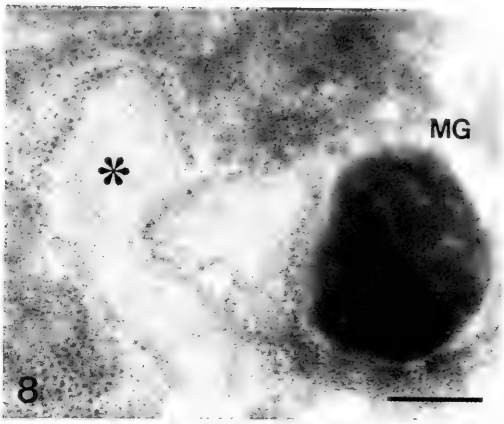
MG
8

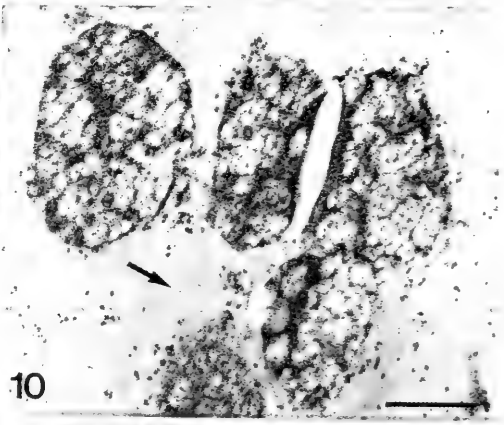
10


Go
MG
9

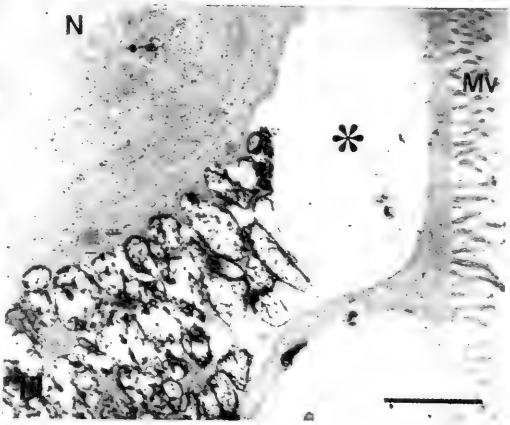
N
Mv

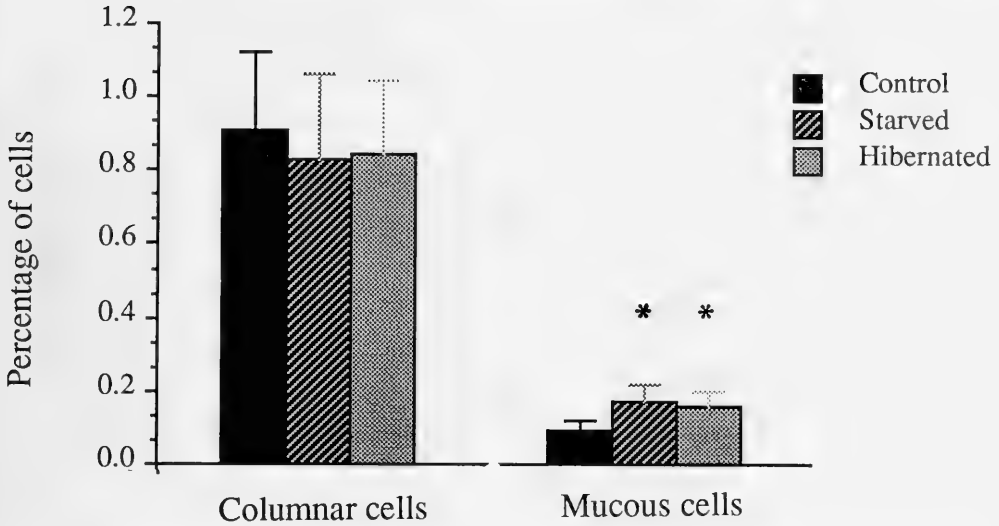

FIG. 12. Percentage (%) of the columnar (ciliated and unciliated cells) and mucous cells in the crop epithelium of *H. lucorum*. Significantly different values ($P<0.05$) between control and starved or control and hibernated snails are indicated by an asterisk.

present study are consistent with the notion (see, for example, Oxford, 1977) that digestive activities in the crop of snails are probably mediated by digestive enzymes regurgitated from the digestive gland or the stomach, rather than by enzymes secreted by the crop cells.

The presence of a large number of glycogen particles in the columnar cells indicates that the cytoplasm of these cells is a site of carbohydrate storage. Because other studies show cellulase and chitinase activity in the crop lumen of *Helix* (Jeuniaux, 1955; Strasdine & Whittaker, 1963; Koopmans, 1967; Flari & Charrier, in press), it is possible that the columnar cells of crop epithelium of *H. lucorum* absorb oligosaccharides from crop lumen, part of which are stored as glycogen particles. In addition, the presence of a very well-developed microvillar border and numerous mitochondria in the apex of crop columnar cells of *H. lucorum,* as well as the presence of moderate quantities of lipid inclusion in their cytoplasm, possibly indicates an extensive absorptive function coexisting with their function as cells that propel mucus. In the snail *Theba pisana,* an absorptive function is also suggested for the crop epithelial cells (Roldan & Garcia-Corrales, 1988).

The dense bodies observed in the digestive cells of *H. lucorum* crop have been also found in the crop or intestinal columnar and mucous cells in different gastropods (pulmonates and prosobranchs) (Carriker & Blistad, 1946; Bowen, 1970; Boquist et al., 1971; Lufty & Demian, 1976; Angulo et al., 1986). In the present study, the positive acid phosphatase reaction established the lysosomal origin of

FIG. 7. Mucous granules (MG) containing a fibrillar matrix without cores inside a mucous cell. Bar = 2 μm.
FIG. 8. Crystalline-like material (asterisk) appears inside the swelled rough endoplasmic reticulum of a mucous cell. MG, mucous granule. Bar = 0.3 μm.
FIG. 9. An intense PA.TCH.SP positive reaction show the saccules of the Golgi complexes (Go), the mucous granules (MG) and the glycogen particles (arrow) in a mucous cell. Un-counterstained section. Bar = 0.6 μm.
FIG. 10. The granules of a mucous cell show a reticulated PA.TCH.SP positive reaction. Note the negative reaction on the crystaline-like inclusions inside the rough endoplasmic reticulum (arrow). Un-counterstained section. Bar = 0, 35 μm.
FIG. 11. A mucous cell located near the apex of the epithelium displays PA.TCH.SP positive mucous granules and a large cisterna showing a negative reaction (asterisk). Mv, microvilli; N, nucleus. Bar = 3 μm.

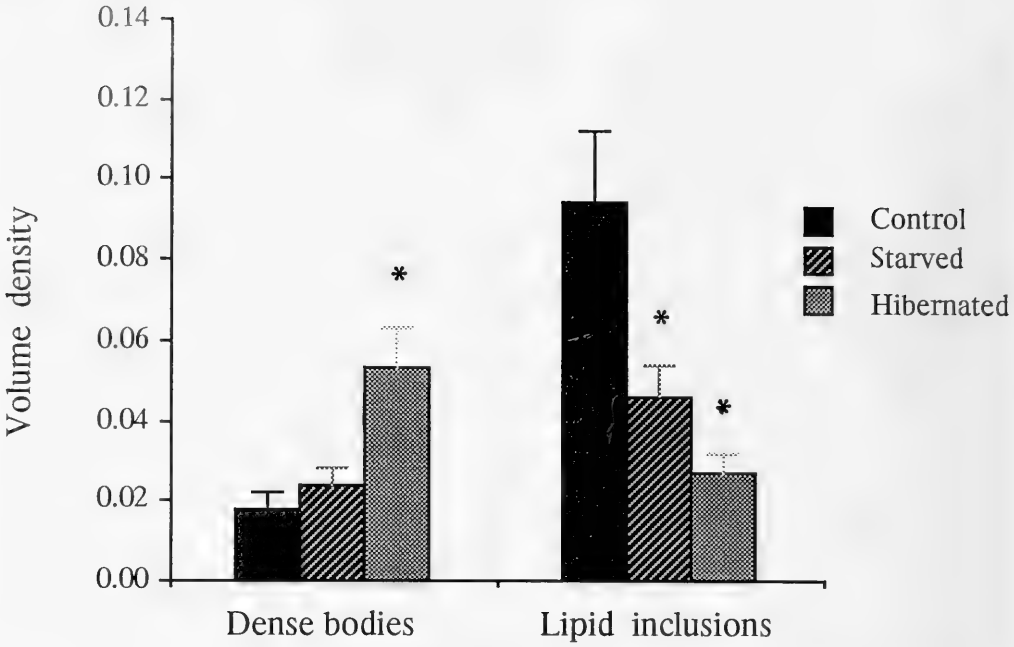

FIG. 13. Volume density of dense bodies and lipid inclusions in the supranuclear cytoplasm of columnar cells (ciliated and unciliated cells). Significant different values ($P<0.05$) between control and starved or control and hibernated snails are indicated by an asterisk.

these structures. A positive acid phosphatase reaction was also observed in apical vacuoles and granules of the crop and intestinal columnar cells, and in all the intestinal gland cells of the slug *Arion ater* (Bowen, 1970; Angulo et al., 1986). The lysosomal origin of the dense bodies of crop digestive cells of *H. lucorum* is additionally supported by the positive PA.TCH.SP, HID.TCH.SP and LID.TCH.SP reactions, indicating the presence of periodate-reactive, sulfated and carboxylated glycoconjugates, respectively. The association of the latter reactions with lysosomal activities is also referred to in studies on mammalian leukocytes (Bruyn et al., 1975, Spicer et al., 1978), as well as in studies on *H. lucorum* digestive gland cells (Dimitriadis & Liosi, in press).

There is little information about carbohydrate histochemistry and cytochemistry of the molluscan digestive epithelium. In the slug *Arion ater* (Angulo et al., 1986), intestinal gland cells showed either a positive reaction for acid and sulphated mucosubstances or a positive one for neutral polysaccharides. In the molluscs *Semerula maculata* (Varute & Patil, 1971) and *Venus mercenaria* (Zacks, 1965), sulfated acid and neutral polysaccharides, respectively, were found in their intestinal mucocytes. The mucous cells of *H. lucorum* crop epithelium, as the present study indicates, were positive to the PA.TCH.SP re-

FIG. 14. 25 days of starvation. Numerous dense bodies (Dbs) are located in the apical portion of certain columnar cells. Bar = 1.9 μm.

FIG 15. 40 days of starvation. A crop epithelial cell in a stage of its lysis. N, nucleus Bar = 1 μm.

FIG. 16. 37 days of hibernation. Cisternae with membranic materials are located in the apex of a ciliated cells. Bar = 1 μm.

FIG. 17. 37 days of hibernation. A columnar cell (asterisk) is extruded into the crop lumen. This phenomenon is more apparent in the experimental snails than in controls. Note the numerous dense bodies (arrows) in the supranuclear cytoplasm of two columnar cells. Mi, mitochondria; Mv, microvilli; N, nucleus. Bar = 1.5 μm.

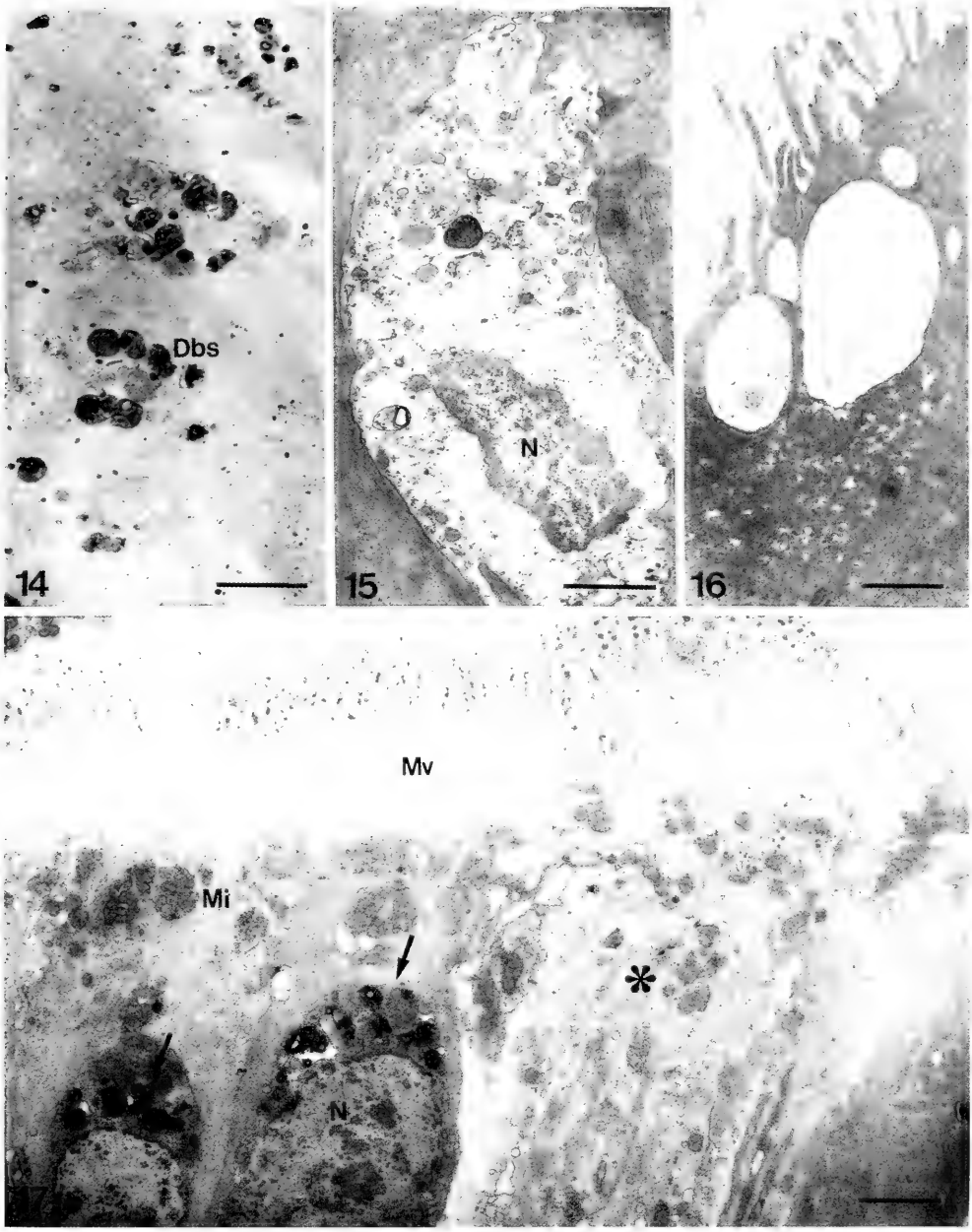
Dbs
14
D
N
15
16
Mv
Mi
N
*

action and negative to both HID.TCH.SP and LID.TCH.SP sequences, indicating periodate-reactive glycoconjugates, which lack sulfated and carboxylated esters. However, it is possible that the polysaccharides of mucous cells in *H. lucorum* crop epithelium contain hyaluronic and sialic acid, which are stained by alcian blue (pH = 2.5), as was demonstrated in mucocytes in the intestinal gland cells of the slug *Arion ater* (Angulo et al., 1986).

Morphology of the Crop Epithelium of Starved and Hibernated Snails

The existing data on morphological changes in the fine structure of the crop epithelial cells of Pulmonata under starvation or hibernation is not sufficient to give a clear insight into the physiology of the cells under these conditions. There are reports indicating biochemical and physiological differences in enzyme secretion, changes in the concentration of the components of extracellular body fluids (Meenakshi, 1956), changes in the osmotic pressure and respiratory rate (Ghiretti, 1966), and changes in major metabolic products (Florkin, 1966) due to hibernation or starvation.

The light and electron microscope observations of the crop cells of *H. lucorum* after 40 days of starvation and 37 days of hibernation showed a significant increase in number of the dense bodies located near the nuclei of the columnar cells compared to controls. This increase probably reflects increased lysosomal activity and/or increased intracellular digestion of nutrients by these cells during starvation and hibernation.

The increased lytic phenomena and extrusions of cytoplasmic regions into the crop lumen of the snails *H. lucorum* during starvation and hibernation compared to controls are probably related to the reduction of the energy requirements and the maintenance of low function activity by the crop epithelial cells during the experimental periods. In contrast to our observations, autophagic vacuoles were formed in tissues of other organisms under starvation (Bowen, 1968; Bauer et al., 1977) that were related to cell autophagy. The nonappearance of autophagic vacuoles in the crop cells of *H. lucorum* during starvation and hibernation probably indicates the snail's adaptation to these conditions.

Another effect that starvation and hibernation induced in the crop epithelium of *H. lucorum* was the increase in the number of mucous cells in the starved and hibernated snails compared to controls. It is uncertain whether the increase in the number of mucous cells in the starved and hibernated snails is a result of increased mucous cell development or of the accumulation of mucous cells in the crop epithelium, reflecting decreased mucous cell secretion due to starvation and hibernation.

In conclusion, by using light and electron microscopic observations, in combination with cytochemical characterization and morphometric evaluation, the present study provides information about the effect of starvation and hibernation on the cells of the crop epithelium of the snail *H. lucorum.* The results of the present study should be considered as preliminary. Additional information, especially by the use of cytochemical techniques, is needed in order to clarify the physiology of snails during such conditions as hibernation and starvation.

ACKNOWLEDGMENTS

This work was financially supported by the Greek Ministry of Agriculture. We are grateful to Dr. M. Lazaridou-Dimitriadou for the provision of the snails and their keep under normal, starvation and hibernation conditions.

LITERATURE CITED

ANGULO, E., J. MOYA & I. de la VEGA, 1986, Histochemical observation on the intestinal epithelium of the slug *Arion ater. Cuadernos Investigacion Biologica* (Bilbao) 9: 59–65.

BARKA, T. & P. J. ANDERSON, 1962, Histochemical methods for acid phosphatase using hexazonium parasolinin as coupler. *Journal of Histochemistry and Cytochemistry,* 10: 141–153.

BAUER, R., W. RUDIN & H. HECKER, 1977, Ultrastructure changes in midgut cells of female *Aedes aegypti* L (Insecta, Diptera) after starvation or sugar diet. *Cell and Tissue Research,* 177: 215–219.

BOQUIST, L., S. FALKEMER & B. K. MEHROTRA, 1971, Ultrastructural search for homologues of pancreatic beta-cells in the intestinal mucosa of the mollusc *Buccinum undatum. General Comparative Endocrinology* 17: 236–239.

BOWEN, I. D., 1968, Electron microscopic studies on autophagy in the gut epithelial cells of the locust *Schistocerca gregaria. Histochemical Journal,* 1: 141–151.

BOWEN, I. D., 1970, The fine structure localization of acid phosphatase in the gut epithelium cells of

the slug *Arion ater* (L.). *Protoplasma* 70: 247–270.

BRUYN, P. P. H. de, S. MICHELSON & R. B. BECKER, 1975, Endocytosis, transfer tubules and lysosomal activity in myeloid sinusoidal endothelium. *Journal of Ultrastructure Research,* 53: 133–151.

CARRIKER, M.R. & N. M. BILSTAD, 1946, Histology of the alimentary system of the snail *Lymnaea stagnalis Transactions. American Microscopical Society* 65: 250–275.

CHARRIER, M., 1990, Evolution, during digestion, of the bacterial flora in the alimentary system of *Helix aspersa* (Castropoda: Pulmonata): a scanning electron microscope study. *Journal of Molluscan Studies,* 56: 425–433.

DIMITRIADIS, V. K. & D. HONDROS, Effect of starvation and hibernation on the fine structural morphology of digestive gland cells of the snail *Helix lucorum. Malacologia* (in press).

DIMITRIADIS, V. K. & M. LIOSI, Ultrastructural localization of periodate-reactive complex carbohydrates and acid-alkaline phosphatases in digestive gland cells of fed and hibernated *Helix lucorum* (Mollusca: Helicidae). *Journal of Molluscan Studies* (in press).

FLARI, V. & M. CHARRIER, Contribution to the study of carbohydrases in the digestive tract of the edible snail *Helix lucorum* L. (Gastropoda: Palmonata: Stylommatophora) in relation to its age and its physiological state. *Journal of Molluscan Studies* (in press).

FLORKIN, M. 1966, Nitrogen metabolism. Pp. 309–351, in: K. M. WILBUR & C. M. YONGE, eds, Physiology of Mollusca. Vol. 2. Academic Press, New York, San Francisco.

FRETTER, V., 1952, Experiments with ^{32}P and ^{131}I on species of *Arion Hellix* and *Agriolimax. Quarterly Journal of Microscopical Science* 93: 133–146.

GHIRETTI, F., 1966, Respiration. Pp. 175–208, in: K. M. WILBUR & C. M. YONGE, eds., Physiology of Mollusca. Vol. 2. Academic Press, New York, San Francisco.

HIRSCH, G. C., 1917, Ernahrungsbiologie fleischfressender Gastropoden. I. Makroskopischer Bau, Nahrung, Nahrungsaufnahme, Verbauung, Sekretion. *Zoologishe Jahrbücher, Abteilung Allgemeine Zoologie und Physiologie* 35: 357–504.

JANSSEN, H. H., 1985, Some histophysiological findings on the mid-gut gland of the common garden snail, *Arion rufus* (L.) *Zoologischez Anzeiger* (Jena) 215: 33–51.

JEUNIAUX, C., 1954, Sur la chitinase et la flore bacterienne intestinale des mollusques gasteropodes. *Bulletin Academie Royale de Belgique, Classe des Sciences 28: F7.*

KARNOVSKY, M. J., 1965, A formaldehyde-glutaraldehyde fixative of high osmolarity for use in electron microscopy. *Journal of Cell Biology* 27: 137A–138A.

KOOPMANS, J. J. C., 1967, The nature and origin of cellulases in *Helix pomatia. Acta Physiologica et Pharmacologica Neerlandica* 14: 349–350.

LAZARIDOU-DIMITRIADOU, M. & D. C. SAUNDERS, 1986, The influence of humidity, photoperiod and temperature on the dormancy and activity of *Helix lucorum* L. (Gastropoda, Pulmonata). *Journal of Molluscan Studies,* 52: 180–189.

LUFTY, R. G. & E. S. DEMIAN, 1976, The histology of the alimentary system of *Marisa cornuarietis* (Mesogastropoda : Ampullariidae). *Malacologia* 5: 375–422.

MEENAKSHI, V. R., 1956, Physiology and hibernation of the apple snail *Pila virens* (L.). *Current Science* 10: 321–322.

OWEN, G., 1966, Digestion. Pp. 53–96, in: K. M. WILBUR & C. M. YONGE, eds., Physiology of Mollusca. Vol. 2. Academic Press, New York, San Francisco.

OXFORD, G. S., 1977, Multiple sources of esterase enzymes in crop juice of *Cepaea* (Mollusca, Helicidae). *Journal of Comparative Physiology* 122: 375–383.

OXFORD, G. S. & L. J. FISH, 1979, Ultrastructural localization of esterase and acid phosphatase in digestive gland cells of fed and starved *Cepaea nemoralis* (L.). *Protoplasma* 101: 186–196.

ROLDAN, C., 1987, Ultrastructural modification of the epithelium in the anterior digestive tract in starved specimens of *Theba pisana* (Mollusca, Gastropada, Pulmonata) *Iberus,* 7: 153–164.

ROLDAN, C. & B. GARCIA-CORRALES, 1988, Anatomy and Histology of the alimentary tract of the snail *Theba pisana* (Gastropoda: Pulmonata). *Malacologia,* 28: 119–130.

RUNHAM, N. W., 1975, Alimentary canal. Pp. 53–105, in: V. FRETTER & J. PEAKE, eds., Pulmonates. Vol. 1. Functional anatomy and Physiology. London, Academic Press.

SANNES, P. L., S. SPICER & T. KATSUYAMA, 1979, Ultrastructural localization of sulfated and complex carbohydrates with a modified iron diamine procedure. *Journal of Histochemistry and Cytochemistry* 27: 1108–1111.

SPICER, S. S., J. H. HARDIN & M. E. SETSER, 1978. Ultrastructural visualization of sulfated complex carbohydrates in blood and epithelial cells with the high iron diamine procedure. *Histochemical Journal,* 10: 435–452.

STEER, M. W., 1981, *Understanding cell structure.* Cambridge University Press, Cambridge.

STRASDINE, G. A. & D. R. WHITTAKER, 1963, On the origine of the cellulase and chitinase of *Helix pomatia. Canadian Journal of Biochemistry and Physiology* 41: 1621–1626.

SUMNER, A. T., 1965, The cytology and cytochemistry of the digestive gland cells of *Helix. Quarterly Journal of Microscopical Science* 106: 173–192.

TAKAGI, M., T. R. PARMLEY, S. S. SPICER, F. R. DENYS & M. E. SETSER, 1982, Ultrastructural localization of acidic glycoconjugates with the low

iron diamine method. *Journal of Histochemistry and Cytochemistry,* 30: 471–476.

THIÉRY, J. P., 1967, Mise en evidence des polysaccharides sour coupes fines en microscopie électronique. *Journal of Microscopie* 6: 987–1018.

VARUTE, A. T. & V. A. PATIL, 1971, Histochemical analysis of molluscan stomach and intestinal alkaline phosphatase: a sialoglycoprotein. *Histochemie,* 25: 77–90.

WEIBEL, E. R., 1979, *Stereological methods.* Vol. 1: Practical methods for biological morphometry. Academic Press, New York and London.

WEEL, P.B. van, 1961, The comparative physiology of digestion in molluscs. *American Zoologist* 1: 245–272.

ZACKS, S. I., 1955, The cytochemistry of the amoebocytes and intestinal epithelium of *Venus mercenaria* (Lamellibranchiata), with remarks on a pigment resembling ceroid. *Quarterly Journal of Microscopical Science, 96: 57–71.*

Revised Ms. accepted 9 March 1992

MALACOLOGIA, 1992, 34(1–2): 355–369

GENETIC SIMILARITIES AMONG CERTAIN FRESHWATER MUSSEL POPULATIONS OF THE *LAMPSILIS* GENUS IN NORTH CAROLINA

Alan E. Stiven[1] and John Alderman[2]

ABSTRACT

The objective of this research was to explore ecological and genetic similarities among several southeastern freshwater mussel populations, focusing especially on two rare and potentially endangered "subspecies" of *Lampsilis radiata* residing in river systems in the Piedmont and coastal plain of North Carolina. Conchological analyses and the examination of genetic identity patterns derived from 11 electrophoretic loci in six different populations or species formed the basis of our interpretations.

Two currently recognized subspecies of *Lampsilis radiata* (*radiata* and *conspicua*) are now quite rare in North Carolina waters, and one, *L. r. conspicua,* may be endemic to the state. However, we find that in spite of the difference in unadjustable sample mean shell length, they do not differ in general shell morphometry. For example, covariance analyses indicated homogeneity of shell length-height regression coefficients, and no difference in adjusted mean lengths. A similar conchological comparison of these two "subspecies" with the smaller sized recently described *Lampsilis fullerkati* of Lake Waccamaw also failed to find any significant conchological differences among these populations.

Nei's unbiased genetic distance and Rogers modified genetic distance derived from electrophoretic analyses consistently separated on established *Ellipito, Leptodea* and *Lampsilis* species. However, these genetic distance measures did not distinguish between the two rare *Lampsilis radiata* "subspecies" nor between these two groups and *Lampsilis fullerkati;* Nei's unbiased identity ranged from 0.945 to 0.978 among these three populations. Phenograms and a Wagner tree derived from Rogers distance supported evolutionary similarities among these three populations.

We also found evidence of site effects (conchological differences in different habitats) in *Lampsilis cariosa* and *Leptodea ochracea,* the two species examined for such a phenomenon. Genetic identity values among these intraspecific but allopatric populations ranged from 0.922–0.982. We suggest that until contrasting genetic and distinctive biological data are forthcoming, the two "subspecies" of *L. radiata* and possibly *L. fullerkati* simply be considered as a multiple population complex of *Lampsilis radiata.*

Key words: freshwater mussel, *Lampsilis radiata,* ecology, genetics, North Carolina, genetic distance, phenogram, Wagner tree.

INTRODUCTION

Freshwater bivalves constitute a large and very diverse assemblage of species in North Carolina and other southeastern states (R.I. Johnson, 1970; Burch, 1975; Davis, 1984). Many of these mussels and clams are highly vulnerable to pollutants, and changes in their abundance, survival and reproductive status can be a warning signal of the declining health of an estuary or river system (Goldberg et al., 1978). Because many freshwater mussels in North Carolina are already in a state of decline (Clarke, 1983), it is imperative that work focus on the assessment of potentially rare and endangered species of freshwater mussels, especially in the genera *Lampsilis, Lasmigona, Elliptio,* and *Alasmidonta* (Clarke, 1983; Keferl & Shelley, 1988; Alderman, 1988). The development and use of the "rare and endangered" classification, however, has been hampered by insufficient ecological, genetic and systematic information, as well as confusion even over the species concept in this group. Many early mussel investigators relied on shell morphology for distinguishing species, but this approach is often suspect, especially in light of the extensive conchological divergence in this group (Davis, 1984).

The freshwater mussel genus *Lampsilis* is probably one of the most successful and specialized groups of the Unionidae (Davis, 1984), with more than 20 living species in North America. At least five of these species

[1]Department of Biology, University of North Carolina, Chapel Hill, North Carolina 27599-3280, U.S.A.
[2]Nongame Program, North Carolina Wildlife Resources Commission, Raleigh, North Carolina 27604–1188, U.S.A.

are found in North Carolina waters and some may be endemic to the state. Currently, the American Malacological Union recognizes two subspecies of *Lampsilis radiata* (Gmelin, 1791), *L. r. radiata* (eastern lampmussel) and *L. r. conspicua* (I. Lea, 1872) (Carolina fatmucket) (Turgeon et al., 1988). The eastern lampmussel is found largely in coastal plain waters and occupies a broad geographic range from the Pee Dee drainage north to the St. Lawrence River. Collections of this "subspecies" in North Carolina waters during the past four years include sites in the Chowan River, Swift Creek, Fishing Creek and the lower main channel of the Tar River (Clarke, 1983; Alderman, 1988). Shelley (1987) lists its occurrence in the Tar, Neuse, and Cape Fear rivers. The second "subspecies," the very rare Carolina fatmucket, is apparently found only in North Carolina and may be endemic to this state. It has been collected in the tributaries of the Pee Dee River drainage (e.g. the Little and Uwharrie rivers), and recently in the Flat River of the upper Neuse River drainage basin (Alderman, 1988, 1989). In prior collections of these two "subspecies," *L. r. radiata* often exhibited smaller shells (Alderman, 1989). *Lampsilis r. radiata* is also found in waters containing anadromous fish, and its larval glochidia may be parasitic on such fish. If these two populations are sufficiently different to warrant "species" status, then the rarer *L. r. conspicua* is a prime candidate for federal listing as "endangered."

This study utilized biochemical and population genetic methods (Rogers, 1972; Davis et al., 1981; Davis, 1984) to probe several questions about the genetic relatedness among certain North Carolina mussel populations. Our prime question dealt with ecological and genetic differences in the two *Lampsilis radiata* "subspecies." In addition, we explored three other questions within this genus. The first focused on the recent discovery of a small population of a *Lampsilis*-like species in the Deep River near its confluence with the Cape Fear River. This population is comprised of only large old specimens and is thought to be declining. Clarification of its genetic structure and possible systematic status is required (Alderman, 1990). The second question related to the genetic and ecological status of *Lampsilis cariosa* (Say, 1817). Mostly large *L. cariosa* are now found in sites formerly containing both young and adults (e.g. Tar and upper Neuse drainages) (Alderman, personal observation), and its level of genetic heterozygosity is unknown. Finally, *Lampsilis fullerkati* R. I. Johnson, 1984, a Lake Waccamaw species, was first discussed by Kat (1983) and then described as a new species by R. I. Johnson (1984). Kat (1983) noted that the genetic structure of this species was similar to *Lampsilis radiata* from New Brunswick and Nova Scotia. To help clarify the systematic status of *Lampsilis fullerkati,* we compared its genetic structure with North Carolina *Lampsilis radiata* specimens as well as other *Lampsilis* species.

METHODS

Study Sites and Collections

The description of all collection sites, as well as the species/populations and numbers of mussels collected, along with their ANSP catalog number (except the two rare *Lampsilis radiata* subspecies as noted below), are given in Figure 1 and Appendix I.

Collections of mussels were made from shallow water by hand and from deeper areas by snorkeling and SCUBA. Mussel species of prime interest to this study were generally too sparse to use quadrat sampling to estimate relative abundance. Specimens of the two rare "subspecies," *L. r. radiata* and *L. r. conspicua,* were returned to their original sites following shell measurements and the removal of a small tissue sample from the mantle for use in genetic analysis. Individuals of all other mussel species collected were sacrificed, tissue samples removed, shell measurements obtained, and shell and remaining soft body tissue preserved. Shell measurements included maximum length, height, and width. *Leptodea ochracea* (Say, 1817), formerly placed in *Lampsilis*, was identified as such by the lack of a distinct mantle flap (this flap is located ventral to the incurrent aperture in *Lampsilis*).

Genetic Methods

All animals were processed within 10 days of collection. Shells were pried open and tissue samples of mantle and liver (hepatopancreas) were removed, combined and processed, except in the case of the rare "subspecies" as noted above. Tissues were chopped on cold glass with a razor blade, then homogenized (sonified) in an equal volume of grinding buffer (0.1 M Tris, 0.001 M

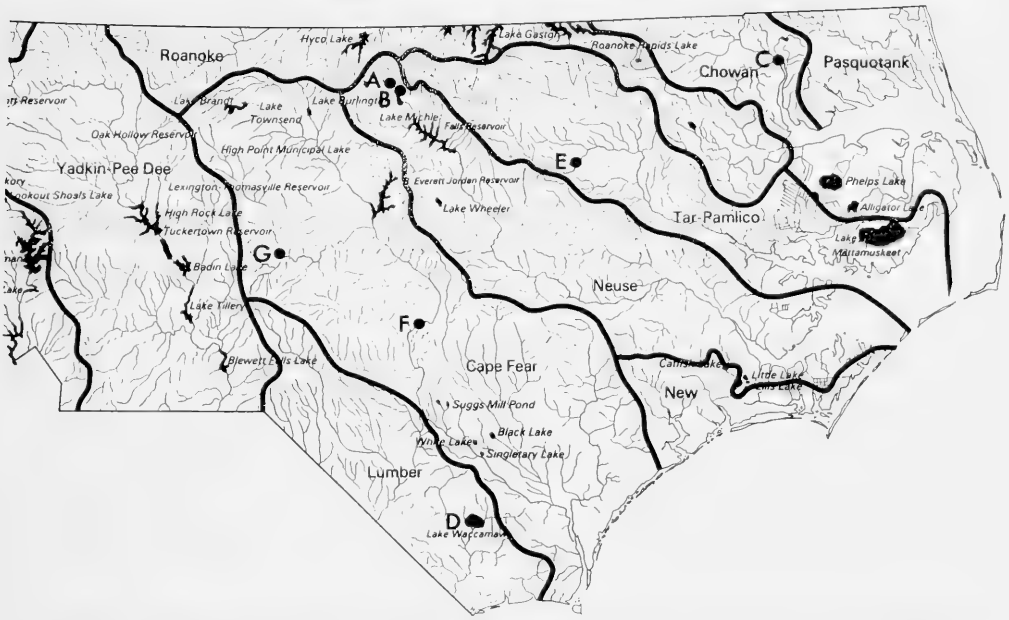

FIG. 1. Map of eastern North Carolina showing major river systems and the location of the collection sites (A-G) for this study. See Appendix I for details of each site.

EDTA, and 5×10^{-5} M NADP, pH 7.0) for about 20–50 sec. The sample was then centrifuged for 30 min at 12,000 *g*. Sample extracts were stored at −70°C. Protein extracts were then analyzed by horizontal starch gel electrophoresis (Electrostarch, Lot 89) following procedures outlined by Shaw & Prasdad (1970), Selander et al. (1971), Davis et al. (1981), Kat (1983), Davis (1984), and Stiven (1989). The 11 enzyme loci used (Table 1) correspond to most of the loci utilized by others in molluscan genetic research (e.g. Davis et al., 1981; Kat, 1983). The numbering of loci and lettering of alleles were from the most anodal region back to the origin on the gel. Sample tissues of *Elliptio complanata* (Lightfoot, 1786) and *Leptodea ochracea* were run with the other species and subspecies to provide allelic consistency. Aminopeptidase 1 and 2 (*Ala-1* and *Ala-2*) are associated with the substrate leucyl-alanine. Leucine aminopeptidase (*Lap*) or α-aminoacyl-peptide hydrolase (cytosol) was resolved using L-leucyl-β-naphthylamide and fast black K salt. The position of this locus differed from the *Ala* loci on the same gel.

The genetic data were analyzed using Swofford & Selander's (1981) BIOSYS-1 computer program. P, the proportion of loci that are polymorphic under the 0.95 criterion, and H, the direct-count heterozygosity, were measures of genetic variability. Levels of heterozygote deficiency were also estimated by $D = (H_O - H_E)/H_E$, where H_O and H_E are the observed and expected frequencies of heterozygotes respectively (Koehn et al., 1973). Departure of genetic frequencies from Hardy-Weinberg expectations were assessed by chi-square analysis adjusted for small sample sizes (Levene, 1949). All statistical analyses were carried out using SYSTAT (Wilkinson, 1990).

Genetic distance/similarity among species-populations were measured by Nei's nonmetric unbiased genetic distance and genetic identity (Nei, 1972, 1978) and Rogers metric modified distance (Rogers, 1972; Wright, 1978). Each has its specific assumptions and limitations, but all are related to F_{ST} (Wright's measure of genetic divergence-Wright, 1978; Hartl & Clark, 1989). Nei's unbiased measures are less sensitive to small sample sizes than are Nei's biased measures (Nei, 1978). There is no upper bound on the magnitude of Nei's genetic distance measure. We note also that when distance measures are relatively large between pairs of species, and heterozygosity is low, the construction of phenograms

TABLE 1. Isoenzymes and buffers utilized in the genetic analysis of freshwater mussels from North Carolina waters.

Locus/Isoenzyme (No. Loci)	Abbrev.	E.C. No.	Buffer
Phosphoglucose isomerase (1)	*Gpi*	5.3.1.9	LiOH[1]
Phosphoglucomutase (2)	*Pgm*	2.7.5.1	LiOH
Peptidase (2)	*Ala*	3.4.1.2	LiOH
Leucine aminopeptidase (1)	*Lap*	3.4.11.1	LiOH
Malate dehydrogenase (1)	*Mdh*	1.1.1.37	CM-6[2]
Phosphogluconate dehydrogenase (1)	*6-Pgd*	1.1.1.43	CM-6
Mannose 6-phosphatase isomerase (1)	*Mpi*	5.3.1.8	CM-6
α-glycerophosphate dehydrogenase (1)	*α-Gpdh*	1.1.1.8	TEB-9[3]
Superoxide dismutase (1)	*Sod*	1.15.11	TEB-9

[1]Selander et al. (1971)
[2]8.4 g citric acid per liter, to pH 6 with N-(3aminopropyl) morpholine. Gel buffer 1 part electrode: 19 parts water.
[3]Davis et al. (1981)

can be carried out fairly reliably with only a few representative individuals for a species (Nei, 1978). Phenograms were constructed for Nei's unbiased genetic distance (Nei, 1978) and for modified Rogers genetic distance (Rogers, 1972; Wright, 1978) using the unweighted pair group method of construction (Sneath & Sokal, 1973). A Wagner tree phenogram (Farris, 1972; Felsenstein, 1983) was also constructed using Rogers modified metric distance coefficient (Wright, 1978), with the tree rooted at the midpoint of the greatest patristic distance. Roger's metric measure satisfies the Wagner requirement of triangle inequality. This method does not assume constant evolutionary rates (Felsenstein, 1983).

RESULTS

Ecological and Shell Parameters

Only nine individuals of the rare *L. r. radiata* were obtained during many searches (by hand during wading, and SCUBA in deeper waters), some lasting many hours. Most were found in fine to medium sand and organic silt substrates. In the lower Chowan River site, *Leptodea ochracea* was about three times as abundant as *L. r. radiata.* In contrast, a 40-min search on 5-17-90 by two persons in the South Flat River yielded 40 *Elliptio complanata* and seven individuals of other species. *Lampsilis r. conspicua,* also rare, was obtained from the Flat River in Durham County. This subspecies was found primarily in coarse sand especially along sand bars.

Figure 2 illustrates the shell length vs. height regressions for *L. r. conspicua* and *L. r. radiata.* Although these "subspecies" differed significantly in mean shell length ($F_{1,30}$ = 29.5, $P<0.0001$) (Table 2), covariance analysis indicated that the length-height regression coefficients did not differ ($F_{1,28}$ = 0.61, P = 0.44), suggesting similar relative conchologies. Shell length, adjusted for differences in shell height, was 105.7 mm and 104.1 mm for *L. r. conspicua* and *L. r. radiata* respectively, and this difference is not significant ($F_{1,28}$ = 0.63, P = 0.43). Shells of *L. fullerkati* from Lake Waccamaw were considerably smaller than the two subspecies (Table 2). However, covariance analysis of length-height regressions among *L. r. conspicua, L. r. radiata,* and *L. fullerkati* indicated no significant differences ($F_{2,61}$ = 0.32, P = 0.49), and adjusted mean lengths also did not differ among these three *Lampsilis* populations ($F_{2,63}$ = 2.72, P = 0.073). In contrast, shell length-height regression comparisons among all combinations of *Elliptio complanata, Lampsilis cariosa,* and *Leptodea ochracea* were significant.

Leptodea ochracea and *Lampsilis cariosa* showed evidence of the "site effects" that arise from conchological differences in populations of the same species drawn from different sites (Kat, 1982; Hinch et al., 1986), or conversely, conchological similarities among different species found in the same site (Horn & Porter, 1981). In *L. cariosa,* mean shell length was larger ($F_{2,31}$ = 46, $P<0.001$; and Tukey test) at the Deep River site (116.4 mm) than at the Cape Fear (60.6 mm) or Tar River (61.1 mm) sites. Similarly, *Leptodea ochracea* was much larger in the Chowan River (92.5 mm) than in Lake Waccamaw (37.6 mm) ($F_{1,72}$ = 847, $P<0.0001$; and Tukey test).

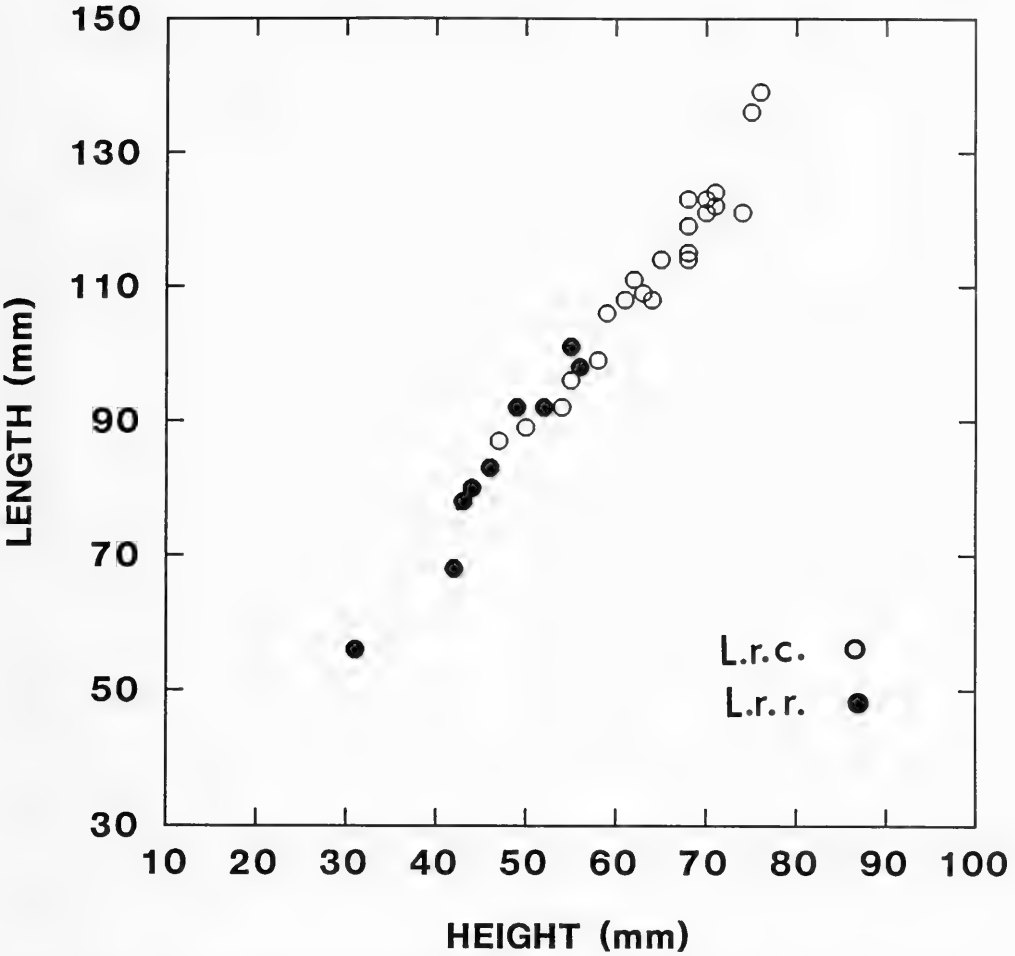

FIG. 2. Plot of shell length against shell height (mm) for samples of the freshwater mussels, *Lampsilis radiata conspicua* (open circles) and *L. r. radiata* (closed circles) from North Carolina waters. Refer to Appendix I for collecting sites.

TABLE 2. Summary of shell measurements for the freshwater mussels *Lampsilis radiata radiata, Lampsilis radiata conspicua,* and *Lampsilis fullerkati* from collections taken in North Carolina waters, 1990. Values are means ± SE.

Shell Parameters	*L. r. conspicua*	*L. r. radiata*	*L. fullerkati*
Sample Size	23	9	35
Length	113.0 ± 2.88	83.1 ± 4.87	47.1 ± 0.89
Height	64.6 ± 1.65	46.4 ± 2.57	23.5 ± 0.44
Width	40.2 ± 1.67	30.0 ± 2.27	15.5 ± 0.25

Genetic Analyses

Diversity and Heterozygosity: Alleleic frequencies and measures of genetic diversity derived from the 11 loci for all populations/species/subspecies are given in Table 3. Average direct-count heterozygosity and P-values were high in the more common and wide-spread species, *Elliptio complanata* and

TABLE 3. Alleleic frequencies, sample sizes, and locus-specific direct-count heterozygosity, along with percentage of loci polymorphic (P at the 0.95 criterion), and mean direct-count heterozygosity (H ± 1 S.E.) for the nine populations/species of freshwater mussels from North Carolina waters.

	Population[1]								
Locus	1	2	3	4	5	6	7	8	9
PGI									
A	0.000	0.125	0.000	0.294	0.000	0.000	0.086	0.000	0.000
B	0.000	0.833	0.929	0.706	0.000	0.000	0.000	0.000	0.000
C	0.000	0.000	0.000	0.000	0.000	0.000	0.729	0.935	1.000
D	0.000	0.000	0.000	0.000	0.000	0.000	0.000	0.000	0.000
E	0.067	0.042	0.071	0.000	0.316	0.718	0.186	0.065	0.000
F	0.767	0.000	0.000	0.000	0.000	0.000	0.000	0.000	0.000
G	0.078	0.000	0.000	0.000	0.000	0.000	0.000	0.000	0.000
H	0.089	0.000	0.000	0.000	0.684	0.282	0.000	0.000	0.000
(N)	45	12	7	17	19	55	35	23	9
H (dc)	0.133	0.333	0.143	.0.235	0.526	0.309	0.314	0.130	0
PGM-1									
A	0.011	0.000	0.000	0.000	0.000	0.000	0.000	0.000	0.000
B	0.744	0.000	0.000	0.000	0.000	0.000	0.000	0.000	0.000
C	0.044	0.167	0.214	0.147	0.000	0.000	0.000	0.000	0.000
D	0.189	0.625	0.571	0.559	0.974	1.000	0.814	1.000	1.000
E	0.011	0.167	0.000	0.294	0.026	0.000	0.171	0.000	0.000
F	0.000	0.042	0.214	0.000	0.000	0.000	0.014	0.000	0.000
(N)	45	12	7	17	19	55	35	23	9
H (dc)	0.356	0.417	0.286	0.471	0.053	0	0.314	0	0
PGM-2									
A	0.000	0.042	0.000	0.029	0.000	0.000	0.000	0.043	0.000
B	0.044	0.000	0.000	0.000	1.000	0.964	0.000	0.022	0.000
C	0.944	0.792	0.857	0.706	0.000	0.027	1.000	0.935	1.000
D	0.000	0.000	0.000	0.000	0.000	0.000	0.000	0.000	0.000
E	0.011	0.167	0.071	0.265	0.000	0.000	0.000	0.000	0.000
F	0.000	0.000	0.071	0.000	0.000	0.009	0.000	0.000	0.000
(N)	45	12	7	17	19	55	35	23	9
H (dc)	0.067	0.250	0.286	0.471	0	0.073	0	0.130	0
ALA-1									
A	0.000	0.000	0.000	0.000	0.053	0.055	0.000	0.000	0.000
B	0.011	0.792	0.714	0.676	0.947	0.936	0.229	0.457	0.722
C	0.067	0.208	0.214	0.324	0.000	0.000	0.029	0.043	0.000
D	0.744	0.000	0.071	0.000	0.000	0.009	0.714	0.500	0.278
E	0.122	0.000	0.000	0.000	0.000	0.000	0.000	0.000	0.000
F	0.056	0.000	0.000	0.000	0.000	0.000	0.029	0.000	0.000
(N)	45	12	7	17	19	55	35	23	9
H (dc)	0.244	0.417	0.429	0.529	0	0.018	0.286	0.391	0.333
ALA-2									
A	0.000	0.000	0.000	0.059	0.000	0.036	0.000	0.348	0.000
B	0.274	0.625	0.643	0.647	1.000	0.964	1.000	0.652	1.000
C	0.726	0.375	0.357	0.294	0.000	0.000	0.000	0.000	0.000
(N)	42	12	7	17	19	55	35	23	9
H (dc)	0.244	0.583	0.714	0.294	0	0	0	0	0
LAP									
A	0.022	0.000	0.000	0.000	0.000	0.000	0.000	0.000	0.000
B	0.678	0.000	0.000	0.000	0.079	0.000	0.000	0.000	0.000
C	0.011	0.000	0.000	0.000	0.000	0.000	0.000	0.000	0.000
D	0.133	0.000	0.000	0.250	0.000	0.000	0.000	0.000	0.000
E	0.011	0.000	0.071	0.313	0.000	0.000	0.000	0.000	0.000
F	0.000	0.375	0.571	0.250	0.000	0.000	0.000	0.109	0.000
G	0.011	0.292	0.214	0.125	0.000	0.000	1.000	0.761	1.000
H	0.067	0.083	0.071	0.063	0.000	0.000	0.000	0.022	0.000
I	0.000	0.000	0.071	0.000	0.000	0.000	0.000	0.000	0.000
J	0.067	0.250	0.000	0.000	0.921	1.000	0.000	0.109	0.000
(N)	45	12	7	16	19	54	1	23	9
H (dc)	0.333	0.667	0.857	0.375	0.158	0	0	0.087	0

TABLE 3. (Continued)

Locus	Population[1]								
	1	2	3	4	5	6	7	8	9
MDH									
A	0.000	0.000	0.000	0.000	0.158	0.009	0.000	0.000	0.000
B	0.012	0.167	0.000	0.000	0.842	0.991	0.214	0.000	0.167
C	0.628	0.833	1.000	1.000	0.000	0.000	0.000	0.000	0.000
D	0.360	0.000	0.000	0.000	0.000	0.000	0.786	1.000	0.833
(N)	43	12	7	17	19	55	35	23	9
H (dc)	0.023	0	0	0	0.316	0.018	0.429	0	0.333
6-PGD									
A	0.000	0.042	0.000	0.059	0.000	0.000	0.000	0.000	0.000
B	0.000	0.000	0.143	0.000	0.000	0.009	0.000	0.000	0.000
C	0.000	0.917	0.786	0.941	0.000	0.000	0.686	0.413	0.500
D	0.000	0.000	0.000	0.000	1.000	0.973	0.000	0.000	0.000
E	0.326	0.042	0.071	0.000	0.000	0.018	0.314	0.587	0.500
F	0.674	0.000	0.000	0.000	0.000	0.000	0.000	0.000	0.000
(N)	43	12	7	17	19	55	35	23	9
H (dc)	0.372	0.167	0.143	0.118	0	0.018	0.514	0.391	0.556
MPI									
A	0.023	0.000	0.000	0.000	0.000	0.000	0.000	0.000	0.000
B	0.682	0.000	0.000	0.000	0.000	0.018	0.000	0.000	0.056
C	0.295	0.792	0.000	0.000	0.974	0.900	0.029	0.348	0.389
D	0.000	0.000	0.000	0.324	0.000	0.000	0.000	0.022	0.000
E	0.000	0.208	1.000	0.676	0.026	0.082	0.971	0.630	0.556
(N)	44	12	7	17	19	55	35	23	9
H (dc)	0.068	0.250	0	0.647	0.053	0.127	0	0.304	0.556
α-PGD									
A	0.000	1.000	1.000	0.765	1.000	1.000	1.000	0.870	1.000
B	1.000	0.000	0.000	0.235	0.000	0.000	0.000	0.130	0.000
(N)	45	12	7	17	19	55	35	23	9
H (dc)	0	0	0	0.353	0	0	0	0.087	0
SOD									
A	0.000	0.000	0.000	0.000	1.000	1.000	0.000	0.000	0.000
B	1.000	1.000	1.000	1.000	0.000	0.000	1.000	1.000	1.000
(N)	45	12	7	17	19	55	35	23	9
H (dc)	0	0	0	0	0	0	0	0	0
P	81.8	81.8	63.6	81.8	36.4	27.3	45.5	72.7	36.4
$\bar{H}$ ±	0.169	0.280	0.260	0.318	0.100	0.051	0.169	0.138	0.162
S.E.	0.044	0.070	0.090	0.064	0.052	0.028	0.061	0.046	0.071

[1]1-*Elliptio complanata,* S. Flat River, Durham Co.
2-*Lampsilis cariosa,* Cape Fear River, Cumberland Co.
3-*Lampsilis cariosa,* Tar River, Nash Co.
4-*Lampsilis cariosa,* Deep River, Moore Co.
5-*Leptodea ochracea,* Chowan River, Gates Co.
6-*Leptodea ochracea,* Lake Waccamaw, Columbus Co.
7-*Lampsilis fullerkati,* Lake Waccamaw, Columbus Co.
8-*Lampsilis radiata conspicua,* Flat River, Durham Co.
9-*Lampsilis radiata radiata,* Chowan River, Gates Co.

Lampsilis cariosa. Lower heterozygosity estimates are associated with the two rare *Lampsilis radiata* "subspecies," *Lampsilis fullerkati* and *Leptodea ochracea,* which exhibited a very low heterozygosity level.

Elliptio complanata from the South Flat River showed the largest number of polymorphic loci deviating from Hardy-Weinberg expectation (six of nine) (0.95 criterion for polymorphic loci), whereas *Leptodea ochracea* from Lake Waccamaw had three of four. *Lampsilis r. conspicua* had three of eight, and *L. r. radiata* none. All significant departures came from deficiencies in heterozygotes. For example, in *E. complanata,* "D" ranged from −0.36 to −0.95 among loci, *Leptodea ochracea* from −0.66 to −1.0, and in *L. r. conspicua* from −0.21 to −1.0.

TABLE 4. Matrix of Nei (1978) unbiased genetic identity (below diagonal) and unbiased genetic distance (above diagonal) for the nine populations/species of freshwater mussels from North Carolina waters.

Population/Species	1	2	3	4	5	6	7	8	9
1. *Elliptio complanata*	*****	0.853	0.902	0.825	2.138	2.179	0.892	0.809	0.927
2. *Lampsilis cariosa*-Cape Fear	0.426	*****	0.082	0.090	0.726	0.729	0.420	0.414	0.345
3. *Lampsilis cariosa*-Tar R.	0.406	0.921	*****	0.041	1.111	1.086	0.350	0.422	0.386
4. *Lampsilis cariosa*-Deep R.	0.438	0.914	0.959	*****	1.146	1.140	0.404	0.477	0.435
5. *Leptodea ochracea*-Chowan R.	0.118	0.484	0.329	0.318	*****	0.018	1.049	0.963	0.823
6. *Leptodea ochracea*-L. Wacc.	0.113	0.483	0.338	0.320	0.982	*****	1.004	0.943	0.819
7. *Lampsilis fullerkati*	0.410	0.657	0.704	0.668	0.350	0.366	*****	0.056	0.049
8. *L. radiata conspicua*	0.445	0.661	0.655	0.621	0.382	0.390	0.945	*****	0.022
9. *L. radiata radiata*	0.396	0.708	0.680	0.647	0.439	0.441	0.952	0.978	*****

Genetic Relatedness Among and Within the Populations: Genetic relatedness among the nine populations was explored through pairwise associations using Nei's (1978) unbiased genetic distance and identity measures (non metric) (Table 4) and Rogers modified distance metric measure (Rogers, 1972; Wright, 1978) (Table 5). Some of the greatest distances were found between species of the two genera, *Elliptio* and *Lampsilis,* confirming prior taxonomic designations based largely upon morphological work. Notably, some of the smallest distance values occurred between *L. r. conspicua* and *L. r. radiata,* the two rare subspecies. In addition, these rare subspecies showed corresponding small distance values with another species, *L. fullerkati,* a mussel first collected from Lake Waccamaw. Kat (1983) provided morphologically and electrophoretic descriptions of this population, and R. I. Johnson (1984) judged it to be sufficiently distinct from *L. r. radiata* to warrant separate species status. Rogers modified distance (Table 5), which produces less compaction at the extremes, yielded corresponding results, with *L. fullerkati* being almost as genetically close to *L. r. radiata* as *L. r. conspicua* is to *L. r. radiata.*

Two species, *Lampsilis cariosa* and *Leptodea ochracea,* were sampled from different river systems (Fig. 1, Appendix I) thus providing measures of intraspecific genetic similarity among sites. Nei's (1978) unbiased genetic identity among the three poulations of *Lampsilis cariosa* from the Cape Fear, Tar, and Deep rivers ranged from 0.914–0.959. Heterozygosity values for these populations (Table 3) were also comparable (0.26–0.32). The populations of *Leptodea ochracea* from the Chowan River and Lake Waccamaw (Fig. 1, Appendix I) were genetically identical (Nei's identity was 0.982; Rogers metric distance was 0.134). However, the Lake Waccamaw population exhibited a low heterozygosity value (0.051, almost half that of the population from the Chowan River), and these within-species genetic distance comparisons essentially correspond to the levels found for the *L. r. conspicua-L. r. radiata-L. fullerkati* association (Tables 4, 5).

Evolutionary relationships among the nine populations were explored by performing a hierarchical cluster analysis using the unweighed pair-group method with arithmetic averaging (Sneath & Sokal, 1973). The resulting phenograms, one based upon Nei's unbiased genetic distance (Nei, 1978) and the other based upon unmodified Rogers genetic distance (Rogers, 1972; Wright, 1978) are given in Figures 3 and 4 respectively. Both confirm the close genetic similarity between the two rare "subspecies" *L. r. conspicua* and *L. r. radiata,* as well as their very close similarity to the Lake Waccamaw *L. fullerkati. Lampsilis cariosa* lies next in genetic relatedness to this group of three "species/subspecies," with *Leptodea ochracea* and *Elliptio complanata* exhibiting significant genetic distance not only from each other but also from the *Lampsilis* group. The phenogram based upon Nei's unbiased distance tended to compact values at the lower end of the scale (Fig. 3), whereas the phenogram derived from modified Rogers distance, a metric scale, provided a less compacted view of the genetic relationships among the *Lampsilis radiata* subspecies and *L. fullerkati* (Fig. 4). Even viewed in this manner, the relationships are still exceedingly close.

A possible evolutionary or phylogenetic pathway among the nine populations is given by the Wagner tree (Fig. 5) (Farris, 1970, 1972). It is based upon Rogers metric modified distance measure. Construction assump-

TABLE 5. Matrix of Rogers modified distance for the nine populations/species of freshwater mussels from North Carolina waters.

Population/Species	1	2	3	4	5	6	7	8	9
1. *Elliptio complanata*	*****								
2. *Lampsilis cariosa*-Cape Fear	0.627	*****							
3. *Lampsilis cariosa*-Tar R.	0.652	0.269	*****						
4. *Lampsilis cariosa*-Deep R.	0.609	0.262	0.211	*****					
5. *Leptodea ochracea*-Chowan R.	0.835	0.647	0.747	0.729	*****				
6. *Leptodea ochracea*-L. Wacc.	0.840	0.650	0.745	0.731	0.134	*****			
7. *Lampsilis fullerkati*	0.665	0.516	0.490	0.500	0.749	0.742	*****		
8. *L. radiata conspicua*	0.629	0.499	0.514	0.518	0.716	0.714	0.219	*****	
9. *L. radiata radiata*	0.680	0.484	0.515	0.522	0.702	0.703	0.213	0.162	*****

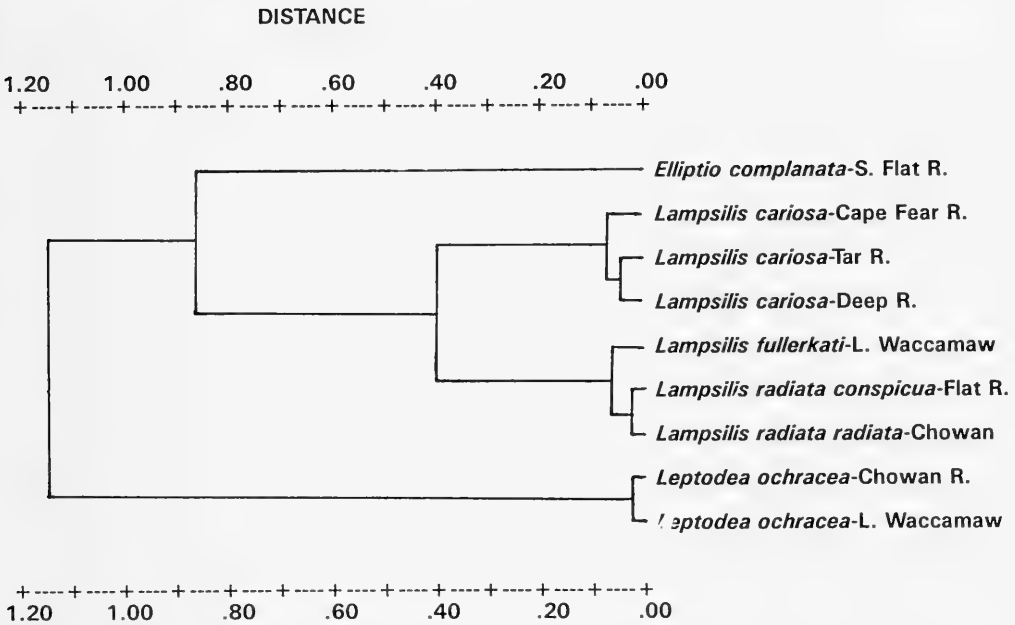

FIG. 3. Phenogram of nine North Carolina freshwater mussel populations based upon Nei (1978) unbiased genetic distance and using the unweighted pair group method of construction. Farris (1972) "f"-value = 4.672.

tions are discussed in Felsenstein (1983) and Swofford & Olsen (1990). The method of rooting is based upon midpoint location (Farris 1972, 1981). This method usually leads to trees having their roots on the branch leading to outgroup species (Felsenstein, 1983). This tree placed the two rare *Lampsilis* subspecies and *L. fullerkati* at approximately the same distance from the root, and into the same common evolutionary assemblage. *Lampsilis cariosa* lies next in genetic relatedness to the three aforementioned species-subspecies. *Leptodea ochracea* and *Elliptio complanata,* as expected, exhibited significant genetic distances not only from each other but also from the *Lampsilis* group. Populations within both *Lampsilis cariosa* and *Leptodea ochracea* have relative distances from the root that differ little from that among the *L. radiata* subspecies-*L. fullerkati* complex.

With respect to specific loci, both *L. radiata* "subspecies" also share the same major (most common) allele for all loci, and do so in approximately the same frequency (Table 3). In six of the loci, slight differences among the two subspecies do exist, ranging from certain

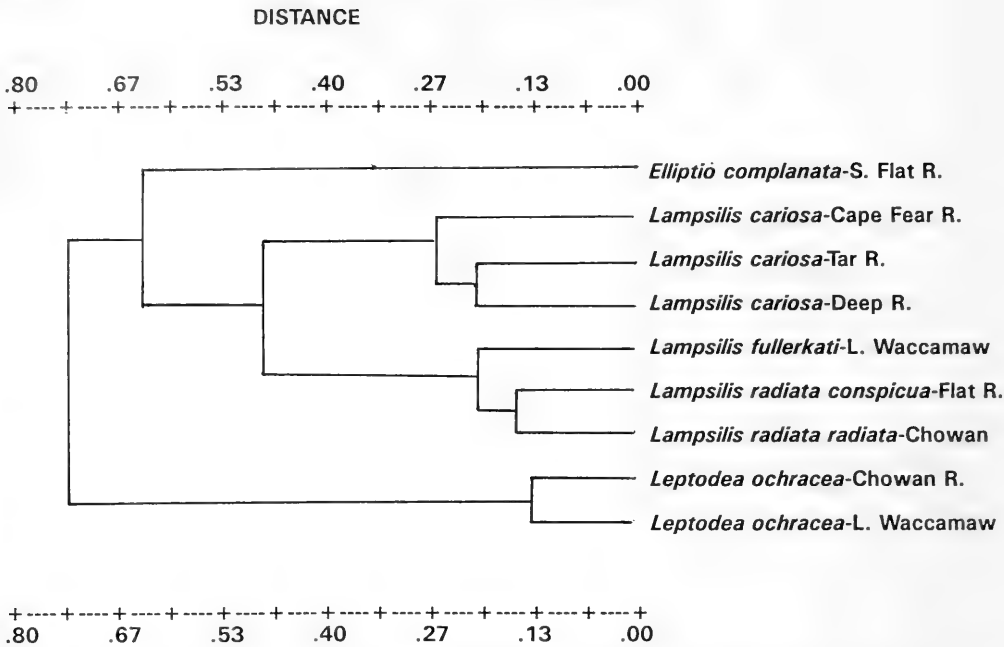

FIG. 4. Phenogram of nine North Carolina freshwater mussel populations based upon modified Rogers genetic distance (Rogers, 1972; Wright, 1978) and using the unweighted pair group method of construction. Farris (1972) "f"-value = 0.780.

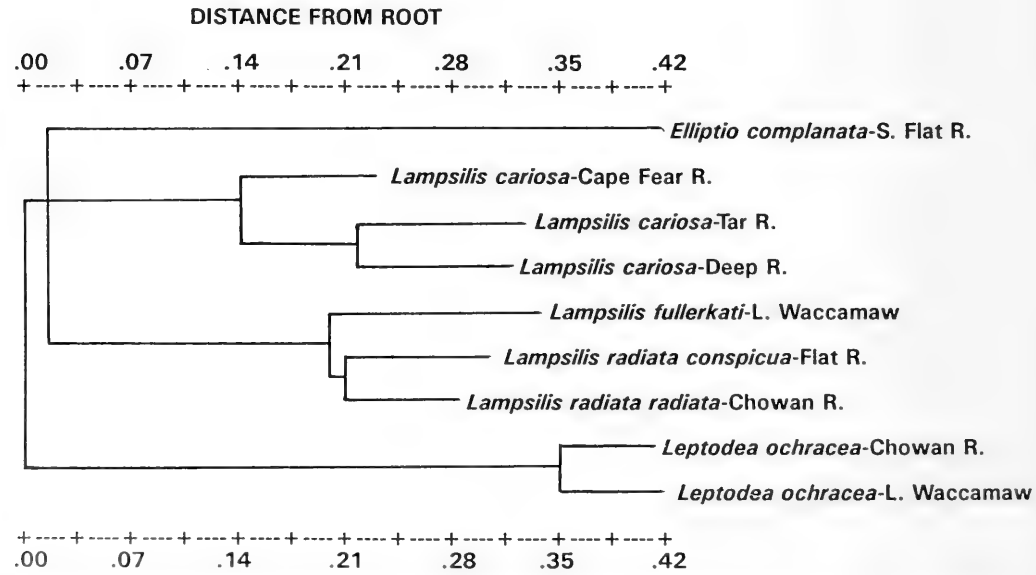

FIG. 5. Wagner tree depicting phylogenetic relationships of nine North Carolina freshwater mussel species and populations. Coefficient used was modified Rogers distance (Rogers, 1972; Wright, 1978). Tree is rooted at midpoint of longest path. Farris (1972) "f"-value is 0.893.

loci being polymorphic in one but not the other (*Pgi, Pgm-1, Pgm-2, α-Pgdh*) to one locus showing an allele in one subspecies that is not present in the other (*Mpi*).

DISCUSSION AND CONCLUSIONS

Genetic Relationships Among *Lampsilis, Leptodea* and *Elliptio* spp.

Freshwater mussels are one of the most diverse and abundant groups of macroinvertebrates in the United States, but also one of the most notorious for lack of systematic agreement among investigators (Davis & Fuller, 1981). Because conchological differences among bivalves are so environmentally dependent, the use of shell morphology in separating groups, especially above the species level, can often be misleading (Davis & Fuller, 1981). Molecular genetic methodologies have grown in importance in helping sort out differences among the Unionacea (Davis et al., 1981; Davis & Fuller, 1981; Kat, 1983; Kat & Davis, 1984). However, opinions differ over the association between genetic distance, level of systematic divergence and speciation, as well as the broader question of the applicability of molecular genetic tools (G.B. Johnson, 1977) and their use in phylogenetic interpretations (Felsenstein, 1988; Swofford & Olsen, 1990). Avise (1976) suggested in general terms that when using Nei's (1972, 1978) genetic identity (I), values of 0.9–1.0 would be expected among populations within a species, 0.8 to 0.89 among subspecies within a species, and a value < 0.8 among different species. Thorpe (1982), in a literature review, found that 97% of Nei I-values used for erecting new species were below 0.85, and 98% of the I-values associated with within species comparisons exceeded 0.85. In freshwater mussels, however, systematic interpretations based upon genetic distances vary, often as a function of allopatry-sympatry. Kat (1983) argued that a value of 0.878 found among *Lampsilis* spp. and *L. radiata* is characteristic of distinct species among radiating clades. This is consistent with Davis et al. (1981), who reported values > 0.9 among apparent sympatric species of *Elliptio* in Florida and Lake Waccamaw in North Carolina. The two "sympatric" *Elliptio* species in Lake Waccamaw had different shell characters states, differed in allelic frequencies at three loci, and preferred different habitats. Habitat differences were not apparent in the two Florida sympatric *Elliptio* species. On the other hand, Kat & Davis (1984) interpretated a value of 0.954 between two allopatric populations of *Elliptio complanata* in adjacent drainages in Nova Scotia as consistent with the Avise (1976) scheme. Thus, Davis et al. (1981) argue that in established conchologically distinct sympatric populations, genetic identity values of >0.9 could indicate different species, yet recognize that in allopatric situations, genetic identity values for different species of the same genus would more likely be less than 0.9.

Our intraspecific work with *Lampsilis cariosa* and *Leptodea ochracea* populations produced unbiased genetic identities (Nei, 1978) among separated sites of 0.922–0.959 and 0.982 for these species, respectively. These values are consistent with those suggested by Avise (1976), Davis et al. (1981), and Thorpe (1982) to encompass the expected variation and range within allopatric populations of a single species. Both phenograms (Figs. 3, 4) illustrate the identical genetic nature of these two species groups. Thus, the large-shelled *L. cariosa* type sampled from the Deep River is probably *L. cariosa.* It is genetically indistinct from the other two populations and also shows no signs of prolonged bottleneck effects (e.g. diminished heterozygosity).

Among paired associations within the four species of *Lampsilis,* we found identity values ranging from 0.357 to 0.863, consistent with Avise's (1976) expectations for variation among different species, as well as values found by Kat (1983) for three distinct species of *Lampsilis.* For example, we found identity values of 0.382 and 0.439 between Chowan River *Leptodea ochracea* and *L. r. conspicua* and *L. r. radiata* respectively, whereas Kat's (1983) value for a comparable association was 0.31. Genetic identity measures between *Leptodea ochracea* and *Lampsilis fullerkati* ranged from 0.35 to 0.366, and Kat's (1983) corresponding value was about 0.49. We also found values from 0.33 to 0.48 between *Leptodea ochracea* and *L. cariosa,* clearly implying distinct species status for each according to guidelines in Avise (1976). Identity values among *Elliptio, Leptodea* and *Lampsilis* genera in our study ranged from 0.115 to 0.445 (Table 4), consistent with Avise (1976) and also Davis et al. (1981). Again the two phenograms (Figures 3, 4) clearly depict these patterns.

Heterozygosity Levels

In examining relative heterozygosity levels among the various populations, we found that the two rare *Lampsilis* "subspecies" had H-values that were about 40% lower than that of populations of the more abundant and common *Lampsilis cariosa.* They were about the same as that of the genetically identical *Lampsilis fullerkati* from Lake Waccamaw and the common *Elliptio complanata.* Thus, we cannot associate these low heterozygosity levels with a prolonged bottleneck effect (Nei et al., 1975). *Leptodea ochracea* populations exhibited even lower heterozygosity levels as well as low polymorphism, a finding consistent with Kat's (1983), especially for Lake Waccamaw. We note that reliability of genetic identity comparisons among populations by genetic distance measures when sample sizes are small is greatly improved when heterozygosity levels are low (Nei, 1978), as in the case of the rare *L. radiata* "subspecies."

One possible explanation for the heterozygote deficiencies may be that a population in any one site is simply a mix of age classes and genotypes derived from a variety of populations some distance away that possess different gene frequencies. Dispersal of mussel larvae may be substantial (river currents, glochidia on fish hosts), and the Wahlund effect may be a partial explanation for heterozygote deficiencies (Dillon, 1988).

The Eastern Lampmussel and the Carolina Fatmucket: Distinct Subspecies?

The two rare *L. radiata* populations (subspecies) are currently recognized by the American Malacological Union as *L. r. conspicua* (Carolina fatmucket) and *L. r. radiata* (eastern lampmussel) (Turgeon et al., 1988). Turgeon et al. (1988) and Alderman (personal observation) have reported that sampled *L. r. conspicua* shells were larger and heavier than *L. r. radiata,* and that differences existed in their current range and preferred habitat. *Lampsilis r. radiata* resides in the lower parts of drainage basins of the eastern North American coastal plain, discontinuously from South Carolina to the St. Lawrence, whereas the very rare *L. r. conspicua* seems endemic to North Carolina and is currently restricted to the Pee Dee River drainage basin and the upper Neuse River basin. Previous work on these populations differentiated substrate affinities (Alderman, 1989), with the Carolina fatmucket found more often in course sands, gravel and cobble substrates, whereas the eastern lampmussel occurred more often in medium to coarse sands. Our own collecting of these two groups was consistent with these reported substrate preferences. Sample shell size data from this study, even though based on relatively small numbers, confirmed prior evidence of a larger *L. r. conspicua,* that is, about 1.4 times greater than *L. r. radiata* (Table 2). There is also strong evidence for "site effects" in the two species examined (*Lampsilis cariosa* and *Leptodea ochracea*) for this phenomenon, and this process cannot be eliminated as a basis of the shell differences. In addition, covariance analysis of shell regressions clearly indicated strong concohological similarities between these two "subspecies."

Nei's (1978) unbiased genetic identity between these two "subspecies" is 0.978 (and an unbiased genetic distance of 0.022) (Table 4). Rogers metric modified distance (Rogers, 1972; Wright, 1978) was 0.162, hardly distinguishable from the value of 0.134 between the two separated populations of *Leptodea ochracea,* and even smaller than 0.211 to 0.229 among the allopatric populations of *Lampsilis cariosa.* Clearly, Nei's (1978) identity between the two "subspecies" is consistent with Avise's (1976) categorization of populations within a species (0.9–1.0). It does not approach the subspecies category (0.80–0.89), let alone values differentiating species ($<$0.8). It is also in the range of values we found among the allopatric populations of *Lampsilis cariosa* and *Leptodea ochracea.* In addition, we note that the distinct Lake Waccamaw species, *Lampsilis fullerkati,* has Nei (1978) unbiased identity values of 0.945 and 0.952 in association with *L. r. conspicua* and North Carolina *L. r. radiata* respectively. Those are above the 0.88 recorded for the same species comparisons by Kat (1983), but Kat's *L. radiata* specimens came from Canada's maritime provinces. Recall also that Davis et al. (1981) argued that values $>$0.9 could be found among sympatric freshwater mussel species that recently underwent speciation. However, these two so-called subspecies of *L. radiata* are currently not sympatric, and, in fact, are found for the most part in different river basins with the exception of the Neuse River (R. I. Johnson, 1970). *Lampsilis r. radiata* seems confined to the coastal plain tidewater areas of the river systems and does not appear to overlap with *L. r. conspicua.*

One may also speculate the most pre-existing *L. radiata* populations above the tidewater areas have simply been extirpated.

Thus, the genetic identity and distance measures (Tables 4, 5), and the graphical illustrations given by the phenograms and Wagner tree (Figs. 3–5) point out the almost identical genetic similarity between the two "subspecies" of *L. radiata,* as well as the negligible genetic distance separating these "subspecies" from the recently designated species, *L. fullerkati.* Conchological data for these three populations are also similar (covariance analysis) and suggest either the beginnings of evolutionary divergence or simply evidence of wide phenotypic plasticity coming from different shell growth rates and patterns in different sites. The genetic similarity of these two *L. radiata* populations differ little from that found among poulations of the same species living in different sites (e.g. *Leptodea ochracea* and *Lampsilis cariosa*). Clearly, research on reciprocal transplant growth of young individuals (preferably of both "subspecies" and *L. fullerkati*) would be useful in clarifying this possible shell phenotypic plasticity. Answers to questions about reproductive isolation and potential hybridization among these populations also would shed further light on this genetically similar complex. Until evidence to the contrary appears, we suggest that *L. r. conspicua* and *L. r. radiata* and perhaps *L. fullerkati* be considered simply as allopatric "populations" of *Lampsilis radiata.*

We are aware that much of the work on the application of molecular genetic techniques to systematic issues has been in one direction, that of defining and erecting new species and subspecies. For example, Ayala (1975) instituted several subspecies of *Drosophila willistoni* based on allozyme techniques and Nei's (1972) genetic distance. Highton et al. (1989), also utilizing allozymes, established 16 species of *Plethodon* salamanders from the single *Plethodon glutinosis* complex based on a minimum Nei distance of 0.15 or an Nei genetic identity (I) of 0.85. Such taxonomic splitting is quite common in the systematic literature, including that of freshwater mussels. Our suggestion, therefore, of regrouping the two and possibly three previously recognized allopatric subspecies/species into one species complex, based upon very high levels of genetic identity as well as similar conchologies, is probably an uncommon event, yet appropriate until more distinctive biological species properties become evident.

ACKNOWLEDGMENTS

Special thanks go to Christopher McGrath for his help with the field work. We are also appreciative of the helpful comments of two reviewers as well as the editor, George Davis. The research was partly supported by a grant from the Nongame Program, North Carolina Wildlife Resources Commission.

LITERATURE CITED

ALDERMAN, J. M., 1988, Tar River spiny mussel annual performance report. *Annual Performance Report for the N. C. Wildlife Resources Commission-Wildlife Management,* October 1987-June 1988, 41: 192–218.

ALDERMAN, J. M., 1989, *Lampsilis radiata* (Gmelin, 1791). Unpublished report to the Nongame Program, North Carolina Wildlife Resources Commission, Raleigh, North Carolina. 6 pp.

ALDERMAN, J. M., 1990, *Lampsilis cariosa* (Say 1817). Pp. 97–100, in *Report on the Conservation Status of North Carolina's Freshwater and Terrestrial Mollusca Fauna,* W. F. ADAMS, ed., North Carolina Wildlife Resources Commission. Mimeo, 245 pp.

AVISE, J. C., 1976, Genetic differentiation during speciation. Pp. 106–122, *Molecular evolution,* F.J. AYALA, ed. Sinauer. Sunderland, Massachusetts.

AYALA, F. F., 1975, Genetic differentiation during the speciation process. *Evolutionary Biology* 15: 151–185.

BURCH, J. B., 1975, *Freshwater unionacean clams (Mollusca: Pelecypoda) of North America,* revised ed. Michigan: Malacological Publications. 204 pp.

CLARKE, A. H., 1983, *Status survey of the Tar River spiny mussel.* Final Project Report for the U. S. Fish and Wildlife Service. Ashville, North Carolina, mimeo.

DAVIS, G. M., 1984, Genetic relationships among some North American Unionidae (Bivalvia): sibling species, convergence, and cladistic relationships. *Malacologia,* 25: 629–648.

DAVIS, G. M. & S. L. FULLER, 1981, Genetic relationships among recent Unionacea (Bivalvia) of North America. *Malacologia,* 20: 217–253.

DAVIS, G. M., W. H. HEARD, S. L. FULLER & C. HESTERMAN, 1981, Molecular genetics and speciation in *Elliptio* and its relationships to other taxa of North American Unionidae (Bivalvia). *Biological Journal of the Linnean Society,* 15: 131–150.

DILLON, R. T., 1988, The influence of minor human disturbance on biochemical variation in a population of freshwater snails. *Biological Conservation,* 43: 137–144.

FARRIS, J. S., 1970, Methods for computing Wagner trees. *Systematic Zoology,* 19: 83–92.

FARRIS, J. S., 1972, Estimating phylogenetic trees from distance matrices. *American Naturalist,* 106: 645–668.

FARRIS, J. S., 1981, Distance data in phylogenetic analysis. In: V. A. FUNK & D. R. BROOKS, eds., *Advances in cladistics:* Proc. First Meeting of the Willie Hennig Soc., N.Y. Botanical Garden, Bronx, New York.

FELSENSTEIN, J., 1983, Parsimony in systematics: biological and statistical issues. *Annual Review of Ecology and Systematics,* 14: 313–333.

FELSENSTEIN, J., 1988, Phylogenies from molecular sequences: inferences and reliability. *Annals of Research in Genetics,* 22: 521–565.

GOLDBERG, E. D., plus nine other authors, 1978, The mussel watch. *Environmental Conservation,* 5: 101–105.

HARTL, D. L. & A. G. CLARK, 1989, *Principles of population genetics,* 2nd ed. Sinauer. Sunderland, Massachusetts. 682 pp.

HIGHTON, R., G. A. MAHA & L. R. MAXSON, 1989, Biochemical evolution in the slimy salamanders of the *Plethodon glutinosis* complex in the eastern United States. *Illinois Biological Monographs,* 57: 1–153.

HINCH, S. G., R. C. BAILEY & R. H. GREEN, 1986, Growth of *Lampsilis radiata* (Bivalvia: Unionidae) in sand and mud: a reciprocal transplant experiment. *Canadian Journal of Fisheries Science,* 43: 548–552.

HORN, K. J. & H. J. PORTER, 1981, Correlation of shell shape in *Elliptio waccamawensis, Leptodea ochracea,* and *Lampsilis* sp. (Bivalvia, Unionidae) with environmental factors in Lake Waccamaw, Columbus County, North Carolina. *Bulletin of the American Malacological Union,* for 1981: 1–4.

JOHNSON, G. B., 1977, Assessing electrophoretic similarity: the problem of hidden heterogeneity. *Annual Review of Ecology and Systematics,* 8: 309–328.

JOHNSON, R. I., 1970, The systematics and zoogeography of the Unionidae (Mollusca: Bivalvia) of the Southern Atlantic Slope region. *Bulletin of the Museum Comparative Zoology,* 140: 263–449.

JOHNSON, R. I., 1984, A new mussel, *Lampsilis (Lampsilis) fullerkati* (Bivalvia: Unionidae) from Lake Waccamaw, Columbus County, North Carolina, with a list of the other unionid species of the Waccamaw River system. *Occasional Papers on Mollusks, Museum Comparative Zoology, Harvard University,* 4: 305–320.

KAT, P. W., 1982, Effects of population density and substratum type on growth and migration of *Elliptio complanatum* (Bivalvia: Unionidae). *Malacological Review,* 15: 119–127.

KAT, P. W., 1983, Morphological divergence, genetics, and speciation among *Lampsilis* (Bilvalvia: Unionidae). *Journal of Molluscan Studies,* 49: 133–145.

KAT, P. W. & G. M. DAVIS, 1984, Molecular genetics of peripheral populations of Nova Scotia Unionidae (Mollusca: Bivalvia). *Biological Journal Linnean Society,* 22: 157–185.

KEFERL, E. P. & R. M. SHELLEY, 1988, *The final report on a status survey of the Carolina heelsplitter, Lasmigona decorata and the Carolina elktoe, Alasmidonta robusta.* Prepared for the U.S. Fish and Wildlife Service and the N.C. State Museum of Natural History.

KOEHN, R. K., F. J. TURANO & J. B. MITTON, 1973, Population genetics of marine pelecypods. II. Genetic differences in microhabitats of *Modiolus demissus. Evolution,* 27: 100–105.

LEVENE, H., 1949, On a matching problem arising in genetics. *Annals of Mathematical Statistics,* 20: 91–94.

NEI, M., 1972, Genetic distance between populations. *American Naturalist,* 106: 283–292.

NEI, M., 1978, Estimation of average heterozygosity and genetic distance from a small number of individuals. *Genetics,* 89: 583–590.

NEI, M., T. MARUYAMA & R. CHAKROBORTY, 1975, The bottleneck effect and genetic variability in populations. *Evolution,* 29: 1–10.

ROGERS, J. S., 1972, Measures of genetic similarity and genetic distance. *Studies in Genetics, University of Texas Publications,* 7213: 145–153.

SELANDER, R. K., M. H. SMITH, Y. YANG, W. E. JOHNSON & J. B. GENTRY, 1971, Biochemical polymorphism and systematics in the genus *Peromyscus.* I. Variation in the field mouse (*Peromyscus polionotus*). *Studies in Genetics* VI, *University of Texas Publications,* 7103: 49–90.

SHAW, C. R. & R. PRASAD, 1970, Starch gel electrophoresis of enzymes-A compilation of recipes. *Biochemical Genetics,* 4: 297–320.

SHELLEY, R. M., 1987, Unionid mollusks from the upper Cape Fear River basin, North Carolina, with a comparison of the fauna of the Neuse, Tar, and Cape Fear drainages (Bivalvia: Unionacea). *Brimleyana,* 13: 67–89.

SNEATH, P. H. & R. R. SOKAL, 1973, *Numerical taxonomy: the principles and practice of numerical classification.* W. H. Freeman, San Francisco. 573 pp.

STIVEN, A. E., 1989, Population biology of two southern Appalachian land snails (*Mesomphix* spp.): variation among six sites with differing disturbance histories. *Oecologica,* 79: 372–382.

SWOFFORD, D. L. & G. J. OLSEN, 1990, Phylogeny reconstruction. Pp: 411–501, D. M. HILLIS & C. MORITZ, eds., *Molecular systematics.* Sinauer, Sunderland, Massachusetts.

SWOFFORD, D. L. & R. B. SELANDER, 1981, Bioysis-1: a Fortran program for the comprehensive analysis of electrophoretic data in population genetics and systematics. *Journal of Heredity,* 72: 281–283.

THORPE, J. P., 1982, The molecular clock hypothesis: biochemical evolution, genetic differentiation and systematics. *Annual Review of Ecology and Systematics,* 13: 139–168.

TURGEON, D. D., plus nine other authors, 1988, *Common and scientific names of invertebrates*

from the United States and Canada: Mollusca. American Fisheries Society Special Publication 16: 277 pp.

WILKINSON, L., 1990, SYSTAT: The system for statistics. SYSTAT, Inc., Evanston, Illinois.

WRIGHT, S., 1978, *Evolution and genetics of populations. Vol. 4. Variability within and among natural populations.* University of Chicago Press, Chicago, Illinois.

Revised MS accepted 24 March 1992

APPENDIX I. Species and ANSP catalog numbers, number electrophoresed, water system, site code (Fig. 1), and description of collecting sites for populations of North Carolina freshwater mussels used in this study. The rate *L. r. radiata* and *L. r. conspicua* were returned alive to collecting site.

Species	ANSP	No.	County	Water System (Code) Location
Lampsilis radiata radiata[1]		9	Gates	Chowan River (C). Below HiWay 13/ 158 bridge, Hertford-Gates county line
Lampsilis radiata conspicua[1]		23	Durham	Flat River (B). HiWay 501, east on SR 1471 to bridge, 200 m below bridge
Elliptio complanata	392038 392039	44	Person	S. Flat River (A). HiWay 501, west on SR 1123, south on SR 1125 to bridge, 200 m below bridge
Leptodea ochracea[2]	392040	19	Gates	Chowan River (C) (see above)
	392041	55	Columbus	Lake Waccamaw (D). Collections just off shore State Park, 2 m depth
Lampsilis cariosa	392042	11	Cumberland	Cape Fear River (F). HiWay 401, site at confluence of Carvers Ck. and Cape Fear R.
	392043	7	Nash	Tar River (E). Main channel from Spring Hope to HiWay 581 bridge
	392044	17	Moore	Deep River (G). Via HiWay 22 west on SR 1456 bridge, upstream 100 m.
Lempsilis fullerkati	392044	35	Columbus	Lake Waccamaw (C) (see above)

[1]Returned alive to collecting site, no ANSP number.
[2]Formerly called *Lampsilis ochracea* (see Turgeon et al., 1988).

MALACOLOGIA, 1992, 34(1-2): 371-376

INDEX

Taxa in **bold** are new; page numbers in **bold** indicate pages on which new taxa are described; underscored pages indicate systematic descriptions of previously named taxa; pages in *italics* indicate figured taxa.

MALACOLOGIA, VOL. 34

CONTENTS

WHY NOT SUBSCRIBE TO MALACOLOGIA?

ORDER FORM

Your name and address _____

_____

_____

Send U.S. $26.00 for a personal subscription (one volume) or U.S. $45.00 for an institutional subscription. Make checks payable to "MALACOLOGIA."

Address: Malacologia, Academy of Natural Sciences
1900 Benjamin Franklin Parkway
Philadelphia, PA 19103-1195, U.S.A.

MALACOLOGIA, 1992, 34(1–2):

INSTRUCTIONS FOR AUTHORS

1. MALACOLOGIA publishes original research on the Mollusca that is of high quality and of broad international interest. Papers combining synthesis with innovation are particularly desired. While publishing symposia from time to time, MALACOLOGIA encourages submission of single manuscripts on diverse topics. Papers of local geographical or systematic interest should be submitted elsewhere, as should papers whose primary thrust is physiology or biochemistry. Nearly all branches of malacology are represented on the pages of MALACOLOGIA.

2. Manuscripts submitted for publication are received with the tacit understanding that they have not been submitted or published elsewhere in whole or in part.

3. Manuscripts may be in English, French, German or Spanish. Papers in languages other than English must include a translation of the Abstract in English. Authors desiring to have their abstracts published in other languages must provide the translations (complete with main titles). Include all foreign accents. Both American and British spellings are allowed.

4. Unless indicated otherwise below, contributors should follow the recommendations in the *Council of Biology Editors (CBE) Style Manual* (ed. 5, 1983) available for U.S. $24.00 from CBE, 9650 Rockville Pike, Bethesda, MD 20814, U.S.A.

5. Be brief.

6. Manuscripts must be typed on one side of good quality white paper, double-spaced throughout (including the references, tables and figure captions), and with ample margins. Tables and figure captions should be typed on separate pages and put at the end of the manuscript. Make the hierarchy of headings within the text simple and consistent. Avoid internal page references (which have to be added in page proof).

7. Choose a running title (a shortened version of the main title) of fewer than 50 letters and spaces.

8. Provide a concise and informative Abstract summarizing not only contents but results. A separate summary generally is superfluous.

9. Supply between five and eight key (topic) words to go at the end of the Abstract.

10. Use the metric system throughout. Micron should be abbreviated μm.

11. Illustrations are printed either in one column or the full width of a page of the journal, so plan accordingly. The maximum size of a printed figure is 13.5 × 20.0 cm (preferably not as tall as this so that the caption does not have to be on the opposite page).

12. Drawings and lettering must be dark black on white, blue tracing, or blue-lined paper. Lines, stippling, letters and numbers should be thick enough to allow reduction by ½ or ⅓. Letters and numbers should be at least 3 mm high after reduction. Several drawings or photographs may be grouped together to fit a page. Photographs are to be high contrast. High contrast is especially important for histological photographs.

13. All illustrations are to be numbered sequentially as figures (not grouped as plates or as lettered subseries), and are to be arranged as closely as possible to the order in which they are first cited in the text. Each figure must be cited in the text.

14. Scale lines are required for all nondiagrammatic figures, and should be convenient lengths (e.g., "200 μm," not "163 μm"). Magnifications in captions are not acceptable.

15. All illustrations should be mounted, numbered, labeled or lettered, i.e. ready for the printer.

16. A caption should summarize what is shown in an illustration, and should not duplicate information given in the text. Each lettered abbreviation labeling an individual feature in a figure must either be explained in each caption (listed alphabetically), or be grouped in one alphabetic sequence after the Methods section. Use the latter method if many abbreviations are repeated on different figures.

17. Tables are to be used sparingly, and vertical lines not at all.

18. References cited in the text must be in the Literature Cited section and *vice versa.* Follow a recent issue of MALACOLOGIA for bibliographic style, noting especially that serials are cited unabbreviated. Supply pagination for books. Supply information on plates, etc., only if they are not included in the pagination.

19. In systematic papers, synonymies should not give complete citations but should relate by author, date and page to the Literature Cited section.

20. For systematic papers, all new type-specimens must be deposited in museums where they may be studied by other scientists. Likewise MALACOLOGIA requires that voucher specimens upon which a paper is based be deposited in a museum where they may eventually be reidentified.

21. Submit each manuscript in triplicate. The second and third copies can be reproductions.

22. Authors who want illustrations returned should request this at the time of ordering reprints. Otherwise, illustrations will be maintained for six months only after publication.

REPRINTS AND PAGE COSTS

23. When 100 or more reprints are ordered, an author receives 25 additional copies free. Reprints must be ordered at the time proof is returned to the Editorial Office. Later orders cannot be considered. For each authors' change in page proof, the cost is U.S. $3.00 or more.

24. When an article is 10 or more printed pages long, MALACOLOGIA requests that an author pay part of the publication costs if grant or institutional support is available.

SUBSCRIPTION COSTS

25. Effective August 1992, personal subscriptions are U.S. $26.00 and institutional subscriptions are U.S. $45.00. Back issues and single volumes: $35.00 for non-institutional purchaser; $45.00 for institutional purchaser. There is a one dollar handling charge for all purchases of single volumes. Address inquiries to the Subscription Office.

VOL. 34, NO. 1–2 MALACOLOGIA 1992

CONTENTS


3 2044 072 160 559